16th European Powder Diffraction Conference

1 - 4 July 2018

John McIntyre Conference Centre

University of Edinburgh, Edinburgh, UK

http://epdic16.efconference.co.uk/

Introduction

Welcome to EPDIC16 at the University of Edinburgh.

The European Powder Diffraction Conference series has been running since 1991. EPDIC is the only European conference completely dedicated to all aspects of the analysis of polycrystalline materials by diffraction methods. The 16th EPDIC meeting will highlight the latest developments in powder diffraction including methodology, data analysis and instrumental advances. EPDIC16 brings together practitioners from institutes, universities and companies to discuss progress in academic and industrial research related to powder diffraction. For more information about EPDIC activities and past meetings see; http://epdic.ing.unitn.it/

We thank all members of the conference committees shown below, the sponsors and exhibitors, the Edinburgh First organizing team, and all attendees for their contributions to the success of EPDIC16.

Conference Co-chairs:
Prof. J. Paul Attfield (University of Edinburgh)
Prof. Robert J. Cernik (University of Manchester)

Exhibition Organiser:
Dr. Caroline Kirk (University of Edinburgh)

Local Organizing Committee:
Prof. J. Paul Attfield (Chair)
Assoc. Prof. Jan Willem Bos (Heriot Watt University)
Dr. Caroline Kirk (University of Edinburgh)
Prof. Phil Lightfoot (University of St. Andrews)
Dr. Abbie McLaughlin (University of Aberdeen)
Prof. Malcolm McMahon (University of Edinburgh)

Programme Committee:

Prof. Robert J. Cernik (Chair) and EPDIC Committee members;

A. Altomare, Bari, Italy

J.P. Attfield, Edinburgh, UK

N. Audebrand, Rennes, France

P. Bordet, Grenoble, France

M. Brunelli, Grenoble, France

R.J. Cernik, Manchester, UK - Vice-Chairman

W.I.F. David, ISIS, Oxon, UK

S. Eriksson, Göteborg, Sweden

A.N. Fitch, ESRF, Grenoble, France

G. Nenert, Malvern Panalytical, Almelo, The Netherlands

A. Goodwin, Oxford, UK

A. Guagliardi, Bari and Como, Italy

J.E. Jorgensen, Aarhus, Denmark

A. Kern, Bruker AXS, Karlsruhe, Germany

A. Kremenovic, Belgrade, Serbia

R. Kuzel, Prague, Czech Republic

I. Margiolaki, Grenoble, France

A. Neels, Dübendorf, Switzerland

W. Paszkowicz, Warsaw, Poland

D. Rafaja, Freiberg, Germany

J. Rius, Barcelona, Spain

P. Scardi, Trento, Italy – Chairman

P. Whitfield, Excelsus SS, Switzerland

Pollock Halls Campus Map

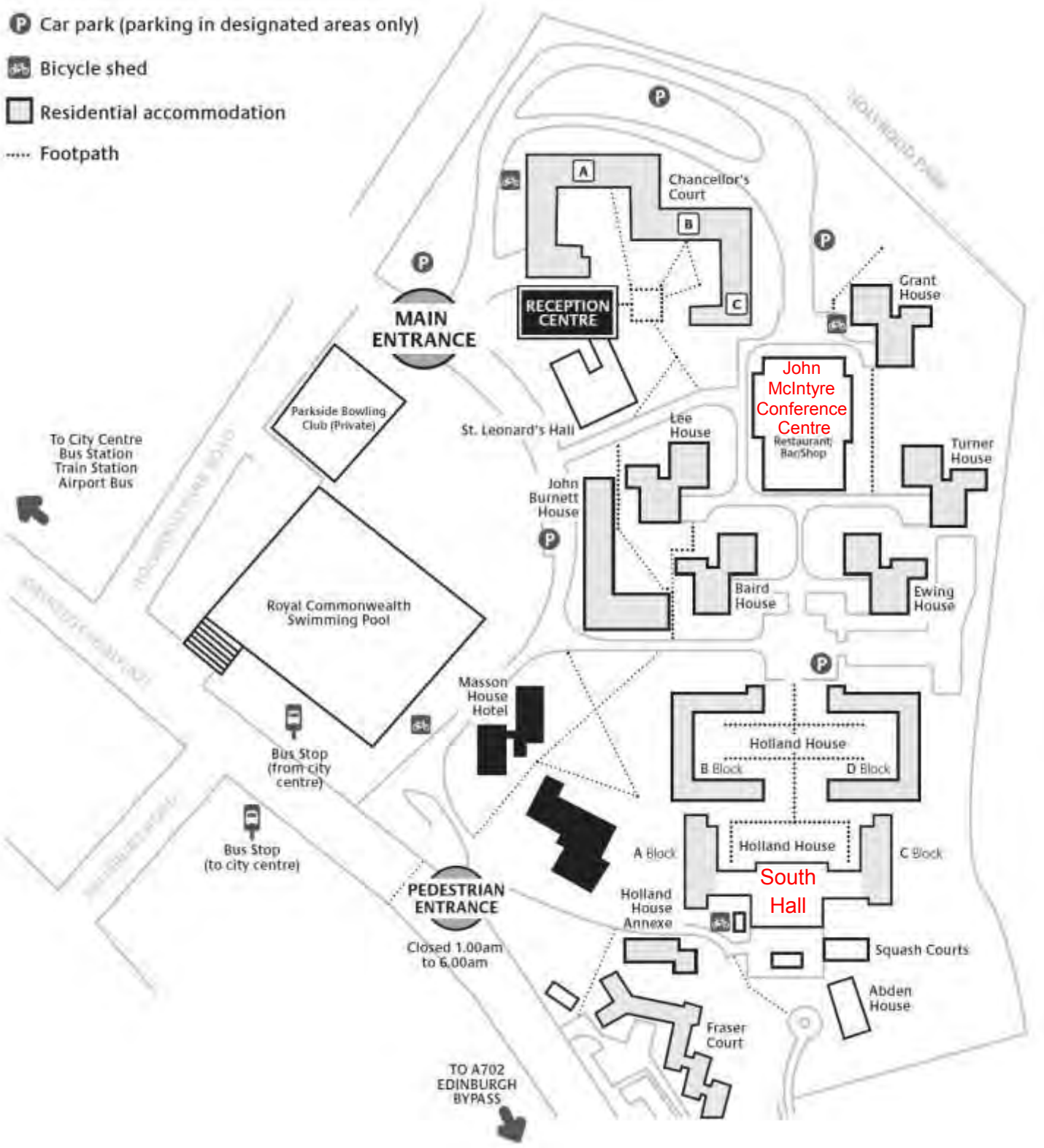

John McIntyre Conference Centre

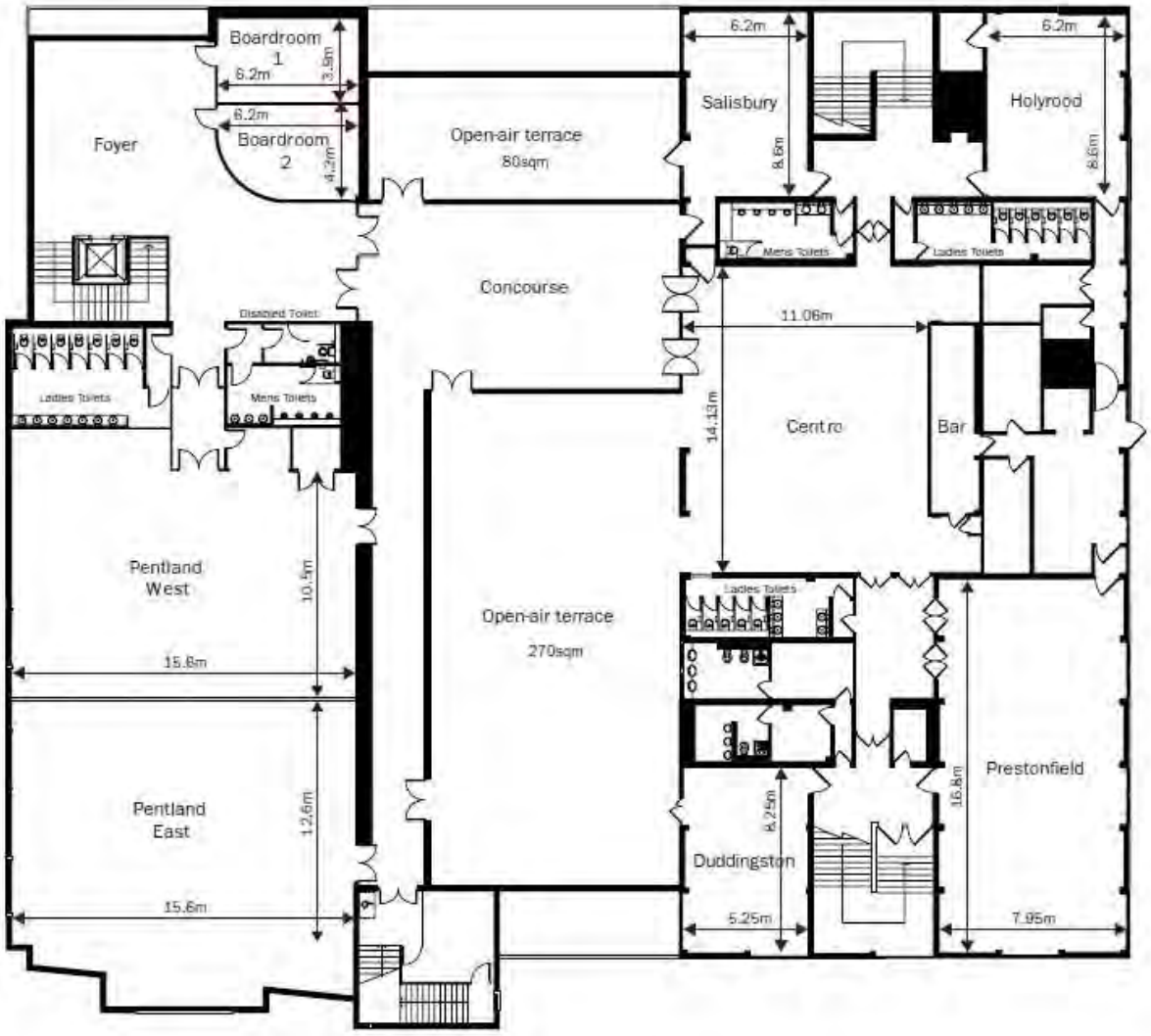

South Hall Complex

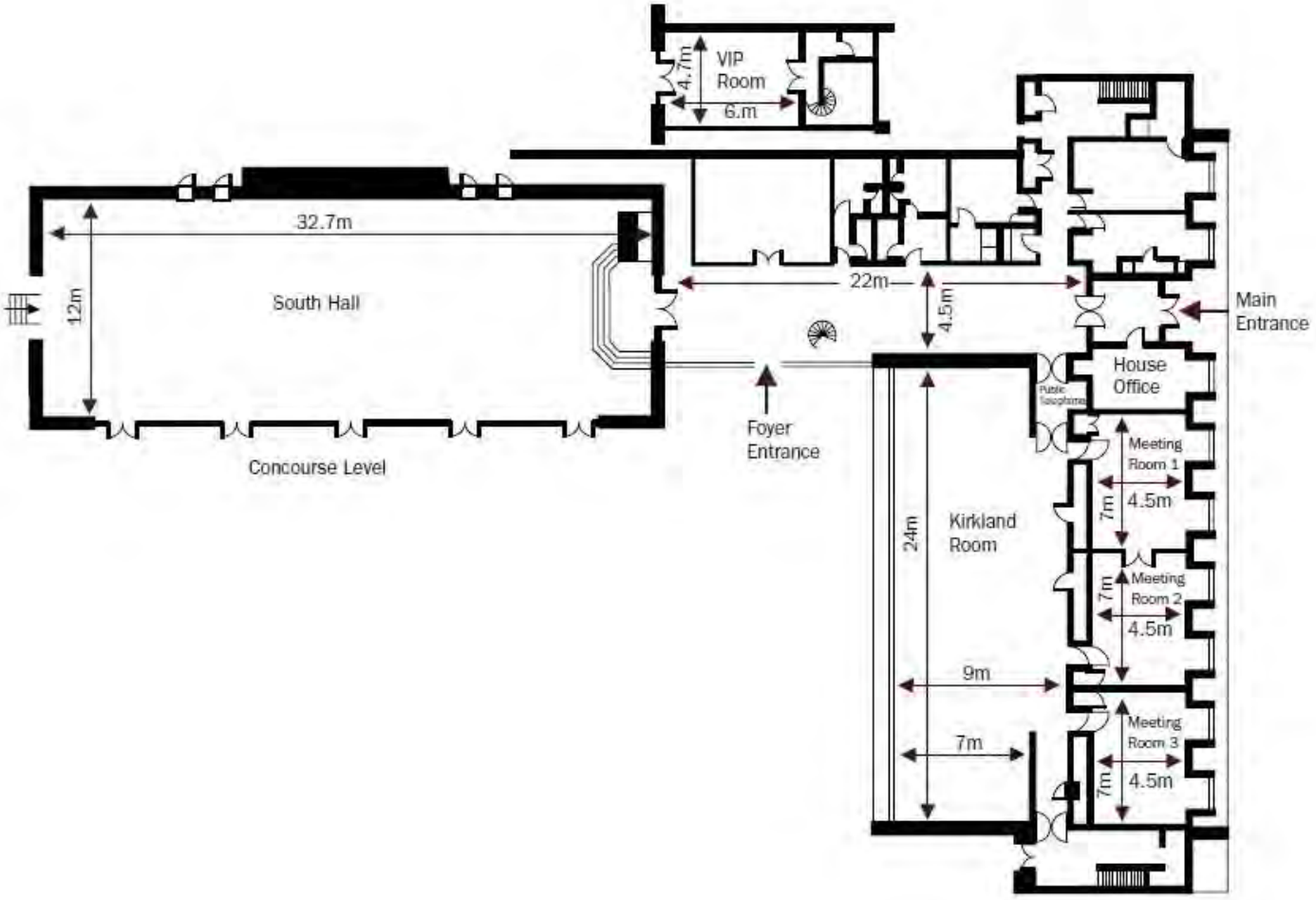

Exhibition Floor Plan

Foyer

Concourse

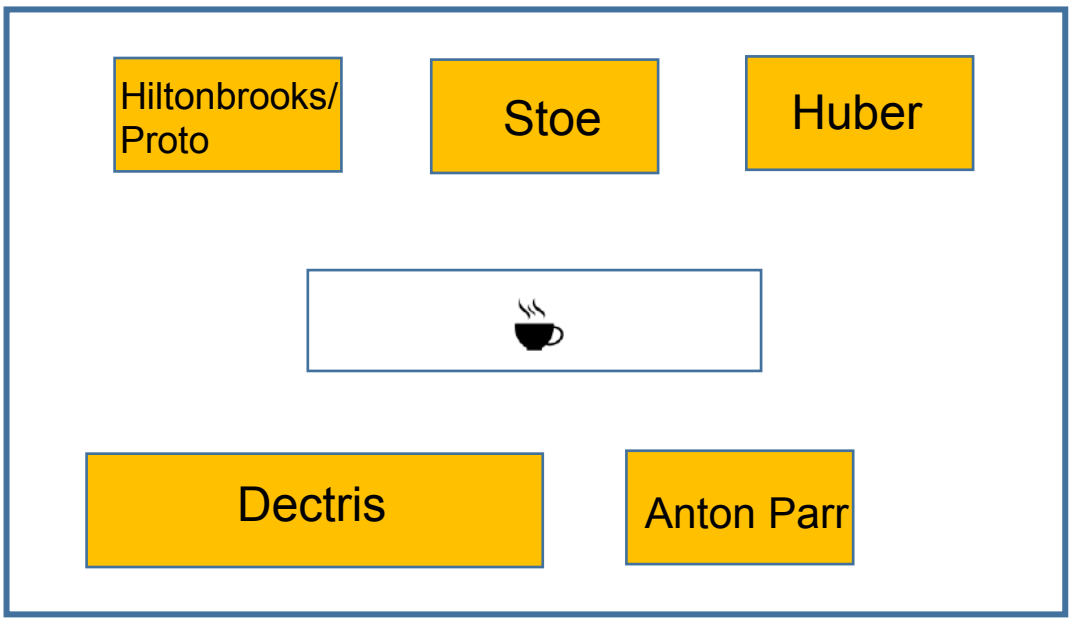

Centro

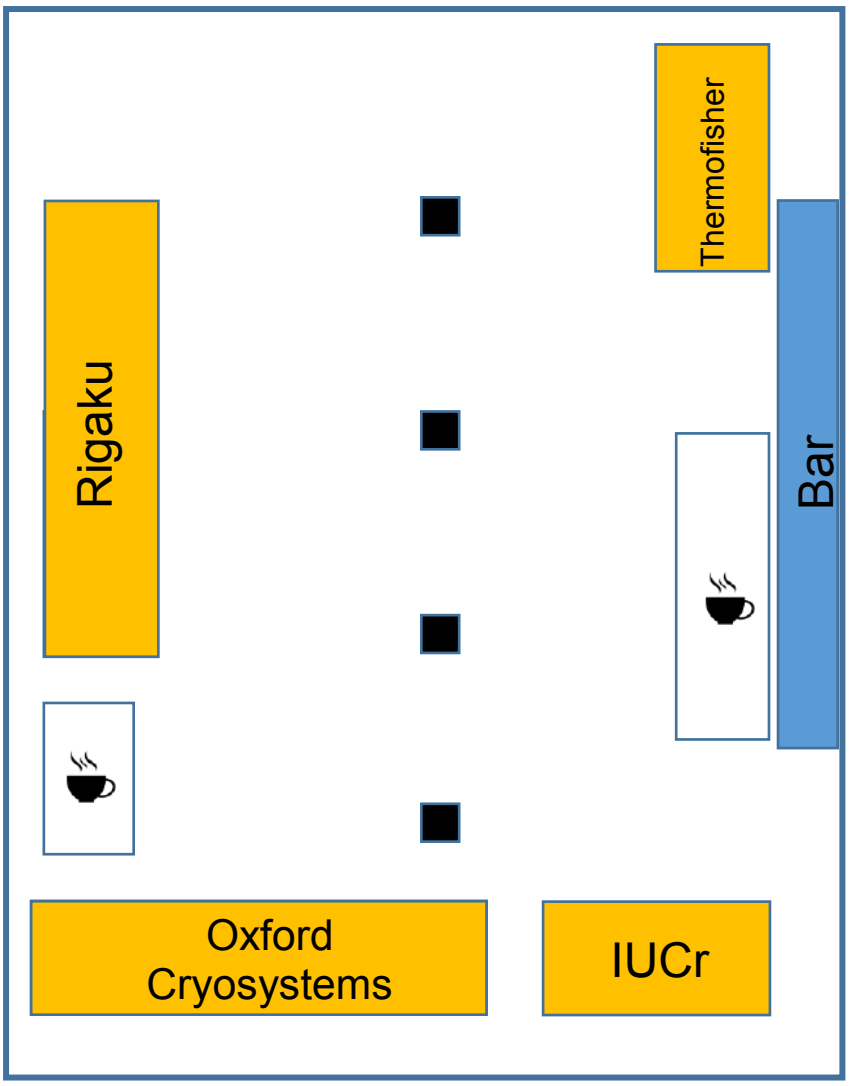

Prestonfield

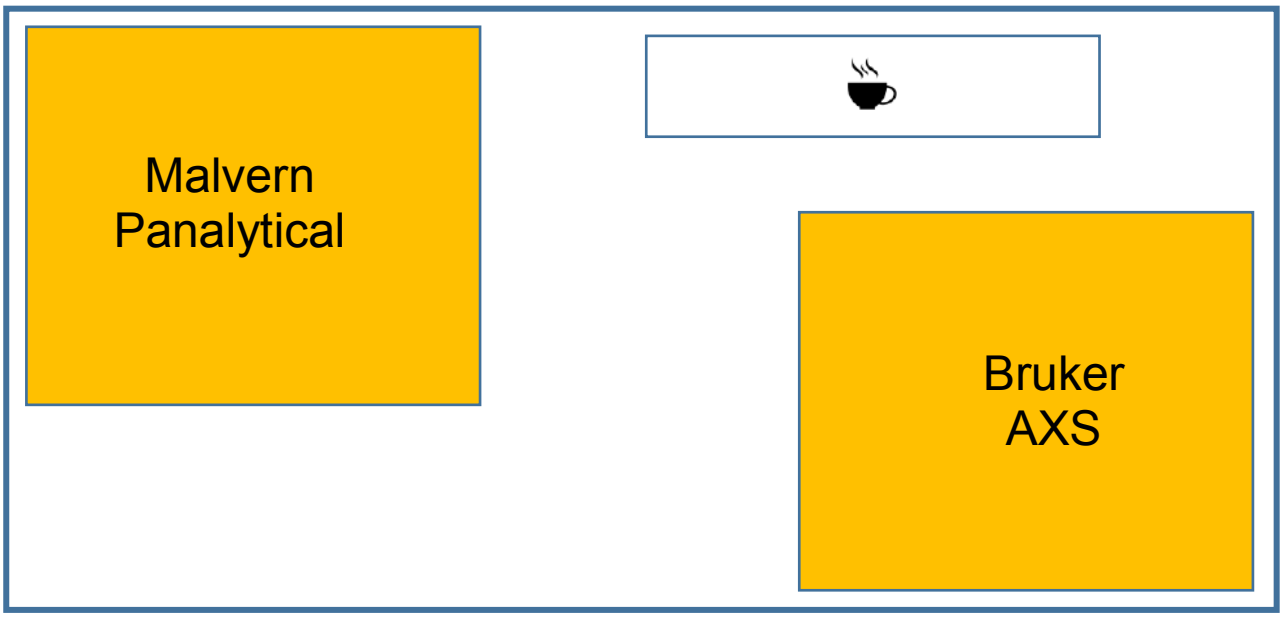

Time	Sunday 1st July	
12.30		EPDIC 16 registration, JMCC
13.00	ICDD workshop Lunch 1 - 2 pm, Marquee Workshop 2 - 5 pm Pentland Room	From 12.30 until 18.00
16.00		
18.00		
18.00 - 19.00	Drinks reception JMCC	
Time	**Monday 2nd July**	
8.30 - 9.00	Opening ceremony, EPDIC awards Chairs: Paul Attfield, Paolo Scardi and Bob Cernik; Pentland	
9.00 - 10.00	Plenary Lecture; New Opportunities at European XFEL Robert Feidenhans'l (FEEL, DE) Chair Andy Fitch; Pentland	
10.00 - 10.30	Tea/coffee break and commercial exhibition	
10.30 - 12.30	MS10 New Sources and Instruments for Powder Diffraction, South Hall Chairs: Paul Henry (ISIS, UK) and Andy Fitch (ESRF, FR)	MS03 Methods in structure solution and refinement, Pentland Chairs: Angela Altomare (Bari, IT) and Jordi Rius (Barcelona, ES)
10.30 - 11.00	POWTEX – Angular- and Wavelength-Dispersive, High-Intensity Neutron TOF Diffractometer Andreas Houben (Aachen, DE)	Bigger structures, faster: optimising simulated annealing to improve structure determination from powder diffraction data Kenneth Shankland - University of Reading
11.00 - 11.30	ESRF ID15 EH3 - A new station dedicated to multi-dimensional operando materials chemistry Marco Di Michiel (ESRF, FR)	Inorganic Materials Serial Crystallography Structure Determination Kenneth Beyerlein - Max Planck Institute
11.30 - 11.50	Multi-Mythen detector for fast, high-resolution, lab-based pair distribution function characterization of nanostructures Maxwell Terban - MPI	Combining Powder & Single-Crystal Diffraction Techniques with DSC Studies to Provide Insights into C-H…F-C Interactions in C6F6:C6H(6−n)Me(n) Co-crystals Jeremy Karl Cockcroft (UCL)
11.50 - 12.10	Combining a nine-crystal multianalyser stage with a Pilatus3 X CdTe detector for high-resolution X-ray powder diffraction at ESRF-ID22 Catherine Dejoie - ESRF	Common rules of systematic absence applied to ab-initio indexing Ryoko Oishi-Tomiyasu - Yamagata Univ.
12.10 - 12.30	DanMAX – The new materials science beamline at MAX IV Mads Jørgensen - Aarhus University	New algorithms for structure solution of polycrystalline materials in EXPO software Rosanna Rizzi (IC-CNR)
12.30 - 14.00	"Discover the new diffraction platforms from Malvern Panalytical" seminar, (lunch sponsored by Malvern Panalytical is included), Kirkland Lunch and commercial exhibition, concourse/ centro/ Prestonfield Lachlan's Software Fayre, Boardroom 2 and Pentland EPDIC committee meeting (lunch included), Holyrood	
14.00 - 16.00	MS08 Total Scattering and Disorder, Pentland Chairs: Matt Tucker (Oak Ridge USA) and Alexsander Kremenovic (Belgrade, RS)	MS06 New developments in instrumentation for sample environments, South Hall Chairs: Paul Attfield (Edinburgh, UK) and Pamela Whitfield (Excelsus SS, CH)
14.00 - 14.30	DISCOVER: ORNL's Diffraction and Total Scattering Beamline for Materials Discovery Katharine Page (ORNL, USA)	In situ studies of mechanochemical milling reactions Ivan Halasz - Ruđer Bošković Institute

14.30 - 15.00	Local Structure Investigations on the XPDF Beamline at Diamond Light Source Philip Chater - Diamond Light Source	In-Situ Diffraction Studies of Uranium Oxides. How to safely reduce SrUO4 at a beamline. Brendan Kennedy - University of Sydney
15.00 - 15.20	Alloying anodes for sodium-ion batteries: insights from pair distribution function analysis and solid-state NMR Phoebe Allan - University of Birmingham	Study of proton conductivity on powder samples using XRD David Havlicek - Charles University
15.20 - 15.40	Diffuse scattering masquerading as Bragg peaks: Low-dimensional magnetic order in a metal–organic framework Andrew Goodwin - University of Oxford	Rotatable load frames for neutron diffraction - analysis of strain, texture, phase transformations and elastic constants Markus Hoelzel - TUM-MLZ
15.40 - 16.00	Planar defects and dynamic disorder in lead halide perovskite nanocrystals unveiled through reciprocal space total scattering methods Federica Bertolotti - Aarhus University	Exploring real time amorphization in organic pharmaceutical compounds via in situ ball milling Mickaël Morin - Excelsus AG
16.00 - 16.30	Tea/ coffee/ commercial exhibition	
16.30 - 17.30	Plenary Lecture; Revealing local orbital degeneracy lifting and local geometric frustration relieving in complex electronic materials with total scattering Emil Bozin (Brookhaven National Lab, USA) Chair : Alexsander Kremenovic; Pentland	
17.30 - 18.30	Poster session 1 for MS01, MS03, MS04, MS06, MS08 and MS10, Marquee Commercial exhibition Beer/ wine/ soft drinks	
19.00 - 20.00	Drinks reception; The Signet Library, Parliament Square, Edinburgh EH1 1RF	
Time	**Tuesday 3rd July**	
8.30 - 9.30	Plenary Lecture; Strengths of neutron powder diffraction Maria Teresa Fernandez-Diaz (ILL, France) Chair: Pamela Whitfield; Pentland	
9.30 - 10.30	Young powder diffractionist award winner; Structure determination of polycrystalline materials using X-rays and electrons Stef Smeets (Stockholm, SE) Chair: Lynne McCusker (Stockholm, SE); Pentland	
10.30 - 11.00	Tea/coffee break and commercial exhibition	
11.00 - 13.00	MS05 XRD diffraction imaging and combined methods, South Hall Chairs: Antonia Neels (Zurich, CH) and Bob Cernik (Manchester, UK)	MS12 Microstructure phenomena in thin films, Pentland Chairs: David Rafaja (Freiberg, DE) and Radek Kuzek (Prague, CZ)
11.00 - 11.30	Materials Imaging Using Synchrotron X-ray Diffraction Jon Wright (ESRF, FR)	Structure formation during sputter deposition of thin films Bärbel Krause (Karlsruhe, DE)
11.30 - 12.00	Coherent X-Ray Diffraction Imaging of Frozen Hydrated Human Erythrocytes Infected by Malaria Parasites Motomu Tanaka (Heidelberg, DE)	Materials science: in-situ, in-operando, time-resolved Jörg Grenzer (HZ Dresden, DE)
12.00 - 12.20	Aberration-corrected scanning transmission electron microscopy imaging and its use in materials science. Thomas Vogt - University of South Carolina	Microstructure and properties of magnetron sputtered Pt, PtCu and PtNi polycrystalline coatings studied by the x-ray scattering methods Milan Dopita - Charles University

12.20 - 12.40	Diffraction imaging of catalytic materials under operating conditions – unrevealing the solid-state chemistry with full pattern Rietveld refinement Dorota Matras - University of Manchester	Film Texture as a Strain Relief Mechanism in the Cubic to Tetragonal Phase Transition in (CH3NH3)PbI3 Kevin Stone - SLAC
12.40 - 13.00	Combined XRD/XRF multivariate analysis for fast chemical and crystallographic surface mapping Mauro Bortolotti - University of Trento	Analysis of functional thin films via in plane diffraction methods Zoltán Balogh-Michels - Empa
13.00 - 14.00	Lunch sponsored by Rigaku, Holyrood Lunch and commercial exhibition, concourse/ centro/ Prestonfield Lachlan's Software Fayre, Boardroom 2 and Pentland	
14.00 - 16.00	MS01 Emerging functional materials, Pentland Chairs: Robert Dinnebier (Stuttgart, DE) and Phil Lightfoot (St Andrews, UK)	MS04 Balancing conventional powder diffraction structural approaches with computation and electron diffraction, South Hall. Chairs: Bill David (STFC, UK) and Andy Goodwin (Oxford, UK)
14.00 - 14.30	Metal-organic Frameworks: Efficient Synthesis, Thermodynamic Stability and Structure Prediction Tomislav Friscic (McGill, USA)	Balancing Powder Diffraction Data and Computational Data Marcus Newmann (AMS Merzhausen, DE)
14.30 - 15.00	Soft Chemical Routes to Novel Ferroelectric and Multiferroic Materials Mike Hayward (Oxford, UK)	Combining the strengths of 3D single crystal electron diffraction and powder X-ray diffraction Xiaodong Zou (Stockholm, SE)
15.00 - 15.20	Unconventional magnetic order in GeFe2O4 and γ-SiFe2O4 Giuditta Perversi - University of Edinburgh	Crystal structure of complex coordination polymers solved from X-ray powder diffraction Luzia S. Germann - Max Planck Institute
15.20 - 15.40	Compositional nanodomain formation in hybrid formate perovskites Emily Reynolds - University of Oxford	Powder-X-ray diffraction analysis of the channel occupation in disordered η-Al5Fe2 and in three of its ordered low temperature phases η', η'' and η''' Hanka Becker - TUB Freiberg
15.40 - 16.00	Luminescent M(I) (M = Au, Ag) Thiophenolate Coordination Polymers: Structures / Properties Relationships Nathalie Guillou - Université Paris-Saclay	Mechanochemical synthesis and structure solution of MOF-74 intermediates by powder solution methods Jethro Beamish-Cook -University of Reading
16.00 - 16.30	Tea/ coffee/ commercial exhibition	
16.30 - 17.30	Plenary Lecture; Structural characterization of ordering phenomena in (multi)ferroic thin films Beatriz Noheda (Groningen, NL) Chair: Bob Cernik; Pentland	
17.30 - 18.30	Poster session 2 for MS02, MS05, MS07, MS09, MS11 and MS12, Marquee Commercial exhibition Beer/ wine/ soft drinks	
Time	**Wednesday 4th July**	
9.00 - 10.00	Plenary Lecture; Structure of Nanoparticles by Small-Angle X-ray Scattering: Application to LDL Lipoproteins and to Refolding of SDS-Denatured Proteins Jan Skov Pederson (Aarhus, Denmark) Chair: Antoinella Guagliardi; Pentland	
10.00 - 10.30	Tea/coffee break and commercial exhibition	
10.30 - 12.30	MS11 Materials under extreme conditions, South Hall Chairs: Malcolm McMahon (Edinburgh, UK) and Wojciech Paszkowicz (Warsaw, PL)	MS07 Nanomaterials: Structural, Microstructural and Surface Aspects, Pentland Chairs: Paolo Scardi (Trento, IT) and Antonietta Guagliardi (Como, IT)

10.30 - 11.00	Multiparametric studies of magnetocaloric materials in the system Mn5-xFexSi3 Karen Friese - T. U. Munchen	Characterizing Disordered Ensembles of 2-D Materials: Massively Defective MnO2 Scott Misture (Alfred, USA)
11.00 - 11.30	Unraveling the mechanical behaviour of an isoreticular family of Metal Organic Frameworks: UiO-66(M) with M=Zr, Hf, Ce Pascal Yot (Monpellier, FR)	Improving magnets through size, shape and texture control Mogens Christensen (Aarhus, DE)
11.30 - 11.50	High Pressure Synthesis and Characterisation of MnFe3O5 Ka Hou Hong - University of Edinburgh	Crystal structure and microstructure of γ-Al2O3 determined by analysing the anisotropic line broadening diffuse scattering Martin Rudolph - TUB Freiberg
11.50 - 12.10	XRD and image based modelling to evaluate turbine blade failures Robert Cernik - Manchester	Quantification of Correlated Disorder in Alloy Systems Through Complex PDF Modelling Robert Koch - Alfred University
12.10 - 12.30	Synthesis and characterization, by high pressure neutron powder diffraction, of the defect perovskite He2-x[CaZr]F6 Angus Wilkinson - Georgia Inst Technology	Mapping the size dependent structure of metal oxides: A new molybdenum oxide nanostructure from X-ray total scattering Kirsten M. Jensen - Copenhagen
12.30 - 13.30	Lunch and Lachlan's Software Fayre, Boardroom 2 and Pentland	
13.30 - 15.30	MS02 Energy Materials, Pentland Chairs: Michele Brunelli (ESRF, FR) and Pierre Bordet (Grenoble, FR)	MS09 Pharmaceutical and biological materials, South Hall Chairs: Fabia Gozzo (Zurich, CH) and Irene Margiolaki (Patras, GR)
13.30 - 14.00	Lithium and sodium electrochemical (de) intercalation in layered molybdenum oxides Marie Guignard (Bordeaux, FR)	Protein Polycrystallography with GSAS-II Bob von Dreele (Los Alamos, USA)
14.00 - 14.30	Operando X-ray Diffraction Studies of Battery Materials David Wragg (Oslo, NO)	14.00 Humidity Induced Structural Changes of a Novel Monoclinic HEWLysozyme Form Investigated by In Situ Laboratory X-Ray Powder Diffraction. Detlef Beckers - Malvern Panalytical 14.15 In-situ powder diffraction study of molecular compounds under high energy milling: from amorphization to solid state transformation. Pierre Bordet - Institut Néel
14.30 - 14.50	Na3V2(PO4)2F3 : an optimal cathode material for high rates In Situ Powder Diffraction studies on Operando battery Francois Fauth - Alba	Expression and preliminary Structural Determination of viral proteins via XRPD Maria Spiliopoulou - University of Patras
14.50 - 15.10	Towards an understanding of the magnetocaloric effect in Fe2P Johan Cedervall - Uppsala University	A New Malaria Pigment Structural Motif and Potential Drug Target Peter Stephens - Stony Brook University
15.10 - 15.30	Structural insights into the lithium amide-imide solid solution Josh Makepeace - University of Oxford	Identification and characterization of pharmaceutical API using Electron Energy Loss Spectroscopy (EELS) and TEM Electron Diffraction Tomography Stavros Nicolopoulos - NanoMEGAS
15.30 - 16.00	Tea/coffee break	
16.00 - 17.00	Plenary Lecture; Batteries: a playground for crystallographers Gwen Rousse (UPMC, Paris, France) Chair Michela Brunelli; Pentland	
17.00 - 18.00	EPDIC distinguished powder diffraction award lecture; The power of powder diffraction Bill David (STFC and Oxford, UK) Chair Paolo Scardi; Pentland	
18.00	Closing Ceremony, Pentland	
19.00	Pre dinner drinks reception, Kirkland Room, South Hall	
19.30 - on	Conference dinner, South Hall followed by Cèilidh (Music and Scottish Dancing)	

Table of Contents

Plenary Lectures

Plenary Lectures

Abstract Number	Title	Author	Corresponding Affiliation
PL1	New Opportunities at European XFEL	Prof Robert Feidenhansl	European XFEL
PL2	Revealing local orbital degeneracy lifting and local geometric frustration relieving in complex electronic materials with total scattering	Dr Emil Bozin	Brookhaven National Laboratory
PL3	Strengths of neutron powder diffraction	Prof Maria Teresa Fernandez-Diaz	Institute Laue Langevin
PL4	Structure determination of polycrystalline materials using X-rays and electrons	Dr Stef Smeets	Stockholm University
PL5	Structural characterization of ordering phenomena in (multi)ferroic thin films	Prof Beatriz Noheda	Zernike Institute for Advanced Materials, University of Groningen,
PL6	Structure of Nanoparticles by Small-Angle X-ray Scattering: Application to LDL Lipoproteins and to Refolding of SDS-Denatured Proteins	Prof Jan Skov Pedersen	Center for Materials Crystallography, Department of Chemistry and Interdisciplinary Nanoscience Center (iNANO), Aarhus University
PL7	Batteries: a playground for crystallographers	Dr Gwenaelle Rousse	Sorbonne Université - Collège de France
PL8	The power of powder diffraction	Prof Bill David	University of Oxford,

New Opportunities at European XFEL

Robert Feidenhans'l
European XFEL, Schenefeld, Germany
robert.feidenhansl@xfel.eu

The European X-ray Free Electron Laser is the brightest X-ray free electron laser in the world. It will be able to deliver up to 27000 intense ultrashort X-ray pulses per second due to its superconducting linear accelerator. The facility started commissioning in 2017 and went into operation July 1 2017. First lasing at hard x-ray energies was observed in May 2017 on the first set of instruments. Lasing was achieved in February 2018 on the second set of instruments.

User experiments have been conducted since September last year. The first two instruments that opened for user experiments were the FXE instrument for ultra-fast x-ray spectroscopy and x-ray scattering and the SPB/SFX instrument for diffractive imaging and structural determination for single particles, clusters and biomolecules. At the end year of this year two more instruments will be taken into operation. The last two instruments will go on-line in 2019. In total the six instruments this will cover a wide range of scientific fields from biology to material science and will open up new areas of science in particular within ultrafast dynamics.

In the talk I will give a description of the facility [1] including a status report of the first year the operation, a glimpse into results from the first experiments and an outlook into the prospects for the coming years.

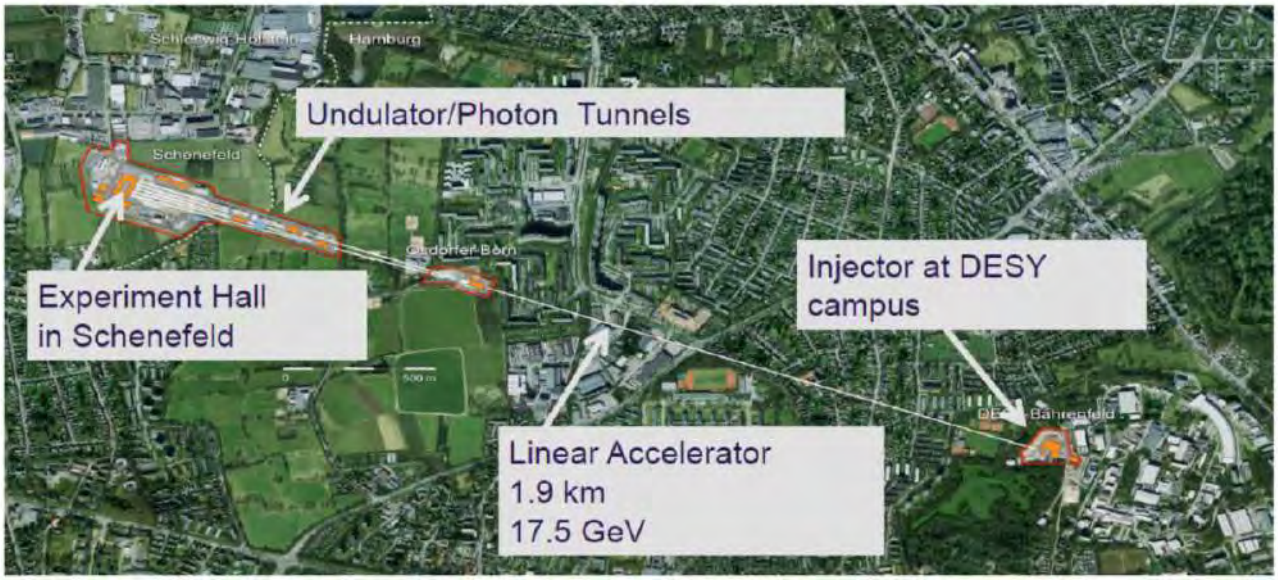

Outline of the European XFEL

[1] T. Tschentscher, C. Bressler, J. Grünert, A. Madsen, A. P. Mancuso, M. Meyer, A. Scherz, H. Sinn, U. Zastrau *Appl. Sci.* 2017, ***7***(6), 592; doi:10.3390/app7060592

Revealing local orbital degeneracy lifting and local geometric frustration relieving in complex electronic materials with total scattering

Emil S. Bozin[a*]
[a] *Condensed Matter Physics and Materials Science, Brookhaven National Laboratory, USA*
** bozin@bnl.gov*

Understanding the interplay of the electronic, orbital, and spin sectors in complex electronic materials, and how this leads to the observed ground states and associated emergent phenomena is among the most challenging tasks in solid state physics and chemistry. The crystal lattice is frequently an integral part of such a complexity, as evidenced through symmetry breaking structural alterations associated with, for example, orbital degeneracy lifting and/or geometric frustration relieving effects. Transition metal chalcogenides (TMC) with partially filled *d*-bands can be considered as exemplar systems in this regard, as they exhibit rich physical phenomena including orbital, charge, and spin orders, as well as structural, electronic, and magnetic phase transitions. More importantly, TMCs display properties that are of interest for applications, such as high-temperature superconductivity, colossal magnetoresistance, metal-insulator transitions, spin-dimerized lattices, and spin and charge glass states.
Most studies focus on the behavior in the low temperature regime, where symmetry broken states order over long range, originating from subtle interplays of competing and/or cooperating tendencies with possible new fundamental interactions. Less is known about what happens upon heating when the long-range order melts or disappears upon doping or other perturbation, yet this is possibly more crucial to understand the physics governing the behavior than the much lower energy effects responsible for the ordering of the broken symmetry states. In most of the TMCs of interest the high temperature regime is characterized by a high crystallographic symmetry structure. The low-temperature symmetry breaking is due to partial filling: the *d*-orbital states are degenerate and are prone to symmetry breaking to lift the degeneracy. We explore the character of the orbital degeneracy lifting and/or geometric frustration breaking of states at high temperature, above the temperature where the broken symmetry states order (i.e., the spin, charge, or orbital ordering).
Tracking the footprints of the broken-symmetry states lacking long range periodicity is difficult by using conventional crystallographic tools. Employing highly complementary total scattering approach based on x-ray and neutron powder diffraction and the associated pair distribution function (PDF) analysis enables in such cases more comprehensive understanding of the properties of complex electronic materials. This presentation will spotlight recent examples demonstrating the important insights that neutron and x-ray PDF analyses can provide into the structure-function relationship in complex electronic materials, with particular focus on local orbital degeneracy lifting and local geometric frustration relieving observed in several TMC families including perovskites, spinels, pyroxenes, and delafossites.

Keywords: electronic materials, orbital degeneracy and frustration, pair distribution function

Strengths of neutron powder diffraction

In spite of the huge evolution in efficiency of x-ray diffraction techniques and their accessibility in the last decades, neutron powder diffraction (NPD) is still a unique tool to extract precious information about the structure and behavior of new materials.
Actually the particular characteristics of the neutron-matter interaction make of NPD an excellent complement to X-ray diffraction for the characterization of materials. The neutron high penetration depth allows in-situ investigations of structural changes as a function of temperature, pressure, or other sample environment as well as studies of active components like charge cycling batteries. Due to the better sensitivity of neutrons to light atoms like H or Li, they are used to explore the properties of different energy-related materials and analyze the relevant physical processes. But it is the magnetic coupling of the neutron magnetic moment with the unpaired electrons in the material that makes of neutron scattering the most powerful tool to study the magnetic structure in solids.
Some examples of recent work mainly carried out at the ILL will be presented, demonstrating the valuable insights that NPD can provide in the understanding of the relationship of crystal and magnetic structure of materials with their physical properties.

Structure determination of polycrystalline materials using X-rays and electrons

S. Smeets[a*]
[a] *Department of Materials and Environmental Chemistry, Stockholm University, SE*
* *stef.smeets@mmk.su.se*

Many industrially and commercially important materials are used and produced in polycrystalline form, and not suitable for standard single-crystal structure analysis. We have been developing methodology to uncover and characterize crystal structures using X-ray powder diffraction (PXRD) data, often by making use of information gleaned from complementary characterization methods such as electron microscopy (HRTEM), electron diffraction (ED), and spectroscopic methods. This will be demonstrated on the basis of a recent example, the structure of calcined high-silica zeolite SSZ-70 [1]. The synthesis of the zeolite SSZ-70 was first reported over 10 years ago, but it proved to be difficult to characterize, because its framework structure is highly disordered. HRTEM images, synchrotron XRPD data, and DNP-enhanced 2D NMR spectra, each providing crucial and complementary insights, were used to probe different structural aspects, ranging from the long-range average structure (> 500 nm) to short-range stacking sequences (ca. 50 nm) to local atomic-level compositions and structures (< 1 nm). This combination is particularly well suited to the investigation of materials with complex partially disordered structures that cannot be resolved with conventional X-ray diffraction analysis alone. On the other hand, electron crystallography methods have now reached a level where high-quality data can be collected quickly and routinely [2]. These methods have opened up a new avenue to study nano- and microcrystalline materials. Our recent efforts have focused on the development of serial crystallograpy using a computer controlled electron microscope, making it possible to collect ED patterns of up to 4000 crystals per hour. This offers new opportunities for screening and phase analysis of polycrystalline materials, complementing the data that can be obtained using XRPD.

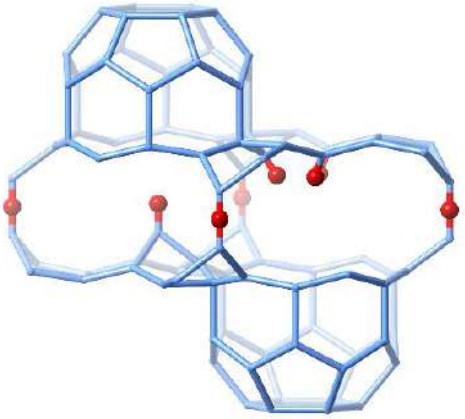

[1] Smeets S., Berkson Z.J., Xie D., Zones S.I., Wan W., Zou X., Hsieh M.-F., Chmelka B.F., McCusker L.B., and Baerlocher C., *J. Am. Chem. Soc.*, 2017, 139, 16803-16812

[2] Yun Y., Zou X., Hovmöller S. and Wan W., *IUCrJ*, 2015, 2, 267–82

[3] Smeets S., & Wan, W., *J. Appl. Crystallogr.*, 2017, 50, 885–92

Keywords: polycrystalline materials, electron diffraction, X-ray powder diffraction

Structural characterization of ordering phenomena in (multi)ferroic thin films

Beatriz Noheda
Zernike Institute for Advanced Materials, University of Groningen, The Netherlands &
Groningen Cognitive Systems and Materials center (CogniGron), University of Groningen, The Netherlands

The field of functional thin films has transformed in the past decade. This is due to the development of experimental techniques that allow synthesizing materials with atomic control, which eventually leads to atomically-defined interfaces, showing the way to much improved devices and, in some cases, to totally new device concepts. Alongside with these developments, a pressing need to achieve atomic characterization of these materials has also motivated huge research efforts towards developing novel structural methods.

Here I will focus on the challenges related to the characterization of ferroic thin films, particularly of oxide thin films, and the ordering phenomena responsible for their large and tunable electrical, mechanical or magnetic responses, which are directly linked to their ferroelectric, ferroelastic or magnetic nature. I will discuss the role of epitaxy on the atomic structure (strain engineering) but also on the microstructure and the properties; and how diffraction-based techniques remain key assets in this field. I will illustrate this with examples of our own work on ferroelectric/piezoelectric PZT and $BaTiO_3$, multiferroic $TbMnO_3$ and $BiFeO_3$ or our most recent work on the newly discovered (by the Namlab team in Dresden) nano-ferroelectric $Hf_{0.5}Zr_{0.5}O_2$. Finally, I will offer my vision about future directions in the field of (multi)ferroic oxides.

Structure of Nanoparticles by Small-Angle X-ray Scattering: Application to LDL Lipoproteins and to Refolding of SDS-Denatured Proteins

Jan Skov Pedersen[a,*]
[a] *Aarhus University, Department of Chemistry and Interdisciplinary Nanoscience Center (iNANO), Gustav wieds Vej 14, DK-8000 Aarhus C, Denmark*
** jsp@chem.au.dk*

During the last two decades, there has been a large progress on small-angle x-ray scattering (SAXS) instrumentation, at synchrotrons as well as at home sources. The development of more powerful home sources and advanced optics means that even weakly scattering samples can be measured at home. And the commercialization of the instruments has led to a large increase in capacity, so that the use has become much more widespread. Simultaneous development of analysis and modelling methods allows extracting more detailed structural information from the SAXS data. At Aarhus University, a SAXS instrument from Bruker AXS [1], which uses a powerful Ga metal jet X-ray source from Excillum, which employs an optimized geometry with homebuilt scatterless slits [2] was installed in 2014.

A brief presentation of the new Aarhus SAXS instrument will be given, and a recent example, where the structure of low-density lipoprotein (LDL) particles [3] as a function of temperature was studied and modelled, will be presented. LDL is involved in atherosclerosis and the build-up of plaque inside the arteries, which is broadly involved in cardio-vascular deceases, the leading cause of death in the western hemisphere. In the work [3], a new model for determination of the structure of the LDL particles based on super ellipsoids was derived. The model allows fitting both size and shape, and to determine the particular internal layering of the fats inside the LDL core. The analysis of the resulting structure gives in addition information on changes in the conformation of the protein component, which wraps the fatty core. The availability of the model now allows monitoring of structural changes in the LDL upon different stresses from the environment, such as changes in temperature, oxidation, or external agents used or currently in development against atherosclerotic plaque build-up.

In another project, protein-detergent interactions have been studied [4]. Globular proteins are usually unfolded and denatured by the anionic surfactant sodium dodecyl sulphate (SDS). This was also fthe case for the four investigated proteins, bovine serum albumin (BSA), α-lactalbumin, (αLA), lysozyme (LYZ), and β-lactoglobulin (βLG), which all form complexes, which are protein-decorated SDS micelles. Somewhat surprisingly, most of these proteins could be refolded by addition of the non-ionic surfactants (NIS), octaethylene glycol monododecyl ether (C12E8) or dodecyl maltoside (DDM). A relatively simple data analysis approach based on linear combinations of SAXS data recorded for, respectively, native protein, complexes, and pure and mixed micelles. The addition of NIS to the protein-SDS samples resulted in extraction of the SDS from the protein-SDS complexes and refolding of βLG, BSA, and LYZ, while αLA changed to its NIS-bound state instead of the native state. It was concluded that NIS competes with globular proteins for association with SDS, making it possible to refold SDS-denatured proteins by adding sufficient amounts of NIS, unless the protein also has significant interactions with the NIS.

[1] Schwamberger, A.; De Roo, B.; Jacob, D.; Dillemans, L.; Bruegeman, L.;. Seo, J.W; Locquet, J.P., *Nuclear Inst. and Methods in Physics Research B*, 2015, 343, 116-122.

[2] Li, Y.; Beck, R.; Huang, T.; Choi, M. C.; Divinagracia, M., *J. Appl. Crystallogr*., 2008, 41, 1134–1139.

[3] Maric, S.; Lind, T.K.; Lyngsø, J.; Cárdenas, M.; Pedersen, J.S., *ACS Nano*, 2017, 11, 1080-1090.

[4] Kaspersen, J.D.; Søndergaard, A.; Madsen, D.J.; Otzen, D.E.; Pedersen, J.S., *Biophysical Journal*, 2017, 112, 609-1620.

Keywords: Small-angle X-ray Scattering, Low-density Lipoproteins, Protein Refolding

Batteries: a playground for crystallographers

G. Rousse[a,*]
[a] *"Chimie du solide et énergie", Sorbonne Université-Collège de France, Paris, France*
** gwenaelle.rousse@upmc.fr*

Research's progresses in rechargeable batteries are driven by ever increasing demands dictated by the energy transition. Rechargeable lithium ion batteries, because of their high energy density, have conquered most of today's portable electronics. The development of electric transportation also largely relies on the development of such devices. Still, there is plenty of room for improvement since the energy density is far from being enough for long-driving distances. The same applies for the sister technology, Na-ion, which could become the technology of choice for stationary storage in a near future. For all these applications, electrode materials have been essential. Identifying new phases and understanding their electrochemical reactivity towards Li or Na, via the help of evolving analytical techniques, including powder diffraction, have contributed to the success of the Li-ion technology. This will be illustrated through a few examples dealing with Li(Na)-ion batteries based on either polyanionic (phosphates, sulphates or borates) or layered compounds [1-5]. Importance of crystallography and diffraction experiments will also be highlighted in the field of ionic conductors, as an important step towards the development of safe all-solid-state batteries. Lastly, it will be shown that other communities – e.g. solid state physicists- may benefit from research in materials for batteries with the discovery of compounds presenting interesting magnetic properties [6-7].

[1] Rousse, G.; Rodríguez-Carvajal, J.; Giacobbe, C.; Sun, M.; Vaccarelli, O.; Radtke, *Physical Review B* **2017**, *95* (14), 144103.

[2] Rousse, G.; Tarascon, J. M. *Chemistry of Materials* **2014**, *26* (1), 394–406.

[3] McCalla, E.; Abakumov, A. M.; Saubanere, M.; Foix, D.; Berg, E. J.; Rousse, G.; Doublet, M.-L.; Gonbeau, D.; Novak, P.; Van Tendeloo, G.; et al. *Science* 2015, 350 (6267), 1516–1521.

[4] Sathiya, M.; Abakumov, A. M.; Foix, D.; Rousse, G.; Ramesha, K.; Saubanère, M.; Doublet, M. L.; Vezin, H.; Laisa, C. P.; Prakash, A. S.; et al. *Nat Mater* **2015**, *14* (2), 230–238.

[5] Sathiya, M.; Rousse, G.; Ramesha, K.; Laisa, C. P.; Vezin, H.; Sougrati, M. T.; Doublet, M.-L.; Foix, D.; Gonbeau, D.; Walker, W.; et al. *Nature Materials* **2013**, *12* (9), 827–835.

[6] Rousse, G.; Rodríguez-Carvajal, J. *Dalton Trans.* **2016**, *45*, 14311–14319.

[7] Vaccarelli, O.; Rousse, G.; Saúl, A.; Radtke, G.. *Physical Review B* **2017**, *96* (18), 180406(R).

Keywords: batteries, electrode materials, nuclear and magnetic structures

.

The power of powder diffraction

Bill David
ISIS Spallation Neutron Source, Rutherford Appleton Laboratory, Harwell Campus, OX11 0QX &
Inorganic Chemistry Laboratory, University of Oxford, South Parks Road, Oxford, OX1 3QR

Abstract

Powder diffraction rules our structural understanding of the materials world around us. It is a technique of remarkable scope that addresses and informs many of the most important technical challenges of our time that include photovoltaic perovskites and pharmaceutical polymorphs, and battery cathodes and heterogeneous catalysis. Moreover, the advances in modern instrumentation and computer software mean that we can now make structural movies of processes as they happen. And with modern analytical tools, a single powder diffraction pattern not only informs us about the average crystal structure but also the local atomic structure, through pair distribution function analysis, and the mesoscale structure, through whole powder pattern modelling. In this presentation, I will talk about some of the more curious things that I have encountered in my forty years of powder diffraction and talk about future opportunities afforded by combining powder diffraction with spectroscopy and thermodynamic measurements, electron microscopy and first principles computational modelling.

MS01 - Emerging functional materials

MSO1

Abstract Number	Title	Author	Corresponding Affiliation
MS01 - K1	Metal-organic Frameworks: Efficient Synthesis, Thermodynamic Stability and Structure Prediction	Dr Tomislav Friscic	McGill University
MS01 - K2	Soft Chemical Routes to Novel Ferroelectric and Multiferroic Materials	Prof Michael Hayward	University of Oxford
MS01 - OR1	Unconventional magnetic order in GeFe2O4 and γ-SiFe2O4	Ms Giuditta Perversi	University of Edinburgh
MS01 - OR2	Compositional nanodomain formation in hybrid formate perovskites	Dr Emily Reynolds	University of Oxford
MS01 - OR3	Luminescent M(I) (M = Au, Ag) Thiophenolate Coordination Polymers: Structures / Properties Relationships	Dr Nathalie Guillou	ILV/UVSQ/Université Paris-Saclay
MS01 - P1	Improper Ferroelectric Polarisation in a Perovskite driven by Inter-site Charge Transfer and Ordering	Dr Mark Senn	University of Warwick
MS01 - P2	Green chemistry and nanotechnology for a sustainable agriculture	Dr Gregorio Dal Sasso	Istituto di Cristallografia, Consiglio Nazionale delle Ricerche
MS01 – P3	Powder diffraction on High Pressure A-site Manganites	Dr Angel Arevalo-Lopez	Universite Lille
MS01 - P4	Synthesis of Ettringite and Thaumasite Analogues and Their Potential Use as Remediation Materials	Ms Rebecca Rae	University of Edinburgh
MS01 - P5	Dynamical Processes in Crystalline Solid Solutions of Ionic Supramolecular Complexes	Mr Luca Fornasari	University of Bologna
MS01 - P6	Evolving spin periodicity and lock-in transition in Mn2InSbO6	Dr Angel Arevalo-Lopez	Universite Lille
MS01 - P7	Pure gyrotropic phase transitions in the arcanite related materials PbMGeO4 (M = Ba, Sr)	Dr Gwilherm Nenert	PANalytical B. V.
MS01 - P8	New luminescent materials based on d10 metal halides	Ms Chiara Cappuccino	Bologna University
MS01 - P9	Powder Neutron Diffraction Studies of New Magnetic Manganites	Dr Graham McNally	Max Planck Institute for Solid State Research
MS01 - P10	Magnetic structures of Co doped materials Ni2-xCoxScSbO6	Mr Kunlang Ji	University of Edinburgh
MS01 - P11	Positive to negative thermal expansion in V2OPO4	Dr Elise Pachoud	University of Edinburgh
MS01 - P12	Structures and magnetic properties of MnRMnSbO6	Dr Elena Solana-Madruga	University of Edinburgh
MS01 - P13	The Synthesis and Characterisation of Goethite Doped with the Critical Metal Cobalt – Implications for Natural Systems	Mrs Sandra Dressler	Loughborough University
MS01 - P14	Phase composition and structure of Ni-doped iron seleno-telluride	Ms Katarzyna Kosyl	Institute of Physics PAS
MS01 - P15	Origin of the phase transition in bismuth hollandite	Dr James Cumby	University of Edinburgh

MS01 - P16	Piezoelectric phase transition in KSrVO4 investigated using the Aeris diffractometer	Dr Jan Gertenbach	Malvern Panalytical B.V.
MS01 - P17	Deformations of the α-Fe2O3 rhombohedral lattice across the Néel temperature	Mr Piotr Fabrykiewicz	University of Warsaw
MS01 - P19	In situ Investigation of Thermomechanical Processing of NiTi Shape Memory Alloys	Mrs Patricia Rodrigues	Universidade Nova de Lisboa

Metal-organic Frameworks: Efficient Synthesis, Thermodynamic Stability and Structure Prediction

T. Friščić*
[a] *Department of Chemistry, McGill University, Canada*
** tomislav.friscic@mcgill.ca*

In contrast to the demonstrated potential in a number of applications, including recently announced commercial uses in food packaging and toxic gas storage,[1] there is still a significant gap in the fundamental understanding of structures and stability of microporous metal-organic frameworks (MOFs). This presentation will outline our group's recent efforts in developing a thorough understanding of factors that guide the formation of topologically different MOFs, and determine their stability. In brief, we will highlight how different types of solvent-free reactivity, such as mechanochemistry or accelerated aging, enable a thorough screening of MOF phase diagrams. Combined with experimental thermodynamic studies of enthalpic stability and heat capacities, such efficient materials screening provides a foundation to begin evaluating how thermodynamic stability of MOFs is related to their porosity, topology and presence of substituents on the organic linkers.[2] Using metal azolate frameworks (MAFs) as model materials, it will also be shown how periodic density functional theory (DFT) enables the accurate evaluation of MOF stability, and even the prediction of preferred structures in not yet synthesized MOF systems.[3]

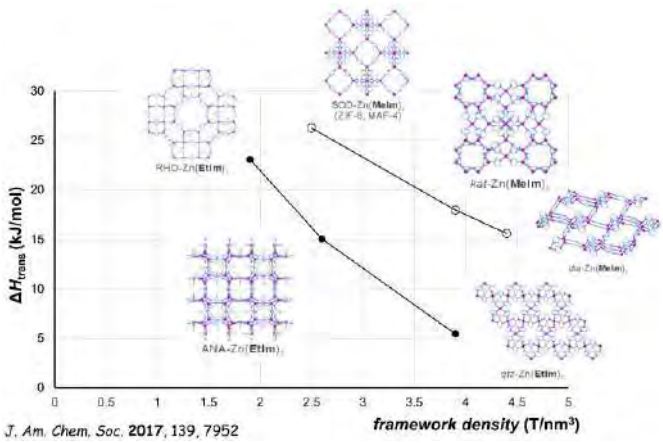

Finally, we will show how the advances in rapid and clean synthesis[4] come together with the described improved theoretical understanding of MOFs to enable new, clean and safer designs for high-energy, environmentally-friendly solid fuels.

[1] *Nature Chem.* 2016, 8, 987.

[2] Akimbekov Z., Katsenis A. D., Nagabhushana GP, Ayoub G., Arhangelskis M., Morris A. J., Friščić T. and Navrotsky A. *J. Am. Chem. Soc.,* 2017, 139, 7952.

[3] Arhangelskis M., Katsenis A. D. Morris A. J. and Friščić T. *Chem. Sci.,* 2018, 9, 3367.

[4] Marrett J. M., Mottillo C., Girard S., Nickels C. W., Do J.-L., Dayaker C., Germann L. S., Dinnebier R. E., Howarth A. J., Farha O. K., Friščić T. and Li C.-J. *Cryst. Growth Des.,* 2018, 18, DOI:10.1021/acs.cgd.8b00385

Keywords: metal-organic frameworks, mechanochemistry, thermodynamics

Soft Chemical Routes to Novel Ferroelectric and Multiferroic Materials

M. A. Hayward
Department of Chemistry, University of Oxford, U.K.
michael.hayward@chem.ox.ac.uk

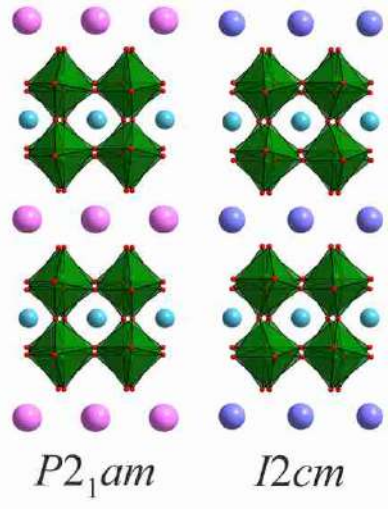

Ferroelectric materials are utilized in a wide variety of technological applications, and as a result have been the focus of prolonged and intense study. Recently there has been much interest in harnessing the collective tilting and twisting distortions of the octahedral units in oxide perovskites, and their layered structural analogues, to induce electrical polarization via a 'hybrid improper' mechanism.

Powder diffraction data, in combination with first-principles DFT calculations have been used to establish the complex and subtle tilting distortions of a series of $A'NdM_2O_7$ (A' = Cs, Rb; M = Nb, Ta) Dion-Jacobson phases, and conclusively demonstrate these phases adopt non-centrosymmetric crystal structures driven by this hybrid improper mechanism.

The extensive cation exchange chemistry of Dion-Jacobson phases can now be utilized to tune the physical properties of these layered materials. A particularly attractive option is the addition of paramagnetic centres which can provide a novel route to multiferroic materials.

[1] Zhu T., Cohen T., Gibbs A. S., Zhang W. G., Halasyamani P. S., Hayward M. A. and Benedek N. A. *Chem. Mater.* 2017, *29*, 9489.

Keywords: Ferroelectric, Dion-Jacobson phase, Transition-metal oxide

Unconventional magnetic order in $GeFe_2O_4$ and γ-$SiFe_2O_4$

G. Perversi[a*], Arevalo-Lopez, Angel M.[b], C. Ritter[c], J. P. Attfield[a]
[a] *Centre for Science at Extreme Conditions and School of Chemistry, University of Edinburgh, UK.*
[b] *Univ. Lille, CNRS, Centrale Lille, ENSCL, Unite´ de Catalyse et Chimie du Solide, France*
[c] *Institute Laue Langevin, BP 156, 38042, Grenoble, France*
* *g.perversi@sms.ed.ac.uk*

The spinel structure is widely occurring in natural and synthetic materials. The oxides of this family exhibit the general formula AB_2O_4, where the oxygen forms a *ccp* arrangement, the B cation coordinates in edge-sharing octahedra and the A cation occupies tetrahedra. The technological and scientific significance of these materials has risen in the last few decades, but their geological relevance had focused their characterisation under high-temperature and high-pressure conditions. The low temperature behaviour of most materials in this class is remarkably under-explored.

$GeFe_2O_4$ and γ-$SiFe_2O_4$ are two normal spinels, where the 3D arrangement of the Fe^{2+} outlines a pyrochlore lattice; as such, the structure has the potential for frustration upon magnetic ordering of the iron moment, which is reported as antiferromagnetic (T_N ~ 10 K and T_N ~ 11 K respectively) by early physical measurements [1]. We report a full magnetic structure solution, derived from neutron powder diffraction data collected at D2B and D20 at the ILL reactor, France.

Contrary to reports on other germanate spinels in the transition metal series ($GeCo_2O_4$, $GeNi_2O_4$ [2][3]), $GeFe_2O_4$ shows no signs of distortion in the crystal structure and remains cubic *Fd-3m* below the Néel temperature. The appearance of magnetic Bragg peaks reveals the ordering temperature to be T_N = 8.6 K. Keeping the cubic symmetry, the magnetic structure was solved with incommensurate propagation vector **k** = [⅔+δ, ⅔+δ, 0], with $\delta_{1.8K}$ = 0.025. γ-$SiFe_2O_4$ is equally undistorted but shows both an incommensurate ordering ($\mathbf{k_1}$ = [¾+δ, ¾+δ, 0], with $\delta_{1.8K}$ = 0.03 at T < 12 K) and an additional commensurate transition ($\mathbf{k_2}$ = [1 0 0] at T < 7 K).

Due to the inherent frustration of the pyrochlore lattice, a complex spin structure is required to achieve antiferromagnetic ordering without distorting the cubic symmetry. This unusual magnetic ordering and its implications will be presented, using $GeFe_2O_4$ as a main case-study.

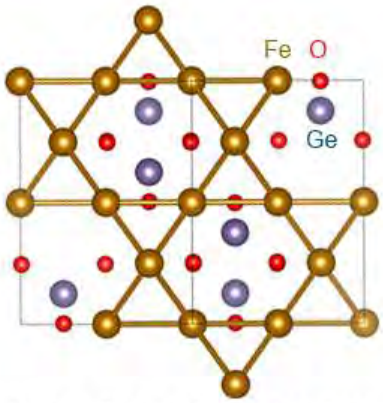

Pyrochlore lattice of edge-sharing iron-iron octahedra

[1] Blasse, G. and Fast, J. F. *Philips Res. Rep.* 1963, **18**, 393;

[2] Barton, P.T *et al. Phys Rev B* 2014 **90**, 064105;

[3] Diaz, S. *et al. Phys. Rev. B,* 2014*,* **74**, 092404

Keywords: neutron powder diffraction, magnetic structures, magnetic frustration

Compositional nanodomain formation in hybrid formate perovskites

E. M. Reynolds[a*], E. A. Donlan[a], H. L. B. Boström[a], H. S. Geddes[a], A. L. Goodwin[a]
[a] *School of Chemistry, University of Oxford, UK*
* *emily.reynolds@chem.ox.ac.uk*

At the heart of creating and developing functional materials is understanding structure - a task often complicated by disorder, be it compositional or orientational, static or dynamic. This challenge is all too familiar in the world of relaxor ferroelectrics, where the observed switchable electric polarization, in for example (1–x)Pb($Mg_{1/3}Nb_{2/3}$)O_3 – x$PbTiO_3$ (PMN-PT),[1] is a result of the inhomogenous distribution of cations and formation of polar nanoregions (PNRs).[2] The compositional disorder itself enhances the polarization and so understanding the delicate balance of atomic interactions that drives PNR formation is of great interest.

Formate perovskites, with formate linkers connecting the B-site cations and organic molecular cations occupying the A-site (Fig. 1a), can exhibit dielectric behavior.[3] In the [Gua]M($HCOO)_3$ [Gua^+ = $C(NH2)_3^+$] system for M = Cu, collective JT order gives rise to a polarization.[4] While the structure and properties of various end-members are relatively well-studied, the mixed-metal formates are not. Substitution of Cu for a JT-inactive cation will disrupt polar order, and if clustering is favourable we might expect to see domain formation, and if so, an associated enhancement in polarization.

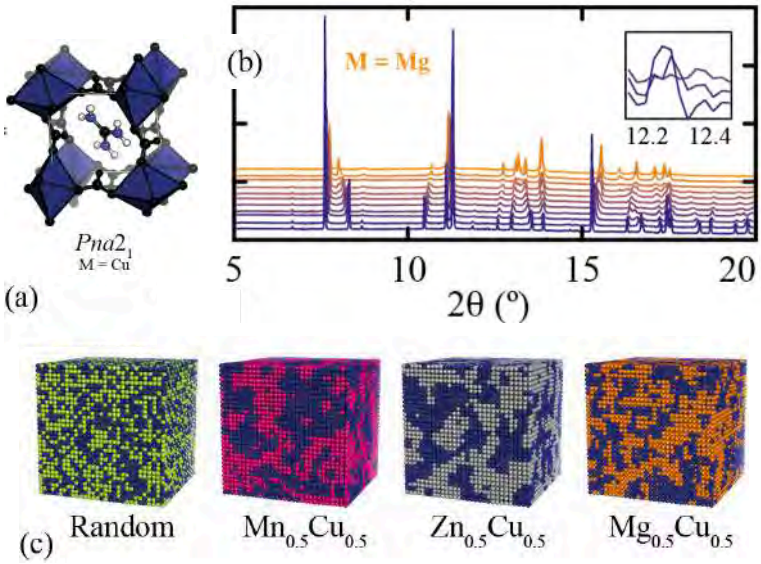

Using powder X-ray diffraction (Fig. 1b) we identified the transition from non-polar *Pnna* to polar *Pna*2_1 for the systems [Gua]$M_{1-x}Cu_x(HCOO)_3$ (M=Mn, Zn, Mg). We then used a newly-developed non-negative matrix factorization (NMF) analysis of IR spectroscopy data in combination with RMC modeling to show the existence of nanodomains in these hybrid formate perovskite systems. The compositional nanodomains in these formates, represented in Figure 1c, are of the same type as those observed in conventional relaxor ferroelectrics such as PMN-PT, and are expected to have large implications for relaxor behavior in these systems.

[1] Burns G. and Dacol F. *Phys. Rev. B.,* 1983, 28, 2527.

[2] Matsura M., Hirota K., Gehring P., Ye Y. G., Chen W. and Shirane G. *Phys. Rev. B.,* 2006, 274, 144107.

[3] Mączka M., Costa N. L. M., Gagor A., Paraguassu W., Sieradzki A. and Hanuza J. *Phys. Chem. Chem. Phys.,* 2016, 18, 13993.

[4] Stroppa A., Jain P., Barone P., Marsman M., Perez-Mato J., Cheetham A. K., Kroto H. W. and Piccozi S. *Angew. Chem. Int. Ed.,* 2011, 50, 5847.

Keywords: Ferroelectricity, nanodomains, perovskite

Luminescent M(I) (M = Au, Ag) Thiophenolate Coordination Polymers: Structures / Properties Relationships

N. Guillou[a*], O. Veselska[b], P. Bordet[c], D. Podbevšek[d], G. Ledoux[d] A. Fateeva[e], A. Demessence[b]
[a] *Institut Lavoisier Versailles, UMR CNRS 8180, UVSQ, Université Paris-Saclay, France*
[b] *IRCELYON, UMR CNRS 5256, Université Claude Bernard Lyon 1, France*
[C] *Institut Néel CNRS/UGA UPR 2940, Grenoble, France*
[d] *ILM, UMR CNRS 5306, Université Claude Bernard Lyon 1, France.*
[e] *LMI, UMR CNRS 5615, Université Claude Bernard Lyon 1, France.*
** nathalie.guillou@uvsq.fr*

Hybrid coinage metal compounds show rich structural diversity and exhibit a large domain of applications such as electronic devices, contrast agents, sensors or photocatalysts, due to the ability of M(I) to form metallophilic interactions implying self-assembly and luminescence.[1] Among them, Ag(I) and Au(I)-thiolates are fascinating compounds with photoluminescence properties that are highly sensitive to the nuclearity of the metal centers, the metal-metal distances and the ligands.[2] Despite they are known for a long time, a little is published about their structures and the relationships with their photophysical properties. Indeed, the strong chemical reactivity of coinage metals with sulfur in solution, leads to a fast precipitation of poorly crystallized compounds, especially for coordination polymers. This study deals with the structural investigation of four coordination polymers based on Au(I) and Ag(I) and two isomers of ($SPhCO_2H$). It has been shown that the two compounds obtained with *p*-($SPhCO_2H$) are lamellar whereas those obtained with *o*-($SPhCO_2H$) exhibit a 1D-structure. $[Au(I)(p\text{-}SPhCO_2H)]_n$ crystallizes in a triclinic unit cell [*S.G.* *P*1, *a* = 4.5181(4), *b* = 5.4084(4), *c* = 14.867(5) Å, α = 84.867(5), β = 86.292(5), γ = 88.256(5) °, *V* = 360.80(5) $Å^3$] and exhibits unique S-Au-S angles due to the presence of aurophilic interactions and uncommon catemeric hydrogen bonds between the layers (see figure below). It is the first coordination polymer displaying intrinsic dual emission in a large temperature range and possessing high potential as an optical temperature sensor.[3] Its analogue $[Ag(I)(p\text{-}SPhCO_2H)]_n$ crystallizes in a orthorhombic unit cell [*S.G.* *Pbca*, *a* = 7.2744(3), *b* = 5.8165(3), *c* = 34.7935(5) Å, *V* = 1472.2(1) $Å^3$] with Ag(I) connected to three ligands generating distorted Ag_3S_3 hexagons and layers connected to their neighbors *via* dimeric hydrogen bonds. The two compounds $[M(I)(o\text{-}SPhCO_2H)]_n$ are isotructural and crystallize in the tetragonal unit cell [*S.G.* $P4_2/n$, *a* = 18.79(1), *c* = 4.531(5) and *a* = 18.439(3), *c* = 4.4375(8) Å, respectively for the Au(I) and Ag(I) analogues]. M(I) are also connected to three ligands generating distorted Ag_3S_3 hexagons, which interconnect to generate an extended ladder like ribbon connected to its neighbors by hydrogen bonds. Knowledge of these structures is of tremendous importance to understand the photoluminescent properties of our materials. The presence of small and large unit cell parameters combined with huge preferred orientation effects, renders these structural determinations challenging.

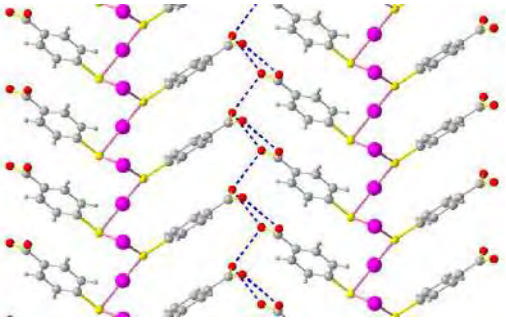

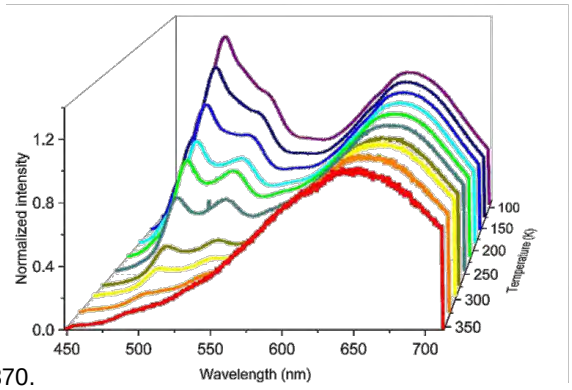

[1] Schmidbaur H., Schier A., *Chem. Soc. Rev.*, 2012, 41, 370.

[2] Veselska O., Demessence A., *Coord. Chem. Rev.*, 2018, 240.

[3] Veselska O., Okhrimenko L., Guillou N., Podbevšek D., Ledoux G., Dujardin C., Chevrier D. M., Yang R., Zhang P., Fateeva A., Demessence A., *J. Mater Chem. C*, 2017, 5, 9843.

Keywords: coordination polymers, d^{10} coinage metal organic thiolates, luminescent materials

Improper Ferroelectric Polarisation in a Perovskite driven by Inter-site Charge Transfer and Ordering

Wei-Tin Chen,[1,2] Chin-Wei Wang, [3] Hung-Cheng Wu,[4] Fang-Cheng Chou,[1,2,3] Hung-Duen Yang,[4] Arkadiy Simonov,[5] Mark S. Senn[6,*]

[1] *Center for Condensed Matter Sciences, National Taiwan University, Taipei 10617, Taiwan*
[2] *Taiwan Consortium of Emergent Crystalline Materials, MOST, Taipei 10622, Taiwan*
[3] *National Synchrotron Radiation Research Center, Hsinchu 30076, Taiwan*
[4] *Department of Physics, National Sun Yat-Sen University, Kaohsiung 80424, Taiwan*
[5] *Department of Chemistry, University of Oxford, South Parks Road, Oxford OX1 3QR, UK*
[6] *Department of Chemistry, University of Warwick, Gibbet Hill, Coventry, CV4 7AL, UK*

It is of great interest to design and make materials in which ferroelectric polarisation is coupled to other order parameters such as lattice, magnetic and electronic instabilities. Such materials will be invaluable in next-generation data storage devices. Recently, remarkable progress has been made in understanding improper ferroelectric coupling mechanisms that arise from lattice and magnetic instabilities. However, although theoretically predicted, a compact lattice coupling between electronic and ferroelectric (polar) instabilities has yet to be realised. Here we report detailed powder diffraction and micro-single crystal diffraction studies of a novel perovskite $Hg^{A}Mn^{A'}_{3}Mn^{B}_{4}O_{12}$ that is found to exhibit a polar ground state on account of such couplings that arise from charge and orbital ordering on both the A' and B-sites, which are themselves driven by a highly unusual $Mn^{A'}$-Mn^{B} inter-site charge transfer. The inherent coupling of polar, charge, orbital and hence magnetic degrees of freedom, make this a system of great fundamental interest, and demonstrating ferroelectric switching in this and a host of recently reported hybrid improper ferroelectrics remains a substantial challenge.

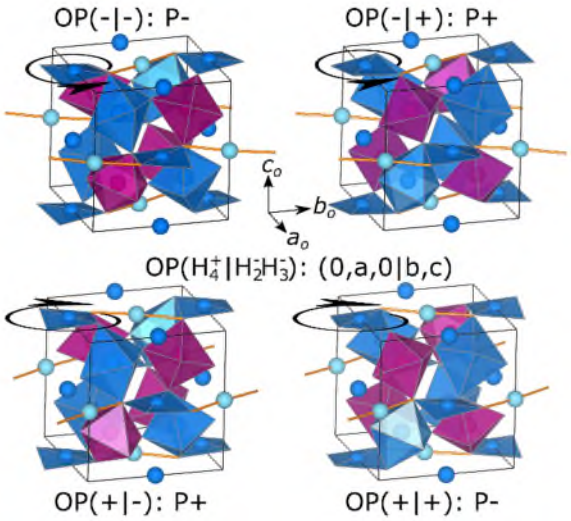

Figure 1: The origin of the improper polarisation in $HgMn_7O_{12}$. The reversal of one or other of the two primary order parameters responsible for the double-charge ordering (H_4^+ and $H_2^-H_3^-$) on the A' and B-sites is sufficient to reverse the direction of the polarisation (P), reversal of both order parameters returns the polarisation to its initial state. The short second nearest neighbor Mn-O distance ($\approx$ 2.4 \AA) that is indicative of the Mn$^{A~2+}$ state is shown in yellow (square-planar nearest neighbour coordination omitted for clarity).

Reference: in press with Phys. Rev. B (http://arxiv.org/pdf/1803.05792.pdf)

Green chemistry and nanotechnology for a sustainable agriculture

G. Dal Sasso[a,b*], F.J. Carmona Fernàndez[b,c], G.B. Ramìrez Rodrìguez[b,c], J.M. Delgado Lopez[d], F. Ferri[b,c], D. Redoglio[b,c], F. Bertolotti[b,e], J.S. Pedersen[f], N. Masciocchi[b,c], A. Guagliardi[a,b]

[a]*Istituto di Cristallografia, Consiglio Nazionale delle Ricerche, Como, Italy.*
[b]*Total Scattering Laboratory (To. Sca. Lab.), Como, Italy.*
[c]*Dipartimento di Scienza e Alta Tecnologia, Università dell'Insubria, Italy.*
[d]*Department of Inorganic Chemistry, Faculty of Science. University of Granada, Spain.*
[e]*Aarhus Institute of Advanced Studies (AIAS), Aarhus University, Denmark.*
[f]*Department of Chemistry, INANO, Aarhus University, Denmark.*
**gregorio.dalsasso@ic.cnr.it*

In the last decades, the massive application of conventional fertilizers, constituted by highly soluble N- and P-rich compounds, caused severe environmental pollution in terms of eutrophication of water bodies. In fact, most of the macronutrients are leached away by rainwater, highlighting the low efficiency of these fertilizers and the wasteful exploitation of non-renewable sources, such as phosphate ores. On a future perspective, considering the unceasing world population growth and the subsequent increase of food demand, increasing the crop yields by intensifying the use of conventional fertilizers is environmental unsustainable. On these bases, this research aims to integrate nanotechnology into the development of more efficient and sustainable fertilizer [1]. Carbonated-calcium phosphate nanoparticles – amorphous and hydroxyapatite-based nanocomposites - are synthetized by chemical precipitation [2] and designed to incorporate N-based macronutrients. Here, we show the results of nanoparticles characterization through synchrotron-based Wide Angle X-ray Total Scattering (WAXTS), Small Angle X-ray Scattering (SAXS) and Static and Dynamic Light Scattering (SLS/DLS) techniques. Advanced modelling techniques based on the Debye scattering equation [3] are applied to diffraction data to extract information on crystallinity degree, crystal structure, size, morphology and composition of nanoapatites obtained at different maturation time and doping. Additional information on the size and shape of nanoparticles is also provided by SAXS analysis. The structural and microstructural information coupled with measurements of stability and nutrients release enables us to control the macronutrients release over time due to the progressive dissolution of nanoparticles by modulating their size, structure and composition. Initial tests on grapevines and wheat plants make these materials highly promising smart fertilizer for future exploitation.

[1] Liu R., Lal R., 2015. The science of the total environment, 514, 131-139.
[2] Delgado-Lõpez J.M., Frison R., Cervellino A., Gõmez-Morales J., Guagliardi A., Masciocchi N., 2014. Advanced Functional Materials, 24 (8), 1090-1099.
[3] Cervellino A., Frison R., Bertolotti F., Guagliardi A., 2015. Journal of Applied Crystallography, 48, 2026-2032.

Acknowledgments: This work has been supported by Fondazione Cariplo, Project n. 2016-0648: Romancing the stone: size-controlled HydroxyaPATItes for sustainable Agriculture (HYPATIA)

Keywords: nano-hydroxyapatite, sustainable agriculture, X-ray total scattering

Synthesis of Ettringite and Thaumasite Analogues and Their Potential Use as Remediation Materials

R. Rae[a*], C. Kirk[a]
[a] *School of Chemistry, University of Edinburgh, UK*
* *rebecca.rae@ed.ac.uk*

Ettringite ($Ca_6[Al(OH)_6]_2(SO_4)_3.26H_2O$) is an important hydration product of Portland cement and also occurs naturally, first being discovered in 1874. It has a well characterised structure crystallising in space group P31c [1]. The structure is cation columns with composition $Ca_3[Al(OH)_6.12H_2O]^{3+}$, that run parallel to the *c* axis, with the sulfate anions and remaining water molecules in channels running parallel to these columns. Ettringite has been shown to accommodate other cations (Fe^{3+}, Ga^{3+}, Mn^{2+}) on the octahedral aluminium sites [2] and other anions (NO_3^-, OH^-, $B(OH)_4^-$) substituting for sulfate [3]. In some cases these analogous phases are found to crystallise in the structure of thaumasite ($Ca_3Si(OH)_6(CO_3)(SO_4).12H_2O$), a mineral which is closely related to ettringite, but crystallises in space group $P6_3$.

The ability of the structure to accommodate a wide range of different ions, of both size and charge, gives it the potential for use in waste remediation. For instance, aluminium present in wastewater from the aluminium anodizing industry has been successfully removed using an ettringite precipitation method [4].

This study is investigating the formation of new ettringite analogues as well as the ideal conditions for synthesis of pure ettringite-type phases. Characterisation of the formed phases was carried out using Powder X-ray diffraction and FTIR spectroscopy. The gallium analogue ($Ca_6[Ga(OH)_6]_2(SO_4)_3.26H_2O$) was found to form almost instantaneously using the saccharate method while other analogues (e.g. Fe, Sn) were found to form over longer periods of time (e.g. the Fe phase ($Ca_6[Fe(OH)_6]_2(SO_4)_3.26H_2O$) only formed after 2 days). Solid solution formation between ettringite and gallium-ettringite ($Ca_6[Al_xGa_{1-x}(OH)_6]_2(SO_4)_3.26H_2O$ $0 \leq x \leq 1$) has also been investigated and a complete solid solution between the end member phases forms. The results from preliminary unit cell refinements will be presented here.

[1] Moore A.E. and Taylor H.F.W. *Acta Cryst.,* 1970, B26, 386

[2] Norman R.L., Dann S.E., Hogg S.C. and Kirk C.A. *Solid State Sci.,* 2013, 25, 110

[3] Pöllman H., Kuzel H.J. and Wenda R. *Neues Jahrbuch Miner. Abh.,* 1989, 160, 133

[4] Álvarez-Ayuso E. and Nugteren H.W. *Water Res*, 2005, 39, 65

Keywords: ettringite, waste remediation, ion replacement

Dynamical Processes in Crystalline Solid Solutions of Ionic Supramolecular Complexes

L. Fornasari[a*], S. D'agostino[a], F. Grepioni[a], D. Braga[a]
[a] *Department of Chemistry "G. Ciamician", University of Bologna, Italy*
* *luca.fornasari3@unibo.it*

Dynamic processes like rotation and libration of molecules within crystals have long attracted the attention of researchers. Partly because this phenomenon undermines what the crystal is considered to be, that is a static entity, in part because the understanding, control, and exploitation of such movements can provide new functional materials. For example, rotation of molecules in crystals has been investigated for applications such as thermal modulation of birefringence, nonlinear optics, switchable ferroelectrics, gas and vapor sensors, and dielectric constant modulation.
Solid solutions can be defined as non-stoichiometric multi-component crystals in which two, or even more, components combine homogeneously in a single crystalline phase[1]. To attain the formation of a solid solution, miscibility of the components is a key condition, which in turn depends on the similarity of the components in terms of size and shape.
We are presently studying the reorientational motions in the crystals of supramolecular complexes comprising crown ethers and halides salts. Their key feature is that a temperature-dependent order-disorder phase transition is associated to the onset of such motions.
This work focuses on the realisation of binary solid solutions of the above-mentioned ionic complexes. Solid solutions over the entire compositional range were prepared by means of mechanochemical methods. Mechanochemistry offered here the advantage of a fast and straightforward synthesis with a precise control over the stoichiometric ratio of the components and the formation of by-products, with respect to the alternative liquid-phase procedure.
Powder XRD analyses and Pawley refinement were employed to probe the accordance of the so obtained solid solutions with Vegard's law[2], while thermal analysis was used to characterise the order-disorder transition. Finally, it was observed that the solid solution approach has a profound influence on the temperature at which the phase transition occurs.

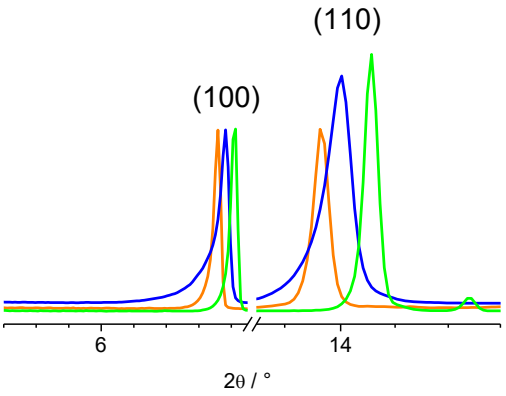

[1] Kitaigorodsky A. I, Mixed crystals, Springer Science & Business Media, 2012, vol. 33

[2] Denton A. R and Ashcroft N. W. *Phys. Rev. A,* 1991, 43, 6, 3161-3164.

Keywords: crystal engineering, supramolecular complexes, solid solutions

Evolving spin periodicity and lock-in transition in Mn_2InSbO_6

A. M. Arévalo-López,[a] E. Solana-Madruga,[b] E. P. Arévalo-López,[c]
D. Khalyavin,[d] M. Kepa,[b] A. J. Dos santos-García,[e] R. Sáez-Puche[f] and J. P. Attfield[b]
[a] *UCCS-UMR 8181, CNRS, Universite de Lille, France.* [b] *CSEC, University of Edinburgh, UK*
[c] *FAM, UNAM, Mexico.* [d] *ISIS Facility, RAL, UK.* [e] *ETSIDI, UPM, Spain.* [f] *UCM, Spain.*

The discovery of new materials with appealing functional properties is challenging and such properties are often observed in complex oxides containing transition metals in intermediate or unusual oxidation states that must be stabilized under special synthetic conditions. ABO_3 compounds present two main structural families, perovskite-like and corundum-like structures, differing on the coordination of the A-site cation. A^{2+} cations in perovskites synthesized at ambient pressures are typically large, nonmagnetic atoms, such as A = Ca, Sr, Ba, Pb. However, materials with the smaller high-spin Mn^{2+} ion at A sites have been synthesized under high-pressure and high temperature conditions. This may introduce additional functionalities as found in $MnVO_3$ perovskite which is metallic but also has coexisting helimagnetic order of localized S = 5/2 Mn^{2+} spins [1]. Corundum type derivatives with Mn^{2+} can be transformed from the ilmenite polymorph ([001] cation order) to the $LiNbO_3$-type ([111] cation order) with high pressure, as demonstrated in $MnTiO_3$, this allows multiferroic properties [2]. More complex functionalities can be envisaged in ordered double oxides AA'BB'O_6 by analogy with the much-studied high-Tc ferrimagnetic magnetoresistive material Sr_2FeMoO_6 [3]. We will present our results in the ordered-ilmenite $(Mn_{0.5}In_{0.5})_2MnSbO_6$ compound obtained with high pressure synthesis. It shows a spin reorientation due to inhomogeneous Dzyaloshinskii-Moriya interactions (DM) from a k_1 = (0 0 0) to a k_2 = (0 0 1/8) through a continuum of helical structures. Figure 1 shows half of the cell of the k_2 magnetic structure and a 2D contour plot with temperature evolution of the magnetic diffraction maxima. The green lines at 38 K, 17 K and 8 K mark the transitions between the different magnetic structures. The panel on the right shows the change on the z component of the propagation vector k_2 = (0 0 k_z).

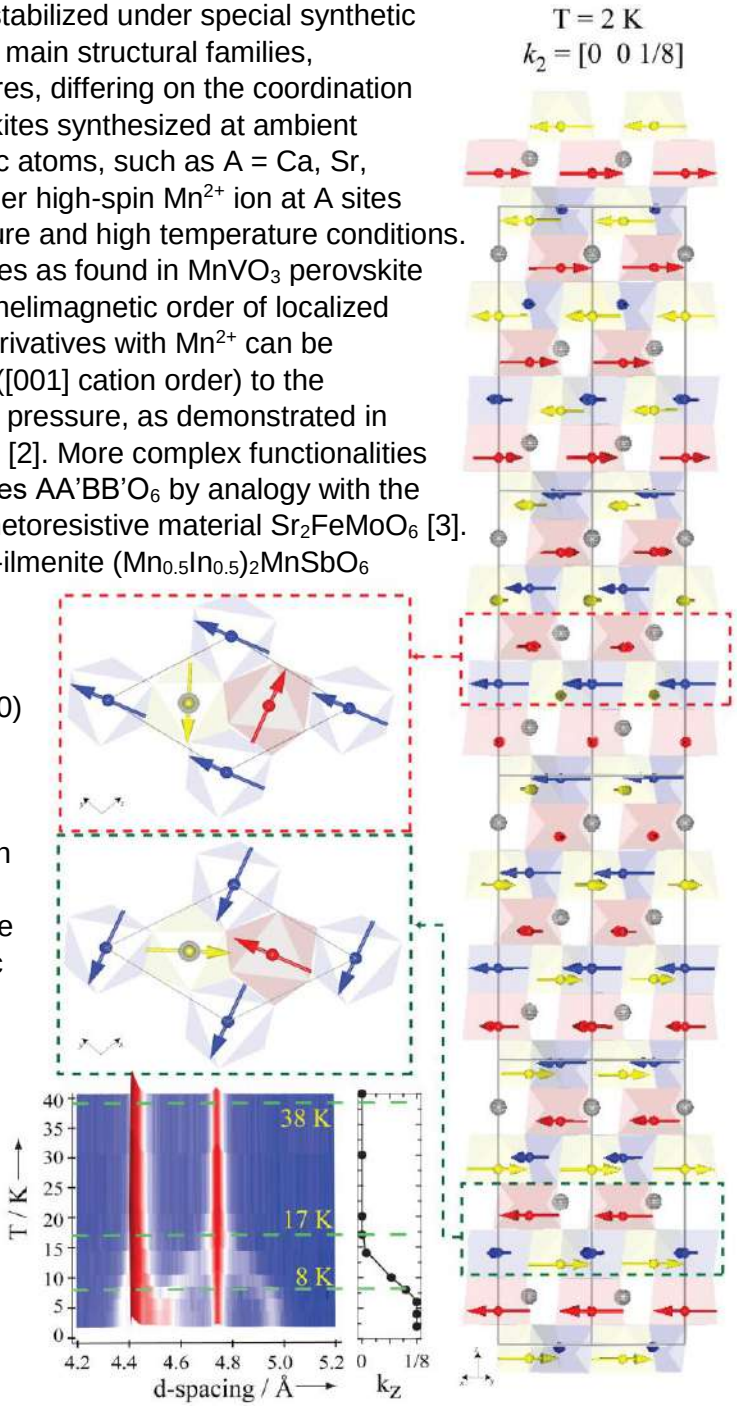

[1] Markkula, M. *et al. Phys. Rev. B,* 2011, 84,094450.
[2] Arevalo-Lopez, A.M. and J. P. Attfield, *Phys. Rev. B*, 2013, 88, 104416.
[3] Kobayashi, K.I. *et al. Nature*, 1988, 395, 677.

Powder diffraction on High Pressure A-site Manganites

A.M. Arevalo-Lopez[a*], E. Solana-Madruga[b],
A. J. Dos santos-Garcia[c], R. Saez-Puche[d], J. P. Attfield[b]
[a]*UCCS-UMR 8181, CNRS, Universite Lille, France*
[b] *CSEC & School of Chemistry, University of Edinburgh, UK*
[c] *ETSIDI, Universidad Politécnica de Madrid, Spain*
[d] *Facultad de Química, Universidad Complutense de Madrid, Spain*
** angel.arevalo-lopez@univ-lille1.fr*

The discovery of new materials with appealing functional properties is challenging and such properties are often observed in complex oxides containing transition metals in intermediate or unusual oxidation states that must be stabilized under special synthetic conditions.
ABO_3 compounds present two main structural families, perovskite-like and corundum-like structures, differing on the coordination of the A-site cation. A^{2+} cations in perovskites synthesized at ambient pressures are typically large, nonmagnetic atoms, such as A = Ca, Sr, Ba, Pb. However, materials with the smaller high-spin Mn^{2+} ion at A sites have been synthesized under high-pressure and high-temperature conditions. This may introduce additional functionalities as found in $MnVO_3$ perovskite which is metallic but also has coexisting helimagnetic order of localized S = 5/2 Mn^{2+} spins [1]. Corundum type derivatives with Mn^{2+} can be transformed from the ilmenite polymorph ([001] cation order) to the $LiNbO_3$-type ([111] cation order) with high pressure, as demonstrated in $MnTiO_3$, this allows multiferroic properties [2]. More complex functionalities can be envisaged in ordered double oxides $AA'BB'O_6$ by analogy with the much-studied high-T_c ferrimagnetic magnetoresistive material Sr_2FeMoO_6 [3].
We will present our results in the ordered-ilmenite $(Mn_{0.5}In_{0.5})_2MnSbO_6$ compound obtained with high-pressure synthesis (Figure 1a). It shows a spin reorientation due to inhomogeneous Dzyaloshinskii-Moriya interactions (DM) from a k_1 = (0 0 0) to a k_2 = (0 0 1/8) through a continuum of helical structures. Figure 1 shows a 2D contour plot with temperature evolution of the magnetic diffraction maxima. The green lines at 38K, 17 K and 8 K mark the transitions between the different magnetic structures. The panel on the right shows the change on the z component of the propagation vector k_2 = (0 0 k_z).

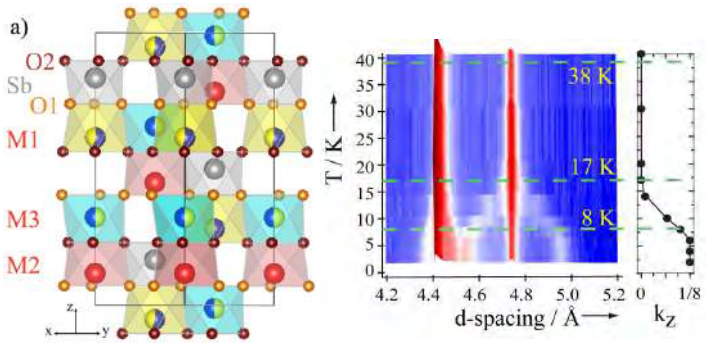

[1] Markkula M., Arevalo-Lopez A. M., Kusmartseva, A., Rodgers J., Ritter R., Wu H., and Attfield J. P. *Phys. Rev. B.,* 2011, 84, 094450.

[2] Arevalo-Lopez A. M. and Attfield J. P. *Phys. Rev B.,* 2013, 88, 104416.

[3] Kobayashi, K. I., Kimura, T., Sawada, H., Terakura, K. and Tokura Y. *Nature*, 1998, 395, 677.

Keywords: high-pressure synthesis, manganites, neutron diffraction.

Pure gyrotropic phase transitions in the arcanite related materials $PbMGeO_4$ (M = Ba, Sr)

G. Nénert
[a] *Malvern Panalytical, Lelyweg 1, 7602 EA, Almelo, The Netherlands*
* *gwilherm.nenert@panalytical.com*

Gyrotropic phase transitions are characterized by the appearance of a spontaneous optical activity [1]. The appearance of such activity is very common in ferroelectric materials. In such materials, the optical activity is a secondary order parameter and is coupled to the primary order parameter which is the electrical polarization. However, only very rare examples are known of a pure gyrotropic phase transition. Among those, one can cite $BiFeO_3$ under strain [2], $(C_5H_{11}NH_3)_2ZnCl_4$ as function of temperature [3]. In both cases, the transition exhibits a change from Pnma to $P2_12_12_1$ symmetry.
In this contribution, we have investigated 2 materials belonging to the $BaNdGaO_4$ structural type, namely $PbBaGeO_4$ and $PbSrGeO_4$ using powder X-ray diffraction as function of temperature. While $PbBaGeO_4$ exhibits a first order phase transition from $P2_12_12_1$ to Pnma symmetry. This behaviour is similar to the one reported for $(C_5H_{11}NH_3)_2ZnCl_4$. However, $PbBaGeO_4$ exhibits phase coexistence and competition over a wide temperature range of about 200°C. On the contrary, $PbSrGeO_4$ shows a 2^{nd} order type phase transition towards a Pnma structure with nearly metrically hexagonal cell.

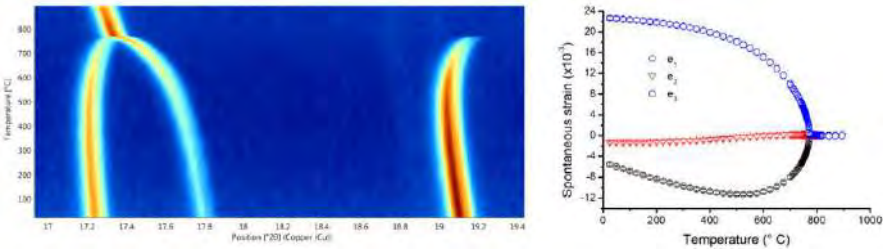

This work demonstrates that both materials are purely gyrotropic and identify $BaNdGaO_4$ structural type as a new source for such materials. Furthermore, those phase transitions seem unusual in light of the complex behavior reported here for these 2 compounds.

[1] C. Konak, V. Kopsky, F. Smutny; *J. Phys. C: Solid State Physics*,1978, 11, 2493

[2] S. Prosandeev, I. A. Kornev, L. Bellaiche; *Phys. Rev. Lett*. , 2011, 107, 117602

[3] A. Gomez Cuevas, J. M. Perez-Mato, M. J. Tello, G. Madariaga, J. Fernandez, L. Echarri, F. J. Zuniga, G. Chapuis; *Phys. Rev. B* , 1984, 29, 2655

Keywords: gyrotropic materials, phase transitions, spontaneous strain

New luminescent materials based on d10 metal halides

C. Cappuccino[a]*, B.Ventura[b], M. Maini[a]
[a]*Chemistry department "G. Ciamician", Bologna University, Italy*
[b]*ISOF - CNR Area della Ricerca di Bologna, Bologna,Italy*
** chiara.cappuccino2@unibo.it*

In recent years, the synthesis of coordination polymers has had a remarkable development, in view of the possibilities of these compounds as multifunctional and multi-responsive materials. The coordination complexes based on Cu(I) halides have for years been subjects of study for their photophysical properties and the large variety of coordination geometries, obtaining a plethora of new compounds with excellent luminescent properties[1].
A similar behaviour is common in Ag(I) halides complexes that present an intense luminescence in the solid state, specially at low temperature. This phenomenon has proved to be particularly evident in crystalline structures with short Ag-Ag contacts, that in some silver compounds could be shorter than the sum of van der Waals radii, effect known as "argentophillic interaction"[2]. The various possible structures of silver(I) halides are typically produced by the condensation of tetrahedral units of $[AgX_4]^{3-}$ that can share corners, sides of faces and form structures from 0 to 3 dimensions.
Combining these advantageous aspects of silver(I) halides with the ability of inserting organic ligand in order to modulate the photophysical properties and modify the crystal structure, we obtaining different luminescent coordination polymers characterised by unidimensinal or bidimensional expansion. The silver(I) tends to bond easily with pyridinic nitrogen, so it was chosen a pyridinic bidentate ligand to act as a bridge between the inorganic atoms, the aminomethyl-pyridine; there were performed various reactions using AgX salts (were X= Cl, Br, I) and three regioisomers of aminomethyl-pyridine.

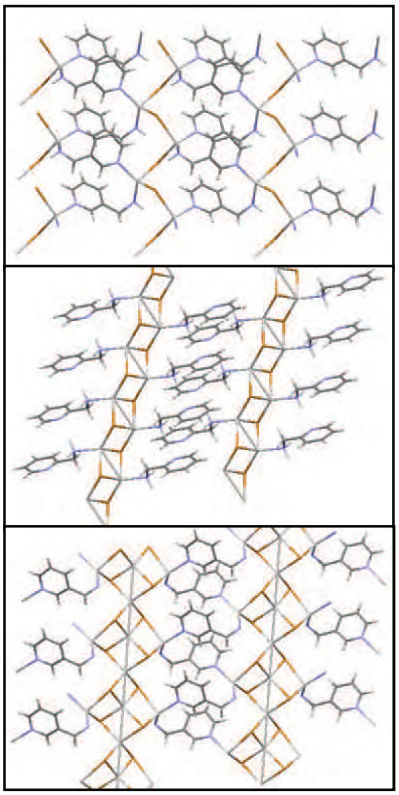

Due to the poor solubility of AgX salts the traditional synthesis methods were difficult to execute, so we tried to overcome this problem using a solvent-free approach. The mechanochemistry permits to perform the reaction directly in solid state and can yield crystal forms that are not obtainable in solution, it also has proved to be extremely effective for the synthesis of Cu(I) halides coordination complexes [3]. The main disadvantage of the mechanochemical approach consists of the formation of microcrystalline powders, unsuitable for single crystal x-ray diffraction, and this could be a problem since the structural solution is a key point for a complete understating of the crystals properties. Nowadays the algorithms for the structural solution from powder diffraction are more and more accurate and permits to obtain the crystal structure of powder samples. There were explored several conditions, varying the stoichiometry ratio and synthetic technique; the compounds obtained are characterized by an infinite chains based on silver halides; this chain can be single, double or in the form of a "saddle polymer". Some of the new compounds present also a bright luminescence following the exposure to UV light, a useful property that could be used in new optoelectronic devices.

[1] R. Peng, M. Li, D. Li, *Coord. Chem. Rev.*, 2010, 254, 1-18

[2] H. Schmidbaur, A. Schier, *Angew. Chem, Int. Ed.*, 2015, 54, 746-784

[3] L. Maini, P. P. Mazzeo, F. Farinella, V. Fattori, D. Braga, Faraday Discuss, 2014, 93-107

Keywords: Coordination Polymer, Mechanochemisty, Luminescent Materials

Powder Neutron Diffraction Studies of New Magnetic Manganites

Graham M. McNally,[a,b]* Ángel M. Arévalo-López,[b,c] Pascal Manuel[d] and J. Paul. Attfield[b]
[a] *Max Planck Institute for Solid State Research, Stuttgart, Germany*
[b] *School of Chemistry & Centre for Science at Extreme Conditions, Univ. of Edinburgh, UK*
[c] *Centre National de la Recherche Scientifique, Lille, France*
[d] *STFC Rutherford Appleton Lab, ISIS Facility, Harwell, UK*
** G.McNally@fkf.mpg.de*

ABO_3 perovskite materials typically contain nonmagnetic A^{2+} cations (e.g. Ba^{2+}, Sr^{2+}, Ca^{2+}), however there are now several examples of materials synthesised at high pressure with A-site Mn^{2+}, which are of fundamental physical interest. Double perovskites of general formula $A_2BB'O_6$ and with rock salt B cation order are one variation on the simple perovskite structure and Sr_2FeMoO_6 is a famous example,[1] with a high Curie temperature (T_c) of 420 K and negative intergrain tunnelling magnetoresistance (MR) at room temperature due to ferrimagnetic order of B-site Fe/Mo. We have recently reported the synthesis of the first all transition metal double perovskite, Mn_2FeReO_6,[2] which combines the novelty of A-site Mn^{2+} ($3d^5$) with ferrimagnetic B-site Fe/Re. This shows a high T_c (520 K) and a switch from negative MR above 75 K to large positive MR at low temperatures due to magnetic frustration between the A and B-site magnetic sublattices.
We have synthesised a set of materials with A-site Mn^{2+} that have general formula $CaABReO_6$ and exhibit 1:1 rock salt order of B cations with an additional 1:1 columnar cation order across A-sites.[3] The coexistence of these two types of cation order in the same material was first discovered only recently in the $MnRMnSbO_6$ (R = La, Pr, Nd, Sm) series, also made under high pressure conditions.[4] Results from neutron data collected using the WISH Diffractometer at the ISIS Neutron Facility concerning the crystal and magnetic structures of perovskites with A-site Mn^{2+} and coexisting A and B-site cation orders will be presented.

[1] Kobayashi K.-I., Kimura T., Sawada H., Terakura K. and Tokura Y. *Nature*, 1998, 395, 677-680.

[2] Arévalo-López Á. M., McNally G. M. and Attfield J. P. *Angew. Chem. Int. Ed.*, 2015, 54, 12074-12077.

[3] McNally G. M., Arévalo-López Á. M., Kearins P., Orlandi F., Manuel P. and Attfield J. P. *Chem. Mater.*, 2017, *29*(20), 8870-8874.

[4] Solana-Madruga E., Arévalo-López Á. M., Dos Santos-García A. J., Urones-Garrote E., Ávila-Brande D., Sáez-Puche R. and Attfield J. P. *Angew. Chem. Int. Ed.*, 2016, 55, 9340-9344.

Keywords: pressure, perovskites, neutrons

Magnetic structures of Co doped materials $Ni_{2-x}Co_xScSbO_6$

K. Ji[a*], E Solana-Madruga[a], A. Senyshyn[b], C. Ritter[c], J.P. Attfield[a]
[a] *Centre for Science at Extreme Conditions and School of Chemistry, University of Edinburgh, UK*
[b] *Forschungsneutronenquelle Heinz Maier-Leibnitz FRM II, Technische Universität München, D-85747 Garching, Germany*
[c] *Institut Laue-Langevin, 38042 Grenoble Cedex, France*
** s1301190@sms.ed.ac.uk*

Multiferroic materials are of much interest as their magnetic properties can be controlled by electric fields, with applications such as transducers, actuators and sensors [1]. Comprehensive studies of structural and magnetic properties of the cation-ordered $LiNbO_3$-type Ni_3TeO_6 (NTO) show an acentric rhombohedral space group *R*3 crystal structure and novel multiferroic properties [2]. Recently an NTO-type material Ni_2ScSbO_6 was reported and found to have a helimagnetic spin order with wavevector (0, 0.036, 0) below T_N = 60 K [3].

We have synthesized a series of new $Ni_{2-x}Co_xScSbO_6$ NTO-type solid solutions with x = 0.5, 1.0, 1.5. DC magnetic susceptibility data indicate a magnetic transition at around 60 K in all samples. Curie-Weiss fits to high temperature data for all samples give Weiss temperatures all around -105 K, which indicates strong antiferromagnetic interactions with some frustration. The effective moment for $Ni_{1.5}Co_{0.5}ScSbO_6$ is μ_{eff} = 4.01 μ_B, comparing to μ_{eff} = 3.22 μ_B for Ni_2ScSbO_6 [2]. Hysteresis measurements at 40 K report another interesting evolution of magnetic properties with increasing Co content. While the x = 0 material is purely antiferromagnetic, metamagnetism is observed for x = 0.5 and 1.0 samples while x = 1.5 appears to be a ferrimagnet or weak ferromagnet with a saturated moment of ~0.2 μ_B/f.u. Hence Co-doping leads to a systematic change from antiferromagnetism to ferro/ferrimagnetism.

Rietveld analysis of neutron powder diffraction data collected at SPODI at the FRMII reactor indicates that the materials have the NTO-type crystal structure with Sb on the Te position and Sc/Ni/Co arranged over the three Ni sites. As an example, $Ni_{1.5}Co_{0.5}ScSbO_6$ has lattice parameters *a* = 5.1777(1) Å, *c* = 14.0053(2) Å at 100 K. Magnetic structure solutions, derived from neutron powder diffraction data collected at SPODI and D20 at ILL reactor, have been solved using the Fullprof program. The figure below shows the Rietveld fit of the nuclear structure and a LeBail fit to magnetic peaks for $Ni_{1.5}Co_{0.5}ScSbO_6$ (pink ticks). The $Ni_{2-x}Co_xScSbO_6$ solid solutions have a more complex incommensurate wavevector (0, *k*y, *k*z) than NTO and magnetic structure results will be presented.

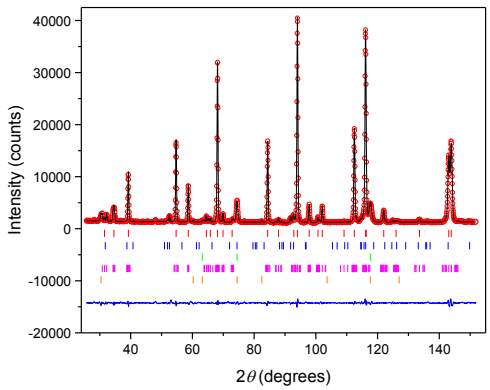

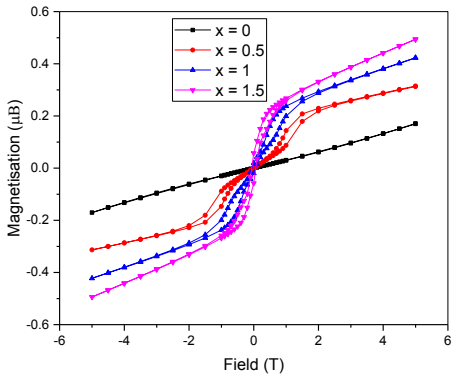

[1] Fiebing M., Lottmoser T., Meier D. and Trassin M, *Nature Reviews Materials*, 2016, 1, 1.

[2] Oh Y.S., Artyukhin S., Yang J.J., Zapf V., Kim J.W., Vanderbilt D. and Cheong S.W. *Nature Communications*, 2014, 5, 3201.

[3] Ivanov S.A., Mathieu R., Nordblad P., Tellgren R., Ritter C., Politova E., Kaleva G., Mosunov A., Stefanovich S. and Weil, M. *Chemistry of Materials*, 2013, 25, 935.

Keywords: neutron scattering, crystal structure, magnetic properties

Positive to negative thermal expansion in V_2OPO_4

E. Pachoud*, J. Cumby, C. T. Lithgow, J. P. Attfield
Centre for Science at Extreme Conditions & School of Chemistry, University of Edinburgh, UK
** elise.pachoud@ed.ac.uk*

Negative thermal expansion (NTE) materials, whose volume contracts upon heating, are of both fundamental and applied interest in creating zero expansion materials [1].
The vanadium oxyphosphate V_2OPO_4 has been previously reported to crystallize in a tetragonal $I4_1/amd$ structure at room temperature [2]. It consists of a stacking along the *c* axis of chains of face-sharing $V^{2.5+}O_6$ octahedra running alternatively along *a* and *b*. Short V-V distances and possible strong orbitals overlap within these chains make this material a promising candidate for 'orbital molecules' [3].
In this communication, we report on its synthesis, structural characterization and properties. Variable temperature neutron and synchrotron X-ray powder diffraction experiments revealed two transitions [4]. High-resolution data from HRPD at ISIS and I11 at Diamond (room temperature Rietveld refinement shown in the picture) enable the observation of a distorted monoclinic structure *C*2/*c* with long range V^{2+}/V^{3+} charge ordering up to T_{CO}=605K. A structural transition to the tetragonal phase occurs at this temperature, accompanied with a switch from positive to negative thermal expansion in the direction of the VO_6 chains. Ferrimagnetic order of V^{2+} spin up and V^{3+} spin down states is observed below T_C=164K from HRPD data, and magnetic susceptibility measurements evidence local spin pairing correlations to higher temperatures. DFT calculations confirm the charge-ordered semiconducting ferrimagnetic ground state.
V−V bonding within the VO_6 chains is proposed as the key factor for this novel switch of thermal expansion behavior, as loss of V−V bonding enables transverse oxygen motions to dominate the thermal expansion at high temperatures.

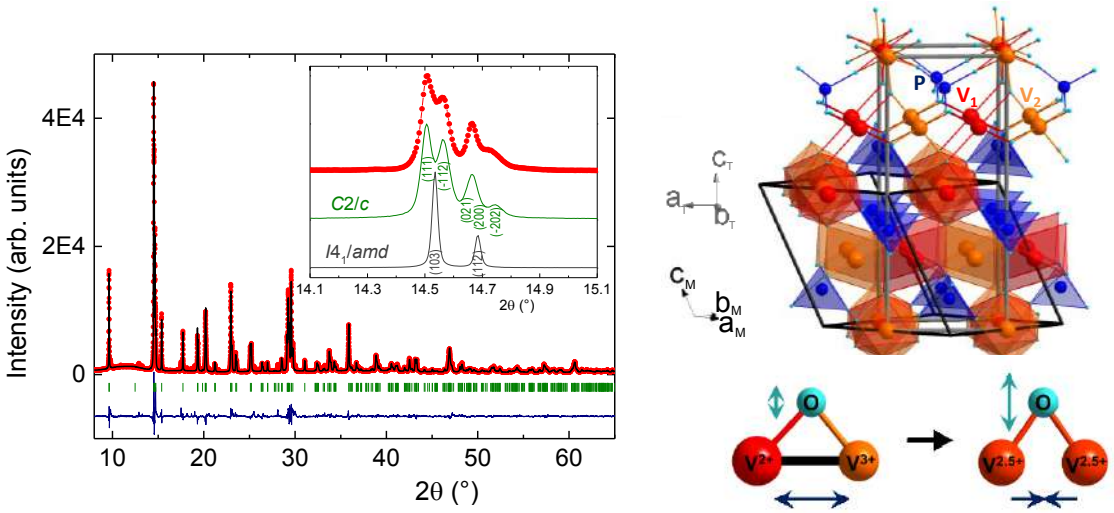

[1] Chen J., Hu L., Deng J., Xing X. *Chem. Soc. Rev.*, 2015, 44, 3522.

[2] Glaum R., Gruehn R. *Z Kristallogr.*, 1989, 91, 186.

[3] Attfield J.P. *APL Materials* 2015, 3, 041510.

[4] Pachoud E., Cumby J., Lithgow C.T., Attfield J.P. *J. Am. Chem. Soc.*, 2018, 140, 636.

Keywords: lazulite-type structure, negative thermal expansion, charge order.

Structures and magnetic properties of $MnRMnSbO_6$

E. Solana-Madruga[a,*], A.M. Arévalo-López[b], A.J. Dos santos-García[c], R. Sáez-Puche[d] and J.P. Attfield[a]

[a] *CSEC and School of Chemistry, University of Edinburgh, Edinburgh, United Kingdom.*
[b] *Univ. Lille, CNRS, ENSCL, Univ. Artois, UMR 8181 – UCCS, Lille, France.*
[c] *Dpto. Ingeniería mecánica, Química y Diseño Industrial, ETSIDI, UPM, Madrid, Spain.*
[d] *Dpto. Química Inorgánica, Fac. Químicas, UCM, Madrid, Spain.*

* *E.Solana@ed.ac.uk*

Compounds of the general formula ABO_3 with perovskite structure and their ordered $A_2BB'O_6$, $AA'B_2O_6$ and $AA'BB'O_6$ derivatives are interesting due to their large variety of electric and magnetic properties. Using high pressure and high temperature (HPHT) synthesis, Mn^{2+} can be stabilised at the A site of the perovskite structure for several compositions, which usually originates exotic magnetic properties and structures [1-3]. The combination of rare earths (R) with Mn under similar HPHT conditions into the $MnRMnSbO_6$ family results in an exciting structural evolution upon substituting R by different rare earths. Synchrotron Powder X-Ray Diffraction data collected using BL09 beamline at ALBA lightsource confirmed the conventional $P2_1/n$ DPv structure of the R = Eu and Gd compounds, with rock-salt order of Mn^{2+} and Sb^{5+} at the B sites. The larger R = La – Sm further order in a columnar fashion with Mn^{2+} at the A sites, giving rise to a new type of double double perovskite structure (DDPv – Fig.1a) crystallising with $P4_2/n$ space group and cell parameters ~ 2a * ~2a * ~2a. Figure 1b shows the emergent (110) peak which accounts for the columnar A-site order of the DDPv structure. This structure, first ever reported in the literature for this family of compounds [4], is notable for having five independent cation sites, three of them occupied by Mn^{2+} in octahedral (B-sites), tetrahedral (A) and square planar (A´) coordinations. Such a distribution of Mn^{2+} and the presence of R^{3+} cations induce complex magnetic behaviours with up to three different anisotropic magnetic structures for the R = La, Pr and Nd compounds [5], determined from the Neutron Powder Diffraction patterns collected at ISIS (WISH) and the ILL (D20).

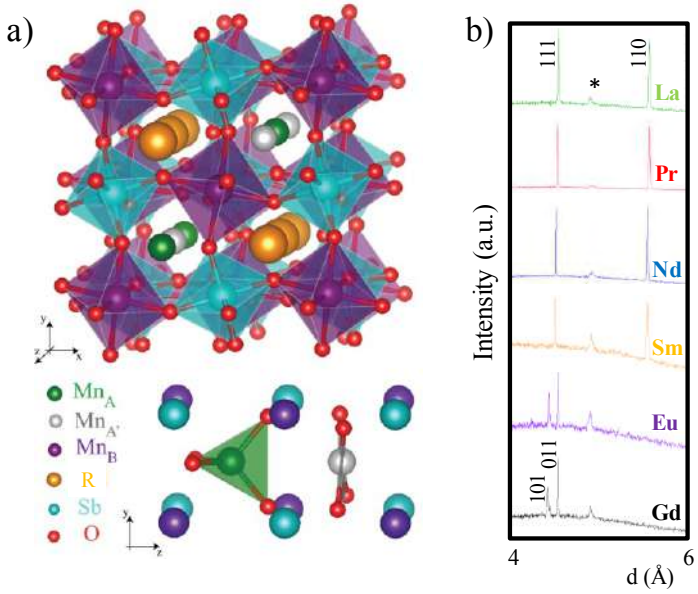

[1] Dos santos-García A.J., Ritter C., Solana-Madruga E. and Sáez-Puche R. *J. Phys. Cond. Matter* 2013, 25, 206004

[2] Arévalo-López A.M., McNally G.M. and Attfield J.P. *Angew. Chemie. Int. Ed.* 2015; 54:12074–7.

[3] Arévalo-López A.M., Stegemann F. and Attfield J.P. *Chem. Comm.* 2016; 147:2–4.

[4] Solana-Madruga E., Arévalo-López A.M., Dos santos-García A.J., Urones-Garrote E., Avila-Brande D., Sáez-Puche and Attfield J.P. *Angew. Chem. Int. Ed.*, 2016, 55, 9340-9344.

[5] Solana-Madruga E., Arévalo-López A.M., Dos santos-García A.J., Ritter C., Cascales C., Sáez-Puche and Attfield J.P. *Phys. Rev. B.* 2018, accepted.

Keywords: Double double perovskites, high pressure, magnetic anisotrpy

The Synthesis and Characterisation of Goethite Doped with the Critical Metal Cobalt – Implications for Natural Systems

S. Dressler[1,3]*, C. A. Kirk[2,3], S. E. Dann[1], R. J. Herrington[3], P. F. Schofield[3]
[1]*Department of Chemistry, Loughborough University, UK*
[2]*School of Chemistry, University of Edinburgh, Edinburgh, UK*
[3]*Department of Earth Sciences, Natural History Museum, UK*
**s.dressler@lboro.ac.uk*

Cobalt is an irreplaceable and strategic element in a diverse range of applications and for many different value chains. It is used in super alloys, in materials which are used in working environments which are aggressive (e.g. hot and acidic) and as well as in the magnet industry. Nevertheless, the globally leading and to date irreplaceable use of cobalt is as a cathode material in lithium rechargeable batteries.[1]

The occurrence of cobalt is variable throughout the Earth's crust. One natural deposit for Co is called laterite, where the iron oxyhydroxide mineral phases goethite (α-FeOOH) and ferrihydrite (ill-defined formula) are the most common minerals found to be present. These iron oxyhydroxides rarely occur with an ideal formula in naturally occurring deposits.[2] This is caused by either substitution processes, where foreign cations can be substituted for Fe, or by the adsorption of cations on the surface of mineral crystallites, due to their small particle size and the resulting high specific surface area. In the case of goethite a range of valencies are possible, e.g. divalent (Ni, Zn), trivalent (Al, Mn, Co) or tetravalent (Si, Ge and Pb).[3] An understanding of elements present in the minerals, their incorporation into the structure and whether they are structurally or surface adsorbed, is vital for optimising extraction processes for the mineral processing industry.

Many of these non-iron-elements associated with natural goethite are present in low concentrations (<2 mol%) and it is often challenging to determine their presence.[4] To investigate the substitution or sorption mechanisms of non-iron-elements, one approach is to use controlled laboratory studies to synthesise goethite materials. Over the last few decades, many laboratory studies of incorporation processes into synthetic FeOOH systems, with variations in the synthesis conditions, e.g. temperature and pH, have been reported. [5] [6] [7] However, little is known about the incorporation process of the critical metal cobalt into goethite and the properties of cobalt containing goethites.

This research is focused on cobalt doped goethite phases and the investigation of the effects of time, cobalt dopant levels, and temperature on the phases formed. Results of Powder X-ray Diffraction (PXRD) and additional techniques, such as Thermogravimetric Analysis (TGA) and Transmission Electron Microscopy (TEM) indicate a multiphase system, where goethite and the poorly crystalline precursor phase, ferrihydrite, are present. Due to this multiphase system the distribution of cobalt in the individual phases is unknown. To determine the partitioning of cobalt between the phases, a separation of the crystalline goethite phase and the poorly crystalline ferrihydrite phase is required. Therefore an EDTA-washing technique was investigated and optimised. During the washing process, PXRD was vital to identify the crystalline phase(s) present and provided information, if the poorly crystalline phase is still present after the EDTA washing. This allowed an optimisation of the washing technique in terms of the duration of the process and the concentration to use. The characterisation of a set of cobalt doped goethite samples using PXRD and complementary techniques such as TGA, Infrared Spectroscopy (IR-spectroscopy) and TEM, will be presented.

[1] Cobalt Development Institute (2006) Available at: http://www.thecdi.com/
[2] Cornell R.M., Schwertmann U. (2003). The iron oxides: structure, properties, reactions, occurrences and uses, 703.
[3] Manceau A., Schlegel M., Musso M., Sole V., Gauthier C., Petit P., Trolard F. (2000). Crystal chemistry of trace elements in natural and synthetic goethite. Geochimica et Cosmochimica Acta, 3643-3661.
[4] Gasser U.G., Jeanroy E., Mustin C., Barres O., Nüesch R., Berthelin J., Herbillon A.J.. (1996). Properties of synthetic goethites with Co for Fe substitution. Clay Minerals, 465-476.
[5] Alvarez M, Rueda EH, Sileo EE. Simultaneous incorporation of Mn and Al in the goethite structure. Geochim Cosmochim Acta. 2007;71(4):1009-1020.
[6] Cornell RM. Simultaneous incorporation of Mn, Ni and Co in the Goethite (a-FeOOH) structure. *Clay Miner*. 1991;26(1):427-430. doi:10.1180/claymin.1991.026.3.11.
[7] Schulze DG, Schwertmann U. The influence of aluminium on iron oxides: X. Properties of Al-substituted goethites. Clay Miner. 1984;19(4):521-539.

Keywords: Cobalt, Goethite, PXRD

Phase composition and structure of Ni-doped iron seleno-telluride

K. M. Kosyl*, W. Paszkowicz , M. Z. Cieplak , I. Zaytseva, D. J. Gawryluk
Institute of Physics, Polish Academy of Sciences, Aleja Lotnikow 32/46, 02-668 Warsaw, Poland
** kosyl@ifpan.edu.pl*

A number of compounds from Fe-Se-Te system are intensively investigated for superconductivity at low temperatures. Among the end members, FeSe has been found to be superconductive (with a critical temperature T_c = 8 K), whereas FeTe at ambient pressures is not exhibiting such properties (similarly $FeTe_{0.82}$ [1]). There have been a lot of attempts for creating various superconducting materials by changing a proportion between elements from the Fe-Te-Se diagram, but also by introducing other doping atoms at the Fe sites (e.g. Co, Ni, Cu, Mn, Zn, Mo, Cd, In, Pb, Hg, V, Ga, Mg, Al, Ti, Cr, Sr or Nd [2]).
The initial structure for those materials is of tetragonal PbO type (space group *P*4/*nmm*), which canpossess a significant non-stoichiometry. When the content of Fe (or dopants introduced in place of iron) exceeds 1 in the formula FeTe, the additional cations are believed to occupy a new site on the out-of-the-plane position [3]. The *c* lattice constant of the tetragonal phase strongly depends on the anionic content and type (it varies by about 0.75 Å from $FeSe_{0.82}$ to $FeTe_{0.82}$ [1]), as well as on a content of the dopant at the Fe site [2, 3].

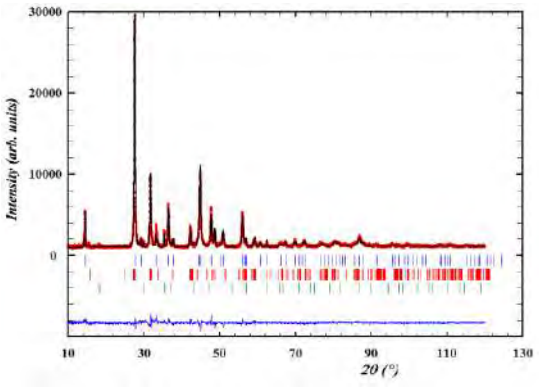

The real origin of the superconductivity in the Fe-Se-Te diagram is still not well understood. Certain interesting dependencies have been noticed recently. The sharpening of the transition to superconducting phase has been reported as a result of worsening of the crystal quality by non-stoichiometry or introducing dopants (e.g. Cu, Co, Ni). However, when the dopant content exceeds a certain level, a suppression of the superconductivity is observed [2]. In case of $FeTe_{0.65}Se_{0.35}$, TEM studies have revealed the presence of hexagonal inclusion of NiAs type (denoted as Fe_7Se_8), as a manifestation of iron non-stoichiometry. The faster growth is applied, the hexagonal inclusions become smaller and the superconductivity is improved [4]. Some theoretical calculation show, that for the strained FeTe, the position of Te atoms has the main contribution to the superconductivity [5]. In case of additional iron atoms, as it takes place in $Fe_{1+x}Te_{1-y}Se_y$ compounds, the removal of those interstitial Fe atoms seems to be crucial for the superconductivity [6].
In this work we present the phase analysis, by powder X-ray diffraction, of $Fe_{1-x}Ni_xTe_{0.65}Se_{0.35}$ crystals grown by Brigdman method, with Ni content in the range from 0% to 6.75%. Two sets of samples, differing by the growth rate (around 1-1.2 mm/h and 15mm/h), exhibit different phase composition. Except the main tetragonal phase, a monoclinic minor phase of Cr_3Se_4 type was found for a number of samples. The observed similarity between diffraction patterns of this phase and the previously reported in $FeTe_{0.65}Se_{0.35}$ hexagonal minor phase (Fe_7Se_8) is not astonishing – some problems with distinction of the hexagonal and monoclinic phase have been already pointed out in a reports of Fe-Te [7] and Fe-Se [8] phase diagrams.

[1] Fang, M. H., Pham, H. M., Qian, B., Liu, T. J., Vehstedt, E. K., Liu, Y., Spinu, L., Mao, Z. Q. (2008). Phys. Rev. B, 78(22), 224503.
[2] Gawryluk, D. J., Fink-Finowicki, J., Wiśniewski, A., Puźniak, R., Domukhovski, V., Diduszko, R., Kozłowski, M., Berkowski, M. (2011). Supercond. Sci. Technol., 24(6), 065011.
[3] Zajdel, P., Zubko, M., Kusz, J., Green, M. A. (2010). Cryst. Res. Technol., 45(12), 1316-1320.
[4] Wittlin, A., Aleshkevych, P., Przybylińska, H., Gawryluk, D. J., Dłużewski, P., Berkowski, M., Puźniak, R., Gutowska M. U., Wiśniewski, A. (2012) Supercond. Sci. Technol., 25(6), 065019.
[5] Ciechan, A., Winiarski, M. J., Samsel-Czekała, M. (2013). J. Phys.: Condens. Matter, 26(2), 025702.
[6] T. M. McQueen, Q. Huang, V. Ksenofontov, C. Felser, Q. Xu, H. W. Zandbergen, Y. S. Hor, J. Allred, A. J. Williams, D. Qu, J. Checkelsky, N. P. Ong, R. J. Cava, Phys. Rev. B 79, 014522 (2009).
[7] Okamoto, H., Tanner, L. E. (1990). Bull. Alloy Phase Diagr., 11(4), 371-376.
[8] Schuster, W., Mikler, H., Komarek, K. L. (1979). Monats.Chem./Chem. Monthly, 110(5), 1153-1170.

Keywords: iron seleno-tellurides, X-ray diffraction, phase analysis

Origin of the phase transition in bismuth hollandite

J. Cumby*, M. Lee, A. Krajewska, J. P. Attfield
CSEC and School of Chemistry, University of Edinburgh, UK
** james.cumby@ed.ac.uk*

Hollandites, $A_xM_8O_{16}$ show a range of potential applications ranging from nuclear waste encapsulation, through organic oxidation catalysts, to potential multiferroics. The structure consists of double-edge-sharing chains of MO_6 octahedra surrounding a square channel occupied by A cations (fig. 1a). A wide range of compositions are known, including A = Na, K, Ba, Bi, Ag and M = Mn, V, Cr and Ti, with the variable A occupation ($1 \leq x \leq 2$) accommodating a range of M oxidation states.
The triangular arrangement of M sites within the octahedral chains (fig. 1b) of the hollandite structure is also of fundamental interest due to competing inter-atomic interactions, with the potential for magnetic and electronic frustration. Hollandite structures are known which exhibit insulating ferromagnetism, frustrated magnetism and metal-insulator transitions (MITs). A key example is $Bi_{1.7}V_8O_{16}$, which undergoes a MIT at 70 K, with a concomitant phase transition [1], although a number of related examples are also known.

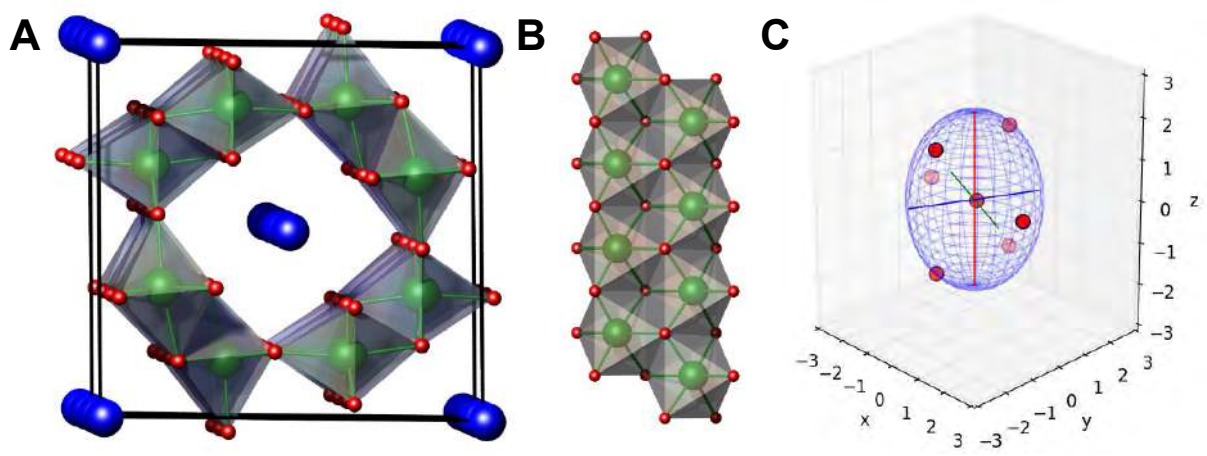

Here we report structural results from powder synchrotron and neutron diffraction data of vanadium hollandite, confirming the transition as isomorphic (symmetry preserving). Using our recently developed ellipsoidal parameterization of distortions in coordination polyhedra (fig 1c) [2], we rationalize the behavior of structural distortions in this and other similar hollandite structures.

[1] Larson A.M., Wilfong, B., Moetakef, P., Brown, C.M., et al. *J Mat. Chem. C*, 2017, 5, 4967.

[2] Cumby, J. and Attfield, J.P., *Nat. Commun*., 2017, 14235.

Keywords: hollandite, metal insulator transition, ellipsoidal analysis

Piezoelectric phase transition in $KSrVO_4$ investigated using the Aeris diffractometer

J. Gertenbach, G. Nénert
[a] *Malvern Panalytical, Lelyweg 1, 7602 EA, Almelo, The Netherlands*
** jan.gertenbach@panalytical.com*

The rich crystal chemistry of $A^IB^{II}XO_4$ (A^I = alkali ion, B^{II} = alkali-earth ion, X = P, V, As) leads to numerous polymorphic phases that have related structural families, such as olivine (e.g. $LiMnPO_4$), arcanite (β-K_2SO_4), glaserite, tridymite, α-K_2SO_4, β-Na_2SO_4 and γ-Na_2SO_4 [1]. Among the various families (X = P, V, As), the phosphates have been most widely studied. In addition to their interesting crystal chemistry behaviour, research on this family of materials is mainly driven by their ferroelectric-, and ferroelastic properties as well as possible applications as phosphors for LEDs [1,2].
In recent years, we have investigated several structural combinations of the $A^IB^{II}VO_4$ type [3,4] and a new crystal type within this family was identified, namely a form of $NaSrVO_4$ that is isostructural to larnite [3]. In this work, we continue our exploration of the $A^IB^{II}VO_4$ family by investigating the composition of $KSrVO_4$. While $NaSrVO_4$ crystallizes in the $P2_1/n$ space group, divergent results are reported for $KSrVO_4$. Single crystal work suggests Pnma symmetry [5], but powder diffraction studies show evidence for $P2_12_12_1$ symmetry with distinct reflections present that are not consistent with Pnma symmetry [6]. These contradictory results prompted us to study the structural composition of the compound as a function of temperature.

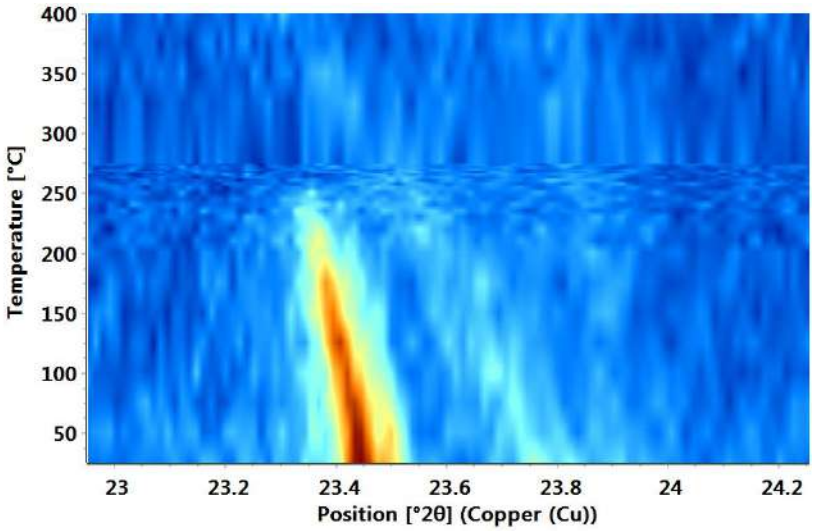

Using the Aeris benchtop diffractometer equipped with the BTS 500 non-ambient chamber, the crystal structure of $KSrVO_4$ was studied in the 25-500°C range. At room temperature the structure is best described as having $P2_12_12_1$ symmetry, allowing for piezoelectricity in this material. By increasing the temperature, it is possible to observe a phase transition to Pnma symmetry. This phase transition appears to be related to the piezoelectric nature of the material and its associated spontaneous strain. This work reports on the first purely gyrotropic phase transitions in the $A^IB^{II}VO_4$ family.

[1] V. A. Isupov *Ferroelectrics* 2002, 274(1), 203

[2] S. Choi, Y. J. Yun, S.J. Kim, H.-K. Jung *Optical Lett.* 2013, 38, 1346

[3] G. Nénert, P. O'Meara, T. Degen *Phys. Chem. Minerals* 2017, 44, 455

[4] G. Nénert, *Z. Kristallogr.* 2017; 232(10), 669

[5] R. Klement, P. Kresse, *Z Anorg Allg Chem* 1961, 310, 53

[6] M. Azrour, L. El Ammari, Y. Le Fur, B. Elouadi , *Materials Research Bulletin* 2000, 35, 263

Keywords: piezoelectricity, phase transitions, spontaneous strain, benchtop XRD

Deformations of the α-Fe_2O_3 rhombohedral lattice across the Néel temperature

P. Fabrykiewicz[a*], M. Stękiel[a,b], I. Sosnowska[a], R. Przeniosło[a]
[a] *Faculty of Physics, University of Warsaw, Poland*
[b] *Institute of Geosciences, Goethe University, Germany*
** Piotr.Fabrykiewicz@fuw.edu.pl*

High-resolution synchrotron radiation powder diffraction patterns of α-Fe_2O_3 measured between room temperature and 1100 K, i.e. above the Néel temperature T_N = 950 K, have been analyzed. The integral breadths of the Bragg peaks show a hkl-dependent anisotropy, both below and above T_N. This anisotropy can be quantitatively described by using a statistical peak broadening model [1]. Model calculations show that the rhombohedral α-Fe_2O_3 lattice is deformed and the deformation leads to a monoclinic lattice with the unique monoclinic axis along the hexagonal [110] direction both below [2,3] and above T_N [4]. The monoclinic symmetry of bulk α-Fe_2O_3 is compatible with α-Fe_2O_3 nanowire growth along the [110] direction reported in Fu et al. [5].
Structural studies of other magnetic materials, e.g. $BiFeO_3$ [6] and Cr_2O_3 [3], have also shown monoclinic deformations of the rhombohedral lattice. The monoclinic symmetry may be related with the magnetic properties of α-Fe_2O_3, but on the other hand a recent study has shown similar monoclinic crystal structure symmetry in the nonmagnetic calcite, $CaCO_3$ [7].

[1] Stephens P.W. *J. Appl. Cryst.*, 1999, 32, 281.

[2] Przeniosło R., Sosnowska I., Stękiel M., Wardecki D., Fitch A., Jasiński J.B. *Physica B*, 2014, 449, 72.

[3] Stękiel M., Przeniosło R., Sosnowska I., Fitch A., Jasiński J.B., Lussier J.A., Bieringer M. *Acta Cryst. B*, 2015, 71, 203.

[4] Fabrykiewicz P., Stękiel M., Sosnowska I., Przeniosło, R. *Acta Cryst. B*, 2017, 73, 27.

[5] Fu Y., Chen J., Zhang H. *Chem. Phys. Lett.*, 2001, 350, 491.

[6] Sosnowska I., Przeniosło R., Palewicz A., Wardecki D., Fitch A. *J. Phys. Soc. Jpn*, 2012, 81, 0446041.

[7] Przeniosło R., Fabrykiewicz P., Sosnowska I. *Physica B*, 2016, 496, 49.

Keywords: high-resolution synchrotron powder diffraction, magnetic ordering, symmetry

In situ Investigation of Thermomechanical Processing of NiTi Shape Memory Alloys

P. Rodrigues[a*], F.M. Braz Fernandes[a], A. S. Paula [b], E. Camacho[a]
[a]*Faculdade de Ciências e Tecnologia, Universidade Nova de Lisboa, Portugal*
b*Mechanical Engineering and Materials Department - SE-4, Instituto Militar de Engenharia – IME, Brazil*
*e-mail: pf.rodrigues@campus.fct.unl.pt

NiTi shape memory alloy (SMA) is a very attractive material due to their shape memory and superelasticity effects. The production of NiTi usually involves several steps of hot or/and cold thermomechanical processing and thermal treatments. However, to control their composition, in terms of the Ni / Ti ratio and the impurities (e.g. carbon and oxygen), during the processing steps is an important challenge in production of these alloys. The thermomechanical process is required to obtain an adequate functional and mechanical characteristic, for their final application.

The characterization of the material was performed by Differential Scanning Calorimetry (DSC) and synchrotron-based x-ray diffraction (SR-XRD) techniques. In situ deformation experiments (Figure 1) were conducted with the high energy X-ray diffraction (HEXRD) setup of the HZG beamline HEMS (P07-EH3) at Petra III, DESY, Hamburg. This study aimed to contribute to the development of processing strategies that will give rise to more consistently uniform characteristics of NiTi shape memory alloys and a minimization of the failures occurring during processing.

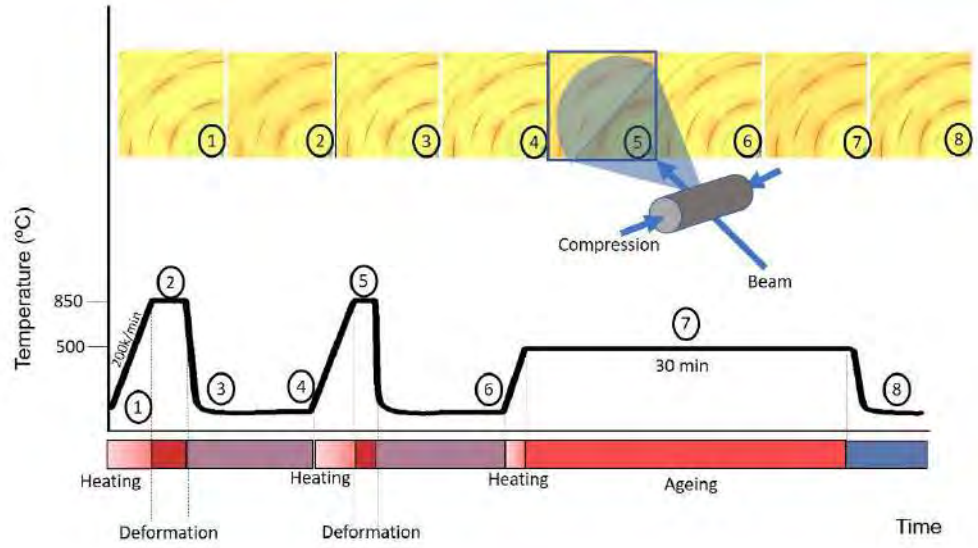

Figure 1 – Scheme of the Thermomechanical Process Applied

Keywords: synchrotron radiation, x-ray diffraction, shape memory alloy.

MS02 - Energy Materials

MSO2

Abstract Number	Title	Author	Affiliation
MS02 - K1	Lithium and sodium electrochemical (de)intercalation in layered molybdenum oxides	Dr Marie Guignard	ICMCB - CNRS
MS02 - K2	Operando X-ray Diffraction Studies of Battery Materials	Dr David Wragg	University of Oslo
MS02 - OR1	Na3V2(PO4)2F3 : an optimal cathode material for high rates In Situ Powder Diffraction studies on Operando battery	Dr Francois Fauth	Alba Synchrotron Light Source
MS02 - OR2	Towards an understanding of the magnetocaloric effect in Fe2P	Dr Johan Cedervall	Uppsala University
MS02 - OR3	Structural insights into the lithium amide-imide solid solution	Dr Josh Makepeace	University of Oxford
MS02 - P97	Mixed-metal amide/imide catalysts for ammonia decomposition applications	Ms Charlotte Kirk	University of Oxford
MS02 - P98	B-site ordered double perovskite, La2(Al0.5MgTa0.5)O6 for thermal barrier applications and its high-temperature phase transition	Dr Yoo Jung Sohn	Forschungszentrum Jülich GmbH
MS02 - P99	Metal Hydro-borates for Li- and Na-ion Batteries	Radovan Cerny	University of Geneva
MS02 - P100	A study of possible extra-framework cation ordering in Pbca leucite structures with stoichiometry RbCsX2+Si5O12 (X = Mg, Ni, Cd).	Dr Tony Bell	Sheffield Hallam University
MS02 - P101	Structural analysis of NaMg(H1-xFx)3 for thermochemical energy storage applications	Dr Matthew Rowles	Curtin University
MS02 - P102	The Crystal Structure and Electrical Properties of the Oxide Ion Conductor Ba3W1.2Nb0.8O8.6	Ms Kirstie McCombie	University of Aberdeen
MS02 - P103	Local structure analysis of titania photocatalysts for light-induced water splitting	Ms Ezgi Onur Sahin	Max-Planck-Institut für Kohlenforschung
MS02 - P104	On the Phase Transitions of NASICON-type compounds	Prof Christian Lengauer	University of Vienna
MS02 - P105	Structural factors enabling fast oxide ion conduction in the hexagonal perovskite derivative Ba3MoNbO8.5	Dr Sacha Fop	University of Aberdeen
MS02 - P106	Phase transformations in Co-Re-Cr-Ni high-temperature superalloys studied by neutron diffraction	Dr Premysl Beran	Nuclear Physics Institute of the CAS
MS02 - P107	In-situ carbonation of SrO and Sr(OH)2·xH2O at 298 K and controlled humidity	Mr Georg Gravogl	University of Vienna
MS02 - P108	Laboratory 2D X-ray diffraction setup for in situ studies on Li-ion battery materials	Dr Holger Geßwein	Karlsruhe Institute of Technology
MS02 - P109	In situ study on reduction of gamma-iron oxides	Mr Pelle Garbus	Aarhus University
MS02 - P110	Operand XRD study of LiMn1.5Ni0.5O4 high-voltage cathode under high-rate charge/discharge reaction	Mr Takayuki Konya	Rigaku Corporation

MS02 - P111	Nanostructured kesterite (Cu2ZnSnS4) for applications in thermoelectric devices	Dr Eleonora Isotta	University of Trento - Department of Civil, Environmental and Mechanical Engineering
MS02 - P112	Structure Property correlation in SOFC & SOEC electrolyte materials	Prof Dave Billing	University of the Witwatersrand
MS02 - P113	Impact of Nb vacancies and p-type doping of the NbCoSn-NbCoSb half-Heusler thermoelectrics	Ms Daniella Ferluccio	Heriot-Watt University
MS02 - P114	Hydrogen induced pase transformations in selected High Entropy Alloys	Mr Gustav Ek	Uppsala University
MS02 - P115	In Operando Characterization of Lithium Batteries using XRD	Dr Geert Vanhoyland	Bruker AXS GmbH
MS02 - P116	X-Ray powder diffraction full profile analysis of thin film absorbers in solar cells	Dr Xavier Alcobé	Universitat de Barcelona
MS02 - P117	Dimensional crossover of correlated anion disorder in oxynitride perovskites	Dr Paula Kayser	University of Edinburgh
MS02 - P118	Structural, microstructural and magnetic evolution in cryo milled carbon doped MnAl	Mr Hailiang Fang	Uppsala University
MS02 - P119	High angular resolution and time-resolved Synchrotron Powder Diffraction experiments revealing inhomogeneous lithiation/delithiation into/from cathode materials during cycling	Dr Mariyam Darma	Helmholtz Institute Ulm
MS02 - P120	The composition-structure-property relationships of Ni(OH)2-based electrochromic materials	Mr Kurt Lawson	Loughborough University
MS02 - P121	In-operando powder diffraction – A powerful tool to study capacity losses in Li-ion batteries at multi-length scales	Dr Karin Kleiner	Diam
MS02 - P122	Structure and magnetic properties of strontium W-type Hexaferrites	Mr Mathias Mørch	Aarhus
MS02 - P123	Controlling cation ordering and oxygen release in LiNi0.5Mn1.5O4 positive electrode materials for tailored electrochemical properties in lithium ion batteries	Dr William Brant	Uppsala University
MS02 - P124	Influence of synthesis routes on the structure and electrochemistry of Li-rich layered oxide cathode materials for Li-ion batteries	Mr Ashok Sreekumar Menon	Uppsala University
MS02 - P125	Speciation of Ni in spent FCC catalysts and its detection limit (by HR powder diffraction and XAS spectroscopy)	Prof Monica Dapiaggi	Università degli Studi di Milano
MS02 - P127	Operando XRD data analysis of Li-ion batteries from laboratory diffractometers	Dr Fabio Masiello	Malvern Panalytical B.V.
MS02 - P128	Comparison of two types of CaCO3 polymorphs synthesized by the mineral carbonation of gaseous carbon dioxide	Kimin Roh	Korea Institute of Geoscience and Mineral Resources
MS02 - P129	In-situ Formation of Fast Lithium Conducting Garnets	Dr Edmund Cussen	University of Strathclyde
MS02 - P130	Controlling H-embrittlement and delamination in Pd – based membrane material	Dr Amarante Bottger	Delft University of Technology

Lithium and sodium electrochemical (de)intercalation in layered molybdenum oxides

M. Guignard[a*], L. Vitoux[a], A. J. Toumar[a], M. R. Suchomel[a], C. Delmas[a], J. C. Pramudita[b], N. Sharma[b]

[a] *ICMCB – CNRS, France*

[b] *School of Chemistry, University of New South Wales, Australia*

* *marie.guignard@icmcb.cnrs.fr*

Lithium and sodium layered oxides, with the general chemical formula A_xMO_2 (A: Li or Na, M: transition element and $0 \leq x \leq 1$), have been studied for 30 years to be used as positive electrode materials in lithium-ion or sodium-ion batteries. Whereas systems containing 3d elements have been intensively studied, systems with 4d transition metal ions have been less investigated due the high molecular weight of 4 d elements. In our laboratory, we have focused recently on layered molybdenum oxides, Li_xMoO_2 or Na_xMoO_2, and we have reinvestigated the structural rearrangements occurring in these compound when they were used as positive electrode material in lithium or sodium batteries, respectively.

We will present first the phase diagram of the system Na_xMoO_2 which has been studied using electrochemistry combined with *in situ* synchrotron X-ray diffraction experiments. The figure shows the X-ray powder diffraction patterns recorded during the electrochemical process at 11-BM beamline (APS, USA). The many steps observed in the electrochemical curve of $Na_{2/3}MoO_2$ during cycling in a sodium battery suggest numerous reversible structural transitions during sodium (de)intercalation $Na_{0.5}MoO_2$ and $Na_{\sim1}MoO_2$. *In situ* X-ray diffraction confirmed the complexity of the phase diagram within this domain, 13 single phase domains with minute changes in sodium contents. Almost all display superstructure or modulation peaks in their X-ray diffraction patterns suggesting the existence of many Na_xMoO_2 specific phases that are believed to be characterized by sodium/vacancy ordering as well as Mo−Mo bonds and subsequent Mo−O distances patterning in the structures. Moreover, a room temperature triclinic distortion was evidenced in the composition range $0.58 \leq x < 0.75$, for the first time in a sodium layered oxide system. Monoclinic and triclinic subcell parameters were refined for every Na_xMoO_2 phase identified. Reversible $[MoO_2]$ slab glidings occur during the sodium (de)intercalation. This level of structural detail provides unprecedented insight on the phases present and their evolution, which may allow each phase to be isolated and examined in more detail.

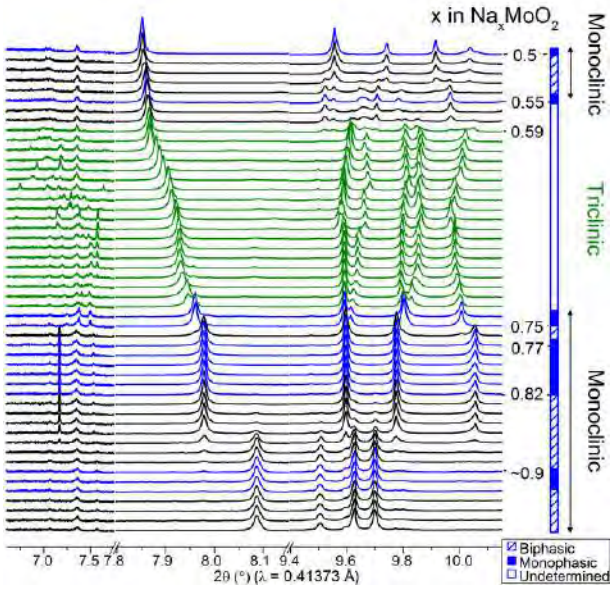

We will present finally the first results that were obtained in the system Li_xMoO_2. It has also been studied using electrochemistry combined with *in situ* laboratory X-ray diffraction experiments. Even if the phase diagram in the Li_xMoO_2 is less complicated than that of the Na_xMoO_2 system, many phase transitions still occur in during the lithium electrochemical (de)intercalation. The large number of phase transitions is usually not observed in lithium layered oxides containing 3d elements, indicating the molybdenum tends to rearranges within the $[MoO_2]$ layers.

The results obtained in our study confirm those reported before [1,2], but they give much more detailed information about the structural modifications occurring in layered molybdenum oxides during the alkali electrochemical (de)intercalation.

[1] Tarascon J.-M., Hull G. W. *Solid State Ion.*, 1986, 22, 85.

[2] Tarascon J.-M. *J. Electrochem. Soc.*,1987, 134, 1345.

Keywords: Lithium and sodium batteries, *in situ* X-ray powder diffraction

Operando X-ray Diffraction Studies of Battery Materials

D.S. Wragg*
Department of Chemistry, University of Oslo, Norway
** david.wragg@smn.uio.no*

Lithium and sodium ion batteries (LIBs and SIBs) are key technologies for renewable energy systems. Despite the widespread application of LIBs there is still significant room for improvement in capacity, lifetime, cycling stability and safety for both LIBs and SIBs. To hasten this improvement we need to examine, understand and control the structure and properties of the battery components. The most accurate information for doing this comes from studying the structures of the materials under working conditions while monitoring the output (*operando* studies). In this lecture I will present a summary of our work on *operando* characterisation of novel electrode systems, including data collected with both the Oslo/Swiss Norwegian beamline cell for combined XRD and XAS[1] and the XRD-CT electrochemical cell which we have developed for tomographic structural studies of batteries with diffraction and total scattering[2]. The work has revealed previously hidden mechanisms (e.g. how phosphorus functions as an anode for SIBs) as well as establishing clear links between structure and properties (e.g. the effects of nanosizing in bismuth anode materials)[3].

Keywords: operando, powder diffraction, total scattering

[1] J. Sottmann, R. Homs-Regojo, D. S. Wragg, H. Fjellvag, S. Margadonna, H. Emerich, *J. Appl. Cryst.* 2016, *49*, 1972- 1981.
[2] J. Sottmann, M. Di Michiel, H. Fjellvåg, L. Malavasi, S. Margadonna, P. Vajeeston, G. B. M. Vaughan, D. S. Wragg, *Angew. Chem. Int. Ed. Engl.* 2017, *56*, 11385-11389.
[3] J. Sottmann, M. Herrmann, P. Vajeeston, Y. Hu, A. Ruud, C. Drathen, H. Emerich, H. Fjellvåg, D. S. Wragg, *Chem. Mater.* 2016, *28*, 2750-2756.

$Na_3V_2(PO_4)_2F_3$: an optimal cathode material for high rates *In Situ* Powder Diffraction studies on *Operando* battery

F. Fauth[1], T. Broux[2], L. Croguennec[2], M. Bianchini[3], C. Masquelier[4]
[1] *CELLS - ALBA synchrotron, E-08290 Cerdanyola del Vallès, Barcelona, Spain*
[2] *CNRS, Univ. Bordeaux, Bordeaux INP, ICMCB UPR 9048, F-33600 Pessac, France*
[3] *Institut Laue-Langevin, 71 Avenue des Martyrs, F-38000 Grenoble, France*
[4] *Lab Réactivité et de Chimie des Solides, CNRS-UMR#7314,Univ. de Picardie Jules Verne, F-80039 Amiens Cedex 1, France*

The phosphate-based polyanionic composition$Na_3V_2(PO_4)_2F_3$ appears as a quite promising positive electrode for Na-ion batteries owing to the ability to reversibly (des-)intercalate two Na ions at voltages of ~3.7 and ~4.2 vs Na^+/Na. Although not achieved so far, a significant maximal theoretical capacity of 192.4 mAh/g could be reached if successfully removing an additional sodium ion. In addition to its high capacity, $Na_3V_2(PO_4)_2F_3$ cathode based batteries exhibit long-term cycling stability and high rate capability.

In the presentation, we will demonstrate how both the high angular resolution and the high throughput offered by synchrotron powder diffraction (SPD) techniques appeared crucial for the exact structure determination of the Na rich composition [1] and intermediate compositions during the $Na_3V_2(PO_4)_2F_3$ - $NaV_2(PO_4)_2F_3$ (des-)intercalation process [2]. SPD data were collected *in Situ* on an *Operando* half-cell battery ($Na_3V_2(PO_4)_2F_3$,on cathode, Na metal on anode) at the BL04-MSPD beamline of the ALBA synchrotron using an ad-hoc cell [3] Surprisingly, the redox process of vanadium is not achieved through V^{3+}/V^{4+} oxidation of the two vanadium ions in the structure but involves the occurrence of V^{5+} ion at the highest voltage. This result was initially guessed from bond valence sum calculations on the refined structure of $NaV_2(PO_4)_2F_3$ composition and later confirmed by X-ray absorption and NMR spectroscopy techniques [4].

As seen in the side figure, battery cycling at various rates, up to an extraordinary maximum of 50C (one full charge and discharge in ~3minutes), have been applied whilst continuously collecting powder patterns, either using standard or microdiffraction powder diffraction techniques (2x0.7 mm^2 or 20x20 μm^2 beamsize).

Latest results as well as actual status of the BL04-MSPD beamline presently intensively used for Operando powder diffaction techniques within batteries will be presented

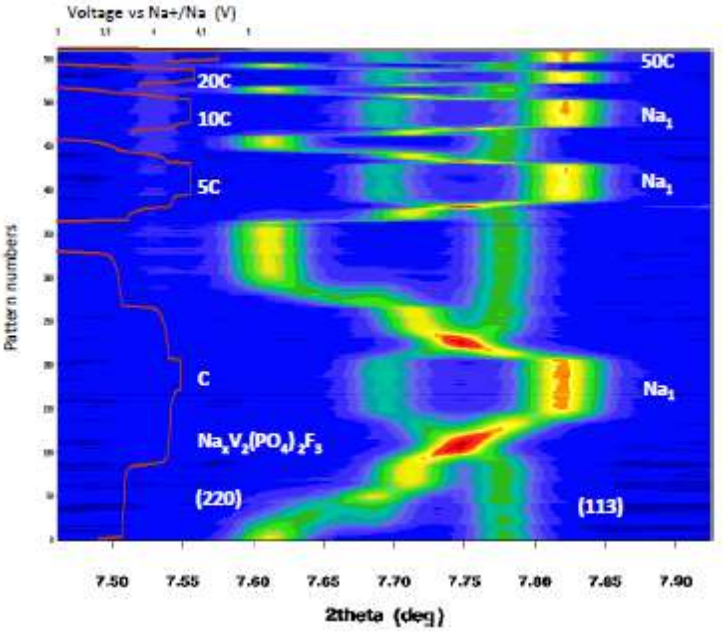

[1] Bianchini, M.; Brisset, N.; Fauth, F.; Weill, F.; Elkaim, E.; Suard, E.; Masquelier, C.; Croguennec, L. *Chem. Mater. 2014*, 26, 4238−4247.
[2] Bianchini, M.; Fauth, F.; Brisset, N.; Weill, F.; Suard, E.; Masquelier, C.; Croguennec, L, *Chem. Mater*. 2015, 27, 3009−3020.
[3] Leriche, J. B.; Hamelet, S.; Shu, J.; Morcrette, M.; Masquelier, C.; Ouvrard, G.; Zerrouki, M.; Soudan, P.; Belin, S.; Elkaim, E.; Baudelet, F. J. Electrochem. Soc. 2010, 157, A606.
[4] Broux T, Bamine T; Simonelli L, Stievano L, Fauth F, Ménétrier M, Carlier D, Masquelier C and Croguennec L, *J. Phys. Chem. C 2017* 121, 4103−4111

Keywords: Operando, Battery, Synchrotron

Towards an understanding of the magnetocaloric effect in Fe_2P

J. Cedervall[a*], M. S. Andersson[b], E. K. Delczeg-Czirjak[c], D. Iuşan[c], M. Pereiro[c], T. Ericsson[c], L. Häggström[c], W. Lohstroh[d], H. Mutka, M[e]. Sahlberg[a], P. Nordblad[b], P. P. Deen[f,g].
[a] *Department of Chemistry - Ångström Laboratory, Uppsala University, Sweden*
[b] *Department of Engineering Sciences, Uppsala University, Sweden.*
[c] *Department of Physics and Astronomy ,Uppsala University, Sweden*
[d] *Technische Universität München, Garching bei München, Forschungsneutronenquelle Heinz Maier-Leibnitz (FRM II), Gemany*
[e] *Institut Laue-Langevin, France*
[f] *ESS, Sweden*
[g] *Nanoscience Center, Niels Bohr Institute, University of Copenhagen,Denmark*
* *johan.cedervall@kemi.uu.se*

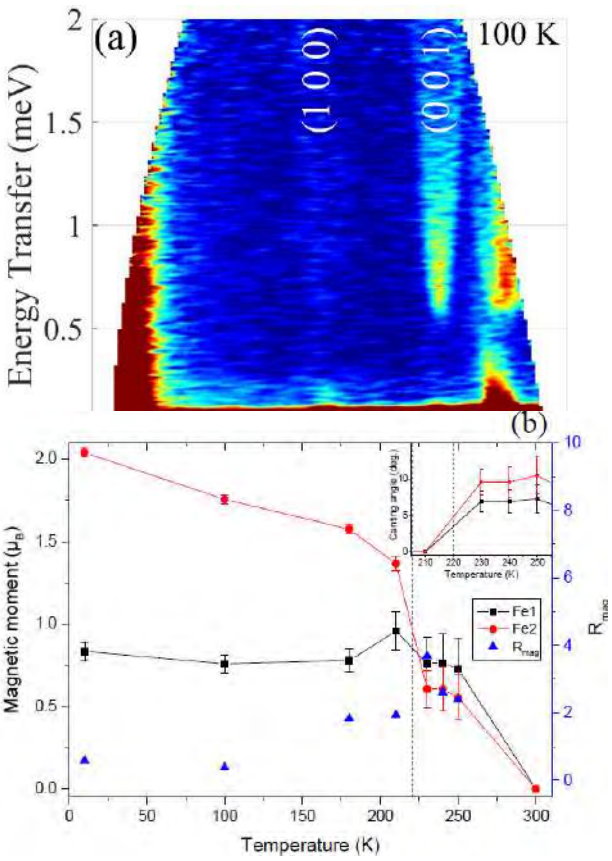

Neutron diffraction and inelastic scattering, Mössbauer spectroscopy and first principles calculations have been used to determine the structural and magnetic state of Fe_2P, a compound that has shown great potential for magnetic cooling devices. In particular when substituted with Mn and Si [1, 2]. In particular it is of great interest to know what drives the first order phase transition (FOPT) that coexist with the strong magnetocaloric effect. The FOTP is concomitant with a canting of ferromagnetic moments away from the principle direction while short range nano clusters develop and vary between antiferromagnetic to ferromagnetic coupling across the FOPT. The canting of the moments where determined from magnetic structure refinements in FullProf [3], where the elastic line where integrated to get conventional diffraction patterns. The refinements also revealed that a significant magnetic moment survives above the magnetic transition temperature where the canting is the largest. From the inelastic scattering data, a gap in the phonon excitation spectrum at low temperatures indicates boundary conditions, possible derived from the nano clusters, while a gap in the spin fluctuations indicates strong magnetic anisotropy within the system. Enhanced electron mobility, as a result of the gap in the phonon excitation, may enhance the magnetocaloric effect. Both excitation gaps disappear at the FOPT. It is clear from these results that the FOPT drives the magnetocaloric effect which is derived from strong magneto-elastic coupling concomitant with significant anisotropy in the studied system.

[1] E. Brück, *Journal of Physics D: Applied Physics,* 2005, 38, R381

[2] V. Höglin, et al. *RSC Advances* 2015, 5, 8278-8284

[3] J. Rodriguez-Carvajal, *Physica B: Condensed Matter,* 1993, 192, 55

Keywords: magnetism, neutron scattering, magnetocaloric effect

Structural insights into the lithium amide-imide solid solution

J.W. Makepeace[a*] and W.I.F. David[a,b]
[a] *Inorganic Chemistry Laboratory, University of Oxford, UK*
[b] *ISIS Neutron and Muon Facility, Rutherford Appleton Laboratory, Harwell Campus, UK*
** josh.makepeace@chem.ox.ac.uk*

Ammonia has significant potential as a sustainable energy store for large-scale grid balancing and transportation. The widespread adoption of ammonia would be promoted by the development of cheap and highly active catalysts for the cracking of ammonia to nitrogen and hydrogen, for use in both low temperature fuel cells and combustion engines. Light metal amides and imides are a new class of ammonia decomposition catalyst showing activities that rival even the most active transition metal catalyst, ruthenium, but with a significant cost advantage as a result of their high natural abundance.[1-3] One of the most active of these new catalysts, lithium imide (Li_2NH), has been shown to exist as an amide-imide solid solution ($Li_{2-x}NH_{1+x}$, $0<x<1$) under ammonia decomposition conditions. This solid solution has also been identified as key to the facile solid state hydrogen storage reactions of lithium imide.[4]

In order to explore the properties of this system, a series of non-stoichiometric samples were synthesised and studied by X-ray and neutron powder diffraction and Raman spectroscopy.[5] The diffraction data show that a non-stoichiometric anti-fluorite phase is present across the solid solution, indicating a high degree of disorder in the long-range structure. While lattice parameter variation gave some indication of stoichiometry variation within this structure, the challenge of obtaining the stoichiometry from Rietveld analysis of the neutron powder diffraction data was addressed by allowing full orientational and occupational variation of the hydrogen positions around the nitrogen. The variation in occupancy, linked to the lithium occupancy, allowed for variation in the stoichiometry. A 'golf ball' array of hydrogen positions around the nitrogen site was used to accommodate the different orientational preferences of amide and imide anions, as well as any disorder in those orientations. Spherical harmonic terms were used to populate the different crystallographic directions on the surface of the 'golf-ball', revealing that the non-stoichiometric hydrogen positions were more disordered than either of the end members, but related strongly to the known hydrogen orientations in each of those phases.

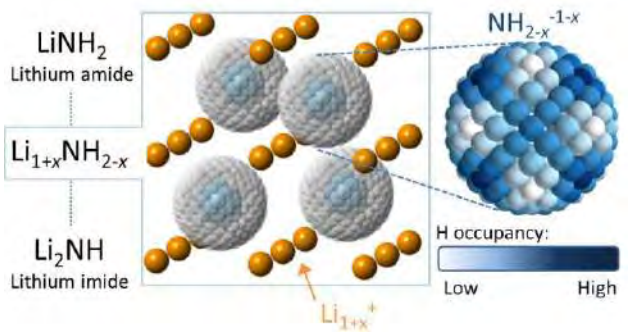

Raman spectroscopy gave further indications of possible local structural variations – indicating the presence of both amide and imide anions in lithium-rich (Li_2NH-like) and lithium poor ($LiNH_2$-like) environments. These results form the basis of an attempt to understand the influence of non-stoichiometry on the function of lithium amide-imide materials in energy storage applicastions. These structural variations dictate important physical properties such as the sample melting point, that has important implications for its use as a catalyst.

[1] David W.I.F., Makepeace J.W., Callear S.K., Hunter H.M.A., Taylor J.D., Wood T.J. and Jones M.O. *J. Am. Chem. Soc.,* 2014, 136(38), 13082-13085.

[2] Makepeace J.W., Wood T.J., Hunter H.M.A., Jones M.O. and David W.I.F. *Chem. Sci..,* 2015, 6, 3805-3815.

[3] Makepeace JW, Hunter HMA, Wood TJ, Smith RI, Murray CA and David WIF, *Faraday Discus.*, 2016, 188, 525-544.

[4] Makepeace J.W., Jones M.O., Callear S.K., Edwards P.P. and David W.I.F., *Phys. Chem. Chem. Phys.*, 2014, 16, 4061-4070.

[5] Makepeace J.W. and David W.I.F., *J. Phys. Chem. C*, 2017, 121(22), 12010-12017.

Keywords: ammonia, non-stoichiometry, hydrogen

Mixed-metal amide/imide catalysts for ammonia decomposition applications

C.Kirk, W.I.F. David
Inorganic Chemistry Department, University of Oxford, UK
ISIS Facility, Rutherford Appleton Laboratory, UK
charlotte.kirk@new.ox.ac.uk

A sustainable hydrogen based economy is seen as one of the necessary options in transitioning away from fossil fuels. There are, however, significant technical and economic challenges in transporting and storing hydrogen at the appropriate industrial scale. Already produced on a global scale, ammonia, with its high gravimetric and volumetric hydrogen density, is an attractive solution to these issues. Its use as a fuel and hydrogen store requires the development of effective and inexpensive NH_3 cracking catalysts. Light-metal amides ($LiNH_2$ [1] and $NaNH_2$ [2]) are a new family of low-cost ammonia cracking catalysts and are likely to surpass the performance of optimised transition metal based catalysts. Creating mixed metal systems is one way to tailor their function as catalysts ($Li_2Ca(NH)_2$ shows the highest activity observed to date [3]). This work reports the results of an investigation into the structural chemistry and ammonia decomposition activity of three mixed group I metal amide systems: Li-Na, Li-K and Na-K. The phase space between the two end members of each system was explored by ball-milling a plethora of molar ratios and analysing the PXRD patterns of the resulting samples. In addition to the known phases, principal component analysis (PCA) elucidated a new phase for each of the Li-K and Na-K systems (figure shown for the Na-K system). $LiK_2(NH_2)_3$ and $NaK_2(NH_2)_3$ have analogous $P4_2/m$ structures so it is likely that the unknown Na-K phase has a similar structure to $Li_3K(NH_2)_4$ given it is most prevalent in the 9:3 and 7:5 $NaNH_2$:KNH_2 molar ratios. For the unknown Li-K phase, the peaks out to a d spacing of 2Å were fitted to pseudo-voigt functions in TOPAS and DICVOL was used to predict a monoclinic cell and determine its dimensions. DASH was used to determine the most likely space group of $P2_1/a$ and the volume of formula units of $LiNH_2$ and KNH_2 used to predict the most likely number of each metal atom present. Finally FOX was used to combine all this information and to predict a crystal structure. Mixed metal amide systems out-perform single metal amides as NH_3 decomposition catalysts across the entire temperature range and particularly at high temperatures. The NH_3 decomposition ability of the Li-Na, Li-K and Na-K mixed metal amide systems was investigated. Common behaviour of particular metal ratios was elucidated for the different families which emphasises the importance of stable imides for active NH_3 decomposition catalysts. Mixed Group I-II metal amide systems were then explored. The K-Mg [4] and Na-Mg [5] systems are of particular importance as the mixed metal amides are known to be metastable kinetic products which can be annealed to form novel mixed amide-imide phases $RMg(NH_2)(NH)$ (R=Na or K) which are stable to higher temperatures. These systems are a new class of NH_3 decomposition catalysts, bridging the intra-Group 1 systems studied so far (Li-Na, Li-K and Na-K) for which no mixed-metal imide exists and those for which only an imide is known (Li-Ca and Li-Mg). Initial results from a neutron powder diffraction investigation on these systems are reported, including attempts to elucidate the crystal structures of $NaMg(NH_2)(NH)$ and $Na_2Mg(NH_2)_4$.

Phase composition of KNH_2 + $NaNH_2$ mixtures derived from PCA of X-ray PXRD data

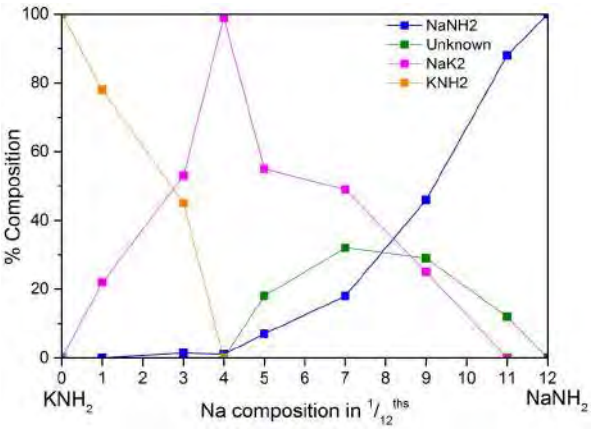

[1] Makepeace, J.; Wood, T.; David, W. I. F. *Chem. Sci.* 2015, 6, 3805
[2] Wood, T.; Makepeace, J.; David, W. I. F. *PCCP*. 2015, 17, 22999
[3] Makepeace, J. *Faraday Discussions.* 2016, 188, 525-544
[4] Santoru, A.; Dornheim, M. *PCCP*. 2016, 18, 3910
[5] Pireddu, G.; Garroni, S.*; Int. J. Hydrogen Energy* 2015, 40, 1829

B-site ordered double perovskite, $La_2(Al_{0.5}MgTa_{0.5})O_6$ for thermal barrier applications and its high-temperature phase transition

Y. J. Sohn[a*], G. Mauer[a], G. Roth[b], O. Guillon[a], R. Vaßen[a]
[a] *Forschungszentrum Jülich GmbH, Institute of Energy and Climate Research, Materials Synthesis and Processing (IEK-1), 52425 Jülich, Germany*
[b] *Institut für Kristallographie, RWTH Aachen University, 52066 Aachen, Germany*
** y.sohn@fz-juelich.de*

An improvement of gas turbine engines can be obtained by increase of the inlet temperatures. The standard thermal barrier coating (TBC) material yttria partially stabilized zirconia (YSZ) decomposes at elevated temperatures into high-yttria and low-yttria phases. The latter transforms upon cooling into the monoclinic phase with an associated large volume increase, which may result in failure of the TBC [1]. Thus, new TBC materials are widely searched to further improve the gas turbine engine efficiency at long-term operation temperatures above 1200 °C. Over the last decades a large amount of candidates have been investigated to identify alternative TBC materials. Among them, the complex rare-earth perovskites gained interest due to their high melting point and possible tailoring properties with *B*-site cation ordering effect [2,3]. Recently, plasma sprayed $La_2(Al_{0.5}MgTa_{0.5})O_6$ (LAMT) coatings showed significantly improved thermal cycling lifetime results, and were suggested to be a promising candidate [4,5]. Up to now, synthesized LAMT-powder was identified to be an orthorhombic phase with the space group symmetry, *Pnma*, which is isostructural to orthorhombic $LaFeO_3$. The Pawley refinement on the measured powder X-ray diffraction (XRD) data revealed no oddity. However, a strong mismatch of the peak intensities was detected during the Rietveld analysis. A possible texture effect was excluded because of the powder morphology, as well as, by trying out the different sample preparation methods. To clarify the correct crystal structure of LAMT and to check the phase stability, in-situ high-temperature XRD was carried out in the temperature range of 25-1200 °C. Unlike reported earlier [4], a structural phase transition was observed at ~ 855 °C upon heating, and this phase transition was completely reversible. The crystal structure of LAMT was then refined by Rietveld analysis in the monoclinic space group symmetry, $P2_1/n$ [6] at room temperature, with β = ~ 90°. In the monoclinic crystal structure, the *B*-site cations are ordering in a rock-salt type arrangement. The Mg^{2+}-ions take the fully occupied 2*c*-Wyckoff position whereas the Al^{3+}- and Ta^{5+}-ions occupy each half of the 2*d*-Wyckoff position. The crystal structure of LAMT becomes rhombohedral with the space group, *R*-3 above ~ 855°C. The unit cell volume changes gradually as a function of temperature without any abrupt jump.

[1] Vaßen R., Jarligo M.O., Steinke T., Mack D.E. and Stöver D. *Surf. Coat. Technol.,* 2010, 205, 938.

[2] Guo R., Bhalla A.S. and Cross L.E. *J. Appl. Phys.,* 1994, 75, 4704.

[3] Tarvin R. and Davies P.K. *J. Am. Ceram. Soc.,* 2004, 87, 859.

[4] Jarligo M.O., Mack D.E., Vaßen R. and Stöver D. *J. Therm. Spray Technol.,* 2009, 18, 187.

[5] Schlegel N., Sebold D., Sohn Y.J., Mauer G. and Vaßen R. *J. Therm. Spray Technol.,* 2015, 24, 1205.

[6] Kim Y.I. and Woodward P.M. *Solid State Chem.,* 2007, 180, 2798.

Keywords: thermal barrier coatings, ordered double perovskite, in-situ high-temperature XRD

Metal Hydro-borates for Li- and Na-ion Batteries

R. Černý*, Y. Sadikin, E. Didelot, M. Brighi, F. Murgia
Department of Quantum Matter Physics, Laboratory of Crystallography, University of Geneva,
Quai Ernest-Ansermet 24, CH-1211 Geneva, Switzerland
**Radovan.Cerny@unige.ch*

Complex hydrides based on light hydro-borate anions such as borohydride BH_4^- or *closo*-borate anion $B_{12}H_{12}^{2-}$ find their place as solid stores for hydrogen, and since recently, also as solid electrolytes in Li- and Na-ion batteries. The mobility of the cations depends on the pathways available in the anion packing, chemical interaction of cations with anions and on the anion thermal motion such as tumbling or rotation. While the latter two require important experimental and theoretical effort, the first parameter can be easily analysed and quantified from the crystal structure data obtained by X-ray powder diffraction. A thorough crystal chemistry analysis of observed crystal structures, allows us to find the structural aristotypes and to draw conclusions about the bonding and building principles in this important category of materials as it was done recently for the borohydrides.[1]
Among others, the modification of $Na_2B_{12}H_{12}$, promising Na-ion solid electrolyte, by anion modification and anion mixing will be shown (Figure 1). [2-4] Novel synthetic way completed by *ab inito* structural characterization using synchrotron X-ray powder diffraction and *ab initio* calculation allowed discovery of several 3*d* transition metal *closo*-borates - potentially battery electrodes (Figure 2).[5]

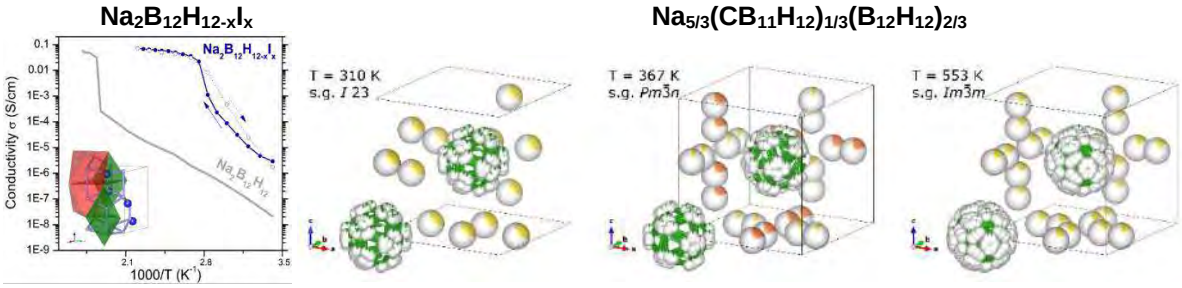

Figure 1: **(left)** Ionic conductivity of a sample containing 52 wt% $Na_2B_{12}H_{12-x}I_x$ and 48 wt% NaI. The conductivity of the precursor $Na_2B_{12}H_{12}$ is shown for comparison. Na-ion conduction channels in *hcp* sublattice with face-sharing T and O interstices sites in *h*-$Na_2B_{12}H_{12-x}I_x$. In blue the static Na positions as optimized by DFT. **(right)** Evolution of anionic and cationic disorder in $Na_{5/3}(CB_{11}H_{12})_{1/3}(B_{12}H_{12})_{2/3}$. Green and yellow spheres represent boron and sodium atoms respectively. Orange spheres indicates a different Wyckoff site for Na (only in *Pm*-3*n*). The colour partial filling indicates the partial site occupation.

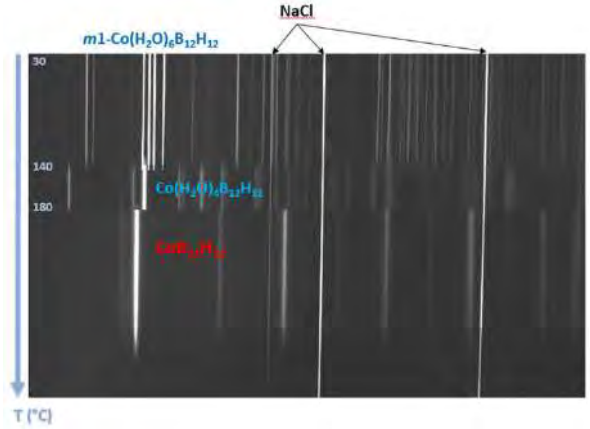

Figure 2: Temperature dependent X-ray powder diffraction patterns (T-ramp) for ball-milled and hydrated $Na_2B_{12}H_{12}$ + $CoCl_2$ mixture (heating rate 10 K/min under dynamic vacuum, λ = 0.7225 Å.

Keywords: solid electrolyte, Na-ion battery, borohydride, *closo*-borate, transition metal

[1] Černý R., Schouwink P. *Acta Cryst. B.* **2015**, *71*, 619-640
[2] Sadikin Y., Brighi M., Schouwink P., Černý R., *Adv. Energy Mater.* **2015**, 1501016
[3] Sadikin Y., Schouwink P., Brighi M., Łodziana Z., Černý R, *Inorg. Chem.* **2017**, *56*, 5006-5016
[4] Brighi M., Murgia F., Łodziana Z., Schouwink P., Wolczyk A., Černý R., submitted to *Adv. Energy Mater.*
[5] Sadikin Y., Didelot E., Łodziana Z., Černý R., submitted to *Dalton Trans.*

A study of possible extra-framework cation ordering in *Pbca* leucite structures with stoichiometry $RbCsX^{2+}Si_5O_{12}$ (X = Mg, Ni, Cd).

A. M. T. Bell[a*], C. M. B. Henderson[b]
[a] *Materials and Engineering Research Institute, Sheffield Hallam University, UK*
[b] *School of Earth and Environmental Sciences, University of Manchester, UK*
** Anthony.Bell@shu.ac.uk*

Leucites are silicate framework structures with some of the silicon framework cations partially replaced by divalent or trivalent cations. A monovalent extraframework alkali metal cation is also incorporated in these structures to balance the charges, these alkali metal cations can be ion-exchanged and these materials are of technological interest as storage media for radioactive Cs from nuclear waste [1].

In 1994 we reported [2] the *Pbca* structure of the leucite analogue $Cs_2CdSi_5O_{12}$. This was the first orthorhombic leucite structure with all the silicon and non-silicon framework cations completely ordered onto separate crystallographic sites. This structure has 5 distinct Si sites and 1 Cd site; there are also 2 distinct sites for the extra-framework Cs. Since then we have reported [3-6] 10 more *Pbca* leucite structures with the stoichiometries $Cs_2X^{2+}Si_5O_{12}$ (X = Mg, Mn, Co, Ni, Cu, Zn) and $Rb_2X^{2+}Si_5O_{12}$ (X = Mg, Mn, Ni, Cd).

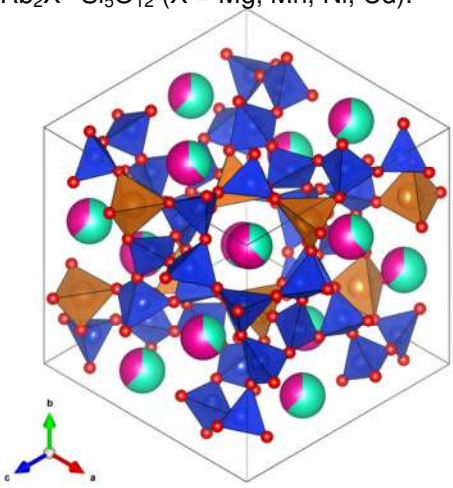

We have recently synthesised leucite analogues with two different extra-framework cations, these have the stoichiometry $RbCsX^{2+}Si_5O_{12}$ (X = Mg, Ni, Cd). Using the Rietveld method [7] crystal structures have been refined from X-ray powder diffraction data collected on these new leucites. The initial Rietveld refinements assumed 50%Cs and 50%Rb on each of the two extra-framework cation sites. The refined structures for X = Ni and Cd have (within error limits) complete disorder of Cs and Rb over these two extra-framework cation sites. However, for X = Mg the occupancies of these two extra-framework cation sites are:- Cs1 0.37(3), Rb1 0.63(3), Cs2 0.63(3), Rb2 0.37(3), there is partial ordering of the occupancies of these two extra-framework cation sites.

[1] Gatta, G. D., Rotiroti, N., Fisch, M., Kadiyski, M. and Armbruster, T. (2008). Phys. Chem. Miner. 35, 521–533.
[2] Bell, A.M.T., Redfern, S.A.T., Henderson, C.M.B., Cernik, R.J., Champness, P.E., Fitch, A.N. and Kohn, S.C. (1994). *Acta Cryst.* B**50**, 560-566.
[3] Bell, A.M.T. and Henderson, C.M.B. (1996). *Acta Cryst.* C**52**, 2132-2139.
[4] Bell, A.M.T. and Henderson, C.M.B. (2009). *Acta Cryst.* B**65**, 435-444.
[5] Bell, A.M.T., Knight, K.S., Henderson, C.M.B. and Fitch, A.N. (2010). *Acta Cryst.* B**66**, 51-59.
[6] Bell, A.M.T. and Henderson, C.M.B. (2016). *Acta Cryst.* E**72**, 249-252.
[7] Rietveld, H.M. (1969). *J. Appl. Cryst.* **2**, 65-71.

Keywords: silicate framework structures, cation ordering, Rietveld method

Structural analysis of $NaMg(H_{1-x}F_x)_3$ for thermochemical energy storage applications

M.R. Rowles[a,b*], M.S. Tortoza[b], T.D. Humphries[b], D. A. Sheppard[b], M. Paskevicius[b], M. V. Sofianos[b], K. F. Aguey-Zinsou[c], C.E. Buckley[b]

[a] *John De Laeter Centre, Curtin University, Australia*

[b] *Hydrogen Storage Research Group, Fuel and Energy Technology Institute, Curtin University, Australia*

[c] *Merlin Group, School of Chemical Engineering, The University of New South Wales, Australia.*

** matthew.rowles@curtin.edu.au*

The use of hydrogen storage materials in concentrated solar thermal applications is an area of active research [1]. These materials must be able to operate over a wide temperature range – room temperature up to 1100 °C – and maintain their capacity over many hundreds or thousands of cycles.

Previous investigations [2,3] have shown that substituting fluorine for hydrogen stabilises NaH and MgH_2, increasing the temperature at which they release hydrogen, increasing the amount of heat able to be stored. This is especially useful for application as a thermal energy storage material. To this end, *in situ* diffraction studies have been undertaken on $NaMg(H_{1-x}F_x)_3$ to study the structural transitions and reactions which occur upon heating in a capillary under dynamic vacuum from room temperature to 600 °C. The experiments were undertaken at the Australian Synchrotron and analysed via a parametric distortion-mode refinement [4-6] in Topas Academic [7,8].

$NaMg(H_{1-x}F_x)_3$ is a perovskite-type structure in the space group *Pnma*, and can be modeled as a distortion of a parent mineral, neighborite ($NaMgF_3$), in *Pm-3m*.There are two distortion modes associated with the Na position, and five with rotations, tilts, and deformations of the MgH/F octahedra. The Mg positions are fixed by symmetry.

In the analysis of the *in situ* heating of $NaMgHF_2$, it was found that at ~320 °C, it starts to release H_2, and dissociates to form NaF, Mg/MgO, and $NaMgF_3$. During this process, the occupancy of the H/F positions remains constant, the lattice expands normally, and all distortion modes are active and linear. The octahedral R^{4-} and M^{3+} modes are nearly zero. At 500 °C, this behavior of $NaMgHF_2$ abruptly changes. The H occupancy tends to zero very quickly, the lattice contracts whilst still being heated, and all distortion modes increase in a sigmoidal fashion. This final expulsion of H from the lattice was unexpected.

The use of distortion-mode refinements can be informative, in only allowing rigid distortions of structural units, whilst maintaining the necessary degrees of freedom, to see how the structure of a material changes with temperature, or some other stimulus. Parametric refinements are very good at stabilising and speeding up refinements, but refinements should initially be undertaken with totally free parameters to ensure that the parameterisations introduced are supported by the data.

[1] Sheppard D.A., Paskevicius M., Humphries T.D., Felderhoff M., Capurso G. *et al. Appl. Phys. A*, 2016, 122, 395.
[2] Humphries T.D., Sheppard D.A., Rowles M.R., Sofianos M.V., Buckley C.E. *J. Mater. Chem. A*, 2016, 4, 12170.
[3] Tortoza M.S., Humphries T.D., Sheppard D.A., Paskevicius M., Rowles M.R. *et al. Phys. Chem. Chem. Phys.*, 2018, 20, 2274.
[4] Stinton G.W., Evans J.S. *J. Appl. Crystallogr.*, 2007, 40, 87.
[5] Campbell B.J., Stokes H.T., Tanner D.E., Hatch D.M. *J. Appl. Crystallogr.*, 2006, 39, 607.
[6] Campbell B.J., Evans J.S.O., Perselli F., Stokes H.T. *IUCr Comput. Comm. Newsl.*, 2007, 8, 81.
[7] Coelho A.A. (2016) Topas Academic. 7b edn.,
[8] Coelho A.A., Rowles M.R. *J. Appl. Crystallogr.*, 2017, 50, 1331.

Keywords: hydrogen storage, thermal energy storage, distortion mode, Rietveld refinement

The Crystal Structure and Electrical Properties of the Oxide Ion Conductor $Ba_3W_{1.2}Nb_{0.8}O_{8.6}$

K.S. McCombie*[a], E. J. Wildman[a], C. Ritter[b], R. I. Smith[c], J. M. S. Skakle[a], A. C. McLaughlin[a]
[a] *Department of Chemistry, University of Aberdeen, UK*
[b] *Institut Laue Langevin*
[c] *ISIS facility, Rutherford Appleton Laboratory*
* *r01ksm15@abdn.ac.uk*

Oxide-ion conducting materials are attracting considerable attention due to their application as electrolytes in solid oxide fuel cells (SOFCs). In order to reduce system costs and increase reliability it is highly desirable to find new materials which exhibit significant ionic conductivity at lower temperatures. Research has been driven into the discovery and development of electrolyte materials which exhibit high ionic conductivities at intermediate temperatures (below 650 °C). Significant oxide ion conductivity has recently been identified in the compounds $Ba_3MoNbO_{8.5}$ [1,2] and $Ba_3WNbO_{8.5}$ [3], which exhibit bulk conductivities of 2.2 x 10^{-3} S cm^{-1} and 1.7 x 10^{-3} S cm^{-1}, respectively, at 600 °C. These compounds both crystallise in a hybrid of the 9R hexagonal perovskite and palmierite structures, containing a mixture of tetrahedral and octahedral geometry (Figure 1).

In order to investigate how the conductivity changes with increasing oxygen concentration, solid solutions of $Ba_3W_{1+x}Nb_{1-x}O_{8.5+x/2}$ (x = 0.05, 0.1, 0.2 and 0.33) were prepared. However, powder X-ray diffraction data showed that only the x = 0.2 phase could be successfully synthesised. Attempts to prepare x = 0.05, 0.1 and 0.33 materials resulted in samples containing impurities of $BaWO_4$. $Ba_3W_{1.2}Nb_{0.8}O_{8.6}$ was discovered as a line phase. $Ba_3W_{1.2}Nb_{0.8}O_{8.6}$ exhibits pure ionic conductivity to low pO_2 (10^{-20} atm) and is stable in reducing atmospheres. At low temperatures, the bulk conductivity is an order of magnitude lower than that of $Ba_3MoNbO_{8.5}$, but the conductivities converge at 600 °C. In order to further investigate the correlation between the structural and transport properties, a variable temperature neutron diffraction study has been performed between 25 and 600 °C. The oxygen/vacancy distribution changes as the temperature increases so that the ratio of $(W/Nb)O_4$ tetrahedra to $(W/Nb)O_6$ octahedra increases upon heating above 300 °C. There is a clear relationship between the ratio of tetrahedra to octahedra and the magnitude of the bulk conductivity in both $Ba_3W_{1.2}Nb_{0.8}O_{8.6}$ and $Ba_3MoNbO_{8.5}$. The increase in the proportion of $(M/Nb)O_4$ tetrahedra (where M = W and Mo) offers a lower energy transition path for the transport of O^{2-} ions, enhancing the conductivity.

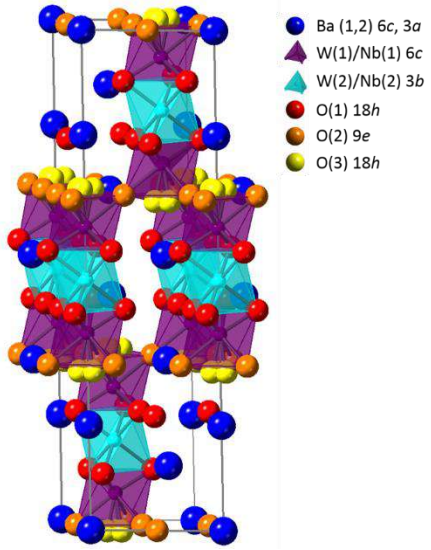

Figure 1. The hybrid crystal structure of $Ba_3W_{1.2}Nb_{0.8}O_{8.6}$.

References

[1] Fop S., Skakle J. M. S., McLaughlin A. C. M., Connor P. A., Irvine J. T. S. and Wildman E. J. *J. Amer. Chem. Soc.,* 2016, 138, 16764.

[2] Fop S., Wildman E. J., Irvine J. T. S., Connor P. A., Skakle J. M. S., Ritter C. and McLaughlin A. C. *Chem. Mater.,* 2017, 29, 4146.

[3] McCombie K. S., Wildman, E. J., Fop S., Smith R. I., Skakle J. M. S. and McLaughlin A. C. *J. Mater. Chem.* 2018, DOI: 10.1039/C7TA08989A

Keywords: hexagonal perovskite, ionic conductor, crystal structure.

Local structure analysis of titania photocatalysts for light-induced water splitting

E. Onur Şahin[a*], H. Tüysüz[a], C. Chan[b], W. Schmidt[a], C. Weidenthaler[a]
[a] *Max-Planck-Institut für Kohlenforschung Germany*
[b] *Department of Materials Science & Engineering, Arizona State University, USA*
** onur@mpi-muelheim.mpg.de*

Titanium-based solids are active photocatalysts for light-induced water splitting. Amorphous titanium oxides synthesized via the direct injection method shows higher photocatalytic activity for H_2 production compared to the crystalline TiO_2 benchmark catalyst P25.[1] All samples introduced in this work were synthesized via the so-called "direct injection method". The method involves injection of a titanium alkoxide precursor (titanium(IV) ethoxide, butoxide, or isopropoxide) into a solution of water and 10% methanol. The solution is mixed in a photoreactor equipped with a UV light source (see figure). TiO_x particles are then formed and split water into hydrogen under UV light. During this process the color of the suspension containing the photocatalyst changes from white to black/blue.[1] This color change indicates a change in the oxidation state of titanium. In order to investigate whether this process also affects the structure of photocatalyst, local and averaged structures of amorphous and partially crystalline titanium oxide-based photocatalysts were investigated by X-ray total scattering. X-ray diffraction showed that the particles prepared by this method are lacking long-range order. Local structures of non-crystalline materials are not accessible by conventional X-ray diffraction methods. Therefore, local probes such as Pair Distribution Function analysis (PDF) are required.[2]

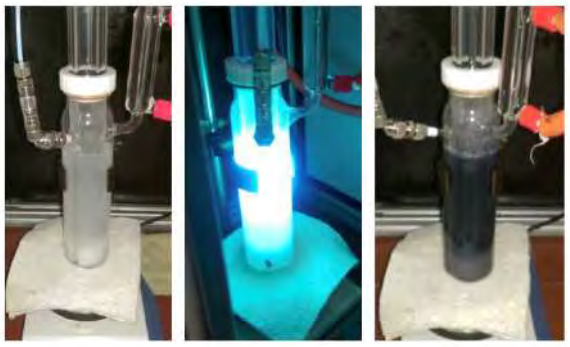

Tracking the changes of the local structure of the synthesized titania materials will help understanding the structure-property relationship for that photocatalyst. The effect of UV light on the titania structures was studied by comparison with samples synthesized without UV light. In addition, the effect of different alkoxide concentrations on the structure of the photocatalysts was investigated as it plays an important role in crystallization process. The state of the photocatalysts were further analysed by complementary characterization techniques including Raman spectroscopy and X-ray photoelectron spectroscopy.

[1] D. Zywitzki, H. Jing, H. Tüysüz, C. K. Chan, *J. Mat. Chem. A*, **2017**, 5, 10957-10967.

[2] P. Juhás, T. Davis, C. L. Farrow, S. J. L. Billinge, *J. Appl. Cryst.*, **2013**, 46, 560–566.

Keywords: photocatalysis, local structure, pair distribution function

On the Phase Transitions of NASICON-type compounds

C. L. Lengauer [a*], *M. Ende* [a], *G. Tippelt* [b], *G. Redhammer* [b]
[a] *Department of Mineralogy and Crystallography, University of Vienna, AT*
[b] *Chemistry and Physics of Materials, University of Salzburg, AT*
** christian.lengauer@univie.ac.at*

NASICON-type materials belong to the group of hetero-polyhedral framework compounds exhibiting ionic conductivity. These 'NAtrium Super Ionic CONductors' were first reported by Goodenough [1] in consequence of a systematic exploration of cubic skeleton structures like pyrochlore and cristobalite-type carnegieite leading to the type material $Na_{1+x}Zr_2P_{3-x}Si_xO_{12}$. Nowadays, NASICONs are classified with the general formula $A_xM_2(XO_4)_3$ (A = Li, Na, K, Mg, Ca; M = Al, Sc, Y, Ti, Zr, V, Nb, Cr, Mn, Fe, Ga, In; X = Si, P, As, S). Due to their physical properties they gained interests as a solid electrolyte over decades, followed up by recent investigations as a potential cathode or anode material for energy storage applications [2].

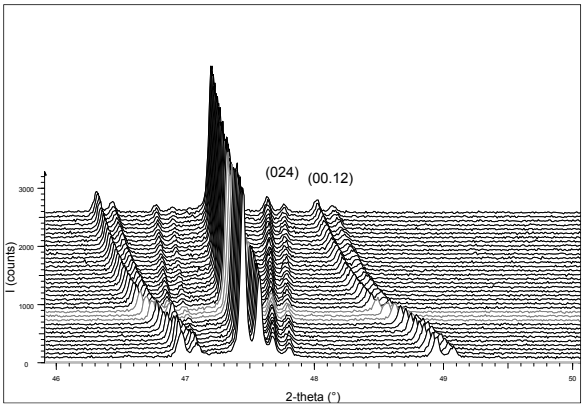

The ionic conductivity is strongly symmetry correlated. Based on the pseudo-cubic, trigonal framework (ideally $R\bar{3}c$) of the corner-linked MO_6 and XO_4 polyhedra three polymorphs are known for $Na_3Sc_2(PO_4)_3$, which exhibit up to now the highest sodium ion conductivity. The reversible states are (i) ionic insulator: monoclinic, low temperature α-phase below ~65 °C, (ii) ionic conductor: average rhombohedral, intermediate β-phase, and (iii) 'superionic' phase: rhombohedral, high temperature γ-phase above ~165 °C. All phase changes are induced by sodium ion order / disorder [3].

DSC measurements, show two distinct and smooth phase transitions (ΔT ~40 °C) at ~10 °C (α→β) and ~160 °C (β→γ) during heating. On cooling the β→α transition is faint, moreover, the unsteady signal from 65 to -20 °C indicates a second β'-type phase. On the dT-PXRD patterns, this temperature range is characterized by the presence of sharp and diffuse incommensurate reflections. As shown in the figure above the β→γ transition between 140 – 180 °C is evident by a discontinuous increase of the ***c***-axis and a small positive anomaly in the basal plane of the trigonal substructure. The general thermal expansion of $Na_3Sc_2(PO_4)_3$ is strongly anisotropic. A similar behaviour can be observed for $Na_3Cr_2(PO_4)_3$, however, the phase transitions are considerably shifted to higher temperatures. This can be explained by the different cation radii of Cr^{3+} and Sc^{3+}, which have a stabilizing impact on the corner-linked zig-zag chains of the MO_6 and XO_4 polyhedra.

[1] Goodenough J.B., Hong H.Y.-P. and Kafalas J.A. *Mater. Res. Bull.*, 1976, 11, 203.
[2] Jian Z., Hu Y.-S., Ji X. and Chen W. *Adv. Mater*., 2017, 29, 1601925.
[3] Collin G., Comes R., Boilot J.P. and Colomban Ph. *J. Phys. Chem. Solids*, 1986, 47, 843.

Keywords: nasicon, energy materials, non-ambient diffractometry

Structural factors enabling fast oxide ion conduction in the hexagonal perovskite derivative $Ba_3MoNbO_{8.5}$

S. Fop [a], J. M. S. Skakle [a], A. C. McLaughlin [a*]
[a] *Department of Chemistry, University of Aberdeen, UK*
* *a.c.mclaughlin@abdn.ac.uk*

Oxide ion conductors have received much attention in recent years due to their application as solid oxide fuel cell (SOFCs) electrolytes and solid oxide electrolysers cells (SOECs). Particular efforts are being made towards the development of materials that exhibit appropriate physical-chemical stability and good ionic conductivity at an intermediate temperature range (400 – 600 °C) [1]. Oxide ion conductivity has been reported in several structural families, demonstrating a strong correlation between the ionic transport and the crystal structure [2].
We have recently identified oxide ion conductivity in the hexagonal perovskite derivative $Ba_3MoNbO_{8.5}$ [3]. $Ba_3MoNbO_{8.5}$ crystallises in a hybrid of the 9R hexagonal perovskite and palmierite structures. $(Mo/Nb)O_4$ and $(Mo/Nb)O_6$ units coexist within the lattice, producing a disordered arrangement of tetrahedral and octahedral domains. Oxide ion diffusion in this system most likely occurs via a cooperative tetrahedral-octahedral interchange mechanism.
Here we present the results of powder neutron diffraction experiments on $Ba_3MoNbO_{8.5}$ and the solid solution $Ba_3Mo_{1-x}Nb_{1+x}O_{8.5-x/2}$ (x = 0.1, 0.2, 0.3). Variable temperature neutron diffraction on $Ba_3MoNbO_{8.5}$ revealed an unusual structural reorganisation of the oxygen/vacancy distribution on the $BaO_{2.5}$ pseudocubic layers above 300 °C [4]. This rearrangement is followed by a concomitant increase in the ratio of $(Mo/Nb)O_4$ tetrahedra and $(Mo/Nb)O_6$ octahedra, enhancing the ionic bulk conductivity. Nb doping decreases the relative number of $(Mo/Nb)O_4$ tetrahedra, as well as the second order Jahn-Teller distortion of the coordination polyhedra, leading to reduced ionic conductivity in the $Ba_3Mo_{1-x}Nb_{1+x}O_{8.5-x/2}$ series [5]. The obtained results evidence the key structural parameters for the ionic conductivity in $Ba_3MoNbO_{8.5}$. The flexibility of the Mo/Nb lattice, a prevalent tetrahedral coordination environment and the off-centre distortion of the *d*-metal polyhedra are fundamental factors in enabling the oxide ion transport. These findings suggest suitable strategies to improve the conductivity of $Ba_3MoNbO_{8.5}$ and for the rational design/discovery of other oxide ion conductors in the hexagonal perovskite family.

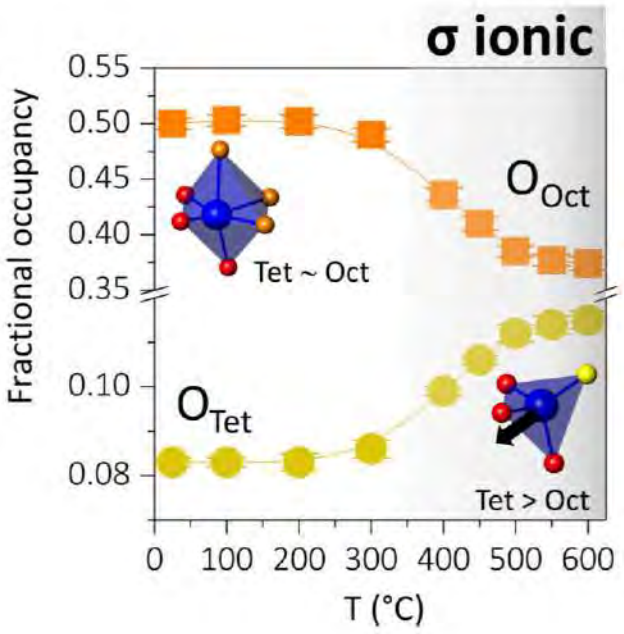

[1] Wachsman E. D. and Lee K. T. *Science,* 2011, 334, 935.

[2] Malavasi L., Fisher C. A. J. and Islam M.S. *Chem. Soc. Rev.,* 2010, 39, 4370.

[3] Fop S., Skakle J. M. S., McLaughlin A. C., Connor P. A., Irvine J. T. S., Smith R. I. and Wildman E. J. *J. Am. Chem. Soc*., 2016, 138, 16764.

[4] Fop S., Wildman E. J., Irvine J. T. S., Connor P. A, Skakle J. M. S., Ritter C. and McLaughlin A. C. *Chem. Mater.*, 2017, 29, 4146.

[5] Fop S., Wildman E. J., Skakle J. M. S., Ritter C. and McLaughlin A. C. *Inorg. Chem*., 2017, 56, 10505.

Keywords: Neutron diffraction, Oxide ion conductor, Perovskite

Phase transformations in Co-Re-Cr-Ni high-temperature superalloys studied by neutron diffraction

Přemysl Beran[a*], Debashis Mukherji[b], Pavel Strunz[a], Ralph Gilles[c], Markus Hölzel[c], Michael Hofmann[c], Lukas Karge[c], Joachim Rösler[b]
[a] *Nuclear Physics Institute of the CAS, Řež near Prague, Czech Republic*
[b] *Technische Universität Braunschweig, IfW, Langer Kamp 8, Braunschweig, Germany*
[c] *Technische Universität München, MLZ, Lichtenbergstr. 1, Garching, Germany*
** pberan@ujf.cas.cz*

Amongst new alloy systems being developed to supplement Ni-based superalloys in gas turbine application, the Co-Re-based alloys show promise because of their excellent specific strength and relatively high melting range (1490°-1560°C) [1]. Alloying elements with various functionality are added to these alloys, for example, Re to increase melting temperature, Cr, Ni, for oxidation resistance, C, Ta to produce high-temperature strengthening phase (TaC) or boron (to improve ductility). The effects of these elements on structure and microstructure were intensively investigated in the past by neutron scattering and other techniques [2-4]. Moreover, since the Co matrix undergoes an allotropic transformation from the low temperature closed packed hexagonal (hcp) structure to the high-temperature face centred cubic (fcc) structure, a two-phase matrix exists in Co-Re alloys at intermediate temperatures [5, 6].
Like other Co-based superalloys presently used in gas turbine static components, the Co-Re alloys use Cr to provide oxidation resistance [7]. Cr addition above 20 at.%, however, pose a challenge – namely the formation of topologically closed packed Cr_2Re_3-type σ-phase. It is generally avoided in high-temperature alloys as its presence causes brittleness. The Co-Re alloys designed presently at TU Braunschweig are now being investigated for improving oxidation resistance and, simultaneously, suppression of σ-phase. It is intended to achieve this goal by a partial replacement of Cr by Ni atoms.
In-situ neutron diffraction measurements were performed during heating to high-temperatures (up to 1500°C) and cooling for a various Ni (8, 15 and 25 at. %) and Cr (18 and 23 at.%) content alloys. The allotropic transformation of the Co-matrix and the evolution of the low-temperature hexagonal and high-temperature cubic Co phases were studied. A surprising observation was the splitting of the fcc Co phase peaks at high temperature during heating as well as cooling. The phase evolution was monitored, and an appearance of the secondary fcc phase could be linked to the formation of σ phase associated with a compositional change in the matrix due to diffusion processes at high temperatures. At a lower content of Ni (8 and 15 at.%) the secondary fcc phase transforms to secondary low-temperature hcp phase with the different chemical composition compared to the primary one. The σ-phase formation and its influence on the matrix phase separation – two fcc/hcp phases – in Co-Re-Cr-Ni alloys are an important discovery for the Co-Re alloy development and deserve further investigation.

[1] D. Mukherji, J. Rösler, J. Wehrs, P. Strunz, P. Beran, R. Gilles, M. Hofmann, M. Hoelzel, H. Eckerlebe, L. Szentmiklósi and Z. Mácsik, *Metall. Mater. Trans. A.*, 2013, 44, 22-30.

[2] R. Gilles, D. Mukherji, L. Karge, P. Strunz, P. Beran, B. Barbier, A. Kriele, M. Hofmann, H. Eckerlebe and J.Roesler, *J. Appl. Cryst.*, 2016, 49, 1253-1265.

[3] P. Beran, D. Mukherji, P. Strunz, R. Gilles, M. Hofmann, L. Karge, O. Dolotko, J. Rösler, *Metals and Materials International*, 2016, 22(4), 562-571.

[4] L. Karge, R. Gilles, D. Mukherji, P. Strunz, P. Beran, M. Hofmann, J. Gavilano, U. Keiderling, O. Dolotko, A. Kriele, A. Neubert, J. Roesler, W. Petry, *Acta Materialia*, 2017, 132, 354-366.

[5] D. Mukherji, P. Strunz, R. Gilles, M. Hofmann, F. Schmitz, J. Rösler, *Mat. Lett.*, 2010, 64, 2608-2611.

[6] D. Mukherji, P. Strunz, S. Piegert, R. Gilles, M. Hofmann, M. Hoelzel and J. Rösler, *Metallurgical and Materials Transactions A*, 2012, 43A, 1834-1844.

[7] T. Depka, *PhD thesis*, Ruhr Universität Bochum, Germany, 2012.

Keywords: phase transformation, high-temperature alloys, neutron diffraction

In-situ carbonation of SrO and $Sr(OH)_2 \cdot xH_2O$ at 298 K and controlled humidity

G. Gravogl[a,b*], C. L. Lengauer[a], D. Müller[b], C. Knoll[b], P. Weinberger[b], R. Miletich[a]
[a] *Institut für Mineralogie und Kristallographie, University of Vienna, AUT*
[b] *Institute of Applied Synthetic Chemistry, TU Wien, AUT*
* *georg.gravogl@univie.ac.at*

In this work the carbonation behavior of SrO and $Sr(OH)_2 \cdot xH_2O$ under humid conditions was studied through *in-situ* pXRD measurements at room temperature conditions (298K) with respect to investigate the potential for thermochemical energy storage (TCES). Carbonates represent a very promising class of TCES materials due to their high energy density, in particular for high temperature storage systems like concentrated solar power plants [1,2].

The experiments were performed on a PANalytical X'Pert Pro diffractometer in Bragg-Brentano geometry using Cu$K\alpha_{1,2}$ radiation and a X'Celerator linear detector with Ni-filter. An Anton Paar XRK 900 reaction chamber was used monitoring *in-situ* the reaction. The pressure within the reaction chamber was adjusted to 8 bar and maintaining a constant CO_2 flow at 0.4 l min^{-1}. In order to investigate the carbonation in the presence of H_2O saturated conditions the CO_2 was previously passed through an external moisturizer.

The study reveals a remarkable carbonation behavior of SrO (see figure, where each curve represents a time period of 48 min). As SrO is very hygroscopic it transforms almost immediately to $Sr(OH)_2$ when getting into contact with the moistened CO_2. It consecutively hydrates yielding $Sr(OH)_2 \cdot H_2O$. This hydration process occurs continuously, and after approximately 500 minutes of reaction time the intermediate $Sr(OH)_2$ is completely converted to $Sr(OH)_2 \cdot H_2O$. Parallel to this hydration the carbonation starts after approximately 180 minutes on achieving a ratio of $Sr(OH)_2$ to $Sr(OH)_2 \cdot H_2O$ = 1:1. Within the next 400 minutes the $SrCO_3$ phase increases up to about 10 wt% of conversion, followed by a significantly accelerated carbonation, which completes the conversion within a short time interval of approximately 15 min (highlighted area of figure).

We conclude, that the reaction starts at the surface of the particles thus forming a carbonate layer, which retards the CO_2 diffusion into the core of the particles. This is the presumable reason for the slow reaction kinetics at the beginning of the carbonation process. At a certain point the comparatively fast transformation of $Sr(OH)_2 \cdot H_2O$ into $SrCO_3$ starts, which can be explained by the formation of micro-cracks and microstructural changes including fragmentation of the particles, volume changes and strain occurring at the interface between the monohydrate and the carbonate.

The experiments were repeated under the same conditions with a mixture of $Sr(OH)_2 \cdot H_2O$ (50 wt%) and $Sr(OH)_2 \cdot 8H_2O$ (50 wt%) as starting material. As a result, the complete amount of $Sr(OH)_2 \cdot 8H_2O$ and 82 % of the $Sr(OH)_2 \cdot H_2O$ phase were converted into $SrCO_3$ within the first 6 min of reaction time. The residual 12 % $Sr(OH)_2 \cdot H_2O$ was found inert towards further carbonation within the next 120 minutes.

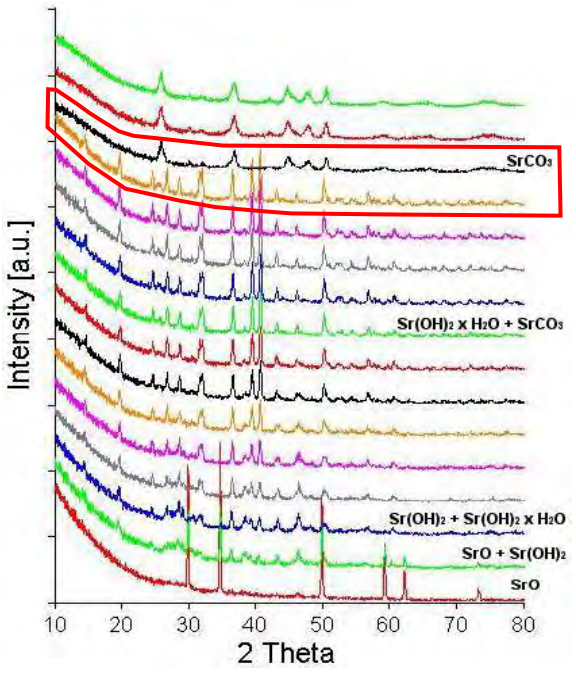

[1] André, L., Abanades, S., *Journal of Energy Storage*, 2017, 13, 193-205.

[2] Cot-Gores, J., Castell, A., & Cabeza, L. F., *Renewable and Sustainable Energy Reviews*, 2012, 16, 5307-5224

Keywords: *in-situ* pXRD, carbonation experiments, thermochemical energy storage

Laboratory 2D X-ray diffraction setup for *in situ* studies on Li-ion battery materials

H. Geßwein [a,c*], A. Stoll [a,c], L. de Biasi [b,a], J. R. Binder [a]
[a] *Institute for Applied Materials, Karlsruhe Institute of Technology (KIT), Germany*
[b] *Battery and Electrochemistry Laboratory, Institute of Nanotechnology, Karlsruhe Institute of Technology (KIT), Germany*
[c] *Helmholtz Institute Ulm for Electrochemical Energy Storage, Germany*
** holger.gesswein@kit.edu*

A laboratory *in situ* X-ray diffraction setup for the structural characterization of electrode materials for Li-ion batteries is described. By means of a high flux X-ray beam arising from a molybdenum-microfocus rotating anode, a collimating 2D multilayer optic as well as a hybrid photon counting, two-dimensional Pilatus 300K-W detector, *in situ* X-ray diffraction studies of battery materials with good time resolution are feasible. The influence of different experimental conditions like the sample or X-ray beam size and sample to detector distance on the instrumental resolution have been evaluated on a standard sample. Two types of cathode materials cycled with different electrochemical *in situ* cells have been used to test the diffractometer performance: a high voltage Ru-Ti codoped $LiNi_{0.5}Mn_{1.5}O_4$ (LNMO) spinel [1] and a layered $LiNi_xCo_yMn_zO_2$ (NCM) cathode material [2]. Rietveld analysis of the integrated diffraction images enables to extract detailed structural information of the changes and processes inside the active materials. The obtained data can be directly related to the simultaneously performed galvanostatic measurements.

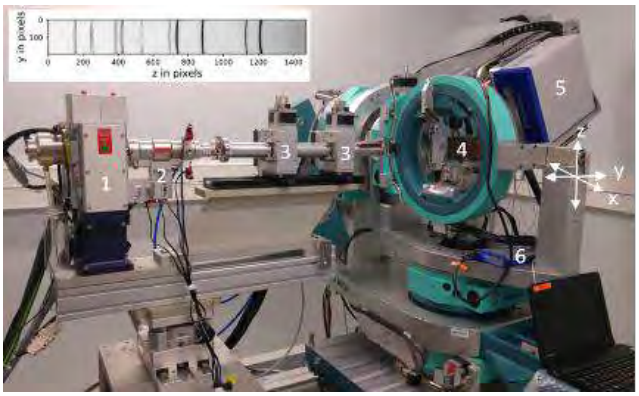

[1] Höweling A., Stoll A., Schmidt D., Geßwein H., Simon U., Binder J. R., , Journal of The Electrochemical Society (2017), 164 (1) A6349-A6358.

[2] de Biasi L., Kondrakov A. O., Geßwein H., Brezesinski T., Hartmann P., Janek J., Journal of Physical Chemistry C (2017), 121(47), 26163-26171

Keywords: Li-ion, cathode materials, in situ powder diffraction

In situ study on the reduction of γ-iron oxides

P.Garbus[a,b*], J.V.Ahlburg[a], H.L.Andersen[a], C. Granados-Miralles[a,c], L.Keller[b], M.Christensen[a]
[a] *iNANO & Department of Chemistry, Aarhus University, DK*
[b] *Laboratory for Neutron Scattering and Imaging, Paul Scherrer Institut, CH*
[c] *Instituto de Cerámica y Vidrio, CSIC, Madrid, ES*
** garbus@inano.au.dk*

Magnetic materials are a hot topic among energy-materials and they find applications in nearly all everyday consumer electronics. Advances in magnetic performance have in particular been made for thin film and nanosized particles in terms of archieving single magnetic domains of typically 10 – 100 nm to increase coercivity [1] and utilizing the exchange spring coupling effect for higher energy product [2]. Therefore, the magnetic properties are strongly related to the size. Iron oxide is cheap and an unreactive precursors for the production of nanosized iron particles. Bulk iron is relatively unreactive, but then nanosized iron particles are highly reactive as a result of the large surface area resulting in a high oxidation potential. This makes nanosized metallic iron ideal for as a starting point to obtain iron nitrides, a group of magnetic materials that do not yet seem to have had a commercial breakthrough [3] despite great potential [4].

In this study, flow synthesized iron oxide (γ-Fe_2O_3) particles (size 8-20 nm) were heated to 400-500°C under a flow of 5% H_2 / Ar, while the process was followed *in situ* using synchrotron X-ray (P02.1, Petra III) or neutron (DMC, SINQ, PSI) powder diffraction. It was found that it is possible to limit the final iron crystallite size by 1) lowering reduction temperature, 2) lowering the initial size of iron oxides and 3) increasing the availability of reducing molecular hydrogen.

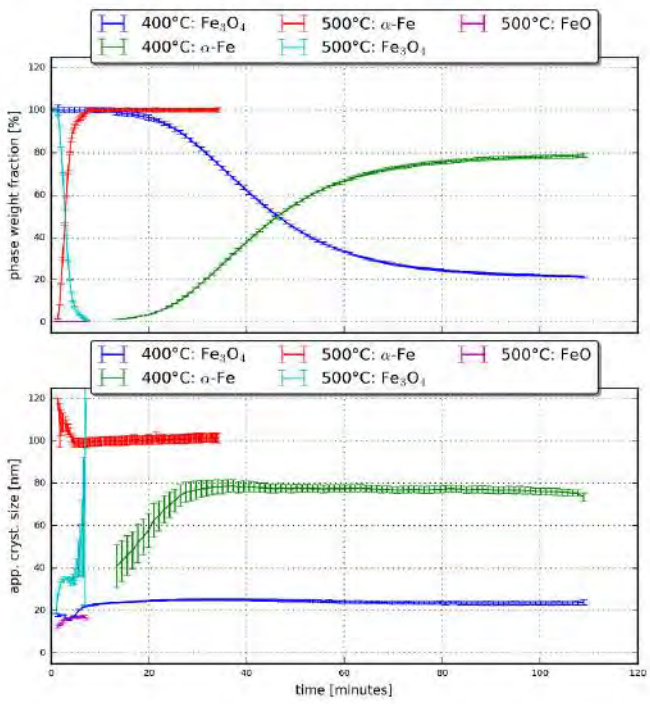

Figure 1: In situ study on the reduction of γ-iron oxide in a reducing flow at elevated temperature, diffraction data collected at the hard X-ray beamline P02.1 at Petra III. Top graph shows phase weight fractions and bottom graph displayes the refined apparent crystalline sizes, both obtained from Rietveld refinement.

[1] Kodama, R. H. “Magnetic nanoparticles.” J. of magnetism and magnetic materials 200.1-3 (1999): 359-372.
[2] Fullerton, Eric E., et al. “Hard/soft magnetic heterostructures: model exchange-spring magnets.” Journal of Magnetism and Magnetic Materials 200.1-3 (1999): 392-404.
[4] Shokrollahi, H. and K. Janghorban, “Soft magnetic composite materials”. Journal of Materials Processing Technology, 2007. 189(1): p. 1-12.
[3] Bhattacharyya, S., “Iron nitride family at reduced dimensions: A review of their synthesis protocols and structural and magnetic properties”. The Journal of Physical Chemistry C, 2015. 119(4): p. 1601-1622

Keywords: Reduction, iron oxides, metallic iron

Operand XRD study of $LiMn_{1.5}Ni_{0.5}O_4$ high-voltage cathode under high-rate charge/discharge reaction

T. Konya[a,b*], Y. Shiramata[a], T. Nakamura[b]
[a] *Rigaku Corporation, Japan*
[b] *University of Hyogo, Dep. Electrical Eng., Japan*
** konya@rigaku.co.jp*

X-ray diffractometer with a 2D detector is one of the most powerful tools for obtaining information of battery materials during charge/discharge process as operand XRD measurement. Lithium ion battery is one of the candidate to meet the demand of power sources with high energy density and high out-put density. The utilization of high-working potential cathode, one of which is $LiMn_{1.5}Ni_{0.5}O_4$ spinel compound, is effective to attain the battery performance.[1, 2] In this presentation, the structural evolution of the spinel compound during the electrochemical Li+ extraction/insertion reaction was discussed, based on the operand X-ray diffraction using the battery cell having specifically designed X-ray window. From the experimental-obtained results, it was found that the electrochemical reactions were composed of two consecutive two-phase reaction, where there are three cubic spinel phases, the lattice parameters of which were 0.8165, 0.8087 and 0.8000 nm. The Li^+ extraction/insertion reaction reversibly progressed in the low current operation. Also, the functionality of new SmartLab StudioII software enabled us to obtain the valuable presentation.

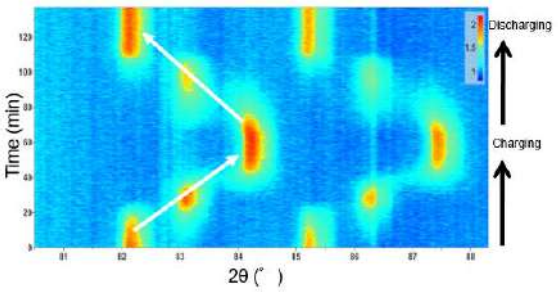

[1] T. Nakamura, M. Tabuchi and Y. Yamada, *J. Appl. Phys.*, Vol. 98 (2005), 093905.

[2] R. Hanafusa, K. Kotani, K. Ishidzu, Y. Oka and T. Nakamura, *Solid State Ionics*, Vol. 288 (2016), 180-183.

Keywords: 2D detector, operand XRD, lithium ion battery

Nanostructured kesterite (Cu_2ZnSnS_4) for applications in thermoelectric devices

E. Isotta[a,b*], N. Pugno[a,b,c,d], P. Scardi[a]
[a] *Department of Civil, Environmental & Mechanical Engineering, University of Trento, Italy*
[b] *Laboratory of Bio-Inspired and Graphene Nanomechanics, Department of Civil, Environmental & Mechanical Engineering, University of Trento, Italy*
[c] *Ket-Lab, Edoardo Amaldi Foundation, Italian Space Agency, Italy*
[d] *School of Engineering and Materials Science, Queen Mary University of London, UK*
** eleonora.isotta@unitn.it*

Thermoelectric generators (TEG) have been known for many years to convert heat, often waste, into electrical energy through the Seeback effect. In recent years material nanostructuring has been proved to enhance the thermoelectric figure-of-merit $zT = (S^2\sigma)/k\ T$ (S is the Seebeck coefficient, k the thermal conductivity, σ the electrical conductivity), by lowering k without penalizing σ.
Most existing materials for efficient TEGs are unfortunately rare, expensive and often toxic. In the quest for viable solutions, kesterite (or CZTS, reference formula Cu_2ZnSnS_4) has been recently proposed for thermoelectric applications for the abundance and low cost of the raw materials, low toxicity and low bulk thermal conductivity. In this work we investigate a relatively simple route to produce bulk nanocrystalline components based on CZTS. Nanocrystalline CZTS powders have been made by reactive ball milling, starting from a mixture of sulfur and elementary metals in the required proportions, eventually pressed into a tablet and thermally treated. First results of the realization process and characterization by XRD and SEM are presented: phase composition and microstructure are the main features of interest.

Keywords: thermoelectric materials, nanocrystalline kesterite, ball milling

Structure Property correlation in SOFC & SOEC electrolyte materials.

D.G. Billing[a*]
[a] *School of Chemistry, University of Witwatersrand, USA*
[b] *Department of Physics, University of xxx, UK*
** dave.billing@wits.ac.za*

Solid Oxide Fuel Cells (SOFCs) and Solid Oxide electrolyser cells (SOECs) are exciting electrochemical devices that could provide unique and revolutionary solutions to some of the renewable energy challenges facing society. The architype materials used as solid electrolyte in most SOFCs include YSZ (Yttrium stabilised Zirconia) and CaSZ (Calcium stabilised Zirconia) with the Y or Ca dopants present at around 8 to 10% level. As the performance characteristics of these materials are not completely satisfactory, there is a definite need for improved alternatives. It is worth noting that although it is well established that these materials are cubic with average structure features consistent with the Flourite structure, there have been no reports of studies into the nano-structure of these materials, as would be revealed by for example PDF studies[1].
Within this context our research has focused on gaining a fundamental understanding of the mechanisms governing the transport properties of these and closely related materials such as δ-Bi_2O_3 as well as doped variants.

Typically the cubic forms of these materials exhibit higher due to the presence of vacant anionic sites. Our research has included the development of suitable synthesis, preparation and processing methodologies, particularly for the more novel materials, followed by structural, crystallographic, electrochemical and spectroscopic characterization.
I will present a selection of our results to date. Analysis of the data for (for example) the $Y_2Zr_2O_7$ as prepared via sol-gel methods case, clearly shows structural differences when comparing the structure as perceived on the nano-scale with the bulk average structure. The implications of this for the transport properties of all energy materials is profound, and will be described.

[1] S. J. L. Billinge, “Nanostructure studied using the atomic pair distribution function”, Z. Kristallogr. Suppl. 26 (2007) 17-26.

Keywords: SOFC, PXRD, electrolyte, PDF analysis

Impact of Nb vacancies and p-type doping of the NbCoSn-NbCoSb half-Heusler thermoelectrics

D. A. Ferluccio[a*], R. I. Smith[b], J. Buckman[c] and J.W.G. Bos[a]
[a] *Institute of Chemical Sciences and Centre for Advanced Energy Storage and Recovery, School of Engineering and Physical Sciences, Heriot-Watt University, Edinburgh, EH14 4AS, UK.*
[b] *ISIS Facility, Rutherford Appleton Laboratory, Harwell Oxford, Didcot, OX11 0QX, UK.*
[c] *Institute of Petroleum Engineering, Heriot-Watt University, Edinburgh, EH14 4AS, UK.*
** daf4@hw.ac.uk*

Thermoelectric generators use semiconductors to convert heat into electricity but are limited to niche applications due to high materials and device costs. The thermoelectric efficiency of a material is determined by a figure of merit, $ZT = S^2\sigma T/\kappa$, where S is the Seebeck coefficient, σ is the electrical conductivity, κ is thermal conductivity and T is the absolute temperature. Thermal stability, low toxicity and the broad scope to optimize the properties through structural modification have driven half-Heusler compounds into the running as potential candidates for device construction, with ZT ~ 1.0 [1].

Good thermoelectric performance has recently been identified, in the understudied NbCoSn and NbCoSb half-Heuslers [2-4]. The discovery of Nb vacancies in NbCoSb is the first of it's kind in this class of compounds, which makes this an interesting prototype material to determine the impact of the vacancies and the potential to exploit them for improved efficiency. Here, we report on the NbCoSn-NbCoSb solid solution [5]. Structural examination using neutron powder diffraction exposes a gradual formation of Nb vacancies to maintain a valence electron count near 18.2.

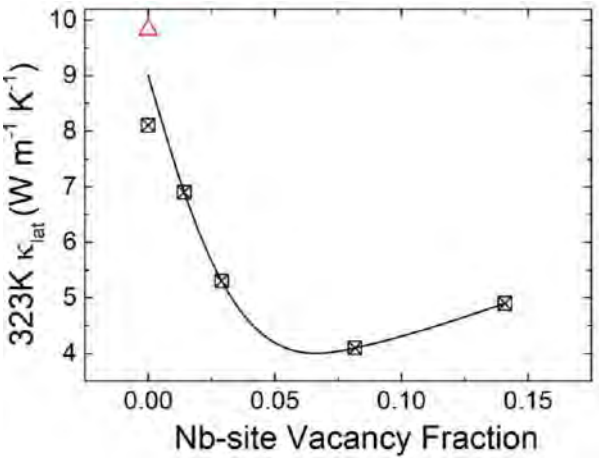

The vacancies cause larger mass disorder on the Nb site which reduces the thermal conductivity from around 10 W m^{-1} K^{-1} (z = 0) to 4.5 W m-1 K-1 (z = 0.5, 1). All samples are degenerate n-type doped, leading to power factor values S^2/ρ = 2.5-3 mW m^{-1} K^{-2} and efficiencies ZT = 0.25-0.33. Attempts at p-type doping using Ti and Zr substitution in $Nb_{0.8}A_{0.2}CoSn$ leads to a low power factors (S^2/ρ = < 0.1 mW m^{-1} K^{-2}) due to a large electrical resistivity, ρ_{323K} = 27-35 mΩ cm. Demonstrating, that effective p-type doping in NbCoSn is hard to achieve.

[1] Bos J.W.G. and Downie R. A. *Journal of Physics-Condensed Matter,* 2014, 26, 433201.

[2] He R., Huang L. H., Wang Y.M., Samsonidze G., Kozinsky B., Zhang Q. Y. and Ren Z. F. *Apl Materials.,* 2016, 4, 104804.

[3] Zeier W. G., Anand S., Huang L. H., Zhang H., Ren Z. F., Wolverton C. and Snyder G. J. *Chemistry of Materials*, 2017, 29, 1210-1217.

[4] Huang L., Zhang Q., Wang Y., He R., Shuai J., Zhang J., Wang C. and Ren Z. F. *Physical Chemistry Chemical Physics,* 2017, 19, 25683-25690.

[5] Ferluccio D. A., Smith R., Buckman J. and Bos J.W.G. *Physical Chemistry Chemical Physics,* 2018, 20, 3979-3987.

Keywords: thermoelectric, half-Heusler, neutron powder diffraction

Hydrogen induced phase transformations in selected High Entropy Alloys

G. Ek[a]*, D. Karlsson[a], C. Zlotea[b], M. Sahlberg[a]
[a] *Department of chemistry – Ångström laboratory, Uppsala University, Sweden*
[b] *Institut de Chimie et des Matériaux Paris-Est, Université Paris Est, France*
* *Gustav.ek@kemi.uu.se*

Hydrogen is now considered one of the most promising solutions as an energy carrier when reducing worldwide fossil fuel consumption to renewable solutions. However, the main setback for hydrogen energy is safety and compact efficiency during storage. Metal hydrides are interesting materials for this application, where they show promise in fields such as anode materials for rechargeable batteries [1], solid hydrogen fuel storage [2] and thermal heat storage [3]. In order to develop functional materials for these applications, the kinetics and phase transformations during hydrogen absorption/desorption are important parameters to understand. In this work, solid-gas reactions have been studied using in-situ X-Ray/neutron diffraction in High Entropy Alloys (HEA). High Entropy Alloys, where five or more elements are mixed in near equimolar concentrations offer good properties for hydrogen storage due to their ability to crystallize in simple cubic structures in the presence of lattice strain originating from the size difference of the elements, both which can help with hydride formation [4], [5]. Hydrides of HEA with composition TiNbZrHfX (X=V, Ta), are here presented to show stable hydrogen cycling (figure 1) and reaching H/M ratios of up to 2.5 (X=V) by tetragonal distortion of the cubic lattice [6], [7]. In addition, when X=Ta, the alloy seem to behave almost identical to the V-H system, with a tetragonal mono-hydride phase although the alloy contains no V.

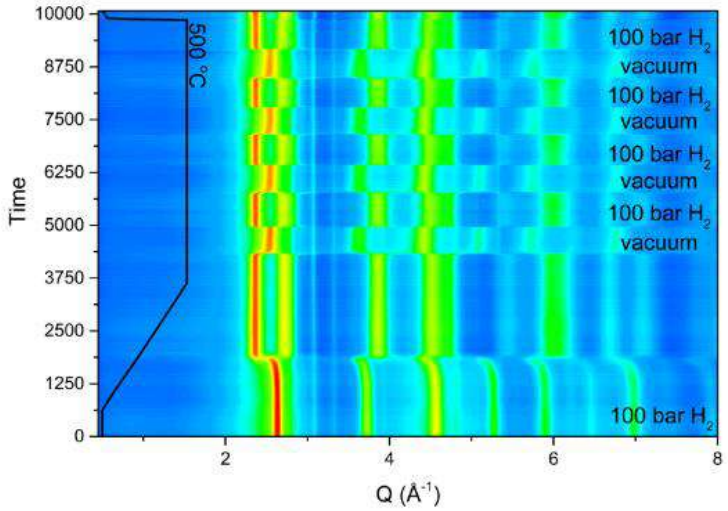

Figure 1: In-situ X-Ray diffraction during hydrogen cycling of TiNbZrHfV

[1] Y. Liu, Y. Cao, L. Huang, M. Gao, and H. Pan, *J. Alloys Compd,* 2011, 509, 3,
[2] L. Schlapbach and A. Züttel, *Nature*, 2001, 414, 6861
[3] D. N. Harries, M. Paskevicius, D. a. Sheppard, T. E. C. Price, and C. E. Buckley, *Proc. IEEE*, 2012, 100, 2
[4] B. Sakintuna, F. Lamari-Darkrim, and M. Hirscher, *Int. J. Hydrogen Energy*, 2007, 9,
[5] X. Xin, R. Johansson, M. Wolff, and B. Hjörvarsson, *Phys. Rev. B*, 2016, 93, 13
[6] M. Sahlberg, D. Karlsson, C. Zlotea, and U. Jansson, *Sci. Rep., 2016,* 6
[7] D. Karlsson *et al.*, *Inorg. Chem.*, 2018, 57, 4

Keywords: Metal-hydride, Energy materials, High Entropy Alloy

In Operando Characterization of Lithium Batteries using XRD

G. Vanhoyland[a*], S. Haaga[a], N. Yang[b]
[a] *Bruker AXS, Karlsruhe, Germany*
[b] *Bruker AXS, Beijing, China*
* *geert.vanhoyland@bruker.com*

Since their commercial introduction beginning of the '90ties, small-size lithium batteries have found wide-spread use in consumer electronics due to their high specific energy and energy density. Recently lithium-ion batteries have also started replacing nickel-metal hydride batteries in hybrid and electric cars. These automotive applications require large-size batteries with high energy density and superb cycle life time. To ensure safe, long-term operation it is important to understand the physical and chemical changes that happen during cycling. In operando X-ray diffraction is an efficient method to probe phase transitions and crystal structure changes that occur in the anode and cathode materials during cycling. This will be demonstrated for a variety of sample systems with different battery cell designs, all measured in operando on a laboratory X-ray diffraction instrument.

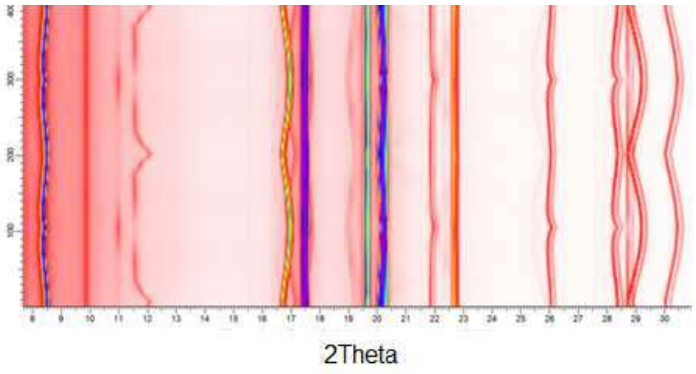

Keywords: Li-ion battery, in operando characterization

X-Ray powder diffraction full profile analysis of thin film absorbers in solar cells

X. Alcobé[a*], T. Jawhari[a], L. Calvo-Barrio[a,b], M. Placidi[c], V. Izquierdo-Roca[c], E. Saucedo[c], A. Perez-Rodríguez[b,c]

[a] *Scientific and Technological Centers (CCiT-UB), Universitat de Barcelona, Spain*
[b] *Departament d'Engenyeria Electrònica i Biomèdica,IN2UB, Universitat de Barcelona, Spain*
[c] *Catalonia Institute for Energy Research (IREC), Spain*
** alcobe@ccit.ub.edu*

Full profile analysis of powder diffraction data [1], [2] enables to check and identify complex mixture of crystalline phases. Moreover, eventually these crystalline phases can be (semi-)quantified [3]. Additionally, structural and microstructural information of the main crystalline phases can be obtained.
The thin film layer of some absorber materials in a solar cell device can be treated as a polycrystalline powder sample and so full profile methodologies can be applied for its fully phase analysis characterization (identification, quantification and structural and microstructural characterization).
Good statistics high resolution, Cu $K\alpha_1$, x-ray diffraction data have been collected on samples of (proto) solar cell devices with absorber polycrystalline material layers of around 1.5 microns of thickness of the systems Cu(In,Ga)Se_2 (CIGS) [4] and $Cu_2ZnSn(S,Se)_4$ ($CZTS_xSe_{1-x}$) [5]. In the former, in chalcopyrite based solar cells, absorbers from Cu-rich to Cu-poor $CuInSe_2$ (CIS) Cu/In=1.4-0.4 have been characterized with the aim to assert and further study the presence of a gradual transition between the stoichiometric CIS, the defective CIS and the formation of OVC (Ordered Vacancies Compounds) phases, also postulated by Raman spectroscopy studies. In the latter system, in kesterite based solar cells, full profile analysis on samples of ion implanted $Cu_2ZnSnSe_4$ (CZTSe) absorbers, with different ions and implantation doses strategies, should help to understand the effect of these implantation technologies applied to find solutions for relevant technological problems, among them the optimization of the buffer/absorber interface.
All the described characterized absorbent layers were grown over Mo back contact layers (around 0.8 microns) onto soda-lime glass substrates. Full profile analysis includes Mo, usually textured and strained, and $MoSe_2$ highly oriented layers (around 0.2 microns), between Mo and the absorbent layers. Eventually in some cases the samples contain the thin buffer and window top layers which phases have also been included in the full profile analysis.

[1] Rietveld, H.M. *J. Appl. Cryst.,* 1969, 2, 65-71

[2] Le Bail, A., Duroy, H., Fourquet, J.L. *Mat. Res. Bull.,* 1988, 23, 447-452

[3] Bisch, D.L., Howard, S.A., *J. Appl. Cryst.,* 1988, 21, 86-91

[4] Jackson, P., Hariskos, D., Wuerz, R., Kiowski, O., Bauer, A., Friedlmeier, T.M., Powalla, M. *Phys. status solidi -Rapid Res. Lett.,* 2015, 9, (1), 28–31

[5] Giraldo, S., Saucedo, E., Neuschitzer, M., Oliva, F., Placidi, M., Alcobé, X., Izquierdo-Roca, V., Kim, S., Tampo, H., Shibata, H., Perez-Rodriguez, A. Pistor, P., *Energy Environ. Sci.,* 2017, DOI:10.1039/C7EE02318A

Keywords: full profile analysis, thin film absorbers, solar cells, chalcopyrite, kesterite

Dimensional crossover of correlated anion disorder in oxynitride perovskites

Paula Kayser,[a] Hannah Johnston,[a] Ashley P. Black, Judith Oró-Solé, [b] David A. Keen, [c] Amparo Fuertes,[*b] and J. Paul Attfield [*a]
[a]*CSEC and School of Chemistry, University of Edinburgh, King's Buildings, Mayfield Road, Edinburgh, EH9 3JZ, U.K.*
[b]*Institut de Ciència de Materials de Barcelona (ICMAB-CSIC), Campus UAB, 08193 Bellaterra, Spain.*
[c]*ISIS Facility, Rutherford Appleton Laboratory, Didcot, OX11 0QX, U.K. School of*
** j.p.attfield@ed.ac.uk *amparo.fuertes@icmab.es*

The combination of the properties of oxides and nitrides makes oxynitrides an important group of materials with great interest. Many of these compounds have shown outstanding electronic, optic and magnetic properties and they have become influential candidates to develop new materials such as photocatalysts, pigments, phosphors, dielectrics and magnetic materials. In particular, oxynitrides with perovskite-like structure have attracted immense attention due to their useful properties as energy materials and intensive research has been made in specific fields such as photocatalysis in water splitting.

The anionic order or disorder play an important role in this family of compounds and a good understanding of the local order is essential to unveil the correlation between the structure and properties and therefore the subsequent study of their applications.

Correlated disorders of atoms or magnetic moments, distributed in two-dimensions (2D) and three-dimensions (3D), have been identified in many crystalline materials, but dimensional crossovers which are associated with changes of chemical or physical properties, as new degrees of freedom become available, are rare for correlated disorder. Here, for the first time, we report an atomic dimensional crossover: a simple strain-driven 2D to 3D crossover on a cubic lattice of correlated disorder of O and N atoms within the $Ba_{1-x}Sr_xTaO_2N$ perovskite series.

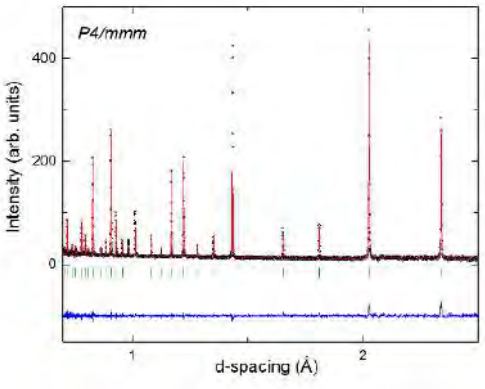

A combination of high resolution x-ray data, collected at the MSPD beamline of the ALBA Synchrotron (Cerdanyola del Vallès, Spain), and neutron diffraction data (see Figure), measured on the High Resolution Powder Diffractometer (HRPD) at the ISIS spallation neutron source, Rutherford Appleton Laboratory (UK), have been used to determine the degree of anionic order of all the samples. The high contrast between the neutron scattering lengths of oxygen (5.83 fm) and nitrogen (9.36 fm) allows us to accurately refine the O/N occupancy over the anionic positions, while the narrower peak width in x-ray data enable to determine any lattice distortion. The Rietveld refinement, done by using FullProf suite software, shows the existence of two polymorphs. The samples with x=0 and 0.2 crystallizes in the cubic $Pm\bar{3}m$ and the other members of the solid solution, with x=0.4-1, adopt tetragonal symmetry (space group $P4/mmm$), which allows for N/O to order over the 1b and 2f Wyckoff positions. Such an anion distribution shows that 2D anion chain layers are present across the tetragonal x = 0.4 – 1 samples while the cubic structure at x = 0 – 0.2 is consistent with a 3D distribution of disordered cis-chains. The absence of an intermediate $P4/mmm$ structure with O/N occupancies between the 2D and 3D distributions indicates that the crossover is relatively sharp with different thermodynamic factors favouring 2D or 3D correlations.

[1] L. Clark, J. Oró-Solé, K. S. Knight, A. Fuertes, and J. P. Attfield, *Chem. Mater*. 2013, 25, 5004.

[2] M. Yang, J. Oró-Solé, J.A. Rodgers, A.B. Jorge, A. Fuertes and J.P. Attfield, *Nat. Chem*, 2011, 3, 47

Keywords: oxynitrides, anion order, powder diffraction

Structural, microstructural and magnetic evolution in cryo milled carbon doped MnAl

Hailiang Fang[a] *, Johan Cedervall[a], Daniel Hedlund[b], Samrand Shafeie[a], Linus von Fieandt[a], Peter Svedlindh[b], Klas Gunnarsson[b] and Martin Sahlberg[a] *
[a].*Department of Chemistry – Ångström Laboratory, Uppsala University, Box 538, 75121 UPPSALA, Sweden*
[b].*Department of Engineering Sciences, Uppsala University, Box 534, 75121 Uppsala, Sweden*
**hailiang.fang@kemi.uu.se*
**martin.sahlberg@kemi.uu.se*

The low cost, rare earth free τ-phase of MnAl has high potential to partially replace bonded $Nd_2Fe_{14}B$ rare earth permanent magnets. However, the τ-phase is metastable and it is experimentally difficult to obtain powders suitable for the permanent magnet alignment process, which requires the fine powders to have a regular round shape and high τ-phase purity. In this work, a high purity τ-phase $Mn_{0.55}Al_{0.45}C_{0.02}$ alloy was synthesized by the drop synthesis method[1, 2]. The drop synthesized material was subjected to cryo milling then followed by a flash heating process[3]. The crystal structure and microstructure of the drop synthesized, cryo milled and flash heated samples were studied by X-ray in situ powder diffraction, scanning electron microscopy, X-ray energy dispersive spectroscopy and electron backscatter diffraction. Magnetic properties and magnetic structure of the drop synthesized, cryo milled, flash heated sample were characterized by magnetometry and neutron powder diffraction, respectively. The results reveal that the 2 and 4 hours cryo milled and flash heated samples both exhibit high τ-phase purity and micron-sized round particle shapes. All the main peaks in the NPD pattern after 4 hours of cryo milling disappear into the background, while the same peaks are broadened in the XRPD data. Moreover, the XRPD data clearly indicates the recrystallization of the τ-phase inside the particles after the flash heating (as evidenced by strong sharp peaks), indicating that the ordering between Mn and Al has been restored,the flash heated samples display high saturation magnetization as well as increased coercivity.

Keywords: permanent magnetic material, metastable, structural change

[1] H. Fang, S. Kontos, J. Ångström, J. Cedervall, P. Svedlindh, K. Gunnarsson, M. Sahlberg, Directly obtained τ-phase MnAl, a high performance magnetic material for permanent magnets, Journal of Solid State Chemistry 237 (2016) 300-306.

[2] H. Fang, J. Cedervall, F.J.M. Casado, Z. Matej, J. Bednarcik, J. Ångström, P. Berastegui, M. Sahlberg, Insights into formation and stability of τ-MnAlZx (Z = C and B), Journal of Alloys and Compounds 692 (2017) 198-203.

[3] H. Fang, J. Cedervall, D. Hedlund, S. Shafeie, S. Deledda, F. Olsson, L. von Fieandt, J. Bednarcik, P. Svedlindh, K. Gunnarsson, Structural, microstructural and magnetic evolution in cryo milled carbon doped MnAl, Scientific reports 8(1) (2018) 2525.

High angular resolution and time-resolved Synchrotron Powder Diffraction experiments revealing inhomogeneous lithiation/delithiation into/from cathode materials during cycling

M. S. D. Darma[a,b*], M. Lang[b], L. Mereacre[b], V. Liebau[c], F. Fauth[d], H. Ehrenberg[b]
[a] Helmholtz Institute Ulm (HIU), Ulm, Germany (current)
[b] *Karlsruhe Institute of Technology, Institute for Applied Materials-Energy Storage System,, Karlsruhe, Germany*
[c] *Bayerische Motoren Werke G, Petuelring 130, 80788, München, Germany (former)*
[d] *CELLS-ALBA Synchrotron, E-08290 Cerdanyola del Valles, Barcelona, Spain*
* *mariyam.darma@kit.edu*

In-situ synchrotron powder diffraction measurements have widely been used by the battery communities mostly to investigate the phase transformation and the evolution of unit cell volume during charging/discharging. In addition to this investigation, we will show here another feature of the powder diffraction technique which contributes to the understanding of the kinetics of charging/discharging process but is less explored.

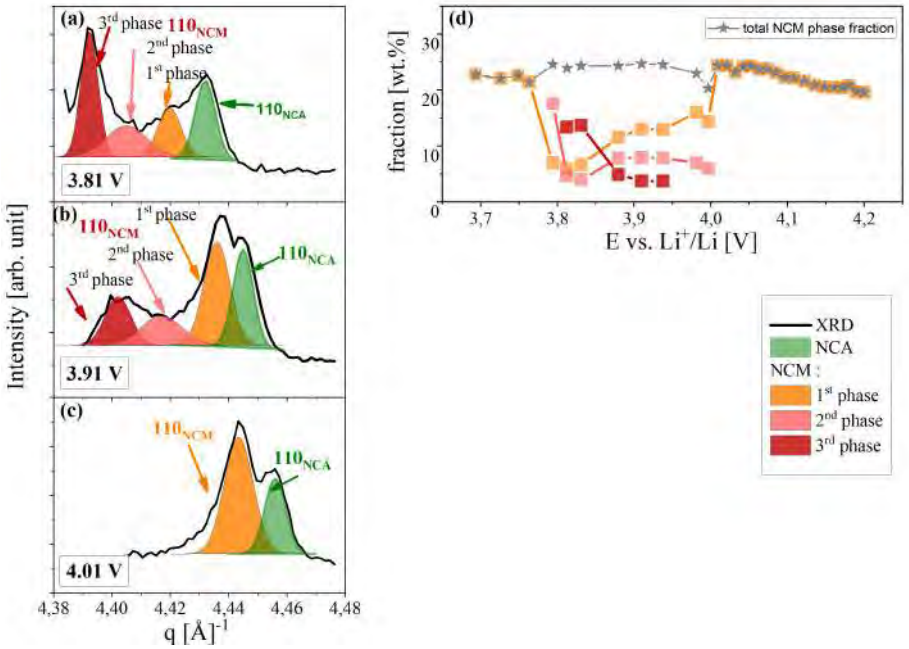

In order to reveal the structural and electrochemical properties of complex samples, i.e. a blended cathode consisting of $LiNi_{0.5}Co_{0.2}Mn_{0.3}O_2$ (NCM), $LiNi_{0.8}Co_{0.15}Al_{0.05}O_2$ (NCA) and $LiMn_2O_4$ (LMO), we performed high resolution, time-resolved X-ray powder diffraction experiments during electrochemical cycling. Some interesting results will be highlighted.

NCM and NCA possess similar crystal structures, unit cell parameters and X-Ray structure factors. Thus, X-Ray Diffraction is not sensitive enough to distinguish both phases. However, complementary analysis of electrochemical and XRD methods enable us to determine reliably phase specific activity of both phases. The inhomogeneous lithiation/delithiation process in the NCM and NCA phases is indicated by analyzing the evolution of peak shape and broadening during cycling. This local variation of state of charge is most likely due to the slow lithium transport inside the cathode materials.

[1] M. S. D. Darma, M. Lang, K. Kleiner, L. Mereacre, V. Liebau, F. Fauth, T. Bergfeldt and H. Ehrenberg, *J. Power Sources* 327 (2016) 1-12.

Keywords: time-resolved synchrotron powder diffraction, inhomogeneous lithiation, blended cathode

The composition-structure-property relationships of $Ni(OH)_2$-based electrochromic materials

K. Lawson[a*], C. A. Kirk[b],
[a] *Department of Chemistry, Loughborough University, UK*
[b] *School of Chemistry, University of Edinburgh, UK*
* *K.Lawson@lboro.ac.uk*

Thin film hydrous NiO ($Ni(OH)_2$) is a commonly used anodically colouring electrochromic material, due to its low cost and excellent electrochromic properties. [1] However, to date, their applicability in devices is poor due to performance issues during cycling and development of more robust films is required. The electrochromic properties have been linked to the hydration state of $Ni(OH)_2$ and we have focused on understanding the structure-composition-property relationships in this system. We have carried out extensive in-house studies into the formation of $Ni(OH)_2$ phases under different conditions. The $Ni(OH)_2$-type phases can be very hydrous, show varying degrees of disorder, resulting in different crystallinities from amorphous in nature to highly crystalline, and display clear peak shape anisotropy. We can now prepare samples to target different degrees of crystallinity/disorder and have found that the samples can be categorised as one of 4 different "types" of nickel hydroxide, labelled α, β, β* and β_{SF}, according to the X ray diffraction patterns (see figure). The high temperature properties of these materials have been characterised using Thermogravimetric Analysis methods and there are clear differences in the dehydration behaviour dependent upon the conditions of synthesis chosen and subsequent $Ni(OH)_2$-type phase formed. Thus, the hydration states and therefore compositions of the 4 "type" samples, are different. Characterisation of the Ni oxyhydroxide phases is difficult due to the high degree of disordered stacking that exists, which results in poorly crystalline/amorphous samples under certain conditions of synthesis. There are reports that the electrochemical activity of the nickel hydroxide samples is linked to their hydration state.[5] It is therefore vital to understand the structures of these phases and investigate how their hydration states vary, to allow enhancement of their properties. We present here X-ray diffraction and X-ray Pair Distribution Function studies on the nickel hydroxide phases.

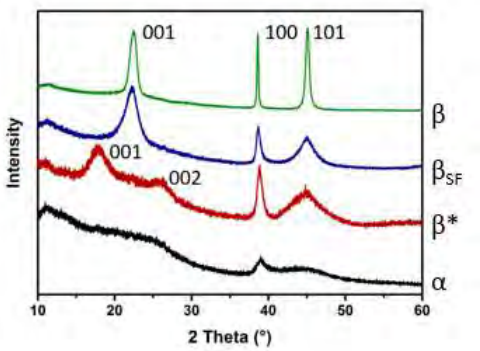

[1] Sialvi, Mortimer, Wilcox, Mat Teridi, Varley, Wijayantha, Kirk, *ACS Appl Mater Interfaces*, 2013 **5**, 5675.

[2] Hall, Lockwood, Bock and MacDougall, *Proceedings of the Royal Society A,* 2015 **A471**, 20140792.

Keywords: X-ray diffraction, X-ray Pair Distribution Function, electrochromic

In-operando powder diffraction – A powerful tool to study capacity losses in Li-ion batteries at multi-length scales

K. Kleiner*, S. J. Day, C. C. Tang

Diamond Light Source
Harwell Science and Innovation Campus, Didcot, Oxfordshire OX11 0DE
E-mail: karin.kleiner@diamond.ac.uk

The degradation issues of Li-ion batteries, tremendously increased by the usage of high energy density materials like Li-rich layered oxides, is studied using *in-operando* synchrotron X-ray powder diffraction (SXPD) at multi-length scales. Atomistic structural changes, electrochemical issues with ion balancing as well as the actual cell design lead to energy density (voltage * capacity) losses which are not yet well understood.[1]

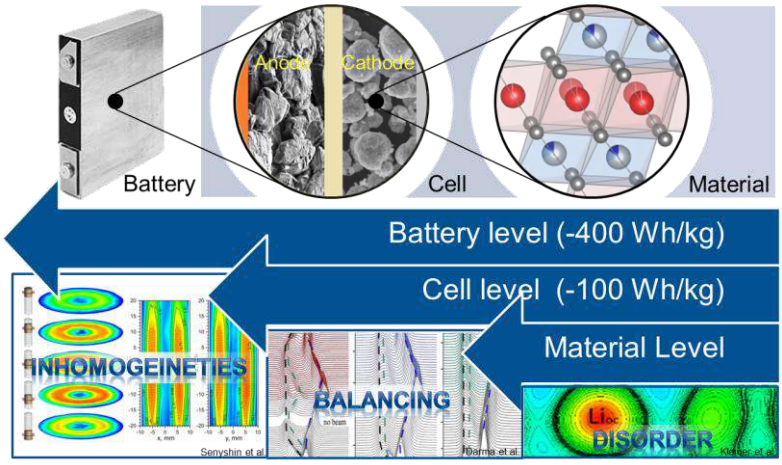

On material level we show that transition metal movements can be analyzed using difference Fourier transform maps and the Rietveld method.[2] Irreversible TM/Li disorder increases continuously upon long term cycling while reversible TM motion stabilizes the materials at high states of charge and therefore ensures higher capacities.

On cell level, all degradation reactions of electrodes lead to a loss of active lithium which shifts or alters the anode and cathode potential curves (changes in ion balancing).[3,4] Therefore, the materials are cycled outside of their stable voltage window and this, in turn, leads to accelerated degradation reactions. By following the state of charge of the electrode materials with SXPD it is possible to deduce the shift/change of the potential curves and thus investigate balancing issues upon operation.[5]

On battery level capacity losses occur due to an inhomogeneous compression and/or inhomogeneities in the current flow (current collector arrangement).[6] Therefore this issue depends on the way the cell components are compressed/stacked and thus on the design of the batteries. Such effects are studied by performing spatial resolved SXPD, which will be briefly outlined

[1] D. Andre, J. Mater. Chem. A 2017, 5, 17174.

[2] K. Kleiner et al, Origin of high capacity and poor cycling stability of HE-NCM - A long-duration in situ synchrotron powder diffraction study, submitted.

[3] Kleiner et al., J. Power Sources 2016, 317, 70.

[4] Kleiner et al., Top. Curr. Chem. (Z) 2017, 375, 54.

[5] Kleiner et al., J. Power Sources 2015, 273, 70.

[6] Senyshin et al., Scientific Reports 2015.

Keywords: Degradation of Li-ion batteries, Li-rich layered oxides, multi-length scales

Structure and magnetic properties of strontium W-type Hexaferrites

M. Mørch[a*], J.V. Ahlburg[a], A. Z. Eikeland[a], M. Christensen[a]
[a]*Department of Chemistry & iNANO, Aarhus University, Denmark*
** mmorch@chem.au.dk*

Permanent magnetic materials are a pillar stone of today's society. Along with the semiconductors, magnets enabled the information age providing logical circuits and data storage, respectively. Additionally permanent magnets can interconvert energy between electricity and motion. By making stronger permanent magnets electronic devices can be downsized and the efficiency improved. Even though hexaferrites are no longer the strongest type of permanent magnets, they are still to this day one of the most important and abundantly used permanent magnetic materials holding the largest share of the market (by volume) [1]. The structure of hexaferrites is best described by closed packed oxygen layers with transition metals, typically Fe, occupying tetrahedral & octahedral sites. Additionally, one Oxygen atom is removed from one or more layers, being replaced by a large cation such as Pb, Ba or Sr. The M-type hexaferrite, e.g. $SrFe_{12}O_{19}$, has undergone a great improvement of its magnetic properties by controlling the size and morphology of nanocrystalline powder samples[2,3]. W-type hexaferrites, e.g. $SrTM_2Fe_{16}O_{27}$, has a higher saturation magnetization than that of the M-type, which makes the upper limit of the permanent magnet properties higher. The magnetocrystalline anisotropy and curie-temperature are like that of the M-type, but the compound has not been studied and optimized to the same extent. W-type hexaferrites belongs to the space group $P6_3/mmc$ and have 7 crystallographically distinct transition metal sites, an ab-axis of 5.89 Å and a c-axis of 32.75 Å and the magnetic ordering is traditionally along the c-axis.

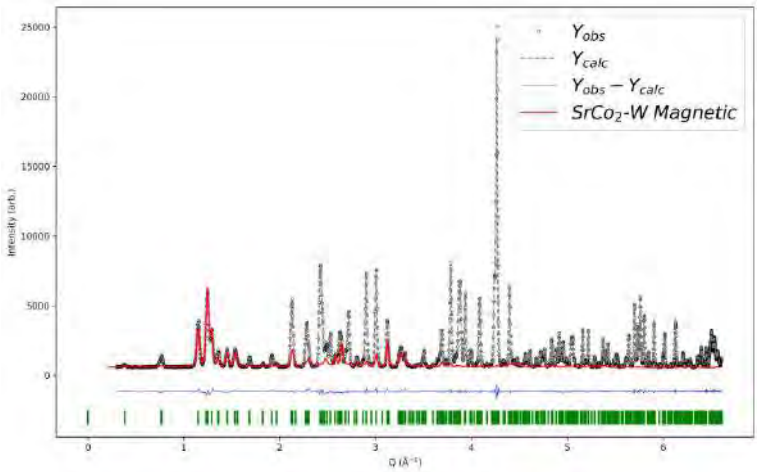

As a starting point for making good permanent magnetic materials, this work used neutron powder diffraction to determine the magnetic structure along with the transition metal occupancies in $SrTM_2Fe_{16}O_{27}$ (TM=Mg, Zn, Ni, Co). All data has been Rietveld refined in FullProff and the magnetic structure has been determined. In the figure the magnetic contribution to the powder diffraction pattern of $SrCo_2Fe_{16}O_{27}$ is highlighted, and it is seen that the magnetic ordering differs from the uniaxial-ordering seen in M-type and the three other W-type hexaferrites examined in this work. The determination of the magnetic ordering in each of the differently doped compounds along with their magnetic structure, enables further tuning of the magnetic properties. This is thought to be done by getting control of size & morphology along with having precise control of the ratio of dopants.

[1] Pullar R.C., *Progress in Materials Science*, 2012, 57, 1191
[2] Eikelend A. Z., *et al.*, *CrystEngComm*, 2017, 19, 1400
[3] Saura-Múzquiz M., *et al. Nanoscale*, 2016 8, 2857

Keywords: neutron diffraction, magnetic scattering, permanent magnets

Controlling cation ordering and oxygen release in $LiNi_{0.5}Mn_{1.5}O_4$ positive electrode materials for tailored electrochemical properties in lithium ion batteries

W. R. Brant[a*], B. Aktekin[a], D. Brandell[a], K. Edström[a]
[a] *Department of Chemistry – Ångström Laboratory, Uppsala University, Sweden*

* *william.brant@kemi.uu.se*

$LiNi_{0.5}Mn_{1.5}O_4$ (LNMO) is a promising spinel-type positive electrode (cathode) material for lithium-ion batteries (LiBs), with a theoretical capacity of 147 mAh/g and an operating voltage around 4.7 V (vs. Li/Li^+). With both high ionic and electronic conductivity it is regarded as a suitable cathode material for high power applications. LMNO can adopt two different structural arrangements, $P4_332$ (cation ordered) or *Fd*-3*m* (disordered) [1]. Generally speaking, it has been observed that batteries incorporating the latter structure exhibit reduced capacity fading during electrochemical cycling. However, synthesis conditions leading to disordering also lead to oxygen deficiency, rock-salt impurities and as a result generate Mn^{3+} [2,3]. Furthermore, while many literature reports categorise the material as either "ordered" or "disordered", the material can adopt varying degrees of ordering. Thus, isolating the exact cause of capacity fade is challenging. In this study, *in-situ* neutron diffraction is performed on disordered and slightly Mn-rich LNMO samples (Mn:Ni ratio of 1.56:0.44) to follow cation ordering-disordering transformations during heating and cooling (see figure). The study shows for the first time that there is not a direct connection between oxygen deficiency and cation disordering. This demonstrates that it is possible to tune disordering in LNMO without inducing oxygen deficiencies or forming the rock-salt impurity phase. Electrochemical testing of samples with different degrees of ordering and oxygen deficiency (i.e. highly ordered, partially ordered and fully disordered) have been performed in LNMO-LTO ($Li_4Ti_5O_{12}$) full cells. It was shown that all cells behave similarly during the initial period of cycling even when discharged at 10C rate, however, over time the disordered sample exhibited the best performance.

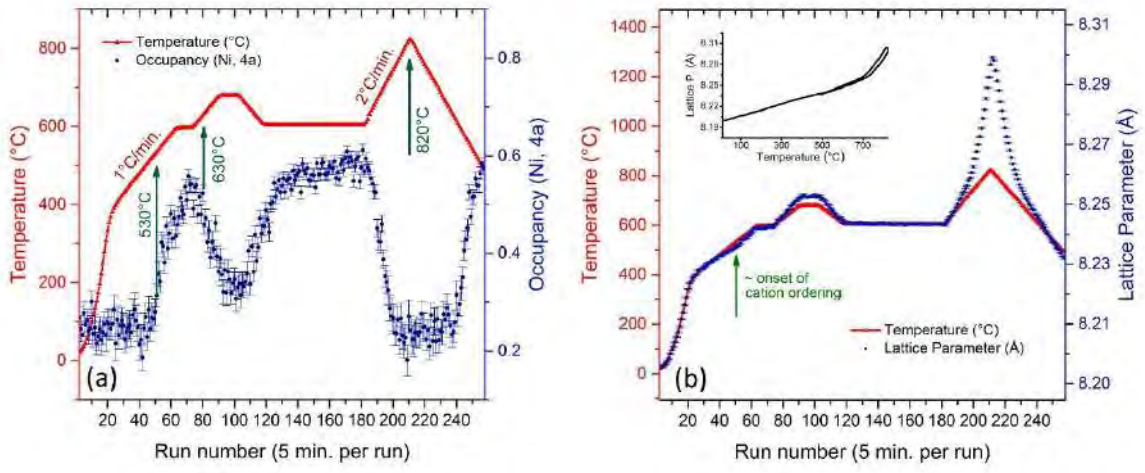

[1] L. Wang, H. Li, X. Huang, E. Baudrin, Solid State Ionics, 2011, 193, 32

[2] J. Song, D.W. Shin, Y. Lu, C.D. Amos, A. Manthiram, J.B. Goodenough, Chem. Mater., 2012, 24, 3101

[3] K.R. Chemelewski, E.S. Lee, W. Li, A. Manthiram, Chem. Mater. 2013, 25, 2890

Keywords: high voltage spinel, *in situ* neutron diffraction, lithium ion battery

Influence of synthesis routes on the structure and electrochemistry of Li-rich layered oxide cathode materials for Li-ion batteries

Ashok S. Menon*, William R. Brant, Cesar Pay Gomez and Kristina Edström
Department of Chemistry – Ångström laboratory, Uppsala University, Uppsala, Sweden
ashok.menon@kemi.uu.se

Lithium rich layered oxides, have generated interest as cathode materials for Li-ion batteries due to their anionic redox behaviour which lends them specific capacities of over 300 mAh/g [1]. Interestingly, there has been a large degree of disagreement among researchers due to the possible presence of superstructure and stacking faults [2, 3]. One possible cause for the uncertainty surrounding the structure is that the presence of stacking faults or structural ordering appears to be highly sensitive to the synthesis routes and the related parameters. The cation mixing as well as the degree of crystallinity will also depend on the synthesis precursors and specific experimental conditions (temperature, time, heating or cooling rates). In this work, a systematic investigation of the major synthesis routes used to produce Li-rich layered oxides was performed with special focus on the crystal structure and resulting electrochemical performance. A model Li-rich layered oxide – $Li_{1.2}Mn_{0.6}Ni_{0.2}O_2$, is synthesized through three different routes – solid state ceramic, sol-gel, and coprecipitation methods. *In-situ* X-ray diffraction was performed to follow the structural evolution of $Li_{1.2}Mn_{0.6}Ni_{0.2}O_2$ synthesized through each of three methods. The final structure of the material has been studied through a combined refinement of X-ray and neutron diffraction data enabling an accurate determination of structure parameters and cation mixing. The influence of synthesis conditions, especially the final heat treatment, on the stacking fault probability have also been investigated. Finally, the impact of synthesis routes on the electrochemical performance of the material system have been studied through galvanostatic cycling techniques. It is envisaged that the results from this work will aid in optimizing the synthesis routes of such material systems.

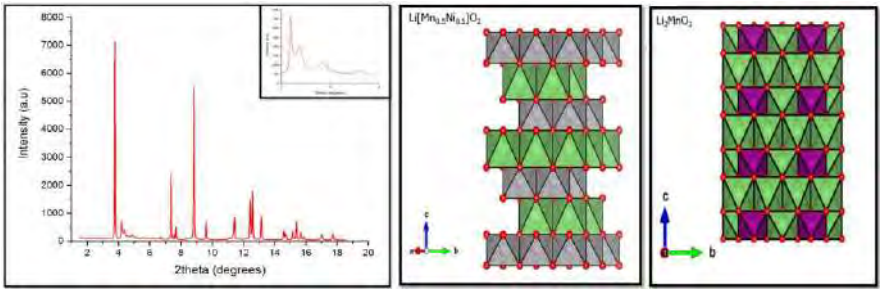

[1] Rozier, Patrick, and Jean Marie Tarascon, *Journal of the Electrochemical Society* 162(14) (2015)

[2] Jarvis, K. A., Deng, Z., Allard, L. F., Manthiram, A., & Ferreira, P. J. *Chemistry of materials*, 23(16), (2011).

[3] Bréger, J., Jiang, M., Dupré, N., Meng, Y. S., Shao-Horn, Y., Ceder, G., & Grey, C. P. *Journal of Solid State Chemistry*, 178(9), (2005)

Keywords: Energy storage, *in-situ* X-ray diffraction, lithium-rich layered oxide

Speciation of Ni in spent FCC catalysts and its detection limit (by HR powder diffraction and XAS spectroscopy)

M. Dapiaggi[a*], G. Buonomo[a], G. Giuli,[b] M. Alloni[c], R. Carli[c], G. Confalonieri[d]
[a] *Dipartimento di Scienze della Terra, Università degli Studi di Milano, Italy*
[b] *Scuola di Scienze e Tecnologie, Università degli Studi di Camerino, Italy*
[c] *Prosimet SpA, Filago (BG), Italy*
[d] *Dipartimento di Scienze della Terra, Università degli Studi di Torino, Italy* *
monica.dapiaggi@unimi.it

Heterogeneous catalysts are widely used in petrochemical processes, and subjected to various regenerating cycles, in order to regain their catalytic activity and to be then re-used or at last disposed as waste. Disposal and more likely re-cycling procedures must cope eventual hazardous nature of spent catalysts to minimize safety and environmental effects. In particular, considering FCC spent catalyst (stabilized H-FAU zeolite), it has to be noted that most of them may contain about 2000–5000 mg kg^{-1} of Ni, with the consequent concerns for their disposal. In fact, a number of nickel compounds are classified as carcinogenic or toxic to reproduction, class 1A or 1B [1]; if nickel is not speciated, it must be supposed to be present as the most dangerous species, i.e. NiO (nickel oxide), with a limit of 0.1 wt%. If nickel is present in larger quantities, the spent catalyst must be classified as hazardous waste (Classification, Labelling and Packaging Regulation 1272/2008/CE and modifications and Regulation 1357/2014/EU). A very nice paper about this subject is the one by Busca et al. [2].
It is then particularly important to understand in which crystalline (or non crystalline) form nickel is present, first of all for environmental reasons, but also for the possibility of re-using it, in the circular economy, as a starting material for other productions.
Here synthetic samples of zeolite Y have been spiked with decreasing quantities of NiO (down to 475 mg kg^{-1} of nickel oxide), of the spinel $NiAl_2O_4$ (which is not classified as hazardous, in the same quantities), and of mixtures of the two phases (their powder diffraction peaks are very close to each other, and for most reflections superposed). These samples were then compared with a spent catalyst with a certified amount of 4800 mg kg^{-1} of NiO. Moreover, a spent catalyst was also studied by means of X-ray absorption spectroscopy (XANES and EXAFS), for a better understand of the oxidation state of nickel, and of its sphere of coordination.
The powder diffraction data were collected at the beamline ID22@ESRF (F) with a wavelength of about 0.35 Å: the beamline has an extremely high resolution, and an excellent signal-to-noise ratio, so it is ideal for this kind of measurement. The XAS data were collected at the beamline BM08@ESRF (F).

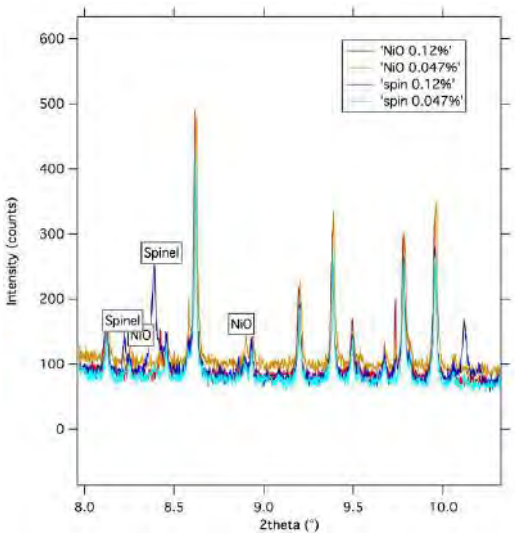

The results showed that the presence of NiO is clearly visible, in the synthetic samples, down to 0.12% wt, and detectable down to 0.047% wt (as shown in the figure). The standard spent catalyst shows no sign of any of the peaks of NiO. This is also supported by the XAS results, which show that nickel is present mainly as tetrahedrally coordinated, while, in nickel oxide, nickel is octahedrally coordinated.

[1] European Union Risk Assessment Report, Nickel and Nickel compounds, 2008. [2] Busca G, Riani P, Garbarino G, Ziemackic G, Gambino L, Montanari E, Millini R, *Applied Catalysis A: General*, (2014), 486, 176–186

Keywords: Nickel oxide detection limit, catalyst, XRPD+XA

Operando XRD data analysis of Li-ion batteries from laboratory diffractometers

F. Masiello[a*], M. Gateshki[a], D. J. Götz[a], M. Hahn[b], M Hahn[b], I. Zanziger[b]
[a] *Malvern Panlytical, Lelyweg 1, 7602 EA, Almelo, The Netherlands*
[b]*EL-CELL GmbH, Tempowerkring 8, 21079 Hamburg, Germany*
**fabio.masiello@malvernpanalytical.com*

X-ray diffraction is a powerful tool for the characterization of battery materials [1,2]. *Operando* X-ray diffraction experiments of Lithium-Ion batteries are typically carried out at high brilliance synchrotron beamlines due to the possibility to use high-energy radiation which allows a very fast collection of diffraction data from rather thick batteries. However, a wealth of information can also be extracted by the analysis of diffraction data collected on a laboratory diffractometer, which is much more accessible compared to a synchrotron source. In this presentation we will show how high-quality diffraction data of Lithium-based batteries can be quickly collected and analyzed during charge/discharge cycles on a laboratory XRD diffractometer equipped with an X-ray tube with silver or molybdenum anode and a CdTe based area detector optimized for high energy X-rays. Two main approaches will be demonstrated, in particular (a) reflection diffraction obtained with customized electrochemical cells which also allows the characterization of half cells and (b) transmission diffraction through single- and multi-layer pouch cells.

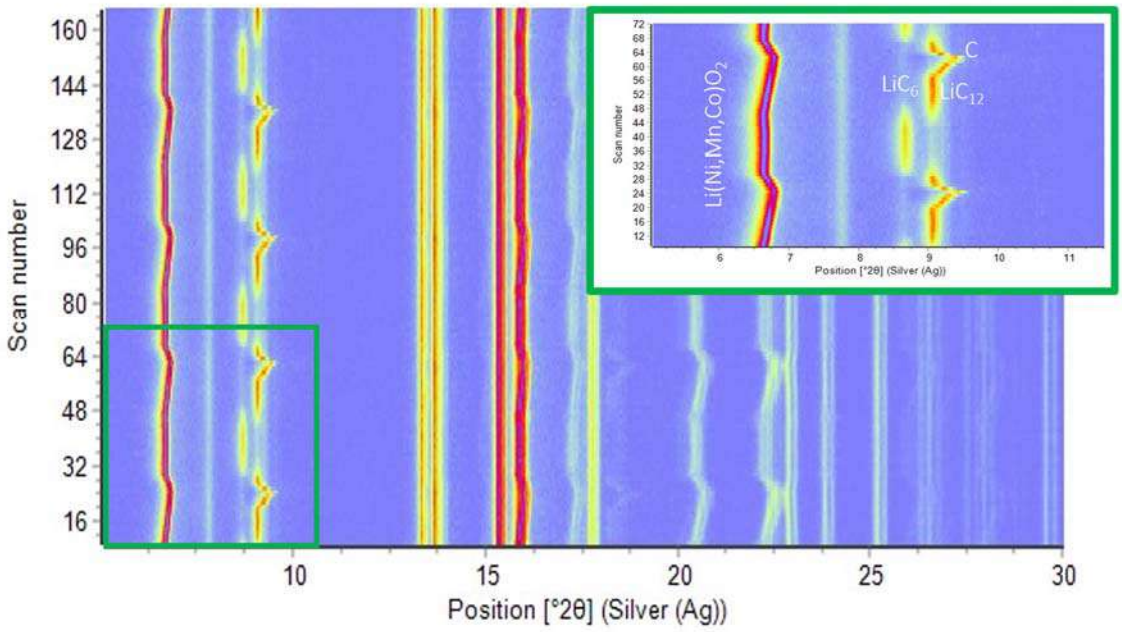

[1] Talaie E., Duffort V., Smith H. L., Fultz B. and Nazar L. F. *Energy & Environmental Science,* 2015, 2512 - 2523.

[2] Liu Z., Hu Y., Dunstan M. T., Huo H., Hao X., Zou H., Zhong G., Yang Y. and Grey C. P. *Chemistry of Materials* 2014, 2513 - 2521.

Keywords: operando, li-ion, battery

Comparison of two types of $CaCO_3$ polymorphs synthesized by the mineral carbonation of gaseous carbon dioxide

K. M. Roh*, D. Y. Kim, S. M. Seong, I. M. Kang
Advanced Geo-materials R&D department, Korea Institute of Geoscience and Mineral Resources, KR
** kmroh@kigam.re.kr*

The mineral carbonation method is still a challenge in practical application owing to: (1) slow reaction kinetics, (2) high reaction temperature, and (3) continuous mineral consumption. These constraints stem from the mode of supplying alkaline earth metals through mineral acidification and dissolution. Here, we attempt to mineralize gaseous carbon dioxide into calcium carbonate, using a cation exchange reaction of vermiculite (a species of expandable clay minerals). The mineralization is operated by draining NaCl solution through vermiculite powders and continuously dropping into the pool of NaOH solution with CO_2 gas injected. The mineralization temperature is regulated here at 293 and 333K for 15 min. As a result of characterization, using an X-ray powder diffractometer and a scanning electron microscopy, two types of pure $CaCO_3$ polymorphs (vaterite and calcite) are identified as main reaction products. We estimated crystallite sizes from the peak broadening of (104), (110), and (113) for calcite and (100), (101), and (102) for vaterite and the abundance of the mineral phases was measured using the reference intensity ratio method. Their abundance and morphology are heavily dependent on the mineralization temperature. Noticeably, spindle-shaped vaterite, which is quite different from a typical vaterite morphology (polycrystalline spherulite), forms predominantly at 333K (~98 wt%).

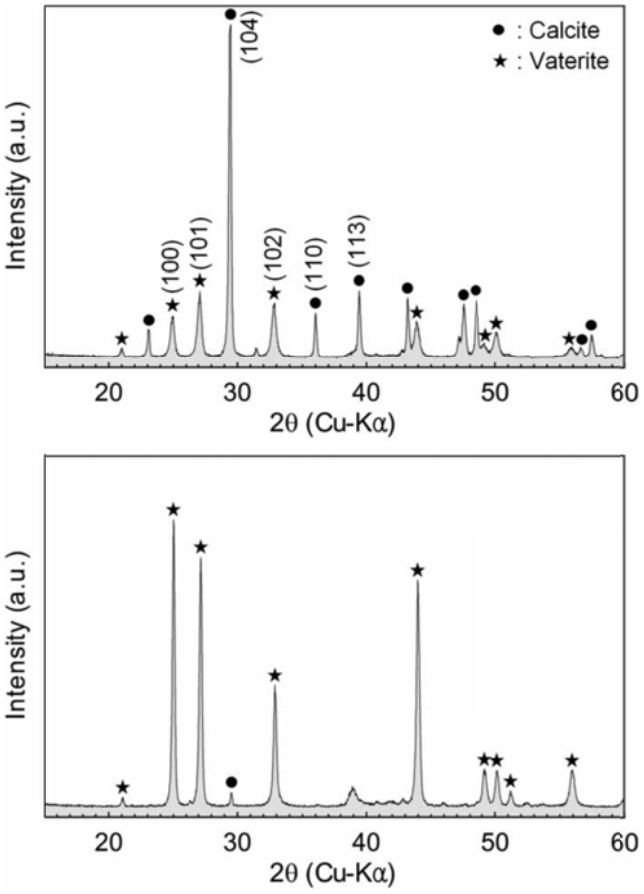

[1] Lackner K.S., Wendt C.H., Butt D.P., Joyce E.L. Jr. and Sharp D.H. Energy, 1995, 20, 1153

[2] Chung F.H. J. Appl. Crystallogr., 1974, 7, 519

Keywords: Mineral carbonation, calcite, vaterite

In-situ Formation of Fast Lithium Conducting Garnets

E. J. Cussen[a,] M. Amores[a,b], S. A. Corr[b]
[a] *Department of Pure and Applied Chemistry, University of Strathclyde, UK*
[b] *School of Chemistry, Glasgow University, UK*
* *edmund.cussen@strath.ac.uk*

The search for new solid state lithium electrolytes has recently gathered impetus from the need to decarbonise the worldwide energy supply and the move towards electric automobiles. Both of these challenges require improvements in battery performance; either to efficiently store the energy harvested from intermittent renewable supplies, such as solar and wind, or to extend the range and reduce charge times for electric automobiles. As energy densities rise, the hazards of uncontrolled battery discharge increase and this is driving research into solid state batteries; devices where the electrolyte and electrodes are all solids. The lithium electrolytes currently in widespread use typically fluid polymers which are often pyrophoric and hazardous. Replacement of these with a fully-oxidised ceramic could transform the risk profile of these devices by introducing an inert, mechanically-robust material capable of acting as a heat sink in the event of battery failure.

Lithium garnet materials have been identified as highly promising all solid state electrolytes. The most effective materials,[1] are based around $Li_7La_3Zr_2O_{12}$, although the most useful polymorph of this can only be stabilised at room temperature by cation doping.[2, 3] The material is conventionally made by heating in air at >1200° for 36 hours and incorporating aluminium into the structure. These materials show a lithium conductivity 10^{-3} S cm^{-1}, with a complex distribution of Li^+ over a range of crystallographic sites. Neutron diffraction has been the crucial tool in unpicking this structural complexity and identifying the pathway for Li^+ conduction.[4] We will present results on the structural analysis of these garnets, our use of microwave,[5] and sol-gel techniques,[6] to reduce the processing time of these materials, and map the reaction pathway during the formation of these materials using x-ray and *in-situ* neutron diffraction to study the phase formation during heating.

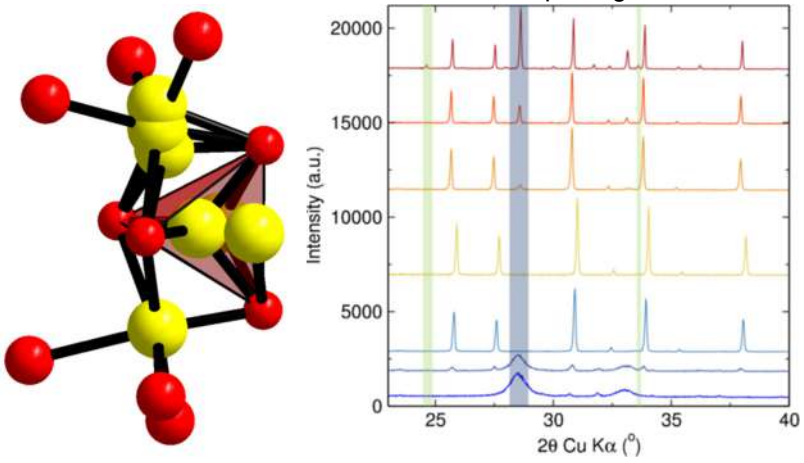

[1] Murugan R.,Thangadurai V.and Weppner W., *Angew. Chem. Int. Ed.* 2007**,** 46.

[2] Buschmann H.,Dolle J.,Berendts S.,Kuhn A.,Bottke P.,Wilkening M.,Heitjans P.,Senyshyn A.,Ehrenberg H.,Lotnyk A.,Duppel V.,Kienle L.and Janek J., *PCCP* 2011**,** 13 (43).

[3] Geiger C. A.,Alekseev E.,Lazic B.,Fisch M.,Armbruster T.,Langner R.,Fechtelkord M.,Kim N.,Pettke T.and Weppner W., *Inorg. Chem.* 2011**,** 50 (3).

[4] O'Callaghan M. P.,Titman J. T.,Chen G. Z.and Cussen E. J., *Chem. Mater.* 2008**,** 20.

[5] Amores M.,Ashton T. E.,Baker P. J.,Cussen E. J.and Corr S. A., *Journal of Materials Chemistry A* 2016**,** 4 (5).

[6] El-Shinawi H.,Paterson G. W.,MacLaren D. A.,Cussen E. J.and Corr S. A., *Journal of Materials Chemistry A* 2017**,** 5 (1).

Keywords: lithium electrolytes, garnets, neutron diffraction

Controlling H-embrittlement and delamination in Pd – based membrane material

A.J.Böttger, N. Verma, N.M. van der Pers
Materials Science and Engineering, Delft University of Technology, The Netherland
** a.j.bottger@tudelft.nl*

Membrane reactors enhance the efficiency of industrially important chemical reactions. Large-scale, commercial application of membrane reactors used to separate hydrogen gas from reaction mixtures is hindered by the limited lifetime of the membrane material and the related costs of downtime and replacement. In high temperature processes mainly Pd-based material is used.
The degradation of metal membrane material in hydrogen is mainly caused by the large volume change that occurs upon absorption of hydrogen. This expansion causes large internal stresses, crack formation and delamination of the membrane layer from its substrate.
Preventing H-embrittlement could be achieved by nano-structuring and delamination from the support can be prevented by using a suitable adhesive layer.
Both aspects will be considered for Pd-based membrane material. The Pd layer is magnetron sputtered in a thickness of about 100 nm on a Ti adhesive layer of several nm, fabricated at various sputter conditions. The interplay between the topography of the adhesive layer and the morphology, texture and stress in the Pd-membrane material will be shown. The findings open a pathway to control the structural properties of a thin layer and also its absorption behaviour in a hydrogen environment.
Prevention of H-embrittlement by choosing particular nano-structures and intermediate (adhesive) layers is demonstrated by (in-situ) X-ray diffraction and SEM analysis.

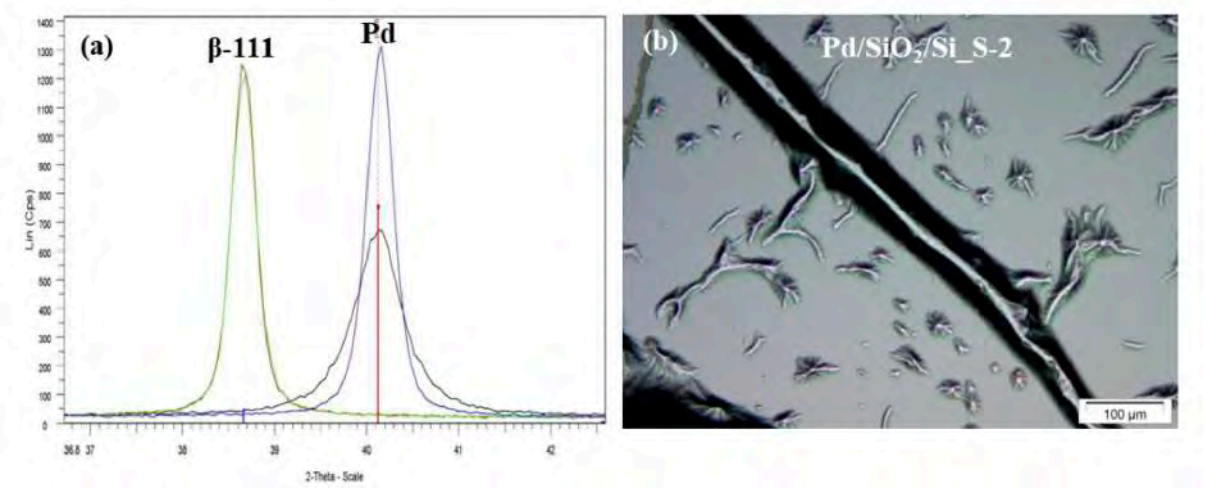

Keywords: H embrittlement, in-situ X-ray diffraction, strain

MS03 Methods in structure solution and refinement

MSO3

Abstract Number	Title	Author	Affiliation
MS03 - K1	Bigger structures, faster: optimising simulated annealing to improve structure determination from powder diffraction data	Dr Kenneth Shankland	University of Reading
MS03 - K2	Inorganic Materials Serial Crystallography Structure Determination	Dr Kenneth Beyerlein	Max Planck Institute for the Structure and Dynamics of Matter
MS03 - OR1	Combining Powder & Single-Crystal Diffraction Techniques with DSC Studies to Provide Insights into C-H…F-C Interactions in C6F6:C6H(6−n)Me(n) Co-crystals	Dr Jeremy Karl Cockcroft	University College London (UCL)
MS03 - OR2	Common rules of systematic absence applied to ab-initio indexing	Dr Ryoko Oishi-Tomiyasu	Yamagata University
MS04 - OR3	New algorithms for structure solution of polycrystalline materials in EXPO software	Dr Rosanna Rizzi	Institute of crystallography (IC-CNR)
MS03 - P20	Proof-of-concept for real-time powder diffraction data workflow at the European Spallation Source: from data streaming to analysis	Dr Celine Durniak	The European Spallation Source ERIC
MS03 - P21	Rietveld Quantitative Phase Analyses of SRM 2686a: a Standard Portland Clinker	Dr Laura Leon-Reina	Universidad de Málaga
MS03 - P22	Framework versatility in metal amino-sulfophosphonates	Ms Estefania Quintero	Universidad de Málaga
MS03 - P23	Study of the Interaction of M1 alite structural model with foreign ions by application of BVS method	Mr William Vieira Fernandes	Universidade Federal da Paraíba
MS03 - P24	Identification of the polytype structure of NiSn4 based on exhaustive generation of possible polytypes and comparison with powder-diffraction patterns	Dr Christian Schimpf	TU Bergakademie Freiberg
MS03 - P25	D2Dplot: 2D X-ray diffraction data processing and analysis for tts-μXRD	Oriol Vallcorba	Alba Synchrotron Light Source
MS03 - P26	Developing Fast Powder Diffraction Analysis for Efficient Characterisation of New Materials	Sophie Hodgkiss	University of Liverpool
MS03 - P27	Extending the limits of powder diffraction data: occupancy defects in NMC cathodes, diffraction parameter space, and the resolution of atomic form factors	Prof Peter Khalifah	Brookhaven National Laboratory / Stony Brook University
MS03 - P28	Rietveld-texture analysis of SRM 1976a: a possible standard for texture measurements?	Dr Mauro Bortolotti	University of Trento
MS03 - P29	Multi-dimensional Rietveld method: Refining angular- and wavelength-dispersive neutron time-of-flight powder-diffraction data	Dr Philipp Jacobs	RWTH Aachen University
MS03 - P30	Combining high resolution powder diffraction and single crystal nano diffraction to study natural fibers	Dr Carlotta Giacobbe	ESRF
MS03 - P31	Quantification of magnetic minerals in activated carbons and biochars	Ms Maggie White	Newcastle University
MS03 - P32	Structural modification of calcium hydroxyapatite cell induced by doping and co-doping of lead and cadmium heavy metal ions	Mohammed Eddya	University of Hassan 1st, FPK, Laboratory of Nanosciences and Modeling, Khouribga, Morocco
MS03 - P185	OChemDb: the free on-line Open Chemistry Database	Dr Nicola Corriero	Institute of crystallography (IC-CNR)

Bigger structures, faster: optimising simulated annealing to improve structure determination from powder diffraction data

K. Shankland[a]*, E. A. Kabova[a], J. C. Cole[b], O. Korb[b], M. López-Ibáñez[c] and A. C. Williams[a]
[a] *School of Pharmacy, University of Reading, UK*
[b] *Cambridge Crystallographic Data Centre, Cambridge, UK*
[c] *Decision & Cognitive Sci. Res. Centre, Alliance Manchester Business Sch., M'chester, UK*
* *k.shankland@reading.ac.uk*

Crystal structure determination from powder diffraction data has benefitted tremendously from the use of global optimization methods. Many computer programs (including, but not limited to, *DASH*, *EXPO*, *PSSP*, *TOPAS* and *FOX*) implement global optimization in the form of simulated annealing and have been used to solve many complex crystal structures from powder data alone [1]. Simulated annealing has many attractive features, not least the small number of "control parameters" that need to be set in order for the algorithm to perform well. However, as it is being applied to increasingly more complex structures, it is valuable to assess whether or not alteration of "default" control parameters can improve program performance. Here we report on the significant improvements in *DASH* [2] performance that were obtained by using the *irace* program [3] to optimize values of three key SA control parameters.

One hundred PXRD datasets, collected from organic molecules spanning a large degrees-of-freedom range were assembled. A training set, consisting of a representative sample of 40 datasets, was used by irace to optimize the SA parameters of *DASH*. The cost function used by *irace* was defined as $100(\chi^2_{SA}/\chi^2_{target})$, where χ^2_{target} was the profile χ^2obtained for the correct crystal structure.

A total of 14 irace runs, consuming 1315 days of CPU time, yielded suggested parameter values substantially different from the *DASH* defaults. The figure to the right shows the significant improvement in *DASH* success rates in solving crystal structures, over the entire range of degrees-of-freedom range present in the PXRD datasets, using the new parameters (right hand curve) as opposed to the defaults (left hand curve). This allows problems of greater complexity to be tackled as a result. The *irace*-derived parameters are now the new defaults for the latest release of *DASH*.

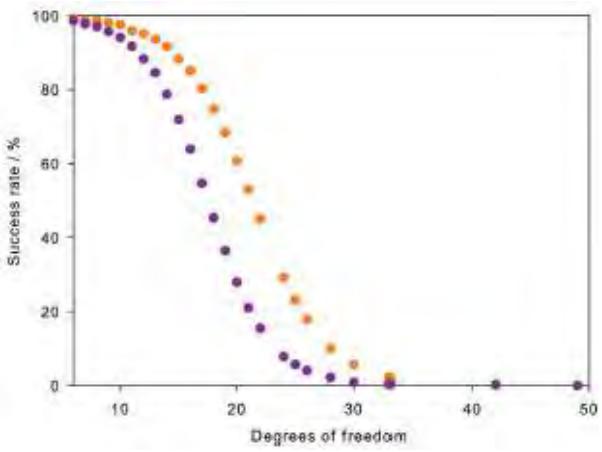

It seems probable that the approach taken in this work can be applied to many other crystallographic programs which rely upon optimization algorithms that have not themselves been optimized in terms of their performance with respect to key control parameters.

[1] Shankland, K., Spillman, M. J., Kabova, E. A., Edgeley, D. S. and Shankland, N. *Acta Cryst. C*, 2013, 69, 1251.

[2] David, W. I. F., Shankland, K., van de Streek, J., Pidcock, E., Motherwell, W. D. S. and Cole, J. C. *J. Appl. Cryst*., 2006, 39, 910.

[3] López-Ibáñez, M., Dubois-Lacoste, J., Pérez Cáceres, L., Birattari, M. and Stützle, T. Oper. Res. Perspect., 2016, 3, 43.

Keywords: simulated annealing, molecular structures, parameter tuning

Inorganic Materials Serial Crystallography Structure Determination

K.R. Beyerlein[a,b*]
[a] *Max Planck Institute for the Structure and Dynamics of Matter, Germany*
[b] *Center for Free-Electron Laser Science, Germany*
** kenneth.beyerlein@mpsd.mpg.de*

As already shown to be true for protein structure determination, serial crystallography offers a new paradigm for inorganic structure and dynamics studies. Bridging powder and single crystal diffraction, this method merges snapshot diffraction patterns collected from thousands of individually measured microcrystals into a complete map of Bragg intensities, which can then be used for structure solution. However, realizing this for inorganic materials requires developing hardware that allows for efficient data collection of these samples, and software that can cope with the challenges of phase mixtures and polycrystallinity.
In this talk I will introduce serial crystallography and present synchrotron measurements that were used to solve the structure of the Terbium complex, $Tb(bipy)_2(NO_3)_3$. The new FELIX indexing algorithm that is able to determine the orientations of multiple crystallites contributing to a single snapshot image will also be discussed. This indexer was critical to obtain a sufficient data quality for structure solution. This study sets an early benchmark for inorganic serial crystallography and points to areas for further development.

Keywords: serial crystallography, polycrystalline indexing, structure solution.

Combining Powder & Single-Crystal Diffraction Techniques with DSC Studies to Provide Insights into C-H…F-C Interactions in C_6F_6:$C_6H_{6-n}Me_n$ Co-crystals

J. K. Cockcroft*
Department of Chemistry, University College London, UK
** j.k.cockcroft@ucl.ac.uk*

Powder X-ray and neutron diffraction (PXRD and PND) are ideal tools for the study of solid-solid phase transitions, especially when complemented by DSC measurements. Similarly, single-crystal X-ray diffraction (SXD) is the method of choice for structure determination, especially given the capabilities of modern X-ray equipment (focussed micro-source X-rays with 2D detectors) combined with state-of-the-art data processing (CrysAlisPro) and analysis (Olex2) software. In addition, variable temperature (VT) crystallography can provide a more detailed understanding of the interactions between molecules than the static one-shot single temperature approach. Combining all of these methods has improved our understanding of the co-crystal system C_6F_6:$C_6H_{6-n}Me_n$ for n=0 to 3.

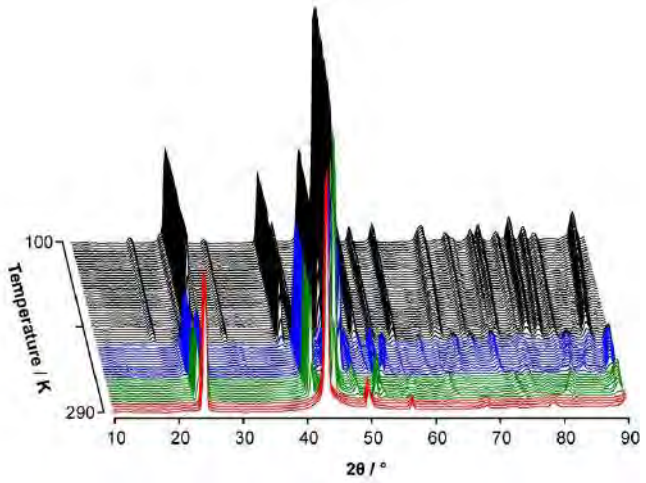

The structure of phase IV of the prototype material C_6F_6:C_6H_6 was solved from combined neutron and synchrotron X-ray powder diffraction a quarter of a century ago[1], but a detailed understanding of the other 3 phases (shown in the VT-PND figure) has remained elusive until now: new laboratory PXRD and SXD data has resulted in the determination of the crystal structures of the unknown phases and a better understanding of the transitions, particularly when combined with DSC measurements[2]. Furthermore, due to the combined use of PXRD, DSC and SXD techniques, the origins of the phase transitions in the related system C_6F_6:$C_6H_3Me_3$ co-crystal system have now been fully understood[3]. More recent studies of C_6F_6:$C_6H_4Me_2$ (p-xylene) using a similar approach has reveal subtleties in the structure of this adduct as a function of temperature which have not previously been seen; it exhibits similarities in structural behaviour to that of the C_6F_6:$C_6H_3Me_3$ adduct. Finally, a preliminary PXRD study combined with low temperature DSC on C_6F_6:C_6H_5Me (toluene) shows that this system is more similar to the prototype material. In each case, an understanding of the changes in symmetry as a function of temperature is essential to solving the structures.

Variable temperature crystallography provides a tool for studying the competing intermolecular interactions in these systems. In all cases, there is a very strong electrostatic interaction from the equal and opposite quadrupolar force between the C_6F_6 and $C_6H_{6-n}Me_n$ rings leading to columns of molecules stacked like dinner plates, but subtle changes in the C-H…F-C interactions between columns of molecules as a function of temperature lead to a variety of phase transformations. Methyl substituted benzene rings cannot rotate about an axis perpendicular to the C_6 ring when $n > 1$, but rotational motion of the methyl groups leads to additional phase transitions not seen in the prototype material driven by changes in bond dipoles interactions as a function of temperature[4].

[1] Williams J.H., Cockcroft J.K. and Fitch A.N. *Angew. Chem. Ind. Ed. Engl.* 1992, 31, 1655-1657.
[2] Cockcroft J.K., Rosu-Finsen A., Fitch A.N. and Williams J.H. 2018, *in preparation*.
[3] Cockcroft J.K., Ghosh R.E., Shephard J.J., Singh A. and Williams J.H. *CrystEngComm*, 2017, 19, 1019-1023.
[4] Cockcroft J.K., Li J., Rosu-Finsen A. and Williams J.H. 2018, *in preparation*.

Keywords: variable temperature powder diffraction, co-crystals, weak interactions

Common rules of systematic absence applied to ab-initio indexing

R. Oishi-Tomiyasu[a*], T. Kamiyama[b]
[a] *Graduate school of science and engineering, Yamagata University, Japan*
[a] *Institute of Materials Science, High Energy Accelerator Research Organization, Japan*
**ryoko_tomiyasu@sci.kj.yamagata-u.ac.jp*

The distribution rules of systematic absence used in the powder indexing software *CONOGRAPH* (https://z-code.kek.jp/zrg/), are introduced. The rules can be described in a picturesque way, by using topographs, which are a graph that was originally invented, based on the lattice-basis reduction theory. In crystallography, topographs were first used in the ab-initio indexing method of *CONOGRAPH*, which attained the highest success ratio, as presented in [1] and the following. The same rules were also recently successfully applied to electron backscattering diffraction, because Kikuchi bandwidths are also influenced by systematic absence. These applications are presented to show that topographs are useful in various types of crystal-lattice determination problems.

Topographs defined for 2D lattices (or sublattices of a 3D lattices), have edges assigned to a set of lattice basis as in Fig.1. The distribution rules predict for example, that there are combinations of four observed reflections (hence, not extinct owing to systematic absence) that can be indexed by l_1, l_2, l_1+2l_2, $2l_1+l_2$, and that similarly, there are combinations of 7 reflections that can be indexed by $l_1 \pm l_2$, $l_1 \pm l_3$, $l_1 \pm (l_2+l_3)$ and either of l_1, l_2, l_3, where l_1, l_2, l_3 are some basis of the reciprocal lattice. Normally a multiple of such combinations are generated from observed reflections. Hence, computation time is also reduced, by using the rules to predict which linear sums of l_1 and l_2, (or l_1 and l_3) are not systematic absence, therefore, probably also in the observed set. All of these predictions are consequences of the theorems in [2], which were proved to hold true regardless of types of systematic absence.

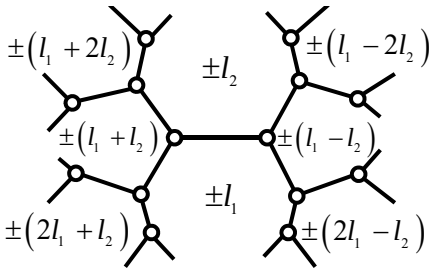

Fig.1 A topograph (each edge are surrounded by two lattice vectors that expand the identical 2D lattice.)

In the *CONOGRAPH* method, the positions of reflections not detected by peak search are sometimes estimated and used, so as to simplify the ab-initio indexing algorithm, without reducing the success ratio. After the process of acquisition for the primitive unit-cell parameters, error-stable Bravais lattice determination [3] is carried out to determine their Bravais types and conventional unit-cell parameters. The part to gain the primitive-cell parameters is completely common to all the crystal systems, and the output unit cells are classified into 14 Bravais types, which are also characteristics of the software.

In [1], the performance of the software was compared to those of *ITO*, *DICVOL* and *N-TREOR,* by using real powder diffraction patterns. The test data also contained difficult cases probably owing to dominant zones or the quality of powder patterns, since they are offered to the authors by collaborators who have experienced difficulty in indexing.

	ITO13	*DICVOL14*	*N-TREOR*	*CONOGRAPH* (quick search)	*CONOGRAPH* (exhaustive search)
Success ratio	15/39	16/39	25/39	24/39	33/39
Mean time ±σ (sec.)	0.04±0.01	1094±1520	51.2±116.1	21.1±12.4	203.9±102.5

With regard to *CONOGRAPH*, users can choose options for “quick search” and “exhaustive search”. In the former setting, *CONOGRAPH* quits the search in short time. Even so, the success ratio is still high. Since each software has very different strategy and algorithms, the setting used for the comparison is clarified in [1] and the presentation.

[1] Esmaeili A., Kamiyama T. and Oishi-Tomiyasu R. *J. Appl. Cryst.,* 2017, 50, pp.651--659.

[2] Oishi-Tomiyasu R. *Acta Cryst. A*69, 2013, pp. 603--610.

[3] Oishi-Tomiyasu R. *Acta Cryst. A*68, 2012, pp. 525--535.

Keywords: powder indexing, ab-initio indexing, Bravais lattice

New algorithms for structure solution of polycrystalline materials in EXPO software

Rosanna Rizzi*, Angela Altomare, Nicola Corriero, Corrado Cuocci, Aurelia Falcicchio, Anna Moliterni
Institute of Crystallography (IC-CNR), Bari, Italy
** rosanna.rizzi@ic.cnr.it*

The increasing interest in crystal structure solution by powder diffraction data is mainly due to the progress of the methodological approaches, the availability of sophisticated software packages and the advances in modern instrumentation, both laboratory X-ray diffractometers and synchrotron radiation [1]. This allowed the use of powder diffraction for solving polycrystalline samples to become almost routine.
Two main alternatives are widely used for solving powder structures: 1) the *ab initio* reciprocal space methods; 2) the direct space methods. The success probability of the first one in getting the correct solution is limited and depends on the experimental resolution, structure complexity, peak resolution, and structure scattering power. On the contrary, the direct space approaches are less demanding on the quality of experimental data but are time consuming and require information on the expected molecular geometry.
In this scenario, methodological and computational progress devoted to overcome the limits of applicability of both approaches is continuously realized.
This is the case of the free EXPO [2] software devoted to the structure solution of polycrystalline compounds. It is able to execute, in a complete automatic way, the full sequence of the powder solution steps from indexation to Rietveld refinement.
EXPO is supported by a user friendly graphic interface and continuously improved and updated. In the last version, two new algorithms for structure solution in reciprocal and direct space [3, 4], have enriched it. Their main aspects will be discussed together with some examples of applications by EXPO.

[1] Dinnebier R.E., Billinge S.J.L. Eds. *Powder diffraction Theory and Practice*, The Royal Society of Chemistry, Cambridge, 2008.

[2] Altomare A., Cuocci C., Giacovazzo C., Moliterni A., Rizzi R., Corriero N., Falcicchio A. *J. Appl. Cryst*., 2013, 46, 1231.

[3] Altomare A., Cuocci C., Moliterni A., Rizzi R., Corriero N., Falcicchio A. *J. Appl. Cryst*., 2017, 50, 1812.

[4] Altomare A., Corriero N., Cuocci C., Falcicchio A., Moliterni A., Rizzi R. *J. Appl. Cryst.* In Press.

Keywords: powder, EXPO software, structure solution

Proof-of-concept for real-time powder diffraction data workflow at the European Spallation Source: from data streaming to analysis

C. Durniak[a*], T. R. Nielsen[a], T. H. Rod[a]
[a] *Data Management and Software Centre, The European Spallation Source ERIC COBIS, Ole Maaløes vej 3, Copenhagen, Denmark*

* *celine.durniak@esss.se*

The European Spallation Source ERIC (ESS), currently under construction in Sweden, will generate a very intense long pulse to feed state-of-the-art instruments. In order to take full advantage of this powerful neutron source and ensure that users can rapidly process meaningful data and leave the facility with useful results, the ESS will implement a data management infrastructure that enables users to perform real-time reduction and analysis of their data during acquisition.

Here we report on the proof-of-concept for real-time refinement of data based on virtual powder diffraction experiments. This is a first step towards a complete data treatment workflow, from data acquisition to analysis, in real time, at the European Spallation Source. The purpose of this workflow is to provide, via a graphical user interface, early qualitative and quantitative hints about the quality of running experiments and some general preliminary characteristics of the investigated sample.

Keywords: real-time analysis, powder diffraction, virtual experiment

Rietveld Quantitative Phase Analyses of SRM 2686a: a Standard Portland Clinker

L. León-Reina[a*], M. García-Maté[b], G. Álvarez-Pinazo[b], A. G. De la Torre[c], M. A. G. Aranda[c,d]
[a] *SCAI, University of Málaga, Spain*
[b] *X-Ray Data Services S.L., Málaga, Spain*
[c] *Dpto. Química Inorgánica, University of Málaga, Spain*
[d] *ALBA Synchrotron, Barcelona, Spain.*
* *lauralr@uma.es*

X-ray powder diffraction (XRPD) data analysed by using the Rietveld methodology is the most widely used methodology to obtain the crystalline mineralogical composition of a sample. Rietveld Quantitative Phase Analysis using laboratory-XRPD was firstly applied to a Portland clinker in 1993. Eight years later, RQPA of Portland cement was obtained by using synchrotron-XRPD. Nowadays, XRPD is routinely used in the cement industry for bulk mineralogical phase analysis [1].

To have a standard reference clinker sample is very important twofold: i) to test the experimental data collection equipment and strategy; and ii) to verify that used Rietveld protocol is adequate. In this context, the National Institute of Standards and Technology (NIST) offers the reference material, SRM 2686a, which is a Portland clinker with a reported mineralogical analysis from XRPD and electron microscopy [2]. Furthermore, the American Society for Testing and Materials (ASTM) C01.23 Compositional Analysis subcommittee developed a test method, ASTM C 1365 [3], entitled 'Determination of the Proportion of Phases in Portland Cement and Portland-Cement Clinker Using X-Ray Powder Diffraction Analysis'. This test method considers the use of XRPD data analysed by the Rietveld method and it is being used for cement industries and related laboratories to self-verify their RQPA procedures. In this protocol, the maximum and minimum ranges for the different crystalline components of SRM 2686a are stated, following the average mineralogical analysis provided by NIST.

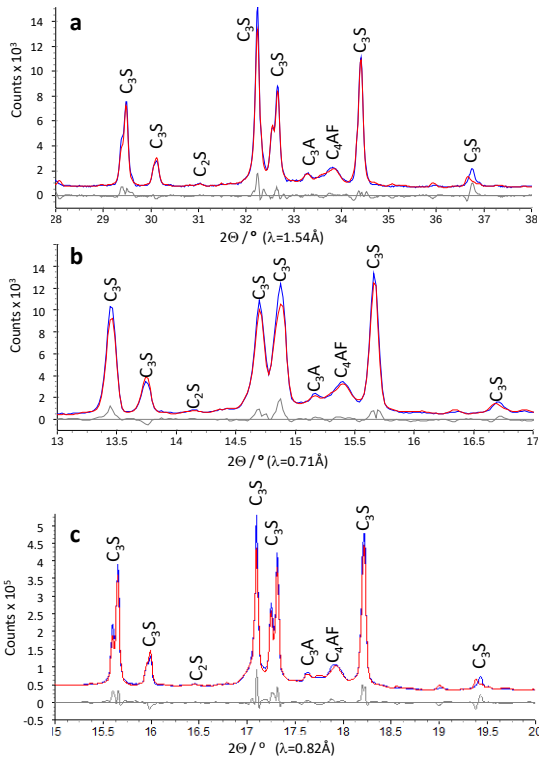

We have analysed SRM 2686a by using three state-of-the-art powder diffraction configurations: a) strictly monochromatic CuKα1 radiation in flat reflection geometry; b) strictly monochromatic MoKα1 radiation in flat transmission geometry; and c) synchrotron radiation in rotating capillary transmission geometry, see figure. The powder patterns were analysed by Rietveld methodology with the best available protocols. The results indicate that the reported NIST analysis overestimate belite content which explains problems found for implementing ASTM C 1365 in some cement manufacturing plants. Further details will be provided in this communication

[1] R. Meier, J. Anderson and S. Verryn, *Rev. Mineral. Geochem.*, 2012, 74, 147.

[2] Certificate of Analysis. Standard Reference Material 2686a. Technical note. National Institute of Standards and Technology; U.S. Department of Commerce: Gaithersburg, MD (2012). Available at: https://www-s.nist.gov/srmors/view_detail.cfm?srm=2686A

[3] ASTM C 1365: Standard Test Method for Determination of the Proportion of Phases in Portland Cement and Portland-Cement Clinker Using X-ray Diffraction Analysis. Annual Book of ASTM Standards. Vol. 4.01. West Conshohocken, PA: ASTM International, 2014. Available at: https://www.astm.org/Standards/C1365.htm

Keywords: clinker NIST, synchrotron radiation, powder diffraction

Framework versatility in metal amino-sulfophosphonates

E. Quintero[a],* I.R. Salcedo[b], M. Bazaga-García[b], R.M.P. Colodrero[c], L. León-Reina[a], K. Xanthopoulos [d], K.D. Demadis [d], E.R. Losilla[b], P. Olivera-Pastor[b], A. Cabeza[b]
[a]SCAI, Universidad de Málaga, Spain
[b] *Departamento de Química Inorgánica, Universidad de Málaga, Spain*
[c] *Wolverhampton School of Sciences, Wolverhampton University, UK*
[d] *Department of Chemistry, University of Crete, Greece*
** estefaniaqm@uma.es*

Coordination polymers possessing acidic groups such (P-OH; SO_3H, COOH, N^+-H…) are potential proton conducting electrolytes for proton exchange membrane fuel cells (PEMFCs). Furthermore, their frameworks can be chemically modified by appropriate structural design and/or the post-synthesis inclusion of guest molecules (H_2O, NH_3, heterocyclics, etc.) that generates extended hydrogen bonding networks [1].

In this work, the crystal structures resulting from the combination of the amino-sulfophosphonate ligand $(H_2O_3PCH_2)_2$-N-$(CH_2)_2$-SO_3H with various transition metal ions, including lanthanide ions, are reported. Optimal synthesis conditions were implemented by high through-put screening. For lanthanide and zinc derivatives, crystal structures were solved from laboratory/synchrotron X-ray powder diffraction data, while for the copper derivative single-crystal data was employed. In layered lanthanide frameworks, the sulfonic group point towards the interlayer region, except the lanthanum derivative, in which the metal ion is linked to both phosphonate and sulfonated groups leaving uncoordinated P-OH groups. Divalent metals give rise to different frameworks. For instance, for Cu(II) the presence of an auxiliary ligand (1,10-phenanthroline) was required to obtain a crystalline compound. As a consequence of this structural variability, different H-bond networks can be generated leading to a wide range of proton conductivity values.

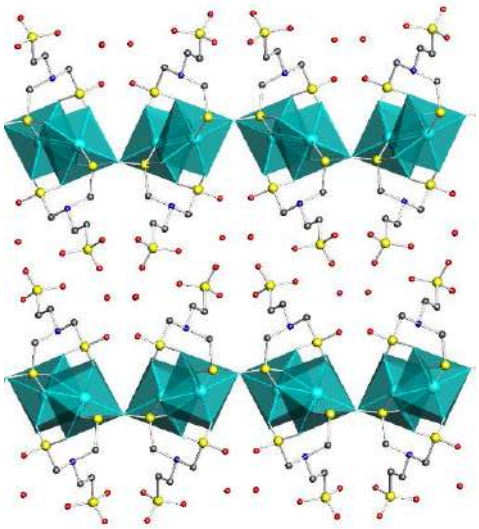

[1] Cabeza, A.; Olivera-Pastor, P.; Colodrero, R. M. P. Tailored Organic-Inorganic Materials, Brunet, E., Colón, J.L., Clearfield, A., Eds.; John Wiley & Sons, Inc. 2015; Ch. 4, 137−191.

Keywords: coordination polymers, phosphonates, proton-conductivity

Study of the Interaction of M1 alite structural model with foreign ions by application of BVS method

W. V. Fernandes[a*], S.M. Torres, C.A. Kirk[b]
[a] *Department of Materials Engineering, Federal University of Paraíba, Brazil*
[b] *School of Chemistry, University of Edinburgh, UK*
**william@prefeitura.ufpb.br*

The use of alternative fuels in cement production is a hot topic with respect to reduction in CO2 emissions of the worldwide cement industry. However, potential changes in the clinker composition due to the incorporation of foreign elements, from the use of alternative fuels, e.g. biomass, coke, must be systematically examined[1], which may possibly influence mechanical properties [2] and durability of concrete mixed with this material [3]. With respect to alite, the major clinker phase, there is evidence that Mg, coming from raw materials, and, S, which is present in some alternative fuels, e.g. coke, together influence the stabilisation of the M3 and M1 polymorphs, respectively [4]. To date, the available alite crystal structure models do not give information about the presence of minor constituents. With the widespread and routine use of phase quantification via Rietveld refinement of PXRD data during cement production for quality control purposes, improved and more realistic structural models are required, which satisfactorily represent phases present. Therefore it is vital to investigate the role minor constituents play in the structural models of alite polymorphs. Despite being recently applied to studies into the influence minor elements have on cement hydration [5], some authors do not agree whether the M1 structural model proposed [6] should be appropriate for Rietveld refinement [7] possibly due its lack of precision. In the work presented here, potential preferential sites in M1 polymorph structural model[6], where substitution of Ca by Mg or S might occur, were studied using the Bond Valence Sum (BVS) technique[8]. This model was then used for structural analysis of an industrial clinker sample, produced using petroleum coke as the kiln fuel and found to contain 6.00 and 1.85 wt.% of MgO and SO_3, respectively, (obtained by x-ray fluorescence (XRF). Rietveld refinement of synchrotron PXRD data, collected on beamline I11 at Diamond Light Source, using the TOPAS software suite was carried out. Refinement of preferential calcium sites occupancy led to equalization of BVS, which became closer to the actual valence of the element, along with an improvement of Rwp. Considerations about possible effects on clinker reactivity towards water were made, highlighting that the doping of the sample is important to take into account when studying the reactivity.

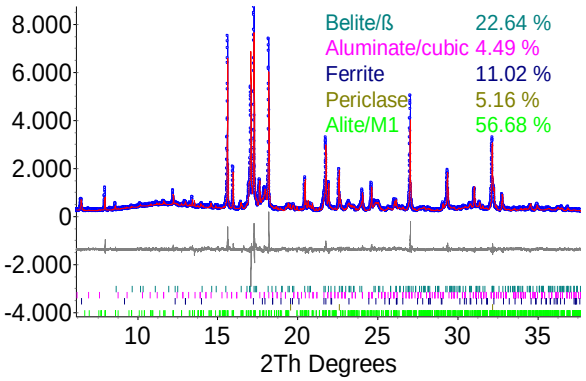

Figure 1 Observed, calculated and difference curves of synchrotron PXRD data collected from clinker sample.

[1] F. Sorrentino, Cem. Concr. Res., vol. 41, no. 7, pp. 616–623, 2011.

[2] T. Staněk and P. Sulovský, Cem. Concr. Res., vol. 32, no. 7, pp. 1169–1175, 2002.

[3] S. M. Torres, C. A. Kirk, C. J. Lynsdale, R. N. Swamy, and J. H. Sharp, Cem. Concr. Res., vol. 34, no. 8, pp. 1297–1305, 2004.

[4] X. Li, W. Xu, S. Wang, M. Tang, and X. Shen, Constr. Build. Mater., vol. 58, pp. 182–192, 2014.

[5] A. Bazzoni, M. Suhua, Q. Wang, X. Shen, M. Cantoni, and K. L. Scrivener J. Am. Ceram. Soc., vol. 97, no. 11, pp. 3684–3693, 2014.

[6] M. N. De Noirfontaine, M. Courtial, M. De Noirfontaine, F. Dunstetter, G. Gasecki, and M. Signes-Frehel, Zeitschrift für Krist., vol. 227, no. 2, pp. 102–112, 2012.

[7] Á. G. De la Torre, I. Santacruz, L. León-Reina, A. Cuesta, and M. A. G. Aranda, in Cementitious Materials, H. Pöllmann, Ed. Berlin, Boston: De Gruyter, 2017, pp. 3–29.

[8] I. D. Brown, The Chemical Bond in Inorganic Chemistry: The Bond Valence Model. 2010.

Keywords: clinker, polymorphism, BVS

Identification of the polytype structure of $NiSn_4$ based on exhaustive generation of possible polytypes and comparison with powder-diffraction patterns

C. Schimpf[a*], M. Motylenko[a], P. Kalanke[a], C. Wolf[a], H. Becker[a], S.L. Shang[b], Z.K. Liu[b], A. Leineweber[a]

[a] *Institute of Materials Science, TU Bergakademie Freiberg, Germany*

[b] *Department of Materials Science and Engineering, The Pennsylvania State University, PA, USA*

**schimpf@iww.tu-freiberg.de*

$NiSn_4$ has recently been shown to possess a heavily faulted microstructure [1]. The structure is a stacking-disordered intermediate of the orthorhombic $PdSn_4$-type structure (space group *Ccce*) and the tetragonal β-$IrSn_4$-type structure (space group $I4_1/amd$). The two structures are composed of a faulted stack (along the crystallographic *c*-axis) of layers consisting of edge-sharing $NiSn_8$-square antiprisms. $NiSn_4$ with this microstructure forms, e.g. after room temperature storage for several weeks, between electrodeposited Sn layers on Ni substrates.

However, annealing of electrodeposited Ni-Sn sandwich structures at T = (333 … 353) K for several days will lead to ordered (i.e. non-random) incorporation of these stacking faults. This process leads to the formation of polytypes, being visible from clear polytype reflections in the XRD patterns, which are shown in the Figure. The Figure also shows the locations of the polytype reflections as dashed lines, which are seen to form in the angular range of a diffuse (21-)diffraction band stemming from uncorrelated stacking faults. The theoretical pattern of the polytype is given by the solid line at the bottom.

We will describe a simple method to generate all unique polytypes with a given number of layers in the unit cell. Their powder diffraction patterns may be easily obtained through the generation of *.cif files in *P*1 setting. Systematic absence/occurrence of polytype reflections will be discussed in terms of layer sequences already visible in the polytype symbol. The polytype reflections are related to crystallographic symmetry elements destroyed or formed by the specific layer sequence in the polytype unit cell. The polytype reflections may serve as a fingerprint of the stacking sequence. Preliminary ground state energy calculations by DFT for several polytypes indicate that the experimentally observed 12-layer polytype with $P4_2/nbc$ symmetry indeed has the lowest energy. It can be shown that the faulted stacking sequence of the $NiSn_4$ formed upon room-temperature storage and that of the ordered 12-layer polytype formed at (333 … 353) K show statistical similarities in the stacking sequences.

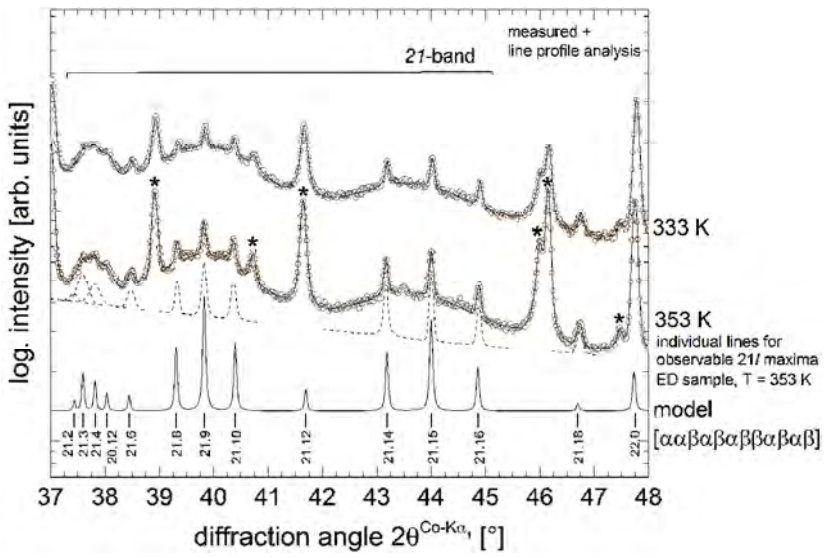

[1] C. Schimpf, P. Kalanke, S.L. Shang, Z.K. Liu, A. Leineweber*. Mater. Design.,* 2016, 109, 324.

Keywords: tin intermetallics, X-ray powder diffraction, polytype reflections

D2Dplot: 2D X-ray diffraction data processing and analysis for tts-*μ*XRD

O. Vallcorba[a*], J. Rius[b]
[a] *ALBA Synchrotron Light Source, Barcelona, Spain*
[b] *Institut de Ciència de Materials de Barcelona (ICMAB-CSIC), Spain*
* *ovallcorba@cells.es*

Collection of diffraction data using 2D detectors is an extensive practice nowadays. In some cases, data reduction of single-crystal diffraction data or circular integration of powder data is automatically performed with almost no visual inspection of the frames. However, for non-routine experiments or when it is necessary to get additional sample information (texture, graininess, mapping of samples) an extended visual inspection of the frames and the capability to work directly on the image becomes essential. Existing software for 2D XRD data processing, such as FIT2D [1] or GSAS-II [2], offers a lot of possibilities and can act as general purpose programs for data analysis. On the other hand, the new *d2Dplot* software has been designed prioritizing the visual inspection of the 2D XRD data frames, including an easy navigation along the images and two specific features: (i) creation of a database for the identification of a subset of compounds and (ii) a peak analysis routine for the through-the-substrate (tts) *μ*XRD methodology [3].

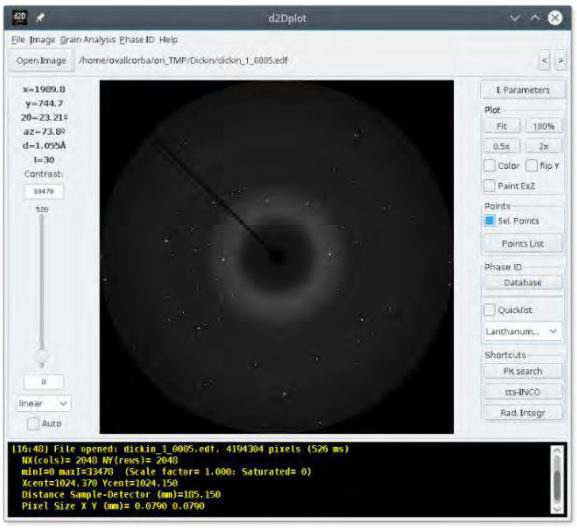

The first specific feature of *d2Dplot* is the possibility to store crystallographic information of compounds in order to plot the expected reflection positions on top of the opened frame. This is useful for example during sample mapping measurements, allowing a quick compound or zone identification. The second specific feature is the tts-*μ*XRD data analysis for single or multiple grain(s). The intensity of the diffraction spots can be extracted to be used in the orientation search by the tts_software [4] and the obtained results can be plotted to check for the correct solution. In addition to these two features, basic data processing operations have been implemented in *d2Dplot* such as the sum or subtraction of frames, radial integration, azimuthal integration, calibration of instrumental parameters using LaB_6 diffraction data, background estimation and a command line mode to run the operations inside data processing pipelines.

D2Dplot can be downloaded from the ALBA Synchrotron Light Source website (https://www.cells.es/en/beamlines/bl04-mspd/preparing-your-experiment) and can be used free of charge for non-commercial and academic purposes.

[1] Hammersley, A.P. *ESRF Internal Report*, ESRF97HA02T, 1997.

[2] Toby B.H., Von Dreele R.B. *Journal of Applied Crystallography*, 2013, 46, 544–549.

[3] Rius J., Vallcorba O., Frontera C., Peral I., Crespi A. and Miravitlles C. *IUCrJ*, 2015, 2, 452-463.

[4] Rius J., Vallcorba O., Frontera C., *TTS_software: A computer software for crystal structure analysis from tts microdiffraction data* [http://departments.icmab.es/crystallography/software], ICMAB-CSIC, 2016.

Keywords: 2D diffraction data, through-the-substrate microdiffraction, computer software

OChemDb: the free on-line Open Chemistry Database

N Corriero*, A. Altomare, C. Cuocci, A. Falcicchio, A. Moliterni, R. Rizzi
Institute of Crystallography, CNR, Bari, Italy
* nicola.corriero@ic.cnr.it

The Open Chemistry Database (OChemDb) is a new free on-line portal which uses an appropriately designed database of already solved crystal structures. It makes freely available computational and graphical tools for searching and analysing crystal-chemical information of organic, metal-organic and inorganic structures, and providing statistics on desired bond distances, bond angles, torsion angles, and space groups. Atom types have been classified by an identifier code containing information about the chemical topology and local environment.
The crystallographic data used by OChemDb are acquired from the CIF files contained in the free small-molecule Crystallography Open Database (COD1). OChemDb offers easy-to- use and intuitive options of searching. It is updated by following the continuous growth of information stored in the COD. It can result of great utility for structural chemistry, in particular in the process of determination of a new crystal structure, and for any discipline involving crystalline structure knowledge.
The OChemDb card contains some of the following information:its identification number which corresponds to the seven-digit number of the deposition of the CIF file in the COD, chemical name, mineral name, chemical formula, space group, crystal system, cell parameters, cell volume, crystal density, linear absorption coefficient, Z value, bibliographic reference. OChemDb incorporates also, for each crystal structure, the bond distances, bond angles, torsion angles and the atom types which are evaluated by the EXPO2 computing program by using its option of reading structure data in CIF format. The use of OChemDb requires only a web browser and an internet connection. Every device (mobile or desktop) and every operating system is able to use OChemDb by accessing to its web page. OChemDb is free for academic use and is available at http://www.ba.ic.cnr.it/ochemdb/ after registration.

[1] Grazulis, S., Chateigner, D., Downs, R.T., Yokochi, A.F.T., Quirós, M., Lutterotti, L., Manakova,E., Butkus, J., Moeck, P. & Le Bail, A. (2009). J. Appl. Cryst. 42, 726-729.

[2] Altomare, A., Cuocci, C., Giacovazzo, C., Moliterni, A., Rizzi, R., Corriero, N. Falcicchio, A. (2013). J. Appl. Cryst. 46, 1231-1235.

Keywords: database, crystal-chemical information, powders

Developing Fast Powder Diffraction Analysis for Efficient Characterisation of New Materials

S. Hodgkiss[a, b], S. Y. Chong[b*]
[a] *Leverhulme Research Centre for Functional Materials Design, UK*
[b] *Department of Chemistry and Materials Innovation Factory, University of Liverpool, UK*
*sgshodgk@liverpool.ac.uk, s.chong@liverpool.ac.uk

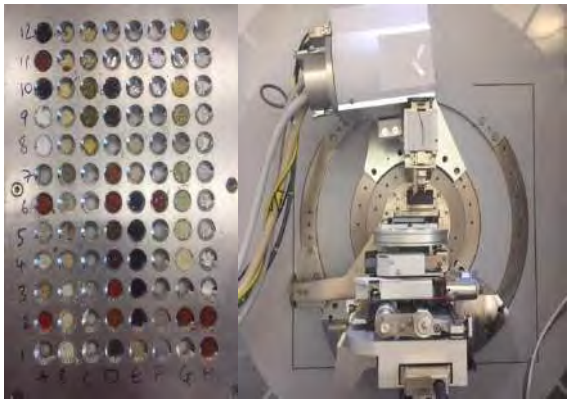

The crystal structure directly influences the crystal and molecular functional properties of a material. Powder X-ray diffraction (PXRD) can be used to obtain structural characterisation of materials where single crystals are not synthetically available. PXRD has also been incorporated alongside high-throughput synthesis 'on-the-fly' due to the efficiency and ease of data collection. [1] Therefore, the limiting factor of many high-throughput techniques becomes the analysis of the data required for characterisation. Computational packages have previously been developed to address the restriction on the rapid analysis of vast quantities of datasets but these tend to be specific to particular types of materials. [1,2] Organic materials however, tend to generate more challenging patterns due to lower intensity peaks and a higher degree of peak overlap. This means the analysis of organic molecular materials tends to be increasingly difficult, slowing down high-throughput techniques significantly.

Work within the group aims to develop methods implemented as a collection of Python scripts to perform rapid processing analysis of PXRD patterns, such as peak identification, which are efficient for the analysis of organic crystals. The scripts developed so far can be used to filter PXRD patterns based on the level of crystallinity of the material and extract peak position data. This will form the basis of future development of rapid diffraction analysis based on statistical analysis and machine learning.

[1] A. G. Kusne, T. Gao, A. Mehta, L. Ke, M. C. Nguyen, K.-M. Ho, V. Antropov, C.-Z. Wang, M. J. Kramer, C. Long and I. Takeuchi, *Sci. Rep.*, 2014, **4**, 6367

[2] D. Lau, D. G Hay, M. R Hill, B. W Muir, S. Furman and D. Kennedy, *Comb. Chem. High Throughput Screen.*, 2010, **14**, 28–35.

Keywords: powder x-ray diffraction, high-throughput, organic crystals

Extending the limits of powder diffraction data: occupancy defects in NMC cathodes, diffraction parameter space, and the resolution of atomic form factors

P. G. Khalifah[a,b*], L. Yin[a,b], G. Mattei[a,b], Z. Li[a,b]
[a] *Department of Chemistry, Stony Brook University, USA*
[b] *Department of Chemistry, Brookhaven National Laboratory, USA*
**kpete@bnl.gov*

Although the Rietveld refinement of powder diffraction data from synchrotron and neutron sources can in theory be used to determine structural models with exquisite sensitivity to crystallographic parameters based on the estimated standard deviations for these parameters, in practice it is found that there are very large systematic errors in the determination of some key parameters, especially in site occupancies and atomic displacement parameters. These problems are most obvious when comparisons are made between the two structural models that are obtained from a single sample when neutron and synchrotron powder diffraction data from the sample are independently utilized for refinements. In this work, it will be shown that with the proper methods for analyzing data, superb agreement (~0.1% absolute) in occupancy-related parameter values can be obtained between structural models refined using neutron and synchrotron data. It is found that the powder diffraction data from modern user facility beamlines is of sufficient quality to allow systematic problems in the standard neutral atomic form factors used in X-ray diffraction data to be discerned. This discrimination is best accomplished using a new intuitive method of visualizing diffraction parameter space that we have developed. These methods have been applied to identify the nature of and to quantify the amount of occupancy defects in layered NMC cathodes with nominal stochiometries of $Li(Ni_xMn_yCo_z)O_2$, providing new general insights into the behavior of defects in this class of materials.

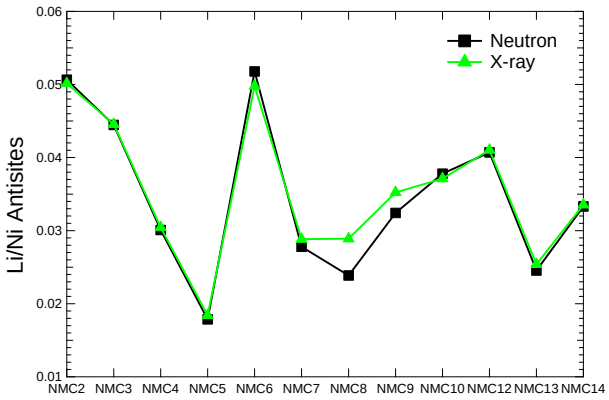

Keywords: batteries, atomic form factors, defects

Rietveld-texture analysis of SRM 1976a: a possible standard for texture measurements?

E. Borovin[a], M. Bortolotti[a*], L. Lutterotti[a]
[a] *Department of Industrial Engineering, University of Trento, IT*
* *mauro.bortolotti@unitn.it*

Measuring texture to determine the ODF (Orientation Distribution Function) of a material requires special instruments able to collect diffraction data over different sample orientations. This is accomplished by the use of goniometers with more “circles” or rotation axis and/or large/1D/2D detectors to speed up the measurement and reduce the number of sample rotations. This kind of diffractometers are more difficult to align and center, but a misalignment or eccentricity in the rotation may compromise the correct measurement. Again, if a traditional point detector and texture measurement is done by pole figures collection the knowledge of the effective defocusing is also fundamental.
Still one of the open questions is what kind of sample/standard can be used to monitor the effectiveness of an instrument to measure texture, its accuracy in the ODF determination and if it can catch correctly sharp textures. The standard procedures developed in the past where to prepare a random sample to measure defocusing and a well-known textured sample shared across different instruments to certify their accuracy in the ODF determination [1]. Labosoft is selling texture reference samples [2], but these come with a lab report and measured pole figures, not a real certification or a standard ODF. These are for sure helpful in the case of a classical texture goniometer measuring pole figures, but not too much with modern instrument measuring images or neutron spectrometers (TOF) where more patterns are measured instead of pole figures.
SRM 1976a [3] is a standard material developed to certify instrument response providing reproducible reflection intensities by an alumina sintered plate. It has been replaced by the more recent and similar SRM 1976b but for the purpose of the work it does not matter. We decided to measure the standard using a special texture goniometer equipped with an Eulerian cradle and large 2D detector.
The ODF determination was performed with the Rietveld texture program MAUD using different inversion methods. In our finding as expected, SRM 1976a has a strong fiber ODF and it may be well suited to be used as a standard for texture. Being a standard material, not a reference, gives it several advantages, for example make it suitable to be used by different labs to certify or monitor their instruments and test different measurement procedures and ODF determination methods. It is not required to share the same sample between different labs as NIST provides a quite narrow standard deviation on relative intensities between samples, sufficient to ensure a reproducible ODF.
A comparison between the different method for ODF determination has been performed as well to show their applicability, limits and relative accuracy.

[1] Wenk H. -R., *J. Appl. Crystallogr.* 1991, 24, 920.
[2] Labosoft, Texture reference samples, http://www.labotex.com/texture_standards.html.
[3] SRM 1976a, 2008, NIST Standard Reference Materials Program, Gaithersburg, MD, USA.
[4] Lutterotti, L., Nuclear Instr. and Methods in Phys. Res. B. 2010, 268, 334.

Keywords: Rietveld texture analysis, ODF, standard reference material, NIST 1976b

Combining high resolution powder diffraction and single crystal nano diffraction to study natural fibers.

C. Giacobbe[a] , N. Bursi Gandolfi[b], J. Wright[a], A.F. Gualtieri[b]

[a]*European Synchrotron Radiation Facility – 71 Avenue des Martyrs, 38040 Grenoble, France*

[b] *Dipartimento di Scienze Chimiche e Geologiche, Università di Modena e Reggio Emilia- Via Giuseppe Campi, 103, 41125 Modena, Italy*

The advent of high-brightness, third generation synchrotron sources and improvements in X-ray focusing optics has enabled new techniques for materials investigations with nanometre spatial resolution. At ID11, the Materials Science beamline at the European Synchrotron Radiation Facility (ESRF), a new end station has recently been built to provide real-space maps of the local lattice structure, crystal orientation and grain morphology.

The characterization of nano- and micro-natural fibres is a promising scientific case, which can benefit by the bright and small beam available in this synchrotron facility.

In fact, despite all the advances in fibres structure analysis, some problems still remain that are very hard to solve. One challenge is the structural analysis of micro- and nano-crystalline natural samples, which do not form crystals large enough for single-crystal X-ray diffraction (SC-XRD), and their analysis is often hampered by reflection overlap and the coexistence of multiple fibres linked together.

This contribution will illustrate the application of the nano-focussing SC-XRD to the case of a fibrous zeolite.

The zeolite ferrierite (FER) is well-known both in nature and as a synthetic material[1]. The crystal structure of ferrierite was first solved by Vaughan *et al.[2]*, in the space group *Immm*, on a magnesium-containing mineral sample from Kamloops Lake, Canada, and has been validated by a number of other workers[3,4].

Open debates, whether deviation from *Immm* symmetry are possible can be found in literarure[5]. We here present a careful high resolution and nano single-crystal diffraction study that aims to clarify the possible lowering of the symmetry to the space group $P2_1/n$.

[1] Wise, W. S et al. *Am. Mineral*. 1976, 61, 60.
[2] Vaughan et al. *Acta Cryst.* 1966, 21, 983-990
[3] Gramlich-Meier, R et al. *Zeit. Kristallogr*. 1984, 169,201
[4] Alberti, . et al. *Zeit. Kristallogr*. 1987, 178, 249.

Keywords: high resolution, single crystal, fibers

Quantification of magnetic minerals in activated carbons and biochars

M. L. White[a*], Z. Han[b], D. Werner[a], A. Neumann[a] , S.S. Pramana[a]
[a] *School of Engineering, Newcastle University, UK*
[b] *Chinese Academy of Geological Sciences, Shijiazhuang, China*
** maggie.white@newcastle.ac.uk*

Recent studies have reported that activated carbons and biochars impregnated with magnetite and/or maghemite produce effective magnetic sorbent materials (MAC and MBC, respectively) and show significant promise for *in-situ* environmental remediation of polluted sediments, due to their potential for recovery and re-use [1,2,3]. However, key to optimising the recovery of these magnetic sorbents (for re-use) is a complete understanding and characterisation of the magnetic mineral component, as each magnetic mineral has a different magnetic susceptibility: for example, maghemite has a weaker magnetic susceptibility than magnetite.

To this end, conventional powder XRD (a PANalytical X'Pert Pro with Cu tube) has shown that magnetite and maghemite are almost certainly both present in the majority of MAC and MBC samples tested (in addition only to quartz), although due to their (spinel) structural similarities it is not possible to accurately determine the proportions of these two iron oxides without careful stripping of $K\alpha_2$ diffraction peaks at moderate to high Bragg angles. This, together with the fluorescence effects encountered when exposing iron-rich samples to copper radiation renders the quantification of magnetite and maghemite in the MAC and MBC samples complex, using conventional XRD alone. To progress this work further, the same MAC and MBC samples will be analysed using two powder diffraction systems: (i) a Rigaku SmartLab fitted with an incident beam monochromator (to eliminate the need for $K\alpha_2$ stripping) and (ii) an X'Pert Pro MPD system ($K\alpha_2$) fitted only with a diffracted beam monochromator, with both XRD systems operated in XRF reduction mode to reduce sample fluorescence. To obtain absolute mineral abundances, samples will be spiked with a known weight percentage of a reference powder and the diffraction data sets refined. Additionally, Mossbauer spectroscopy will be used to confirm that magnetic minerals are present in samples and investigate their associated Fe(II)/Fe(III) ratios.

It is anticipated that a combination of these analytical techniques will yield the data necessary to determine the absolute abundances of magnetite and maghemite and more fully characterise these minerals within the MAC and MBC samples. The results to date will be presented.

[1] Han Z., Sani B., Mrozik W., Obst M., Beckingham. B, Karapanagioti H. K. and Werner D. *Water Res.,* 2015, 70(1), 394.

[2] Han Z., Sani B., Akkanen J., Abel S., Nybom I., Karapanagioti H. and Werner D. *J. Hazard. Mater*., 2015, 286, 41.

[3] Han Z, Abel S, Akkanen J, Werner D. *J. Chem. Technol. Biotechnol*., 2017, 92, 1938.

Keywords: refinement, magnetite, Mossbauer

Structural modification of calcium hydroxyapatite cell induced by doping and co-doping of lead and cadmium heavy metal ions

M. Eddya and K. El-hami*

University of Hassan 1st, FPK, Laboratory of Nanosciences and Modeling, Khouribga, Morocco

** khalil.elhami@uhp.ac.ma*

Contamination of water and soil with heavy metals is particularly dangerous for living organisms. Different studies have shown that hydroxyapatite has a high removal capacity for divalent heavy metal ions in contaminated waters and soils [1]. We try by this study to shown de structural properties change after incorporating lead and cadmium ions into a calcium hydroxyapatite structure and his affect in optical properties. The calcium hydroxyapatite was obtained by ceramic route at high temperature, using $CaCO_3$ and $(NH_4)_2HPO_4$ as sources of calcium and phosphorus. Metal ion (Cd^{2+},Pb^{2+}) incorporation was carried out by dint of grinding and high temperature effect for remove all impurity. All sample were characterized by X-ray diffraction (XRD), and Uv-visible spectroscopy (Uv-visible) analysis to evaluate the structural and light behavior changes. A Rietveld refinement has shown that doping with these ions affects the volume unit cell of hydroxyapatite. The only phase present in pure hydroxyapatite sample stabilize in the hexagonal system and samples doped by (Cd^{2+},Pb^{2+}) stabilizes only in the orthorhombic phase. The Abstract photograph show the rietveld refinement profil matching of hydroxyapatite co-doped by (Cd^{2+},Pb^{2+}) metal ions.

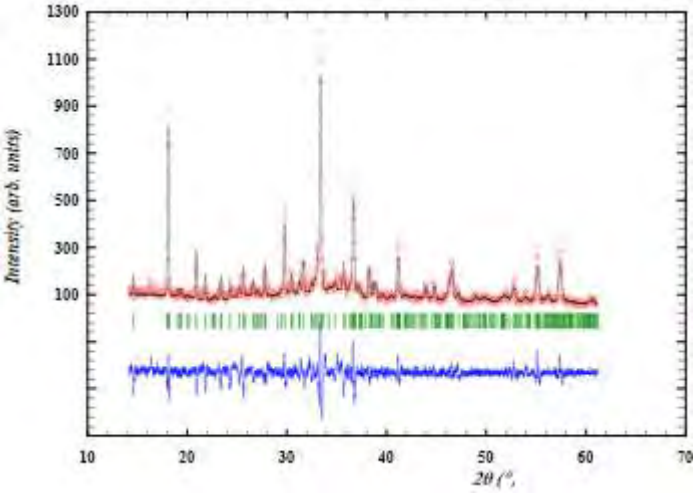

[1] CORAMI A, MIGNARDI S, and FERRINI V. *Journal of Colloid and Interface Science*, 2008, vol. 317, no 2, p. 402-408..

Keywords: Hydroxyapatite, Rietveld refinement, heavy metals ions

.

Multi-dimensional Rietveld method: Refining angular- and wavelength-dispersive neutron time-of-flight powder-diffraction data

P. Jacobs[a*], A. Houben[a], W. Schweika[b,c], A. L. Tchougréeff[a,d] and R. Dronskowski[a]

[a] *Chair of Solid-State and Quantum Chemistry, Institute of Inorganic Chemistry, RWTH Aachen University, 52056 Aachen, Germany*
[b] *Jülich Centre for Neutron Science JCNS and Peter Grünberg Institut PGI, JARA-FIT, Forschungszentrum Jülich, 52425 Jülich, Germany*
[c] *European Spallation Source ESS, SE-22100 Lund, Sweden*
[d] *A.N. Frumkin Institute of Physical Chemistry and Electrochemistry of Russian Academy of Science, 119002 Moscow, Russia*
**philipp.jacobs@ac.rwth-aachen.de*

With increasing solid-angle coverage and the trend to cost-effective designs of modern large-area detectors for neutron time-of-flight powder diffractometers, the present approach to generate one-dimensional data sets as used by existing Rietveld software necessitates more and more tradeoffs. Not only is the pristine data compromised by the reduction steps due to information loss and mixing effects but it is also negatively affected by the varying resolution which most likely results in complex peak-shape variations.

We thus present an extension of the well-established Rietveld refinement method for modeling two-dimensional neutron time-of-flight powder-diffraction data, i.e., intensity as a function of diffraction angle 2θ *and* wavelength λ.

For the future instrument POWTEX [1] at MLZ/FRM II and also for the future powder diffractometer DREAM at the ESS, this novel approach will fully exploit the varying resolution with 2θ and λ, which is otherwise lost when integrated by using today's standard refinement procedures.

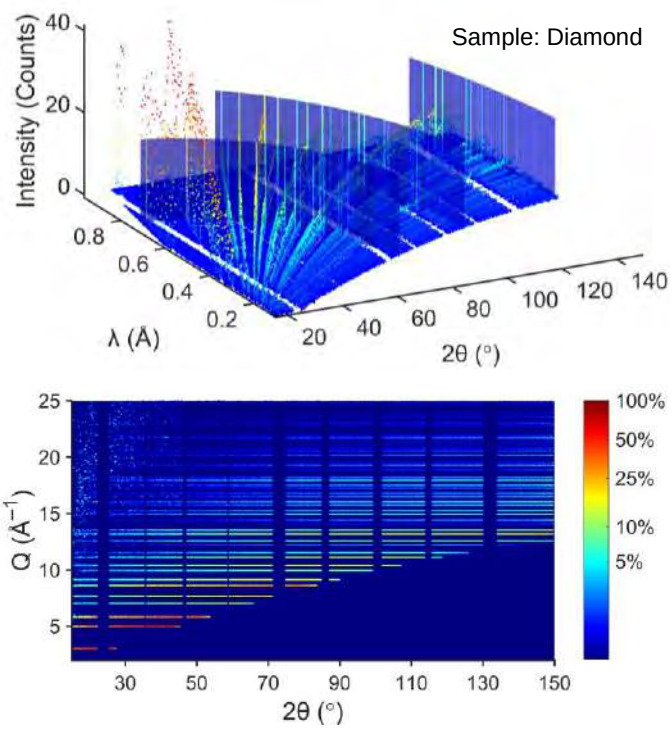

For a proof-of-concept, powder diffraction data of CuNCN, NAC and diamond were collected at POWGEN, SNS, Oak Ridge. The major steps of this new analysis are outlined below. For the refinement procedure, we consider a coordinate system that features axes running parallel and perpendicular to the *d*-spacing profiles and in which the POWGEN event data are binned linearly and logarithmically, respectively [2]. The two-dimensional (2D) pattern is corrected for 2D-background and calibrated by a 2D-vanadium pattern to account for detector efficiency and the wavelength-dependent intensity distribution. The 2D-analytical peak profile function describing the instrument characteristics has been established using reference data sets from diamond and NAC [3]. The 2D profile function is based on physical and geometrical properties of the instrument POWGEN and can now be provided to the user as an instrumental resolution file.

First steps towards and implementation of the multi-dimensional refinement procedure into common Rietveld program suites have been taken by incorporating a read-in-routine for GSAS II and allowing first basic refinements of these 2D data sets. This new development is open for joint activities with program authors of existing user software.

[1] Conrad H., Brückel T., Schäfer W. and Voigt, J. *J. Appl. Cryst*. **2008**, *41*, 836.
[2] Jacobs P., Houben A., Schweika W., Tchougréeff A.L. and Dronskowski R. *J. Appl. Cryst.* **2015**, *48*, 1627.
[3] Jacobs P., Houben A., Schweika W., Tchougréeff A.L. and Dronskowski R. *J. Appl. Cryst.* **2017**, *50*, 866.

Keywords: Rietveld refinement, two-dimensional, neutron diffraction

MS04 - Structure solution and refinement of complex structures

MSO4

Abstract Number	Title	Author	Affiliation
MS04 - K1	Balancing Powder Diffraction Data and Computational Data	Dr Jacco van de Streek	Avant-garde Materials Simulation
MS04 - K2	Combining the strengths of 3D single crystal electron diffraction and powder X-ray diffraction	Prof Xiaodong Zou	Stockholm University
MS04 - OR1	Crystal structure of complex coordination polymers solved from X-ray powder diffraction	Ms Luzia S. Germann	Max Planck Institute for Solid State Research
MS04 - OR2	Powder-X-ray diffraction analysis of the channel occupation in disordered η-Al5Fe2 and in three of its ordered low temperature phases η', η'' and η'''	Ms Hanka Becker	Technical University Bergakademie Freiberg
MS04 - OR3	Mechanochemical synthesis and structure solution of MOF-74 intermediates by powder solution methods	Mr Jethro Beamish-Cook	University of Reading
MS04 - P34	Structure, infrared and Raman spectroscopic studies of new BaSbV2/3MII1/3(PO4)2 (MII = Cu, Co, Mn) yavapaiite type-phases	Hajar Bellefqlh	University of Hassan II/Faculty of sciences Ben M'sik/ Chemistry departement
MS04 - P35	Study of cation site occupancies of apatite-type structures through powder X-ray diffraction and Rietveld refinement	Dr Zhili Dong	Nanyang Technological University
MS04 - P36	Rietveld refinement for a comercial Clinker, Appilacation for quantitative analysis	Mrs dounia Tlamsamani	University of Moulay Ismail
MS04 - P37	Structural review of tricalcium silicate, principal phase in cement clinker Portland	Mrs dounia Tlamsamani	University of Moulay Ismail
MS04 - P38	Challenging structure determination from powder data: Two pharmaceutical salts with Z' = 2	Mrs Carina Schlesinger	Goethe-Universität, Frankfurt am Main
MS04 - P39	Structure and spectroscopic characterization of the monoclinically distorted Double Perovskite, Sr2Co1-xFexTeO6 (x = 0.25, 0.5 and 0.75)	Ms Asmaa Zaraq	University Hassa
MS04 - P40	Structure solution of complex minerals from PD data with EDT-assisted full-symmetry Patterson function direct methods: The decrespignyite-(Y) case	Prof Jordi Rius	Institut Ciència de Materials de Barcelona (CSIC)
MS04 - P41	Porous complex structure of Eu(III)5(EG2-)6(Ac-)3 (EG = C2H4O2, Ac = CH3COO) by X-ray powder diffraction	Prof Michel Francois	Université de Lorraine
MS04 - P42	Crystal structure solution of complex corrosion products of heritage objects	Dr Sebastian Bette	Max Planck Institute for Solid State Research
MS04 - P43	Reference metal carboxylates for identification of metal soaps in historic paintings: synthesis and difficulties in the structure determination	Dr Jiri Plocek	Institute of Inorganic Chemistry of the Czech Academy of Sciences
MS04 - P44	Structural Trends in AReO4 Scheelite Type Oxides A = Na, K, Rb, Cs, Ag, Tl	Mr Sean Injac	University of Sydney
MS04 - P45	Influence of Microstructure on Symmetry Determination of Piezoceramics	Dr Manuel Hinterstein	Karlsruhe Institute of Technology
MS04 - P46	Crystal Structure of Calcium Vanadate-Phosphate Fluoride	Dr ZHILI DONG	Nanyang Technological University
MS04 - P47	Molecular packing determination of Organogel fibers	Mr Danilo Rosa Nunes	Laboratoire de Physique des Solides, CNRS, Université Paris-Sud, Université Paris- Saclay
MS04 - P48	The Study of Layered AA'BO4 Perovskites	Ms Yuanyuan Guo	University of St Andrews
MS04 - P49	High-resolution Powder Diffraction Study of Ca9La(VO4)7 Crystals	Prof Wojciech Paszkowicz	Institute of

MS04 - P50	Chemical characterization of dust calcium phosphate obtained from baghouse dust collector during drying process	Ms Ikram Labtaini	University of Hassan 1st, Faculty of Khouribga, Laboratory of Nanosciences and Modeling, Khouribga, BP.145
MS04 - P51	Crystal Structure of Aluminosilicate EU-12 Zeolite	Dr Sung Man Seo	Korea Institute of Geoscience and Mineral Resources (KIGAM)
MS04 - P52	Mineral phase composition of the surface mud sediment in the city of Ekaterinburg, Russia	Dr Daria Kiseleva	Institute of Geology and Geochemistry, UB RAS
MS04 - P53	The crystal structure of trisodium hexachloroiridate (Na3IrCl6)	Dr Martin Etter	Deutsches Elektronen-Synchrotron, Hamburg

Balancing Powder Diffraction Data and Computational Data

J. van de Streek[a*], Marcus A. Neumann[a]
[a] *Avant-garde Materials Simulation, Germany*
** jacco.vandestreek@avmatsim.eu*

In 2010, we validated dispersion-corrected density functional theory (DFT-D) against 200 molecular single-crystal structures and found that DFT-D is able to reproduce these crystal structures very accurately to within a root-mean-square Cartesian displacement of 0.1 Å [1]. DFT-D therefore grants us access to a "virtual single-crystal structure": a crystal structure that is very close to what the single-crystal structure of the polymorph would look like. This means that given a structural model obtained from powder diffraction data, a simple energy-minimisation with DFT-D provides us with a fairly accurate picture of the corresponding (unknown) single-crystal structure according to a quantum-mechanical energy potential that is independent of the diffraction experiment. If the structure from the Rietveld refinement and the energy-minimised structure agree within a certain tolerance, the structure is most likely to be correct. If the experimental structure distorts upon energy minimisation, then this is a strong hint that the experimental structure may be incorrect. Modified structural models can be prepared and tested against energy minimisations with DFT-D until a satisfactory structural model has been identified. The DFT-D energy minimisations were then used to validate (and, where necessary and possible, correct) 200 molecular crystal structures determined from powder diffraction data [2]. It was found that preferred orientation can correlate with the molecular geometry, obscuring the preferred orientation. We have meanwhile found three such cases where a seemingly negligible amount of preferred orientation leads to an incorrect molecular geometry that is easily detected with DFT-D, but may be very hard to detect by other methods.
Furthermore, it will be shown how the information about the molecular geometry from the DFT-D can be used to derive restraints and constraints for the Rietveld refinement, to arrive at a final structure that agrees extremely well with both the experimental powder diffraction data and the computational DFT-D data.
Recently, using a third set of 200 molecular crystal structures, we have established the tolerances required to determine possible missing space-group symmetry in crystal structures solved from powder diffraction data [3].

[1] Van de Streek J. and Neumann M. A. *Acta Cryst*., 2010, B66, 544.

[2] Van de Streek J. and Neumann M. A. *Acta Cryst*., 2014, B70, 1020.

[3] Hempler D., Schmidt M. U. and Van de Streek J. *Acta Cryst*., 2017, B73, 756.

Keywords: DFT-D, Rietveld refinement, validation

Combining the strengths of 3D single crystal electron diffraction and powder X-ray diffraction

Xiaodong Zou*
Department of Materials and Environmental Chemistry, Stockholm University, Sweden
** xzou@mmk.su.se*

Electron diffraction (ED) and powder X-ray diffraction (PXRD) are complementary for structural analysis of powders. Crystalline powders behave like single crystals in a transmission electron microscope and 3D rotation electron diffraction (RED) data can be collected [1]. Software developed for X-ray crystallography can be directly used for data processing and structure determination. 3D electron diffraction has shown to be powerful for structure determination and phase analysis of poly-crystalline materials [2]. One drawback is that the intensities of electron diffraction suffer from dynamical effects, which led to high R-values in the structure refinements. Another drawback is the electron beam damage, which reduces the data resolution and data completeness.

Powder X-ray diffraction, on the other hand, can overcome these drawbacks, and provide kinematic intensities and complete data. Therefore, Rietveld refinement is often combined with electron diffraction, to determine structural details including possible missing atoms/molecules and atom occupancies. I will present how 3D ED and PXRD are combined for structural analysis of novel polycrystalline materials such as zeolites [3], metal-organic frameworks and oxides (Fig. 1).

The recent development of continuous rotation electron diffraction (cRED) in combination with high sensitive and low background camera with short read-out time made it possible to collect high quality and nearly complete 3D cRED data in short time (15-150 seconds), which is especially useful for studying beam sensitive materials. A complete structure determination by electron diffraction may be achieved within a few hours, from data collection and processing to structure solution and refinement. The refined structural models are within an accuracy of 0.02 - 0.10 Å.

While PXRD provides the bulk information of a sample, ED represents only the local information. It is therefore important to combine the two techniques. An example will be given [4]. Finally I will show the latest development towards automated 3D ED data collection, so that a large number of particles can be analysed, and phase analysis will become possible.

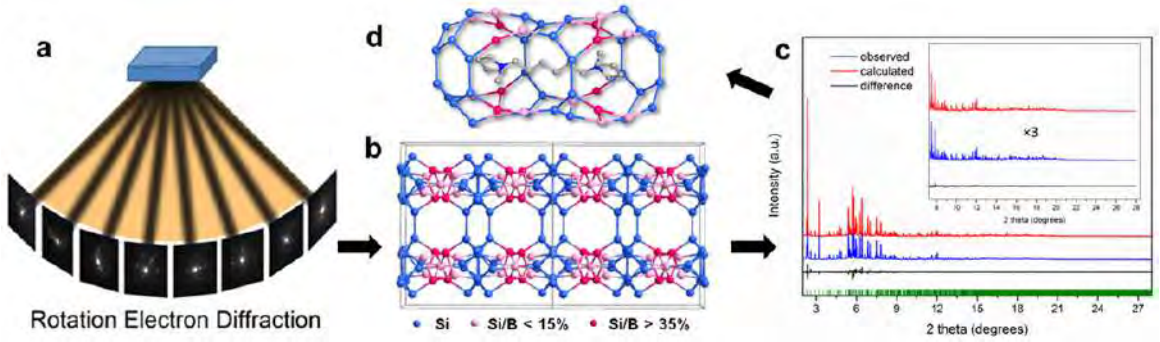

Fig. 1 (a) Illustration of rotation electron diffraction (RED) data collection (a). (b) A structural model is obtained from RED data using methods and software developed for single crystal X-ray diffraction. (c) The structure was refined against powder diffraction (c) from which the missing structural information (d, here an organic template in the pore) can be located. The example is a borosilicate zeolite EMM-26 [3]. Only the Si/B connections are shown, and oxygen atoms are omitted. Compared to those determined from the PXRD data, the atomic positions determined from the RED data differ on average by less than 0.04 Å for Si/B and 0.07 Å for oxygen; the locations and occupancies of boron are also similar, showing that accurate structural model can be obtained from the RED data.

[1] W. Wan, J. Sun, J. Su, S. Hovmöller, X. Zou, *J. App. Crystallogr.* 2013, 46, 1863.
[2] Y. Yun, X. Zou, S. Hovmöller, W. Wan, *IUCrJ*, 2015, *2*, 267.
[3] Guo, P.; Strohmaier, K.; Burton, A.W.; Zou, X. et al. *Inorg. Chem. Front.* 2016, *3*, 1444.
[4] Y. Yun, W. Wan, F. Rabbani, J. Su, S. Hovmöller, M. Johnsson, X. Zou *J. Appl. Crystallogr.* 2014, 47, 2048.

Keywords: continuous rotation electron diffraction (cRED), structure determination, Rietveld refinement

Crystal structure of complex coordination polymers solved from X-ray powder diffraction

L. S. Germann[a*], T. Neumann[b], S. Suckert[b], I. Jess[b], I. Moudrakovski[a], C. Näther[b] and R. E. Dinnebier[a]

[a] *Max Planck Institute for Solid State Research, Stuttgart, Germany,* [b] *University of Kiel, Kiel, Germany*

** l.germann@fkf.mpg.de*

To understand physicochemical properties of emerging materials such as coordination polymers, it is essential to know the crystal structure.[1] From systematic studies of these compounds it is possible to assign certain physical properties such as magnetism or luminescence to binding moieties, functional groups or the nature of metal cations.[2-4] As single crystals cannot always be obtained, X-ray powder diffraction is the method of choice for *ab initio* crystal structure solution.

Different coordination polymers with the general composition $[M^{2+}X_2L_n]$ {M = Co, Cd, Ni; X = NCS or halogens and L = pyridine or pyrazine derivatives} were synthesized from solution or thermal decomposition. For the latter no single crystals were obtained, thus the structures were solved from XRPD data. Novel and unexpected connectivities were observed for different coordination polymers. Further, symmetry reduction as well as symmetry relations were studied in coordination polymers.[1-3] Solid state NMR was used as complementary analytical method to confirm the derived crystal structures.

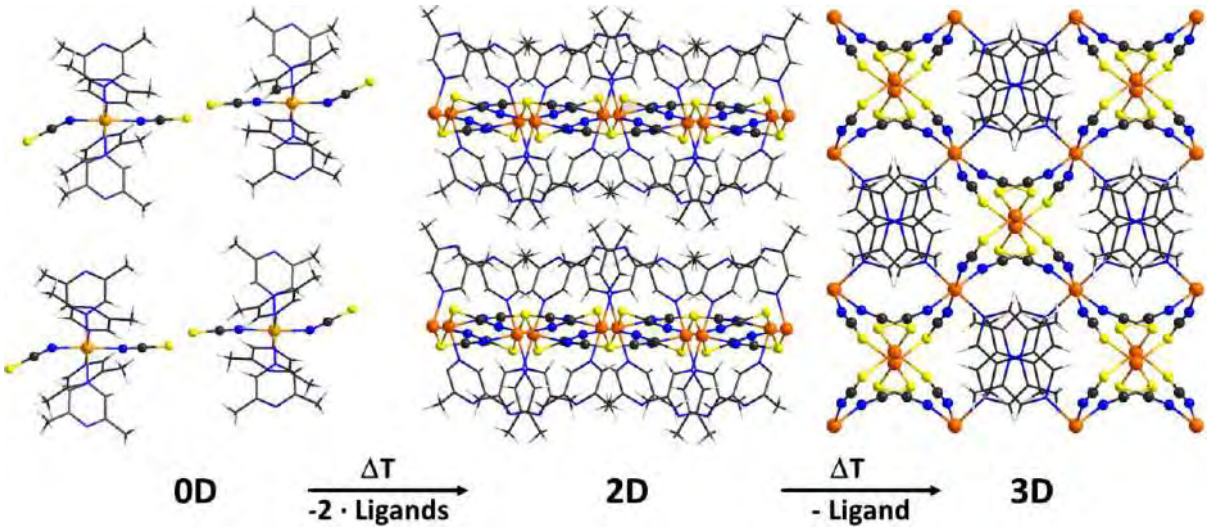

[1] C. Näther, I. Jess, L. S. Germann, R. E. Dinnebier, M. Braun and H. Terraschke, *Eur. J. Inorg. Chem*., **2017**, 1245.

[2] S. Suckert, M. Rams, L. Germann, R. Dinnebier, C. Näther, *Cryst. Growth. Des.,* **2017**, 17, 3997.

[3] Tristan Neumann, L. S. Germann, I. Moudrakovski, R. E. Dinnebier, C. dos Santos Cunha, H. Terraschke and C. Näther, *Z. Anorg. Allg. Chem.*, **2017**.

[4] S. Suckert, M. Rams, M. Boehme, L. S. Germann, R. E. Dinnebier, W. Plass, J. Werner and C. Näther, *Dalton Trans.*, **2016**, 45(45), 18190.

Keywords: X-ray Powder Diffraction, Complex Coordination polymers, Crystal Structure Solution

Powder-X-ray diffraction analysis of the channel occupation in disordered η-Al_5Fe_2 and in three of its ordered low temperature phases η', η'' and η'''

H. Becker[a*], A. Leineweber[a]
[a] *TU Bergakademie Freiberg, Institute of Material Science, 09599, Freiberg, Germany*
** hanka.becker@iww.tu-freiberg.de*

η-Al_5Fe_2 evolves during galvanizing processes [1] and bonding of steel and Al-alloy components [2] or occurs in bulk lightweight iron aluminides which provide excellent high temperature strength and corrosion resistance [3]. Successful processing and application in presence of the η phase require thorough understanding of the underlying crystal structures including low temperature ordering.
Arc- and induction-melted Al-Fe alloys with 70.6 at.% Al - 73.0 at.% Al [4,5] including a 72.8 at.% Al alloy [6] were used. After homogenization at 1000°C for 120 h and at 750°C for 48 h, the compact material was milled by hand. The powders were annealed at 750°C for 24 h followed by heat treatment at 250°C for 624 h or 350°C for 332 h. During all heat treatments, the material was encapsulated in fused silica tubes under Ar atmosphere which were quenched in water after each heat treatment step. Powder-X-ray diffraction (P-XRD) was conducted using a Bruker D8 diffractometer working in Bragg-Brentano reflection geometry being equipped with a Co tube, a quartz-crystal Johannson monochromator in the primary beam and a LYNXEYE position sensitive detector for recording the diffracted radiation. The P-XRD data were evaluated by Rietveld refinement using TOPAS and Jana2006 software to determine channel site occupation parameters of the disordered η phase quenched from 750°C and the ordered crystal structures forming at 350°C and 250°C.

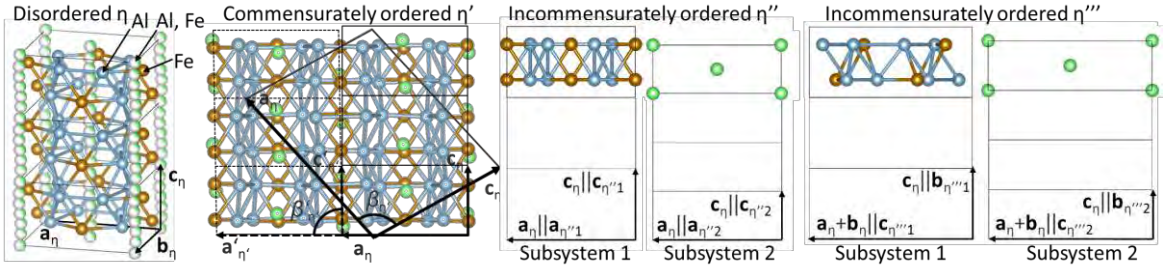

The high temperature η phase has been previously described as orthorhombic (*Cmcm*) structure consisting of a framework structure of Al and Fe atoms forming channels along the **c** axis with disorder of Al atoms [7]. Revision revealed a composition-dependent mixed occupation of the channels by both Al and Fe atoms with a number of atoms per channel and unit cell *N* of approx. 1.5 in the whole homogeneity range [5]. Below about 350 °C, four distinctly different phases exhibit long-range order of the channel atoms and three of four are reported here [4,5]. The monoclinic (*C*2/*c* symmetry) crystal structure of the previously reported [8] η'-Al_8Fe_3 phase was confirmed and refined [4]. A smaller value of *N* of 1.33 is accompanied by a 1.4% decrease of the unit cell volume. The Al-poorest and Al-richest of the low-temperature phases, η″ and η‴ can be characterized as incommensurately modulated composite crystal structures [5]. In both phases, the first composite subsystem contains atoms of the framework structure generating channels which are filled by atoms described by the second composite subsystem. The subsystems of the η″ phase have orthorhombic superspace groups *Xmcm*(00*g*)0*s*0 and *Immm*(00*g*)0*s*0 keeping the basic metric of the parent η phase. The subsystems of the η‴ have monoclinic superspace groups $P2_1/c(0b0)00$ and $P2_1/c(0b0)s0$. The lattice correspondence of subsystem 1 to the parent η phase is $\mathbf{a}_{\eta'''1}=1/2(\mathbf{a}_\eta+\mathbf{b}_\eta)$, $\mathbf{b}_{\eta'''1}=\mathbf{c}_\eta$ and $\mathbf{c}_{\eta'''1}=\mathbf{a}_\eta+\mathbf{b}_\eta$. The channels are differently correlated in η″ and η‴ phases which is attributed to different Fe content in the channels inherited from the channel occupation in the η phase although *N* remains approx. 1.5.

[1] Takata N., Nishimoto M., Kobayashi S. and Takeyama M., *Intermetallics*, 2015, 67, 1.
[2] Watanabe M., Feng K., Nakamura Y. and Kumai S., *Mater. Trans.*, 2011, 52, 953.
[3] Hirose S., Itoh T., Makita M., Fujii S., Arai S., Sasaki K. and Saka H., *Intermetallics*, 2003, 11, 633.
[4] Becker H., Amirkhanyan L., Kortus J. and Leineweber A., *J. Alloys Compd.*, 2017, 721, 691.
[5] Becker H. and Leineweber A., *Intermetallics*, 2018, 93, 251.
[6] Li X., Scherf A., Heilmaier M. and Stein F., *J. Phase Equilib. Diff.*, 2016, 37, 162.
[7] Burkhardt U., Grin Y., Ellner M. and Peters K., *Acta Cryst. B*, 1994, 50 313.
[8] Okamoto N. L., Okumura J., Higashi M. and Inui H., *Acta Mater.*, 129, 2017, 290.

Keywords: η-Al_5Fe_2, channel occupation, ordering

Mechanochemical synthesis and structure solution of MOF-74 intermediates by powder solution methods

J.Beamish-Cook[a*], P.Vaqueiro[a], K.Shankland[a]
[a] *School of Chemistry, Pharmacy, and Food University of Reading, UK*
** j.beamish-cook@pgr.reading.ac.uk*

Metal-organic frameworks (MOFs) are materials with potential applications ranging from fuel cells [1] to drug delivery [2]. MOFs are constructed by connecting metal centres through bridging linkers to form porous frameworks. Solvothermal synthesis is the most common route for MOF synthesis, but reaction times are long and often use large volumes of toxic solvents to produce small amounts of product. Mechanochemistry offers a scalable and environmentally-friendly alternative which is increasingly being used. As it usually produces polycrystalline powders unsuitable for single-crystal analysis, crystal structure determination must be performed directly from powder X-ray diffraction data, using programs such as DASH or EXPO.

The isoreticular MOF-74 family is attractive for drug delivery applications due to its tuneable pore sizes, coupled with the presence of uncoordinated metal sites. We have succeeded in the mechanochemical synthesis of MOF-74 ((Zn_2(dhta); [dhta =2,5-dihydroxyterethphalate]) and of an isoreticular MOF-74 framework, by replacing dhta with a longer linker, 4,4'-[oxalylbis(imino)]bis(2-hydroxybenzoate). During the synthesis of these materials, a number of intermediate phases are formed with increasing grinding times, prior to the formation of the final framework. We have used laboratory powder X-ray diffraction data, together with high-resolution synchrotron data collected on beamline I11 at the Diamond Light Source, to solve the crystal structures of these intermediates, using direct methods (EXPO [3]) and simulated annealing (DASH [4]). We have discovered that during the mechanochemical synthesis of MOF-74, a solvate of the linker, $(H_4dhta)_2(DMF)_3$, is formed after only two minutes of grinding. This rapidly reacts further to produce two polymorphs of a one-dimensional coordination polymer, $Zn(H_2dhta)(DMF)_2(H_2O)_2$, after 4 and 15 minutes of grinding, with two additional phases forming between 50 and 110 minutes, prior to the crystallization of MOF-74. These results demonstrate the feasibility of determining the structure of intermediates formed during the mechanochemical synthesis of MOFs, even when these are present in a mixture of phases.

[1] Adhikari A. K. and Lin K. S., *Journal of Nanoscience and Nanotechnology*, 2014, 14, 2709-2717.
[2] Miller S. R., Heurtaux D., Baati T., Horcajada P., Greneche J. M. and Serre C., *Chemical Communications*, 2010, 46, 4526-4528.
[3] Altomare A., Cuocci C., Giacovazzo C., Moliterni A., Rizzi R., Corriero N. and Falcicchio A., *Journal of Applied Crystallography*, 2013, 46, 1231-1235.
[4] David W. I. F., Shankland K., van de Streek J., Pidcock E., Motherwell W. D. S. and Cole J. C., *Journal of Applied Crystallography*, 2006, 39, 910-915.

Keywords: MOF, Powder solution, mechanochemistry

Structure, infrared and Raman spectroscopic studies of new $BaSb^{V}_{2/3}M^{II}_{1/3}(PO_4)_2$ (M^{II} = Cu, Co, Mn) yavapaiite type-phases

H. Bellefqih*, A. Aatiq

University Hassan II of Casablanca, Faculty of Sciences Ben M'Sik, Chemistry Department. Laboratory of Physical-Chemistry of Applied Materials, Avenue Idriss El Harti, B.P. 7955, Casablanca, Morocco

**Hajar.bellefqih@gmail.com*

Barium double phosphates, with general formula $Ba^{II+}M^{IV+}(PO_4)_2$ (M^{IV} = Ti, Zr, Hf, Ge, Mo, Sn) [1-7] belonging to the yavapaiite family, have been studied over the two last several decades for their potential applications as ionic conductors, catalysts, ion exchanges, and also used in medical imaging to reduce the exposure of the patient to X-rays while maintaining the structural features of the X-ray image. These types of compounds crystallize in the ordinary yavapaiite (Y.O.) structural-type with the *C*2/*m* space group. Their structure is formed by layers of Ba^{II} cations in tenfold coordination, alternating with dense slabs built up of corner-connected of $M^{IV}O_6$ octahedra and PO_4 tetrahedra. Two years ago, we have studied, the effect of substitution of M^{IV+} tetravalent cation, within the yavapaiite $Ba^{II+}M^{IV+}(PO_4)_2$ by tri- $_{0.5}M'^{III+}$and penta-valent $_{0.5}M''^{V+}$. Results of investigations led some of us to synthesis and characterization of $Ba(M^{V+}_{0.5}M'^{III+}_{0.5})(PO_4)_2$ (M^{V} = Sb M^{III} = Fe) phases series [8]. In a continuation of our scientific search, we synthesized, for a first time, new $BaSb^{V}_{2/3}M^{II}_{1/3}(PO_4)_2$ (M=Co^{II},Cu^{II},Mn^{II}) yavapaiite-phases containing a divalent cation. The three materials, which are abbreviated as [Cu], [Co] and [Mn], were obtained by solid state reaction in air atmosphere at 1173 K. Their structures are characterized by the Rietveld refinement analysis of their XRD powder data. Structural analysis showed that all samples are isostructural and crystallizes with a monoclinic symmetry (space group *C*2/*m*, Z = 2). Obtained unit cells parameters are a = 8.0692(4)Å; b = 5.2348(3)Å ;c =7.8784(4)Å ; β= 95.291(3)°for [Cu] a = 8.1446(5)Å; b = 5.2220(4)Å ;c = 7.8554(5)Å; β = 94.688(4) for [Co], and a = 8.1981(3)Å; b = 5.23996(18)Å ;c = 7.8808(3)Å; β = 94.4523(19)°for [Mn]. Sb^{V+} and M^{II+} cation, in $BaSb^{V}_{2/3}M^{II}_{1/3}(PO_4)_2$, are statistically distributed over the octahedral sites. Raman and Infrared spectroscopic study was used to obtain further structural information about the nature of bonding in selected compositions.

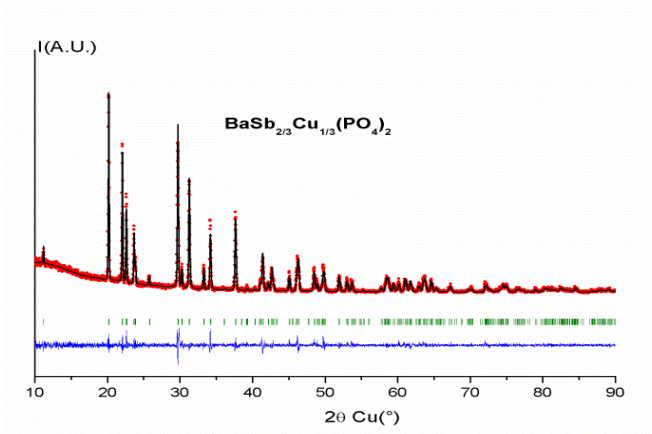

[1] Blasse, G. and Dirksen G. J. *J. Chem. Phys. Lett.,* 1979, 62, 19.
[2] Leclaire, A., Borel, M. M., Chardon, J. and Raveau, B. *J. Solid State Chem.,* 1995,116, 364-368.
[3] Popa, K., Wallez, G., Bregiroux, D.and Loiseau, P. *J. Solid State Chem.,* 2011, 184, 2629-2634.
[4] Zhao, D., Zhang, H., Xie, Z., Zhang, W. L., Yang, S. L.and Cheng, W. *D. Dalton Trans.,* 2009, 27, 5310-5318.
[5] Popa, K., Konings, R. J. M., Beneš, O., Geisler, T.and Popa, A. F. *J. Thermochimica. Acta.,* 2006, 451,1-4.
[6] Zhao, D., Ma, F. X., Yang, H., Wei, W., Fan, Y. C., Zhang, L.and Xin, X. *J. Phys. Chem. Solid.,* 2016, 99, 59-65.
[7] Popa, K., Wallez, G., Bregiroux, D.and Loiseau, P. *J. Solid State Chem.,* 2011, 184, 2629-2634.
[8] Aatiq, A., Tigha, M.R., Fakhreddine, R., Bregiroux, D.and Wallez, G. *J. Solid. State. Sci.,* 2016, 58, 44-54.

Keywords: Yavapaiite-structure, Raman and IR spectroscopy, Rietveld refinement.

Study of cation site occupancies of apatite-type structures through powder X-ray diffraction and Rietveld refinement

Z. L. Dong
School of Materials Science and Engineering, Nanyang Technological University, 50 Nanyang Avenue, Singapore 639798
zldong@ntu.edu.sg

Apatite-type materials can be used as bioceramics, phosphors, ultrafast laser hosts and ionic conductors, depending on their chemical composition. The control of cation site occupancy in apatite-type materials is of great importance for tuning their properties. With the aid of powder X-ray diffraction, Rietveld refinement and high resolution microscopy imaging techniques, it is possible to retrieve information on cation order-disorder, and cation site occupancies of apatite-type ceramics. This work reports the analysis of cation site occupancies of silicate apatite and phosphate apatite with different cation valences.

Apatite material has a general formula $A^{I}_4A^{II}_6(BO_4)_6X_2$, in which A can be occupied by large mono-, di-tri- and tetra-valent cations, B by metalloids, like Si, P, V, As, and X by halides and anion radicals, such as F, Cl, I, O, OH. $P6_3/m$ (hexagonal symmetry) is the most common space group for apatites. In our experiments, apatites with different compositions were synthesized, each of the apatites incorporated two or three of the following cations: Cs, Sr, Ca, Pb, Y, Ce, Nd, Eu, Yb and Th. Our studies show that when A^{I} and A^{II} are filled by divalent cations, smaller cations prefer occupying A^{I} sites rather than A^{II} sites. On the other hand, larger cations prefer A^{II} sites to A^{I} sites [1]. When A^{I} and A^{II} are occupied by cations of different valences, both charge and size need to be considered for the interpretation of site occupancies [2]. In the above analysis, bond valence calculations can help understand whether the X (e.g., oxygen) located in the channel is overbonded or underbonded [3].

The cation site occupancy also influences the HRTEM image contrasts. Therefore, our research results can provide guidance to the experimental HRTEM studies to identify the cation locations in apatite-type materials when site occupancy varies from one region to another. The control of cation distribution in apatites can further help to optimise apatite performance in real-world applications.

[1] Dong. Z. L., White, T. J., *Acta Crystallographica B*, 2004, 60, p138-145.
[2] Shen Y. Q., Chen R., Sun H. D., Tok A., Dong Z. L. *Journal of Solid State Chemistry*, 2010, 183, 3093-3099.
[3] Brown I. D. and Altermatt. D., *Acta Crystallographica B.* 1985, B41, 244-247.

Keywords: apatite, site occupancy, bond valence

Rietveld refinement for a comercial Clinker, Appilacation for quantitative analysis

Dounia Tlamsamani[a]*, K. Yamni[a], M. Angeles G. De La Torre[b], D. Londoño-Zuluaga[b]
[a] *Inorganique Chemistry Dpt, Faculty of sciences, Moulay Ismail University, Meknes Morocc*
[b] *Dpt. Química Inorgánica, Cristalografía y Mineralogía, Facultad de Ciencias, Universidad de Málaga Spain*
** dtlamsamanis@edu.umi.ac.ma*

Cement Portland is the most usual construction material in the world, it's a hydraulic sociable, made from a mixture of calcite and clay brought to 1450°, but surprisingly its composition steel misunderstood. Clinker, which is the main constituent of cement, is composed from four various phases are: impure tricalcium silicate (C3S) called alite; impure di-calcium silicate (C2S) or belite, tricalcium aluminate (C3A) and tetracalcium alumino-ferrite (C4AF).

Recently, the use of Rietveld refinement of powder diffraction data increased in cement components quantitative analysis. The aim of the structure determination by XRD is to know the crystallographic parameters of the compound under study, which mean the symmetry of the lattice, the space group and the mesh content as well as the positions.

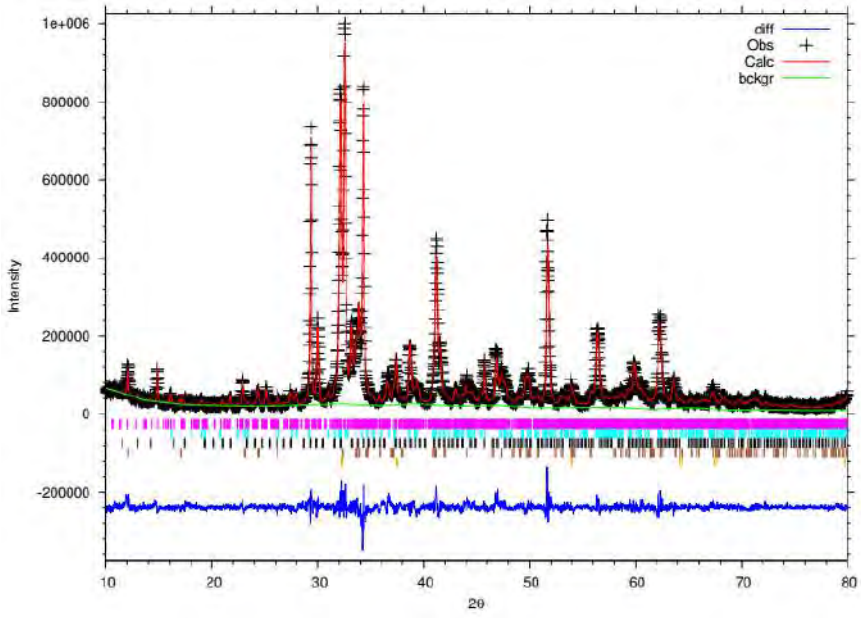

Fig: Gsas refinement of an industrial clinker cement Portland

Keywords: cement Portland, calcite, clay, clinker, phase, alite, belite, rietveld refinement, and XRD

NOTE: Abstract must be in English and converted to a PDF before uploading to the abstract submission system.

Structural review of tricalcium silicate, principal phase in cement clinker Portland

Dounia Tlamsamani[a]*, K. Yamni[a], M. Angeles G. De La Torre[b], D. Londoño-Zuluaga[b]
[a] *Inorganique Chemistry Dpt, Faculty of sciences, Moulay Ismail University, Meknes Morocc*
[b] *Dpt. Química Inorgánica, Cristalografía y Mineralogía, Facultad de Ciencias, Universidad de Málaga Spain*
** dtlamsamanis@edu.umi.ac.ma*

In our day, cement became the most usual material in our life, which explains the big number of studies done on it and its phases to understand its morphology by controlling the mineralogy of cement phases.
Clinker is the principal compound of cement Portland, it composed from four phases which crystallized in different forms: alite (impure C3S) has seven polymorphs between ambient temperature and 1400°C, belite (impure C2S) has five, aluminate (C3A) is always in the same shape and alumino-ferrite (C4AF) has no polymorphs. So this variability judges the difficulty of cement phase's analysis.

From 1952 to now (2018) uncountable number of study are worked on cement and clinker phases, to understand the reactions of their constituents and the arrangement of atomic positions, but the structure of the four main phases of clinker are still misunderstood.

Keywords: cement Portland, clinker, phase, alite, belite, atomic positions and structure**.**

NOTE: Abstract must be in English and converted to a PDF before uploading to the abstract submission system.

Challenging structure determination from powder data: Two pharmaceutical salts with *Z*' = 2

Carina Schlesinger[a*], Michael Bolte[a], Martin U. Schmidt[a]
[a]*Institut für anorganische und analytische Chemie, Goethe-Universität, Frankfurt am Main, Germany*
** c.schlesinger@chemie.uni-frankfurt.de*

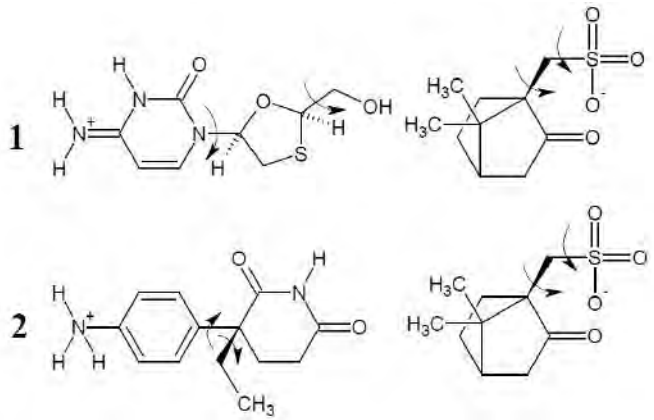

Structure solution of molecular compounds from powder data by real-space methods becomes challenging when the total number of parameters (for molecular position, orientation and intramolecular torsions) exceeds a value of 20 to 25 [1,2]. The structure determination from powder data of two pharmaceutical camphor-sulfonate salts is described, each with four molecules per asymmetric unit on general position: Lamivudine camphorsulfonate (**1**, $P2_1$, $Z = 4$, $Z' = 2$; 31 parameters), and Aminoglutethimide camphorsulfonate (**2**, $P2_1$, $Z = 4$, $Z' = 2$; 31 parameters). The cations and anions have two intramolecular degrees of freedom each (marked by arrows in the figure).

The structure of **1** could be solved without problems by *DASH* [3] using simulated annealing; in contrast, the structure of **2** resisted all attempts for structure solution from powder data. [4]

By chance, a single crystal of **2** was obtained and the structure was determined by single crystal X-ray diffraction. A post-analysis revealed that the failure of the real-space method was not caused by an insufficient powder data quality or not by wrong assumptions on the molecular geometry. The structure could only be solved from powder data by reducing the number of parameters from 31 to 21 by treating the molecules as rigid and fixing the position of one of the two cations. This shows that the simulated-annealing procedure reached its limits in this particular case.

[1] P. Fernandes, K. Shankland, A. J. Florence, N. Shankland, A. Johnston, *J. Pharm. Sci*. 2007, 96, 1192.
[2] W. I. F. David, K. Shankland, *Acta Cryst.* 2008, *A64*, 52.
[3] W. I. F. David, K. Shankland, J. Van de Streek, E. Pidcock, W. D. S. Motherwell, J. C. Cole, *J. Appl. Cryst*. 2006, *39*, 910.
[4] C. Schlesinger, F. Fischer, M. Bolte, M.U. Schmidt, *submitted*.

Keywords: X-ray powder diffraction, **Structure determination**, **Pharmaceutical compounds**

Structure and spectroscopic characterization of the monoclinically distorted Double Perovskite, $Sr_2Co_{1-x}Fe_xTeO_6$ (x = 0.25, 0.5 and 0.75)

A.Zaraq[a*], B. Orayech[b], J. M. Igartua[c], A. El bouari[a].

a. *Laboratory of Physico-Chemical of Materials Applied (LPCMA), Faculty of Sciences Ben M'sik, University HASSAN II of Casablanca, 20670, Morocco*
b. *CICenergigune, Albert Einstein 48, 01510 Miñano, Alava, Spain.*
c. Fisika Aplikatua II Saila, Zientzia eta Teknologia Fakultatea, Euskal Herriko Unibertsitatea, P.O.Box 644, Bilbao 48080, Spain.
** assmaa.zaraq@gmail.com*

Double perovskites are of interest due to their diverse properties that are of potential use in technological applications [1]. In this work we have been interested in double perovskites based on tellurium that exhibit interesting magnetic properties [2]. The compounds $Sr_2Co_{1-x}Fe_xTeO_6$ with (x = 0, 0.25, 0.5, 0.75 and 1) were synthesized by conventional solid state reaction techniques at 1100°C in air atmosphere, as polycrystalline powders. Their crystallographic structures were determined at room temperature from X-ray powder diffraction (XRPD) data using the Rietveld analysis.The Rietveld refinements studie showed that the composition [x=0] and the others compositions with [x=0.25, 0.5, 0.75 and 1] crystallize in monoclinically system with P12/n and I 2/m space group respectively. Cell parameters when x = 0.25, 0.5 and 0.75 are a = 5.6382(1), b = 5.6069(1), c = 7.9191(1), β = 90.0302(1); a = 5.6268(1), b = 5.6026 (1), c = 7.9158(1), β = 89.9925 (1) and a = 5.6076(1), b = 5.5930(1), c = 7.9056(1), β = 90.0064(1), respectively. A Raman spectroscopic study was used to obtain further structural information about the nature of bonding in the selected compositions and confirm that a phase transitions occurred depending on the addition of Iron; from monoclinic P121/n1 to monoclinic I12/m1 symmetry (M–M transition). The analysis of refined crystallographic parameters in $Sr_2Co_{1-x}Fe_xTeO_6$ (x = 0.25; 0.5 and 0.75) indicates that the (Co^{2+}/Fe^{2+}) and Te^{6+} are octahedrally coordinated with the oxygen atoms. The $(Co/Fe)O_6$ and TeO_6 octahedra are alternatively connected and extended in three dimensions. The oxygen atoms connect the $(Co/Fe)O_6$ and TeO_6 octahedra along the three directions.

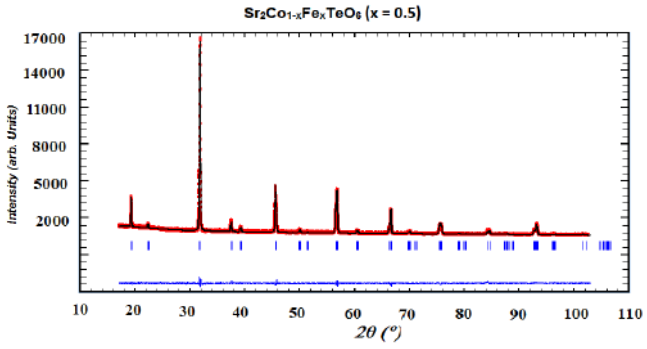

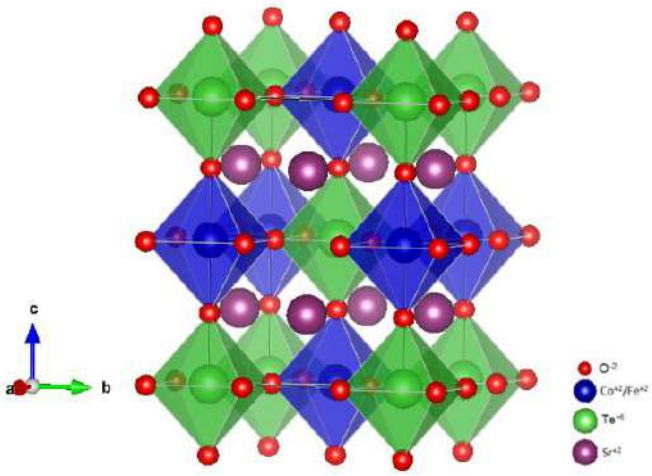

.

[1] B. Orayech, I. Urcelay-Olabarria, G. A. Lopez, O. Fabelo, A. Faik and J. M. Igartua, Dalton Trans (2015) 44 13867-13880.

[2] B. Orayech, A. Faik, G. A. Lopez, O. Fabelo and J. M. Igartua, J. Appl. Cryst. (2015) 48 318-333.

Keywords: $Sr_2Co_{1-x}Fe_xTeO_6$ double perovskites oxides; X-ray diffraction; Rietveld refinements; Raman spectroscopy; crystal structure.

Structure solution of complex minerals from PD data with EDT-assisted full-symmetry Patterson function direct methods: The decrespignyite-(Y) case

J. Rius[a*], F. Colombo[b], O. Vallcorba[c], E.Mugnaioli[d], M. Gemmi[d]
[a] *Materials Science Institute of Barcelona (CSIC), Catalonia, Spain*
[b] *CICTERRA-CONICET. FCEFyN – Universidad Nacional de Córdoba, Argentina*
[c] *Experiments Division-ALBA Synchrotron Light Source-CELLS, Barcelona,Spain*
[d] *Center for Nanotechnology Innovation@NEST, Istituto Italiano di Tecnologia, Pisa, Italy*
** jordi.rius@icmab.es*

In the last years, electron diffraction tomography (EDT) has become a routine tool for collecting 3D diffraction data of complex minerals ordered only in the nanometric range [1,2,3]. Often, these minerals are based on self-assembly of metal clusters via H bond networks and, consequently, are prone to vacuum induced dehydration and electron beam damage [4,5] . Although recent technical advances have considerably reduced the damage either by using weaker electron beams or by reducing the exposure time taking advantage of fast read-out detectors enabling 'continuous' scans, there are still cases where part of the structure can be significantly altered by the ED experiments. In such cases application of Patterson-function direct-methods (PF_DM) [6,7] to EDT data is more complicate since significant parts of the structure will not show up in the Fourier map.

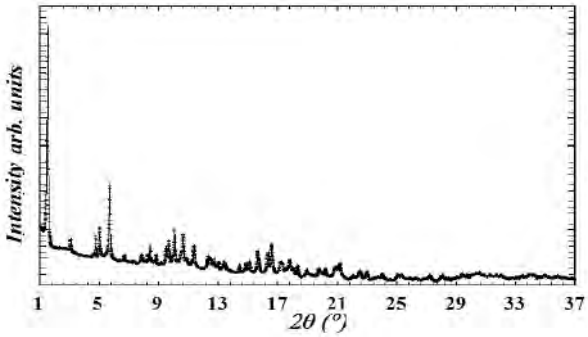

Powder diffraction pattern of decrespignyite (λ= 0.6191 Å)

In any case, even if EDT data fail to supply the structure model, they do provide relevant information on the metric and the space group symmetry which can then be used to advantage by PD full-symmetry DM like the S_P-FT algorithm [8] implemented in XLENS_PD6 [9]. Unlike direct-space structure solution methods, DM algorithms are especially well-suited for crystal structures containing cations with irregular or unpredictable coordination polyhedra or when some structural disorder is present. This will be illustrated on the solution of the unknown crystal structure of decrespignyite-(Y), a new complex copper yttrium rare-earth carbonate chloride from Paratoo (South Australia) first characterized by Wallwork, Kolitsch, Pring and Nasdala [10]. The public financial support through project MAT2015-67953-P of MINECO/FEDER is gratefully acknowledged.

[1] Kolb, U., Gorelik, T., Kübel, C., Otten, M. T. and Hubert, D. *Ultramicroscopy*, 2007, 107, 507.
[2] Kolb, U., Gorelik, T. & Otten, M. T. *Ultramicroscopy*, 2008, 108.
[3] Kolb, U., Mugnaioli, E., Gorelik, T. E. *Cryst. Res. Technol.*, 2011, 46, 542-554.
[4] Capitani, G.C., Mugnaioli, E., Rius, J., Gentile, P., Catelani, T., Lucotti, A., Kolb,U. *American Mineralogist,* 2014, 99, 500.
[5] León-Reina, L., Cabeza, A., Rius, J., Maireles-Torres, P.J., Alba-Rubio, A.C., López-Granados, M. *Journal of Catalysis*, 2013, 300, 30.
[6] Rius, J. *IUCrJ* , 2014. 1, 291.
[7] Rius, J., Mugnaioli, E., Vallcorba, O., Kolb, U. *Acta Cryst*., 2013, A69, 396.
[8] Rius, J. *Acta Cryst*., 2011, A67, 63–67
[9] retrievable from https://departments.icmab.es/crystallography/software
[10] Wallwork K., Kolitsch U., Pring A., Nasdala L. *Mineralogical Magazine*, 2002, 66, 181.

Keywords: direct methods, ab-initio structure solution, powder diffraction

Porous complex structure of $Eu(III)_5(EG^{2-})_6(Ac^-)_3$ (EG = $C_2H_4O_2$, Ac = CH_3COO) by X-ray powder diffraction

Michel François[a]*, Amal Abdallah[b], Voraksmy Ban[c], Romain Sibille[c] and Souad Ammar[b]

[a]*Institut Jean Lamour, CNRS et Université de Lorraine, BP 70239, Vandoeuvre-lès-Nancy, 54506, France*
[b]*ITODYS, CNRS-UMR 7086 et Université Paris Diderot, 15 rue Jean Antoine de Baïf, Paris, 75205, France*
[c]*Paul Scherrer Institut, 5232 Villigen PSI, Switzerland*

The polyol process [1] is used for synthesizing nanoparticles composed of metals, metal oxides or hydroxides. Competition between reduction and hydrolysis is easily controlled by adjustment of the hydrolysis ratio. Alkoxides or intermediate alkoxy-salt complexes precursors subject to these reactions are formed in situ. Such precursors with magnetic elements (3d, 4f) are also studied for their magnetic properties linked to their crystallographic structure [2]. Here, the compound **$Eu(III)_5(EG)_6(Ac)_3$** was obtained using hydrate europium (III) acetate (Ac^- = $C_2H_3O_2^-$) and ethyleneglycol (EG = $C_2H_6O_2$) as reactants. A structural model was achieved *ab initio* from synchrotron powder diffraction data (SLS, Switzerland) using optimization methods and FOX program. The model was refined using the Fullprof_suite software. EG and Ac molecules were considered as a rigid bodies. The final Rietveld plot is shown in the figure. We obtained a Metal-Organic Framework (MOF) with a zeolitic porous structure as shown on the figure. This highly 3D arrangement with EG connector is rather astonishing as only lower dimensional structures (1D or 2D) have been formed with such connectors to the best of our knowledge. Numerous porous MOFs have been built from much more complicated and heavy connectors as polycarboxylate (di or tri carboxylate) and polyamine with O and N atoms acting as electron donors, respectively. Here the connector EG is very simple and associated with Ac. The pore size in the structure is about 80 $Å^3$ and thus is enough for a potential insertion of small molecules (H_2, CO, CO_2…). Especially H_2 could lower the valence from III to II and, in turn, modify the magnetic properties. Hydrogen sensing could be a potential application of this compound.

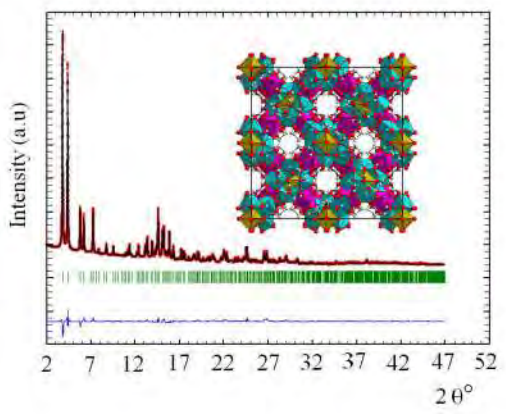

The structure has a relatively high complexity, with a huge unit volume of V = 23657 $Å^3$ (Dx = 2.838 g/cm^3), but fortunately a high symmetry (SG = *Ia*-3*d*, n°230). The model contains three independent sites for the Eu atoms, Eu1 (96*h*), Eu2 (48*g*), Eu3 (16*a*), and three independent molecules in the general position 96*h*, two molecules of ethylene glycolate and one acetate molecule. Thus, the lattice contains 160 Eu trivalent cations, 192 ethylene glycolate and 96 acetate molecules. The following structural formula '$Eu_5(EG)_6(Ac)_3$' with Z = 32 is deduced from crystallography only. Some difficulty for obtaining the true chemical formula is due to the fact that EG and Ac molecules have quasi identical molecular weight. Thus, exact interpretation of the weight loss in thermogravimetric analysis was quite difficult. Also, indexing such a big lattice led to space group determination ambiguity, especially between *Ia*-3*d* and *I*-43*d*. Mössbauer spectroscopy clearly indicates that europium is trivalent in this structure.

[1] Poul L., Noureddine Jouini and Fernand Fiévet, Chem. Mater. 2000, 12, 3123-3132
[2] A. Abdallah, T. Gaudisson, R. Sibille, S. Nowak, W. Cheikhrouhou-Kouba, K. Shinoda, M. François and S. Ammar, Dalton Trans., 2015, 44, 16013–16023

Keywords: porous MOF, polyol process, trivalent europium

Crystal structure solution of complex corrosion products of heritage objects

S.Bette[a*], R.E. Dinnebier[a], G. Eggert[b]
[a] *Max Planck Institute for Solid State Research, Stuttgart, Germany*
[b] *State Academy of Art and Design, Stuttgart, Germany*
** S.Bette@fkf.mpg.de*

Heritage objects are stored in museums and collections for centuries. During that time the objects are exposed to aggression by moisture and atmospheric gases like CO_2 or acetic and formic acid, which is emitted by wooden showcases and furniture. This leads to various corrosion phenomena like the occurrence of efflorescence crystals (Fig 1a) on calcareous objects, which has been known as Byne's disease[1] since the 19th century. Corrosion leads to severe damage of the objects, but sometimes has also been intended, e.g. for the production of synthetic pigments (Fig 1c)[2] like Verdigris. This is a collective term for green and blue copper based pigments known since antiquity, in particular for neutral and basic copper(II) acetates.
Crystallographic knowledge of the corrosion products supports the detailed understanding of corrosion processes or ancient pigment production as it is the basis for reliable reference data for phase identification and quantitative phase analysis. Crystal structure solution of these phases, however, is not trivial, as single crystals usually can neither be found nor grown, the phase compositions of the corrosion products aren't known exactly and the simultaneous occurrence of acetates, formates and nitrates impedes structure solution and refinement from XRPD data.
In our current work, we present the crystal structure solution of various verdigris and efflorescence phases. Indexing, structure solution and refinement was complicated for various reasons: The unit cell volumes of the investigated phases were up to 3500 Å³, crystal symmetry ranged from triclinic to trigonal and in case of the efflorescence phases differentiation between acetate, nitrate and formate was sometimes impossible, even when using the difference Fouríer map. A pronounced tendency towards polymorphism additionally impeded the structure elucidation. In consequence many correlated methods like IR- and Raman-spectroscopy, thermal, elemental and EDX analysis or ion chromatography had to be employed to derive phase compositions or coordination modes that could be used for con- and restraints in the structure solution or refinement or to confirm the obtained structural model. This lead to the successful determination of the crystal structures of the pigment phases: $Cu(CH_3COO)_2$, $1Cu(CH_3COO)_2{\cdot}2Cu(OH)_2$[3] (Fig 1d), $2Cu(CH_3COO)_2{\cdot}1Cu(OH)_2{\cdot}5H_2O$[4] and of the efflorescence phases: $Ca(CH_3COO)_2{\cdot}0.5H_2O$, $Ca(CH_3COO)_2{\cdot}0.25H_2O$, α-, β-, high-temperature-γ-, low-temperature-γ-$Ca(CH_3COO)_2$[5], $Ca(CH_3COO)(HCOO){\cdot}H_2O$, $Ca_2(CH_3COO)(HCOO)(NO_3)_2{\cdot}4H_2O$[6] (Fig 1b).

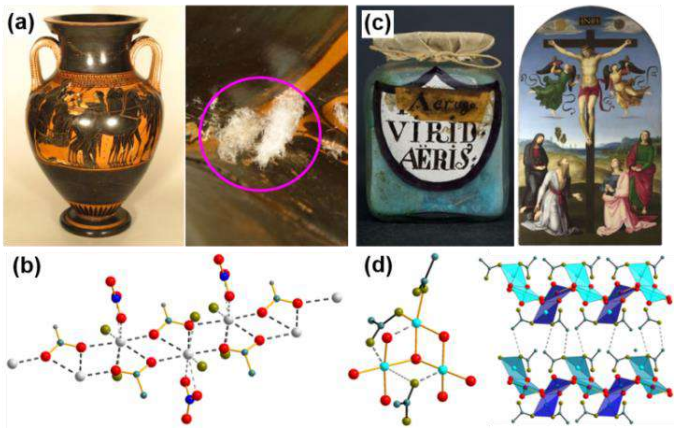

Figure 1
(a) Attic black figured amphora with white efflorescence crystals,
(b) main motif of the crystal structure of the efflorescence phase $Ca_2(CH_3COO)(HCOO)(NO_3)_2{\cdot}4H_2O$,
(c) historic vessel containing verdigris and historic painting by Raphael © National Gallery London made by using verdigris pigments,
(d) motifs in crystal structure of $Cu_3(CH_3COO)_2(OH)_4$, a blue copper pigment.

[1] Byne L.F.G. *Journal of Conchology* 1899, 9, 172.
[2] Scott D.A., Taniguchi Y.and Koseto E. *Rev. Conserv.* 2001, 2, 73.
[3] Bette S., Kremer R.K., Eggert G., Tang C. C. and Dinnebier R.E. *Dalton Trans.* 2017, 46, 14847.
[4] Bette S., Kremer R.K., Eggert G. and Dinnebier R.E. *Dalton Trans.* submitted for publication.
[5] Bette S., Müller, M.X., Eggert G. and Dinnebier R.E. *Chem. Eur. J.* 2018, in preparation.
[6] Bette S., Eggert G., Fischer A., Stelzner J. and Dinnebier R.E. *Corr. Sci.* 2018, 132, 68.

Keywords: corrosion products, crystal structure solution, correlated methods

Reference metal carboxylates for identification of metal soaps in historic paintings: synthesis and difficulties in the structure determination

Jiří Plocek[1*], Assel Zhankina[1,2], Petr Bezdička[3], Silvie Švarcová[3], Michal Dušek[4]
[1]*Institute of Inorganic Chemistry of the Czech Academy of Sciences, Czech Republic*
[2]*Karaganda State University of the name of academician E.A. Buketov, Kazakhstan*
[3]*Institute of Inorganic Chemistry of the Czech Academy of Sciences, ALMA Laboratory, Czech Republic*
[4]*Institute of Physics of the Czech Academy of Sciences, Czech Republic*
**plocek@iic.cas.cz*

Study of saponification phenomena in paintings is a worldwide concern of high relevance today. Saponification is one of the undesirable degradation processes, leading to loss of mechanical integrity and changes of appearance of historic and modern paintings. [1] Some pigments (typically Pb-, Zn- or Cu-based) react with fatty acids in oils used as binding media, resulting in formation of carboxylates - metal soaps. Despite the increasing interest, there is still a gap of knowledge of both, the mechanism of formation and the nature of various metal soaps. Missing structural data of pure reference compounds complicate the identification of metal carboxylates in secondary soaps in paintings as well as the description of the behaviour of particular component in model experiments.

There is a lack of relevant and reliable reference data concerning the crystal structures of metal soaps. There is only few information in the literature and structural databases. Pb carboxylates were studied recently by Martinez-Casado et al [2] including some attempts to prepare single crystals of *C8 – C10* carboxylates. All other structures were deduced by analogy. Similar attempts were performed for Cu carboxylates [3]. However, in the case of zinc, there are no information about structures of higher carboxylates.

We prepared three series of samples of Pb, Zn and Cu carboxylates starting from *C6* to *C18*. We studied and evaluated their X-ray powder patterns to create sets of reference data for determining the products of degradation of subsequent paint layers

Then we attempted to prepare single crystals of selected members e.g. Pb(*C16*)$_2$, Pb(*C18*)$_2$, Zn(*C18*)$_2$, Cu(*C18*)$_2$. However, the properties of as prepared single crystals were not sufficient for successful determination of their structure. A very long unit cell parameter (5 nm), presence of a heavy atom (Pb) bound to a very long chain of light atoms (*C16 – C18*) producing structural disorder caused these complications. Even in the case of electron diffraction, the very long unit cell parameter hindered the analysis by exceeding the instrumental limits of this technique.

[1] Cotte M., Checroun E., De Nolf W., et al., *Studies in Conservation,* 2017, 62(1), 2.

[2] Martınez-Casado F. J., Ramos-Riesco M., Rodrıguez-Cheda A., et al., *Phys. Chem. Chem. Phys.*, 2017, 19, 17009.

[3] Ramos-Riesco M., Martínez-Casado F. J., Rodríguez-Cheda J. A., et al., *Cryst. Growth Des.,* 2015, 15, 2005.

Keywords: metal carboxylates, saponification, paintings degradation

Structural Trends in *A*ReO_4 Scheelite Type Oxides *A* = Na, K, Rb, Cs, Ag, Tl

S. Injac[a], C. Chay[b], M. Avdeev[c], B. J. Kennedy[a]*

[a] *School of Chemistry, University of Sydney, Australia*
[b] *Faculty of Natural and Environmental Sciences, University of Southampton, UK*
[c] *Australian Nuclear Science and Technology Organisation, Lucas Heights, Australia*
* *brendan.kennedy@sydney.edu.au*

This works details the structural investigation of a number of perrhenate (Re^{7+}) compounds taking the form *A*MO_4 where *A* is a 1+ cation, in particular A = Na, K, Rb, Cs, Ag, Tl. Re is often studied as a non-radioactive analogue to Tc, given their similar range of oxidation states and ionic radii resulting in similar chemical behaviour. Evidence is emerging that this may not be the case for solid state materials. The *A*ReO_4 oxides were studied in order to allow for comparison with the analogous pertechnetates as well as to investigate structural trends within the scheelite class of oxides. These compounds were synthesised by neutralisation of perrhenic acid with the appropriate metal carbonate and investigated by a combination of powder synchrotron x-ray diffraction, neutron powder diffraction and single crystal x-ray diffraction both under ambient and variable temperature conditions. The increasing size of the *A*-cation drives a series of structural phase transitions with increased distortion of the unit cell with increasing *A* cation radius; for *A* = Na, Ag, K, Rb the structures crystalise in the archetypal scheelite structure in the tetragonal space group $I4_1/a$, while $CsReO_4$ crystallises as a distorted scheelite in the orthorhombic space group *Pnma*. Upon heating $CsReO_4$ undergoes a 1st order phase transition to a tetragonal structure. A similar transition was observed for the series $Rb_{1-x}Cs_xReO_4$ which induces this transition through chemical pressure as a result of doping at the *A* site. $TlReO_4$ was determined to be monoclinic in space group $P2_1/a$ at room temperature by a combination of x-ray powder, neutron powder and x-ray single crystal diffraction techniques. Variable temperature PXRD studies reveal the presence of a re-entrant phase transition at 380 and 100 K to a tetragonal $I4_1/a$ phase, these tetragonal phases were determined to be isostructural with the only difference being rotation of the tetrahedra. All phase transitions were determined to be 1st order and reversible with a slight thermal hysteresis. Interestingly no orthorhombic structure was observed over this temperature range. Increased tetrahedral distortion was observed in $TlReO_4$ compared to the group 1 metals, suggesting that the Tl $6s^2$ lone pair electrons play a role in the observed distortion. In order to probe the possibility of a charge transfer between Tl and Re driving the re-entrant phase transition DC magnetic susceptibility data were collected, $TlReO_4$ was found to be diamagnetic for all temperatures, suggesting that the Re cation remains 7+ and no charge transfer occurs. This is further supported by the small change (4%) in tetrahedral volume across the transitions, which is inconsistent with a Re^{7+} → Re^{5+} transition.

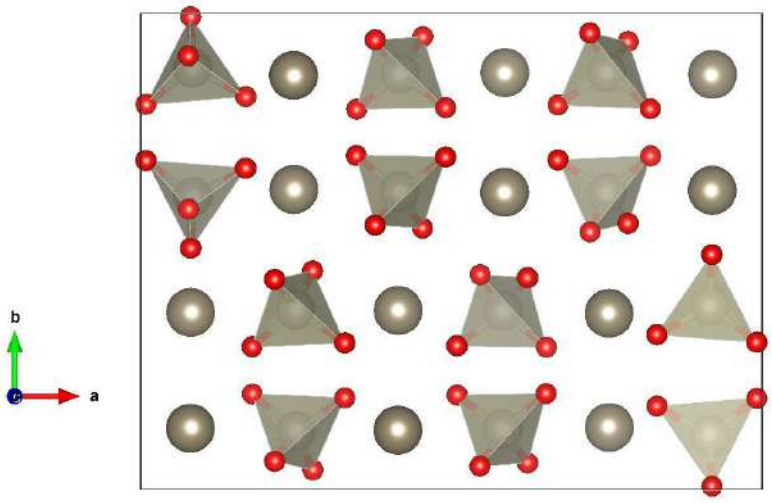

Keywords: Oxides, Phase Transitions, Scheelite

Influence of Microstructure on Symmetry Determination of Piezoceramics

M. Hinterstein[a,b], H.E. Mgbemere[c], M. Hoelzel[d], E. Adabifiroozjaei[b], C.C. Sorrell[b] and M. Hoffman[b]

[a] *Institute for Applied Materials, Karlsruhe Institute of Technology, 76131 Karlsruhe, Germany*
[b] *School of Materials Science and Engineering, UNSW Sydney, Sydney, Australia*
[c] *Department of Metallurgical and Materials Engineering, University of Lagos, Akoka, Lagos, Nigeria*
[d] *Heinz Maier-Leibnitz Zentrum, Technische Universität München, Garching, Germany*

Frequently symmetry determination in studies is based on the discussion of agreement factors or the quality of the refinements, rather than on the basis of physical arguments. Especially in the field of piezoceramics this can be observed in the discussion whether monoclinic symmetry can be observed or not.

In this study we could show with temperature-dependent high-resolution X-ray and neutron diffraction that based on agreement factors alone the physical origin of observations cannot be revealed. Only in combination with additional electron microscopy and electron probe microanalysis we could elucidate that a segregation of substituents results in a complex reflection splitting and phase coexistence that can be misinterpreted as monoclinic symmetry. This single-phase monoclinic *Pm* model is able to perfectly reproduce the diffraction patterns and is known from literature [1,2]. A model with phase coexistence of two classical orthorhombic *Amm*2 phases can reproduce the diffraction data with equal accuracy.

This demonstrates the need of comprehensive analyses with complementary methods to cover a broad range of length scales as well as considering both average and local structure. The conclusions drawn from this work will have an impact on a broad range of research areas where inhomogeneities cannot be ruled out. The underlying mechanisms of the extraordinary properties of some functional materials originate not just in their structures but also their complex microstructures. Consequently, knowledge of both features of materials may be essential for the exploitation and development of their functionalities as well as improvement of material properties.

[1] H. E. Mgbemere, M. Hinterstein, and G. A. Schneider, J. Eur. Ceram. Soc. **32**, 4341 (2012).

[2] L. Liu, X. Ma, M. Knapp, H. Ehrenberg, B. Peng, L. Fang, and M. Hinterstein, Europhys. Lett. **118**, 47001 (2017).

Crystal Structure of Calcium Vanadate-Phosphate Fluoride

Z. L. Dong and T. J. White
School of Materials Science and Engineering, Nanyang Technological University, 50 Nanyang Avenue, Singapore 639798
zldong@ntu.edu.sg

Apatite-type materials $A^{I}_4A^{II}_6(BO_4)_6X_2$ have two unique cations sites "A^{I}" and "A^{II}", which can host large mono-, di- tri- and tetra-valent cations. The average cation radii will affect the twist angle and lattice constants. However, there are few reports on the influence of "B' site substitutions on the twist angle and lattice parameters. It is believed that the lattice constant variation as a function of "B" site substitutions may not follow the same twist-angle model as proposed for "A" site [1]. This work reports our results on the crystal chemistry of synthetic apatite $Ca_{10}(V_xP_{1-x}O_4)_6F_2$ obtained through the crystal structure characterization using Rietveld refinement and high-resolution transmission electron microscopy. The quantification of vanadium/phosphorus partitioning in "BO_4" tetrahedra showed that equilibrium with more than 70% substitution of phosphorous by vanadium was difficult to achieve unless longer annealing (about one week at 900°C) was employed [2 -5]. In comparison with the apatites with different ionic radii at "A^{I}" and "A^{II}" sites, $Ca_{10}(V_{0.9}P_{0..1}O_4)_6F_2$ apatites with different ionic radii at "B" site show little twist angle variation for the whole series, which indicates that the dilation of unit cell constants is mainly due to the expansions of "BO_4" tetrahedra when "A" site cation is fixed.

[1] T. J. White, Z. L. Dong, Acta Crystallographica B, 2003, 59 (1), 1 - 16.
[2] Z. L. Dong, J. Kim, S. H. Lim, K. Laursen and T. J. White, Proceedings of the 2nd International Conference on Materials for Advanced Technologies, MRS Singapore, Dec 2003, Singapore, p736.
[3] P. H. J. Mercier, Z. L. Dong, T. Baikie, Y. L. Page, T. J. White, P. S. Whitfield, L. D. Mitchel, Acta Crystallographica B, 2007, 63, 37 - 48.
[4] Z. L. Dong and T. J. White, Microscopy and Microanalysis 14 (Suppl2), 2008, 210 – 211.
[5] Z. L. Dong, "X-ray diffraction, Rietveld crystal structure refinement and high-resolution transmission electron microscopy of nano-structured materials" in Handbook of Nanoceramics and Their Based Nanodevices, Vol. 3, p 303-336. American Scientific Publishers 2009, ISBN: 1-58883-117-5.

Keywords: apatite, Rietveld refinement, twist angle, high-resolution transmission electron microscopy.

Molecular packing determination of Organogel fibers

D.R. Nunes[ab*], L. Bouteiller[b], P. Foury-Leylekian[a] and P.A. Albouy[a]
[a] *Laboratoire de Physique des Solides, CNRS, Université Paris-Sud, Université Paris-Saclay, 91 400, Orsay, France*
[b] *Sorbonne Université, CNRS, Institut Parisien de Chimie Moléculaire (IPCM), Equipe Chimie des Polymères, F-75005 Paris, France*
** danilo.nunes@u-psud.fr*

Organogels are formed by the unidirectional self-assembly of low molecular weight gelators (LMWG) in organic solvents. They are obtained by the dissolution of LMWGs at high temperature and the subsequent cooling results in the formation of network of fibers, strands, or tapes that trap the solvent. [1-4]
Up to now determining which solvent forms a gel with a given LMWG is largely based on trial-and-error. Several efforts have been made to rationalize this choice and one of us devised a method based on the Hansen Solubility Parameters to determine a thermodynamic domain that includes the liquids that are gelled by a specific LMWG. [5-6]
A deeper understanding of the process involved implying a knowledge of the molecular packing within the LMWG macrostructures that grow during gelation. We observed for instance that within particular thermodynamic gelation domains, x-ray powder patterns of partially dried gels from different liquids may present different structures.
The amount of dried fibers that can be recovered from a gel is quite limited which obliges to use small-diameter glass capillaries as sample holders; this procedure is also necessary to maintain fibers in contact with the solvent vapour. We used a home-made powder diffractometer in parallel beam geometry and mounted on a rotating anode generator. Good-quality powder patterns could be collected within a few hours with a glass capillary filled sample. The automatic indexation is made with the program DIVCOL [7] and the simulation of the molecular packing is obtained by simulating annealing using the EXPO 2014 crystallography suite. [8-9]
We will show how this procedure allowed a better understanding of how the molecular packing of LMWGs within the fibers can get correlated with the Hansen thermodynamic gelation domain.

[1] P. Terech and R. G. Weiss, Chem. Rev., 1997, 97, 3133–3160. [2] O. Gronwald, E. Snip and S. Shinkai, Curr. Opin. Colloid Interface Sci., 2002, 7, 148. [3] N. M. Sangeetha and U. Maitra, Chem. Soc. Rev., 2005, 34, 821. [4] M. George and R. G. Weiss, Acc. Chem. Res., 2006, 39, 489. [5] M. Raynal and L. Bouteiller, Chem. Commun., 2011, 47, 8271. [6] J. Bonnet, G. Suissa, M. Raynal and L. Bouteiller, Soft Matter, 2014, 10, 3154. [7] A. Boultif and D. Louër, J. Appl. Cryst. 2004, 37, 724. [8] A. Altomare, C. Cuocci, C. Giacovazzo, A. Moliterni, R. Rizzi, N. Corriero and A. Falcicchio, J. Appl. Cryst., 2013 46, 1231-1235. [9] Altomare, A., Corriero, N., Cuocci, C., Moliterni, A., Rizzi, R. J. Appl. Cryst. 2013, 46, 779-787.

Keywords: Organogel, simulated annealing, structural resolution.

The Study of Layered $AA'BO_4$ Perovskites

Y. Guo, A. K. Cochrane, M. Telfer, K. J. Cordrey, P. Lightfoot*
School of Chemistry, University of St Andrews, UK
** pl@st-andrews.ac.uk*

Compared with cubic ABO_3 perovskites, layered perovskites contains a number of outstanding polar and ferroelectric materials.[1] In 2016, Cochrane *et al.*[2] showed that the new Fujii $NdBaInO_4$ structure was more like another series of layered perovskites which derives from slicing the perovskite parent phase along *cis*-vertices and might regarded as '<110>-cut' layered perovskites.[3] Both structure types are 'sliced' through octahedral edges rather than corners. Cochrane *et al*. successfully synthesized a new Fujii structure with a Sc^{3+} ion in place of In^{3+} at the B site, $NdBaScO_4$ and a series $LnBaScO_4$, and discussed the close relationship between the Fujii structure $NdBaInO_4$, $NdBaScO_4$ and the '<110>-cut' layered perovskite structure $LaTaO_4$. It can be seen that the ABO_4 structure can be transformed to the $AA'BO_4$ type by insertion of an additional A' layer. The aim of this project is trying to modify A, A' or B sites to find polar and ferroelectric materials like O-$LaTaO_4$.

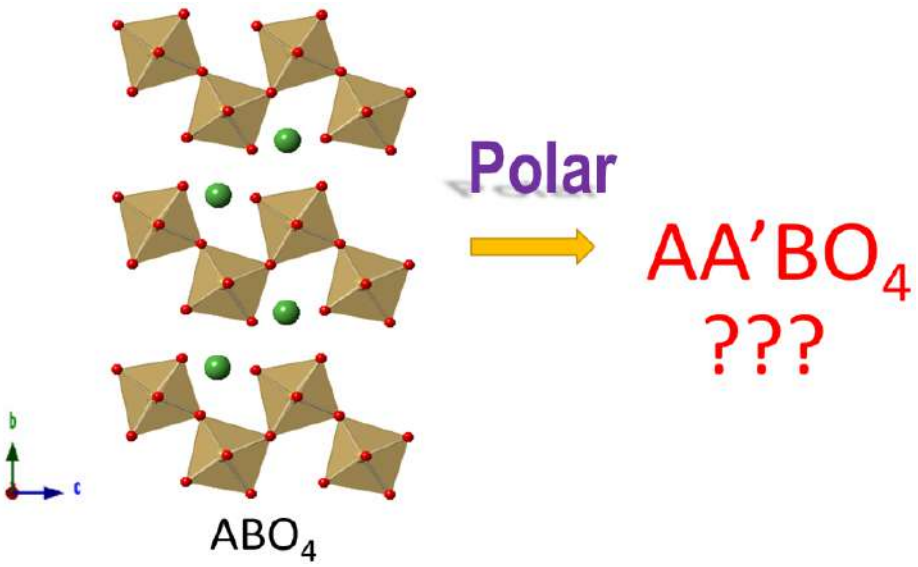

[1] Benedek N.A., Rondinelli J.M., Djani H., Ghosez P. and Lightfoot P. *Dalton Trans.*, 2015, 44, 10543.

[2] Cochrane A.K., Telfer M., Dixon C.A.L., Zhang W., Halasyamani P. S., Bousquet E. and Lightfoot P. *Chem. Commun.*, 2016, 52, 10980.

[3] Lichtenberg F., Herrnberger A. and Wiedenmann K. *Prog. Solid State Chem.*, 2008, 36, 253.

Keywords: Layered perovskites, Fujii $NdBaInO_4$ structure, Ferroelectric

High-resolution Powder Diffraction Study of $Ca_9La(VO_4)_7$ Crystals

W. Paszkowicz[a*], A. Shekhovtsov[b], M. Kosmyna[b], A. Behrooz[a], A. Fitch[c]
[a] *Institute of Physics PAS, PL-02668 Warsaw, Poland,*
[b] *Institute for Single Crystals, NAS of Ukraine, 61001, Kharkov, Ukraine*
[c] *European Synchrotron, ESRF, Grenoble, France*
* *paszk@ifpan.edu.pl*

Whitlockite ($Ca_9(MgFe)(PO_4)_6PO_3OH$, *R*3*c* space group) is one of multiple hydrated phosphate minerals. Whitlockite-related phosphates, vanadates and arsenates form an extended family of compounds, such as $Ca_9X(VO_4)_7$ (with trivalent X atoms), or $Ca_{10}M(VO_4)_7$ (with monovalent M atoms), all crystallizing in structures derived from that of whitlockite. A number of non-hydrated multicomponent members of this family are frequently term ased merrillites. Those belonging to a subfamily of $Ca_9R(VO_4)_7$ formula (R = Y or La - Lu) are considered for applications in optoelectronic devices (white-light emitting diodes, lasers). Their structure is most similar to $Ca_9Fe^{3+}(PO_4)_7$ phosphate, reported in Ref. [1]. In the $Ca_9R(VO_4)_7$ disordered structure, the R atoms substitute a small part of the Ca atoms at the Ca sites; the partial occupancy value at the given site depends on the R atom.

The structure of $Ca_9La(VO_4)_7$, synthesized by solid state reaction, has been studied for the first time, using a conventional laboratory diffractometer, in Ref. [2]. In this work, Czochralski-grown undoped and Yb-doped $Ca_9La(VO_4)_7$ single crystals are studied. The fine-grained samples were prepared using an agate mortar. The crystal structure is refined, using the powder diffraction data collected at a high-resolution synchrotron beamline ID22 (ESRF, Grenoble, France); the wavelength of 0.354201(4) Å was applied. Details of the crystal growth and diffraction measurement have been described in a high-resolution diffraction study of $Ca_9Gd(VO_4)_7$ [3]. The crystal structure was refined by the Rietveld method using the FullProf v.5.30 program [4]; the result for the undoped sample is illustrated in the figure, presenting a comparison of the low-angle part of the experimental and model pattern.

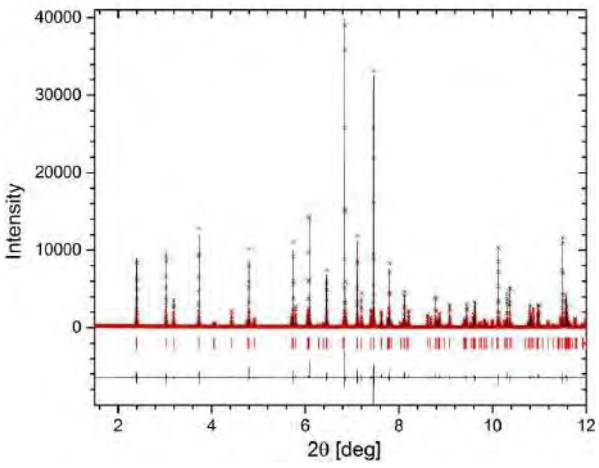

Values of lattice parameters and other details of the refined structure are consistent with literature data. The advantages of the use of the high-resolution synchrotron beam include the excellent counting statistics and improved resolution: leading to peak overlap being considerably smaller in respect to that observed in laboratory data. Consequently, a high-accuracy information on the crystal structure is obtained.

[1] Lazoryak B. L., Morozov V. A., Safonov M. S. and Khasanov S. S., *Mater. Res. Bull*. 1995, 30, 1269.

[2] Belik A.A., Morozov V.A., Khasanov S.S. and Lazoryak B.L., *Crystallogr. Rep*. 1997, 42 (5), 751.

[3] Paszkowicz W., Shekhovtsov A., Kosmyna M., Loiko P., Vilejshikova E., Minikayev R., Romanowski P., Wierzchowski W., Wieteska K., Paulmann C., Bryleva E., Belikov K. and Fitch A., *Nucl. Instrum. Meth. Phys. Res. B* 2017, 411, 100.

[4] Rodríguez-Carvajal J., *Physica B* 1993, 192, 55.

Keywords: vanadate, whitlockite, high resolution

Chemical characterization of dust calcium phosphate obtained from baghouse dust collector during drying process

I. Labtaini[a*], K. Elhami [a]
[a] *University of Hassan 1st, Faculty of Khouribga, Laboratory of Nanosciences and Modeling, Khouribga, BP.145, Morocco*
** ikram.labtaini@gmail.com*

Baghouse dust collectors are using in the unit of drying located in Beni-Idir Khouribga Morocco, to remove phosphates particles from dust air drying before its expellation through the smokestacks. This energetic process is accompanied by the generation of particle puffs emitted during pulse jet cleaning of the baghouse phosphate dust collector. A small dust phosphate part penetrates to the inside of the filter bag and causes the clogging depth. During maintenance of baghouse phosphate dust collectors, 3 samples were collected: untreated calcium phosphate dust, calcium phosphate dust from the outside of filter media and calcium phosphate dust from the inside of filter media which causes clogging depth. Thus the aim of this study is the chemical characterization of the three samples. Chemical investigation was conducted using: scanning electron microscopy (SEM) coupled with the energy dispersive X-ray spectroscopy (EDS), X-ray diffraction (XRD) and X-ray fluorescence (XFR), Raman spectroscopy and Infrared spectroscopy (FTIR). The obtained results suggested that there were differences observed regarding the chemical parameters during the drying process.

Keywords: Dust calcium phosphate, Drying Process, Characterization

Crystal Structure of Aluminosilicate EU-12 Zeolite

S. M. Seo*, I.-M. Kang
Advanced Geo-materials R&D Department, Pohang Branch, Korea Institute of Geoscience and Mineral Resources, Pohang 37559, Republic of Korea
** smseo@kigam.re.kr*

EU-12 Zeolite was first reported by Araya and Lowe in 1986 [1,2], but its structure has remained unknown. In this study, crystal structure of EU-12 synthesized in the mixed Ch^{+}-Na^{+}-Rb^{+} structure-directing agent system has been determined by synchrotron powder X-ray diffraction (XRD) and Rietveld analyses. The micropore volume of its proton form (H-EU-12) determined by N_2 adsorption is 0.09 cm^3/g, which, in principle, makes EU-12 fall into the microporosity boundary between channel-based small-pore and medium-pore zeolites. The synchrotron powder XRD pattern of dehydrated H-EU-12 was successfully indexed as orthorhombic, with *a* = 17.89757 Å, *b* = 28.87473 Å, and *c* = 7.46527 Å. The systematic extinctions were consistent with *Amam* as the best space group. Then, a model for the SiO_2 structure with six symmetry-independent tetrahedral atoms (T-atoms, T = Si or Al) and 14 such O atoms was achieved by direct methods using the program EXPO2014 [3]. After being optimized using the program GULP [4], this model was used as a starting point for the Rietveld refinement of the structure of dehydrated H-EU-12. Final R_{wp} and R_p values of 7.5 and 5.7% were achieved, respectively. The average T-O bond length (1.596 Å) and average O-T-O and T-O-T angles (109.47° and 156.5°, respectively) were found to be in good agreement with those expected for zeolitic materials. The framework structure of EU-12 (framework type code ETL [5]) zeolite can be constructed using two composite building units (CBUs), that is, [5^4] (*mor*) and [$4^1 5^2 8^2$] (*t-kdk*) CBUs. Each *mor* CBU connects to two neighbor *mor* CBUs by sharing 5-ring edges in the opposite direction to form a zigzag chain along the *c* axis. This chain connects to *t-kdk* CBUs by sharing 5-ring edges perpendicular to *c* axis to form the repeating unit of the EU-12 structure. Then, the two repeating units connects to each other via their 8-rings to form a [$4^2 5^4 8^2$-a] (*ygw*) unit [6], coherently creating the EU-12 sheet. Finally, each sheet extends along the *b* axis and is linked to each other in the *ab* plane via T-O-T linkages across mirror planes that are perpendicular to the *a* axis to complete the framework structure. EU-12 has a new unusual framework topology that contains two types of straight 8-ring (4.6×2.8 and 5.0×2.7 Å) channels along the *c* axis, as well as sinusoidal 8-ring (4.8×3.3 Å) channels along the *a* axis. While the smaller 8-ring channels intersect with sinusoidal channels, the other larger 8-ring channels connect to sinusoidal channels by sharing their 8-rings (4.8×2.6 Å) in the *ac* plane. This zeolite is characterized by a framework density (defined as the number of T-atoms per 1,000 $Å^3$) of 18.6, which is relatively high for small-pore materials, mainly due to its channel-based structure.

[1] Araya A., Lowe B. M. US Pat 4581211, 1986.

[2] Araya A., Blake A. J., Harrison I. D., Leach H. F., Lowe B. M., Whan D. A., Collins S. P. *Zeolites* 1992, 12, 24.

[3] Altomare A., Cuocci C., Giacovazzo C., Moliterni A., Rizzi R., Corriero N., Falcicchio A., *J. Appl. Crystallogr*. 2013, 46, 1231.

[4] Gale J. D., Rohl A. L. *Mol. Simul*. 2003, 29, 291.

[5] Baerlocher, C., McCusker, L. B.: Database of Zeolite Structures (2016): http://www.iza-structure.org/databases/

[6] Han S., Smith J. V. *Acta Crystallogr. Sect. A* 1999, 55, 360.

[7] Bae J., Cho J., Lee J. H., Seo S. M., Hong S. B. *Angew. Chem. Int. Ed*. 2016, 55, 7369.

Keywords: EU-12 Zeolite, structure determination, Rietveld analysis

Mineral phase composition of the surface mud sediment in the city of Ekaterinburg, Russia

A. Ryanskaya[a], A. Seleznev[b], E. Ilgasheva[c], I. Yarmoshenko[b], D. Kiseleva[a*], T. Gulyaeva[a], O. Galakhova[a], E. Shagalov[a]
[a] *Institute of Geology and Geochemistry, UB of Russian Academy of Sciences, Russia*
[b] *Institute of Industrial Ecology, UB of Russian Academy of Sciences, Russia*
[c] *Ural State Mining University, Russia*
**kiseleva@igg.uran.ru*

In recent decades, in an urban environment, there has been a steady increase in dust and particle content of various origins as a result of erosion processes of soils and grounds, destruction of various surfaces, constructions and materials. In local microrelief depressions, due to insufficient attention to the planning of the territories, the anthropogenic processes and the disturbance of the atmospheric precipitation runoff, surface mud sediment is formed (one of the types of contemporary anthropogenic sediments). The life-time of such sediments varies from several months to several decades [1], with their thickness reaching up to 5 cm. The sedimentary material is represented by mineral and technogenic formations, particles of soil, sand, peat and small debris. The formation of sediment occurs from the surface including the territory of the residential blocks having the different time of construction (sometimes with a difference of several decades). The surface mud sediment in urban areas is a pollution transporting medium, a secondary and non-point source of pollution, and reflects the geochemical conditions of the environment and its changes.

The aim of the study was to determine the mineral phase composition of surface mud sediment in the city of Ekaterinburg in order to identify the sources of its origin.

Totally 60 samples of superficial mud sediment (30 collected in summer 2016 and 30 in winter 2016/2017) from different parts of residential areas such as traffic-ways, outer sidewalks and lawns, inner yard area with authorised and non-authorised parkings, as well as children playgrounds and green areas were investigated. The four samples of gravel chippings used for treating the slippery sidewalk surfaces during winter were studied as well. Mud sediment samples were separated into fractions according to particle size by dry (>1mm) and wet sieving (0.05-0.1 mm, 0.1-0.25 mm, 0.25-1 mm) and by decantation followed by vacuum filtration (0.002-0.01 mm and 0.01-0.05 mm).

Further the samples (if needed) were powdered manually in a jasper mortar and analysed by X-ray diffraction (XRD) using Shimadzu XRD-7000 powder X-ray diffractometer with Cu Kα radiation (λ=1.5406 Å) and power of 40 kV and current of 30.0 mA. XRD patterns were collected with 1°/min step across the angular range of 3-70°. The preliminary qualitative phase analysis of the samples was carried out by the main reflections using the Powder Diffraction File-2 database (ICDD). To perform the quantitative full profile analysis the diffractograms were analysed according to the Rietveld method [2] using the SiroQuant software (Sietronics, Australia [3]).

The investigated particle size fractions are the complex multi-phase mixtures, similar in mineral composition (quartz, microcline, plagioclase, magnetite, talc, serpentine, micas – muscovite and biotite, chlorite, calcite and dolomite), but having different proportions. Gravel chippings consist of amphibole, chlorite and magnetite.

The results of XRD phase analysis may allow the source of the superficial mud sediment in the city of Ekaterinburg to be determined and quantitatively characterised as well as the share of the anthropogenic input into this source to be evaluated.

The reported study was carried out at the Geoanalyst Center for Collective Use and partially funded by RFBR according to the research project № 16-35-60044 mol_a_dk.

[1] Seleznev A. PhD Thesis, 2015

[2] Rietveld H.M. *Acta Crystallographica,* 1967, 22, 151

[3] Taylor J.C. Canberra, Australia: Sietronics Pty Limited, 2004.

Keywords: mud sediment, city, XRD

The crystal structure of trisodium hexachloroiridate (Na_3IrCl_6)

M. Etter[a*], M. Müller[b], S. Bette[c]
[a] *Deutsches Elektronen-Synchrotron, Hamburg, Germany*
[b] *Department of Physics, University Duisburg-Essen, Duisburg, Germany*
[c] *Max Planck Institute for Solid State Research, Stuttgart, Germany*
** martin.etter@desy.de*

Strongly hygroscopic inorganic compounds exhibit a rich field of unsolved crystal structures as often several hydrated forms exist. However, solving these crystal structures is challenging, since single crystals are in many cases not available and powders usually consist of several hydrated phases at the same temperature and moisture conditions. Such a challenging compound is for instance the highly hygroscopic trisodium hexachloroiridate (Na_3IrCl_6) which possess multiple hydrated phases and a so far unsolved crystal structure even of the anhydrous phase.
Here, the crystal structure of the anhydrous phase of trisodium hexachloroiridate (Na_3IrCl_6) at room temperature was solved after a dehydration process using laboratory powder X-ray diffraction. It was found that the crystal structure of Na_3IrCl_6 crystallizes in space group $P\bar{3}1c$ isostructural to the crystal structures of Na_3CrCl_6, Na_3InCl_6 and Na_3MoCl_6 as well as to the recently found crystal structure of trisodium hexachlororhodate (Na_3RhCl_6) [1] (see figures below).
In this presentation structural details about the dehydrated compound will be given as well as an outlook to the variety of hydrated phases.

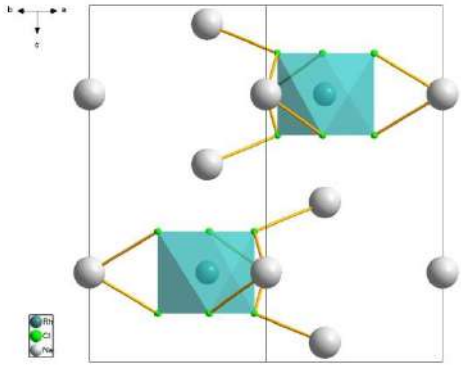

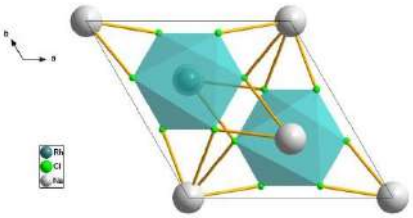

[1] Etter M. *Powder Diffraction,* 2018, 33, 1, pp. 62-65.

Keywords: Na3IrCl6, Iridate, Hydrated phases

MS05 - 3D XRD imaging and combined methods

MSO5

Abstract Number	Title	Author	Affiliation
MS05 -K1	Materials Imaging Using Synchrotron X-ray Diffraction	Dr Jonathan Wright	ESRF
MS05 - K2	Coherent X-Ray Diffraction Imaging of Frozen Hydrated Human Erythrocytes Infected by Malaria Parasites	Prof Motomu Tanaka	Heidelberg University
MS05 - OR1	Aberration-corrected scanning transmission electron microscopy imaging and its use in materials science.	Prof Thomas Vogt	University of South Carolina
MS05 - OR2	Diffraction imaging of catalytic materials under operating conditions – unrevealing the solid-state chemistry with full pattern Rietveld refinement	Ms Dorota Matras	The University of Manchester
MS05 - OR3	Combined XRD/XRF multivariate analysis for fast chemical and crystallographic surface mapping	Dr Mauro Bortolotti	University of Trento - Department of Industrial Engineering
MS05 - P131	Express diagnostics of mineral phases by factor analysis of X-ray diffraction patterns	Ms Ekaterina Fomina	Geological Institute, Kola Science Centre RAS
MS05 - P132	Laboratory based spectral CT	Prof Robert Cernik	The University of Manchester

Materials Imaging Using Synchrotron X-ray Diffraction

J. P. Wright[a*], T. Buslaps[a], C. Giacobbe[a], W. Ludwig[a], M. Majkut[a] and P. Sedmak[a].
[a] *ESRF, 71 Avenue des Martyrs, Grenoble, 38000 FRANCE*
** wright@esrf.fr*

You can quickly collect data from tiny samples using fast detectors at synchrotron radiation sources. Many samples in materials science are not uniform they contain several different substances. In some cases, you can cut up the sample and measure the individual parts separately. The aim of this talk is to review the emerging methods that offer diffraction data from the inside of a sample while keeping it in the original state.

We have many acronyms for the recipes in use at different facilities and beamlines (XRDCT, PDFCT, DCT, XDT, 3DXRD, HEMD, TEDDI, μ-Laue, and so on). We often use a “T” in the name when a Computed Tomography (CT) software package does a reconstruction. Some approaches treat single crystal data from particles inside the material instead of using CT reconstructions. We have experience with several of these methods at the Materials Science Beamline at the ESRF (where the authors work). During the same experiment, you might also be able to do X-ray imaging using absorption or phase contrast without dismounting the sample.

We will try to make sense of the different approaches by comparing the crystallite size in the sample to the size of the X-ray beam and detector pixel. Our X-ray beam size limits the spatial resolution for methods based on scanning samples across the beam. The best resolution is currently similar to optical microscopes (hundreds of nm) but we can still expect improvements in the future. When the sample contains crystallites that are “large enough” then we can measure diffraction spots and adapt single crystal methods to process the data. For liquids, glasses, nanoparticles and finer powders then we turn to powder diffraction or PDF methods instead.

The kinds of results that we can extract, and the difficulties to overcome, are similar to the feature lists you find in established Rietveld refinement software. Be prepared that the software for diffraction tomography is somewhat less user friendly and you might need to write some missing pieces yourself. Even with that in mind, there are now many examples in the literature for mapping out phase fractions, lattice parameters, crystallite sizes, orientations etc. We can also look at effects like site occupancies, atomic positions, preferred orientation, particle sizes, peak shapes, absorption, extinction and stress/strain.

Some physical effects can create problems for reconstructions and might result in artifacts. In general, we can extract parameters that do not depend on the sample orientation quite directly using computed tomographic approaches. When a single projection from the sample only measures a small part of a parameter space then you tend to run into problems. For example, we can measure components of texture or strain parallel to a rotation axis during a single rotation scan for CT methods, but this does not give the full picture in other directions in the sample. There are still many opportunities for developments in this area; improving experiments, reconstruction algorithms and software should all lead to new science.

Keywords: synchrotron, diffraction, tomography

Coherent X-Ray Diffraction Imaging of Frozen Hydrated Human Erythrocytes Infected by Malaria Parasites

M. Tanaka[a,b*]
[a] *Physical Chemistry of Biosystems, Heidelberg University, Germany*
[b] *Center fo Integrative Medicine and Physics, Kyoto University, Japan*
* *tanaka@uni-heidelberg.de*

Mounting evidence has indicated that malaria infection causes the remodeling of various membrane-associated proteins, alters cytoadhesiveness, and mechanical properties of human erythrocytes [1]. To date, the imaging of whole human cells under cryogenic conditions has been performed mostly by Cryo-TEM of thin sections due to the limited penetration depth of electron beams.

In recent years, lensless, coherent X-ray diffraction microscopy has been drawing considerable attentions for tomographic imaging of whole human cells. Recently, we performed cryogenic coherent X-ray diffraction imaging of human erythrocytes with and without malaria infection at ESRF ID10 [2]. To shed light on structural features near the surface, "ghost cells" were prepared by the removal of cytoplasm. From two-dimensional projections, we found that the surface of erythrocytes after 32 h of infection became much rougher compared to that of healthy, uninfected erythrocytes. The Gaussian roughness of an infected erythrocyte surface (69 nm) is about two times larger than that of an uninfected one (31 nm), reflecting the formation of protein “knobs” expressed on infected erythrocyte surfaces.

Three-dimensional tomography further enables to obtain images of the whole cells with no remarkable radiation damage, whose accuracy was estimated using phase retrieval transfer functions to be as good as 64 nm for uninfected and 80 nm for infected erythrocytes, respectively.

Future improvements in phase retrieval algorithm, increase in degree of coherence, and higher flux in combination with complementary X-ray fluorescence are necessary gain both structural and chemical details of mesoscopic architectures, such as cytoskeletons, membraneous structures, and protein complexes, in frozen hydrated human cells, especially under diseased states. In my talk, I will also present some of our recent data on the concentrations of specific target elements in intracellular compartments calculated from scanning X-ray fluorescence images.

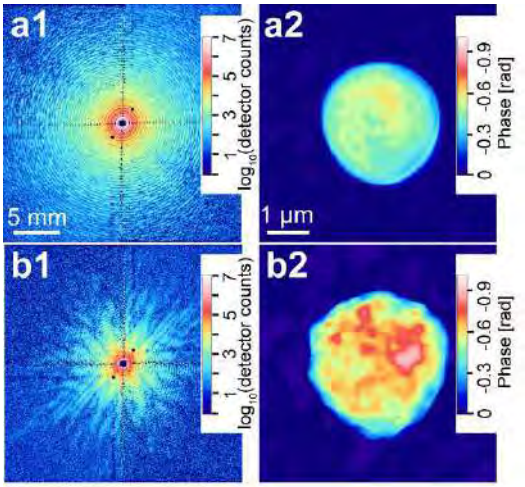

Two-dimensional, real space image reconstructions. (a1) Diffraction pattern measured by a two-dimensional detector and (a2) reconstructed real space image of a healthy, uninfected erythrocyte ghost kept in a cryo-loop. The corresponding data set of a human erythrocyte ghost infected by *P. falciparum* (t = 32 h) are presented in panels (b1) and (b2), respectively.

[1] Rieger, H., Yoshikawa, H., Quadt, K., Nielsen, M., Salanti, A., Sanchez, C., Tanaka, M.* and Lanzer, M.* *Blood,* 2015, 125, 383.

[2] Frank, V., Chushkin*, Y. Froehlich, B., Abuillan, W., Rieger, H., Becker, A., Yamamoto, A., Kaufmann, S. Lanzer, M., Zontone, F., Tanaka, M.* *Sci. Rep.,* 2017, 7, 14081.

Keywords: diffraction imaging, human erythrocyte, malaria

Diffraction imaging of catalytic materials under operating conditions – unrevealing the solid-state chemistry with full pattern Rietveld refinement

D.Matras[a,b*], S.D.M. Jacques[c], A. Vamvakeros[c,d], H.R. Godini[e], R.J. Cernik[a], A.M. Beale[b,f]
[a] *School of Materials, University of Manchester, UK*
[b] *Research Complex at Harwell, Harwell Science and Innovation Campus, UK*
[c] *Finden Ltd., UK*
[d] *ESRF- The European Synchrotron, France*
[e] *Technische Universität Berlin, Germany*
[f] *Department of Chemistry, University College London, UK*
* dorota.matras@rc-harwell.ac.uk

X-ray diffraction computed tomography is a technique that combines powder X-ray diffraction (PXRD) with computed tomography (CT). In contrast to conventional X-ray absorption-contrast computed tomography (CT), which is based on the difference in the attenuation of X-rays from the components present in the sample, XRD-CT is based on the difference in the diffraction signals from the crystalline materials present in the sample. Therefore, additional physico-chemical information is obtained. In the reconstructed image, each pixel corresponds to a complete diffraction pattern, and thus different crystalline chemical species can be mapped inside the cross section of a bulk object [1]. XRD-CT technique is most often applied in synchrotrons (such as the ESRF and the ID15A beamline), due to the remarkable properties (high flux, monochromatic beam, state-of-the-art detector, etc.) and was found to be a very promising technique for *in situ* studies of heterogeneous catalysts, providing high temporally and spatially-resolved data [2]. A diffraction pattern can provide a great number of information not only about the chemical composition but also about the unit cell parameters and crystallite sizes for each crystalline component present in the sample under investigation. These can be extracted by performing a full pattern Rietveld analysis that can be also applied to XRD-CT data [3]. Such information is highly desirable to understand the relationship between the catalyst structure and its role in chemical reaction (structure-function relationships). Since the structure/composition of solid catalysts is rarely uniform, single point measurements are usually insufficient to capture the evolving solid-state chemistry occurring during the chemical process inside the catalytic reactor.

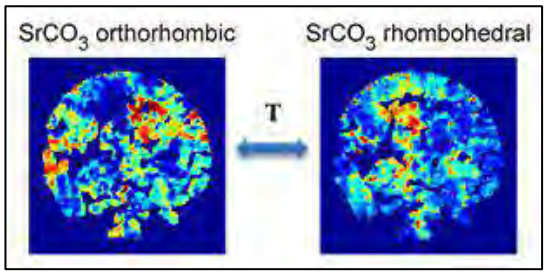

The purpose of this work is to demonstrate the principles of the XRD-CT technique and the batch full profile Rietveld analysis on data collected during the *operando* study of catalytic materials. As an example, a La-Sr/CaO catalyst was studied during the oxidative coupling of methane reaction with XRD-CT. The results obtained from the Rietveld analysis of the XRD-CT data allowed us to capture the transition between two polymorphs of the $SrCO_3$ phase (orthorhombic and rhombohedral). The derived phase distribution maps, which could only be observed by the combination of XRD-CT technique and Rietveld analysis, are directly linked to local temperature gradients inside the catalyst bed as well as the gas-phase composition (partial pressure of CO_2) [3]. We therefore show, for the first time, that the XRD-CT technique coupled with Rietveld analysis can provide unprecedented spatially-resolved physico-chemical information from working reactors and functional materials.

Acknowledgement

This project has received funding from the European Union's Horizon 2020 research and innovation programme under grant agreement No 679933 (MEMERE project).

[1] Jacques S.D.M., et al., *Angew. Chem*., 2011, 50, 10148.

[2] Vamvakeors A., et al., *ChemComm*., 2015, 51, 12752.

[3] Matras D., et al., .*J Chem Phys C,* 2018, 122, 2221.

Keywords: XRD-CT, Rietveld refinement, Catalysis

Combined XRD/XRF multivariate analysis for fast chemical and crystallographic surface mapping

M. Bortolotti[a*], L. Lutterotti[a], E. Borovin[a]
[a] *Department of Industrial Engineering, University of Trento, IT*
* *mauro.bortolotti@unitn.it*

When dealing with the crystallographic characterization of inhomogeneous sample surfaces, it is often desirable to perform a preliminary qualitative screening to locate regions of particular interest. In the case of large areas and/or high resolution mappings, a full Rietveld analysis of each data point becomes impractical; on the other hand, traditional qualitative approaches based on automated peak position extraction and comparison (a.k.a. *search match*), although quite fast and convenient, can pose serious problems in terms of accuracy, especially when dealing with difficult samples and related effects such as complex microstructure and the presence of preferred orientation. In such circumstances, the adoption of non-parametric statistics, in which no *a-priori* assumption is made about the underlying model, can offer an alternative, robust approach for data classification, allowing to sort the patterns in related clusters, some of which can eventually be selected for further quantitative analysis [1].
In a previous paper [2], we have shown how X-Ray Diffraction (XRD) and X-Ray Fluorescence (XRF) can be combined inside a Rietveld/Fundamental Parameters modeling framework to improve the accuracy in both the chemical and crystallographic quantitative analysis of homogeneous samples; in this work, we propose to combine XRD and XRF surface mappings data inside a non-parametric, multivariate analysis approach, to reinforce the classification performance and error tolerance of the single techniques. To achieve this goal, the significant statistical features obtained from the standalone XRD and XRF datasets (correlation and/or distance matrices) are combined together and then used as a single source for multivariate and cluster analysis to classify the data; relevant clusters can then be visually assigned to related surface regions and further selected for an accurate quantitative analysis.
The examples shown are related to XRD/XRF surface mappings of synthetic test samples as well of samples of engineering interests.

[1] Barr G., Dong W., Gilmore C.J., J. *Appl. Crystallogr.* 2004, 37, 2.

[2] Bortolotti M., Lutterotti L., Pepponi G., *Powder Diffraction*, 2017, 32, S1.

Keywords: combined XRD-XRF, multivariate analysis, surface mappings

Express diagnostics of mineral phases by factor analysis of X-ray diffraction patterns

E. N. Fomina[a*], E. N. Kozlov[a]
[a] *Geological Institute, Kola Science Centre RAS, Russia*
* *fomina_e.n@mail.ru*

When studying carbonatites of the Vuoriyarvi massif (NW Russia), the interpretation of geochemical data required information on mineral sets in each sample. The rocks of interest are very heterogeneous, polymineral and hard to study petrographically. In this regard, the choice of X-ray powder diffraction as a source of mineralogical information is obvious. Nevertheless, to meet the study goal (statistical comparison of geochemical and mineralogical data), the usual intermediate interpretation of individual diffraction patterns of each phase is not appropriate. An individual approach to each sample is too laborious for a large set of samples. We managed to avoid this procedure owing to the following fundamental properties of the diffractograms [1]: (a) intensities of peaks of each mineral are proportional to each other and thus correlated; (b) X-ray diffraction spectrum of a phases mixture is a superposition of their diffraction spectra. Hence, it is possible to obtain mineralogical information about the object of investigation by "separating" X-ray data, generalized throughout the sampling, into correlated parts related to particular minerals. We used factor analysis as a tool for solving this problem [2]. The nuances of preparing diffractograms, integrating them with geochemical data, as well as description of the statistical processing technique are given in [3]. The calculations revealed 14 factors that correspond to major and secondary minerals in the rocks. Mineralogical interpretation of the factors was simple. First, these factors are marked by high factor loadings (r^{FA}) of geochemical variables, reflecting the chemical specificity of a mineral. For example, "apatite factor" has high loadings of P, F, HREE, U and Th. Second, peak positions on the graphs of intensity loadings on "factors-minerals" coincide with peak positions on diffractograms of the corresponding minerals from the reference databases. It is shown in the diagram [ibid.] comparing the graph of "apatite factor" r^{FA} (blue line) and the diffraction pattern of fluorapatite from the RRUFF database (analysis R050529, red line). The results of compared mineralogy and geochemistry, based on the analysis of factors-minerals, are also provided in [3]. Importantly, peaks of the r^{FA} graphs coincide with those of diffractograms of the standards not only visually. The difference between their positions does not exceed ±0.05° (2Θ), i.e. peaks of r^{FA} graphs precisely position maximums of diffractograms. Locations of both intense and weak lines of diffractograms are equally well identified on the r^{FA} graphs. The high resolution of the proposed approach is confirmed by clear separation of Fe-dolomite and ankerite, which have extremely close position of all the lines. These data can be used for further detailed study of the samples, e.g. for quantitative XRD in order to correct positions of peaks determined by traditional methods.

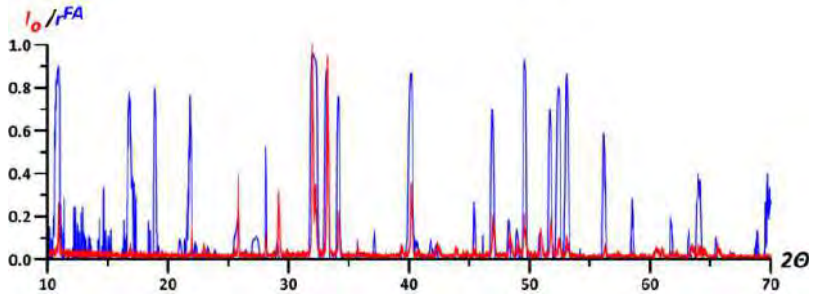

This work was supported by the Russian Foundation for Basic Research (project No. 18-35-00068).

[1] Klug HP, Alexander LE. *X-Ray Diffraction Procedures for Polycrystalline and Amorphous Materials*. New York: John Wiley & Sons, 1974.

[2] Le Maitre RW. *Numerical Petrology: Statistical Interpretation of Geochemical Data*. Amsterdam: Elsevier Scientific Pub. Co, 1982.

[3] Kozlov E. N., Fomina E. N. *Subbmitted*.

Keywords: powder diffraction, factor analysis, express mineral diagnostics

R J Cernik and C Egan

School of Materials, University of Manchester, UK

X-ray computed tomography (XCT) can reveal the internal three-dimensional (3D) structure of an object, with most notable application to medical imaging. However it finds many more areas of application beyond this, such as in security scanning, industrial inspection, materials science, and archaeology. In XCT, the measured contrast is proportional to both density and atomic number variations, with high density regions appearing brighter than low density regions. However it is very difficult to obtain the exact chemical speciation due to the polychromatic nature of the X-ray beam from laboratory X-ray tubes. There are methods, such as dual energy scanning, that can be used to obtain some pseudo chemical sensitivity which are finding increasing application to the medical imaging sector. But still the exact chemical speciation is unavailable. An alternative approach is to use the X-ray fluorescence (XRF) signal emitted from an object. However due to the weak intensity this method is generally limited to very bright synchrotron sources which have a major limitation from
a throughput and access point of view. Laboratory-based CT instruments are cheap and widely available, but due to the low intensity of radiation it is very time-consuming to undertake XRF imaging. Over recent years, a range of pixelated spectroscopic X-ray detectors have been actively researched and developed which have the ability to measure X-ray energy of individual photons with positional sensitivity. It is therefore possible use these types of detectors to measure the full attenuation spectrum and map chemical elements based on the K-edge position. Combining this with CT and using a microfocus source it is possible to identify multiple chemical elements simultaneously in 3D without prior knowledge of sample composition and with high spatial resolution.

MS06 - New developments in instrumentation for sample environments

MSO6

Abstract Number	Title	Author	Affiliation
MS06 - K1	In-Situ Diffraction Studies of Uranium Oxides. How to safely reduce SrUO4 at a beamline.	Prof Brendan Kennedy	The University of Sydney
MS06 - K2	In situ studies of mechanochemical milling reactions	Dr Ivan Halasz	Ruđer Bošković Institute
MS06 - OR1	Study of proton conductivity on powder samples using XRD	Dr David Havlicek	Charles University, Faculty of Science
MS06 - OR2	Rotatable load frames for neutron diffraction - analysis of strain, texture, phase transformations and elastic constants	Dr Markus Hoelzel	Technische Universität München, MLZ
MS06 - OR3	Exploring real time amorphization in organic pharmaceutical compounds via in situ ball milling	Dr Mickaël Morin	Excelsus Structural Solutions (Swiss) AG Empa, Swiss Federal Instititue for Materials Science and Technology
MS06 - P54	Chemical reaction chamber for surface treatments	Dr Zoltán Balogh-Michels	
MS06 - P55	In-situ XRD Analysis of the Rate of Formation of Zinc Ammonium Phosphate with Relative Humidity	Mr Mark Raven	CSIRO Land and Water
MS06 - P56	Monitoring the formation of CuO nanowires using in-situ high temperature X-ray diffraction	Dr Andreas Pein	Anton-Paar GmbH
MS06 - P57	Development of a Laboratory XRD-Raman Setup in Bragg-Brentano Geometry and its Application in In-Situ Studies of Heterogeneous Catalysts.	Dr Henrik Lund	Leibniz-Institute for Catalysis
MS06 - P58	Rapid crystallization of metallic glasses studied by in-situ XRD flash-annealing	Dr Jozef Bednarik	Deutches Elektronen-Synchrotron DESY
MS06 - P59	Implementation of a time-resolved X-Ray Diffractometer having a Ag-source and two Mythen detectors dedicated for battery-related materials	Dr Michael Knapp	KIT

In situ study of mechanochemical milling reactions

I. Halasz[a*], T.Friščić[b], K. Užarević[a]
[a] *Division of Physical Chemistry, Ruđer Bošković Institute, Croatia*
[b] *Department of Chemistry, McGill University, Canada*
** ihalasz@irb.hr*

With mechanochemical solid-state reactions commonly conducted in moving vessels made from some hard and non-transparent material and with the reaction mixture being exposed to violent impacts of the milling media, the milling reaction environment has long been sort of a black box. Recently, the study of mechanochemical milling reactions has been augmented by a methodology to study these reaction in situ and without the need to interrupt the milling process or open the reaction vessel for sampling [1]. First was powder X-ray diffraction which employed high-energy synchrotron X-rays to penetrate the reaction vessel while being shaken by an operating mill and thus providing, in time-resolution of seconds, a direct insight into the evolution of crystalline phases during milling. This revealed a dynamic reaction environment with reactions that often proceed via intermediate phases, can be complete within minutes of milling, it enabled the discovery of new and unusual phases [2], revealed a strong influence of temperature on reaction kinetics [3] and, through the use of a crystalline internal standard, shown a large amorphous fraction of the reaction mixture [4]. PXRD was soon followed by the introduction of a complementary technique not reliant on the crystallinity of the reaction mixture—in situ Raman spectroscopy [5]. The two techniques are ideally used in tandem. This is particularly useful for extraction of concentration profiles in reactions that have a large amorphous fraction or contain structurally unknown phases [6]. Future development and application of in situ monitoring techniques should enable formulation of a comprehensive mechanistic framework, as the one already existing for solution reactions, for mechanochemical solid-state reactions which is a necessary prerequisite for the systematic use of these increasingly important reactions for an efficient and sustainable chemical synthesis.

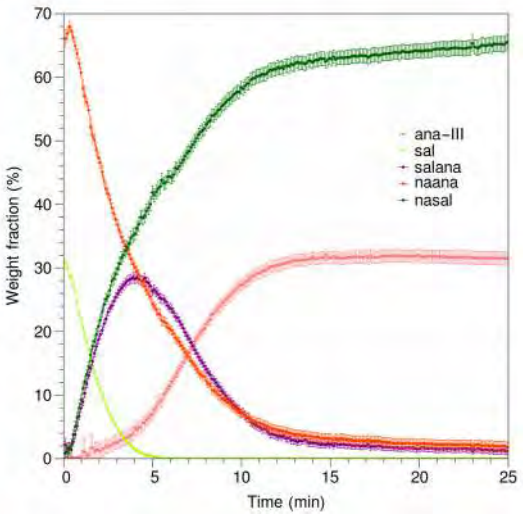

[1] Friščić T., Halasz, I, Beldon P. J., belenguer A., Adams F., Kimber S. A. J., Honkimäki V., Dinnebier R. E. *Nature Chem.* 2013, 5, 66.

[2] Katsenis, A. D. , Puškarić A., Štrukil V., Mottillo C., Julien P. A., Užarević K., Pham M.-H., Do T.-O., Kimber S. A. J., Lazić P., Magdysyuk O., Dinnebier R. E., Halasz I., Friščić T. *Nat. Commun.* 2015, 6, 6662.

[3] Užarević K., Štrukil V., Mottillo C., Julien P. A., Puškarić A., Friščić T., Halasz I. *Cryst. Growth Des.* 2016, 16, 2342.

[4] Halasz I., Friščić T., Kimber S. A. J., Užarević K., Puškarić A., Mottillo C., Julien P., Štrukil V., Honkimäki V., Dinnebier R. E. *Faraday Discuss. 2014,* 170, 203.

[5] Gracin D., Štrukil V., Friščić T., Halasz I., Užarević K. *Angew. Chem. Int. Ed.* 2014, 53, 6193.

[6] Lukin S., Stolar T., Tireli M., Blanco M., Babić D., Friščić T., Užarević K. Halasz I. *Chem. Eur. J.* 2017, 23, 13941.

Keywords: mechanochemistry, kinetics, in situ

In-Situ Diffraction Studies of Uranium Oxides. How to safely reduce $SrUO_4$ at a beamline.

B. J. Kennedy[a*], G. L. Murphy[a,b], Z. Zhang[b]
[a] *School of Chemistry, The University of Sydney, Sydney, NSW 2006 Australia*
[b] *Australian Nuclear Science and Technology Organisation, Lucas Heights, NSW 2234, Australia*
** Brendan.Kennedy@Sydney.edu.au*

Ternary uranium oxides are of interest in context of both the development of nuclear wasteforms and to further understand the properties of materials containing, or which can access, 5f electrons. $SrUO_4$ is one such oxide, it is postulated to form from the reaction of spent UO_{2+x} and the fission daughter Sr-90 under oxidising conditions. Power diffraction studies have shown that $SrUO_4$ undergoes an irreversible phase transformation between its rhombohedral, α-$SrUO_{4-d}$, and orthorhombic, β-SrUO4, forms, where the former contains oxygen vacancies and, by extension, reduced uranium valence states, whereas β-$SrUO_4$ is stoichiometric [1]. These changes are clear in the contour map of the diffraction patterns. The importance of oxygen vacancies in controlling the transformation and precise structure have been studied using a combination of *in-situ* neutron and synchrotron X-ray diffraction, supplemented by X-ray spectroscopy and DFT calculations [2]. These studies reveal oxygen-vacancy ordering can occur in α-$SrUO_{4-d}$ at high temperatures, provided sufficient anion vacancies are generated. This is achieved by reducing α-$SrUO_{4-d}$ with flowing hydrogen using a Norby-type flow cell. The steps necessary to ensure the safety of these experiments will be discussed. The structure and stability of this new, high temperature, phase of $SrUO_4$ will be described. The importance of the Sr cation has also been investigated. We have found, using *in situ* neutron powder diffraction measurements, that heating $CaUO_4$ in an ILL-type vacuum furnace results in the reduction of the Uranium yielding $CaUO_{3.7}$, similar to that seen for α-$SrUO_4$, although we find no evidence for the formation of an analogous β-phase. *In-Situ* Synchrotron X-ray diffraction measurements show evidence for oxygen vacancy ordering.

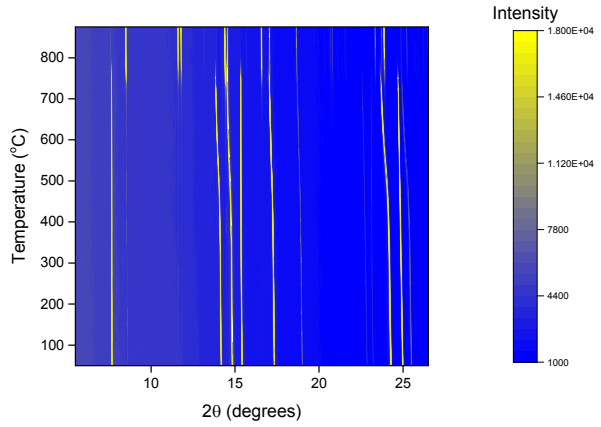

[1] Murphy G., Kennedy B.J., Johannessen B., Kimpton J.A., Avdeev M., Griffith C.S., Thorogood G.J. and Zhang Z. *J. Solid State Chem.,* 2016 86-92.

[2] Murphy G., Kennedy B.J., Kimpton J.A., Gu Q-F., Johannessen B., Beridze G., Kowalski P., Bosbach D., Avdeev M., and Zhang Z. *Inorganic Chemistry* 2016 **55** 9329

Keywords: uranium oxide, in-situ reduction, phase transformation

Study of proton conductivity on powder samples using XRD

D. Havlíček[a], J. Plocek[b], M. Nižňanský[a]
[a] *Dept. of Inorg. Chemistry, Charles University, Prague, Czech Republic*
[b] *Inst. of Inorg. Chem. ofthe ASCR, v.v.i., Husinec - Řež, Czech Republic*
** havlicek@natur.cuni.cz*

The study of proton conductivity is important in many different fields and disciplines. This property can be used in sensors, electrodes to determine glucose or cholesterol, in chemical reactors for hydrogenation and dehydrogenation industries and as materials for so called “Proton Exchanging Membranes” (PEM) in hydrogen fuel cells or “Solid Oxide Fuel Cells” (SOFC). The large family of proton conductors includes also salts of oxoacids, which have been studied in our department for several years. Proton conductivity was observed in crystals of hydrogen phosphates, sulfates, selenates or dihydrogen phosphates, where the cation was a nitrogen-containing organic base. The conductivities, whilst not high, were still several orders of magnitude higher than for insulators. We have prepared and described these new compounds, studied their structural properties by single crystal X-ray and neutron diffraction in combination with molecular spectroscopy and measured proton conductivity on oriented crystals. We were able to define the direction of conductivity in these crystals.

The conductivity mechanism in this type of crystals is not definitely clear. Proton transfer could occur via either the vehicle mechanism or the Grotthus mechanism. In anhydrous salts, the lack of water molecules excludes application of vehicle mechanism. But the application of Grotthus mechanism should cause disorders of the ions through which the protons are transferred at the conditions of proton conductivity. The best way how to study this phenomenon should be single crystal structure determination under the conditions of proton conductivity. But the realization of such experiment is not technically simple task.

For the first information, about existence of proton conductivity in any compound, we have tried to study this property by measurement on powder samples. The results are given in this presentation. Among our (mostly first prepared) samples we have also studied well known proton conductor $CsHSO_4$. This sample exhibit proton conductivity in powder form, and the value is comparable with measurement on single crystal. We have adapted our sample holder in PANalytical X´Pert Pro MPD diffractometer to be possible to keep the sample under high voltage (DC) during measurement. And we have studied its diffraction pattern without and under the conditions of proton conductivity.

Keywords: proton conductivity, powder samples, in situ XRD measurement

Rotatable load frames for neutron diffraction – analysis of strain, texture, phase transformations and elastic constants

M. Hoelzel[a*], M. Hofmann[a], W.M. Gan[b], A. Heldmann[a], W.W. Schmahl[c]
[a] *Heinz Maier-Leibnitz Zentrum (MLZ), Technische Universität München, Germany*
[b] *German Engineering Materials Science Centre, Helmholtz-Zentrum Geesthacht, Germany*
[C] *Department für Geo- und Umweltwissenschaften, Ludwig-Maximilians Universität München, Germany*
** markus.hoelzel@frm2.tum.de*

In this contribution we present unique load frames which allow an orientation of the load axis by an Eulerian cradle type design (ω, χ and ϕ axis) [1] and examples of their applications. One version ("uniaxial version") of the rig is optimized for texture analysis allowing a free sample rotation around the ϕ axis under uniaxial tension or compressive stress. By this design a movement of the load frame columns through incident or scattered beam during the measurements can be avoided. Thus complete pole figures under mechanical load can be derived. A second version ("multiaxial version") enables torsion in addition to tension or compression. The load frames were designed at Heinz Maier-Leibnitz Zentrum (MLZ / FRM II, Garching near Munich) for routine usage at the diffractometers SPODI (high resolution diffractometer) and STRESS-SPEC (strain scanner and texture diffractometer). However, their compact design allows a usage also on other neutron or synchrotron diffractometers.

In addition to layout and specifications of the load frames we present selected examples which benefit from the load frame design:

- Intensity and strain pole figures in austenitic stainless steels were derived under mechanical load, elucidating the orientation distribution of crystallites as well as lattice strains in one experiment [2].
- Diffraction elastic constants and single-crystalline elastic constants in polycrystalline steels and titanium alloys could be determined under a defined mechanical stress in a method which can be regarded as a reverse of classical stress analysis.
- In monoclinic nickel-titanium shape memory alloys the contributions of domain switching and lattice strains to the macroscopic strain were determined by diffraction under mechanical load.
- The evolution of martensite variants in polycrystalline NiMnGa under thermo-mechanical load was investigated [3].

[1] M. Hoelzel, W.M. Gan, M. Hofmann, C. Randau, G. Seidl, Ph. Jüttner, W.W. Schmahl, *Nucl. Instr*. 2013, A711, 101–105.

[2] W.M. Gan, C. Randau, M. Hofmann, H.G. Brokmeier, M. Mueller, A. Schreyer, *J. Phys. : Conf. Ser.* 2012, 340, 012100.

[3] Z. Li , N. Zou , B. Yang , W.M. Gan, L.H., X. Li, Y. Zhang, C. Esling, M.Hofmann, X. Zhao, L. Zuo, *J. Alloys Comp.* 2016, 666, 1-9

Keywords: load frame, tensile rig, engineering alloys

Exploring real time amorphization in organic pharmaceutical compounds via *in situ* ball milling

M.Morin[a], A.Grandeury[b], M.Juhnke[b], N.Casati[c], M.Wilke[c], M.Lange[c], Pomjakushina E[d], P.S. Whitfield[a], M.Reinle-Schmitt[a], and F.Gozzo[a*]

[a] *Excelsus Structural Solutions Swiss AG, Park Innovaare, Villigen, CH*

[b] *Novartis Pharma AG, Basel, CH*

[c] *Paul Scherrer Institut, Laboratory for Synchrotron Radiation – Condensed Matter, Villigen, CH*

[d] *Paul Scherrer Institut, Laboratory for Multiscale materials eXperiments, Villigen, CH*

* *fabia.gozzo@excels.us*

Amorphization of crystalline powder is known in the pharmaceutical industry to increase the solubility of the Active Pharmaceutical Ingredient (API). Amorphization can be achieved by different routes, among which the mechanical comminution of the powders, which however requires the detailed understanding of mechanochemical processes involved so to gain control on the process and it effect on the API. *In situ* materials characterization techniques are extensively used, as they offer the advantage to get a description of possible reactive intermediate states in a sample without risk of reaction/ relaxation by interrupting the process.

A protocol was developed by Halasz et al. [1] for *in situ*, real time monitoring of mechanochemical reaction using synchrotron X-ray powder diffraction and later used by Bordet et al. [2] to investigate the amorphization process of a powder with high energy *in situ* ball milling. However, the ball mill consisting of a Perspex vessel require to be placed in the path of a high-energy X-ray beam (90keV). Under these conditions, the signal by the extrinsic contribution of the grinding media and outer walls of the vessel strongly interfere with the intrinsic signal from the materials under investigation with the risk of hindering relevant information due to peaks overlapping and high level of background.

Recently a new type of *in situ* ball mill [3] was developed at the Materials Science beamline (Paul Scherrer Institute, SLS, Switzerland) with a particular geometry allowing one to obtain data with a lower background and much sharper Bragg peaks using Si-based single photon counting detectors operated at lower photon energies (<30keV). This geometry has advantages in the study of the amorphization process of organic pharmaceutical compounds which usually scatter weakly and thus require a fine control of the background.

However, progress in studying *in situ* amorphization of pharmaceutical compounds were hindered by the tendency of organic compounds to agglomerate while milling, giving rise to inhomogeneous backgrounds and inhomogeneous amorphization processes.

We describe novel strategies allowing improvements in real time monitoring of the amorphization of pharmaceutical compounds. In particular, we present recent results where we show significant improvements for in-situ ball milling using an anti-caking agent to prevent agglomeration of the powder in the ball milling setup. We believe that these improvements could enable systematic and reliable studies of amorphization in pharmaceutical compounds.

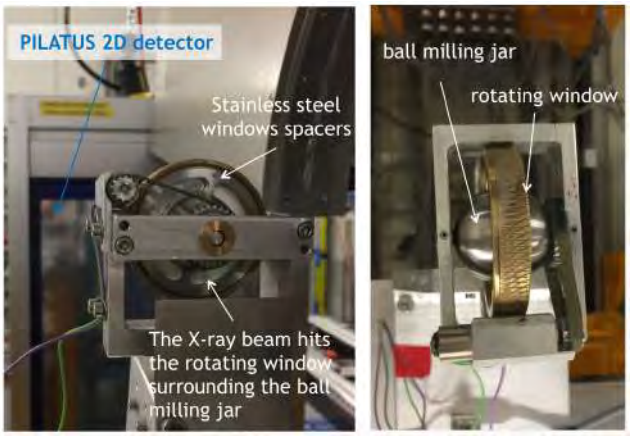

[1] Halasz I., Kimber S. A. J., Beldon P. J., Belenguer A. M., Adams F., Honkimäki V., Nightingale R.C., Dinnebier R. E., Friščić T., Nature Protocols 2013 (8), 1718–1729

[2] Bordet P., Bytchkov A., Descamps M., Dudognon E., Elkaïm E., Martinetto P., Pagnoux W., Poulain A., and Willart J. F., Crystal Growth & Design 2016 16 (8), 4547-4558

[3] Ban V., Sadikin Y., Lange M., Tumanov N., Filinchuk Y., Černý R., and Casati N., Analytical Chemistry 2017 89 (24), 13176-13181

Keywords: in-situ ball milling, amorphization, pharmaceutical compounds

Chemical reaction chamber for surface treatments

Z. Balogh-Michels[a*], S. Kleiner[b], A.Faeht[b], M. Ammann[b], E. Hadjixenophontos[c], A. Neels[a]
[a] *Center for X-ray Analytics, Empa, Switzerland*
[b]*Institute for Applied Laser, Bern University of Applied Science, Switzerland*
[c]*Chair of Materials Physics, University of Stuttgart,Germany.*
** zoltan.balogh@empa.ch*

In this work we are presenting our chemical reaction chamber allowing in situ XRD observation of surface treatments using aggressive gases. Specimens up to 20 mm diameter and 6 mm height can be processed under the NH_3, C_2H_4, N_2 and H_2 at atmospheric pressure. Pretreatment of the specimen surface with HCl gas based on the decomposition of PVC is also possible. In the current stage the maximal temperature is 600 °C, but developments for higher processing temperatures are underway. The chamber can be attached to a Bruker D8 Advance and a Panalytical X'Pert^3 Powder X-ray diffractometer. The "*z*" (height) position of the specimens can be adjusted by a step motor built in the chamber. The figure shows a CAD image of the chamber as well as the measurement setup on a Bruker D8 Advance XRD instrument.

The chamber was already used for two types of experiments. In the first set we measured the growth of the expanded austenite on AISi 316L steels during nitrocarburizing and nitriding [1,2]. We estimated the thickness of the growing layer by the attenuation of the γ-Fe signal. We also fitted the expanded austenite peak with a multilayer model. Both approaches have shown a diffusion controlled growth with 165±12 kJ/mol activation energy for the nitrocarburizing. The layer growth in the nitriding experiment was one order of magnitude slower. This is in agreement with the expected behavior [3].

In the second set of experiments we studied the transport of hydrogen in titanium. It is well known that the interstitially diffusing H is very fast in metals, especially in Ti [4]. Indeed ex situ measurement gave a strong indication that in thin films the absorption from the gas and not the diffusion in the bulk metal is the rate limiting step [5]. Our first in situ experiments have proven that both the intercalation and the phase transformation to a hydrate phase are characterized by a linear kinetics, a typical feature of the supply limited transport due to the naturally occurring surface oxide layer [6]. Furthermore the full width half maximum of the peaks remained constant during the experiment indicating an efficient redistribution of the H and no composition or stress gradient.

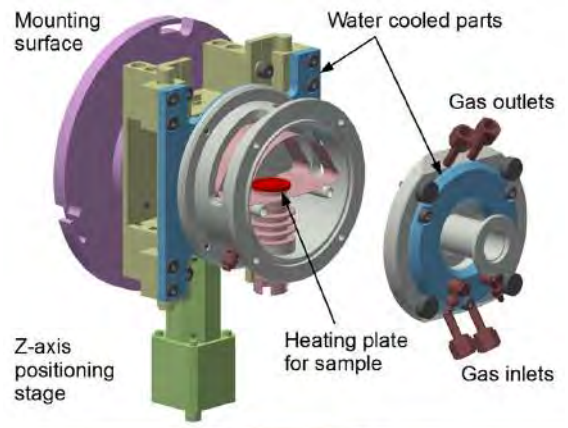

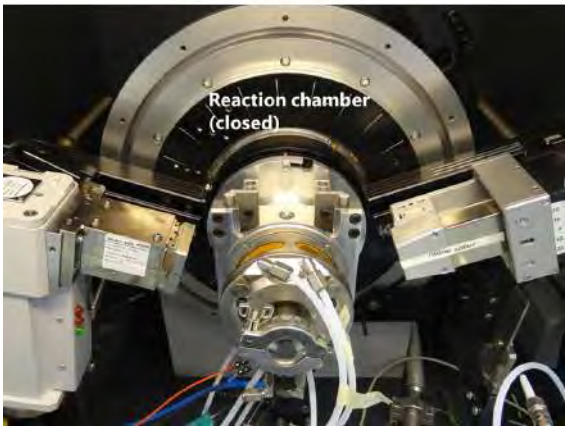

[1] Z. Balogh-Michels, A. Faeht, S. Kleiner, A. von Känel, J.-M. Rufer, A. Dommann, P. Margraf, G. Tschopp, A. Neels, *J. Appl. Phys*., 2017, 122, 025111.

[2] Z. Balogh-Michels, A. Faeht, S. Kleiner, P. Margraf, A. Dommann, A. Neels, *Def. Diff. Forum*, 2018, 383, 142.

[3] D. Wu, Y. Ge, H. Kahn, F. Ernst, A.H. Heuer, *Surf. Coat. Technol*. 2015, 279, 180-180.

[4] U. Kaess, G.Majer, M. Stoll, D.T. Peterson, R.G. Barnes, *J. Alloys Compd*., 1997, 259, 74.

[5] E. Hadjixenophontos, L. Michalek, M. Roussel, M. Hirscher, G. Schmitz, *Appl. Surf. Sci.*, 2018, 441, 324.

[6] B.E. Deal, A.S. Grove, *J. Appl. Phys*., 1965, 36, 3770.

Keywords: non-ambient XRD, surface treatment, hydrogenation

In-situ XRD Analysis of the Rate of Formation of Zinc Ammonium Phosphate with Relative Humidity

M.D. Raven[a*] and P.G. Self[a]
[a] *CSIRO Land and Water, Australia*
[*] *mark.raven@csiro.au*

Zinc is an essential micronutrient that plants require for healthy growth and development. Zinc deficiency in plants is recognised as one of the most widespread causes of poor crop quality and quantity. Over half of the world's cereal crops are grown on soils that are identified as zinc deficient either due to low total zinc concentration or low plant available zinc [1]. Subsequent consumption of grains and other plant based foods is a major source of zinc for maintaining animal and human health. Therefore zinc deficiency in soils has a direct impact on animals and humans which is becoming a serious worldwide health issue.
Application of suitable treatments for zinc deficient soils and plants are varied, depending on the soil and crop type. Zinc sulfate or zinc oxide applied directly to the soil are the two most widely used treatments for zinc deficiency, however, alkaline soils inhibit zinc absorption so alternative methods are required. A simple method of efficiently adding zinc to existing fertilizers is to coat monoammonium phosphate granules with zinc oxide. However, this composite material, when exposed to water or high relative humidity rapidly precipitates zinc ammonium phosphate with a substantially lower solubility than the original zinc oxide.
In-situ X-ray diffraction (XRD) analysis of mixtures of zinc oxide with monoammonium phosphate at various levels of relative humidity at 25°C were performed on a PANalytical X'Pert Pro with an Anton Paar CHC plus$^+$, cryo and humidity chamber. The XRD data showed an increasing rate of formation of orthorhombic zinc ammonium phosphate (OZAP) with increasing relative humidity. When the relative humidity approaches the critical relative humidity of monoammonium phosphate (i.e. 91.9% at 25°C) the formation of OZAP is rapid with >90 wt.% forming after 25 minutes. At 95% RH over 95 wt.% OZAP forms after just 3 minutes. The level of OZAP remains at 100 wt.% for up to 90 minutes before the structure transforms to the monoclinic zinc ammonium phosphate (MZAP) form. Use of the Anton Paar CHC plus$^+$ cryo and humidity chamber is ideally suited for in-situ studies on phase transformations during processing, storage and application of fertiliser formulations.

[1] Alloway, B.J. 2008. Zinc in soils and crop nutrition. Paris, France: IFA; and Brussels, Belgium: IZA

Keywords: in-situ, XRD, humidity, zinc ammonium phosphate

Monitoring the formation of CuO nanowires using in-situ high temperature X-ray diffraction

A.Pein [a]*, A. Jones [a]
[a] *Anton Paar GmbH, Austria*
* *andreas.pein@anton-paar.com*

Nanostructured semiconductors have a wide variety of potential applications ranging from photovoltaic devices (e.g. solar cells) to gas / liquid sensors. To be used on a commercial scale, fast and reproducible methods for nanostructure formation must be developed. In this context, in-situ measurements allow detailed information to be obtained during formation which could allow for new and better methods to be developed.

Cuprous oxide (Cu_2O) and cupric oxide (CuO) are the two naturally occurring oxide forms of copper which can grow as nanoscale crystals. Both display semiconducting properties and their band gaps (2.0 and 1.2 eV, respectively) mean that they can be applied in various fields. [1],[2] Of particular interest are nano-wires of the two oxide forms. While both oxides can form nanowires, CuO nanowires can be produced more easily and are the subject of this study.

Several methods are possible for the growth of CuO nanowires, but the simplest relies on only heating a pure Cu foil in air to a sufficiently high temperature for a certain length of time. The temperature at which nanowire growth occurs is in the region from 300 – 800 °C, and the time required is typically a few hours. Generally, it has been reported that higher temperatures result in larger nanowire diameters, while longer annealing times result in an increase in the length of the wires. [3]

During heating it is expected that Cu_2O first forms as a layer on the foil surface and from this layer CuO nano-wires grow when held at higher temperatures for a longer period of time. [3] The goal of the present study is to find the optimum conditions for the growth of CuO nanowires with regards to temperature and annealing time. This information can then be used to optimize the process so that nanowires can be produced in the rapid and efficient manner that is required for the commercialization of nanowire devices.

[1] S. Steinhauer, E. Brunet, T. Maier, G. C. Mutinati, A. Köck, O. Freudenberg, C. Gspan, W. Grogger, A. Neuhold, R. Resel, Sens. Actuator B-Chem. (2013), 187, 50-57.

[2] S. Steinhauer, A. Chapelle, P. Menini, M. Sowwan, ACS Sens. (2016), 1, 53-507.

[3] G. Filipic, U. Cvelbar, Nanotechnology (2012), 23, 194001.

Keywords: in-situ X-ray diffraction, nanowires, copper oxide

Development of a Laboratory XRD-Raman Setup in Bragg-Brentano Geometry and its Application in In-Situ Studies of Heterogeneous Catalysts.

H. Lund[a*], M. Schneider[a]
[a]*Leibniz-Institute for Catalysis, Albert-Einstein Straße 29a, 18059 Rostock, Germany*
**henrik.lund@catalysis.de*

The investigation of heterogeneous catalysts by in-situ or in-operando techniques is widely used nowadays to understand the role of the catalysts in the chosen chemical reaction [1]. Here, the investigations are focussed on either the synthesis of the catalysts or on the observation of the catalytic system under working conditions to obtain a structure-activity relationship. Powder diffraction is mostly applied to identify the phases present and obtain microstructural properties. In case of the presence of amorphous materials, Raman spectroscopy offers an additional access to structural information. Various in-situ studies, including XRD-Raman coupling have been reported so far, e.g. on working catalysts or crystallisation processes [2]. However, most of these studies have been done using synchrotron radiation for X-ray diffraction. Due to the limited accessibility of synchrotron sources, in-house laboratory solutions are highly beneficial. So far, only a few solutions have been established which are mostly using capillary reactor systems in Transmission/Debye-Scherrer-Geometry [3].
In order to provide an improved ability to study heterogeneous catalysts under non-ambient conditions a XRD-Raman coupling was developed. Powder diffraction data are acquired by a standard laboratory diffractometer in Bragg-Brentano geometry. Simultaneously, Raman data are obtained in 180° backscattering setting. The directly heated sample can be investigated under various gas atmospheres by an attached mass flow controller system. Several standard materials have been investigated to proof the equal response of both methods over a temperature range from 100 to 800 °C. To proof the setups capability the synthesis and reaction behavior of transition metal molybdate based catalysts, which are widely applied in industry and research, were investigated. In detail, the calcination process during the synthesis, phase transitions and reduction-oxidation behavior of $Fe_2(MoO_4)_3$ are studied.

[1] Rodriguez J. A., Hanson J. C. and Chupas P. J. *In-situ Characterization of Heterogeneous Catalysts*, 2013, Wiley.

[2] a) Patlolla A., Carino E. V., Ehrlich S. N., Stavitski E and Frenkel A. I. *ACS Catal*. 2012, *2*, 2216; b) Klimakow M., Leiterer J., Kneipp J., Rössler E., Panne U., Rademann K. and Emmerling F. *Langmuir* 2010**,** 26, 11233; c) Radnik J.,Bentrup U., Leiterer J., Brückner A. and Emmerling F., *Chem. Mater*. 2011, 23, 5425.

[3] a) Cats K. H. and Weckhuysen B. M. *ChemCatChem* 2016, 8, 1531; b) Depla A., Verheyen E., Verfeyken A., Gobechiya E., Hartmann T., Schaefer R., Martens J. A. and Kirschhock C. E. A. *Phys. Chem. Chem. Phys*. 2011, 13, 13730; c) Schneider M., Winkler S. and Brückner A. *ChemieIngenieurTechnik*, 2008, 80, 1323.

Keywords: In-situ studies, Catalysis, XRD-Raman coupling

Rapid crystallization of metallic glasses studied by in-situ XRD flash-annealing

J. Bednarcik[a*], K. Kosiba[b], S. Pauly[b], A. Rothkirch[a]
[a] *Deutches Elektronen-Synchrotron DESY, FS-PE, Notkestr. 85, 22603, Hamburg, Germany*
[b] *Institute for Complex Materials, IFW Dresden, Helmholtzstr. 20, 01069 Dresden, Germany*
** jozef.bednarcik@desy.de*

Bulk metallic glasses (BMGs) are known to exhibit the highest yield strength of any metallic material (up to 5 GPa) and show large elastic strain at ambient conditions. A very effective way to suppress their brittle behavior is to incorporate crystals into the glass. The resulting BMG composites exhibit high strength as well as plasticity. Nowadays, it is very difficult, if not impossible, to prepare BMG composites with uniformly distributed crystals in a reproducible manner by melt-quenching, which is the standard preparation method. Direct current fast Joule heating (flash-annealing) represents an alternative way to overcome such deficiency. Achieving high heating/cooling rates (well above 1000 °C/s) by flash-annealing opens up new possibilities for study of fast kinetics. Phase composition and microstructure of a material can be tailored by proper heat-treatment in order to improve its overall performance. In this contribution we will introduce a novel setup for studying rapid crystallization of metallic glasses using an in-situ X-ray diffraction flash-annealing. Capabilities of the in-situ XRD flash-annealing with high temporal resolution will be demonstrated by studying crystallization behavior of selected CuZr- and Fe- based metallic glasses.

Keywords: crystallization, flash-annealing, in-situ XRD

Implementation of a time-resolved X-Ray Diffractometer having a Ag-source and two Mythen detectors dedicated for battery-related materials

M. Knapp[a*], M.S.D. Darma[b], M. Yavuz[a], L. Mereacre[a], R. H. Schneider[a], T. Hartmann[c], H. Ehrenberg[a]

[a] *Institute for Applied Materials, Karlsruhe Institute of Technology (KIT), Karlsruhe, Germany*
[b] *Helmholtz Institute Ulm (HIU), Ulm, Germany*
[c] *STOE & Cie GmbH, Darmstadt, Germany*
** michael.knapp@kit.edu*

A high energy and high angular resolution powder diffractometer optimized for time-resolved X-Ray Diffraction experiments has been successfully commissioned at the Karlsruhe Institute of Technology (KIT) in cooperation with the STOE & Cie GmbH. The diffractometer has a Silver source (E = 22.123 keV, λ = 0.55942 Å) with focusing Ge 111 monochromator. A Dectris MYTHEN 2 2K double detector with a fixed distance between both detectors of a little less than the width of a module (appr. 18° 2θ) is mounted at a radius of 130 mm from the centre axis of the goniometer, enabling a simultaneous intensity counting covering the angular range from 0° to 36°. The use of two Mythen detectors considerably decreases the measurement time. The effective angular resolution is 0.005° in 2θ.
A dedicated sample holder for in-situ powder diffraction experiments during electrochemical cycling of Li-ion cells has been developed in-house. A rotation motor is integrated into this sample holder, ensuring a good orientation statistics of the powder samples and the electrical contacts allow good quality of the electrochemical signal at the same time.
The implementation of this in-house time-resolved X-Ray Diffractometer allows investigations in the field of battery research performing intermittent in-situ XRD experiments during long-term cycling (over hundreds of cycles) or long term storage tests of Li-ion coin cells, a unique feature that cannot be offered by synchrotron facilities due to the limited beam time. The relatively slow cycling rate of C/10 or slower ensures better chemical equilibrium inside the cell compared to typically faster measurements at the synchrotron. Complementary analysis of the intermittent powder diffraction and the long-term electrochemical tests (e.g. by monitoring the coulombic efficiency over time) will certainly shed more light into the comprehensive understanding of competing degradation mechanisms, e.g. to investigate the development of coexisting electrode degradation and lithium loss over time.

Keywords: time-resolved X- Ray diffractometry, intermittent in-situ XRD experiment, battery research

MS07 - Nanomaterials: Structural, Microstructural and Surface Aspects

MSO7

Abstract Number	Title	Author	Corresponding Affiliation
MS07 - K1	Characterizing Disordered Ensembles of 2-D Materials: Massively Defective MnO2	Prof Scott Misture	Alfred University
MS07 - K2	Improving magnets through size, shape and texture control	Dr Mogens Christensen	Aarhus University
MS07 - OR1	Crystal structure and microstructure of γ-Al2O3 determined by analysing the anisotropic line broadening diffuse scattering	Mr Martin Rudolph	TU Bergakademie Freiberg
MS07 - OR2	Quantification of Correlated Disorder in Alloy Systems Through Complex PDF Modelling	Dr Robert Koch	Alfred University
MS07 - OR3	Mapping the size dependent structure of metal oxides: A new molybdenum oxide nanostructure from X-ray total scattering	Dr Kirsten Marie Jensen	University of Copenhagen
MS07 - P133	Study of Nanoalloys CoxPt1-x Formation Mechanism from Single-Source Precursors	Evgeny Filatov	Nikolaev Institute of Inorganic Chemistry SB RAS
MS07 - P134	New insights on Structure and Morphology of Defective CdSe Colloidal Quantum Dots combining DNP-NMR and Advanced Small and Wide Angle X-ray Scattering Techniques	Mr Daniele Moscheni	University of Insubria and To.Sca.Lab
MS07 - P135	Size and strain induced anisotropic XRPD line broadening in Fe3-xYxO4 (x=0.00, 0.05, 0.10) nanorods and nanospheres mixtures	Prof A Kremenovic	University of Belgrade
MS07 - P136	X-ray characterization of dielectric layers of crosslinked methacrylate copolymers for application in organic electronics	Dr Dieter Jehnichen	Leibniz-Institut für Polymerforschung Dresden e.V.
MS07 - P137	Syntheses and Characterization of Iron Oxide Nanoparticles functionalized with biocompatible molecules	Prof Paula Haddad	Universidade Federal de São Paulo
MS07 - P138	Room temperature aging and tempering of highly nitrogen-supersaturated ferritic solid solutions	Mr Marius Wetzel	TU Bergakademie Freiberg
MS07 - P139	Toward Smart and Eco-friendly Nanofertilizers: Structural and Physico-Chemical Characterization of N-doped Calcium Phosphates	Prof Norberto Masciocchi	Univeristy of Insubria and To.Sca.Lab
MS07 - P140	Synthesis of cobalt molybdenum nitrides from cobalt(II) acetate and ammonium heptamolybdate – in-situ XRD study	Mr Paweł Adamski	Institute of Inorganic Chemical Technology and Environment Engineering, Faculty of Chemical Technology and Engineering, West Pomeranian University of Technology, Szczecin, Poland
MS07 - P141	Application of Debye Scattering Equation on laboratory XRPD data of TiO2 NPs	Dr Paul O'Meara	Malvern Panalytical Ltd
MS07 - P142	Crystal-, magnetic- and micro-structure of spinel ferrite nanocrystallites	Mr Henrik Lyder Andersen	Aarhus University
MS07 - P143	Microstructure and cation distribution in magnetic Ni1-xZnxFe2O4 nanocrystallites	Ms Jennifer Hoelscher	Aarhus University
MS07 - P144	Combustion assisted preparation of single-domain high coercivity SmCo5	Mr Hao Tang	Aarhus University
MS07 - P145	Structural characterization of superparamagnetic iron oxide nanoparticles for potential biomedical applications	Prof Fabio Furlan Ferreira	Federal University of ABC

MS07 - P146	Structure, texture and properties of SrFe12O19 magnets	Dr Matilde Saura-Múzquiz	Aarhus University
MS07 - P147	The Orange framework for line profile analysis: integration of WPPM with advanced instrumental modelling	Dr Luca Rebuffi	Elettra Sincrotrone-Trieste
MS07 - P148	The study of monolithic silicon nanowires: Correlation of structural and physical behavior	Simone Dolabella	Empa, Swiss Federal Instititue for Materials Science and Technology
MS07 - P149	X-ray and neutron diffraction magnetostructural investigations on exchange-coupled nanocomposite magnets	Mr Priyank Shyam	Center for Materials Crystallography, Department of Chemistry and Interdisciplinary Nanoscience Center (iNANO), Aarhus University
MS07 - P150	Optimization of spring exchange coupled ferrites, studied by in situ neutron diffraction	Mr Jakob Voldum Ahlburg	Center for Materials Crystallography, Department of Chemistry and Interdisciplinary Nanoscience Center (iNANO), Aarhus University
MS07 - P151	Mathematical model for iron non-destructive testing for anti-corrosion metallurgic application	Mr Abouharim Abdelhafid	University of Hassan 1st, FPK, Laboratory of Nanosciences and Modeling, Khouribga, Morocc
MS07 - P152	XRD investigation of severe plastic deformation, strain and temperature induced nanocrystalline TiNiCu shape memory alloy	Dr Rajath Hedge	JAWAHARLAL NEHRU NATIONAL COLLEGE OF ENGINEERING
MS07 - P153	Coercivity enhancement of strontium hexaferrite nano-crystallites through morphology-optimizing annealing	Mr Frederik Gjørup	Center for Materials Crystallography, Department of Chemistry and Interdisciplinary Nanoscience Center (iNANO), Aarhus University
MS07 - P154	Synthesis and Characterization of Cancrinite Zeolite from Natural Bentonite	Mr Daeyoung Kim	University of Science and Technology
MS07 - P155	Facile Synthesis and Characterization of Mesoporous Iron Nanocomposites for Environmental Applications	Dr Jaehwan Kim	Korea Institute of Geoscience and Mineral Resources (KIGAM)
MS07 - P156	Application of Powder X-ray Diffraction in Studying the 3D Self-assembled Structure of Peptide Foldamers	Dr Jintaek Gong	Natural Science Research Institute, Korea Advanced Institute of Science and Technology
MS07 - P157	Refining Nanocrystalline and Amorphous like ZrO2 with MSTRUCT	Dr Zdeněk Matěj	Lund University / MAX IV Laboratory
MS07 - P158	Evolution of Crystalline Microstructure of Mullite in Triaxial Whiteware Porcelains	Marek Kojdecki	Military University of Technology
MS07 - P159	Results of a Round Robin on Line Profile Analysis (LPA): separation of size and strain broadening	Prof Paolo Scardi	University of Trento
MS07 - P160	Switching Between the Superparamagnetic and Ferrimagnetic Ordering: Structural, Microstructural and Magnetic Study of CoMn2O4 Spinels	Dr Jasminka Popović	Ruđer Bošković Institute

Characterizing Disordered Ensembles of 2-D Materials: Massively Defective MnO_2 Nanosheet Assemblies

S.T. Misture*[a]
[a] *Kazuo Inamori School of Engineering, Alfred University, Alfred, NY*
* *misture@alfred.edu*

X-ray total scattering was teamed with Raman and X-ray spectroscopy and related tools to probe both the mesostructure and the atomic defects of MnO_2 nanosheet assemblies, revealing a direct link between surface-displaced Mn cations and pseudocapacitance, for example. To demonstrate the efficacy of the new approach, we use data calculated for graphene with various types of stacking disorder. Next, nominally defect-free MnO_2 nanosheets were reassembled into 3-D porous structures, followed by controlled reduction of some of the tetravalent Mn. As might be expected for a system of this complexity, nano and meso-scale disorder complicates the X-ray scattering data, making traditional approaches to quantification of defects impossible. X-ray PDF studies were used to quantify the Mn surface Frenkel defects by developing a new modelling approach for optimizing the fit of the model to the data. A refineable stacking model provides a mechanism to propagate the 2D sheet motif, where the critical feature of our new approach is the ability to refine a relatively small number of physically meaningful parameters for a massively defective atomic ensemble using only modest computing power. The approach is generally applicable to layered systems of any type, and we demonstrate that statistical modelling can be used to quantify the uncertainties in refined model parameters.

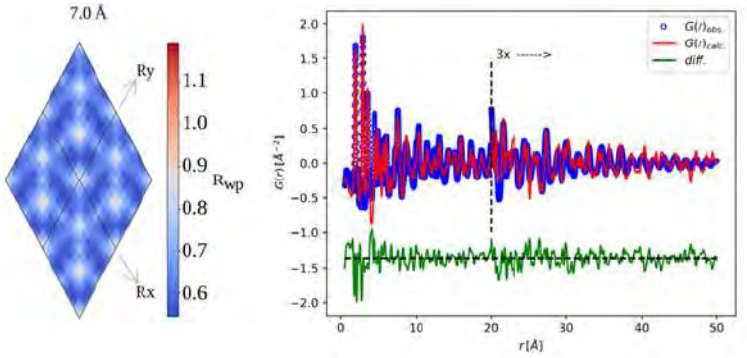

Keywords: PDF, stacking disorder, complex modeling

Improving magnets through size, shape and texture control

M. Saura-Muzquiz[a], C. Granados-Miralles[a,b], A. Eikeland[a], F. Gjørup[a] & M. Christensen[a*]
[a]*Department of Chemistry and iNANO, Aarhus University, Denmark*
[b]*Current address: Instituto de Cerámica y Vidrio, CSIC, Madrid, Spain*
** mch@chem.au.dk*

Magnetic materials are found everywhere in our daily life, ranging from electromotors converting electricity to kinetic energy to data stored on computer hard drives. Magnetism is a quantum mechanical phenomenon related to the number of unpaired electrons on the atomic level. When magnetic particles are reduced in size they go from multiple magnetic domains to being single domain nanoparticles and finally ending up in a superparamagnetic state. The figure below gives an overview of the length scales involved in making high performance magnets. Understanding and controlling structures at the nanolevel allows the design and building of better performing magnetic materials. We have extensively investigated strontium hexaferrites prepared through bottom-up synthesis.

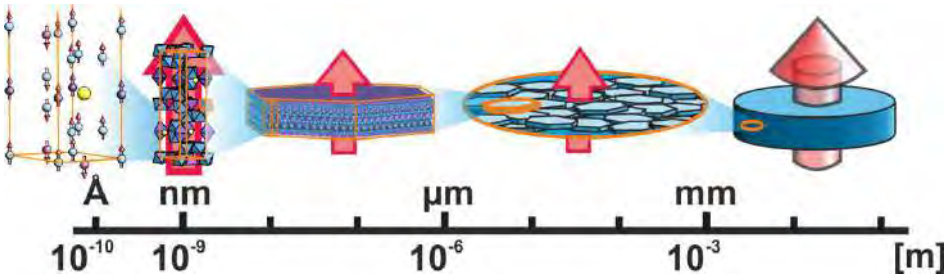

The presentation gives an overview of the effects relating size and texture to magnetic properties. The size, shape, and composition are crucial for making a competitive magnetic material. Many of these parameters are controlled through the synthesis conditions, which we have followed *in situ* using synchrotron radiation.[1] The *in situ* studies allow us to optimize the synthesis conditions.
After having prepared nanocrystallites with specific size and shape, it is necessary to compact them into bulk magnets usable for actual applications. Controlling the pressing process is of paramount importance as the heating may alter the nanocrystallites.[2] In an effort to understand the process, we have designed a special diamond anvil cell to observe the heating and pressing process *in situ*. Hereby we get a better handle of what happens during the compaction process.
The structure under investigation, $SrFe_{12}O_{19}$, is hexagonal with largely different unit cell parameters (ab-axis = 5.88 Å and the c-axis = 23.09 Å). Using a bottom-up synthesis approach the resulting crystallites are thin platelets with hexagonal shape. The magnetic easy axis is aligned along the c-axis. The highly anisotropic shape of the nanoparticles causes the nanopowder to significantly align when pressed into pellets.[3] Preferred orientation is normally considered a nuisance, but for magnetic material it is an absolute must for obtaining good magnetic properties.
All processes have been followed using X-ray diffraction to get information about size, shape, and texture. The obtained information is utilized to improve the processes and enhance the magnetic performance.

[1] Granados-Miralles C., Saura-Múzquiz M., Jensen K. M. Ø., Bøjesen E. D., Andersen H. L. and Christensen M. *J. Mater. Chem. C*, 2016 *4*, 10903-10913

[2] Saura-Múzquiz M., Granados-Miralles C., Stingaciu M., Bøjesen E. D., Li Q., Song J., Dong M., Eikeland E. and Christensen M. *Nanoscale*, 2016 8, 2857-2866

[3] Eikeland A. Z., Stingaciu M., Granados-Miralles C., Saura-Múzquiz M., Andersen H. L., Christensen M. *CrystEngComm*, 2017, 19, 1400-1407

Keywords: Magnetic materials, nanocrystallites, texture

Crystal structure and microstructure of γ-Al_2O_3 determined by analysing the anisotropic line broadening diffuse scattering

M. Rudolph[a*], M. Motylenko[a], D. Rafaja[a]
[a] *Institute of Materials Science, TU Bergakademie Freiberg, DE*
* *m.rudolph@iww.tu-freiberg.de*

The intermediate alumina phase γ-Al_2O_3 plays a key role in the industrial catalysis, because it possesses a large specific surface area and a high catalytic activity. Currently, this phase is also considered as a key material for production of functional coatings for metal melt filtration, as it can attach ceramic inclusions and remove them from the metallic melt. At high temperatures, however, the metastable γ-Al_2O_3 phase, which is usually described as a defect spinel like structure, transforms to corundum (α-Al_2O_3) and loses its beneficial properties. As this transformation is accompanied and facilitated by changes in the defect structure of γ-Al_2O_3, a reliable and quantifiable structure and microstructure model of γ-Al_2O_3 is required to understand and to delay the phase transition of γ-Al_2O_3 to α-Al_2O_3 and thus to stabilize metastable γ-Al_2O_3.
In the selected area electron diffraction (SAED) and X-ray diffraction (XRD) patterns, the defect structure of γ-Al_2O_3 produces prominent broadening of particular diffraction lines. The SAED disclosed that the reciprocal lattice points of γ-Al_2O_3 are broadened in the ⟨001⟩ direction. Crystallographic considerations revealed that the broadening of particular diffraction lines is caused by the atomic disorder concerning exclusively on the cation sublattice. For advanced interpretation of the observed diffraction phenomena, a computer routine was developed that allows a concurrent modelling of the defect structure and microstructure of γ-Al_2O_3, and a subsequent simulation of the corresponding diffraction patterns by means of the Debye equation.
It will be demonstrated that γ-Al_2O_3 consists of nano-crystallites with a spinel like structure, which are additionally fragmented by antiphase boundaries (APBs) into small nano-domains. For distinct reflections, these APBs break the coherence of neighbouring domains for SAED and XRD that results in a selective anisotropic broadening of the reciprocal lattice points. The quantitative modelling of the defect structure revealed fundamental parameters of γ-Al_2O_3 like the mean size of the nano-domains, the specific type of the APBs and the degree of ordering of the structural vacancies within the cation sublattice. Finally, the effect of these microstructure defects on the thermal stability of γ-Al_2O_3 and the consecutive phase transition to α-Al_2O_3 will be discussed.

Keywords: disordered structure, phase transition, Debye equation

Quantification of Correlated Disorder in Alloy Systems Through Complex PDF Modelling

Robert J. Koch[a*], Shubham Pandey[b], Guangfang Li[c], Hui Wang[c], Simon R. Phillpot[b], and Scott T. Misture[a]

[1]*Inamori School of Engineering, Alfred University, Alfred, NY 14802, USA*

[2]*Department of Materials Science and Engineering, University of Florida, Gainesville, FL 32611, USA*

[3]*Department of Chemistry and Biochemistry, University of South Carolina, Columbia, SC 29208, USA*

**kochr@alfred.edu*

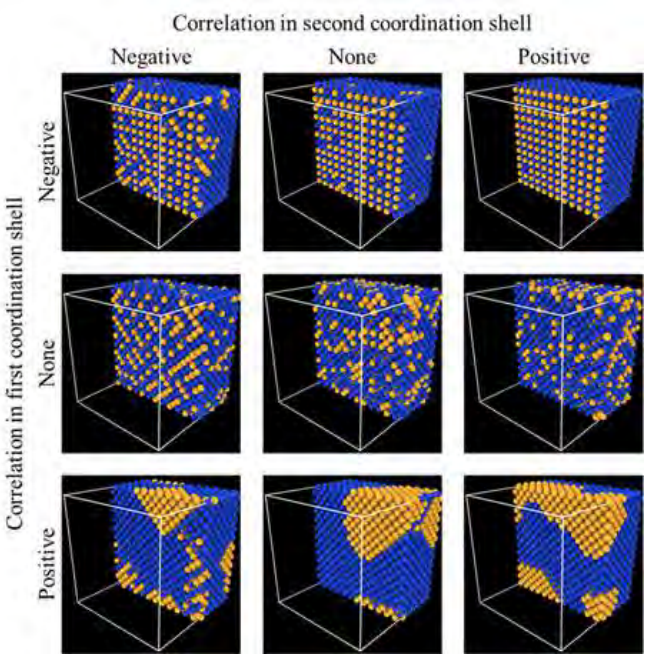

Detailed information on atomic scale ordering and nanostructure in order-disorder (intermetallic-solid solution) phase transitions is not easily accessible. This is a result of the "nanostructure problem" [1] within the field of classical crystallography. The depth and inverse nature of this problem requires complex modelling [2] to fit observed data, so that structure – processing - property relationships can be leveraged to tailor material performance. Here we probe the correlated nature [3] of chemical short-range order and displacement disorder in prototypical order-disorder (o-d) Au-Cu systems. We achieve this through a novel approach, by tuning an evolutionary algorithm for global optimization of large atomic ensembles to fit the measured total scattering pair distribution function (PDF). These models are further refined using density functional theory (DFT) to elucidate the subtle bond-length fluctuations associated with correlated disorder. Applications of this technique to both ambient and high-temperature conditions are discussed.

[1. S. J. L. Billinge, I. Levin, *Science*. **316**, 561–565 (2007).
2. P. Juhás, C. L. Farrow, X. Yang, K. R. Knox, S. J. L. Billinge, *Acta Crystallogr. Sect. A Found. Adv.* **71**, 562–568 (2015).
3. D. A. Keen, A. L. Goodwin, *Nature*. **521**, 303–309 (2015).

Keywords: total-scattering, chemical-short-range-order, differential evolution

Mapping the size dependent structure of metal oxides: A new molybdenum oxide nanostructure from X-ray total scattering

Kirsten M. Ø. Jensen*[a], Troels L. Christiansen[a], Espen D. Bøjesen[b], Mikkel Juelsholt[a]
[a] *Department of Chemistry and Nanoscience Center, University of Copenhagen, Denmark*
[b] *Monash Centre for Electron Microscopy, Monash University, Australia*
* *kirsten@chem.ku.dk*

Mapping the structure/property relations in new nanomaterials have for a long time been a challenge for structural chemists, and on an atomic scale, even the smallest nanoparticles are often seen as 'cut-outs' of bulk materials, where the atomic structure known from bulk chemistry is used to describe the atomic arrangement. With the development of new methods for structural characterization, in both scattering, spectroscopy and microscopy, the influence of nanosize on structure has recently been realized and studied in metallic nanoparticles.[2,3] Here, we extend this field to the study of oxides, and show that nanoparticles of molybdenum oxides with sizes under 5 nm ubiquitously take new structural motifs not seen in any reported bulk molybdenum oxides, regardless of the synthesis method applied.[1] The realisation of a new structure in nanoscale molybdenum oxides explains several observations of altered material properties in e.g. battery materials and catalysis, and knowledge of the structure is crucial to improve the material performance in any application.[4]
The building blocks for bulk molybdenum oxide structures are $[MoO_6]$-octahedra, which share corners and edges to form different crystal structures, giving rise to very rich structural chemistry. Early studies of these structures found a large homologous 'Magneli' series of molybdenum oxide phases (Mo_nO_{3n-m}) where the structures vary by the introduction of shear planes.[5] Using PDF analysis, we show that the known molybdenum oxide Magneli series cannot describe the atomic arrangement in nanostructured molybdenum oxides. Instead, the atomic arrangement is related to the distorted rutile MoO_2 structure with a high concentration of shear planes which greatly alters the both the local and average structure in the particles. This structure has so far not been seen in molybdenum oxides but is related to the shear planes sometimes observed in bulk rutile titanium oxides. PDF analysis allows us to develop a new structural model for even the smallest nanoparticles of MoO_2 and understand the size/structure relation in the system. As the particle size increases, the concentration of shear planes decreases, and alters only the local structure but not the long-range order, as characterized by PDF and Rietveld refinement. The PDF analysis and modelling is supported by HR-TEM which confirms the model developed from X-ray total scattering on an atomic scale. Finally, *in situ* studies of the formation of oxides from polyoxometalate ions give hints to the formation of defects in the structure as well as their degradation.

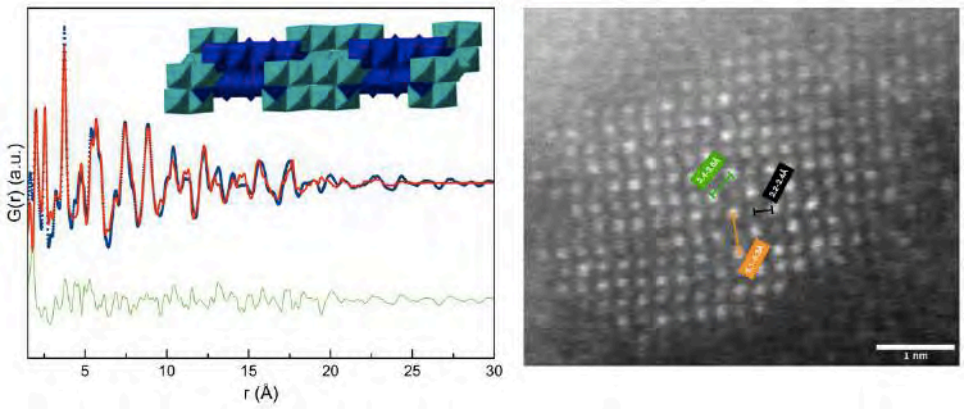

[1] Christiansen, T. L.; Bøjesen, E.D. Juelsholt, M., Jensen, K.M.Ø., Submitted, 2018
[2] Jensen, K. M. O.; Juhas, P.; Tofanelli, M. A.; Heinecke, C. L.; Vaughan, G.; Ackerson, C. J.; Billinge, S. J. L. *Nat Commun* 2016, 7.
[3] Doan-Nguyen, V. V. T.; Kimber, S. A. J.; Pontoni, D.; Hickey, D. R.; Diroll, B. T.; Yang, X. H.; Miglierini, M.; Murray, C. B.; Billinge, S. J. L. *ACS Nano* 2014, 8, 6163-6170.
[4] Koziej, D. *Chem. Mater.* 2016, 28, 2478-2490.
[5] Magneli, A. *Acta Crystallogr* 1953, 6, 495-500.

Keywords: Pair Distribution Function, Nanostructure, defects, size/structure relation

Study of Nanoalloys Co_xPt_{1-x} Formation Mechanism from Single-Source Precursors

E. Yu. Filatov[a,b], A. V. Zadesenets[a,b], S.V. Korenev[a,b]
[a] *Nikolaev Institute of Inorganic Chemistry SB RAS, 630090 Novosibirsk, Lavrentjiev Ave. 3*
[b] *Novosibirsk State University, 630090 Novosibirsk, Pirogova str. 2*
E-mail: decan@niic.nsc.ru

This work is devoted to the study of the metals solid solutions formation mechanism in the Co-Pt system, in which a wide region of superstructural ordering is present. The CoPt alloys, which are closed to equiatomic composition, have a very high energy of crystallographic magnetic anisotropy ($K_1 \approx 5 \cdot 10^7$ erg/cm^3) and, as a result, high hysteresis properties, which makes them attractive for use as nanomagnets. In the literature there are also scientific works showing high catalytic activity of this system. Our task was to study the formation mechanism of nanoscale equiatomic bimetallic solid solutions $Co_{0.5}Pt_{0.5}$ using *in situ* diffractometry, investigation of their magnetic and catalytic properties.

To get equiatomic nanoalloys $Co_{0.5}Pt_{0.5}$, two double complex salts (DCS) $[Pt(NH_3)_4][Co(C_2O_4)_2(H_2O)_2]\cdot 2H_2O$ and $[Co(H_2O)_6][Pt(NO_2)_4]$ were synthesized and characterized by a set of physical and chemical methods. The thermolysis of DCS at relatively low temperatures (350°C and 140°C for the first and second salts, respectively) in a hydrogen atmosphere produces disordered solid solutions of $Co_{0.5}Pt_{0.5}$ with crystallite sizes of 2-4 nm.

In an inert atmosphere the decomposition mechanism is quite complex and after the dehydration stage is determined by two parallel processes. The course of the mass loss curve in the thermogravimetric analysis $[Pt(NH_3)_4][Co(C_2O_4)_2(H_2O)_2]\cdot 2H_2O$ in a hydrogen atmosphere repeats this one in an inert atmosphere. This fact should indicate that the stage mechanism of thermolysis in the inert and reducing atmospheres is the same. Differences are manifested only at the temperatures of the beginning and the end of the stages: in a reducing atmosphere the temperatures of the stages are shifted to a region of lower temperatures. However, diffraction patterns of the thermolysis products of the precursor compound obtained *in situ* upon heating in a hydrogen atmosphere show a significant effect of the second metal reduction process. When the temperature reaches 450°C, only reflexes of the disordered equiatomic solid solution of cobalt and platinum remain on the diffraction pattern.

The subsequent annealing of the obtained samples leads to a time-extended superstructural ordering process, which makes it possible to prepare solid solutions with different degrees of superstructural ordering (α): from a completely disordered $Co_{0.5}Pt_{0.5}$ (α = 0) to a fully ordered solid solution (intermetallic compound) CoPt (α = 100%).

The work is supported by the RFBR Grant 17-03-00950-a.

Keywords: nanoalloys, in situ XRD, ordering, platinum, cobalt.

New insights on Structure and Morphology of Defective CdSe Colloidal Quantum Dots combining DNP-NMR and Advanced Small and Wide Angle X-ray Scattering Techniques

D. Moscheni,[a*] F. Bertolotti,[a,b] L. Protesescu,[c] D. N. Dirin,[c] L. Pivateau,[c] B. Benin,[c] A. Cervellino,[d] M. V. Kovalenko,[c] J. S. Pedersen,[b] N. Masciocchi,[a] A. Guagliardi [e]

[a] *Università degli Studi dell'Insubria and To.Sca.Lab, Como, Italy*
[b] *Aarhus University, Aarhus, Denmark*
[c] *ETH Zürich and EMPA, Dübendorf, Switzerland*
[d] *Paul Scherrer Institut, PSI, Villigen, Switzerland.*
[e] *Istituto di Cristallografia, CNR, and To.Sca.Lab, Como, Italy.*
* d.moscheni@studenti.uninsubria.it

Cadmium Selenide Colloidal Quantum Dots (cQDs) are one of the most promising class of luminescent nanocrystalline materials [1,2]. The reduced crystalline domains at the nanoscale, together with the presence of structural or compositional defects (i.e. point or planar defects, such as dislocations or stacking faults, SF) and of surface relaxation phenomena, cause a significant amount of diffuse scattering and unpredictable peaks broadening and shifts in the diffraction patterns, no longer interpretable by the conventional crystallographic laws [3,4].
Not being restricted to ideally periodic and ordered materials, the Debye Scattering Equation (DSE)-based approach, treats Bragg and diffuse scattering on equal basis and allows the modeling of the total scattering pattern of nanocrystals. Since the computation operates starting from real space atomistic models, structural and microstructural information can be simultaneously derived within a unified approach [5]. However, when dealing with highly defective materials such as CdSe cQDs [6], disentangling size- from defects-induced peaks broadening is not a trivial task and deem it necessary resorting to complementary, "structure insensitive", techniques, such as Small Angle X-ray Scattering (SAXS) [7].
In this work, we investigated the effects of different SF types and probabilities in cQDs of 3÷6 nm in diameter and nanoplatelets (nPLs) of 1.5÷2.5 nm in thickness, by the synergic combination of SAXS and DSE. Starting from the Warren theory [8], modeling has been tailored towards an original method for the SF interpretation and quantification in nanoparticles. By this innovative approach, we were able to determine the non-isotropic morphology of CdSe cQDs, to unveil the presence of planar defects in the zinc blend crystal structure and an additional SF-induced anisotropic strain.
To complete this picture, Dynamic Nuclear Polarization - ^{113}Cd NMR measurements [9] were performed on cQDs and nPLs, in order to provide additional information on the different chemical environments of the atoms between the core and the surface of the nanocrystals.

[1] Talapin D. V., Lee J., Kovalenko M. V. and Shevchenko E. V. *Chem. Rev.,* 2010, *110*, 389.

[2] Kovalenko M. V., Manna L., Cabot A., Hens Z., Talapin D. V., Kagan C. R., Klimov V. I., Rogach A. L., Reiss P., Milliron D. J., Sionnest P. G., Konstantatos G., Parak W. J., Hyeon T., Korgel B. A., Murray C. B. and Heiss W. *ACS Nano,* 2015, *9(2)*, 1212.

[3] Billinge S. J. L. and Levin I. *Science,* 2007, *316*, 561.

[4] Palosz B.; Grzanka E., Gierlotka S., Stelmakha S., Pielaszek R., Bismayer U., Neuefeind J., Weber H.-P. and Palosz W. *Acta Phys. Pol. A,* 2002, 102, 58.

[5] Bertolotti F., Dirin D. N., Ibanez M., Krumeich F., Cervellino A., Frison R., Voznyy O., Sargent E. H., Guagliardi A. and Masciocchi N. *Nat. Mater.,* 2016, *15*, 987.

[6] Masadeh A. S., Božin E. S., Farrow C. L., Paglia G., Juhas P. and Billinge S. J. L. *Phys. Rev. B,* 2007, *76*, 115413.

[7] Gagin A., Allen A. J. and Levin I. *J. Appl. Cryst.,* 2014, 47, (2), 619.

[8] Warren B. E. *X-Ray Diffraction* 1990, *Dover Publications, Inc., New York, 275.*

[9] Piveteau L., Ong T. C., Rossini A. J., Emsley L., Copéret C. and M. V. Kovalenko *J. Am. Chem. Soc.,* 2015, *137, 13964*.

Keywords: Nanomaterials, Quantum-dots, Total Scattering

Size and strain induced anisotropic XRPD line broadening in $Fe_{3-x}Y_xO_4$ (x=0.00, 0.05, 0.10) nanorods and nanospheres mixtures

A. Kremenović [a*], B. Antić [b]
[a] *University of Belgrade, Serbia*
[b] *The "Vinča" Institute of Nuclear Sciences, Belgrade, Serbia*
[*] *aleksandar.kremenovic@rgf.bg.ac.rs*

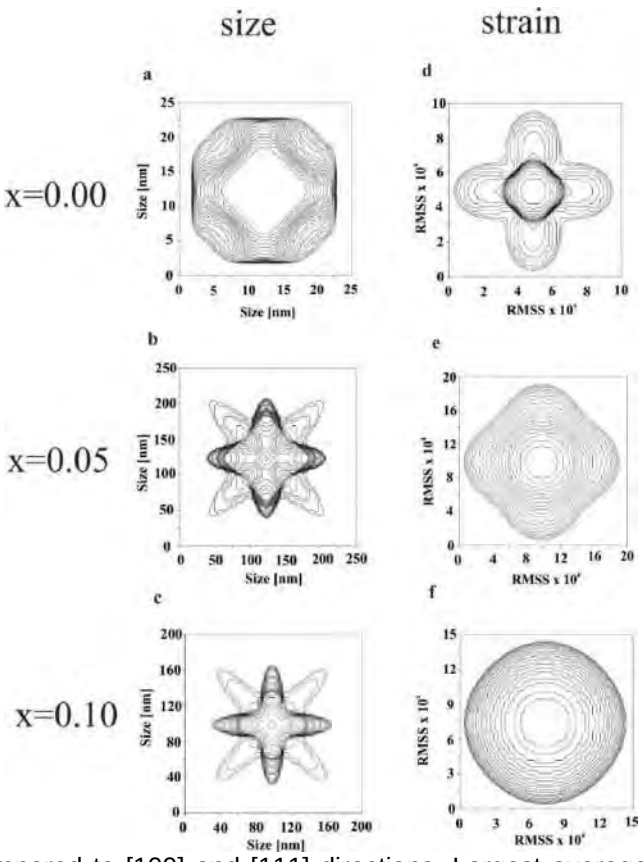

Laboratory XRPD data collected on $Fe_{3-x}Y_xO_4$ (x=0.00, 0.05, 0.10) nanorods and nanospheres mixtures were refined by the program FullProf [1], which enables to refine simultaneously both structural and microstructural parameters. Beside atomic coordinates, unit cell, site occupation and thermal vibration parameters anisotropic size parameters K_{00}, K_{41}, K_{61}, K_{81}, as well as anisotropic strain parameters S_{400}, S_{200}, L_σ (applied Laue class $m\bar{3}m$) were refined simultaneously till convergence was reached. Identical XRPD patterns for $Fe_{3-x}Y_xO_4$ (x=0.00, 0.05, 0.10) nanorods and nanospheres in a mixture, within instrument resolution, limits refinements of separate contribution of nanorods and nanospheres to overall XRPD line broadening. Therefore, interpretation of obtained results as averaged over all nanospheres and nanorods is important step in microstructure characterization. Results show that addition of Y provokes increase of both apparent strain and crystallite size values in all directions. Largest average apparent crystallite size is in [110] direction for all compositions. Only when Y exchange Fe in Fe_3O_4 structure average apparent crystallite size in [110] direction increases 2-3 times compared to [100] and [111] directions. Largest average mixing strain for Fe_3O_4 is in [100] direction and lowest in [111] direction. With Y concentration increase difference in average strain in different directions decreases and is negligible for $Fe_{2.90}Y_{0.10}O_4$.

[1] Rodriguez-Carvajal, J. *Physica B*, 1993, 192**,** 55.

Keywords: size-strain, anisotropic, line broadening

X-ray characterization of dielectric layers of crosslinked methacrylate copolymers for application in organic electronics

D. Jehnichen[a*], D. Pospiech[a], A. Berndt[a], S. C. Gomoll[a], E. Natkowski[a], M. Plötner[b]
[a] *Leibniz-Institut für Polymerforschung Dresden e.V., Germany*
[b] *Institute of Semiconductors and Microsystems, Technische Universität Dresden, Germany*

* *djeh@ipfdd.de*

Poly(methyl methacrylate) (PMMA) is one of the most important polymers for application as dielectric layer in organic electronics devices, e.g. in organic field effect transistors (OFETs). The key to improve the transistor performance, expressed e.g. by charge carrier mobility and on/off ratio, is the design and optimization of the interface between semiconductor and dielectric layer where charges are accumulated and move [1]. The order in this interface plays an important role. Usually, the semi-conductor polymer has a high order due to its chemical structure, while the dielectric used has not.

Therefore, PMMA copolymers were designed in this study that are able to introduce self-organization when the semiconductor is applied on top of dielectric. Semifluorinated methacrylates (sfMA) with different sf chains were used as comonomer for MMA dielectric layers. PMMA itself is amorphous, but incorporation of sf side chains is expected to induce self-organization as reported earlier [4] and should enhance the order. The copolymers additionally contain crosslinkable monomer units to improve the chemical stability of the layers against inks, semiconductor solvents and other solvents used during processing, and to allow multilayer preparation. The chemical structure of the copolymers which were obtained by radical copolymerization was tuned to achieve this combination of properties [2,3].

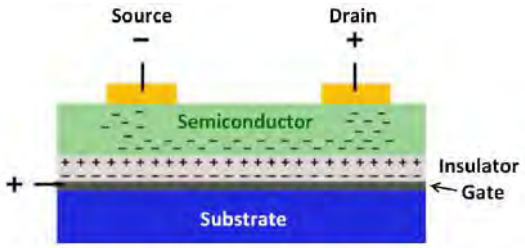

Scheme of OFET with bottom-gate / top-contact structure

Sf dielectrics with stepwise varied chemical were investigated. The copolymers contained MMA, a crosslinker (4-benzoylphenyl MA), and a sfMA with either -0-$(CH_2)_{10}$-$(CF_2)_{10}$F, -0-$(CH_2)_2$-$(CF_2)_8$F or -0-$(CH_2)_2$-$(CF_2)_6$F side chains as comonomers. As a result, both concentration as well as length of the sf substituent influenced the degree of order, i.e. generation of layered structures [2,4,5,7].

Thin dielectric films were prepared by spin-coating of polymer solutions onto silicon wafer. For suitable electric properties the films are required to be defect-free. It was found that the film quality depended strongly on the type of solvent. As semiconductor, poly(3-hexylthiophene-2,5-diyl) (P3HT) was employed, its ordering behavior has been reported in literature [8]. The ordering behavior of the sf units in the dielectric layers was studied by a combination of methods. Thin films (single films of dielectric, double layers of dielectric on the semiconductor layer) were investigated by X-ray reflectometry (XRR). Additionally, film thicknesses were determined by ellipsometry. As in the bulk, the length of the sf substituent as well as their concentration determines the structure formation in thin films. This will be illustrated by XRR measurements. The same parameters influence the film quality, the wetting of P3HT with the dielectric layer, and the electrical properties and OFET quality.

[1] Brinkmann M., Gonthier E., Bogen S. et al. *ACS Nano*, 2012, 6, 10319.

[2] Berndt A., Pospiech D., Jehnichen D. et al. *ACS Appl. Mater. Interfaces*, 2015, 7, 12339.

[3] Al-Hussein M., Berndt A., Jehnichen D. et al. *Colloid Polym. Sci.*, 2016, 294, 1475.

[4] Jehnichen D., Friedel P., Selinger R. et al. *Powder Diffraction*, 2013, S2, S144.

[5] Jehnichen D., Pospiech D., Friedel P. and Funari S.S. *Z. Kristallogr. Proc.*, 2011, 1, 487.

[6] Pospiech D. and Jehnichen D., Chpt. 11 in: *Handbook of Fluoropolymer Science & Technology*, ed. by D. W. Smith Jr., S. T. Iacono and S. S. Iyer (Wiley) 2014, pp. 235-290.

[7] Pospiech D., Jehnichen D., Chunsod P., Friedel P., Simon F. and Grundke K., Chapt. 8 in: *Fluorinated polymers: From fundamental to practical synthesis and applications*, ed. by B. Ameduri and H. Sawada (RSC Press), 2016, Vol.1, pp. 235-275.

[8] Colle R., Grosso G., Romzani A. and Zicovich-Wilson C.M. *Phys. Status Solidi B*, 2011, 248, 1360.

Keywords: dielectric layers, PMMA copolymer, multilayer characterization

Syntheses and Characterization of Iron Oxide Nanoparticles functionalized with biocompatible molecules

P.S. Haddad*, I.S. Campos
[a] *Department of Chemistry, Federal University of São Paulo, Brazil*
* *haddad.paula@unifesp.br*

Magnetic iron oxide nanoparticles (NPs), with appropriate surface coatings, are commonly used in biomedical applications [1], such as drug delivery. For the successful application of these nanoparticles, it is necessary they have well-defined structural and magnetic characteristics, in addition to high stability and biocompatibility in biological environments. Therefore, the present work is focused on the synthesis and structural characterization of Fe_3O_4 nanoparticles coated with mercaptosuccinic acid (MSA) and chitosan (CS) polymer with great potential as drug-delivery. Magnetite nanoparticles (Fe_3O_4 NPs) were synthesized by mixture of Fe^{2+} and Fe^{3+} chlorides in the presence of a base (NH_4OH) by the co-precipitation method and by thermal decomposition of acetylacetonate iron ($Fe(acac)_3$). These nanoparticles were coated with the thiol-containing molecule MSA and with CS polymer leading to Fe_3O_4-MSA and Fe_3O_4-CS NPs, respectively. The obtained NPs were characterized by different techniques such as Fourier transform infrared spectroscopy (FTIR), X-ray diffraction (XRD), dynamic light scattering (DLS) and SQUID magnetic measurements. The results showed that the Fe_3O_4-MSA NPs obtained have a mean diameter of 11 nm, while Fe_3O_4-CS NPs presented a crystallite diameter of 14 nm. The average hydrodynamic sizes of Fe_3O_4-MSA and Fe_3O_4-CS nanoparticles were 87 ± 17 and 124 nm ± 15 nm. The nanoparticles presented magnetic behavior at room temperature due to the presence of Fe_3O_4 core. Due to the superparamagnetic behavior of Fe_3O_4-MSA or Fe_3O_4-CS nanoparticles, upon the application of an external magnetic field, those nanoparticles can be guided to the target site yielding with minimal side effects to normal tissues, highlighting the promising uses of iron oxide nanoparticles in biomedical applications as drug carrier vehicles.

[1] Gonçalves L.C, Seabra A.B., Pelegrino M.T., de Araujo D.R., Bernardes J.S. and Haddad P.S. *RSC. Advances*, 2017,7, 14496.

Keywords: superparamagnetic iron oxide nanoparticles, chitosan, X-ray diffraction

Room temperature aging and tempering of highly nitrogen-supersaturated ferritic solid solutions

M. Wetzel[a*], A. Leineweber[a]
[a] *Institute of Materials Science, TU Bergakademie Freiberg, Freiberg, Germany*
** marius.wetzel@iww.tu-freiberg.de*

High-energy ball milling of one or more substances leads to a mechanically driven redistribution of their atoms. As a result, the thereby mechanically alloyed components may form solid solutions or novel metastable phases. For the system Fe-N it has been shown that ball milling of α-Fe in N_2 or NH_3 atmosphere [1,2] as well as mixtures of α-Fe and iron nitrides [3,4] leads to the formation of a bcc-like solid solution containing up to 15.6 at.% N [4] which is several orders of magnitude more than the equilibrium solubility of N in α-Fe.

In this work, powder mixtures of bcc α-Fe and fcc γ'-Fe_4N containing up to 10 at.% N have been mechanically alloyed in either a shaker or a planetary ball mill. The resulting samples were investigated by means of powder X-ray diffraction. Changes in line profiles and positions were determined in order to characterize the diffraction phenomena related to nitrogen supersaturation of ferrite and their evolution during aging and tempering of the solid solutions.

When sufficiently homogenized, the milled powder mixtures appear to be single-phase bcc-like α-(Fe,N) solid solution. Only in some cases minor amounts of residual fcc γ-(Fe,N) were observed. The diffraction patterns of α-(Fe,N) are characterized by pronounced line broadening and asymmetries, both increasing with increasing nitrogen content. More interestingly, the solid solution phase shows peculiar anisotropic peak shifts. If the peak position data are interpreted in terms of a bcc solid solution, the observed peak shifts cannot be explained by a mere cubic anisotropy in lattice strain. Room-temperature aging experiments have shown that the anisotropy in the line shifts reduces with aging time. The distortion vanishes entirely upon tempering at temperatures above 200°C as soon as enhanced γ'-Fe_4N formation sets in.
Although both models are not mutually exclusive, peak shifts and asymmetries have so far been interpreted to indicate either a tetragonal distortion of the bcc crystal structure [2] or the occurrence of planar faults [4] predominantly causing these effects. Both approaches are reassessed taking into consideration the aging behavior of N-supersaturated ferrite.

[1] T. Koyano, C. Lee, T. Fukunaga and U. Mizutani, *Mat. Sci. For.*, 1992, 88-90, 809.

[2] J. Rawers, D. Govier and D. Cook , *J. Mater. Synth. Process.*, 1995, 3, 263.

[3] T. Koyano, T. Takizawa, T. Fukunaga and U. Mizutani, *Jpn. J. Appl. Phys.,* 1993, 32, L1524.

[4] J. Aufrecht, A. Leineweber, J. Foct and E.J. Mittemeijer, *Phil. Mag*., 2008, 88, 1835.

Keywords: mechanical alloying, aging, peak shifts

Toward Smart and Eco-friendly Nanofertilizers: Structural and Physico-Chemical Characterization of N-doped Calcium Phosphates

N. Masciocchi,[a,*] F. Carmona,[a] G. Dal Sasso,[b] G.B. Ramírez Rodríguez,[a,c] D. Redoglio,[a] F. Ferri,[a] J.M. Delgado López[c] and A. Guagliardi[b]

[a]*University of Insubria and Total Scattering Laboratory (To.Sca.Lab.), Como, Italy*
[f]*Istituto di Cristallografia, CNR, and Total Scattering Laboratory (To.Sca.Lab) Como, Italy*
[c] *University of Granada, Granada, Spain*
** norberto.masciocchi@uninsubria.it*

Hydroxyapatite [$C_{10}(OH)_2(PO_4)_6$] (HA), the mineral component of bone and teeth, is known to naturally occur as fluo- or chloro-substituted crystalline phases. As many inorganic ionic solids, HA is easily converted into multicomponent systems by including exogenous ions substituting the original ones. The structural ability of incorporating different kinds of ions makes HA-based materials a very interesting platform to engineering the properties, a strategy that is particularly effective at the nanoscale while adopting a biomimetic synthesis approach. However, the in-depth comprehension of how ions incorporation structure takes place within the HA crystal framework, is not a trivial task, considered the intrinsic enhanced complication of structural analysis at the nanoscale. As an example, in bio-apatite the well known carbonate-to-phosphate substitution, heavily influencing the mechanical bone properties, is still highly debated.
In this study, nanosized-HA versatility has been the starting point for addressing the effect of N-containing ions (ammonium and/or nitrate), for the application of engineered nano-apatites (E-nAp) as smart nanofertilizers (N and P are the plants macronutrients). NO_3^- and NH_4^+ are found to strongly influence the nature and the microstructural properties of nanocomposites obtained by controlled precipitation, at physiological conditions, of more that 80 batches of doped materials, obtained by varying ions concentration, pH, and Ca(II) complexing agents (citrate). [1] Our structural studies, mostly relying on synchrotron-based X-ray total scattering methods and Debye Scattering Equation modeling [2] of the entire set of nanocomposites, revealed the appearance of subtle, but distinct, structural/microstructural features induced by the incorporation of different ions. Complemented by a number of independent physico-chemical analyses such as elemental, ICP-MS, IR and DLS characterization, and by an extensive electrochemical study of the release kinetics of the ions upon suspending the dry materials in aqueous media, the in-depth characterization enables a comprehensive understanding of the structure-property dependency. The obtained results indicate that a differential behavior of the whole solubility process can be addressed by the careful control of the synthetic conditions, therefore validating a synthesis-by-design approach for eco-friendly, easily scalable E-nAp to be used as smart nanofertilizers.

[1] J.M. Delgado-López, R. Frison, A. Cervellino, J. Gómez-Morales, A. Guagliardi, N. Masciocchi. *Adv. Funct. Mater.* **2014**, *24*, 1090.

[2] A. Cervellino, R. Frison, A. Guagliardi, F. Bertolotti. *J. Appl. Cryst.* **2015**, *48*, 2026.

Acknowledgments: This work was supported by Fondazione Cariplo, "Integrated research on industrial biotechnologies". Project No. 2016-0648*. HYPATIA, Size-controlled HYdroxyaPATItes for sustainable Agricultur*e.

Keywords: Calcium Phosphates, Ion Doping, Nanocrystals, Total Scattering Methods

Synthesis of cobalt molybdenum nitrides from cobalt(II) acetate and ammonium heptamolybdate – in-situ XRD study

P. Adamski[a*], A. Sarnecki[a], M. Nadziejko[a], A. Komorowska[a], A. Albrecht[a], D. Moszyński[a]
[a] *Institute of Inorganic Chemical Technology and Environment Engineering, Faculty of Chemical Technology and Engineering, West Pomeranian University of Technology, Szczecin, Poland*
** adamski_pawel@zut.edu.pl*

Ternary nitrides exhibit very promising catalytic and magnetic properties [1]. Among them cobalt molybdenum nitrides, Co_2Mo_3N, Co_3Mo_3N and Co_6Mo_6N, are compounds of the special interest. Cobalt molybdenum nitrides are catalysts in such processes as the ammonia synthesis and decomposition, hydrodesulphurization or NO reduction [2]. The typical synthesis procedure has two steps. Bimetallic oxide precursor is synthesized, usually from cobalt(II) nitrate and ammonium heptamolybdate. It is further transformed into nitride during a temperature-programmed ammonolysis. In this work the second step was investigated with the use of a reaction chamber attached to a laboratory diffractometer. This approach allows to handle the ammonolysis process and acquire diffraction data simultaneously. Cobalt(II) nitrate was substituted with cobalt(II) acetate. Since an obtained diffraction pattern of precursor was not identified with use of ICDD PDF 4+ 2018 database the structure solution procedure was used to determine its atomic arrangement. It was found that the precursor contains lamellar phase similar to $NH_4H_3Cu_2Mo_2O_{10}$ described earlier [5], but with copper sites substituted with cobalt atoms. Under the ammonolysis conditions the precursor underwent several structural transformations as shown in the picture below. Intermediate phases were identified as: $CoMoO_4$, $Co_2Mo_3O_8$, Co, Mo_2N. Final product was stable under synthesis conditions and it is a mixture of Co_2Mo_3N and Co_3Mo_3N.

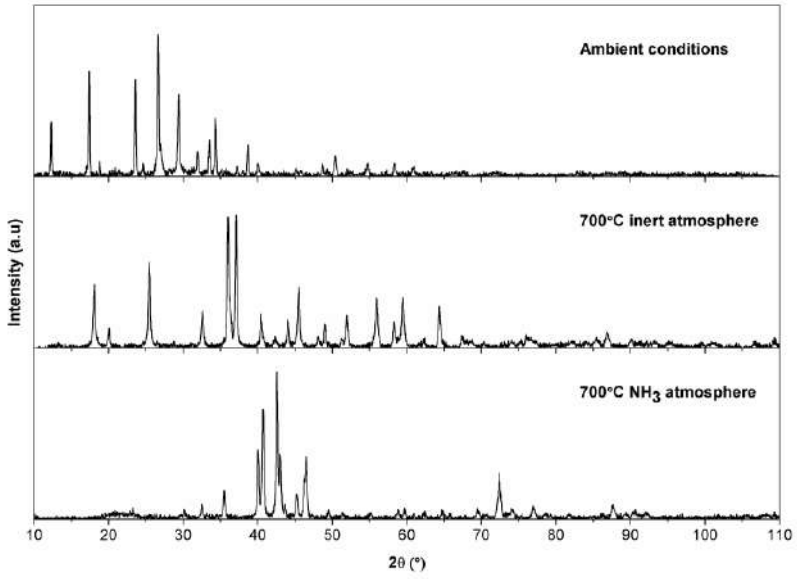

[1] Moszyński D. *Int. J. Refract. Met. Hard Mater.,* 2013, 41, 449.

[2] Moszyński D., Jędrzejewski R., Ziebro J., Arabczyk W. *Appl. Surf. Sci.,* 2010, 256, 5581.

[3] Kojima R., Aika K. *Appl. Catal. A.,* 2001, 215, 149.

[4] Moszyński D., Adamski P., Nadziejko M., Komorowska A., Sarnecki A. *Chem. Pap.,* 2018, 72, 425.

[5] Wu C.D., Lu C.Z., Lin X., Lu S.F., Zhaung H.H., Huang J.S. *J. Alloys. Compd.,* 2004, 368, 342.

Keywords: cobalt molybdenum nitrides, ammonolysis, XRD in-situ

Application of Debye Scattering Equation on laboratory XRPD data of TiO_2 NPs

P. O'Meara[a*], M. Sommariva[b], M. Gateshki[b], F. Bertolotti[c], A. Guagliardi[d], A. Cervellino[e], N. Masciocchi[f]

[a] *Malvern Panalytical Ltd., Royston Hertfordshire, UK*
[b] *Malvern Panalytical BV, Almelo, The Netherlands*
[c] *Aarhus University, Århus, Denmark*
[d] *Institute of Crystallography-CNR and To.Sca.Lab, Como, Italy*
[e] *Swiss Light Source, Paul Scherrer Institut, Switzerland*
[f] *Insubria University, Como, Italy*
* *Paul.OMeara@malvernpanalytical.com*

The direct application of the Debye Scattering Equation (DSE) [1] is increasing its popularity as a tool for the analysis of defective and nanocrystalline materials, see for instance [2]: starting from a structural model in the real space, the (X-ray or neutrons) total scattering pattern of a defective or nanocrystalline system can be calculated by using the DSE, and microstructural information such as the crystallite size distribution or the size-dependence of lattice parameters can be extracted [3]. In recent times the main limiting factor in the direct application of the DSE has been overcome by the widespread availability of high computing power, and also by smarter implementation of the DSE approach in programs such as the Debussy suite of programs [4]. This opens-up the doors to the advanced characterization of nanocrystalline materials below 10 nm, which is the size range in which the traditional crystallography starts to lose accuracy due to extreme peak broadening and overlap [5].
The DSE is also the theoretical foundation of the more popular Pair Distribution Function (PDF) method [6], which is an atomistic analysis of the local structure directly in the real space, after Fourier transformation of total scattering data collected till the highest values of scattering vector.
Total scattering experiments are typically carried out at high brilliance synchrotron beamlines, but in this study we report the application of DSE analysis implemented in the Debussy suite [4], based on X-ray powder diffraction data collected on a X-ray laboratory equipment. Photocatalytic TiO_2 nanoparticles in the range 7-10 nm have been used as a case study, in order to illustrate the possibilities to determine microstructural information. The results from laboratory data have been confirmed with analysis in Debussy suite of synchrotron data collected on the same samples at the Swiss Light Source.
The work has been complemented by a comparison of the DSE results with the crystallite size values obtained from conventional line profile analysis of XRPD data, with the refinement of the structural coherent length by PDF analysis, and correlating the results with the particle size distribution obtained by Small-Angle X-ray Scattering (SAXS) data obtained with the same laboratory instrument.

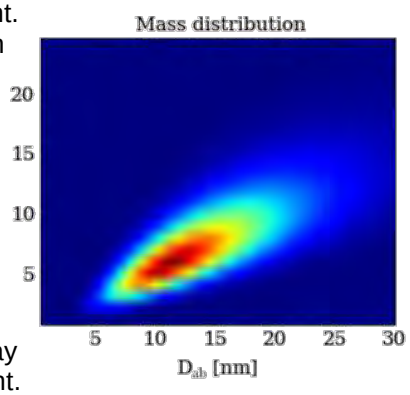

[1] Debye, P. *Ann. Phys.*, 1915, 351, 809.

[2] Liu J. *et al.*, *Chem. Mater.,* 2017, 29, 5591.

[3] Frison R., Cernuto G., Cervellino A., Zaharko O., Colonna G.M., Guagliardi A. and Masciocchi N., *Chem. Mater.*, 2013, 25, 4820.

[4] Cervellino A., Frison R., Bertolotti F. and Guagliardi A. *J. Appl. Cryst.*, 2015, 48, 2026.

[5] Grey I.E. and Wilson N.C. *J. Sol. State Chemistry*, 2007, 180, 670.

[6] Egami T. and Billinge S.J.L. Elsevier, 2012.

Keywords: DSE, PDF, SAXS

Crystal-, magnetic- and micro-structure of spinel ferrite nanocrystallites

Henrik L. Andersen,[a]* Matilde Saura-Múzquiz,[a] Cecilia Granados-Miralles,[a,b] Marian Stingaciu,[a] Frederik M. Søndergaard-Pedersen,[a] Jakob V. Ahlburg,[a] Emmanuel Canévet,[c] Nina Lock[d] and Mogens Christensen[a]

[a]Center for Materials Crystallography, Department of Chemistry and Interdisciplinary Nanoscience Centre, Aarhus University, DK-8000 Aarhus C, Denmark

[b]Current address: Electroceramic Department, Instituto de Cerámica y Vidrio, CSIC, Madrid, Spain

[c]Laboratory for Neutron Scattering and Imaging, Paul Scherrer Institut, 5232 Villigen, Switzerland

[d]Carbon Dioxide Activation Center, Interdisciplinary Nanoscience Centre and Department of Chemistry, Aarhus University, DK-8000, Aarhus C, Denmark

hla@chem.au.dk

The macroscopic performance of magnetic materials is inherently rooted in their atomic- and nano-scale structures. Understanding their crystal- and micro-structure is therefore essential for designing and tailoring magnetic materials with certain properties. The magnetic properties of spinel ferrites, MFe_2O_4 (M= Mn^{2+}, Co^{2+}, Ni^{2+}, Zn^{2+}), depend on the constituent elements, the cation distribution in the structure, and the size of the nanocrystallites. It is thus necessary to develop highly flexible synthesis procedures, which can be easily manipulated into yielding specific products. In this context, hydrothermal synthesis under near- or supercritical conditions is a promising method It has the benefit of being relatively simple, cheap, energy-efficient and easily scalable, and in many cases the product characteristics can be tuned by performing simple adjustments to the reaction parameters.[1-3]
Here, the crystal-, magnetic-, and micro-structures of hydrothermally synthesized spinel ferrite nanocrystallites have been examined by a number of complementary techniques. In particular, a robust structural characterization is achieved by combined Rietveld refinement of a constrained structural model to powder X-ray diffraction and high-resolution neutron powder diffraction data. The structural modeling of $MnFe_2O_4$, $CoFe_2O_4$ and $ZnFe_2O_4$, reveals different affinities of the divalent 3d transition metals for the specific crystallographic sites in the nanocrystalline structures compared to the bulk counterparts, while $NiFe_2O_4$ exhibits the typical 100% inverse spinel structure. The substitution of Zn^{2+} into $Zn_xCo_{1-x}Fe_2O_4$ leads to a decrease in crystallite size and fading of the magnetic long-range order. Comparison with field-dependent magnetization curves illustrates, how the nanocrystallite sizes, the distinct magnetic natures of the constituent ions, and the cation distribution in the spinel structure directly alter the macroscopic magnetic properties.

[1] Andersen H. L., Jensen K. M. Ø., Tyrsted C., Bøjesen E. D. and Christensen M., *Cryst. Growth Des.* 2014, 14, 1307-1313.
[2] Andersen H. L. and Christensen M., *Nanoscale,* 2015, 7, 3481-3490.
[3] Stingaciu M., Andersen H. L., Granados-Miralles C., Mamakhel A. and Christensen M., *CrystEngComm,* 2017, 19, 3986-3996.

Keywords: spinel ferrites, nanoparticles, magnetic structure

Microstructure and cation distribution in magnetic $Ni_{1-x}Zn_xFe_2O_4$ nanocrystallites

Jennifer Hoelscher[a], Henrik Lyder Andersen[a], Matilde Saura-Múzquiz[a], Pelle Gorm Garbus[a], Mogens Christensen[a]
[a] *Department of Chemistry & iNANO, Aarhus University, Denmark*
** j.hoelscher@inano.au.dk*

The cubic spinel ferrites are iron-containing ferromagnetic oxides with the chemical formula MFe_2O_4 (*M*=divalent cation). The magnetic properties of spinel ferrites can be optimized by controlling the type of cations and their relative site distribution within the structure. While the bulk structure of the soft magnetic $Ni_{1-x}Zn_xFe_2O_4$ has been extensively investigated, there are only few studies on the cation site distribution in nano-sized particles using Rietveld refinement.
In this study, we investigate the atomic- and micro-structure of $Ni_{1-x}Zn_xFe_2O_4$ (*x*=0-1) nanoparticles, prepared by a hydrothermal synthesis method in a Teflon lined steel autoclave, using combined Rietveld refinement of neutron powder diffraction, high resolution synchrotron powder X-ray diffraction (PXRD) and in-house PXRD data. The combined Rietveld refinement of the different diffraction datasets obtained at different beam energies provides a robust structural model of the investigated samples making use of resonant scattering contrast to discern between Ni, Zn and Fe atoms. As a consequence, the site occupancies can reliably be deduced from the refinement model. The results show that the crystallite size of the synthesized $Ni_{1-x}Zn_xFe_2O_4$ (*x*=0-1) nanoparticles decreases with increasing zinc content (~7-27 nm) and that Vegard's law is roughly followed. From the peak broadening it is observed that the samples exhibit microstrain due to an uneven distribution of the cations leading to local variations of the lattice constant. Moreover, this study supports that the cation distribution of the crystallographic sites in nanoparticles can deviate from the bulk material as Zn seems to occupy octahedral sites in addition to the tetrahedral sites, which are the preferred position in the bulk structure.

Keywords: rietveld refinement, magnetic nanoparticles, cation distribution

Combustion assisted preparation of single-domain high coercivity $SmCo_5$

H. Tang[a*] and M. Christenen[a]
[a] *Department of Chemistry and iNANO, Aarhus University, Denmark*
** hao@inano.au.dk*

Permanent magnetic materials are widely used in modern technologies, where they are responsible for interchanging between electrical and kinetic energy. One example is the electric car driven by an electric motor, which is partly made of hard magnetic materials. Hard magnetic materials are defined as materials with coercivity >50 kA/m. Another important parameter for hard permanent magnets is the energy product, which described the energy stored in the magnetic fieldlines outside the magnet. $Nd_2Fe_{14}B_3$ magnets show the highest energy product, while its ability to resist demagnetization is relative weak, especially at the working temperature of a motor [1]. The low coercivity is due to a low Curie temperature. Magnets made from $SmCo_5$ on the other hand have a very high Curie temperature (1015 K), which results in a high coercivity and a high resisteance to thermal demagnetization, when functioning in a motor [2]. In previous works, the traditional method to synthesize $SmCo_5$ is melting high purity metals with a stoichiometric ratio at high temperature, forming a size of above 200 µm.[3] Several chemical methods have been developed in recent years for synthesizing $SmCo_5$ nanoparticles with sizes below 100 nm.[4] Either of them, however, are smaller or bigger than calculated single domain size (~0.8 µm), and show relative low coercivity, compared to theoretical predictions.[2-5] Therefore, we have developed a chemical synthesis route to make single-domain size of $SmCo_5$. The method uses assisted solution combustion to obtain a very high coercivity. The powder X-ray diffraction pattern and SEM image of $SmCo_5$ are displayed in the figure below. The coercivity of prepared-$SmCo_5$ particles with size of ~0.8µm reaches to 27 kOe at 300 K and 54 kOe at 10 K. In addition, Prepared-$SmCo_5$ powder can be directly compacted and sintered to form bulk material with a good energy product.

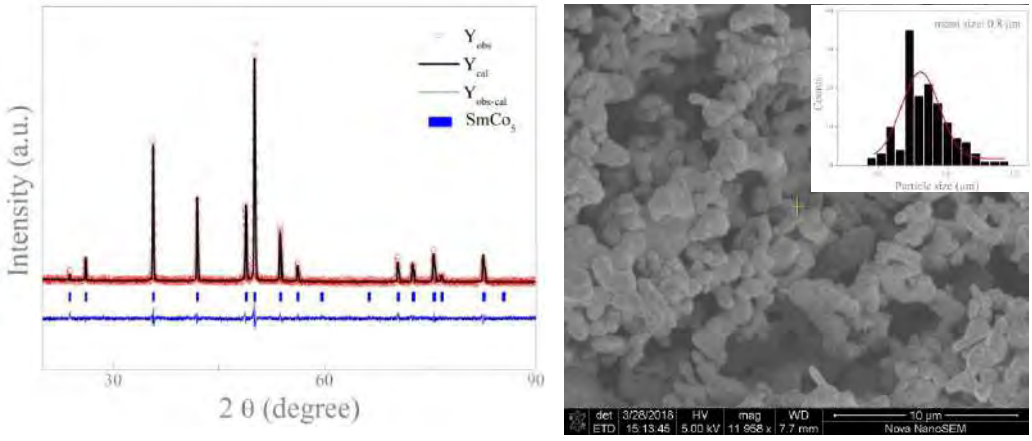

[1] Gutfleisch O. Willard M. A. , Brück E., Chen C. H., Sankar S. G., and Liu J. P. Adv. Mater. 2011, 23, 821-842.
[2] Nassau K. Cherry L. V. and Wallace W. E. J. Phys. Chem. Solids. 1960, 16, 131-137.
[3] Shen Y. H. Leontsev S. O., Turgut Z., Lucas M. S., Sheets A. O., and Horwathet J. C. IEEE Transactions on Magnetics, 2013, 49 (19), 3244-3247.
[4] Zhang H. W., Peng S., Rong C. B., Liu J. P., Zhang Y., Kramer M. J. and Sun S. H. J. Mater. Chem., 2011, 21, 16873-16876.
[5] Tetsuo I., Goto K. and Sakurai T. J. Appl. Phys. 1983, 22, 695-697.

Keywords: $SmCo_5$ particles, single-domain, combustion method

Structural characterization of superparamagnetic iron oxide nanoparticles for potential biomedical applications

F. F. Ferreira[a*], B. L. Henrique[a], F. N. Costa[a], D. R. Araujo[a], T. N. Britos[b], P. S. Haddad[b]
[a] *Center for Natural and Human Sciences, Federal University of ABC, Brazil*
[b] *Department of Chemistry, Federal University of São Paulo, Brazil*
** fabio.furlan@ufabc.edu.br*

In recent years, the use of superparamagnetic iron oxide nanoparticles (SPIONs) – mainly magnetite – has received increasing attention of the scientific community due to its potential biomedical applications [1]. The functionalization of the SPIONs' surface with organic or inorganic ligands is an important task to promote biocompatibility. Oleic acid (OA), tetraethyl ammonium (TEA), cysteine (CYS) and some block copolymers (e.g. Poloxamer 407 – PL407) are among the most used organic ligands, while gold can be employed in a core/shell-like system. Magnetite structure consists of octahedral and mixed tetrahedral and octahedral layers stacked along the [111] direction and its chemical formula is written as $Y(XY)O_4$, where X = Fe^{2+} and Y= Fe^{3+}, displaying superparamagnetic behaviour at room temperature (when synthetized in nanoscale), high effective surface area and low sedimentation rates. Magnetite (Fe_3O_4) crystallizes in a cubic crystal system with space group $Fd\bar{3}m$ and unit cell parameters *a* = 8.3941 Å. Maghemite (γ-Fe_2O_3) crystallizes in a cubic crystal system with space group $P4_332$ and unit cell parameters *a* = 8.3474 Å. Due to the broadened diffraction peaks characteristic of nanoparticulated systems, differentiation between magnetite and maghemite patterns becomes difficult to achieve using conventional X-ray powder diffraction experiments. In this work we have used a combination of X-ray powder diffraction (XRPD), transmission electron microscopy (TEM) and pair distribution function (PDF) to characterize the structure of Au-, CYS-, OA-, TEA- and PL407-covered SPIONs. For the specific case of SPIONs@Au we could identify the quantify the amounts of Fe_3O_4, Au and CTAB (cetyltrimethylammonium bromide) – one of the organic compounds used to synthesize the nanoparticles – using PDF analyses. TEM images revealed the nanoparticles are covered by an amorphous shell, which is responsible for ~64 wt% according to the results obtained from PDF and XRPD. For the OA-SPIONs and TEA-SPIONs we have performed *in situ* XRPD experiments – with temperatures ranging from 303 – 1223 K – and studied how the oxidation state of Fe^{2+} ions varied in the different systems, parameterising them using parametric Rietveld refinements [2].

Acknowledgments: The authors thank the financial supported provided by FAPESP (grants # 2011/19924-2, # 2015/26233-7 and # 2017/15601-6), CNPq (grants # 402289/2013-7 and # 307664/2015-5), the Brazilian Nanotechnology National Laboratory (LNNANO) and the Multiuser Experimental Centre (CEM) of UFABC.

[1] Mohammed L., Gomaa H.G., Ragab D. and Zhu J., *Particuology*, 2017, 30, 1.

[2] Pereira G.F.L., Costa F.N., Souza J.A., Haddad P.S. and Ferreira F.F., *J. Magn. Magn. Mater.*, 2018, 456, 108.

Keywords: iron oxide nanoparticles, x-ray powder diffraction, pair distribution function

Structure, texture and properties of $SrFe_{12}O_{19}$ magnets

M. Saura-Múzquiz[a,b*], A. Z. Eikeland[a], M. Stingaciu[a], H. L. Andersen[a], C. Granados-Miralles[a,c], V. Luzin[b], M. Avdeev[b] & Mogens Christensen[a]

[a] *Center for Materials Crystallography, Department of Chemistry and iNANO, Aarhus University Langelandsgade 140, DK-8000 Aarhus C, Denmark*

[b] *Bragg Institute, Australian Nuclear Science and Technology Organisation (ANSTO), New Illawarra Road, Lucas Heights NSW 2234 Australia*

[c] *Current address: Instituto de Cerámica y Vidrio, Consejo Superior de Investigaciones Científicas (CSIC), Kelsen 5, 28049 Madrid, Spain*

** msaura@inano.au.dk*

Permanent magnets (PMs) play a key role in modern society, as they are indispensable in an enormous variety of applications.[1, 2] Hexaferrite magnets, while much weaker than the rare-earth PMs, account for 85% (by weight) of the global sales of all PMs.[1] In particular, the M-type ferrite $SrFe_{12}O_{19}$ is a widely used rare-earth free, low-cost, chemically stable and non-toxic hard magnetic material with a relatively large magnetocystalline anisotropy and a high Curie temperature.[3] However, its magnetic performance has not been significantly improved within the last 20 years.[4] Nanostructuring has the potential of improving its performance by optimizing its structural characteristics at the atomic, nano- and microscopic scale.

We have developed a bottom-up nanostructuring protocol for preparation of high-performance $SrFe_{12}O_{19}$ PMs.[5, 6] Phase pure, highly crystalline $SrFe_{12}O_{19}$ nanoparticles have been synthesized by hydrothermal and sol-gel synthesis methods. By varying synthesis parameters and method, $SrFe_{12}O_{19}$ nanoplatelets of various sizes and morphologies are obtained. Combined Rietveld refinement of neutron and X-ray powder diffraction data reveal a clear correlation between crystallite size and long-range magnetic order in the structure, which influences the macroscopic magnetic properties of the sample. The tailor-made powder samples have been compacted into dense magnets (>90% of the theoretical density) by spark plasma sintering (SPS). Powder diffraction as well as X-ray and neutron pole figure analyses have been carried out on the compacted magnets in order to characterize the nuclear and magnetic alignment of the crystallites within the dense magnets. The obtained results, combined with macroscopic magnetic measurements, reveal a direct influence between nanoparticle morphology, texture, crystallite growth during compaction and macroscopic magnetic performance.[5, 6] An increasing diameter-to-thickness aspect ratio of the nanoplatelets leads to increasing degree of crystallite alignment achieved by SPS. As a consequence, magnetically aligned, highly dense magnets with excellent magnetic performance are obtained by nanostructuring means, without application of an external magnetic field before or during compaction.

[1] Lewis L. H. and Jiménez-Villacorta F., *Metall Mat Trans A*, 2013, 44, 2-20.

[2] Coey J. M. D., *J Magn Magn Mater*, 2002, 248, 441-456.

[3] Pullar R. C., *Prog Mater Sci*, 2012, 57, 1191-1334.

[4] Coey J. M. D., *IEEE Trans Magn*, 2011, 47, 4671-4681.

[5] Saura-Múzquiz M., Granados-Miralles C., Stingaciu M., Bojesen E. D., Li Q., Song J., Dong M., Eikeland E. and Christensen M., *Nanoscale*, 2016, 8, 2857-2866.

[6] Eikeland A. Z., Stingaciu M., Granados-Miralles C., Saura-Muzquiz M., Andersen H. and Christensen M., *CrystEngComm*, 2017, 19, 1400-1407.

Keywords: anisotropic nanoparticles, texture, magnetism

The Orange framework for line profile analysis: integration of WPPM with advanced instrumental modelling

L. Rebuffi[a*], A. Flor[b], & P. Scardi[b]
[a] *Elettra-Sincrotrone Trieste S.C.p.A., Trieste, Italy*
[b] *Department of Civil, Environmental & Mechanical Engineering, University of Trento, Italy*
* *luca.rebuffi@elettra.eu*

Reliable and robust beamline design is nowadays based on sophisticated computer simulations only possible by lumping together different simulation tools. This led us to develop OASYS (OrAnge SYnchrotron Suite), a completely new, intuitive and easy-to-use graphical environment for modelling X-ray experiments [1].

This new approach has been successfully used in the conceptual design of beamlines and optical design for the upgrade of ESRF and Elettra-Sincrotrone Trieste. Specific applications have been reported for the instrumental profile of typical beamlines for powder diffraction, MCX at Elettra-Sincrotrone Trieste and 11bm at APS-Argonne [2,3], to investigate the contribution of each optical component and of the X-ray absorption in the traditional capillary (Debye-Scherrer) geometry.

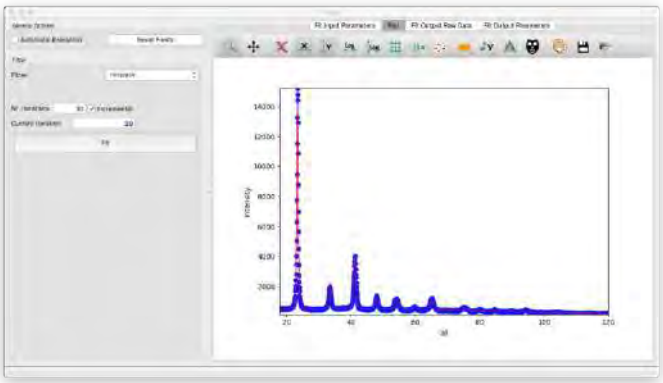

The present contribution introduces the next and most natural step toward an integration of the Whole Powder Pattern Modelling (WPPM) [4], to describe the contribution of the material microstructure to the line profile.

Flexibility and expandability are greatly increased compared to the existing WPPM software, with the fundamental improvement multicore parallelization, already provided by the OASYS environment.

A test case will be illustrated concerning a nanocrystalline materials used in a recent Round-Robin project on line profile analysis [5]

[1] Rebuffi L. & Sánchez del Río M., *J. Synchrotron Rad.,* 2016, 23, 1357.

[2] Rebuffi L., Sánchez del Río M., Busetto E. & Scardi P. *J. Synchrotron Rad.,* 2017, 24, 622.

[3] Rebuffi L., Plaisier J.R., Abdellatief M., Lausi.A. & Scardi P. *Z. Anorg. Allg. Chem. 2014, 640, 3100*.

[4] Scardi, P., (2008). Powder Diffraction: Theory and Practice, edited by R. E. Dinnebier & S. J. L. Billinge, ch. 13, pp. 376–413. Cambridge: Royal Society of Chemistry.

[5] Scardi P., Ermrich M., Fitch A., Huang E-Wen, Jardin R., Kuzel R., Leineweber A., Mendoza Cuevas A., Misture S.T., Rebuffi L., Schimpf C. *J. Appl. Crystallography*, 2018. Submitted.

Keywords: line profile analysis, nanocrystalline materials, algorithm and software development

The study of monolithic silicon nanowires: Correlation of structural and physical behavior

Simone Dolabella[a*], Zuhal Tasdemir[c], Oliver Braun[a], Jan Overbeck[a], Yusuf Leblebici[b], Erdem Alaça[c], Gilbert Chahine[d], Michel Calame[a], Alex Dommann[a], Antonia Neels[a]
[a] *EMPA – Swiss Federal Laboratories for Materials Science and Technology, Dübendorf,*
[b] *EPFL – Swiss Federal Institute of Technology Lausanne, Switzerland,*
[c] *Department of Mechanical Engineering, Koç University, Istanbul, Turkey*
[d] *ID01 X-ray Nanodiffraction beamline, European Synchrotron Radiation Facility, Grenoble, France*
** simone.dolabella@empa.ch*

In the last decades the wide field of applications of electronic devices and the miniaturization of materials brought us to study and develop devices such as MEMS and NEMS especially due to the increase in demand from the medical and aerospace sectors. The applicability of Nanoelectromechanical systems (NEMS) is based on their ability to operate reliability over time under service conditions.

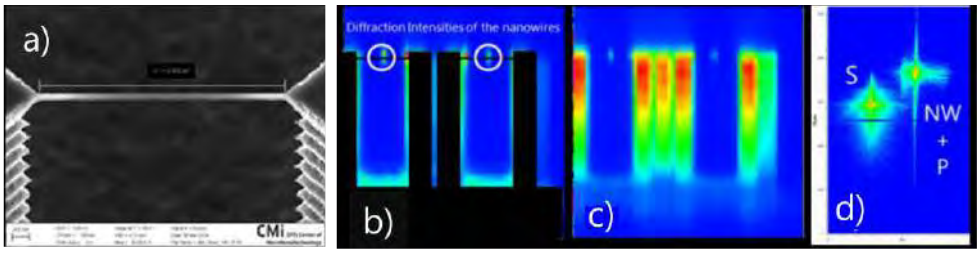

The purpose is to link atomic structure and physical properties for silicon NEMS. The object under investigation - the nanowire system - is shown in *figure a*. A monolithic fabrication has been performed. Structural analysis such as High Resolution X-ray Diffraction (HRXRD) for defect and strain analysis has been applied and performed using the nano-beamline ID01 at the ESRF. HRXRD is used as a non-destructive method to gather more structural information on the inner part of the material framework[1]. The performed experiments show us that the intensity of the diffracted X-ray beam of the Si-nanowire can be probed on the given setup (*figure b*). The y and z scanning of the sample (K-Map in *figure c*) shows that the Si-pillars and nanowires exhibit inhomogeneous strain, defect and tilt states. The reciprocal space map (RSM) shows the 2D diffraction peaks of the substrate S and for the Si-nanowires NW superposed with the Si-pillars P (*figure d*).

In addition, the use of nano-Raman spectroscopy will support the discussion about local strain[3] within the nanowires. These methods are also combined with FEM simulations in order to evaluate diffraction patterns with respect to material parameters such as Poisson's ratio, Young's modulus etc.. This approach allows us to go one step further in understanding mechanical, electrical or thermal behaviors of this class of nanowires.

[1] Schifferle A., Dommann A. and Neels A. *Science and Technology of Advanced Materials,* 2017, 12, 1.

[2] Tasdemir Z., Wollschläger N., Österle W., Leblebici Y. and B Erdem Alaca. *Nanotechnology,* 2016, 2, 8.

[3] Yazji S., Hoffman E. A., Ercolani D., Rossella F., Pitanti A., Cavalli A., Roddaro S., Abstreiter G., Sorba L. and Zardo. *Nano Research,* 2015, 9, 28.

Keywords: silicon nanowires, HRXRD, nano-Raman

X-ray and neutron diffraction magnetostructural investigations on exchange-coupled nanocomposite magnets

P. Shyam[a], A. Eikeland[a], M. Saura-Múzquiz[a], J. Ahlburg[a], M. Christensen[a*]
[a] *Center for Materials Crystallography, Department of Chemistry and Interdisciplinary Nanoscience Center (iNANO), Aarhus University, Langelandsgade 140, 8000 Aarhus C, Denmark.*
**mch@chem.au.dk*

Rare-earth based permanent magnets (such as $Nd_2Fe_{14}B_3$ magnets) exhibit superior performance characteristics but are limited by their high costs and low corrosion resistance. Volatile geopolitical circumstances and high environmental costs associated with rare-earth mining are additional concerns. These factors have given impetus to the development of permanent magnets that are free of rare-earth elements. Magnetic ferrites have emerged as viable alternatives, with the hexaferrite $SrFe_{12}O_{19}$ being an excellent candidate. [1] While $SrFe_{12}O_{19}$ has high coercivity (due to pronounced magnetocrystalline anisotropy) – making it a 'hard magnetic' phase, but it lacks a high magnetic saturation value. Spinel ferrites (AB_2O_4 type) on the other hand, are 'soft magnetic' phases *i.e.* low coercivities, but potentially strongly magnetic. Mixing the hard and soft phases at the nanoscale level results in an exchange-spring nanocomposite magnet where the soft phase enhances magnetization of the composite and the hard phase stabilizes the composite against demagnetization.[2,3] The resultant magnetic properties of such composites would be hierarchically emergent – arising from the underlying atomic structure, via the nanoscale morphology of the individual particles, to the microscopic structural coupling of the different phases. While various studies have focused on the synthesis of exchange-spring magnets and their magnetic characterizations, detailed structural investigations are limited.[3–5] In the present study, we report a comparative investigation on nanocomposites of $SrFe_{12}O_{19}$ (hard phase) and $Zn_{0.2}Co_{0.8}Fe_2O_4$ (soft phase) prepared by two different techniques: mechanical powder mixing and sol-gel coating. Hysteresis loops from VSM magnetometry showed a dependence of the exchange-coupling behavior on the technique used for nanocomposite formation. Crystallographic and magnetic structure of the composites (and the parent phases) was obtained by combined Rietveld refinement of data from synchrotron X-ray diffraction (SR-XRD performed at MS X04SA beamline at the Swiss Light Source) and thermal neutron powder diffraction (NPD performed using the HRPT diffractometer at SINQ spallation source, Paul Scherrer Institute). The difference in the scattering interaction for X-rays and neutrons allows for complementary, robust & accurate structural analysis.[5,6] Combined Rietveld refinement of SR-XRD and NPD data of the nanocomposites enabled extraction of accurate values for lattice parameters, atomic positions, thermal motion, cation distribution, magnetic moments and microstructure. As the crystallographic and magnetic structures of exchange-spring nanocomposite systems dictate their observed magnetic properties, a detailed understanding of the intertwined magnetostructural properties would be a key enabler towards engineering better permanent magnets.

[1] Pullar R. C., *Prog. Mater. Sci.*, 2012, 57, 1191.
[2] Kneller E. F., and Hawig R., *IEEE Trans. Magn.*, 1991, 27, 3588.
[3] Liu F., Hou Y., and Gao S., *Chem. Soc. Rev.*, 2014, 43, 8098.
[4] Hirosawa S., *J. Magn. Soc. Japan*, 2015, 39, 85.
[5] Yusuf S. M., and Kumar A., *Appl. Phys. Rev.*, 2017, 4, 31303.
[6] Solano E., Frontera C., Puig T., Obradors X., Ricart S., and Ros J., *J. Appl. Crystallogr.*, 2014, 47, 414.

Keywords: exchange-spring nanocomposite, neutron diffraction, X-ray diffraction

Optimization of spring exchange coupled ferrites, *studied by in situ* neutron diffraction

Jakob V. Ahlburg[a*], Cecilia Granados[c], Henrik L. Andersen[a], Emmanuel Canévet[b] and Mogens Christensen[a]

[a]*Center for Materials Crystallography, Department of Chemistry and iNANO, Aarhus University, DK-8000 Aarhus C, Denmark.* [b]*Laboratory for Neutron Scattering and Imaging, Paul Scherrer Institut, 5232 Villigen, Switzerland.* [c]*Current address: Electroceramic Department, Instituto de Cerámica y Vidrio, CSIC, Madrid, Spain*
[*]*Jakob.ahlburg@inano.au.dk*

Exchange-spring magnets are a hot topic in permanent magnet research. The concept was coined by Kneller et al. in 1991. [1] The idea is coupling hard and soft magnetic materials at the nanoscale to improve the magnetic performance. An effective coupling locks the magnetization of the soft to that of the hard. It is a very short range effect; therefore, the size of the particles needs to be controlled including the weight fractions of hard and soft phase. The concept has the potential to enhance the magnetic performance of permanent magnets. However, achieving effective exchange-spring magnets appears more challenging than expected. We have overcome this challenge and successfully prepared exchange-spring magnets by using the magnetic nanocomposite $CoFe_2O_4/CoFe_2$.

The composites are prepared directly from hard-ferromagnetic cobalt spinel, $CoFe_2O_4$, by reduction into $CoFe_2$ using 5% H_2 in Ar at elevated temperatures. The results reveal remarkable changes in coercivity and remanence, both parameters are dependent on both the weight fractions and the size of the particles constituting the sample. This gives a 10-fold increase of the energy product for the best sample compared to pristine $CoFe_2O_4$ [3].

The reduction process has been earlier been followed *in* situ with x-ray powder diffraction using the beamline P2.1 at Petra [4] but in order to obtain information about occupancies and the evolution of magnetic moments (Information about exchange coupling) the process has now been followed by neutron powder diffraction at the DMC instrument at PSI (see figure). All data has been sequentially refined using Rietveld refinement and from the refinements we can follow the evolution of weight fractions, crystallite size, occupation of Co^{+2} and Fe^{+3} and the atomic magnetic moments for both the spinel and the metal.

In the figure the reduction mechanism can be seen. The transition from spinel to pure metal goes through an intermediate step of a metal monoxide before being fully reduced. These metal monoxides are antiferromagnetically ordered and are therefore considered a parasitic phase. The white lines correspond to the numbers in the spheres. These represent the evolution of a $CoFe_2O_4$ particle through the reduction process. The colors green, yellow and brown corresponds to $CoFe_2O_4$, $Co_{(1-z)}Fe_zO$ and $CoFe_2$ respectively. However, by fine-tuning the reaction temperature and hydrogen flow rate the occurrence of the phase can be minimized. To understand the reaction mechanism, a series of experiments *with varying temperature (fixed flow) or varying flow (fixed temperature) has been performed. To optimize the exchange-coupling several experiments with fixed temperature and flow, have been performed to control the conversion rate from spinel to metal.*

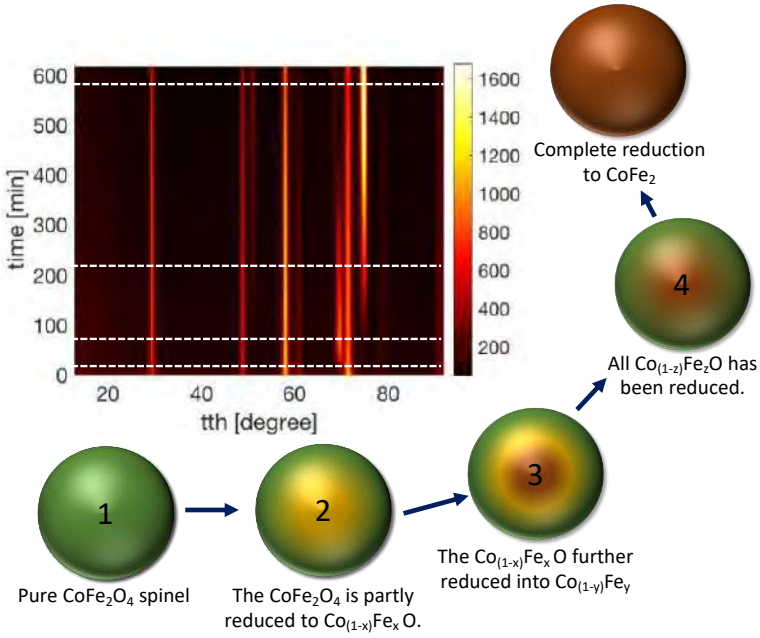

[1] E. F. Kneller and R. Hawig, IEEE Trans. Magn., 27, 3588 (1991).
[3] A. Quesada, C. Granados-Miralles et al,. Adv. Electron. Mater., 2, 1500365 (2016)
[4] C. Granados-Miralles, M. Saura-Múzquiz, H. L. Andersen, A. Quesada, J. V. Ahlburg, A.Dippel, E. Canévet, and M. Christensen, A step forward on ferrite-based exchange-coupled nanocomposites (to be submitted to Chemistry of Materials)

Keywords: ***in situ, neutron diffraction, magnetic exchange-coupling***

Mathematical model for iron non-destructive testing

for anti-corrosion metallurgic application

A. Abouharim[a] , K. El-hami[b]
[a] *University of Hassan 1st, FPK, Laboratory of Nanosciencesand Modeling, Khouribga, Morocc*
**khalil.elhami@uhp.ac.ma*

Our aim is to innovate in terms of mathematical model for non-destructive testing of iron anti-corrosion using the ultrasonic waves, to detect any measured interface variation which can be furtherly processed by means of physical equations. As known, the iron is very sensitive to oxygen water and acid tobe converted into iron oxide (Fe2O3,nH2O) and thus, caused damaged of materials.The iron corrosion exhibits an irregularity of iron interface and provokes an additional volume into iron surface. This volume parameter is our indicator of the rate of corrosion appearance which can be used to follow corrosion velocity and thus the speed at which a metal deteriorates in a specific environment.

Keywords :Iron, Ultrasonic waves, Interface corrosion,

XRD Investigation of Severe Plastic Deformation, Strain and Temperature Induced Nanocrystalline TiNiCu Shape Memory Alloy

M. M. Rajath Hegde[a *], N. B. Pradeep[a], M. Shanthikiran[a]
[a]*Department of Mechanical Engineering*
Jawaharlal Nehru National College of Engineering Shimoga (JNNCE)
*rajathhegdemm63@gmail.com

X-ray diffraction (XRD) analysis of elemental (Ti, Ni and Cu) powders subjected to high energetic ball milling showed transition from crystalline to partial amorphous structure during midway through the process. Formation of alloyed (TiNiCu, TiNi, NiCu, tenorite and NiCuO) phases too are observed in addition to traces of undissolved Ni and Cu during milling. Energy dispersive x-ray spectroscopy (EDS) analysis using scanning electron microscopy (SEM) revealed the composition during milling and consolidation process. Prolonged ball milling induces strain hardening, severe plastic deformation (SPD) and increased temperature inducing the formation of austenite (B2) and martensite (B19) phases. Crystallite size and lattice strain are 9 nm and 1.45 % respectively at the end of prolonged milling process indicating nano and SPD induced amorphous structure. Amorphous structure morphs the B2 and B19 phases. Traces of undissolved Ni and Cu in TiNiCu suppresses the propagation of shear bands resulting in enhanced mechanical properties in bulk alloyed glass. It's a huge challenge to retain non-equilibrium structures and phases synthesized during milling in bulk form. Mechanically alloyed (MA) amorphous powder is consolidated by cold isostatic pressing (CIP) followed by microwave sintering. Partial transition from amorphous to crystalline structure occurred during microwave sintering of CIP compacts as revealed by XRD analysis. Sintering process triggered the formation of intermetallic phases (Cu_3Ti_2 and $Ni_{90}Cu_{10}O$) with marginal grain growth (≤ 100 nm). Strain, temperature and SPD induced B2→B19→B19' transitions are observed from XRD evaluation, revealing susceptibility towards shape memory effect (SME) [1]. SME, crystallite size and texture has a vast influence on mechanical properties as revealed by nanoindentation. Gibbs free energy (ΔG) evaluation reveals a more stable and stronger (ΔH) TiNiCu (B19') phase than NiTi and CuTi. Selected area diffraction pattern (SADP) of transmission electron microscopy (TEM) concurs with XRD results. However, the amorphization during MA is unfavourable to shape recovery, hence crystallization of amorphous phase attained during sintering favours SME [2].

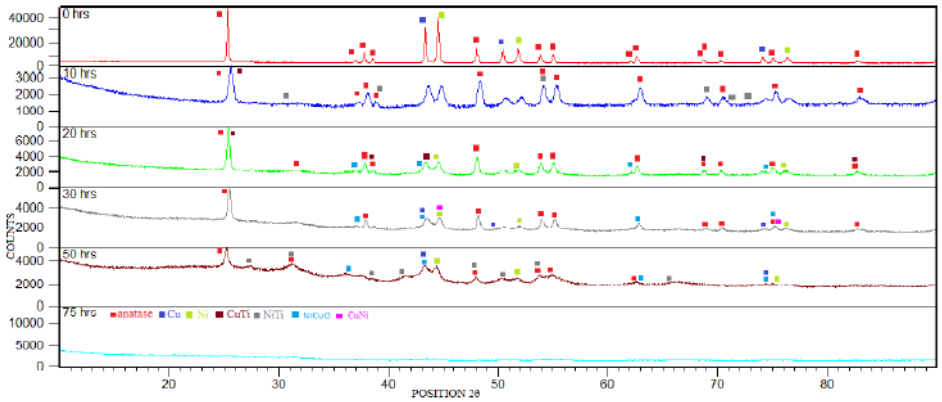

[1] Kai-Nan Lin and Shyi-Kaan Wu. *The Japan Institute of Metals,* 2007, 805-808.

[2] Chang SH, Wu SK, Kimura H. Crystallization Kinetics of Ti50Ni25Cu25. *Mater Trans* 2006;47(10):2489–92.

Keywords: TiNiCu, Shape memory effect, Mechanical alloying

Coercivity enhancement of strontium hexaferrite nano-crystallites through morphology-optimizing annealing

F. H. Gjørup[a*], M. Saura-Múzquiz[a], J. V. Ahlburg[a], H. L. Andersen[a], M. Christensen[a]
[a] *Department of Chemistry and iNANO, Aarhus University, Denmark*
** fgjorup@chem.au.dk*

Permanent magnets are found in countless forms in most modern electronics, from tiny speakers in smart devices to massive magnets in giant wind turbines. The strongest magnets currently available on the marked contain rare-earth elements like neodymium or dysprosium. However, political and economic circumstances surrounding rare-earth containing magnets have led to an increased interest in rare-earth-free alternatives, such as the inexpensive yet relatively strong ferrites.[1] Strontium hexaferrite, $SrFe_{12}O_{19}$, has been used as a permanent magnet for decades, but recent improvements gained through nanostructuring have sparked a renewed interest in the material. A promising approach to optimize the magnetic performance of a compound is by matching its crystallite size to that of a Stable Single Domain (SSD). At the SSD size, the nanoparticles only contain a single magnetic domain [2], meaning that no domain walls are present within the particle. This in turn leads to an increase in the magnetic coercivity, i.e. the magnets ability to retain its magnetic moment in an opposed external magnetic field. At crystallite sizes below the SSD, the energy of the magnetic domains become smaller than the energy associated with thermal fluctuations and, consequently, the particles become superparamagnetic and hold no magnetic moment. At sizes above the SSD, several magnetic domains start forming within the particles, which leads to a "short-circuit" of the net magnetization. In other words there exists a crystallite size, where the magnetic properties are optimal.

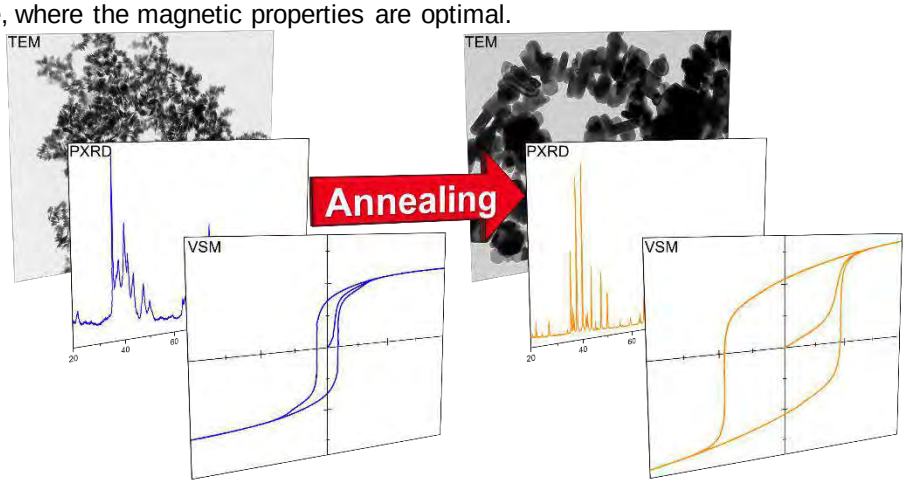

The study presented here uses a bottom-up approach based on hydrothermal synthesis of ultra-thin platelet-shaped nanoparticles of $SrFe_{12}O_{19}$.Subsequent annealing at different temperatures and times are used in order to control and optimize the size and morphology of the magnetic nanoplatelets. The resulting sizes are determined by a combination of crystallite analysis by Rietveld refinement of Powder X-Ray Diffraction data (PXRD) and particle analysis by Transmission Electron Microscopy (TEM). The magnetic properties of the annealed powders are determined by measuring magnetic hysteresis loops using a Vibrating Sample Magnetometer (VSM). By combining the size analysis with macroscopic magnetic measurements, the SDD size of $SrFe_{12}O_{19}$ nanoplatelets is elucidated, allowing tuning and optimization of the magnetic performance.
Once the optimal particle size is known, it can be applied to the next step in the process of making permanent magnets, namely the compaction process during which the nanopowders are hot-pressed into very dense pellets.

[1] Jones N. *Nature News,* 2011, 472, 22-23.

[2] Leslie-Pelecky, D. L. and Rieke, R. D. *Chemistry of Materials.,* 1996, 8.8, 1770-1783.

Keywords: permanent magnets, single domain nano-particles, coercivity

Synthesis and Characterization of Cancrinite Zeolite from Natural Bentonite

D. Kim[a,b], S. M. Seo[b], D. Kim[b], I.-M. Kang[b], J.-H. Kim[b], K.-M. Roh[a,b*]
[a] *Department of Nanomaterials Science and Engineering, University of Science and Technology, Daejeon 34113, Republic of Korea*
[b] *Advanced Geo-materials R&D Department, Pohang Branch, Korea Institute of Geoscience and Mineral Resources, Pohang 37559, Republic of Korea*
** kmroh@kigam.re.kr*

A nearly pure, pale brown, spherical, nitrate cancrinite (CAN) zeolite was successfully synthesized from natural bentonite as starting material with acidic activation treatment via hydrothermal method at 368 K for 24 h. The effect of different NaOH concentrations (pH at around 12) was investigated without addition of silica and aluminium sources. The final solids were characterized by powder X-ray diffraction (XRD), scanning electron microscopy (SEM), elemental and thermal analyses, and infrared (IR) spectroscopy. From powder XRD pattern, four strong peaks around 2θ = 13.9, 18.8, 24.2, and 27.4° respective to the (110), (101), (300), and (211) reflections of the CAN structure [1,2] revealed the corresponding material. The calculated cell parameters are a = 12.661(2) Å and c = 5.1853(10) Å in the hexagonal space group $P6_3/mmc$ (#194), which are in agreement with previously reported values of a = 12.668(2) Å and c = 5.166(1) Å for nitrate cancrinite determined by single-crystal X-ray technique [2] and a = 12.6802(7) Å and c = 5.1872(3) Å for nitrate cancrinite determined by Rietveld analysis [3], respectively. While the Si/Al ratio of ideal cancrinite is 1.0, the Si/Al ratio of the product framework is approximately 1.76 analysed by energy dispersive X-ray fluorescence spectrometry, apart from trace components. Unique single nitrate band was observed in both IR and thermogravimetric measurements, indicating that pure cancrinite was synthesized. This study showed that pure nitrate cancrinite was obtained with NaOH concentrations from 8 to 12 M, independent of NaOH contents on crystallization. Through this study, we proposed a simple synthesis method for pure nitrate cancrinite from bentonite for the purpose of recycling natural clay minerals.

[1] Baerlocher C., McCusker L., Data of zeolite structures, http://www.iza-structure.org/databases

[2] Buhl J.-Ch, Stief F., Fechtelkord M., Gesing T.M., Taphorn U., Taake C., *J. Alloys Compd*. 2000, 305, 93.

[3] Liu Q., Xu H., Navrotsky A., *Microporous Mesoporous Mater*. 2005, 87, 146.

Keywords: cancrinite, hydrothermal method, powder diffraction

Facile Synthesis and Characterization of Mesoporous Iron Nanocomposites for Environmental Applications

J. H. Kim[a*], S.M. Seo[a], K.M. Roh, I.M. Kang.
[a] *Advanced Geo-materials R&D Department, Pohang Branch, Korea Institute of Geoscience and Mineral Resources, South Korea*
**jaehwankim@kigam.re.kr*

Iron nanoparticles have been received considerable attention in the environmental engineering because they provide novel functions not available in their counterparts in micro-size such as injection into aquifer or rapid kinetics for pollutants removal [1]. Nano zero-valent iron (nZVI) is one of the most representative nano materials in groundwater remediation for *in-situ* chemical reduction [2]. However, there has been compatibility issue on practical application of nZVI in respect to their reactivity and mobility. In this study, we describe a facile method for the preparation of iron/iron oxide composites using co-solvent system that can be one of alternatives for the issue. As-synthesized iron nanocomposites showed both better dispersibility in aqueous phase and performance in chromate (Cr(VI)) removal due to its highly porous and acicular iron oxides structure. Interestingly, more dramatic morphological change was observed with increase of organic solvent concentration, and X-ray powder diffraction (XRD) analysis was employed to investigate what changes were in crystal structure. At 0% of organic solvent, a peak at 44˚ indicating the presence of Fe^0 as the single phase was presented. However, the intensity of the Fe^0 peak decreased for samples by increasing concentration of organic solvent. Simultaneously, a new peak at 11˚ attributed to an iron oxide precursor was presented which was known to be indicative of phase transformation of iron metal into iron oxides [3], and iron oxides corresponding to magnetite (Fe_3O_4) and lepidocrocite (γ-FeOOH) appeared in XRD pattern. As a result, the iron nanocomposites have not only very larger specific surface area in accordance with the concentration of organic solvent, also its physical properties such as crystal structure and surface area could be controlled with a new one-pot method. In addition to this, X-ray photoelectron spectroscopy analysis of Cr(III) on the iron nanocomposite surface confirmed that Cr(VI) removal from solution was achieved by sequential adsorption–reduction.

[1] Mathoeson L. J. and Tratnyek P.G. *Environ. Sci. Technol.*, 1994, 28

[2] Wang C. and Zhang W. *Environ. Sci. Technol.*, 1997, 31, 7

[3] Pike J., Hanson J., Zhang L. and Chan SW. *Chem Mater.*, 2007, 41

Keywords: Iron nanocomposites, Co-solvent system, Acicular iron oxides.

Application of Powder X-ray Diffraction in Studying the 3D Self-assembled Structure of Peptide Foldamers

J. Gong[a], H.-S. Lee[b]*
[a] *Natural Science Research Institute, KAIST, Republic of Korea*
[b] *Department of Chemistry, KAIST, Republic of Korea*
* *hee-seung_lee@kaist.ac.kr*

Peptide foldamers with rigid secondary structure can self-assemble to make well-defined 3D nano-/micro-sized architectures, called “foldecture” [1]. This foldecture research was attracted the attention for unprecedented morphology such as molar-tooth shape controlled by the experimental conditions of self-assembly [2]. It is also, furthermore, reported that some foldectures have unique physical properties that are able to be lined up with the direction of external magnetic field [3]. These interesting characteristics were predicted to be derived from the high-level crystallinity, despite the rapid formation process which is differentiated from common crystallisation process. In this context, powder x-ray diffraction (PXRD) was selected as the most suitable analytical tool for structure determination of solid-state structure of foldecture in molecular-level.

The molecular packing structures obtained from the structure determination from powder diffraction data (SDPD) have consequently supported various properties of the foldecture. Firstly, the correlation between symmetry inside the unit cell and symmetry of the external appearance of foldecture could be derived. Based on the texture due to the unique 3D morphology of foldecture and the March-Dollase preferred orientation approximation model [4,5], the functional group exposed to the specific face of the foldecture was predicted [6]. The characteristics of the foldecture showing the alignment in the magnetic field could be proved theoretically through the structure obtained through SDPD [3]. In addition, the type of intermolecular interaction was able to be designated by anisotropic micro-strain analysis [7]. Thus, PXRD analysis has not only been used to characterize the structural properties of the peptide self-assembled structure, but it has increased the overall understanding of the organic material of the new concept, foldecture.

[1] Yoo S. H. and Lee H. -S. *Acc. Chem. Res.*, 2017, 50, 832.

[2] Kwon S., Shin H. S., Gong J., Eom J. –H., Jeon A., Yoo S. H., Chung I. S., Cho S. J. and Lee H. –S. *J. Am. Chem. Soc.*, 2011, 133, 17618.

[3] Kwon S., Kim B. J., Lim H. –K., Kang K., Yoo S. H., Gong J., Yoon E., Lee J., Choi I. S., Kim H. and Lee H. –S. *Nat. Commun.*, 2015, 6, 8747.

[4] March A. *Z. Kristallogr.*, 1932, 81, 285.

[5] Dollase W. A. *J. Appl. Cryst.*, 1986, 19, 267.

[6] Yoo S. H., Eom T., Kwon S., Gong J., Kim J., Cho S. J., Driver R. W., Lee Y., Kim H., Lee H. –S. *J. Am. Chem. Soc.*, 2015, 137, 2159.

[7] Gong J., Eom J. –H., Jeong R., Driver R. W. and Lee H. –S. *Solid State Sci.*, 2017, 70, 1.

Keywords: powder x-ray diffraction, peptide foldamer, self-assembly

Refining Nanocrystalline and Amorphous like ZrO_2 with MSTRUCT

Z. Matěj[a*], J. Wollmann[b], J. Endres[b], M. Dopita[b], L. Matějová[c], R. Kužel[b]
[a] *MAX IV Laboratory, Lund University, SE*
[b] *Faculty of Mathematics and Physics, Charles University, Prague, CZ*
[c] *Institute of Environmental Technology, VŠB – Technical University of Ostrava, CZ*
* *zdenek.matej@maxiv.lu.se*

Uniform microstructure is a common assumption in diffraction data analysis. However it is often not the case in nature. Bimodal grain size and interaction between two-microstructures with same or very similar atomic structure is a key point driving properties of catalytic nanoparticles, nucleation and crystallization processes or structural changes of pigments in ancient paintings. The diffraction method [1] was shown to be very robust for refinements of bimodal microstructure of recrystallized fined grained metals and nanocrystalline metal oxides catalysts. A different common case when a part of the sample is amorphous and the conventional diffraction analysis can hardly give information about non-crystalline fraction of the sample is discussed here for the case of nanostructured ZrO_2 synthesized by using pressurized and supercritical fluids [2]. The sample state is clear even from low energy (8-15 keV) or laboratory data. An amorphous-like oxide is present in the sample together with two additional crystalline phases. Scattering from such the amorphous-like materials can be simulated by setting extremely small crystallites size (D ~ 0.8 nm). In spite of a good fit the phase can not be considered as crystalline as the potential crystal would consist only from about 8-12 molecules. Also the refined model (lattice) parameters can be subjected to systematic deviations [3]. Using this simple model microstructure and lattice parameters and relative fractions of crystalline phases can be reliably refined. Including amorphous-like contribution allows then determination of the amorphous content without any external standard. The scattering from structures with atomic clusters of <~ 2 nm in size is not the strongest point of the MSTRUCT [4] software used. And so our recent contribution is its Python extension allowing for more general usage. One application is combing with the state-of-art methods for scattering from such amorphous-like materials.

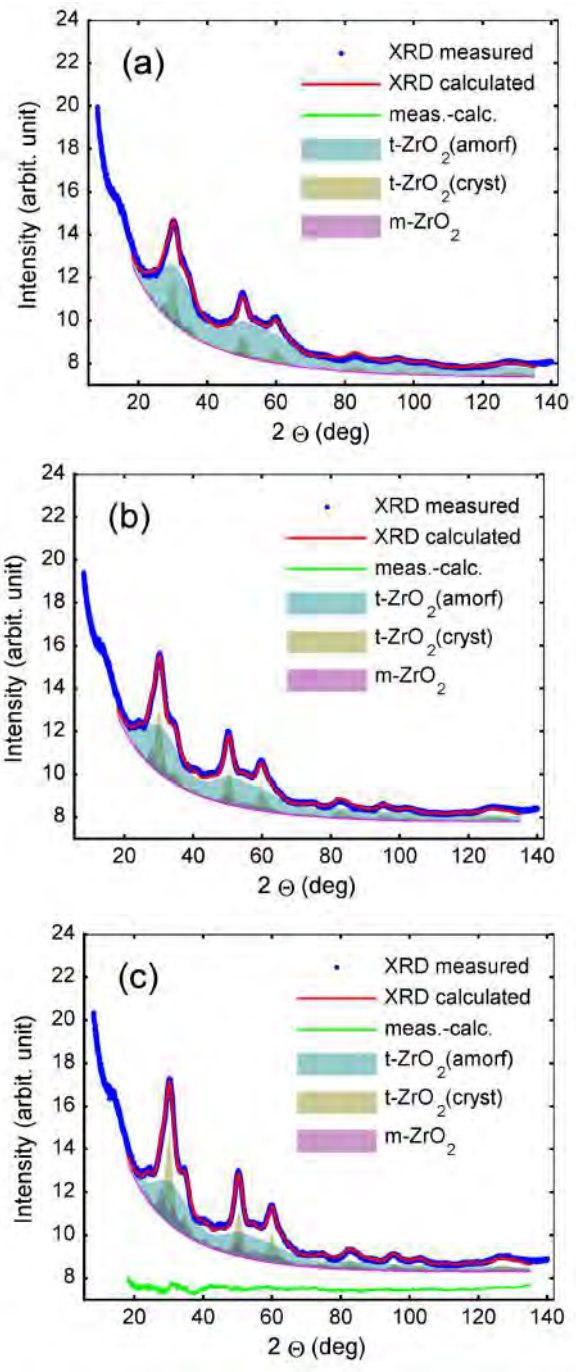

[1] Matěj Z., Kadlecová A., Janeček M., Matějová L., Dopita M., Kužel R., *Powder Diffraction*, 2014, 29 S2, S35. doi: 10.1017/S0885715614000852
[2] Matějová L., Matěj Z., *J. Supercritical Fluids*, 2017, 128, 182. doi: 10.1016/j.supflu.2017.05.029
[3] Grey I., Wilson N.C., *J. Solid State. Chem.*, 2007, 180, 670. doi: 10.1016/j.jssc.2006.11.028
[4] Matěj Z., Kužel R., Dopita M., *MSTRUCT*, www.xray.cz/mstruct (Apr 8, 2018).

Keywords: ZrO2, bimodal, microstructure

Evolution of Crystalline Microstructure of Mullite in Triaxial Whiteware Porcelains

M. A. Kojdecki[a*], A. Sanz[b], J. Bastida[b], A. Caballero[c]
[a] *Institute of Mathematics and Cryptology, Military University of Technology, Poland*
[b] *Geology Unit , University of Valencia, Spain*
[c] *Institute of Ceramics and Glass, CSIC, Spain*
* *Marek.Kojdecki@wat.edu.pl*

The development of mullite in triaxial whiteware porcelains produced of mixtures containing 53% weight of kaolin (of "high crystallinity kaolinite" B, or of "low crystallinity kaolinite minerals" M), 14% of quartz (of small grains P or of big grains G) and 33% of feldspar (with lithium content C or without S) were studied. Cylindrical samples were prepared by casting and subsequent drying. Samples were treated at two firing cycles: slow (L) with heating rate of 2ºC/min and held at maximal temperature for 180 minutes or fast (R) with heating rate of 5ºC/min and held at maximal temperature for 90 minutes, both at one of four maximal temperatures: T1=1270ºC, T2 = 1300ºC, T3 = 1320ºC, T4 = 1340ºC (all typical of industrial processing). In this way sixty-four different porcelain specimens were obtained (labelled as e.g. BGCL1, MPSR2) [1]. Porcelain samples were ground and investigated by X-ray diffraction and other techniques. Influence of firing temperature and different compositions on crystalline microstructure of mullite was observed. Size distributions and shapes of crystallites and second-order strain distributions were determined by applying multi-peak analysis of X-ray diffraction patterns [2] [3]. Crystallites were modelled in form of spheres, cylinders or prisms. Prisms (found to be most probable shape) were modelled with edges parallel to main crystallographic axes of corresponding lengths A, B, C with B/A=1.02 fixed and aspect ratio C/A modelled. Mean volume-weighted standardised crystallite size [Å] (equal to cube root of volume) of mullite for all samples is shown in table.

Cycle	T max	BGS	BGC	BPS	BPC	MGS	MGC	MPS	MPC
L1	1270	601	666	313	488	517	468	559	810
L2	1300	597	898	411	663	546	474	467	404
L3	1320	547	710	422	530	464	770	504	504
L4	1340	514	563	462	777	460	837	514	535
R1	1270	500	625	380	417	378	435	496	382
R2	1300	509	556	437	518	437	568	546	616
R3	1320	625	532	403	688	451	519	464	507
R4	1340	607	478	489	650	565	543	563	495

All samples featured bimodality of volume-weighted size distributions of mullite crystallites. All firing cycles produced secondary mullite ($3Al_2O_3 \cdot 2SiO_2$) but primary mullite ($2Al_2O_3 \cdot SiO_2$) appeared also at early stages of processing and finally transformed into secondary one. These processes resulted in formation of two fractions of crystallites with logarithmic-normal size distributions. Mean standardised sizes [Å] of crystallites for whole sample and for each fraction, mean-absolute second-order strain [%] and mean aspect ratio of prismatic crystallites for BPS series of samples were collected as in table below to illustrate complex dependence of mullite microstructure on composition and firing cycle.

	BPSL1	BPSL2	BPSL3	BPSL4	BPSR1	BPSR2	BPSR3	BPSR4
Mean size: total	313	411	422	462	380	437	403	489
first fraction	273	321	180	355	291	176	246	343
second fraction	377	521	493	567	454	467	517	606
Mean strain	0.099	0.080	0.086	0.080	0.089	0.087	0.085	0.082
Prism aspect ratio	1.4	2.0	1.7	1.9	1.7	1.7	1.8	1.5

[1] Sanz A. *Study of crystallite size in industrial porcelains,* PhD thesis (in Spanish), 2015, University of Valencia (Spain).

[2] Kojdecki M.A., Bastida J., Pardo P. and Amorós P. *J. Appl. Cryst*,, 2005, 38, 888-899.

[3] Kojdecki M. A., Ruiz de Sola E., Serrano F.J. Delgado Pinar V,, Raventós M., Esteve V.J. *J. Appl. Cryst.*, 2007, 40, 260–276.

Keywords: crystalline microstructure, X-ray diffraction, mullite

Results of a Round Robin on Line Profile Analysis (LPA): separation of size and strain broadening

P. Scardi[a*], M. Ermrich[b], A. Fitch[c], E-Wen Huang[d], R. Jardin[e], R. Kuzel[f], A. Leineweber[g], A. Mendoza Cuevas[h,i], S.T. Misture[j], L. Rebuffi[k], C. Schimpf[g]

[a] *Department of Civil, Environmental & Mechanical Engineering, University of Trento, Italy*
[b] *Röntgenlabor Dr. Ermrich, Am Kandelborn 7, D - 64354 Reinheim, Germany*
[c] *ESRF, 71, avenue des Martyrs, CS 40220, 38043 Grenoble Cedex, France*
[d] *Bruker AXS GmbH, Oestliche Rheinbrueckenstrasse 49, 76187 Karlsruhe, Germany*
[e] *Department of Materials Science & Engineering, National Chiao Tung University, Hsinchu, Taiwan*
[f] *Department of Condensed Matter Physics, Charles University, Prague, Czech Republic*
[g] *Institute of Materials Science, TU Bergakademie Freiberg, D-09599 Freiberg, Germany*
[h] *Archaeometry Laboratory, Havana's Historian Office, University San Geronimo de La Habana, Habana Vieja, Cuba*
[i] *Multidiscipilanary Laboratory, ICTP, I-34151, Trieste, Italy*
[j] *Alfred University, Alfred, NY 14802, USA*
[k] *Elettra-Sincrotrone Trieste, Trieste, Italy*
* *Paolo.Scardi@unitn.it*

This contribution presents the main results of a recently concluded Round Robin project on the separation of size and strain effects on diffraction line profiles [1]. The study has involved 10 different laboratories, testing both laboratory instruments and synchrotron radiation (SR) beamlines. The operating conditions involved different radiation, optics and detectors, for a total of 12 experimental configurations, 5 with SR and 7 with laboratory sources, including an energy-dispersive set-up.
The case study is an iron alloy powder, extensively deformed by high-energy ball milling. The sample was available in large quantity, to be distributed to all participants (a large amount is still available), in a stable form of ferritic (bcc) iron with a minor amount of austenite (fcc), making an ideal test case for LPA, as domain size broadening and strain broadening are of comparable size.
As expected SR provides the best conditions for an accurate analysis of the line profiles, but quality information on domain size distribution and microstrain can also be obtained with standard laboratory equipment, provided that data quality is good, in terms of counting statistics, and low and smooth background. All results are analyzed by two different approaches, respectively based on the use of peak width (integral breadth) and Fourier Analysis of the line profiles, with due consideration of the Instrumental Profile component

[1] Scardi P., Ermrich M., Fitch A., Huang E-Wen, Jardin R., Kuzel R., Leineweber A., Mendoza Cuevas A., Misture S.T., Rebuffi L., Schimpf C. *J. Appl. Crystallography*, 2018. In press.

Keywords: line profile analysis, nanocrystalline materials, plastically deformed materials, size-strain separation

Switching Between the Superparamagnetic and Ferrimagnetic Ordering: Structural, Microstructural and Magnetic Study of $CoMn_2O_4$ Spinels

J. Popović[a*], M. Jurić[a], M. Vrankić[a], D. Pajić[b], J. Zavašnik[c]
[a] *Ruđer Bošković Institute, Zagreb, Croatia*
[b] *Department of Physics, Faculty of Science, University of Zagreb, Croatia*
[a] *Centre for Electron Microscopy, Jožef Štefan Institute, Ljubljana, Slovenia*
* *jpopovic@irb.hr*

Spinel materials represent an important class of compounds that as a result of their unique chemical, electric, magnetic, and mechanical properties have a wide range of potential applications ranging from energy storage and conversion to magnetism, electronics, and catalysis. Among many spinel materials cobalt manganite ($CoMn_2O4$) attracted great attention as a new advanced anode material for lithium-ion batteries [1], an electrocatalyst for oxygen reduction/ evolution reactions [2] and a catalyst in CO oxidation [3]. The majority of the recent reports appears to be strongly focused on the electrochemical properties while magnetic studies have been scarce in spite of a few papers reporting on an intriguing and complex but still poorly understood magnetic behaviour.

$CoMn_2O_4$ samples were prepared by thermal decomposition of single-source molecular precursor, $\{[Co(bpy)_3]^-[Mn_2(C_2O_4)_3]\cdot H_2O\}_n$ at T= 500, 700, 800, and 1000 °C in a stream of synthetic air a heating rate of 10 °C min^{-1} [4]. Structural changes of the cobalt manganite samples caused by different temperatures of a heat treatment have been studied in detail by PXRD. The increase of lattice parameters has been observed; this increase of the unit-cell parameters was a first indication that the heat treatment induced significant structural changes within the lattice, specifically in the cation distribution between octahedral and tetrahedral sites. Rietveld refinement reviled an increase in the octahedral bond lengths, while the interatomic distances in the tetrahedral coordination decreased as a result of thermally enhanced substitution of Co^{2+} by smaller Mn^{3+} cations at the 4a site of the spinel structure. On the other hand, the octahedral 8d site becomes partially occupied by Co^{2+} as a consequence of transferred Mn^{3+} cations from the octahedral site to the tetrahedral site; the substitution of smaller Mn^{3+} cations by larger Co^{2+} led to an increase of the octahedral bond lengths.

Changes in the thermal treatment, besides influencing the structural features, also had a strong impact on the microstructural properties of the prepared samples. Size−strain analysis showed that the average crystallite size of $CoMn_2O_4$ can easily be tuned in the range of 8−40 nm depending on the temperature of annealing.

While thermal treatment was expected to influence both structural and microstructural features, we found that the magnetic behaviour of $CoMn_2O_4$ can be successfully tailored as well; depending on the heat treatment it is possible to switch between the superparamagnetic and ferrimagnetic ordering and to tailor the magnetic transition temperatures, i.e., the boundaries between the hard and soft magnetic behaviour.

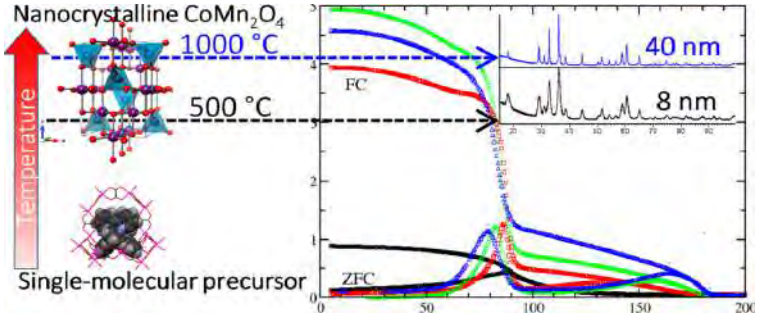

[1] Bijelić,M., Liu,X., Sun,Q.m Djurišić, A., Xie,M.H., Ng, A., Suchomski, C., Djerdj, I., Skoko, Ž.; Popović, J. *J. Mater. Chem. A* 2015, 3, 14759.

[2] Cheng, F., Shen, J., Peng, B., Pan, Y., Tao, Z., Chen, *Nat. Chem.* 2011, 3, 79.

[3] Liu, L., Yang, Y. *Superlattices Microstruct.* 2013, 54, 26.

[4] Popović, J., Jurić, M., Vrankić, M., Pajić, D., Zavašnik, J. *Inorg. Chem.* 2017, 56, 3983.

Keywords: spinel, $CoMn_2O_4$, magnetism

MS08 - Total scattering studies and disorder

MSO8

Abstract Number	Title	Author	Corresponding Affiliation
MS08 - K1	DISCOVER: ORNL's Diffraction and Total Scattering Beamline for Materials Discovery	Dr Katharine Page	Oak Ridge National Laboratory
MS08 - K2	Local Structure Investigations on the XPDF Beamline at Diamond Light Source	Dr Philip Chater	Diamond Light Source
MS08 - OR1	Alloying anodes for sodium-ion batteries: insights from pair distribution function analysis and solid-state NMR	Dr Phoebe Allan	University of Birmingham
MS08 - OR2	Diffuse scattering masquerading as Bragg peaks: Low-dimensional magnetic order in a metal–organic framework	Prof Andrew Goodwin	University of Oxford
MS08 - OR3	Planar defects and dynamic disorder in lead halide perovskite nanocrystals unveiled through reciprocal space total scattering methods	Dr Federica Bertolotti	Aarhus University
MS08 - P60	Evidence of anatase intergrowths formed during slow cooling of reduced ilmenite	Dr Anita D'Angelo	CSIRO
MS08 - P61	SYNCHROTRON X-RAY PAIR DISTRIBUTION FUNCTION: A tool to characterize cement gels	Dr Ana Cuesta	Universidad de Málaga
MS08 - P62	Elevated temperature in-situ PDF analyses of Anatase Nanoparticles	Mr Stefan Diez	Friedrich-Alexander University Erlangen-Nuremberg
MS08 - P63	EPSR-derived structure of functionalised geopolymers	Prof Monica Dapiaggi	Università degli Studi di Milano
MS08 - P64	XPDF at DLS: Physics-based reduction of pair-distribution function data	Dr Timothy Spain	Diamond Light Source
MS08 - P65	Orbital order-disorder and defects in molecular perovskites	Ms Hanna Boström	University of Oxford
MS08 - P66	Investigations on crystal structures and planar defects of heavily stacking faulted honeycomb iridates	Dr Sebastian Bette	Max Planck Institute for Solid State Research
MS08 - P67	Unravelling the local structure of zeolite precursor aluminosilicate gels by neutron total scattering	Dr Iara gigli	Elettra Sincrotrone-Trieste
MS08 - P68	Structural Insights into Semicrystalline States of Electrospun Nanofibers by X-ray Scattering	Dr Amin Sadeghpour	Center for X-ray Analytics, Empa
MS08 - P70	Crystal structure solution of organic compound without prior knowledge of space group and lattice parameters by a global fit to the pair distribution function	Dr Dragica Prill	Goethe University Frankfurt am Main
MS08 - P71	Orbital Molecules in Vanadium Spinels	Mr Alexander Browne	University of Edinburgh
MS08 - P72	Following the Formation of Tungsten Oxide Nanostructures from Polyoxometalates Through In Situ Pair Distribution Function Analysis	Mr Mikkel Juelsholt	University of Copenhagen
MS08 - P73	Understanding the Mechanism of Sodium Insertion in Hard Carbon Through Operando Pair Distribution Function Analysis	Ms Jette Mathiesen	University of Copenhagen
MS08 - P74	Exploration of the structure of a series of UiO-66(M)s (M = Zr, Ce, Hf), using the pair distribution function analysis	Dr Pascal G. Yot	Universite de Montpellier

MS08 - P75	Atomic Pair distribution function analysis by high power Mo Kα radiation and focusing mirror	Dr Jungeun Kim	Rigaku Corporation
MS08 - P76	Differential anomalous scattering study of binary Cu-Hf based metallic glasses	Dr Stefan Michalik	Diamond Light Source
MS08 - P77	Combining PDF and DFT to resolve defect configurations in La1-xBa1+xGaO4-x/2 ionic conductors	Dr Mauro Coduri	ESRF
MS08 - P78	Operando PDF/DRIFTS/MS experiments at the beamline ID15A at ESRF: investigating the structure and reactivity of catalytic nanomaterials	Stefano Checchia	ESRF
MS08 - P79	Study on scattering origins for profiling basal reflections of 1:1 regularly interstratified illite and smectite (rectorite)	Dr Il Mo Kang	Korea Institute of Geoscience and Mineral Resources (KIGAM)
MS08 - P80	Thermoresponsive behaviour of (NH4)0.5Co1.25(H2O)2[BP2O8].(H2O)0.5 with CZP framework topology	Dr Mashikoane Wilson Mogodi	European Synchrotron Radiation Facility (ESRF)
MS08 - P81	Routine quantification of stacking disordered kaolinites by the Rietveld method	Dr Kristian Ufer	Federal Institute for Geosciences and Natural Resources
MS08 - P82	Toward solution of locally ordered polymer domain structures using pair distribution function analysis	Dr Maxwell Terban	Max Planck Institute for Solid State Research
MS08 - P83	Total Scattering at the X04SA beamline of SLS	Dr Antonio Cervellino	Photon Science Division, Paul Scherrer Institute
MS08 - P84	Applications of PDF Analysis to Organic Molecular Compounds	Dr Pamela Whitfield	Excelsus Structural Solutions (Swiss) AG
MS08 - P85	The New Pair Distribution Function Beamline, PDF (28-ID-1) at the NSLS-II	Ms A. M. Milinda Abeykoon	National Synchrotron Light Source II, Brookhaven National Laboratory
MS08 - P86	Early hydration study of standard and active Belite-Alite-Ye'elimite (BAY) cements by Synchrotron Radiation	Mr Jesus David Zea-Garcia	Departamento de Química Inorgánica, Cristalografía y Mineralogía, Universidad de Málaga,

DISCOVER: ORNL's Diffraction and Total Scattering Beamline for Materials Discovery

K. Page[a*], T. Huegle[a], V. Graves[a], M. Tucker[a], P. Woodward[b]
[a] *Neutron Science Directorate, Oak Ridge National Laboratory, USA*
[b] *Chemistry Department, The Ohio State University, USA*
**pagekl@ornl.gov*

Many modern materials classes, from semiconductors and superconductors, to relaxor ferrolelectrics and ionic conductors, are defined by self-organization of atoms, spins, or charges occuring on length scales requiring understanding of both atomic and intermediate (several hundred Ångstrom) range order. There are a multitude of theories for such phenomena, but little in the way of experimental verification. For several years the Materials Chemistry and Quantum Condensed Matter communities have advocated for a rapid acquisition but medium-resolution and low background diffractometer for the First Target Station (FTS) at the Spallation Neutron Source (SNS), Oak Ridge National Laboratory (ORNL). DISCOVER, ORNL's Diffraction and Total Scattering Beamline for Materials Discovery, will be optimized for studying real materials in their operating environments from day one, and is intended to supply the scientific community with a platform for front-line investigations of the delicate interplay of global symmetry and local symmetry, for examining how order evolves from the atomic to macroscale, and for discovering how these features respond to external perturbation to deliver new functionality. The instrument has come into focus recently as plans to build out the FTS suite at ORNL have evolved. In this contribution we will describe the science mission, early experiment opportunities, and key design criteria for the beamline concept. We will present several design alternatives, informed by neutronics calculations and comparisons with current US diffraction capabilities, inviting further input from the community.

Keywords: neutron diffraction, total scattering, instrumentation

Local Structure Investigations on the XPDF Beamline at Diamond Light Source

P. A. Chater[a*], D, S. Keeble[a], T, Spain[a], J, Filik[a], H. Wilhelm[a]
[a] *Diamond Light Source, Harwell Science and Innovation Campus, Didcot, OX11 0DE, UK*
** philip.chater@diamond.ac.uk*

The XPDF beamline at Diamond Light Source is committed to the fast and reliable production of pair distribution function (PDF) data. In its first year of operation XPDF has welcomed users from a diverse range of disciplines such as materials science, energy materials, earth sciences and pharmaceuticals. Here we present a selection of studies performed using the XPDF beamline and highlight the hardware and software developments which have made these studies possible.

XPDF operates with two large area detectors with one placed close to the sample to the provide the large *Q* range required for quality PDF data (Q_{max} up to 40 $Å^{-1}$) and one mounted further from the sample for simultaneous higher-resolution Bragg data. This set-up is particularly valuable when studying disordered crystalline systems such as multiferroics or alloys.

Battery materials can be studied *in-situ* during electrochemical cycling. The small vertical beam size of XPDF means that contributions from just the active material of interest can be isolated. Tools such as principle component analysis are available within the DAWN software package [1] which allow you to quickly visualize what is happening with the sample in real time.

The high throughput capabilities offered by beamlines such as XPDF mean that new modelling tools are required to rapidly analyse the PDF data generated. The presentation will conclude by using XPDF data to demonstrate the speed and flexibility of the computer program TOPAS for PDF analysis [2], using a variety of examples such as small-molecule rigid-body refinements and nano-structured multi-component systems.

[1] Filik J. *et al. J. Appl. Cryst.*, 2017, 50, 959.

[2] Coelho A. A., Chater P. A. and Kern A. *J. Appl. Cryst.*, 2015 48, 869.

Keywords: pair distribution function, total scattering, beamline

Alloying anodes for sodium-ion batteries: insights from pair distribution function analysis and solid-state NMR

P. K. Allan[a*], J. M. Stratford[b], J. M. Griffin[c], O. J. Borkiewicz[d], K. M. Wiaderek[d], K. W. Chapman[d], P. J. Chupas[d], A. J. Morris[e], L. Monconduit[f], C. P. Grey[b]

[a] *School of Chemistry, University of Birmingham, UK*
[b] *Department of Chemistry, University of Cambridge, UK*
[c] *School of Chemistry, University of Lancaster, UK*
[d] *Advanced Photon Source, Argonne National Laboratory, USA*
[e] *School of Metallurgy and Materials, University of Birmingham, UK*
[f] *Institut Charles Gerhardt Montpellier, Université Montpellier, France*
* *p.allan@bham.ac.uk*

Sodium-ion batteries have attracted attention in recent years because of the high natural abundance of sodium compared to lithium, making them particularly attractive in applications such as large-scale grid storage where low cost and sustainability, rather than energy density is the key issue. Several materials have been suggested as cathodes but far fewer studies have been done on anode materials and, because of the reluctance of sodium to intercalate into graphite, the anode material of choice in commercial lithium-ion batteries, the anode represents a significant challenge to this technology. Materials which form alloys with sodium, particularly tin and antimony, have been suggested as anode materials; their ability to react with multiple sodiums per metal-atom give potential for high gravimetric capacities. However, relatively little is known about the reaction mechanism of these materials in the battery, primarily due to drastic reduction in crystallinity during (dis)charging conditions, but also because the structures formed on electrochemical cycling may not be alloys known to exist under ambient conditions.

We present a study of elemental antimony and tin anodes in sodium-ion batteries, using operando pair distribution function (PDF) analysis combined with solid-state nuclear magnetic resonance (NMR) studies[1,2]. Inclusion of diffuse scattering in analysis is able to circumvent some of the issues of crystallinity loss, and gain information about the local structure in all regions, independent of the presence of long-range order in the material. As a result, we are able to isolate the crystalline and amorphous phases present in the Na-Sb and Na-Sn systems and probe the nature of previously uncharacterised intermediate phases. This analysis has been linked with ^{23}Na solid-state NMR experiments to examine the local environment of the sodium. In the Na-Sb system, results provide evidence of known Na_xSb phases but indicate additional metastable phases are also present at partial discharge. The electrochemical signatures are linked with structural processes taking place in the battery to show that the different electrochemical profile observed on the second sodium insertion cycle is a result of complex multiphase electrode formed after sodium removal. In more recent work, we explore how factors such as battery (dis)charge rate might affect the phases formed, as well as the effect of using binary alloys, for example SnSb.

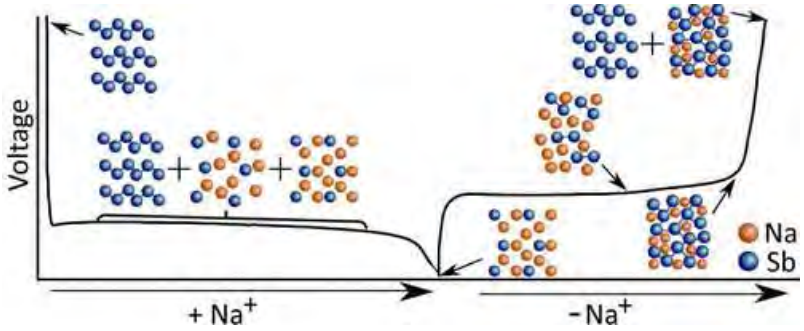

[1] Allan, P. K., Griffin, J. M., Darwiche, A., Borkiewicz, O. J., Wiaderek, K. M., Chapman, K. W., Morris, A. J., Chupas, P. J., Monconduit, L., Grey, C. P., *J. Am. Chem. Soc.,* 2016, 138, 2352

[2] Stratford, J. M., Mayo, M., Allan, P. K., Pecher, O., Borkiewicz, O. J, Wiaderek, K. M., Chapman, K. W., Pickard, C. J., Morris, A. J., Grey, C. P., *J. Am. Chem. Soc.*, 2017, 139, 7273

Keywords: PDF analysis, sodium-ion batteries, operando studies

Diffuse scattering masquerading as Bragg peaks: Low-dimensional magnetic order in a metal–organic framework

D. R. Harcombe,[a] P. G. Welch,[a] P. Manuel,[b] P. J. Saines,[c] A. L. Goodwin[a*]
[a] *Inorganic Chemistry Laboratory, University of Oxford, UK*
[b] *ISIS Facility, Rutherford Appleton Laboratory, UK*
[c] *School of Physical Sciences, University of Kent, UK*
* *andrew.goodwin@chem.ox.ac.uk*

Terbium formate, $Tb(HCOO)_3$, is a metal–organic framework of current interest as a candidate magnetocaloric.[1] Its structure consists of columns of Tb^{3+} ions, which are arranged on a triangular lattice and connected *via* flexible anionic formate linkers. It has long been known that the system exhibits antiferromagnetic ordering at very low temperatures (T_N ~ 1.6 K).[2] The magnetic diffraction pattern within the antiferromagnetic regime is peculiar because it exhibits both strong diffuse scattering and a series of Bragg-like reflections. Conventional magnetic symmetry analysis and magnetic structure determination gives two structural models that provide equally convincing fits to the Bragg component of this diffraction pattern.[1,3] Both models indicate ferromagnetic order *along* Tb chains but differ in the nature of the antiferromagnetic order between chains: in one model, one third of the chains has twice the ordered moment of the other two thirds, and the magnetization directions of these two components are opposite; in the other model one third of the chains has no ordered moment, and the other two thirds alternate their magnetization directions. This second model is the so-called "partially disordered antiferromagnet" (PDA) state, which is thought to be relevant to a large number of magnetically frustrated systems.[4]

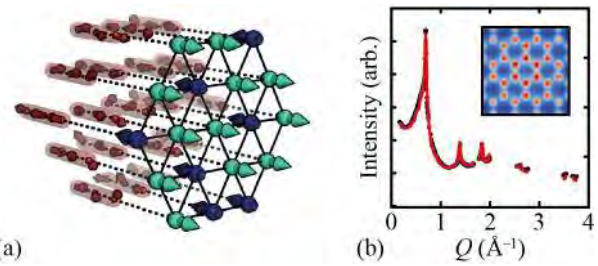

Using magnetic total scattering measurements and SPINVERT analysis,[5] we have shown that the full diffraction pattern (Bragg + diffuse scattering) is actually characteristic of a fundamentally different partially-ordered magnetic state related to the triangular Ising antiferromagnet (TIA).[6] In this model, the each Tb chain has the same ordered magnetization. The direction of chain magnetization tends to alternate between neighbouring chains but this alternation is frustrated and is not itself ordered. This same state also emerges from simple direct Monte Carlo configurations. Importantly, despite the absence of three-dimensional magnetic order, this TIA state gives rise to Bragg-like diffraction features which — if analysed in isolation — give spurious and unphysical magnetic structure solutions.[7] We discuss the implications for analysis of non-magnetic diffraction patterns for TIA-type states in systems with unusual charge and compositional (dis)order.

[1] Saines P. J., Paddison J. A. M., Thygesen P. M. M. and Tucker, M. G. *Mater. Horiz.,* 2015, 2, 528.

[2] Trounov V., Tserkovnaya E., Gavrilov S. and Vahrushev, S. *Physica B* 1997, 234-236, 679.

[3] Kurbaokv A. I., Rodriguez-Carvajal J., Trounov V. A. and Starostina N. V. *Mater. Sci. Forum*, 2000, 321-324, 971.

[4] Mekata M. *J. Phys. Soc. Jpn.*, 1977, 42, 76.

[5] Paddison J. A. M. and Goodwin A. L. *Phys. Rev. Lett.*, 2012, 108, 017204.

[6] Harcombe D. R., Welch P. G., Manuel P., Saines P. J. and Goodwin A. L. *Phys. Rev. B,* 2016, 94, 174429.

[7] Wojtas D. H. and Millane R. P. *Phys. Rev. E*, 2009, 79, 041123.

Keywords: frustrated magnetism, diffuse scattering, metal–organic frameworks

Planar defects and dynamic disorder in lead halide perovskite nanocrystals unveiled through reciprocal space total scattering methods

F. Bertolotti[a,b*], L. Protesescu[c], M.I. Bodnarchuk[c], M.V. Kovalenko[c], A. Cervellino[d], N. Masciocchi[b,e] and A. Guagliardi[b,f]

[a]*Aarhus Institute of Advanced Studies, Aarhus University, Aarhus C, Denmark*
[b]*Total Scattering Laboratory (To.Sca.Lab), Como, Italy*
[c]*ETH-Zürich and EMPA, Zürich, Switzerland*
[d]*Swiss Light Source, Paul Scherrer Institut, Villigen, Switzerland*
[e]*University of Insubria, Como, Italy*
[f]*Istituto di Cristallografia, CNR, Como, Italy*
* fbertolotti@aias.au.dk

Lead halide perovskites (LHP) are long-known crystalline materials with ABX_3 general formula (where A=Cs^+, MA:$CH_3NH_3^+$ or FA:$CH(NH_2)_2^+$, B=Pb^{2+} and X=Cl^-,Br^-,I^-), characterized by a three-dimensional interconnection of $[PbX_6]^{4-}$ octahedra and a large A cation residing the cuboctahedra cavities in between. These materials in form of nanocrystals (NCs) are considered ideal candidates to be integrated in television displays and LEDs, due to their high photoluminescence QYs (up to 95%-100%), very narrow emission bandwidths (FWHM<100meV, ensuring highly saturated colors) and an impressive gamut, achieving up to 140% of the North American Television Standard Committee (NTSC).[1] Due to the dynamic nature of the perovskite lattice preventing the charge carriers from trapping, LHP NCs are highly tolerant to structural defects and surface states that are considered benign with respect to their electronic and optical properties.[2]

The flexible nature of the perovskite framework, very prone to structural defectiveness, coupled with the reduced size of the crystalline domains, makes these materials unsuitable for conventional crystallographic methods, unable to properly account for deviations from ideally infinite periodic structures. At this purpose total scattering techniques based on the Debye Scattering Equation (DSE), considering both Bragg and diffuse scattering on equal foot, have been established as effective methods for characterizing nanoscale materials and taking into account size-induced structural defects emerging with downsizing.[3] Through the DSE-based method developed by some of us,[4] starting from real space atomistic models, structural (intended both as periodic crystal structure and structural defectiveness or disorder) and microstructural information on NCs can be simultaneously derived within a unified approach, with all the well-known advantages associated to the use of reciprocal space methods.

Using newly developed defective models within the DSE-based approach, we were able to unveil the presence of locally ordered subdomains in all-inorganic LHP ($CsPbX_3$) NCs, characterized by the orthorhombic tilting of the $[PbX_6]^{4-}$ octahedra.[5] These subdomains are hinged together by a network of two-dimensional twin boundaries (identified by specific *k*<*hkl*>{*hkl*} slip planes, modulating the number and the type of superstructure peaks visible in the powder diffraction patterns of $CsPbX_3$), through which the coherent arrangement of Pb^{2+} ions is nearly preserved. The density of these twin boundaries, migrating trough the particles via cooperative rotations of the octahedra, determines the size of the subdomains and increases upon temperature increase, due to the entropic stabilization of the polyfragmented NCs. These synchronized movements modify the domains sizes and orientations, leading to an “apparent” higher crystal symmetry (tetragonal or cubic) on average, while keeping locally (at the subdomains scale) the tilted “orthorhombic” arrangement of the octahedra.

The extension of this approach to the modelling of temperature dependent (in the 30K-300K range) X-ray total scattering data of hybrid organic-inorganic LPH is currently under development.

[1] Akkerman Q. A., Rainò G., Kovalenko M. V. and Manna L., *Nat. Mater.* 2018, https://doi.org/10.1038/s41563-018-0018-4.
[2] Kovalenko M. V., Protesescu L. and Bodnarchuk M.I., *Science,* 2017, 358, 745.
[3] Bertolotti F., Dirin D.N., Ibáñez M., Krumeich F., Cervellino A., Frison R., Voznyy O., Sargent E.H., Kovalenko M.V., Guagliardi A. and Masciocchi N., *Nat. Mater.* 2016, 15, 987 *and references therein.*
[4] Cervellino A., Frison R., Bertolotti F. and Guagliardi A., *J. Appl. Cryst.* 2015, 48, 2026.
[5] Bertolotti F., Protesescu L., Kovalenko M. V., Yakunin S., Cervellino A., Billinge S.J.L., Terban M.W., Pedersen J.S., Masciocchi N. and Guagliardi A., *ACS nano*, 2017, 11, 3819.

Acknowledgments: Part of this work has been financially supported by the European Union and the Aarhus Institute of Advanced Studies (Aarhus University) under the EU-FP7 framework program (Grant Agreement No. 609033, Marie Skłodowska-Curie AIAS-COFUND grant).

Keywords: total scattering, twin boundaries, lead halide perovskites

SYNCHROTRON X-RAY PAIR DISTRIBUTION FUNCTION: A tool to characterize cement gels

Ana Cuesta[a*], Jesus D. Zea-Garcia[a], Diana Londono-Zuluaga[a], Angeles G. De la Torre[a], Isabel Santacruz[a], Miguel A. G. Aranda[a.b]
[a] *Departamento de Química Inorgánica, Universidad de Málaga, Spain.*
[b] *ALBA synchrotron, Carrer de la Llum, Barcelona, Spain.*
** a_cuesta@uma.es*

Cement matrices contain large amounts of crystalline phases jointly with amorphous and/or nanocrystalline phases. Consequently, their analyses are very challenging. Synchrotron powder diffraction in combination with the pair distribution function (PDF) methodology is very useful to characterize such complex cement pastes. This work is focused on the study of the short and medium range atomic arrangement(s) in the different nanocrystalline gels which are present in the cement pastes through total scattering Pair Distribution Function quantitative phase analyses.
Powder diffraction data of cement pastes were collected in BL04-MSPD beamline at ALBA Synchrotron (Barcelona, Spain). They have been analyzed by PDF and Rietveld methodologies in order to determine the nanocrystalline and microcrystalline contents, respectively. This methodology allows obtaining a better understanding of the binding gels. Three sets of hydrated model samples have been studied: i) monocalcium aluminate, $CaAl_2O_4$, the main component of calcium aluminate cements [1,2], ii) ye'elimite, $Ca_4Al_6SO_{16}$, the main component of calcium sulfoaluminate cements [2] and iii) tricalcium silicate [2,3], Ca_3SiO_5, the main component of Portland cements. For i) and ii) samples, the influence of some selected parameters were investigated; for instance, different water-to-solid (w/s) mass ratios and temperatures. Moreover, the diameter of the nanoparticles of the aluminum hydroxide nanocrystalline gels have been investigated and compared in these pastes.
For the PDF analyses of Ca_3SiO_5 pastes [2,3], a multi r-range approach was followed: a higher r-range, above 40 Å, was used to determine the microcrystalline phase contents, portlandite and residual alite; then, the intermedium r-range (10-25 Å) allowed characterizing the atomic ordering in the nanocrystalline gels; and finally, the low r-range, below 10 Å, gave insight about the chemical nature of the amorphous component. It is important to highlight that the analysis of the data in the 10-25 Å r-range indicated that a defective clinotobermorite crystal structure fitted the total scattering data of C-S-H gel better than others crystal structures, Figure left. Moreover, the analysis of the PDF data in the 2-10 Å r-range showed that an amorphous component was needed to justify the residual scattering data. This contribution was justified with monolayer calcium hydroxide, Figure right.

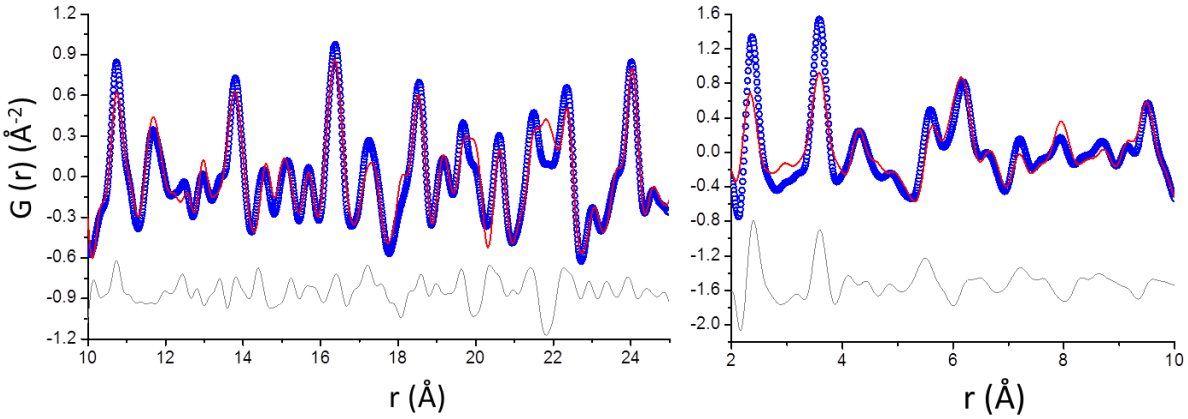

[1] Cuesta, A., et al. *Cem. Concr. Res.,* 2017, 96, 1, doi: 10.1016/j.cemconres.2017.02.025

[2] Cuesta, A., et al. *Crystals,* 2017, 7, 317, doi: 10.3390/cryst7100317

[3] Cuesta, A., et al. *Sci. Rep.,* 2018, 8, 8544, doi: 10.1038/s41598-018-26943-y

Keywords: pair distribution function, cementitious materials, nanocrystaline gels

Elevated temperature in-situ PDF analyses of Anatase Nanoparticles

S. Diez[a*], C. Schieber[a], M. V. Blanco[b], R. B. Neder[a]
[a] *Crystallography and Structural Physics, Erlangen, De*
[b] *European Synchrotron Radiation Facility (ESRF), Grenoble, Fr*
** Stefan.Diez@fau.de*

Pair distribution Functions (PDFs) are a decent means to develop structural models of nanomaterials as well as X-ray amorphous appearing substances. In the latest studies we advanced an in-situ approach on syntheses of nanoparticles in liquid phase with the objective of explaining nucleation processes and particle growth kinetics [1]. To this end, current practice comprises the analysis of synchrotron data on the second timescale throughout the course of a synthesis. The background corrected data modelling is in particular sophisticated at early stages of a reaction when syntheses give rise to small clusters and intermediates.
The synthesis of TiO_2 nanoparticles was chosen in this work for closer investigation due to the myriad of applications of anatase in photovoltaic cells [2]. As rather well investigated material TiO_2 nanoparticles grow to crystalline domain sizes of up to 7 nm representing the ideal size range for full structure modelling with DISCUS [3]. The main focus in the present route of synthesis rests on obtaining phase pure anatase nanoparticles since additional other polymorphic phases of TiO_2 (mainly rutile and brookite) veil modeling efforts which target intermediates. Moreover, in later stages of the reaction the slow aging process of nanoparticles is monitored and interrupted eventually. For this purpose, various reactants are introduced to the solution in order to inhibit the particle growth and the corresponding PDFs are deployed to sketch the inhibition mechanism.

[1] M. Zobel, H. Chatterjee, G. Matveeva, U. Kolb, R. B. Neder, *J Nanopart Res* 2015, *17*.

[2] Z. Q. Li, Y. Zhu, L. W. Wang, J. T. Wang, Q. Guo, J. G. Li, *Appl Surf Sci* 2015, *355*, 1051-1056.

[3] T. Proffen, R. B. Neder, *J Appl Crystallogr* 1997, *30*, 171-175.

Keywords: PDF, Nanoparticles, Anatase

Early hydration study of standard and doped Alite-Belite-Ye'elimite (ABY) cements through Synchrotron Radiation

J. D. Zea-Garcia[a*], A. Cuesta[a], A. G. De la Torre[a], M. A. G. Aranda[b], O. Vallcorba[b], I Santacruz[a]

[a] *Departamento de Química Inorgánica, Cristalografía y Mineralogía, Universidad de Málaga, Spain.*

[b]*ALBA Synchrotron, Carrer de la Llum 2-26, Barcelona, E-08290 Cerdanyola, Spain.*

** jdavidzea@uma.es*

The manufacturing of ye'elimite-rich cements releases from 15 to 37%, depending on their composition, less CO_2 to the atmosphere than ordinary Portland cement (OPC). BYF cements containing belite, ye'elimite and ferrite as main crystalline phases, are promising eco-friendly binders. Nevertheless, belite, its main phase, shows a slow hydrating behaviour and the mechanical strengths are lower than OPC at early ages. Some alternatives to solve this problem are: i) forming alite jointly with belite and ye'elimite during clinkering, Alite Belite Ye'elimite (ABY) clinkers. The hydration of alite and ye'elimite would develop high mechanical strengths at early ages, and belite contributes to later curing times; ii) a second alternative is the stabilisation of alpha forms of belite using dopants such as boron named here after dABY.

In this work, two different types of ABY clinkers (standard and doped) have been prepared and characterized to understand their different hydration mechanisms at the same water-to-cement (w/c) ratio. The clinkers have been prepared using CaF_2 and ZnO as mineralizers, and borax as dopant agent to stabilize alpha forms of belite (α'_H-C_2S). Afterwards, 14 wt% of anhydrite (as soluble sulphate source) was added to prepare the corresponding cements. Finally, the hydration study was performed at w/c ratio of 0.5. Here, an in-situ hydration study using synchrotron X-ray powder diffraction (SXRPD) for the first 14 hours of hydration is reported. Moreover, these results will be combined with the ex-situ laboratory X-ray powder diffraction study (LXRPD) at 1 day of hydration and calorimetric results. Rietveld quantitative phase analysis has been used to establish the phase evolution across the time.

Keywords: clinkering, hydration properties, ABY cements, mineralogical behaviour, Rietveld quantitative phase analysis, synchrotron radiation.

EPSR-derived structure of functionalised geopolymers

M. Dapiaggi[a*], A. Bernasconi[b], M. Nazzaro[c], H. Farina[c], F. Demartin[c], G. Confalonieri[d]
[a] *Dipartimento di Scienze della Terra, Università degli Studi di Milano, Italy*
[b] *Dipartimento di Chimica, Università degli Studi di Pavia, Italy*
[c] *Dipartimento di Chimica, Università degli Studi di Milano,*
[d] *Dipartimento di Scienze della Terra, Università degli Studi di Torino, Italy*
* *monica.dapiaggi@unimi.it*

Geopolymers can be defined as amorphous analogues of crystalline natural tectosilicates (like zeolites, for example), and have received a lot of attention in the recent years, due to their technological properties, such as low weight, mechanical resistance and extreme versatility.
They are obtained through a polycondensation reaction from silico-aluminate raw materials, with the aid of basic solutions containing cations such as Na, Ca and/or K. They have an amorphous or semi-crystalline structure, which strongly depends on the synthesis conditions (type and amount of activator, pH and calcination temperature). Various geopolymers were produced, with different Si/Al ratios, and different cations (K^+or Na^+). In order to produce hybrid geopolymers, the starting source of silica was APTES ((3-aminopropyl)triethoxysilane) instead of the usual TEOS (tetraethyl orthosilicate). Various amounts of functionalised silicon were tried (from 0 to 100% wt), with Na^+ and/or K^+ as the balancing cation for Al/Si substitution.
The local structure of geopolymers is usually studied by means of solid state NMR, but it may also be useful to understand more about the relationship between the very local (as shown by NMR) and the medium-range structure. They both can be obtained by means of total scattering measurements (either X-ray or neutron) and subsequent EPSR (Empirical Potential Structure Refinement [1], and references therein) modeling approach. So far, there are only a few papers in the literature using the total scattering approach (see [2] and references within), mainly studying geopolymers local structure as a function of temperature, concentrating mainly on the onset of crystallisation and on the fully crystallised sample. They showed that there is a strong dependence of the structure on the presence of Na^+ or of K^+ in their samples. No paper is reported for EPSR approach on the amorphous or semi-crystalline geopolymer, which is in fact the most interesting one for the possible practical applications. The samples were analysed by means of high-energy X-ray total scattering (at the beamline ID11@ESRF in Grenoble), and the corresponding Pair Distribution Functions (PDF) were produced. The data were modelled with EPSR, and produced very interesting results.

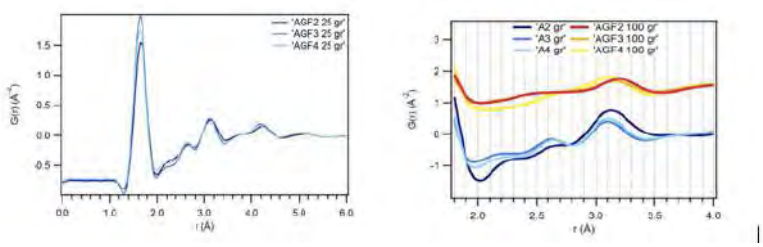

The figures show the different behavior of the geopolymer structure as a function of Si/Al ratio (equal to 2, 3, or 4, on the left hand side; the peak below 2 Å corresponds to Si-O and Al-O bonds) and as a function of the amount of functionalised silicon (equal to 0 in the blue samples and 100% in the red-yellow samples, on the right hand side; the bond corresponding to the peak at about 3 Å corresponds to Si-Al, Si-Si and/or Al-Al bonds). EPSR modeling showed a strong dependence of the Si-O bond length (and bond length distribution) as a function of the amount of functionalised silicon; Al-O bond results more disordered than Si-O one, while Na^+ and K^+ actually behave as charge-compensating cations. This preliminary work allowed to better understand how the organic substitution influences the local and medium-range structure of the geopolymer, with the aim of using this knowledge to produce tailored hybrid geopolymers.

[1] Soper, AK, *J. Phys.: Condens. Matter*, 2007 19, 415108 http://dx.doi.org/10.1088/0953-8984/19/41/415108.
[2] White, CE, Provis, JL, Bloomer, B, Henson, NJ, Page, K, *Physical Chemistry Chemical Physics,* 2013, 15(22), 8573-8582.

Keywords: geopolymers, PDF, EPSR

XPDF at DLS: Physics based reduction of pair-distribution function data

T. Spain[a*], D. Keeble[a], J. Filik[a], P. Chater[a], A. Ashton[a], H. Wilhelm[a]
[a] *Diamond Light Source, Harwell Campus, UK*
**timothy.spain@diamond.ac.uk*

The XPDF software project on the I15-1 beamline at Diamond Light Source aims to produce fully reduced pair distribution function (PDF) data for all users at the point of data collection, making this widely-applicable technique more accessible to non-experts. A key part of this is the data processing pipeline that takes in scattering data and returns pair distribution function data that the users are able analyse without requiring further processing.

The conventional approach to reducing X-ray PDF data frequently involves making empirical adjustments to the data to obtain normalized, background-free data that can be Fourier transformed to the PDF; these methods often rely on manual tweaking to obtain fully quantitative PDF data. Here we describe two new methods aimed at reducing the need for manual intervention which have been employed on data produced as part of the XPDF software project and implemented in the Dawn data analysis software [1].

The first is based on empirical simulation of the fluorescence and absorption from the properties of the sample and its environment using the estimated fluorescence and known absorption cross-sections of the atoms in the material. This method, similar to that employed in GudrunX [2], allows removal of the scattering from objects other than the sample (such as any containers) and correction for the absorption of the scattered radiation by all the objects in the beam path, including the sample itself.

The second method replaces the estimations using the known cross-sections with a Monte Carlo based ray tracing of the scattered radiation. This is achieved by simulating the sample and its environment using the X-ray Monte Carlo (XRMC) package [3]. This simplifies the processing at the expense of additional computation, which can be performed before the data is collected.

These two methods will be described, along with details of the automation of the data processing, which will ultimately allow sample data to be collected and the data processed with minimal intervention.

[1] Filik J. *et al*., *J. Appl. Cryst*., 2017, 50
[2] Soper, A. K, Barney, E. R., *J. Appl. Cryst.*, 2011, 44, 714
[3] Golosio, B. *et al.*, *Computer Physics Communications*, 2014, 185, 3

Keywords: PDF, analysis, software

Orbital order-disorder and defects in molecular perovskites

H. L. B. Boström[a*], A. Simonov[a,b], C. S. Coates[a], E. M. Reynolds[a] , Andrew L. Goodwin[a]

[a] Department of Chemistry, *University of Oxford, Oxford, UK.*

[b] *Institut für Geo- und Umweltnaturwissenschaften, Universität Freiburg, Freiburg, Germany.*

* *hanna.bostrom@chem.ox.ac.uk*

The reduced point symmetry of Jahn–Teller distorted cations leads to a wealth of orbitally ordered and disordered phases in transition metal oxides with Cu^{2+} or Mn^{3+} at high-symmetry sites. This degree of freedom is crucial to the functionality of many perovskites and a particularly notable example is the well-studied $La_{1-x}Ca_xMnO_3$, famous for its colossal magnetoresistance.[1] In recent decades, molecular perovskites — coordination polymers with the perovskite topology — have attracted considerable research attention for their structural diversity.[2] However, the orbital correlations in doped series of these materials have been little investigated, despite being of profound importance in several compounds. For example, the hybrid improper ferroelectricity in $[C(NH_2)_3]Cu(HCOO)_3$ and the anisotropic thermal expansion in $CuPt(CN)_6$ are both direct consequences of the Jahn–Teller distortion.[3,4]

We present a comparative study of the three doped molecular perovskites $[C(NH_2)_3]Mn_{1-x}Cu_x(HCOO)_3$, $Mn_{1-x}Cu_xPt(CN)_6$ and $(Mn_{1-x}Cu_x)_3[Co(CN)_6]_2$ using a combination of PXRD and Monte Carlo simulations.[5] The orbital (dis)order and its compositional tolerance varies significantly between the three families: $[C(NH_2)_3]Mn_{1-x}Cu_x(HCOO)_3$ exhibits an orbital order-disorder transition at high values of x; $Mn_{1-x}Cu_xPt(CN)_6$ segregates into an orbitally ordered Cu-rich phase ($I4/mmm$) and a Cu-poor disordered phase ($Fm\bar{3}m$); and the defective Prussian blue analogue $(Mn_{1-x}Cu_x)_3[Co(CN)_6]_2$ remains disordered with space group symmetry $Fm\bar{3}m$ across the entire compositional range. By way of context, the orbitally disordered state $LaMnO_3$ only appears above 750 K and, hence, this provides an opportunity to study orbital disorder in a similar system at ambient conditions. The Monte Carlo simulations explain the discrepant behaviours of the various molecular perovskites in terms of the connectivity of the lattice as well as the presence of defects. The energy scale of the orbital order in these systems is reduced relative to inorganic perovskites and hence may be amenable to control by judicious choice of synthetic conditions.

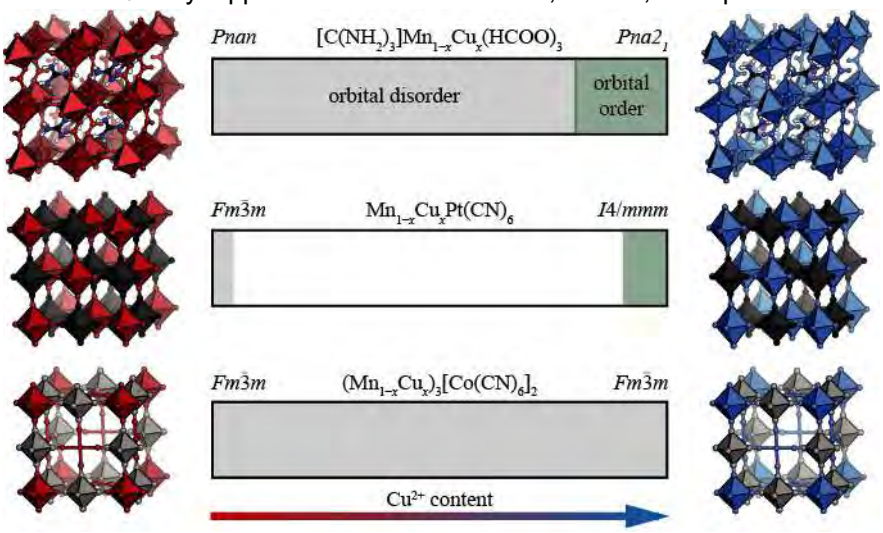

[1] Saitoh E., Tomioka Y., Kimura T. and Tokura Y., *J. Magn. Magn. Mater.*, 2002, 239, 170–172.

[2] Li W., Wang Z., Deschler F., Gao S., Friend R. H. and Cheetham A. K., *Nat. Rev. Mater.*, 2017, 2, 16099.

[3] Stroppa A., Jain P., Barone P., Marsman M., Perez-Mato P. M., Cheetham A. K., Kroto H. W. and S. Picozzi, *Angew. Chem. Int. Ed.*, 2011, 50, 5847–5850.

[4] Chapman K. W., Chupas P. J. and Kepert C. J., *J. Am. Chem. Soc.*, 2006, 128, 7009–7014.

[5] Donlan E. A., Boström H. L. B., Geddes H. S., Reynolds E. M. and Goodwin A. L., *Chem. Commun.*, 2017, 39, 11233–11236.

Keywords: orbital order-disorder, hybrid perovskites, Monte Carlo simulations

Investigations on crystal structures and planar defects of heavily stacking faulted honeycomb iridates

S.Bette[a*], R.E. Dinnebier[a], T. Takayama[a], H.Takagi[a]
[a] *Max-Planck-Institute for Solid State Research, Stuttgart, Germany*
* *S.Bette@fkf.mpg.de*

Iridates with honeycomb like structural motifs recently attracted significant interest due to their promising physical and chemical properties. In alkaline metal iridates correlated electrons and a strong spin orbit coupling was discovered[1] and honeycomb like α-Li_2IrO_3 and $H_3LiIr_2O_6$ were revealed to show pH-sensing properties and therefore to be potential alternatives for glass electrodes.[2] Finally, by using the latter material, $H_3LiIr_2O_6$, a quantum spin liquid state that has been only predicted by theoretical calculations before, was experimentally confirmed for the first time.[3]
Due to their layered constitution the occurrence of stacking fault disorder is a common phenomenon in honeycomb-like iridates.[1,2] The diffraction effects, i.e. anisotropic peak broadening, seriously impeded the structural characterization of this material. In consequence the constitution of the layers has been only roughly described for many iridates, yet.[1,2] A detailed knowledge of the layer constitution and of the type and degree of faulting, however, is essential for the understanding of the physical and chemical properties of the materials.
In our current work[4] we describe the determination of the ideal, i.e. faultless, crystal structure of $H_3LiIr_2O_6$ as well as of the real structure, i.e. the kind and degree of faulting. Due to pronounced anisotropic, peak broadening because of stacking faults, the ideal crystal structure could not be solved by *ab-initio* methods; instead the layer constitution of α-Li_2IrO_3 was used as a starting model for a Rietveld refinement. In order to stabilize the refinement restraints on M-O bond lengths were introduced, that were derived from the low radii region of the measured PDF-curve (Fig. 1, a). The ideal crystal structure indicates that the stacking order is governed by strong O···H-O contacts. Hence several alternative stacking orders were derived that lead to a similar number of favorable O···H-O interlayer contacts (Fig 1, b, c). The derived microstructural model was confirmed by systematic *DIFFaX* simulations[5]. A Rietveld compatible approach[6] was employed to globally optimize a 12*c*, i.e. 12 layer, supercell. By treating each layer as a rigid body like unit, a superstructure was obtained that represents a suitable approximation of the microstructure of the sample. PDF-analysis, in particular in the high radii region, was employed a complementary tool to confirm the optimized super structure.

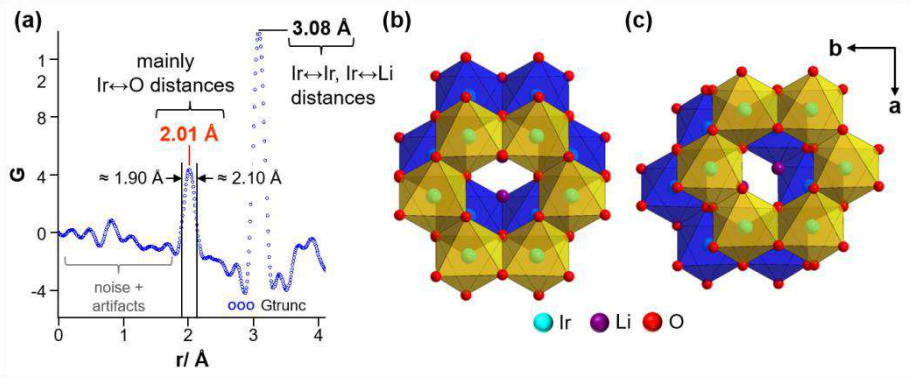

Fig. 1. (a) Low r-region of the measured PDF-curve of $H_3LiIr_2O_6$, (b) stacking of the $Ir_6O_{18}^{12-}$-honeycombs, (c) alternative stacking order.

[1] Wallace D.C. and McQueen T.M. *Dalton Trans.* 2015, 44, 20344.
[2] O'Malley M.J., Woodward P.M. and Verweij H. *J. Chem. Mat.* 2012, 22, 7782.
[3] Kitagawa K., Takayama T., Matsumoto Y., Kato A., Takano R., Kishimoto Y., Bette S., Dinnebier R.E., Jackeli G. and Takagi H. *Nature* 2018, 554, 341.
[4] Bette S., Takayama T., Kitagawa K., Takano R., Takagi H. and Dinnebier R.E. *Dalton Trans.* 2017, 46, 15216.
[5] Treacy M.M.J., Newsam J.M. and Deem M.W. Proc. R. Soc. London, Ser. A 1991, 433, 499.
[6] Bette S., Dinnebier R.E. and Freyer D. *J. Appl. Cryst.* 2015, 48, 1706.

Keywords: honeycomb iridates, stacking faults, PDF-analysis

Unravelling the local structure of zeolite precursor aluminosilicate gels by neutron total scattering

L. Gigli[a*], D. Bowron[b], S. Imberti[b], S. Quartieri[c], F. Di Renzo[d], R. Arletti[e,f]

[a] *Elettra-Sincrotrone Trieste, Basovizza, Trieste, Italy*
[b] *ISIS Rutherford Appleton Laboratory, Didcot, UK*
[c] *Dpt Mathematics, Computing, Physical and Earth sciences, University of Messina, Italy*
[d] *Institut Charles Gerhardt, UMR5253 UM-CNRS-ENSCM, Montpellier, France*
[e] *Department of Earth Sciences, University of Turin, Italy*
[f] *Nanostructured Interfaces and Surfaces IC, Turin, Italy*
* *lara.gigli@elettra.eu*

Amorphous aluminosilicates hydrogels find important applications as glazers, binders and concrete additives, often under the name of geopolymers. They are also intermediates in the hydrothermal synthesis of most zeolites, ordered microporous materials produced at million-ton scale for ion exchange, catalysis and adsorption applications. The structure of the amorphous precursors has always been considered as having a paramount influence in the nucleation and growth of zeolites, especially as a controlling factor in the selectivity of phases formation.

A series of sodium aluminosilicate hydrogels with different Si/Al ratios, representing the precursors of zeolites X, Y, mordenite and ZSM-5, have been prepared by mild hydrothermal synthesis. Powder XRD confirmed the amorphous nature of the materials. ^{27}Al MAS-NMR indicated that all aluminium was in tetrahedral coordination and ^{29}Si MAS-NMR data were compatible with a largely connected network of tetrahedra with a uniform distribution of lattice Al and silanol defects.

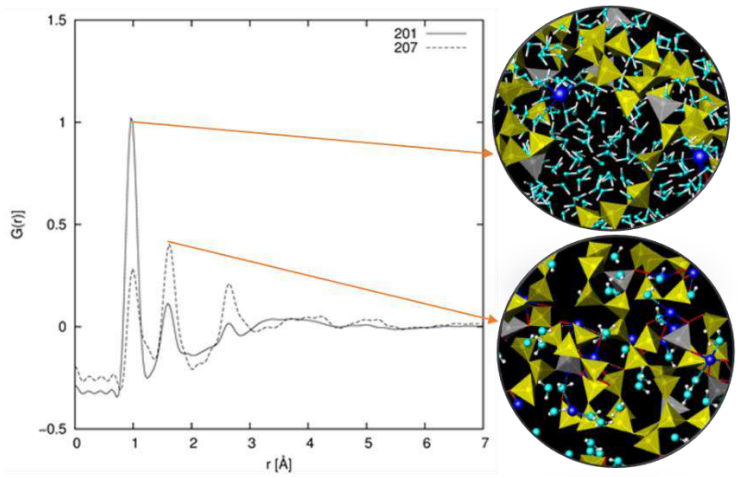

Amorphous precursor samples were deuterated and total scattering neutron diffraction data were collected at SANDALS beamline at ISIS Rutherford Appleton Laboratory.

The empirical potential structure refinement (EPSR) of the neutron total scattering data provided three-dimensional atomistic model of the aluminosilicate gels. Samples 201 and 207, with Al/(Si+Al) ratio 0.05 and 0.22 respectively, present different connectivity and organisation.

The silicon-rich sample (top right in the figure) present 0.8 network interruptions per tetrahedron. Na cations are poorly coordinated to the framework and are surrounded by nearly 7 water molecules, indicating that they don't play a significant silicate structure-directing role. In some ways, the organisation of the silica-rich hydrogel corresponds to a frequently interrupted network of common silica gel. The network of the most Al-rich sample (bottom right in the figure) is more connected, with 0.35 interruptions per tetrahedra. Each sodium cation is coordinated to five-to-six network oxygen atoms and to two water molecules. This strictly corresponds to the common configuration of hydrated cations as structure-directing agents of zeolite cages and confirms the interest of structural studies of the precursors for better understanding of zeolite crystallisation.

Keywords: gels, aluminosilicate, total scattering

Structural Insights into Semicrystalline States of Electrospun Nanofibers by X-ray Scattering

A. Sadeghpour[a,b*], Anjani K. Maurya[a,b,c], L. Weidenbacher[b], F. Spano[b], G. Fortunato[b], R. Rossi[b], A. Dommann[a,b], M. Frenz[c], A. Neels[a]

[a] *Center for X-ray Analytics, Empa, Dübendorf, Switzreland*

[b] *Laboratory for Biomimetic Membranes and Textiles, Empa, St. Gallen, Switzerland*

[c] *Cellular and Biomedical Sciences, Faculty of Medicine, University of Bern, Bern, Switzerland*

* *amin.sadeghpour@empa.ch*

Electrospinning is a versatile technique to produce polymer matrices of highly entangled nanofibers with great potential applications in wound dressing, tissue engineering and controlled drug release [1]. It is well established that their functions are highly correlated with their morphology as well as molecular arrangement in nanometer and sub-nanometer scale [2]. Despite significant advances on understanding the structure and morphology of electrospun nanofibers by various methods like electron microscopy, atomic force microscopy and X-ray based techniques, their detailed structural features and the fiber formation process at the nanoscale has not been fully described yet.

In this contribution, our recent advancement in understanding the structure of fibers in molecular level will be presented. By applying small angle X-ray scattering techniques (SAXS), the nanofibers with varying degree of alignment, processed under different electrospinning conditions, are used to attain new structural insights. Crystalline/amorphous domains in nanometer range are quantitatively analyzed by applying a global analysis method in which the SAXS profile over the whole experimental range for magnitude of scattering vector, q, is simulated. The correlations with the orientation of nanofibers will be demonstrated using the relevant theoretical approaches. The crystallinity and the crystal structure in Angstrom scale will also be discussed considering the patterns obtained from X-ray diffraction methodology. The outcomes will be compared with structural features obtained by other microscopic techniques like electron microscopy (EM) and atomic force microscopy (AFM).

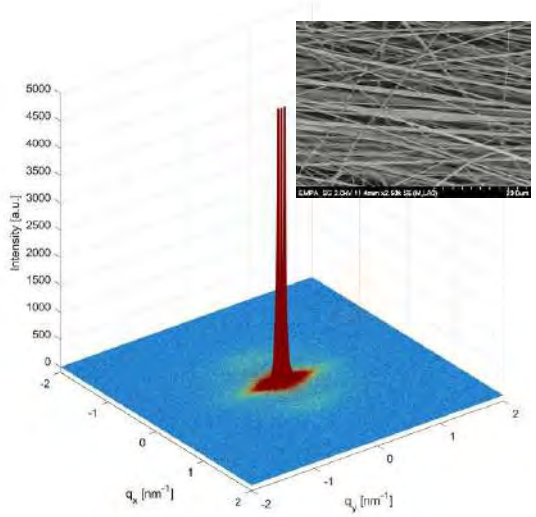

[1] Greiner, A. and Wendorff, J. H. *Angew. Chem. Int. Ed.* 2007, *46*, 5670.

[2] Kołbuk, D.,Sajkiewicz, P.,Maniura-Weber, K. and Fortunato, G. *Eur. Polym. J.* 2013, *49*, 2052.

Keywords: SAXS, electrospun nanofibers, semi-crystalline states

Crystal structure solution of organic compound without prior knowledge of space group and lattice parameters by a global fit to the pair distribution function

D. Prill*, C. Schlesinger, M. U. Schmidt
Institute of Inorganic and Analytical Chemistry, Goethe University, Frankfurt am Main, Germany
** prill@chemie.uni-frankfurt.de*

Local structures in crystalline, nanocrystalline and amorphous organic compounds can be investigated using pair distribution functions (PDFs). For organic compounds, the experimental determination of the PDF curves of organic compounds is very similar to that of inorganic compounds. Nevertheless, the fit of structural models to the PDF curve has rarely been done for organic compounds. In our previous research, the method developments for structure determination from PDF of organic compounds were successful with determination of molecular position and orientation starting from random values. However, the lattice parameters and space group were given as an input[1]. For nanocrystalline compounds the space group and lattice parameters are typically unknown. Therefore, we developed a global procedure in which the lattice parameters, space group, molecular position and orientation are determined from PDF-data[2]. The calculations were carried out with TOPAS 6 Software[3]. The optimisation initiates with a large set of random starting structures in various space groups. The space groups are chosen according to the space group frequency of the corresponding compound class, regarding the chemical class and the molecular symmetry[4]. The optimisation of lattice parameters starts from random values within the sensible range. The ranges are automatically chosen depending on the size of the investigated molecule and space group in which the calculations are preformed. At the present stage of the development, the molecules are treated as rigid bodies. However, intramolecular degrees of freedom should not be a major problem, given the good functionalities provided by TOPAS Software. Barbituric Acid and other small organic molecules were chosen as examples. Synchrotron powder patterns were recorded at the NSLS (Brookhaven, USA) with the wavelength of 0.18 Å. The experimental PDF curve were derived with PDFgetX3 Software[5]. Results of the global fit to the PDF data will be shown.

[1] D. Prill, P. Juhás, S. J. L. Billinge, M. U. Schmidt, *Acta Cryst. A* , 2015, 72, 62.

[2] D. Prill, C. Schlesinger, M. U. Schmidt, in preparation.

[3] A. A. Coelho, *J. Appl. Cryst.*, 2018, 51, 210.

[4] E. Pidcock, W. D. S. Motherwell, J. C. Cole, *Acta Cryst. B*, 2003, 59, 634.

[5] P. Juhás, T. Davis, C. L. Farrow, S. J. L. Billinge, J. Appl. Cryst. , 2013, 46, 560.

Keywords: organic compounds, pair distribution function, structure solution

Orbital Molecules in Vanadium Spinels

A. J. Browne[a*], C. Lithgow[a], S. A. J. Kimber[b], J. P. Attfield[a]
[a] *Centre for Science at Extreme Conditions and School of Chemistry, University of Edinburgh, UK*
[b] *Neutron Sciences Division, Oak Ridge National Laboratory, USA*
* *A.J.Browne@sms.ed.ac.uk*

The use of local structure methods to study short-range charge, spin and orbital ordering has become increasingly important in the characterisation of transition metal oxides and the understanding of phenomena such as colossal magnetoresistance [1]. In systems with short metal-metal separations, ordering of directly interacting *d* orbitals can result in the formation of clusters of transition metal cations called orbital molecules [2]. Vanadium oxides exhibit an especially rich variety of orbital molecule states, with the V-V dimerisation that accompanies the metal-insulator transition in VO_2 a particularly well-known example [3].

V_7 'heptamer' orbital molecules have been reported to form in the spinel AlV_2O_4 below a long-range ordering transition at 700 K [4]. We have used X-ray total scattering data, collected at ESRF beamline ID22, to investigate the nature of the V-V bonding in this material through its effect on the local structure. Pair distribution function analysis shows that the heptamers actually comprise ordered pairs of V_3 trimers and V_4 tetramers (Figure). Furthermore, local ordering is stable to at least 1100 K and the orbital molecules persist into a structurally disordered high-temperature phase [5].

We have also synthesised a new spinel, GaV_2O_4. X-ray powder diffraction and total scattering data collected at ID22, neutron powder diffraction data collected at ISIS beamline HRPD, and magnetic and transport property measurements reveal that this material has orbital molecule states analogous to those in AlV_2O_4 but with a lower order-disorder transition temperature, of 415 K [6]. These are the first examples of vanadium oxides in which the orbital molecules are found to have a high-temperature disordered state, showing that the electronic instabilities that cause V-V bonds to form in these materials can vary considerably from the Peierls-type mechanism normally considered for VO_2.

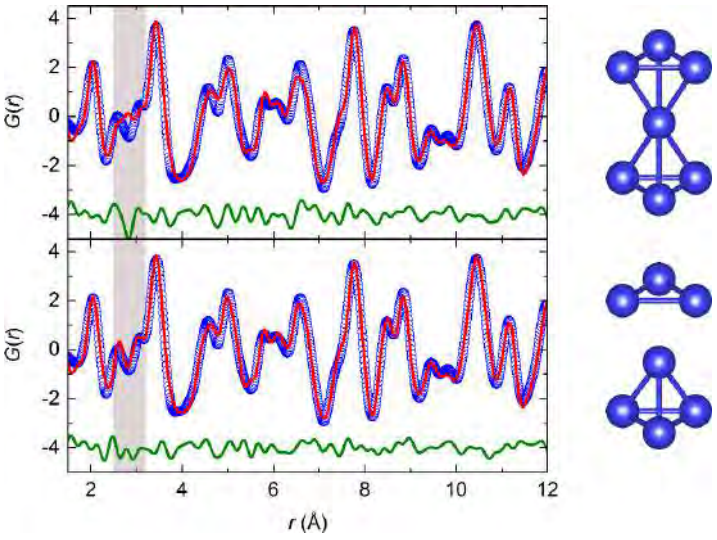

[1] Billinge S.J.L. *et al*., *Phys. Rev. Lett.*, 1996, 77, 715-718.

[1] Attfield J.P., *APL Mater.*, 2015, 3, 041510.

[2] Goodenough J.B., *J. Solid State Chem.*, 1971, 3, 490-500.

[3] Horibe Y. *et al*., *Phys. Rev. Lett.*, 2006, 96, 086406.

[4] Browne A.J., Kimber S.A.J. and Attfield J.P., *Phys. Rev. Mater.*, 2017, 1, 052003(R).

[5] Browne A.J., Lithgow C., Kimber S.A.J. and Attfield J.P., *Inorg. Chem.*, 2018, 57, 2815-2822.

Keywords: orbital ordering, vanadium oxides, pair distribution function

Following the Formation of Tungsten Oxide Nanostructures from Polyoxometalates Through *In Situ* Pair Distribution Function Analysis

Mikkel Juelsholt[a*], Troels Lindahl Christiansen[a], Kirsten M. Ø. Jensen[a]
[a] *Department of Chemistry, University of Copenhagen, DK.*
* *mikkel.juelsholt@chem.ku.dk*

Nanoparticles of tungsten oxides have a range of important applications in e.g. gas-sensing, catalysis and in supercapacitors[1]. Tungsten oxides show rich structural chemistry due to rich redox chemistry and a range of stable crystal structures. The properties are highly dependent on the size and structure of the material, and in order to obtain a 'tailor-made' material, it is crucial to understand the mechanisms that dictate the formation of the material during synthesis. X-ray total scattering with Pair Distribution Function (PDF) analysis allows following the structural changes that take place all the way from precursor cluster over nucleation clusters to the final crystalline particles[2].

We here present a study of WOx nanostructures formed in a solvothermal synthesis by thermal decomposition of ammonium metatungstate hydrate under different experimental conditions. Using Ex Situ and In Situ X-ray Total Scattering and Pair Distribution Function analysis, we study how different experimental conditions induces changes in the final size and crystal structure of the nanomaterials. We also observe how different reaction conditions influence the precursor and induce two distinct crystallization pathways. We determine the changes in molecular geometries as the system moves from polyanion clusters to crystalline nanoparticles. We determine the structure of the ionic clusters present at all stages of the reaction, revealing complex equilibria between different polyoxometalate structures. Furthermore, we determine the atomic structure of the crystalline nanoparticles.

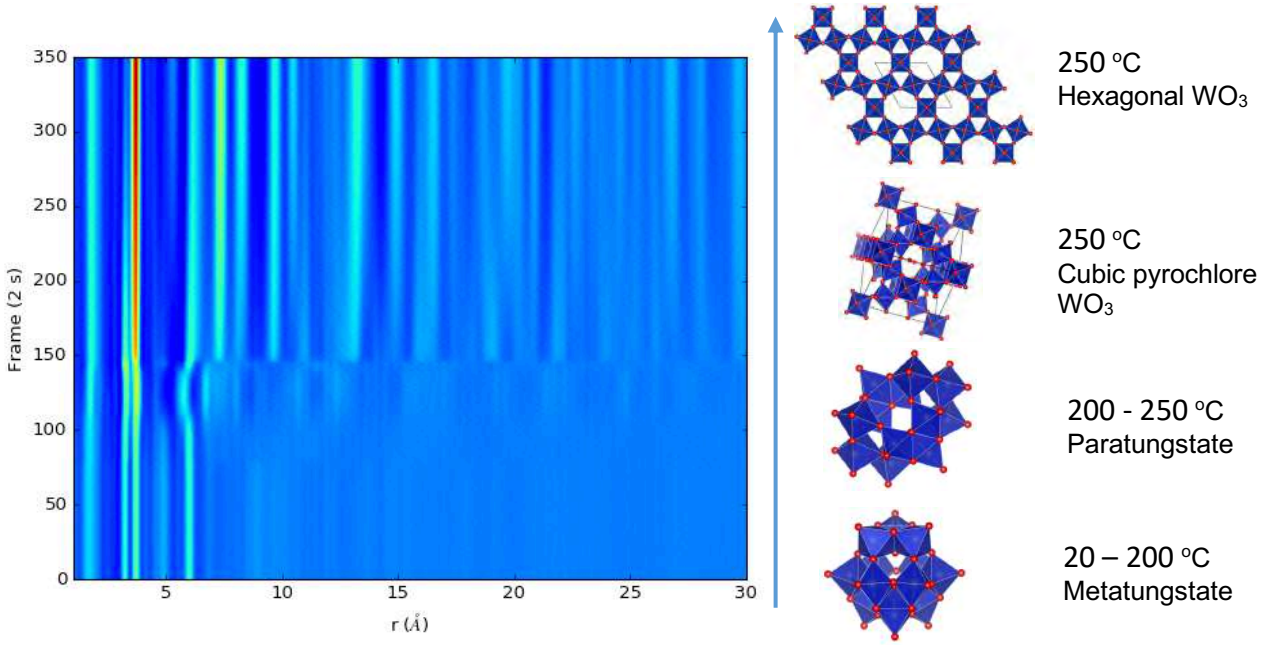

Keywords: crystallization, in situ, pair distribution function

[1] H. Zheng, J. Z. Ou, M. S. Strano, R. B. Kaner, A. Mitchell and K. Kalantar-zadeh, *Advanced Functional Materials*, 2011, 12, 2175.

[2] M. Ø. Jensen Kirsten, C. Tyrsted, M. Bremholm and B. Iversen Bo, *ChemSusChem*, 2014, 6, 1594.

Understanding the Mechanism of Sodium Insertion in Hard Carbon Through *Operando* Pair Distribution Function Analysis

J. K. Mathiesen[1*], P. Norby[2] & K. M. Ø. Jensen[1]
[1]*Dept. of Chemistry and Nanoscience, University of Copenhagen,*
[2]*Dept. of Energy, Technical University of Denmark,*
**jkm@chem.ku.dk*

The interest in new battery materials, which are able to "follow in the footsteps" of the superior lithium ion batteries (LIBs), has increased the recent years. As a suitable candidate for the replacement of LIB employing graphite as the negative electrode, sodium-ion batteries (SIB) have long been investigated due to their intrinsic similarity to LIB, e.g. comparable electrode potentials to that of LIBs. However, due to unfavorable thermodynamics, sodium ions have been found unable to intercalate into graphite unless electrolyte solvents are co-intercalated. Fortunately, hard carbons, or non-graphitic carbons, have been successfully used as anodes. Previous studies proposed the sodiation mechanism to follow a three-stage mechanism characterized by absorption of sodium ions onto pore surfaces, at defect sites and between expanded layers of graphene [1, 2]. However, the continuous, dynamical structural changes have not yet been addressed and are essential to fully understand the sodiation mechanism.
Using *operando* X-ray total scattering and Pair Distribution Function (PDF) analysis utilizing a capillary-battery cell, the mechanism of hard carbon sodiation has been investigated. The results obtained provides information about the local structural changes of the disordered material, which are difficult to address using conventional crystallographic methods due to the amorphous state of the material. The PDF data reveals that inter- and intralayer expansions appear upon sodiation, suggesting the possibility for intercalating behavior. The expanding behavior corresponds to a reversible charge transfer between the σ-orbitals of sodium and the antibonding orbitals in the upper π-band of the graphene sheet resulting in bond reduction. Consequently, in-plane elongation and contraction are observed upon discharge and charge, respectively. However, the data also reveals that the hard carbon structure becomes increasingly disordered upon discharge, in which the initial structure is never fully recovered. Additionally, an overestimation of high-*r* data fitting compared to low-*r* fitting reveals the presence of graphene sheet curvature. As an attempt to disentangle overlapping contributions from the C-C correlation distances and possible sodium-sodium or sodium-carbon bonds, an *operando* experiment of lithiated hard carbon was performed. Intercalation behavior was also clearly identified with expanding cell parameters, but at a much lower rate than as seen upon sodiation. The more pronounced structural impact upon sodiation suggests a larger electron transfer impact on the structure by influencing the π-orbitals of the neighboring, conjugated benzene rings. This means that the electron transfer cannot be described as a local electron transfer contribution as might be the case of lithium, but instead as a more delocalized contribution.

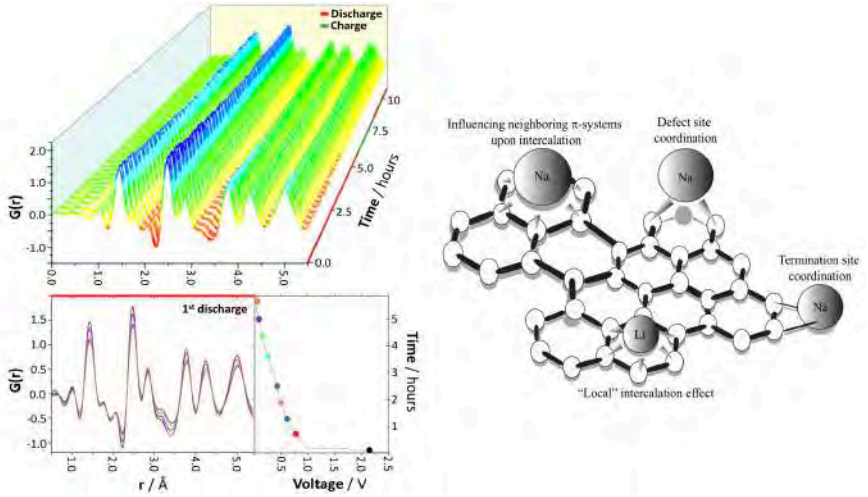

[1] Bommier, C., Surta, T. W., Dolgos, M., & Ji, X., *Nano letters*, *15*(**9**), 5888-5892 (2015).
[2] Stratford, J. M, Allan, P. K., Pecher, O., Chater, P. A. & Grey, C. P., *Chem. Commun.*, *52*, 12430-12433 (2016).

Keywords: *operando,* total scattering, battery materials

Exploration of the structure of a series of UiO-66(M)s (M = Zr, Ce, Hf), using the pair distribution function analysis

V. Ortiz[a], J. Jacobsen[b], J. Dannewerk[b], E. Elkaïm[c], S. Devautour-Vinot[a], P.G. Yot[a*], N. Stock[b] and G. Maurin[a]
[a] *Institut Charles Gerhardt, Université de Montpellier, France*
[b] *Institut für Anorganische Chemie, Christian Albrechts Universität zu Kiel, Germany*
[c] *Synchrotron Soleil, Saint-Aubin, France*
* *pascal.yot@umontpellier.fr*

Metal organic frameworks (MOF) are the object of intensive research since more than twenty years. The success of this family of porous hybrid crystalline materials could be explained by the huge chemical versatility resulting from the large number of possible combinations between the metal centers and the organic linkers. The porous volumes, pores size and shape etc make such solids as very promising candidates for a large variety of applications such as catalysis [1], storage, separations and sequestration of fluids and gases [2,3], proton conduction [4], mechanical energy storage [5], ...

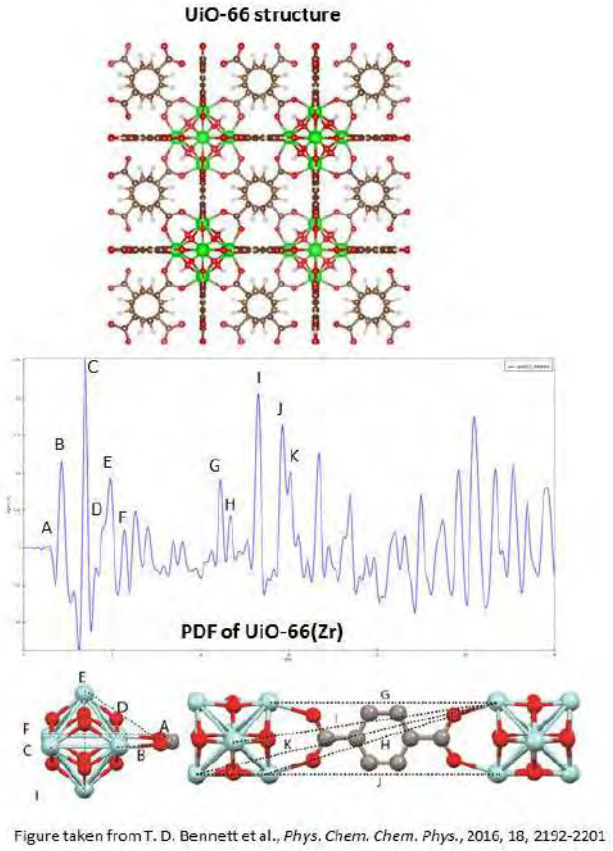

Figure taken from T. D. Bennett et al., *Phys. Chem. Chem. Phys.*, 2016, 18, 2192-2201

Structural model, Radial Distribution Function and schematic representation of the correlations in UiO-66(Zr) MOF.

Amongst the large number of existing MOFs, the UiO-66(Zr) (UiO stands for University of Oslo) has demonstrated promising performances in different fields exposed before, due to its good thermal and mechanical stability. As known, UiO-66(Zr) results of $Zr_6O_4(OH)_4$ octahedras connected together by benzene-1,4-dicarboxylate linkers. In this work, we studied the local structure of the well-known zirconium-based MOF and the isostructural analogues including (i) the pure Ce- and Hf-based UiO-66 and (ii) the mixed Zr/Ce and Zr/Hf based UiO-66 (with Zr/M = 1/1). Structure factors have been determined for all these solids from patterns recorded on CRISTAL beam line at Soleil Synchrotron (Saint-Aubin, France) and treated using the Pair Distribution Function (PDF) analysis with the xPDFSuite software [6]. Using PDF analysis [7] it was possible (i) to probe the modification of the local structure of UiO-66(Zr) upon total substitution of Zr by Ce or Hf and (ii) to determine the ratio of pure $M_6O_4(OH)_4$/$Zr_3M_3O_4(OH)_4$ clusters (with M = Ce or Hf) in the mixed Zr/Ce and Zr/Hf based UiO-66s. In addition, the mechanism of the structural collapse (defect creation and/or amorphisation) of the UiO-66s upon ball-milling was also investigated compared according to the nature of the metallic center.

[1] A. Corma, H. García, F. X. Llabrés i Xamena, *Chem. Rev*., 2010, 110, 4606.
[2] J.-R. Li, J. Sculley, H.-C. Zhou, *Chem. Rev*., 2012, 112, 869.
[3] X. Li, Y. Liu, J. Wang, J. Gascon, J. Li, B. Van der Bruggen, *Chem. Soc. Rev*., 2017,46, 7124.
[4] X. Meng, H.-N. Wang, S.-Y. Song, H.-J. Zhang, *Chem. Soc. Rev*., 2017,46, 464.
[5] P. G. Yot, K. Yang, F. Ragon, V. Dmitriev, T. Devic, P. Horcajada, C. Serre, G. Maurin, *Dalton Trans*., 2016, 45, 4283 and references there in.
[6] X. Yang, P. Juhas, C. L. Farrow, S. J. L. Billinge, J. Appl. *arXiv*, 2014, 1402, 3163.
[7] T. D. Bennett, T. K. Todorova, E. F. Baxter, D. G. Reid, C. Gervais, B. Bueken, B. Van de Voorde, D. De Vos, D. A. Keen, C. Mellot-Draznieks, *Phys. Chem. Chem. Phys*., 2016, 18, 2192.

Keywords: UiO-66, Chemical modification, Mechanical Stability, Pair Distribution Function analysis

Atomic Pair distribution function analysis by high power Mo Kα radiation and focusing mirror

J. Kim[a*], Y. Shiramata[a], K. Nagao[a], A. Yamano[a]
[a] *Application Laboratories, Rigaku Corporation, Japan*
* *jungeun@rigaku.co.jp*

X-ray diffraction has been generally used to probe average crystal structure of long range atomic arrangement of powder crystallite sample. The X-ray diffraction profile contains diffuse scattering caused by disordered local structure besides Bragg reflection by average crystal structure of long range atomic order. Using profile of total scattering of both Bragg and diffuse scattering, local structure information such as structural deviation, structural defect, or disordered structure can be obtained in addition to average crystal structure. These structures are analyzed by atomic Pair Distribution Function (PDF, G(r)) [1]. So far, total scattering data for PDF analysis was generally obtained from synchrotron X-ray and neutron source by reason that an accuracy of inter-atomic distance is significantly depended on the intensity of source and the range of scattering vector Q(=4πsinθ/λ).

In recent, Rigaku Co. has developed CBO-E(Cross Beam Optics of Elliptical multilayer mirror) [2] for use in high-power Mo radiation of which maximum X-ray tube voltage/current is 60kV/150mA. We attempted a possibility of PDF analysis for several powder materials by using the optics of rotating anode type Mo tube with CBO-E focusing mirror for use in high-power Mo radiation. Rigaku's original software, PDF plug-in of SmartLab Studio II, was used for PDF analysis. Reverse Monte Carlo (RMC) modeling and simulation [3] was additionally carried out in order to compare between G(r) transformed from total scattering data and simulation result.

Figure 1 shows G(r) obtained from total scattering data of SiO_2 and $0.9SiO_2$-$0.1Na_2O$ glass by Mo radiation. The experimentally visualized results are in good agreement with G(r) reproduced by RMC simulation. In the presentation, PDF analysis apply to several powder materials, which are measured by high power Mo Kα radiation combined with focusing mirror. Based on the results, we discuss applicability of combination of general-purpose X-ray diffractometry and PDF analysis in powder materials of short-range charge ordering and/or complex disordered structure.

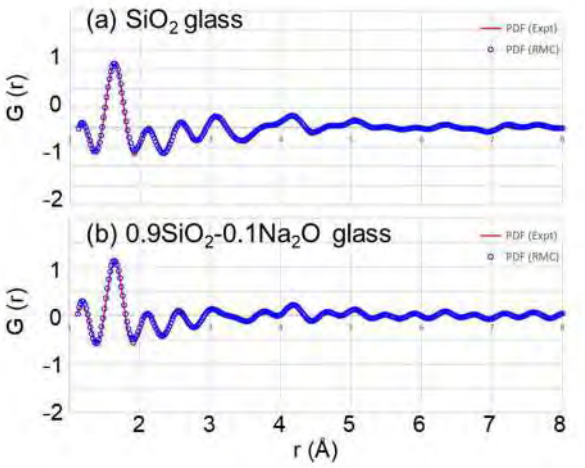

Figure 1. G(r) of SiO_2 and $0.9SiO_2$-$0.1Na_2O$ glass by Mo Kα radiation and RMC simulation

[1] Proffen, Th. & Billinge, S. J. L. *J. Appl. Cryst*. 1999, 32, 572–575.

[2] T. Osakabe, *Rigaku J.* 2017, 33, 1.

[3] R. L. McGreevy, *J.Phys.: Condens. Mat*. 2001, 13, R877–R913.

Keywords: Mo and Ag Kα radiation, Pair distribution function, Total X-ray scattering

Differential anomalous scattering study of binary Cu-Hf based metallic glasses

S. Michalik[a*], K. Saksl[b,c], P. Jóvári[d], A. Lachová[c], M. Fejerčák[b,c], M. Šuliková[c], K. Šuľová[b,e], M. Drakopoulos[a]

[a] *Diamond Light Source Ltd., UK*

[b] *Institute of Materials Research, Slovak Academy of Sciences, Slovak Republic*

[c] *Institute of Physics, Faculty of Science, P.J. Šafárik University in Košice, Slovak Republic*

[d] *Wigner Research Centre for Physics, Hungarian Academy of Sciences, Hungary*

[e] *Faculty of Materials Metallurgy and Recycling, Technical University, Slovak Republic*

* *stefan.michalik@diamond.ac.uk*

Metallic glasses (MGs) are a progressive type of engineering alloys in which the structure consisting of metal elements does not have a long range atomic order and their properties are strongly determined by the local atomic environment. Considering where and what the neighboring atoms are the chemical/compositional (CSRO) and physical short range order (SRO) can be defined. The X-ray diffraction (XRD) gives access to the total structure factor, S(Q), which is mostly sensitive to the SRO. For a *N*-component alloy $N(N+1)/2$ structure partials can be distinguished. The drawback of XRD is its lack of a chemical sensitivity. The exceptions can be found for systems where the bond lengths are so different that each peak in the pair distribution function (PDF) obtained after the Fourier transformation of S(Q) can be assigned chemical identity.

Differential anomalous scattering (DAS) allows one to obtain the differential structure factor, $\Delta S_A(Q)$, which contains structural information about the surrounding of a particular atomic species *A* in the sample by performing X-ray diffraction measurements at two different energies near the absorption edge of the atomic type *A* [1]. The obtained chemical contrast is due to the strong energy dependence of the anomalous dispersion term close the absorption edge of this atomic type A. The standard setup for performing of DAS uses an energy sensitive semiconductor detector, such as a pure Ge detector. However we performed DAS measurements using a large 2D flat-panel detector to speed-up data collection. The main disadvantage of flat-panel detectors is their inability to distinguish between elastically scattered and fluorescence photons. We show the constant fluorescence contribution could be subtracted during data processing reflecting the fact that S(Q) and $\Delta S_A(Q)$ should oscillate around 1 and 0 for high *Q* values, respectively.

In this work we applied a DAS technique near the Hf absorption *K*-edge (65.351 keV) to investigate the CSRO around Hf atoms in binary MGs of the composition of $Cu_{54}Hf_{46}$, $Cu_{61}Hf_{39}$ and $Cu_{69}Hf_{31}$ (in at. %). DAS measurements were carried out in a transmission geometry using a 2D Pixium RF4343 detector at the I12-JEEP beamline at Diamond Light Source. Figures show obtained $\Delta S_{Hf}(Q)$ (left side) and their corresponding differential pair distribution functions $DPDF_{Hf}(r)$ (right side). Focusing on the first coordination shell, it can be recognized the maximum around 3.18 Å is much more pronounced in the respect to the shoulder at 2.72 Å for samples with higher Hf concentration. Furthermore the obtained $DPDF_{Hf}(r)$ using the DAS technique are confronted with ones obtained from a Reverse Monte Carlo (RMC) simulated configuration box of atoms using X-ray diffraction data collected at 80 keV, neutron diffraction data and Cu K-edge X-ray absorption spectroscopy data as inputs for the RMC simulation.

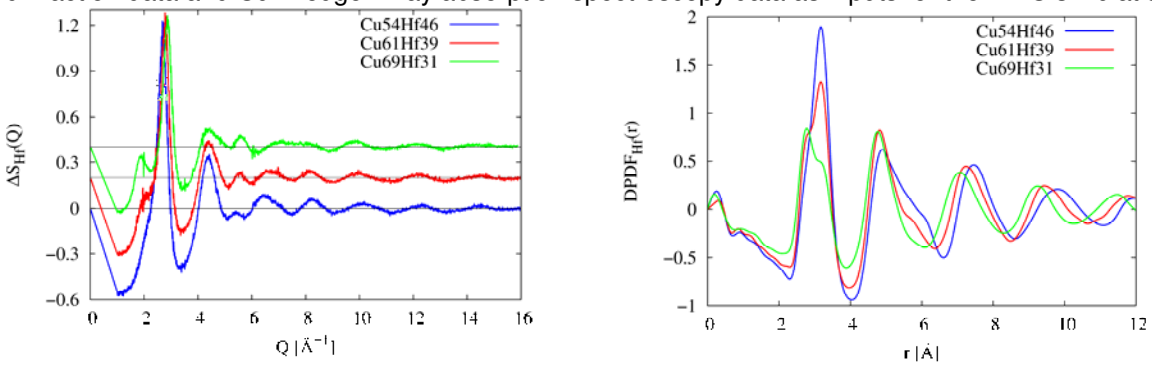

[1] Waseda Y. *Anomalous X-Ray Scattering for Materials Characterization, Springer Tracts in Modern Physics 179*, Springer, Berlin, 2002.

Keywords: differential anomalous scattering, metallic glasses, short range order

Combining PDF and DFT to resolve defect configurations in $La_{1-x}Ba_{1+x}GaO_{4-x/2}$ ionic conductors

M. Coduri[a*], S. Casolo[b], N. H. Jalarvo[c], M. Scavini[b]
[a] *ESRF, Grenoble, France*
[b] *Universita' degli studi di Milano, Italy*
[c] *Oak Ridge, USA*
** coduri@esrf.fr*

$La_{1-x}Ba_{1+x}GaO_{4-x/2}$ is a family of ionic conductors that can exhibit both proton and oxygen vacancies diffusion. The former can be triggered by the incorporation of water into the oxygen vacancies (V_O) introduced by substituting Ba for La (Ba_{La}') [1]. Undoped $LaBaGaO_4$ has orthorhombic structure (s.g. $P2_12_12_1$) composed of GaO_4 distorted tetrahedral units not directly connected with each other. The substitution of Ba for La induces significant disorder, which cannot be modeled properly with the long range orthorhombic structure. The local structure of $La_{1-x}Ba_{1+x}GaO_{4-x/2}$ is here studied by combining X-ray Pair Distribution Function (PDF) and Density Functional Theory (DFT) calculations. DFT was used to simulate defect arrangements differing for the relative position of Ba_{La}' with respect to V_O. All the models result in the formation of Ga_2O_7 corner-sharing dimers, with the Ga-O bonds elongated along the major axis. As the average structure is orthorhombic with none of the cations lying in special positions, the explicit description of the local structure through lower symmetry models would require intensive parameters constrains. This problem was overcome by using the models calculated by DFT, fixing all atomic positions and displacement parameters, thus refining only lattice parameters. The DFT models were used to refine experimental PDF data separately at the very local scale (r < ~6 Å) and on a larger interatomic distance range up to 13 Å. The most stable model according to DFT, which accounts for Ba_{La}' as 1st and 2nd neighbor of the vacancy and of the O bridge in the dimer, is the one giving the best fit of the PDF local scale. As a general trend, the lower the energy of the DFT structure, the smaller the fit residual of PDF data. it turned out that the introduction of BaLa' and VO promotes the disorder of the La substructure and in general it affects the distribution of distances involving Ba and La, towards which X-ray PDF is strongly sensitive. Above 6 Å the average orthorhombic structure fits the PDF better than the DFT models, thus suggesting that Ga_2O_7 units are not correlated with each other.

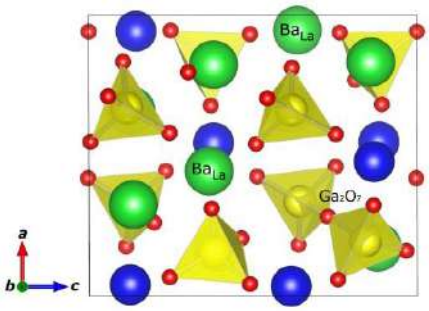

The synergy between DFT simulations and XRD-PDF proved to be successful to model structural features in disordered systems.

[1] Kendrick E., Kendrick J., Knight K. S., Islam M. S., Slater P. R., Nature Materials 2017, 6, 871.

Keywords: Pair Distribution Function, Density Functional Theory, gallate conductors

Operando PDF/DRIFTS/MS experiments at the beamline ID15A at ESRF: investigating the structure and reactivity of catalytic nanomaterials

S. Checchia [a*], M. A. Newton [b], A. J. Knorpp [b], J. Meyet [b], P. Sot [b], M. Di Michiel [a], C. Coperet [c], and J. A. van Bokhoven [b]
[a] *European Synchrotron Radiation Facility, France*
[b] *ETH Hönggerberg - Institute for Chemical & Bio-engineering, Switzerland*
[c] *ETH Zürich - Institute for Inorganic Chemistry, Switzerland*
* *stefano.checchia@esrf.fr*

The study of catalysts under operating conditions leads to a better understanding of how catalytic processes work. At the same time, correlating information from multiple probes on a coincident sample volume has become inevitable to understand increasingly complex heterogeneous catalysts [1,2]. Synchronous X-ray diffraction and vibrational spectroscopy are an example of gathering complementary structural and chemical information [3]. An effective combined *operando* setup must reproduce real-world conditions and evidence different key aspects of a material without compromising data quality.
Pair Distribution Function (PDF) analysis is probably the most insightful synchrotron X-ray technique, probing structures up to the nanometre scale regardless of long-range order and with high time-resolution. Combining PDF analysis with Diffuse Reflectance Infrared Spectroscopy (DRIFTS), subtle structural changes can be linked to a host of chemical information such as formation and sorption of surface species, thus forming a coherent image of intermediates and products of the catalytic process.
We present recent results obtained with the *operando* PDF/DRIFTS/MS setup at the high-energy beamline ID15A at ESRF. First, we show the sensitivity of the method to structural and chemical responses of catalytic Cu/Fe nanoclusters supported on Omega zeolite frameworks and amorphous silica under several catalytic conditions (Figure). Next, we discuss the challenges in data collection and analysis specific to *operando* total scattering experiments.

[1] Newton M.A., Di Michiel M., Kubacka A., Fernandez-Garcia M., J. Am. Chem. Soc., 2010, 132(13), 4540.

[2] Kalantzopoulos G., Lundvall F., Checchia S., Lind A., Wragg D.S., Fjellvåg H., Arstad B., ChemPhysChem, 2017, 19(4), 519.

[3] Beyer K.A., Zhao H., Borkiewicz O., Newton M.A., Chupas P.J., Chapman K. W., J. Appl. Cryst., 2014, 47, 95.

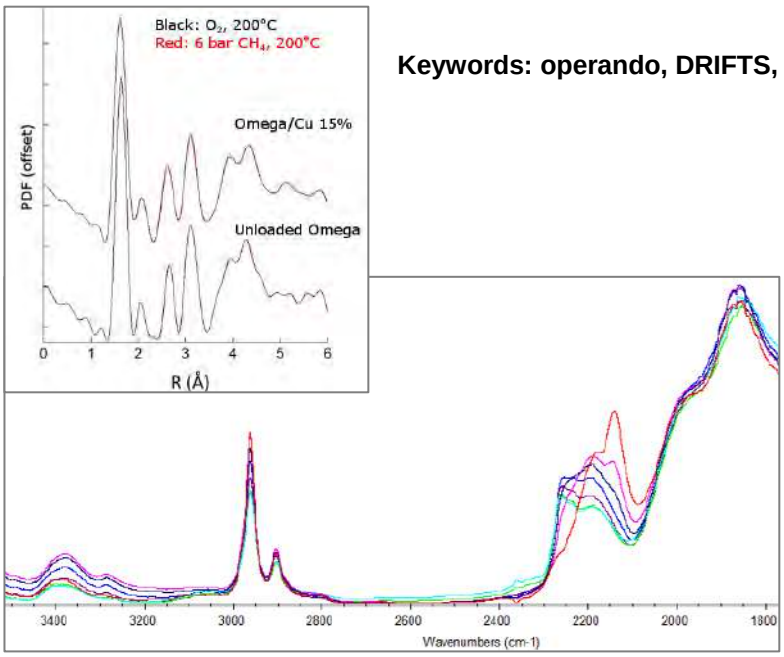

Keywords: operando, DRIFTS, catalysis.

Study on scattering origins for profiling basal reflections of 1:1 regularly interstratified illite and smectite (rectorite)

I. M. Kang[a*], M. H. Kim[b], H. S. Moon[b]
[a] *Advanced Geo-materials Department, Korea Institute of Geoscience and Mineral Resources, Korea*
[b] *Department of Chemistry, Yonsei University, Korea*
[c] *Department of Earth System Sciences, Yonsei University, Korea*
** imkang@kigam.re.kr*

Interstratified illite and smectite (I-S) progressively reacts to form more illite-rich phases as burial depth increases. Therefore, the smectite-to-illite transition is used for evaluating a potential of hydrocarbon source rock because the transition temperature corresponds to oil formation temperature, so-called oil window. The I-S array is often described using a MacEwan crystallite concept which views I-S as a finite Markov chain of illite and smectite. This crystallite concept is useful for theoretically profiling the basal reflections of I-S using a junction probability depicted by layer proportion and stack ordering [1]. We calculate here the basal peak profiles of Na-rectorite (1:1 regular interstratification of illite and Na-smectite) with two different scattering origin choices based on the octahedral cationic plane and on the basal oxygen plane of tetrahedral sheet. Our calculation shows that the scattering origin of the octahedral cationic plane, which has been often used in previous diffraction models, is ineffective for profiling the measured peak skewness and irrationality. Alternatively, the calculation using the scattering origin of basal oxygen plane better mimics the measured peak profiles, and provides more reliable crystallite thickness distributions for Bertaut-Warren-Averbach analyses [2]. The origin is also useful for demonstrating the scattering sequence, the layer chemistry heterogeneity, and the effect of the crystallite margin on rectorite scattering. More details are described in [3].

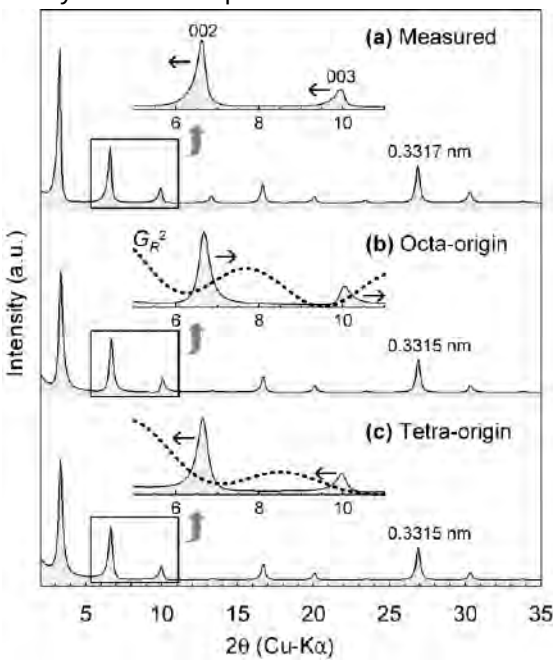

[1] Reynolds R.C. *Crystal structures of clay minerals and their X-ray identification*, 1980, 249.

[2] Drits V.A., Eberl D.D. and Środoń J. *Clays and Clay Minerals*, 1998, 46, 38.

[3] Kang I.M., Kim M.H. and Moon H.S. American Mineralogist, 2009, 94, 1411.

Keywords: rectorite, scattering origin, basal reflection

Thermoresponsive behaviour of $(NH_4)_{0.5}Co_{1.25}(H_2O)_2[BP_2O_8].(H_2O)_{0.5}$ with CZP framework topology

M. W. Mogodi[a*], D. G. Billing[b], M. A. Fernandes[b]
[a] *European Synchrotron Radiation Facility (ESRF), Grenoble, France*
[b] *School of Chemistry, University of the Witwatersrand, Johannesburg, South Africa*
* *mogodi@esrf.fr*

Four CZP (chiral zincophosphate) zeolite topology compounds [1] with the general formula $M^{I}M^{II}(H_2O)_2[BP_2O_8].yH_2O$ (M^{I} = Na, NH_4 and M^{II} = Mn, Co, y = 0.5, 1) have been prepared under mild hydrothermal conditions (at 180 °C). Such microporous compounds with aesthetically interesting crystal structures can have interests in fields such as catalysis, storage, separation and ion-exchange. One compound of this family, $(NH_4)_{0.5}Co_{1.25}(H_2O)_2[BP_2O_8].(H_2O)_{0.5}$, has been studied by variable temperature high resolution powder X-ray diffraction experiments carried out from 298 to 1073 K. Complete Rietveld refinements were achieved by combining stereochemical restraints with the powder diffraction data. At room temperature, this compound crystallizes in the $P6_5$ (No. 170) space group with Z = 4 belonging to the hexagonal system. The unit cell parameters obtained were: a = 9.4330(2) Å, c = 15.5203(2) Å, V = 1196.01(5) Å^3. The crystal structure consists of a helical anionic framework, $\infty[BP_2O_8]^{3-}$, composed of corner sharing BO_4 and PO_4 tetrahedra. Water and ammonia molecules are found within the helical channels running along the [001] direction. This compound undergoes a series of dehydration, de-ammoniation (analysis augmented by thermogravimetric experiments) and finally long range structural decomposition into an amorphous phase. Total scattering analysis [2] was applied for the first time coupled to the above conventional structural refinement approach to further unravel this gaseous dissociation and subsequent decomposition pathway of the rigid host structure.

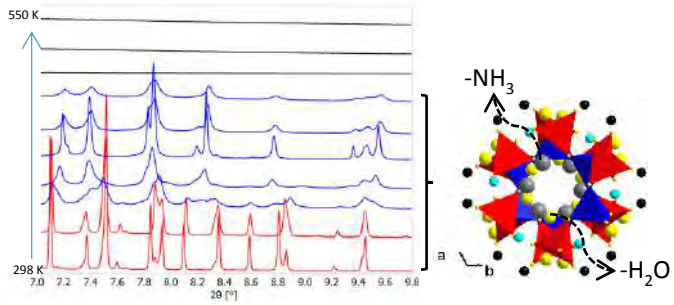

[1] Kniep, R., Will, H.G., Boy, I. and Röhr, C. *Angewandte Chemie International Edition*, 1997, 36, 1013.

[2] Egami, T. and Billinge, S.J. *Elsevier*, 2003.

Keywords: borophosphates, high-temperature, in-situ synchrotron XRPD

Routine quantification of stacking disordered kaolinites by the Rietveld method.

K. Ufer[a*], R. Kleeberg[b]
[a] *Federal Institute for Geosciences and Natural Resources, Germany*
[b] *TU Bergakademie Freiberg, Germany*
** Kristian.ufer@bgr.de*

The mineral kaolinite $Al_4Si_4O_{10}(OH)_8$, a 1:1 layer silicate, is of economic interest due to its relevancy as raw material and as indicator of hydrothermal alterations of noble metal deposits [1]. Therefore a correct quantification of kaolinite contents is eligible.
Kaolinite occurs in a wide variability of disorder, mainly caused by faults in layer stacking. It was recently demonstrated that quantitative XRD by the Rietveld method can be used as a tool for the quantification of kaolinite contents [1]. However, the structural description of stacking disorder in Rietveld refinements is computationally time consuming and in case of co-existing disordered layer silicates it is leading to strong correlation effects.
One possibility to avoid these drawbacks is to fixate all refineable structural parameters by the refinement of standard materials. This reduces the effect of correlations, but the extensive calculations are still severe, especially in case of large sample series. Other Rietveld refinement techniques use the approach to generate lists of *hkl*-dependent structure factors [2]. These Le Bail-like approaches [3] use refinements of reference sample materials with a limited use of structural parameters.
It will be demonstrated here that structurally based calculations by using disorder models can also be used to generate lists of structure factors. This makes it possible to generate collections of calculated patterns even without the availability of reference materials.
It will be shown that these models are stable and feasible for the quantification of kaolinite contents in reference mixtures (figure, blue pattern) as well as in bulk samples of kaolinite deposits.

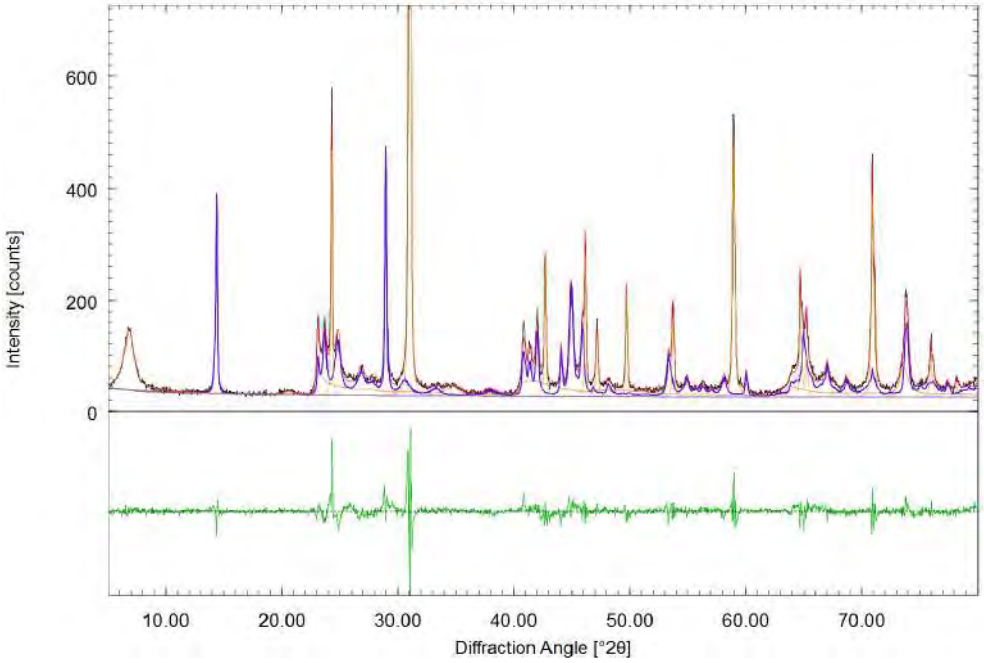

[1] Ufer K., Kleeberg R. and Monecke T. *Powder Diffraction, 2015,* 30 (S1), 111.

[2] Scarlett N.V.Y. and Madsen I.C. *Powder Diffraction,* 2006, 21, 278.

[3] Le Bail A., Duroy, H. and Fourquet, J.L. *Mater. Res. Bull.*, 1988, 23, 447.

Keywords: kaolinite, stacking disorder, quantitative phase analysis

Toward solution of locally ordered polymer domain structures using pair distribution function analysis

M. W. Terban[a*], B. Hinrichsen[b], R. E. Dinnebier[a]
[a] *Max-Planck-Institute for Solid State Research, Stuttgart, Germany*
[b] *BASF, Ludwigshafen, Germany*
* *M.Terban@fkf.mpg.de*

The characterization of polymer structures from X-ray diffraction data is difficult due to the low level of crystallinity in many as-produced samples. Structure determination can be hindered by low resolution and poor quality data. Furthermore, drawing and annealing treatments for fiber diffraction studies may modify the sample structure in undesirable ways, leaving structure probes and modeling techniques for disordered materials to be desired.
The total scattering pair distribution function (PDF) method provides a high resolution means to analyzing a material's local structure. It can therefore provide a measure for determining bonding characteristics, molecular conformation, and domain structure even when no long-range order is present. While it has already been demonstrated for distinguishing proposed models and structure determination without extensive sample preparation [1], there are still only a few examples of its use, and mostly qualitative, for polymers currently in the literature [2,3].
Here, we have implemented model construction and refinement methods for performing polymer structure solution driven by PDF data. Methodologies concerning different construction methods will be discussed with respect to different use-cases. In particular, extensive analysis of Nylon 6 (polycaprolactam 6, $[C_6H_{11}NO]_n$), a well known synthetic thermoplastic polymer, has been undertaken. Despite its extensive research over many decades, there are only a few examples of detailed structural modeling available [4,5]. Here, we demonstrate PDF characterization of the α form, through a variety of processing treatments, and use it as a model compound for constrained structure solution using the PDF when *Q*-space data is too diffuse for standard crystallographic methods. Fine structural details and the interplay of ordered and disordered components will be discussed with respect to previous models, along with the benefits of coupling iterative energy optimization with the refinements.
High real-space resolution allows direct visualization of nearest neighbor bond distances, providing constraints for average intrachain bond lengths. Sharp features indicate highly correlated atom-pairs due to bonding along the chain, and give a direct measure of chain persistence. Broader features at higher distances help to distinguish and constrain various chain packing motifs, while simultaneously giving distinct information about the domain size and shape. Implications of the diffraction resolution on obtaining valuable information at intermediate length scales will be discussed, as well as the possibilities for extracting useful information from lab-based diffraction methods.

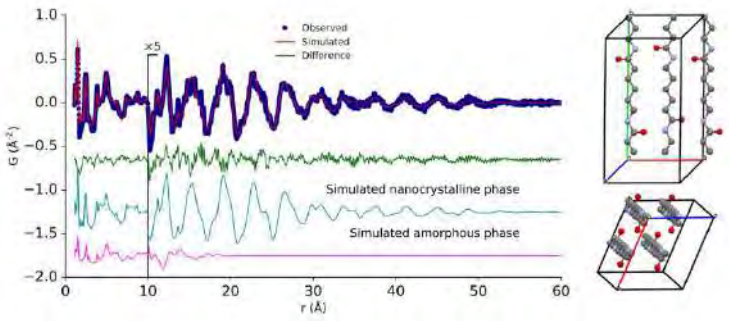

Fig. 1. Co-modelling and refinement of locally ordered and disordered phases to nylon PDF data, and the resulting small-box model structure.

[1] Terban M. W., Dabbous R., Debellis A. D., Pöselt E. and Billinge S. J. L. *Macromol.,* 2016, 49, 7350-7358.

[2] Narten A. H., Habenschuss A., Xenopoulos A. *Polymer*, 32, 1923-1927.

[3] Maron J., Winokur M. J. and Mattes B. R. *Macromol.*, 1995, 28, 4475-4486.

[4] Holmes D.R., Bunn C. W. and Smith D. J. *J. Poly. Sci.,* 1955, 17, 159-177.

[5] Malta V., Cojazzi G., Fichera A., Ajò D. and Zannetti R. *Eur. Poly. J.*, 1979, 15, 765-770.

Keywords: PDF-analysis, polymers, structure

Applications of PDF Analysis to Organic Molecular Compounds

P. S. Whitfield*, M. Reinle-Schmitt, M. Morin, F. Gozzo
Excelsus Structural Solutions, PARK innovAARE, Villigen 5234, Switzerland
** pamela.whitfield@excels.us*

Total scattering methods have been used for many years to study short-range behaviour in liquids and glasses. The Pair Distribution Function (PDF) methodology gained popularity when nanomaterials became a popular area for study, and continued when local-range effects in inorganic functional materials were recognized as important factors.
The application of the technique to organic molecular systems has traditionally been a more modest area of study but is growing in importance as the use of amorphous materials in pharmaceuticals has grown rapidly. Where structural and quantitative phase analysis using reciprocal space data has become a routine tool for crystalline materials and formulations, PDF may provide some of the same information for nanoscale, amorphous and mixed formulations. The more limited potential information available in a PDF versus a Bragg dataset increases the tendency to over-parameterization and challenges the analyst to become more imaginative with respect to the possible physically and chemically-reasonable restraints and constraints that may be applied.
The study of organic molecular systems via PDF present some additional problems over and above the more familiar systems. The reduced scattering power of the samples means accurate corrections for background, multiple scattering and Compton scattering are increasingly important compared to many semiconductors and oxides for instance. The non-spherical shape of many of the molecules makes r-dependent corrections for factors such as Uiso less useful than for other systems due to the significant overlap in r between intra- and inter-molecular interactions. The approach published by Prill et al [1] offers a work-around to better fit this troublesome region. This presentation will give examples showing the problems that may be encountered, some of the approaches that may be used to overcome them, and where further developments may be required to fully realize the technique's potential.

[1] Prill D., Juhás P., Schmidt M.U., Billinge S.J.L. *Acta Cryst.,* 2016, A72, 62.

Keywords: PDF, molecular systems, pharmaceuticals

The New Pair Distribution Function Beamline, PDF (28-ID-1) at the NSLS-II

Milinda Abeykoon, Eric Dooryhee
National Synchrotron Light Source II, Brookhaven National Laboratory
**aabeykoon@bnl.gov*

The Pair Distribution Function (PDF) has recently emerged as a powerful technique to study local structural fluctuations in complex materials, which are very often responsible for tuning their interesting properties. For this very reason, today there is an increasing demand for instrumentation that are capable of producing high-quality powder diffraction data up to high momentum transfer. The existing total scattering synchrotron beamlines are oversubscribed, and there is a great need for the development of new beamlines. I will present the design and capabilities of the newly built PDF beamline that is currently being commissioned at the NSLS-II. The new beamline is optimized for total scattering measurements over a large Q-range with very low background. The experimental setup of the PDF can provide data for multiple techniques (Ex: PDF, WAXS, SAXS) during the same beamtime opening the door for complex modelling approach. The new beamline also facilitates combining sample environments: for example, temperature and magnetic field. PDF offers rapid data acquisition rates (15-30 frames/s) and high flux required for *in situ* and operando studies of variety of materials in a suite of sample environments. Technical commissioning of the beamline started in April of 2018. Currently, PDF is accepting science-commissioning proposals for the cycle, 2018-3. I will present several sciences cases highlighting the strength of the beamline and discuss its scientific mission.

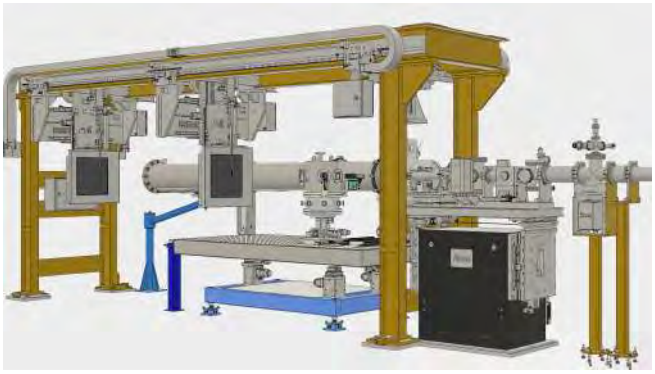

Keywords: PDF, Total Scattering, Complex Materials

Evidence of anatase intergrowths formed during slow cooling of reduced ilmenite

A. M. D'Angelo[a*], N. A. S. Webster[a]
[a] *Minerals Resources, CSIRO, Australia*
** anita.dangelo@csiro.au*

Reduced ilmenite (RI) is the main feedstock for production of TiO_2 pigment that has applications in sunscreen, paints and photocatalysis. RI is typically comprised of metallic Fe and M_3O_5, where M^{2+}= Mg, Mn and/or Fe and M^{3+}=Ti and/or Al, and is produced industrially by reacting ilmenite at high temperatures and under highly reducing conditions in a rotary kiln. The phases that form during the reduction and cooling stage have an effect on the plant process that follows and potentially the final TiO_2 grade. Controlling the parameters during synthetic rutile production is essential to minimise production costs and ensure final product quality. Powder X-ray diffraction (PXRD) is typically used within the industry to guide process control.

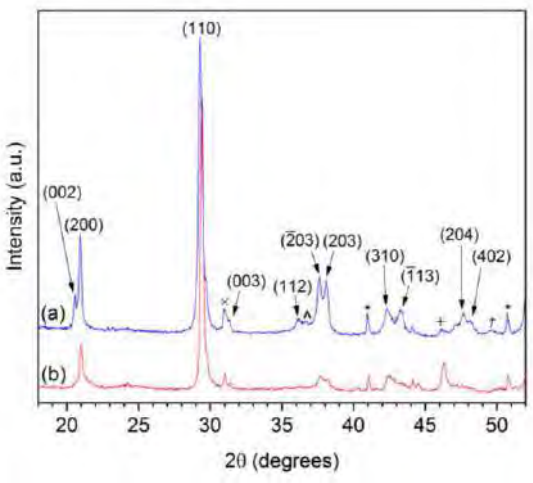

This work investigated the source of unusual features observed in the PXRD pattern of a slow-cooled RI, which were not observed for a rapid-cooled RI [1]. Experimentally in our work, the most noticeability affected are the M_3O_5 peaks of the slow cooled sample at 20.8° (002), 37.9° ($\bar{2}$03) and 38.3° (203), and 47.9° (204) and 48.4° (402) 2θ, when compared to the rapid cooled sample. The diffraction pattern of the rapid-cooled RI is labelled (a) in the Figure, and the slow-cooled RI is labelled (b). The pattern of the rapid cooled sample contained the expected M_3O_5 peaks, however, the (002) peak at 20.6° 2θ was not apparent in the trace collected for the slow cooled sample, and the peaks at 37.9° ($\bar{2}$03) and 38.3° (203), and 47.9° (204) and 48.4° (402) 2θ had significantly decreased in intensity.

A major challenge in differentiating between anatase and M_3O_5 through Bragg scattering is that both structures possess common *d*-spacings of 1.9 and 3.5 Å (for M_3O_5 these correspond to the (020) and (110) planes, respectively, and for anatase the (020) and (011) planes, respectively). Crystallographically, these structures are only able to be differentiated when viewed down their *b*-axis.

Using transmission electron microscopy (TEM), selected area electron diffraction (SAED) and pair distribution function (PDF) analysis, we attribute these features to M_3O_5–anatase intergrowth formation, which causes a loss in long-range order along the M_3O_5 *c*-axis. TEM investigations revealed the existence of regular thin grey bands of an intergrowth phase, and strong diffuse streaking in the SAED patterns supported the presence of disordered intergrowths from the oxidation of M_3O_5. PDF analysis showed a significant improvement in the fit to the data for the slow-cooled RI, primarily in the <17 Å region, when anatase was added to the PDF model. The results presented here highlight the importance of the reduction and cooling stages during the formation of these industrially relevant RI minerals, which may be used to direct the production process and final TiO_2 product quality.

[1] D'Angelo A. M. and Webster N. A. S. *J. Appl. Cryst.*, 2018, 51, 185–192.

Keywords: anosovite; intergrowth; pair distribution function

MS09 - Pharmaceutical and biological materials

MSO9

Abstract Number	Title	Author	Corresponding Affiliation
MS09 - K1	Protein Polycrystallography with GSAS-II	Dr Robert Von Dreele	Advanced Photon Source/Argonne National Labortory
MS09 - K2	Humidity Induced Structural Changes of a Novel Monoclinic HEWLysozyme Form Investigated by In Situ Laboratory X-Ray Powder Diffraction	Dr Detlef Beckers	Malvern Panalytical B.V.
MS09 - OR1	In-situ powder diffraction study of molecular compounds under high energy milling: from amorphization to solid state transformation.	Dr Pierre Bordet	CNRS, Institut Néel, Grenoble
MS09 - OR2	Expression and preliminary Structural Determination of viral proteins via XRPD	Mrs Maria Spiliopoulou	University of Patras, Department of Biology
MS09 - OR3	A New Malaria Pigment Structural Motif and Potential Drug Target	Prof Peter Stephens	Stony Brook University
MS09 - OR4	Identification and characterization of pharmaceutical API using Electron Energy Loss Spectroscopy (EELS) and TEM Electron Diffraction Tomography	Dr Stavros Nicolopoulos	NanoMEGAS SPRL
MS09 - P161	Probing a "CH-pi zipper" with a CH-pi donor/acceptor guest molecule	Mr Giovanni Pierri	University of Salerno
MS09 - P162	Trust your powder data	Mr Lukas Tapmeyer	Goethe University Frankfurt am Main
MS09 - P163	Crystal structures of Large-Volume Commercial Pharmaceuticals	Dr James Kaduk	North Central College
MS09 - P164	Powder Diffraction File™ Coverage of Polymers used in Pharmaceutical and Biomedical Applications	Dr Tom Blanton	International Centre for Diffraction Data
MS09 - P165	Fast PDF screening of amorphous pharmaceuticals in the laboratory	Dr Michael Evans	Bruker AXS GmbH
MS09 - P166	Determination of nanocrystalline organic crystal structures from unindexed powder data by global fit	Prof Martin U. Schmidt	Goethe University Frankfurt am Main
MS09 - P167	Quantitative phase analysis of pharmaceutical materials containing known structure, unknown structure, and high and low crystalline components by using the direct derivation method	Dr Hideo Toraya	Rigaku Corporation
MS09 - P168	Combining experimental and computational techniques for polymorph screening	Dr Dubravka Sisak Jung	DECTRIS
MS09 - P169	An XRD study of Permian fossil bone tissue	Ms Anastasia Ryanskaya	Institute of Geology and Geochemistry, UB of RAS
MS09 - P170	Crystal structure determination of ciprofibrate and preliminary evaluation of its functionalization using Pluronic	Dr Fanny Costa	UFABC
MS09 - P171	pH-triggered release of the anti-tumour drug gefitinib through metal-organic crystal engineering	Dr Liana Vella-Zarb	University of Malta
MS09 - P172	Limit tests by XRPD – ensuring consistency in Drug Substances and Drug Products	Dr Clement Haeck	Department of Physical Sciences, Almac Sciences, Craigavon

Protein Polycrystallography with GSAS-II

Robert Von Dreele[a*]
[a] *Advanced Photon Source, Argonne National Laboratory, Lemont, IL, USA*
** vondreele@anl.gov*

The GSAS-II software package is a fully developed, open source, crystallographic data analysis system written almost entirely in Python. For powder diffraction, it encompasses the entire data analysis process beginning with 2D image integration, peak selection, fitting and indexing, followed by intensity extraction, structure solution and ultimately Rietveld refinement, all driven by an intuitive graphical interface. Significant functionality of GSAS-II also can be scripted to allow it to be integrated into workflows or other software. For protein studies, it includes restraints on bond distances, angles, torsions, chiral volumes and coupled torsions (e.g Ramachandran Φ/Ψ angles) each with graphical displays allowing visual validation. Each amino acid residue (and any ligands) can be represented by flexible rigid bodies with refinable internal torsions and optionally fully described TLS thermal motion. The least-squares algorithm invokes a Levenberg-Marquart minimization of a normalized double precision full matrix via Singular Value Decomposition (SVD) providing fast convergence and high stability even for a large number of parameters. Protein validation via a python implementation of the errat and errat2 routines [1] is also available. GSAS-II interfaces with the coot protein visualization and building package [2] via exported PDB coordinate and omit map files built within GSAS-iI. The protein structure rebuilt via coot can then be imported back into GSAS-II for continued refinement thus closing the protein refine-rebuild loop.

[1] Colovos, C. & Yeates, T. O., *Protein Science* 1993, 2, 1511-1519.

[2] Emsley, P. et al., Acta Cryst. 2010, D66, 486-501.

Keywords: protein, powder diffraction, python

Humidity Induced Structural Changes of a Novel Monoclinic HEWLysozyme Form Investigated by In Situ Laboratory X-Ray Powder Diffraction

D. Beckers[a*], G. Nénert[a], T. Degen[a]
S. Trampari[b]
S. Logotheti[c], A.Valmas[c], S. Saslis[c], F. Karavassili[c], I. Margiolaki[c]
[a]*Malvern Panalytical B.V., Almelo, The Netherlands*
[b]*Kapodistrian University of Athens, Greece*
[c]*University of Patras, Greece*
**detlef.beckers@panalytical.com*

Proteins often crystallize in microcrystalline precipitates. The protein molecules are then surrounded by solvent and their packing arrangement is retained by limited intermolecular contacts. A change in the crystal environment first affects the bulk solvent that fills the intermolecular space, with resulting changes in the crystal structure. In literature it is reported that protein crystals in controlled humidity environments can show a large change in unit-cell parameters when the humidity is decreased [1-2]. When a protein crystal is carefully dehydrated, it is in a metastable state in which the crystal initially still retains the original packing structure [2]. Further dehydration may cause the collapse of the crystal lattice: the crystal no longer maintains its packing structure because of the loss of a large amount of bulk solvent. However in some crystals, the dehydration induces a molecular arrangement change resulting in a new crystal structure.
In this study we investigated the effect of relative humidity (rH) on the crystal structures of hen egg-white lysozyme (HEWL) polycrystalline precipitates via in-situ laboratory X-ray Powder Diffraction (XRPD) measurements. We focused on the effects of rH variation on a novel monoclinic crystal form (space group *P*21) of HEWL which was crystallized at room temperature and pH 4.5. and - to our knowledge - has not been observed before. The structural changes were investigated both during direct and gradual dehydration of the crystals to certain humidity levels in the relative humidity range 55% - 95%.
These observations, on a well-studied molecule such as HEWL, underlie not only the high impact of humidity on biological crystal structures, but show also the significance of in-house XRPD as an analytical tool in industrial drug development and its potential to provide information for enhancing manufacturing of pharmaceuticals.

[1] Kiefersauer, R., et al. (2000). J. Appl. Cryst. 33, 1223–1230.

[2] Dobrianov, I., et al.(1999). J. Cryst. Growth, 196, 511–523.

Keywords: powder diffraction, protein crystallization, humidity variation

In-situ powder diffraction study of molecular compounds under high energy milling: from amorphization to solid state transformation.

P. Bordet[1*], P. Martinetto[1], W. Pagnoux[1,2], J.F. Willart[2], M. Descamps[2], E. Dudognon[2]
[1] *Univ. Grenoble Alpes, CNRS, Grenoble INP, Institut Néel, 38000 Grenoble, France*
[2] *UMET, UMR CNRS 8207, Université de Lille, France*
**pierre.bordet@neel.cnrs.fr*

High energy milling is often used in the pharmaceutical industry to reduce the particle size of drug powders, with the expected effect of enhancing solubility and bioavailability of APIs. This mechanical processing can have drastic effects on the physical state of the powder, and may lead to amorphization or solid state polymorphic transformations of the starting material [1]. Amorphization is generally observed when milling is performed below the glass transition temperature (Tg) of the material. Otherwise, polymorphic transformations may occur. However, little is known about the physical mechanisms responsible for these physical transformations. Here we investigate the behaviour of two pharmaceutical compounds: trehalose and mannitol, which have very different fates when submitted to milling at room temperature (as shown by DSC and laboratory DRX measurement, among others): trehalose becomes progressively amorphous while mannitol undergoes a polymorphic β->α transformation (Figure 1).

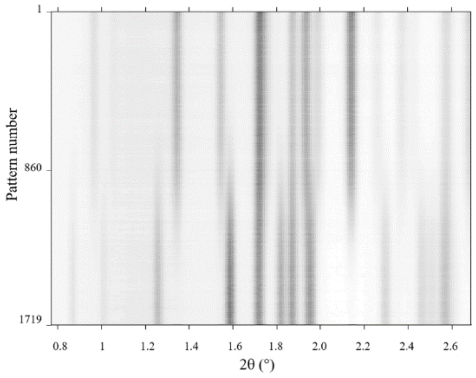

Figure 1: the polymorphic β->α transformation of mannitol as observed by synchrotron powder diffraction during *in situ* milling at the ID15-ESRF beamline. Diffraction patterns are recorded every ~12s. The whole experiment time is ~5.8h

The transformations under mechanical milling of these two compounds were studied *in situ* by synchrotron powder diffraction at the ID15-ESRF beamline using an oscillatory mill of the type described by Friscic et al. [2]. The data consisting of a diffraction image every 12s were integrated and analyzed by sequential Rietveld refinement, allowing to observe the fine details of the evolution of phase fractions and coherent domain sizes. Based on these data, we proposed physical interpretation and numerical simulations to understand the transformation kinetics in both cases.
The amorphization of trehalose can be described as a two-phase process with a crystalline core surrounded by an amorphous shell. The crystalline phase fraction decreases exponentially while its coherent domain size first rapidly decreases to few 100Å and then more slowly.
For mannitol, the transformation begins with an extended incubation phase during which a small fraction of the final phase unexpectedly rapidly appears. This is followed by the transformation itself showing a sigmoidal-shape evolution of the phase fractions. We propose a physical mechanism at the crystallite level to understand this behavior. A constant and relatively large domain size of 500 Å is observed during the whole transformation and no transient amorphous phase can be detected. This surprising behavior can be understood by noticing the topologic relations between the two phases, and close melting temperatures.

[1] J. F. Willart and M. Descamps, Molecular Pharmaceutics 5, 905 (2008)
[2] T. Friščič, W. Jones, V. Štrukil, I. Halasz, Angew. Chemie, 52 (44), 11538-11541. (2013)
[3] P. Bordet, A. Bytchkov, M. Descamps, E. Dudognon, E. Elkaïm, P. Martinetto, W. Pagnoux, A. Poulain, and J. F. Willart, Crystal Growth and Design 16, 4547 (2016)
[4] P. Martinetto, P. Bordet, M. Descamps, E. Dudognon, W. Pagnoux, and J.-F. Willart, Crystal Growth & Design 17, 6111 (2017)

Expression and preliminary Structural Determination of viral proteins via XRPD

M. Spiliopoulou[a*], A. Valmas[a], C. Kosinas[a], M. Balasi[a], S. Vlachos[a], M. Ntouni[a], S. Fili[a], N. Nikolopoulos[a], J. Lichière[b], F. Karavassili[a], E. Rosmaraki[a], A. Fitch[c], D. Beckers[d], T. Degen[d], G. Nenert[d], R. Hilgenfeld[e], N. Papageorgiou[b], B. Canard[b], B. Coutard[b], I. Margiolaki[a]

[a] *Department of Biology, Section of Genetics, Cell Biology and Development, University of Patras, Greece*
[b] *Aix Marseille Université, CNRS, Architecture et Fonction des Macromolécules Biologiques (AFMB), France*
[c] *European Synchrotron Radiation Facility (ESRF), Grenoble, France*
[d] *PANalytical B.V, Almelo, Netherlands*
[e] *Institute of Biochemistry, Center for Structural and Cell Biology in Medicine, University of Lübeck, 23562, Lübeck, Germany*

* mary.spiliopoulou94@gmail.com

Viral infections can result in life-threatening diseases of epidemic magnitudes, thus extensive research is currently on-going towards the development of efficient vaccines and approved antiviral compounds [1]. Proteases are proteolytic enzymes that orchestrate the assembly of viral components during the viral life cycle and proliferation [2]. In this study, the expression, purification, crystallization and preliminary X-ray diffraction analysis are presented of protease 3C, the main protease of an emerging enterovirus, coxsackievirus B3 that is responsible for many cases of viral myocarditis. Additionally, the same series of experiments was conducted on one of the components of the flavivirus replication complex, the non-structural protein 5 (NS5) mRNA methyltransferase (MTase) domain, from an emerging pathogenic flavivirus, Dengue virus 3 (DENV3).
In the case of protease 3C, polycrystalline protein precipitates suitable for X-ray powder diffraction (XRPD) measurements [3, 4] were produced in the presence of 22–28% (w/v) PEG 4000, 0.1 M Tris–HCl, 0.2 M $MgCl_2$ in a pH range from 7.0 to 8.5 [5]. A polymorph of monoclinic symmetry (space group *C*2, unit-cell parameters *a* = 77.9, *b* = 65.7, *c* = 40.6 A ˚, *β* = 115.9˚) was identified via XRPD [5]. Regarding DENV3 MTase, polycrystalline samples suitable for XRPD measurements were also produced in the presence of PEG 8000 (25-32.5% (w/v)), 0.1 M Tris-Amino, in a pH range from 7.0 to 8.0 [1]. A polymorph of orthorhombic symmetry (space group: $P2_12_12$, *a* = 61.9 Å, *b* = 189.6 Å, *c* = 52.4 Å) was successfully identified [1].
These results constitute the first step towards the complete structural determination of the aforementioned virus protein domains via XRPD and demonstrates in parallel the efficiency and the accuracy of the method.

[1] Valmas, A., Fili, S., Nikolopoulos, N., Spiliopoulou, M., Christopoulou, M., Karavassili, F., Kosinas, C., Bastalias, K., Rosmaraki, E., Lichiére, J., Fitch, A., Beckers, D., Degen, T., Papageorgiou, N., Canard, B., Coutard, B., Margiolaki, I. (2017). Dengue virus 3 NS5 methyltransferase domain: expression, purification, crystallization and first structural data from microcrystalline specimens. *Zeitschrift für Kristallographie-Crystalline Materials*.

[2] Lin, J. Y., Chen, T. C., Weng, K. F., Chang, S. C., Chen, L. L., & Shih, S. R. (2009). Viral and host proteins involved in picornavirus life cycle. *Journal of biomedical science*, *16*(1), 1.

[3] Margiolaki, I., & Wright, J. P. (2008). Powder crystallography on macromolecules. *Acta Crystallographica Section A: Foundations of Crystallography*, *64*(1), 169-180.

[4] Karavassili, F., & Margiolaki, I. (2016). Macromolecular Powder Diffraction: Ready for genuine biological problems. *Protein and peptide letters*, *23*(3), 232-241

[5] Fili, S., Valmas, A., Christopoulou, M., Spiliopoulou, M., Nikolopoulos, N., Lichière, J., Logotheti, S., Karavassili, F., Rosmaraki, E., Fitch, A., Wright, J., Beckers, D., Degen, T., Nenert G., Hilgenfeld, R., Papageorgiou, N., Canard, B., Coutard, B., Margiolaki, I. (2016). Coxsackievirus B3 protease 3C: expression, purification, crystallization and preliminary structural insights. *Acta Crystallographica Section F: Structural Biology Communications*, *72*(12), 877-884.

Keywords: 3C protease, non structural protein 5, powder diffraction

A New Malaria Pigment Structural Motif and Potential Drug Target

*Peter W. Stephens** [a], *Liliana Suárez* [b], *Erin L. Dodd* [b], *David Kuter* [b,c], *and D. Scott Bohle* [b]

[a] *Department of Physics and Astronomy, Stony Brook University, USA;*
[b] *Department of Chemistry, McGill University, Montreal H3A 0B8 CANADA;*
[c] *Dept. of Chemistry and Polymer Science, Stellenbosch University, South Africa.*
**pstephens@stonybrook.edu*

It is well established that the structure of both natural and synthetic hemozoin (malaria pigment or hematin anhydride, HA) is a chain of proprionate-linked dimers of iron(III)(protoporphyrin-IX); this is true also of solvated crystals, and of the partially soluble mesoporphyrin analog in which the vinyl groups are hydrogenated. It is widely regarded, that the quinoline family of antimalarials inhibits of the formation of hemozoin, although the mechanism is still unclear. We have recently obtained the structure of another slightly soluble analog, iron(III)(deuteroporphyrin-IX), in which the vinyl groups are replaced by hydrogen atoms. As determined from powder diffraction data, the crystal is monoclinic, with $Z = 4$.

The deuterohematin anhydride (DHA) structure also comprises proprionate-linked dimers, but the intra-dimer geometry and inter-dimer interactions are significantly different than hemozoin. Influencing heme precipitation in the direction of the DHA binding motif in place of hematin anhydride could be a complementary new approach to seeking drug targets based on binding to the facets of the growing hemozoin crystal in the parasite's digestive vacuole.

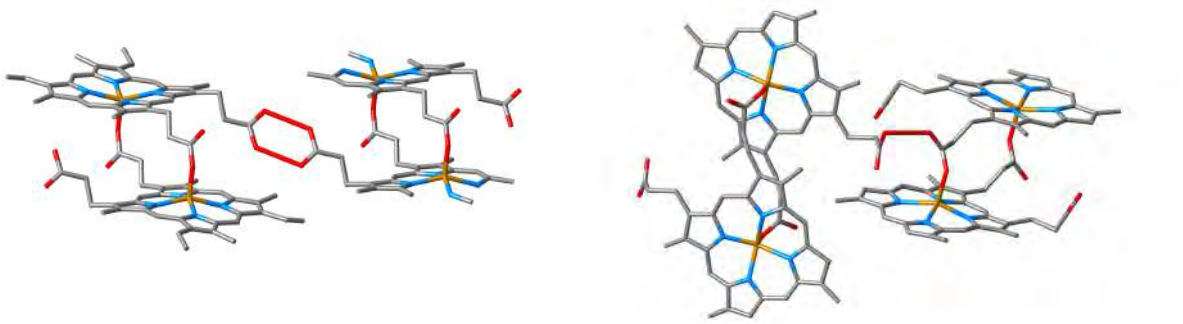

Left: Structure of hematin anhydride. Right: Structure of deuterohematin anhydride

We gratefully acknowledge support from the Burroughs Wellcome Fund, NSERC, FQRNT, CRC, and the South African NRF. Use of the National Synchrotron Light Source, Brookhaven National Laboratory, was supported by the U.S. Department of Energy, Office of Basic Energy Sciences, under Contract No. DE-AC02-98CH10886.

Keywords: malaria, hemazoin, deuteroporphyrin

Identification and characterization of pharmaceutical API using Electron Energy Loss Spectroscopy (EELS) and TEM Electron Diffraction Tomography

S. Nicolopoulos[a*],G. Guzzinati[b], A. Gomez[a], P. Das[a], A.Galanis[a] ,S. Bals [b],
[a] *NanoMEGAS SPRL,Brussels,Belgium*
[b] *EMAT, University of Antwerp, Antwerp,Belgium*
* *info@nanomegas.com*

Pharmaceutical compounds can exist in different polymorph forms which can have different physical properties. In a synthetic preparation more than one polymorph of the desired compound/ impurities can be present in small amount (e.g. less than 1-5%wt), and standard techniques like conventional powder X-ray diffraction or Raman techniques may fail reliably identity and characterize them at nm scale.
TEM microscopy can efficiently characterize nm size crystals. In case of active pharmaceutical ingredients (API) identification of various nm size phases can be possible using EELS in the low loss < 50 eV, where each API may show a different response (for instance plasmon π^* transition) [1]. We have further confirmed this in our study using different organic compounds (hexacarboxycyclohexane, tannin and small peptide γGlu-Cys(Trt)-Gly). The TEM used was a Titan (300 kv) with a monochromated electron source (0.2 eV effective resolution); all studied compounds revealed different unique signature of EELS peaks at low loss/plasmon region (figure on the left shows low loss tannin EELS spectra with plasmon peaks at 4.5, 5.9 and 7.2 ev, figure of the center shows hexacarboxycyclohexane with peak/shoulder at 8 eV).

An alternative way to identify and fully characterize API nanocrystals is the 3D automated (electron) diffraction tomography (ADT). The principle of the method is sampling the reciprocal space in small steps (usually 1 degree tilt) using precession electron diffraction (PED) of 1 degree, which can be used to determine unambiguous determination of unit cell, space group and structure.
In this work, structure solution of small pharmaceuticals compounds (e.g. carbamazepine, nicotinic acid) to complex API having long unit cell parameters (>35 Å) with complex structures, having 2 molecules in the asymmetric unit will be presented [2]. ADT can be used with any TEM microscope with enough tilt range available (±60^{o} is preferred) regardless of the acceleration voltage (120-300kv).To avoid sample beam damage during data collection, is important to apply low dose conditions (i.e. Cumulated dose in the sample ≤ 6 e^{-}. $Å^{-2}$); the use of new generation Direct Electron detectors in combination with Cryo-cooling holders is highly recommendable to avoid structure integrity loss during data collection (figure on right shows 3d electron diffraction dataset of carbamazepine crystal).

The combination of TEM-EELS spectroscopy with ADT can help to finely characterize API at nm scale and help distinguish finely between various phases of organic compounds.

[1] Ricarte R., Lodge T., Hillmyer M. *Langmuir 2016,* 32, 7411
[2] van Genderen, E., Clabbers, M. T. B., Das, P. P., Stewart, A., Nederlof, I., Barentsen, K. C., Portillo, Q., Pannu, N. S., Nicolopoulos, S., Gruene, T. & Abrahams, J. P. Acta Cryst. 2016, A72, 236.

Keywords: EELS, Diffraction Tomography, Pharmaceuticals

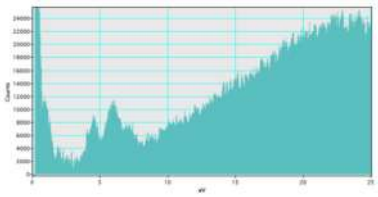
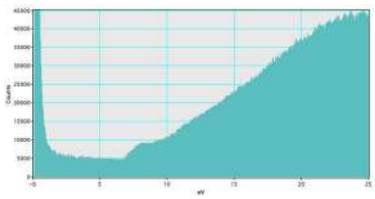
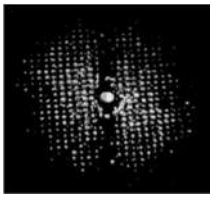

Acknowledgments: The authors acknowledge financial support from the European Commission under the Horizon 2020 Programme by means of the grant agreement No. 731019 EUSMI

Probing a "CH-pi zipper" with a CH-pi donor/acceptor guest molecule

G. Pierri[a*], V. Iuliano[a], E. Macedi[b], C. Dejoie[c], A. N. Fitch[c], I. Izzo[a], F. De Riccardis[a], C. Tedesco[a]
[a]*Department of Chemistry and Biology "A. Zambelli", University of Salerno, Italy*
[b]*Department of Chemistry "Ugo Schiff", University of Florence, Italy*
[c]*European Synchrotron Radiation Facility, 38043 Grenoble, France*

*gpierri@unisa.it

Porous molecular materials gained recently considerable attention as a promising alternative to zeolites, MOF, etc [1]. Our results showed recently that cyclic peptoids revealed the potential to be developed into selective hosts.
Cyclic alpha-peptoids are peptido-mimetic compounds which represent interesting building blocks for the design and synthesis of artificial systems at the frontier between materials science and biology [2]. Peptoids differ from peptides in the side chains, which are shifted by one position along the peptide backbone to the nitrogen atom to give N-substituted oligoglycine. The lack of the amide proton prevents the formation of NH•••OC hydrogen bonds and weaker interactions, as CH•••OC hydrogen bonds and CH-pi interactions, play a key role [3]. The possibility of varying the size of the ring [4] and the type of side chains makes cyclic peptoids extremely interesting as building blocks for engineering porous molecular structures in the solid state [5].
It was widely demonstrated that cyclic peptoids decorated with methoxyethyl and propargyl side chains can form porous structures and perform guest exchange [6].
Here we describe the behaviour of the compound cyclo-(Nme-Npa$_2$)$_2$ (**1**) (Figure 1) during the adsorption of propyne gas by *in-situ* HR X-ray powder diffraction measurements at the ESRF beamline ID22.

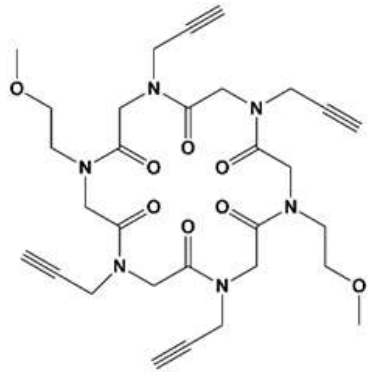

Figure 1. Cyclo-(Nme-Npa$_2$)$_2$ (**1**). Nme = *N*-(methoxyethyl) glycine, Npa = *N*-(propargyl) glycine.

[1] Holden D., Chong S. Y., Chen L., Jelfs K. E., Hasell T., Cooper A. I. *Chem. Sci*., 2016, 7, 4875-4879.

[2] Sun J., Jiang X., Lund R., Downing K. H., Balsara N. P., Zuckermann, R. N. *Pnas*, 2016, 113, 3954-3959.

[3] Tedesco C., Erra L., Izzo I., De Riccardis F. *CrystEngComm*, 2014, 16, 3667-3687.

[4] Tedesco C., Meli A., Macedi E., Iulliano V., Ricciardulli A. G., De Riccardis F., Vaughan G. B. M., Smith V. J., Barbour L. J., Izzo I. *CrystEngComm*, 2016, 18, 8838-8848.

[5] Macedi E., Meli A., De Riccardis F., Rossi P., Smith V. J., Barbour L., Izzo I., Tedesco C. *CrystEngComm*, 2017, 19, 4704-4708.

[6] Meli A., Macedi E., De Riccardis F., Smith V. J., Barbour L. J., Izzo I., Tedesco C. *Angew. Chem. Int. Ed.*, 2016, 55, 4679-4682.

Keywords: peptidomimetic, cyclic peptoids, gas absorption

Trust your powder data

Lukas Tapmeyer[a*], W. Maximilian Hützler[b], Martin U. Schmidt[a]

[a]*Institute of Inorganic and Analytical Chemistry, Goethe University, Frankfurt am Main, Germany*
[b]*Institute of Organic Chemistry and Chemical Biology, Goethe University, Frankfurt am Main, Germany*
** tapmeyer@chemie.uni-frankfurt.de*

The di-sodium salt of an organic sulfonate was recrystallized from glacial acetic acid. The resulting X-ray powder diffraction pattern was of good quality. Indexing was straightforward, and led to a reliable unit cell. Comparison of the cell volume with values from Hofmann's volume increments [1] led to a mono-sodium salt as most plausible match. The calculated cell volume was slightly too large for a mono-sodium salt, but the difference was less than the volume of an additional sodium ion or a solvent molecule (acetic acid).
The structure was solved by real-space methods with DASH [2]. However, all structural models with (relatively) low Chi^2 values exhibited voids, and were therefore regarded as generally incorrect. Trials with a di-sodium salt failed completely. In a benighted consideration, the powder data were discarded as being "unreliable". Several months of laboratory work were invested in various attempts to grow single crystals. Finally, needle-shaped single crystals were obtained by repeated thermal cycling of a suspension of the di-sodium salt in glacial acetic acid.
The structure determined by single-crystal diffraction revealed that the compound is actually a monohydrate of the mono-sodium salt. The single-crystal structure was very similar to the powder structure, which had been disregarded earlier. The additional water molecule simply occupied the previously "scaring" voids. Obviously the "glacial" acetic acid, used for crystallization, contained traces of water or acquired moisture from its environment.
Conclusion: Trust your powder data! If the structure does not meet your expectations, do not distrust the powder data. Reconsidering your perception might save you some time and spare you grief!

[1] D.W.M. Hofmann*, Acta Cryst. B*, 2002, 58.
[2] W. I. F. David *et al.*, *J. Appl. Cryst.,* 2006, 39.

Keywords: structure determination from powder data, organic compounds, singe-crystal structure determination

Crystal Structures of Large-Volume Commercial Pharmaceuticals

J. A. Kaduk[a*], A. M. Wheatley[a], A. M. Gindhart[b], T. N. Blanton[b]
[a] *Department of Physics, North Central College, USA*
[b] *International Centre for Diffraction Data, USA*
** kaduk@polycrystallography.com*

As part of a continuing project, the room-temperature crystal structures of several commercial pharmaceutical APIs have been solved using synchrotron X-ray powder diffraction data (11-BM at APS), and optimized using density functional techniques. All of the structures presented have features which made their solution and refinement non-routine. The molecules to be discussed include: 1. terazosin hydrochloride dihydrate (Hytrin), which was originally solved (but only approximately) using data contained in the Powder Diffraction File database. 2. bretylium tosylate (Bretylol and others), which exhibited significant decomposition in the beam. 3. oxybutynin hydrochloride hemihydrate (Dytropan and Lyrinel XL), which has not been described as a hemihydrate, and which exhibits X-ray induced photoreduction of a triple bond. 4. levocetirizine dihydrochloride (Xyzal), which solves and refines better in $P2_1/n$ rather than the true space group $P2_1$. The presentation may also include progress (or lack thereof) on febuxostat Form G (Uloric and Adenuric), as well as other new structures as they are solved.

Keywords: pharmaceuticals, Rietveld refinement, density functional theory

Powder Diffraction File™ Coverage of Polymers used in Pharmaceutical and Biomedical Applications

T.N. Blanton*, S. Gates-Rector
International Centre for Diffraction Data, Newtown Square, PA, USA
** tblanton@icdd.com*

Polymers show a range of order from amorphous to semi-crystalline. Traditional organic analytical techniques, such as infrared spectroscopy (IR), differential scanning calorimetry (DSC), thermal gravimetric analysis (TGA), and nuclear magnetic resonance (NMR), are typically used for polymer analysis. Though X-ray diffraction (XRD) is not commonly used as the primary technique for polymer characterization, XRD does provide unique information about a polymer particularly when assessing crystallinity and crystallite size. In medical applications, polymers are often used as excipients in pharmaceuticals, and the base material for delivery devices used in biomedical applications.
ICDD has been adding polymer diffraction data to the Powder Diffraction File™ (PDF®) with the focus on adding raw data diffraction patterns (1D and 2D) as part of the PDF entry. The inclusion of the raw data diffraction pattern is important in correctly identifying the polymer contribution to a composite material diffraction pattern. A traditional d-spacing/intensity stick pattern or simulated diffraction pattern is not capable of accounting for the full-pattern diffraction profile of polymers since all polymers have some amorphous component.

Poly(R)-3-hydroxybutyrate

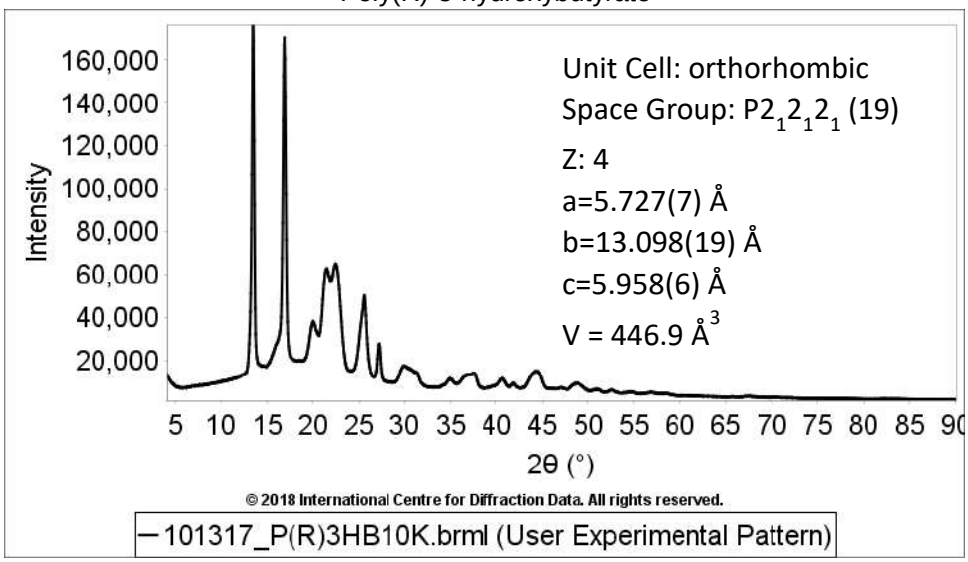

The ICDD polymer project focuses on industrially important polymers with an added emphasis on polymers used in medical and biomedical applications. New entries resulting from this project will be presented along analysis results including an interesting finding for a change in the polymers used in the formulation of opioid based oxycodone pain medication.

Keywords: pharmaceutical excipient, polymer, XRD

Fast PDF screening of amorphous pharmaceuticals in the laboratory

M. Evans[a*], C. Drathen[a]
[a] *Bruker AXS GmbH, Karlsruhe, Germany*
**Michael.Evans@bruker.com*

In an effort to increase the binding specificity to protein-targets active pharmaceutical ingredients (APIs) are becoming more complex and less soluble. One route to increased solubility is via polymorph screening, since different molecular packings may have different dissolution properties. Another approach is to reduce the particle/ crystallite size of the API, possibly even to an amorphous state.
In those cases, the long-range crystal structure breaks down, resulting in broad features in the diffraction pattern that are not easily interpretable and as such do not provide sufficient information for identification. A diffraction pattern of an amorphous compound does, however, contain valuable information in the diffuse scattering. This information can be accessed through the Fourier transform of corrected and normalized diffraction data, which gives the pair distribution function (PDF) suitable for fingerprinting APIs [1].
Experimentally the PDF requires good counting statistics to a high Q-range (Q_{max} > 12.5 Å) [2], which generally necessitates the use of hard radiation (Mo, Ag) and long measurement times on laboratory instruments, making this technique less suitable for screening. To considerably reduce the measurement time, we have used an EIGER2 R 500K 2-dimensional detector in combination with a focusing Goebel mirror on a Bruker D8 ADVANCE diffractometer. PDF data for a series of weakly diffracting crystalline and amorphous pharmaceutical compounds was collected in 1h. Here, we evaluate if these rapidly measured PDF data contain sufficient information for finger-printing using cluster analysis. Further, we demonstrate that the PDF patterns of molecular compounds, including their intra- and intermolecular interactions, were modelled and refined with DIFFRAC.TOPAS [3]. This is a key step for further development in modelling the PDF data of organic materials.

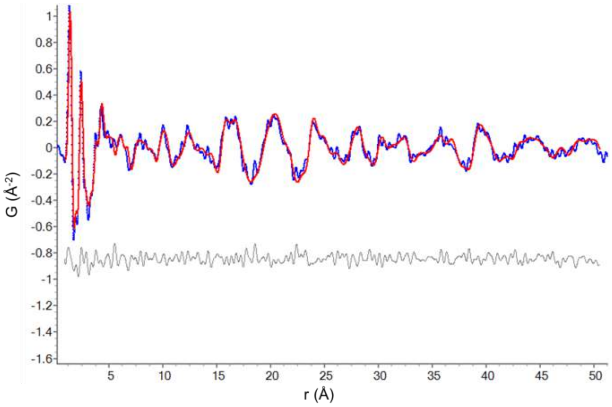

Figure 1 - Experimental G(r) (blue), calculated PDF (red) and difference curve (grey) of ketoprofen (1h dataset) using two different displacement parameters to model inter- and intramolecular interactions.

[1] Billinge, S.J.L., Dykhne, T., Juhás, P., Božin, E., Taylor, R., Florence, A.J. and Shankland, K. *CrystEngComm*, 2010, 12, 1366-1368.

[2] Dykhne, T., Taylor, R., Florence, A. and Billinge, S.J.L. (2011). *Pharm. Res.*, 2011, 28, 1041-1048.

[3] DIFFRAC.TOPAS, Bruker AXS, 1999-2017, Version 6 (Computer Software)

Keywords: pair distribution function (PDF), amorphous, fingerprinting of pharmacueticals

Determination of nanocrystalline organic crystal structures from unindexed powder data by global fit

Martin U. Schmidt[a*], Stefan Habermehl[a]
[a]*Institut für Anorganische und Analytische Chemie, Goethe-Universität, Frankfurt am Main, Germany*
** m.schmidt@chemie.uni-frankfurt.de*

Crystal structures of nanocrystalline organic compounds can be determined from unindexed powder diffraction data by a global fit to the powder data using an algorithm called FIDEL ("Fit with Deviating Lattice parameters) [1]. The molecular geometry is used as input. The optimisation starts from random crystal structures with random lattice parameters in various space groups. For the optimisation, FIDEL uses a similarity index based on cross-correlation functions, which allows a comparison of simulated and experimental powder data even if the lattice parameters do not match [1,2]. The lattice parameters, molecular position and spatial orientation as well as selected intramolecular degrees of freedom are optimised simultaneously in an elaborated multi-step procedure. Subsequently, the promising hits are subjected to an automated Rietveld refinement with TOPAS [3]. Finally, a user-controlled Rietveld refinement with TOPAS is performed.
Examples of organic compounds, including quinacridones (see Figure) and metal complexes are shown.

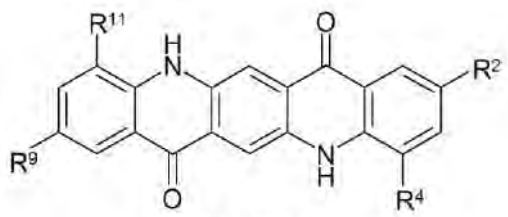

Quinacridone

R = H, F, Cl

[1] Habermehl, S., Mörschel, P., Eisenbrandt, P., Hammer, S.M. and Schmidt, M.U. *Acta Cryst.,* 2014, B70, 347.

[2] Gelder, R., Wehrens, R. and Hageman, J.A. *J. Comput. Chem.,* 2001, 22, 273.

[3] Coelho, A.A. *TOPAS-Academic*, Coelho Software, Brisbane, Australia.

Keywords: Structure determination from powder data, FIDEL, Cross-correlation functions

Quantitative Phase Analysis of Pharmaceutical Materials Containing Known Structure, Unknown Structure, and High and Low Crystalline Components by Using the Direct Derivation (DD) Method

Hideo Toraya*, Yukiko Namatame
Rigaku Corporation, Japan
** toraya@rigaku.co.jp*

Rietveld refinement technique is nowadays widely used for quantitative phase analysis (QPA) of many kinds of materials not only in research and development but also in quality control of natural resources and industrial products. For conducting Rietveld QPA, crystal structure parameters of component materials are required. When structural data are not available, observed diffraction intensities can be used in place of calculated ones by equalizing them in their magnitudes by using standard reference material as in the PONKCS method.

The direct derivation (DD) method for QPA can derive weight fractions of individual crystalline phases in a mixture from sets of observed intensities, measured in a wide 2θ-range, and chemical composition data [1 – 3]. The sum of squared structure amplitudes, calculated for each phase in Rietveld refinement, can be replaced with the sum of squared numbers of electrons belonging to atoms in the chemical formula unit. Therefore, the DD method can conduct QPA of Rietveld equivalent without referencing to structural data. Moreover, observed quantities are total sums of diffracted intensities of component phases, and any form such as the sum of integrated intensities and/or the integrated profile intensities can be used irrespective of profile models used for deriving the total sums. The DD method can quantify mixture samples containing known structure, unknown structure, and high and low crystalline component materials.

One of the applications, to be shown in this report, is QPA of lanthanum carbonate hydrate $La_2(CO_3)_3.xH_2O$ (LCH), which is used as a phosphate binder in the medicines for the treatment of hyperphosphatemia. LCH is known to have several forms with different numbers of water molecules. Some are unknown structure and some of them give degraded powder diffraction patterns, making difficult to apply Rietveld QPA. QPA of some other pharmaceutical samples by the DD method will also be shown.

[1] Toraya, H. (2016). *J. Appl. Cryst*., **49**, 1508 – 1516.
[2] Toraya, H. (2017). *J. Appl. Cryst*., **50**, 820 – 829.
[3] Toraya, H. (2018). *J. Appl. Cryst*., **51**, 446 – 455.

Keywords: the DD method, quantitative phase analysis, pharmaceutical materials, lanthanum carbonate hydrates

Combining experimental and computational techniques for polymorph screening

D. Šišak Jung[a*], I. Halasz[b], D. McDonagh[c], G.M. Day[c]
[a] *DECTRIS, Switzerland*
[b] *Division of Physical Chemistry, Ruđer Bošković Institute, Croatia*
[c] *School of Chemistry, University of Southampton, UK*
* *dubravka.sisak@dectris.com*

Among organic and pharmaceutical molecules, adenine has one of the simplest, small and rigid, molecular structures. However, its crystal structure has been tackled only relatively recently and has yielded two polymorphs, a monoclinic (**I**) [1] and an orthorhombic (**II**) [2] form. This fact may come as surprising, given that adenine is a commercial sample, featuring a simple powder X-ray diffraction (PXRD) pattern. However, PXRD patterns of several batches of commercial samples reveal that adenine usually, if not preferably, crystallizes as a mixture of the two polymorphs. Pure phases (**I**) and (**II**) can be obtained from a solution or by slurrying, while further polymorph screening revealed no additional crystal forms. Both phases were found to be bench-stable at ambient conditions. However, at temperatures above 280 °C phase (**I**) transforms into phase (**II**).

While this seems to have exhausted the polymorphism of this simple molecule, recent *in situ* PXRD measurements carried out with an optimized laboratory diffractometer indicate two new phases (**III** and **X**) at higher temperatures. Phase (**III**) occurs above 300 °C, and is characterised with a single-peak PXRD pattern. This phase is stable upon cooling and its structure features randomly oriented adenine layers [3]. At about 200 °C, several low-intensity peaks indicated a new phase, (**X**). Although these peak positions could be indexed with a triclinic cell of a favourable volume, the data did not allow for cell validation or refinement. To complement the diffraction study, crystal structure prediction was carried out for adenine using quasi-random sampling in a large number of space groups [4, 5]. This has generated a set of structures energetically close to the two known polymorphs. A few of these computer-generated structures could correspond to the phase (**X**) observed in the PXRD patterns. Calculations are ongoing.

[1] Mahapatra, S.; Nayak, S. K.; Prathapa, S. J.; Guru Row, T. N. *Cryst. Growth Des*. 2008, 8, 1223.

[2] Stolar T. et al. *Cryst. Growth Des*. 2016, 16, 3262.

[3] Proffen, T.; Neder, R.B. J. Appl. Cryst. 1997, 30, 171-175.

[4] Case, D. H. et al. J. Chem. Theory Comput. 2016, 12, 910-924.

[5] Price, S. L. et al. *Phys. Chem. Chem. Phys.* 2010**,** 12, 8478-8490.

Keywords: crystal structure prediction, in situ, polymorph screening

An XRD study of Permian fossil bone tissue

A. Ryanskaya[a*], D. Kiseleva[a], O. Shilovsky[b,c], E. Shagalov[a]
[a] *Institute of Geology and Geochemistry, UB of Russian Academy of Sciences, Russia*
[b] *Kazan Federal University, Russia*
[c] *Natural History Museum of Tatarstan, Russia*
**tosenka2008@gmail.com*

The bone tissue of vertebrates is considered to be a composite material formed by inorganic apatite crystallites embedded in an organic matrix. It has a hierarchical structure composed of different structural units at different size scales. It is generally recognised that the microstructure of fossil bones is quite well preserved. The Kotelnich location of vertebrates (river Vyatka, Russia), one of the richest of the Permian period, is characterised by the excellent preservation of fossil remains due to burial in a silty anaerobic environment similar to modern bogs.

The aim was to carry out an XRD study of bone structure and phase composition of *Deltavjatia vjatkensis* pareiasaurus, a Permian parareptile, for the restoration of fossilisation processes.

Two pareiasaurus bone fragments (sample mass 500 mg) were powdered manually in a jasper mortar and analysed by X-ray diffraction (XRD) using Shimadzu XRD-7000 powder X-ray diffractometer with Cu Kα radiation (λ=1.5406 Å). The X-ray generator worked at a power of 40 kV and current of 30.0 mA. XRD patterns were collected during 8 hours with 0.1°/min step across the angular range of 20-70°. The preliminary qualitative phase analysis of the bones was carried by the main reflections using the Powder Diffraction File-2 database (The International Centre for Diffraction Data, ICDD). To perform the quantitative full profile analysis and unit cell lattice parameters determination of the bone, digitised diffractograms were analysed according to the Rietveld method [1] using the SiroQuant software (Sietronics, Australia [2]).

Bone phase composition was defined as calcite (55.1-52.4)%, fluorapatite (44-37.2)%, quartz (0.7-6.2)%, and dolomite (0.2-4.2)%. The refined fluorapatite unit cell parameters of *a* and *b*-axis (9.3526-9.3587) Å and c-axis (6.8930-6.8968) Å correspond to carbonate F-apatite (francolite) [3]. Crystallinity index (CI) was determined as the full width at half maximum (FWHM) of the 002 reflection in degrees 2θ [4] and comprised 0.266-0.250, which was typical for Mesozoic vertebrate bones [4].

Apatite has a hexagonal crystallographic structure with [001] crystallographic direction aligned along the length of the crystals. Based on this structure, the average size of coherently diffracting domains (otherwise referred to as crystallites) can be determined: the length from the 002 reflection, and the width from the 300 reflection.

The FWHMs of 002 and 300 principal reflections corresponding to apatite crystallites were measured after the background subtraction. Considering that the strain broadening is negligible [5], the true crystallite sizes t were determined from the Scherrer equation with the Scherrer's constant K = 2 for the (002) reflection and K = 1 for the (300) reflection [5]:

$t = K\varepsilon = 2\lambda/(FWHM \cdot \cos\theta)$

The error of crystallite sizes was obtained from the error of the FWHM provided by the curve fitting program Peakfit V.4.0.

Francolite apparently is of a diagenetic origin and could grow from groundwater and from dissolution of bone crystallites. After burial, francolite grew on crystallite seeds, filling the space formerly occupied by collagen and dissolved crystallites.

The reported study was carried out at the Geoanalyst Center for Collective Use and funded by RFBR according to the research project № 18-35-00462.

[1] Rietveld H.M. *Acta Crystallographica,* 1967, 22, 151

[2] Taylor J.C. Canberra, Australia: Sietronics Pty Limited, 2004.

[3] Stathopoulou et al. *Palaeogeography, Palaeoclimatology, Palaeoecology,* 2008, 266, 168

[4] Elorza et al. *Cretaceous Research,* 1999, 20, 169

[5] Dumont et al. *Palaeogeography, Palaeoclimatology, Palaeoecology,* 2011, 310, 108

Keywords: fossil bone, Permian, apatite

Crystal structure determination of ciprofibrate and preliminary evaluation of its functionalization using Pluronic

F. N. Costa[a]*, R. dos Santos[a], M. T. Peligrino[a], A. B. Seabra[a], F. F. Ferreira[a]
[a] *Centro de Ciências Naturais e Humanas, Universidade Federal do ABC, Brazil*
* *fannycosta@yahoo.com.br*

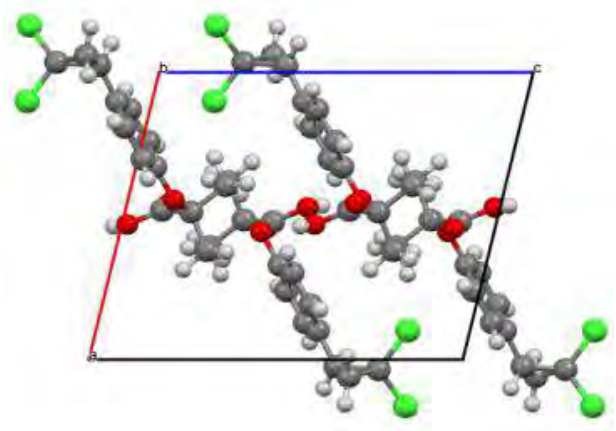

Ciprofibrate (CIP) is a drug used in the treatment of dyslipidemia, a chronic degenerative disease characterized by abnormal levels of lipids in the blood. It is a relevant risk factor for the development of cardiovascular diseases that nowadays are considered as the biggest cause of deaths worldwide [1, 2]. In this work, X-ray powder diffraction data were used to determine the crystal structure of ciprofibrate. The sample was gently hand-ground in an agate mortar and packed between two 0.014-mm thick cellulose-acetate foils in a sample holder that was held spinning during data collection. X-ray powder diffraction data were collected at room temperature on a STADI-P powder diffractometer in transmission geometry by using CuKα_1 (λ= 1.54056 Å) wavelength. CIP crystallizes in a monoclinic crystal system with space group $P2_1/c$ and unit cell parameters a = 10.7576(3) Å, b = 10.2652(2) Å, c = 12.7973(3) Å, β = 102.9356(11)°, V = 1377.33(6) Å^3, Z = 4, Z' = 1. The R-factors indicate a good agreement between the experimental data and the model. R_{exp} = 2.637 %, R_{wp} = 5.746 %, R_{Bragg} = 2.984 % and χ^2 = 2.179 %.

As ciprofibrate is poorly soluble in water, which can lead to poor bioavailability, we investigated the use of micelles prepared with a mixture of two nonionic block copolymer surfactants (Pluronic F127® and Pluronic P123®) as a drug-delivery system. The micelles were prepared using 100 mg of Pluronic mixture (proportion 2:1 – F127:P123) that was dissolved in an organic solvent, resulting in a stock solution. Then, for drug-loaded micelles, different amounts of CIP were dissolved in this solution providing samples in different concentrations (5.0, 2.5, 1.0, 0.5 and 0.1 mgL^{-1}). The characterization of the obtained samples was performed using dynamic light scattering (DLS) to evaluate the hydrodynamic diameter of the micelles as well as the polydispersity index; zeta potential (a physicochemical parameter) measurements revealed the potential stability of nanoparticles. These experiments were performed in triplicate. Nanoparticle tracking analysis (NTA) was carried out to determine the size distribution profile. The preliminary results show a mean size around 31.4 nm for unloaded micelles and ~150 nm for loaded micelles in different concentrations. The resulting zeta potential was negative for all samples, with a polydispersity index of ~0.3.

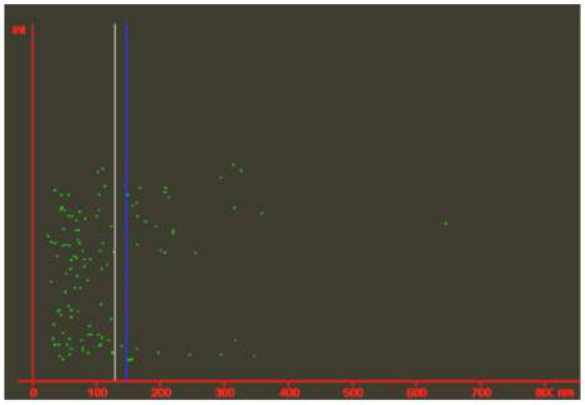

Acknowledgments: We thank the financial support provided by FAPESP (grant nr. 2015/26233-7), CNPq (grants nr. 402289/2013-7, 037664/2015-5) and CAPES (postdoctoral fellowship no. 23038007044201108).

[1] Staels B., Dallongeville J., Auwerx J., Schoonjans K., Leitersdorf E. and Fruchart J. C., *Circulation*, 1998, 98, 2088.

[2] World Health Organization, eds. S. Mendis, P. Puska and B. Norrving, WHO Press, Geneva, Switzerland (2013).

Keywords: ciprofibrate, crystal structure determination, Pluronic micelles

pH-triggered release of the anti-tumour drug gefitinib through metal-organic crystal engineering

L. Vella-Zarb[a*], C. Vella[a]
[a] *Department of Chemistry, University of Malta, Malta*
* *l.vella-zarb@um.edu.mt*

Gefitinib, a potent anti-neoplastic agent, is widely used in patients diagnosed with various advanced cancers.[1] However, as with many other active pharmaceutical ingredients, its bioavailability, and therefore its efficacy, is restricted to a specific narrow pH range. [2]
We present a study involving crystal engineering and complexation of gefitinib with lanthanide coordination compounds, with the aim of synthesizing a more pH labile, tunable, and hence potentially more bioavailable, complex of the drug. All ligands and complexes used are pharmaceutically acceptable and generally regarded as safe for human consumption.
Although structure determination proved to be challenging due to the presence of very heavy atoms together with organic ligands, all crystal structures were successfully solved from laboratory powder X-ray diffraction data.

[1] Tanaka, R., Haramakura, M., Tanaka, A. And Hiragama, N. *Analytical Sciences,* 2004**,** 20, 173.

[2] Prakash, K., Jieun, R.et al. *Asian Journal of Pharmaceutical Sciences*, 2014, 9, 304.

Keywords: crystal engineering, cancer, pharmaceutical

Limit tests by XRPD – ensuring consistency in Drug Substances and Drug Products

Clement M. Haeck[a,*], Ashley McMichael[a], Catherine McClorey[a], Edislav Lekšić[a]
[a] *Department of Physical Sciences, Almac Sciences, Craigavon, Northern Ireland, UK*
* clement.haeck@almacgroup.com

To ensure the quality of pharmaceutical products, manufacturers must characterise and quantify their physical nature throughout all phases of development: from the Drug Substance (DS) to the final Drug Product (DP) and over the product's entire shelf life. Preferably, the substance registered with regulators will be of a single stable polymorph such that there is no possible variation in the drug product's stability, dissolution, and bioavailability. However, at various stages of DS isolation, DP formulation, production, and storage, other physical forms can be induced to form unintentionally. When these different polymorphic forms do not share the same physical properties, their presence can affect the product's safety, quality and efficacy. Manufacturers must, therefore, be aware of such possibilities and have methods for detecting and controlling the degree to which the DS, on its own or in a finished DP, converts to another form.

When it is possible for different polymorphs to be formed, a quantitative test, such as a limit test, should be applied to ensure that the degree of polymorphism falls within specified limits [1]. Since the conversion to other polymorphic forms can happen over time, limit tests must be applied over the product shelf-life. Guidelines from the International Council for Harmonisation specify that manufacturers must have validated and reproducible methods for characterising and controlling polymorphs throughout the approved expiry date of a drug [2, 3].

Almac successfully validated a detection limit method for four polymorphic impurities in a fixed-dose combination tablet containing two drug substances. Each form has a specific limit which has been validated via XRPD using reference standards.

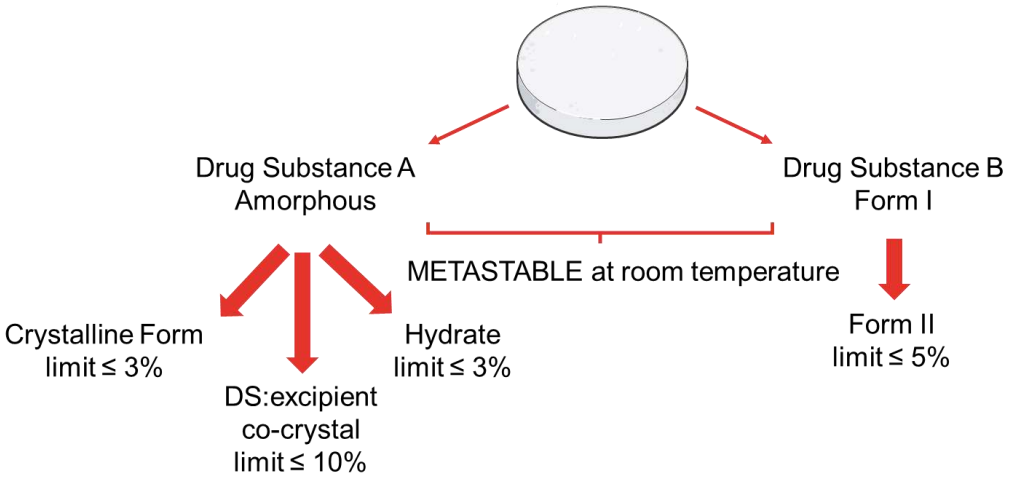

XRPD is a recommended methodology for performing limit tests as it has the advantage of being relatively fast, easy, and inexpensive.

[1] FDA. ANDAs: Pharmaceutical Solid Polymorphism, *Guidance for Industry*, July 2007

[2] ICH Q2 (R1), Validation of Analytical Procedures: Text and Methodology, *ICH Harmonised Tripartite Guideline*, June 1995

[3] ICH Q6A, Specifications: Test Procedures and Acceptance Criteria for New Drug Substances and New Drug Products: Chemical Substances, *ICH Harmonised Tripartite Guideline*, October 2009

Keywords: Pharmaceutical, Limits, Regulations

MS10 - New Sources and Instruments for Powder Diffraction

MS10

Abstract Number	Title	Author	Corresponding Affiliation
MS10 - K1	POWTEX – Angular- and Wavelength-Dispersive, High-Intensity Neutron TOF Diffractometer	Dr Andreas Houben	RWTH Aachen University
MS10 - K2	ESRF ID15 EH3 - A new station dedicated to multi-dimensional operando materials chemistry	Dr Marco Di Michiel	ESRF, FR
MS10 - OR1	Multi-Mythen detector for fast, high-resolution, lab-based pair distribution function characterization of nanostructures	Dr Maxwell Terban	Max
MS10 - OR2	Combining a nine-crystal multianalyser stage with a Pilatus3 X CdTe detector for high-resolution X-ray powder diffraction at ESRF-ID22	Dr Catherine Dejoie	ESRF
MS10 - OR3	DanMAX – The new materials science beamline at MAX IV	Dr Mads Jørgensen	Aarhus University / MAX IV Laboratory
MS10 - P87	A High-Resolution Non-Invasive XRD Technique for Cultural Heritage	Dr Graeme Hansford	University of Leicester
MS10 - P88	Handheld XRD Methods for Applications in Mining and Metals Analysis	Dr Graeme Hansford	University of Leicester
MS10 - P89	High resolution dispersive double bent crystal monochromators Si(111)+Si(311) and Si(111)+Si(400) with a strongly asymmetric diffraction geometry of the analyzer for powder diffractometry	Dr Pavol Mikula	Nuclear Physics Institute ASCR, v.v.i.
MS10 - P90	The novel EIGER2 R 500K for Powder X-ray Diffraction	Dr Stefan Brandstetter	Dectris Ltd.
MS10 - P91	Event Based Powder Integration	Dr Jonathan Wright	ESRF
MS10 - P92	Beamline P02.1: A Workhorse for High-Resolution Powder Diffraction & Total Scattering Experiments at PETRA III, DESY	Michael Wharmby	Deutches Elektronen-Synchrotron DESY
MS10 - P93	New developments at the neutron powder diffraction facility of SAFARI-1	Dr Andrew Venter	Necsa SOC Ltd
MS10 - P94	Is there a future for monochromatic neutron powder diffractometers at large-scale facilities	Prof Paul Henry	STFC/ISIS
MS10 - P95	Developments in Certification of NIST SRMs for Lattice Parameter Dimensions	Dr James Cline	National Institute of Standards and Technology
MS10 - P96	SI Traceable X-ray Wavelength Metrology at NIST	Dr James Cline	National Institute of Standards and Technology

POWTEX – Angular- and Wavelength-Dispersive, High-Intensity Neutron TOF Diffractometer

A. Houben[a*], P. Jacobs[a], W. Schweika[b], Th. Brückel[b], R. Dronskowski[a]
[a] *Chair of Solid-State and Quantum Chemistry, Institute of Inorganic Chemistry, RWTH Aachen University, 52056 Aachen, Germany*
[b] *Jülich Centre for Neutron Science JCNS and Peter Grünberg Institut PGI, JARA-FIT, Forschungszentrum Jülich, 52425 Jülich, Germany*
** andreas.houben@ac.rwth-aachen.de*

POWTEX is a TOF neutron powder diffractometer [1] under construction at MLZ/FRM II. Funded by Germany's Federal Ministry of Education and Research (BMBF), it is built by RWTH Aachen University and FZ Jülich, with contributions for texture analysis and dedicated sample environments from the Geo Science Centre of Göttingen University.

An overview on the instrument specification and the advances made in neutron instrumentation will be presented. Several new concepts were developed including a novel ^{10}B detector and a double-elliptic neutron-guide system sharing focal points at the positions of pulse chopper and sample. The common focal point is an "eye of a needle" in time and space, optimizing time resolution and reducing the source background. The guide features an octagonal cross section with graded super-mirror coating, which results in Gaussian intensity and divergence distributions [2]. The innovative jalousie detector based on solid ^{10}B is specifically being developed for POWTEX [3] achieving high efficiency for a remarkably large coverage of nine steradians with almost no blind spots. The depth-resolved volume-detector will open new opportunities in powder diffraction, e.g., in discriminating background.

For powder diffraction, POWTEX aims for short measurement times and large sample throughput. It will also give access to *in situ* chemical experiments, e.g., to characterize phase transitions as a function of T, p, and B_0. The diffractometer will accommodate large sample environments, e.g., a unique uniaxial deformation apparatus (Göttingen). For texture analysis, *in situ* deformation, annealing, simultaneous stress, etc., the large angular coverage drastically reduces the need for sample tilting/rotation.

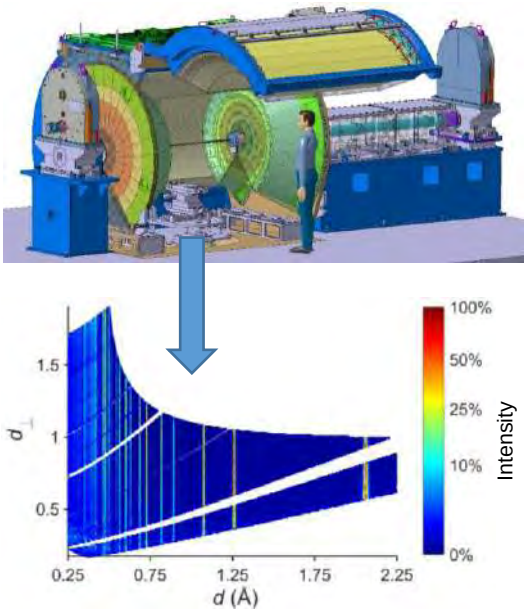

To exploit the POWTEX powder-data, we developed new algorithms for a multi-dimensional Rietveld refinement of angular- and wavelength-dispersive data sets (intensity as function of 2θ *and* λ). More precisely, we determine analytically the multidimensional-resolution function of the instrument [5 and abstract/poster of P. Jacobs], and we refine the parameters based on a diamond reference measurement. The multi-dimensional approach was tested successfully on two data sets (CuNCN, diamond) measured at POWGEN (SNS, Oak Ridge) [4].

[1] Conrad H., Brückel Th., Schäfer W. and Voigt J. *J. Appl. Cryst.*, 2008, 41, 836.

[2] Houben A., Schweika W., Brückel Th. and Dronskowski R. *Nucl. Instr. and Meth. A*, 2012, 680, 124.

[3] Modzel G., Henske M., Houben A., Klein M., Köhli M., Lennert P., Meven M., Schmidt C. J., Schmidt U. and Schweika W. *Nucl. Instr. Meth. A*, 2014, 743, 90.

[4] Jacobs P., Houben A., Schweika W., Tchougréeff A.L. and Dronskowski R. *J. Appl. Cryst.*, 2015, 48, 1627.

[5] Jacobs P., Houben A., Schweika W., Tchougréeff A.L. and Dronskowski R. *J. Appl. Cryst.*, 2017, 50, 866.

Keywords: POWTEX, neutron time-of-flight, multidimensional Rietveld

ESRF ID15 EH3 - A new station dedicated to multi-dimensional *operando* materials chemistry

M. Di Michiel, ESRF, Grenoble, France

In the context of the ESRF Upgrade Phase I, a station has been developed for *operando* multi-dimensional materials chemistry. Novel focusing optics provide very intense sub-micron high energy x-ray beams. Combined with a new CdTe photon counting area detector this allows full three-dimensional characterization by X-ray diffraction of heterogeneous, real working systems with a combination of high spatial, temporal and structural resolution. A wide variety of sample environments and simultaneous ancillary probes (X-ray imaging, IR spectrometry, Mass Spectrometry, X-ray fluorescence) are routinely available for all users. We will discuss studies of several systems of importance to the chemical and energy sectors, such as batteries and catalytic reactors, which have been studied under in situ/operando conditions.

Multi-Mythen detector for fast, high-resolution, lab-based pair distribution function characterization of nanostructures

M. W. Terban[a*], S. Bette[a], R. E. Dinnebier[a]
[a] *Max-Planck-Institute for Solid State Research, Stuttgart, Germany*
* *m.terban@fkf.mpg.de*

Characterization of nanoscale features in materials is critical to understanding synthetic mechanisms and functional properties in novel materials. In recent years, the power of total scattering pair distribution function analysis has been demonstrated for understanding local structure and chemical interactions in complex materials [1,2]. While significant advances in measurement protocol and data reduction have occurred, difficulty still exists in obtaining access to synchrotron or neutron sources for the measurements, or test measurements for optimizing experimental conditions prior to beamtime.
Lab-PDFs can be measured using Mo or Ag anode diffractometers [3], but typically require long scan times between 20 and 40 hours, pushing this method outside the realm of routine laboratory techniques. With the triple-Mythen detector array, scan times for lab-PDF experiments can be reduced down to 1 hour or less for crystalline materials. Hence, test measurements of samples that are candidates for synchrotron measurements or *in situ* studies of slow processes can be performed in the lab. Our work demonstrates that the quality of lab-PDF data is comparable to synchrotron data especially in terms of resolution. In order to demonstrate the viability of these laboratory PDF-measurements, we investigated 3 showcase examples: Nickel standard material, inorganic and organic nanocrystalline powders, and stacking faulted layered materials both by laboratory and synchrotron PDF-analysis and compared the results from both approaches.
In the case of nanocrystalline materials, the Triple-Mythen setup allows for high momentum transfer measurement for high real-space resolution of defects and nanoscale features. The increased *Q*-resolution in comparison to rapid acquisition setups also allows for more detailed analysis of effects due to crystallite size and shape. PDF-analysis was found to be a suitable complementary tool for investigations on the microstructure of stacking faulted layered materials. In Rietveld compatible approaches [4] microstructures are approximated by supercells containing a limited number of layers and therefore a limited number of faultless stacked sections and defects. PDF-analyses from synchrotron data were successfully applied as a complementary tool to confirm the obtained supercells [5,6]. In some cases PDF-analysis was also applied to derive essential information on the layer constitution [6]. Samples of NiCl(OH) and of the honeycomb iridate $H_3LiIr_2O_6$ were reinvestigated by high resolution laboratory XRPD using a device equipped with a Ag-source and a triple Mythen detector array. We show that comparable high-resolution structure interrogation and solution can be achieved in a reasonable time-frame with a routine in-lab setup.

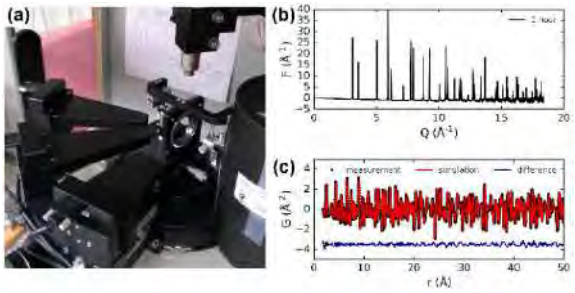

Fig. 1. (a) Triple-MYTHEN detector setup on Ag source diffractometer. **(b)** Structure function of Ni obtained after just 1 hour sufficient for accurate Fourier transformation. **(c)** Good fit to local structure of Ni for only 1 hour of measurement.

[1] Terban M. W., Dabbous R., Debellis A. D., Poselt E. and Billinge S. J. L. *Macromol.*, 2016, 49, 7350.
[2] Terban M. W., Banerjee D., Ghose S., Medasani B., Shukla A., Legg B. A., Zhou Y., Sushko M. L., De Yoreo J. J., Liu J., Thallapally P. K. and Billinge S. J. L. *Nanoscale,* 2018, 10, 4291.
[3] Dykhne T., Taylor R., Florence A. and Billinge S. J. L. *Pharm. Res.*, 2011, 28, 1041.
[4] Bette S., Dinnebier R.E. and Freyer D. *J. Appl. Cryst.* 2015, 48, 1706.
[5] Kudielka A. ,Bette S., Dinnebier R. E., Abeykoon M., Pietzonka C. and Harbrecht B. *J. Mater. Chem., C.* 2017, 5, 2899.
[6] Bette S., Takayama T., Kitagawa K., Takano R., Takagi H. and Dinnebier R.E. *Dalton Trans.,* 2017, 46, 15216.

Keywords: PDF-analysis, laboratory X-ray diffraction, materials characterization

Combining a nine-crystal multianalyser stage with a Pilatus3 X CdTe detector for high-resolution X-ray powder diffraction at ESRF-ID22

C. Dejoie[a*], M. Coduri[a], C. Giacobbe[a], D. Sisak-Jung[b], A. N. Fitch[a]
[a] *European Synchrotron Radiation Facility, Grenoble, France*
[b] *Dectris, Baden, Switzerland*
** catherine.dejoie@esrf.fr*

The high-resolution powder diffraction beamline at ESRF (ID22), built with a dual-undulator source on the 6 GeV storage ring, combines a wide continuous range of incident energy (6-80 keV) with high brightness, offering the possibility to carry out high-flux, high-resolution powder diffraction measurements above 30 keV. In routine operation, a bank of nine scintillation detectors is scanned vertically to measure the diffracted intensity as a function of 2θ, each detector being preceded by a Si 111 analyzer crystal. The current detector system has operated successfully for the past 20 years. Nevertheless developments in detector technology can be exploited to improve the overall performance. In particular, at low diffraction angle, the axial acceptance of the detectors results in broadened and asymmetric peaks owing to the curvature of the Debye-Scherrer cones. At high diffraction angles, detection efficiency could be improved by up to an order of magnitude by increasing the axial acceptance of the detectors as the scattering power of the sample falls off naturally. In order to improve the detection efficiency behind the 9 analyzer crystals, a Pilatus3 X CdTe 300K-W was mounted on the arm of the diffractometer, and used for standard continuous-scanning acquisition on several test samples (Si, LaB6, ceria, ZSM-5 zeolite). By using a small area detector, the axial aperture can be varied with 2θ, narrow at low angles where the curvature is most marked, and wider at higher angles, where the curvature is less. In this way, as well as increasing overall counting efficiency, resolution and peak shapes at low angle are improved as compared to the current fixed, 4-mm-wide receiving aperture. In addition, by carefully selecting the diffraction region on the 2D images, parasitic signals can be avoided. Combining the high efficiency of a hybrid photon-counting area detector with the high resolution given by analyzer crystals is an effective approach to improving the overall performance of high resolution powder diffraction.

Keywords: high-resolution powder diffraction, Pilatus detector

DanMAX – The new materials science beamline at MAX IV

M. R. V. Jørgensen[a,c*], I. Kantor[b,c]
[a] *Department of Chemistry & iNANO, Aarhus University, DK*
[b] *Department of Physics, Technical University of Denmark, DK*
[c] *MAX IV Laboratory, SE*
* *mads@chem.au.dk*

The DanMAX beamline[1] currently under construction at the new 3 GeV MAX IV synchrotron facility[2] is presented. The beamline will be highly versatile and perform both PXRD and full-field imaging experiments in the energy range 15-35 keV. The very brilliant X-ray source and a flexible optics system allows for both three different band pass modes, and focusing of the beam from ~5 µm up to ~ 1 mm.
DanMAX will have two instruments for PXRD; a high resolution instrument and an instrument with an area detector and large sample environments. The high resolution instrument will use a strip detector with large angular coverage. This will enable fast experiment with high resolution. The instrument will have a robotic sample changer and use computer vision to align the samples, thus ensuring the optimal data quality.
The area detector instrument will be built around a hexapod that can accommodate bulky and heavy sample environments. For this setup one or more large area detectors will be used to record the diffraction data. The detector positioning stage will offer large flexibility in both sample to detector distance and in detector tilt to increase the attainable Q range.
A wide range of advanced sample environments will be available at the beamline. Open standards will be available, both mechanical and software, for fast and easy integration of custom-built sample environments at the beamline. To enhance the user experience and the success of experiments at DanMAX, the user software will be tailored to give the users direct feedback, i.e. on-the-fly integration of 2D data and on-the-fly modelling. DanMAX is expected to be available for users in 2020.

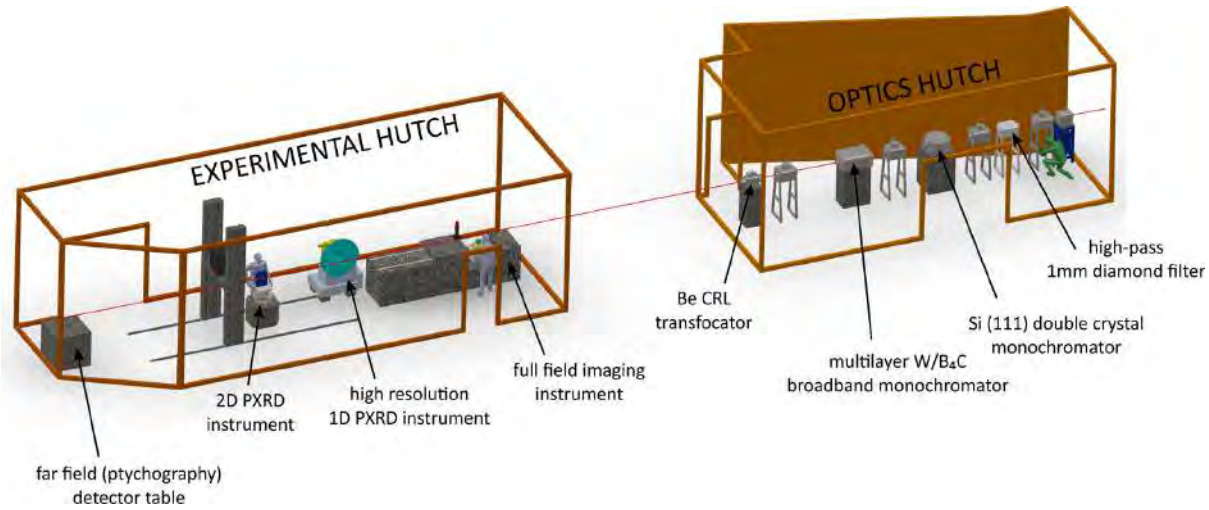

[1] www.maxiv.lu.se/danmax

[2] Tavares, P. F., Leemann, S. C., Sjöström, M. and Anderson, Å. *J. Synchrotron Rad.*, 2014, 21, 862-877.

Keywords: in-situ PXRD, Synchrotron beamline, high-resolution PXRD

A High-Resolution Non-Invasive XRD Technique for Cultural Heritage

G. M. Hansford[a*], S. M. R. Turner[a], P. Degryse[b] and A. J. Shortland[c]
[a] *Space Research Centre, University of Leicester, UK*
[b] *Centre for Archaeological Science, K.U. Leuven, Belgium*
[c] *Centre for Archaeological and Forensic Analysis, Cranfield University, UK*
** gmh14@leicester.ac.uk*

Energy-dispersive X-ray diffraction (EDXRD) implemented in a back-reflection geometry is extremely insensitive to sample morphology and positioning even in a high-resolution configuration [1,2]. This technique allows high-quality XRD analysis of samples that have not been prepared in any way and is therefore completely non-invasive. The experimental technique was implemented on beamline B18 at the Diamond Light Source synchrotron in Oxfordshire, UK. The majority of the experiments in this study were performed with pre-characterised geological materials in order to elucidate the characteristics of this novel technique and to develop the analysis methods. Sample d-spacings were extracted from the data with a typical accuracy of 2 x 10^{-4} Å, enabling phase identification and the derivation of precise unit-cell parameters, yielding insights into the sample material. The data is also of sufficient quality to allow the investigation of microstructural properties such as crystallite size and shape, and microstrain. A particular highlight was the identification of a specific polytype of a muscovite in an unprepared mica schist sample (see figure). The technique was also demonstrated in application to a small number of fossil and archaeological samples; details of these analyses will be given in the presentation.
Back-reflection EDXRD implemented in a high-resolution configuration shows great potential in the crystallographic analysis of cultural heritage artefacts for the purposes of archaeological research such as provenancing, as well as contributing to the formulation of conservation strategies. Future plans will be discussed, including possibilities for moving the technique from the synchrotron into museums. The avoidance of the need to extract samples from high-value and rare objects is a highly significant advantage, applicable also in other potential research areas such as palaeontology, and the study of meteorites and planetary materials brought to Earth by sample-return missions.

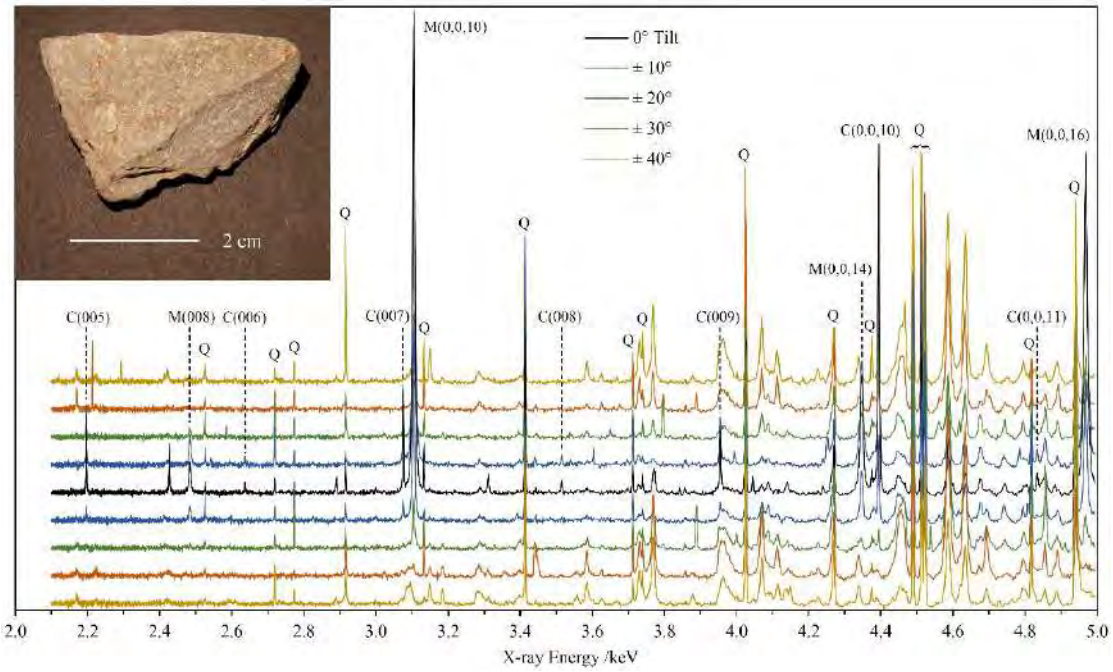

[1] Hansford G. M. *J. Appl. Cryst.*, 2011, 44, 514.

[2] Hansford G. M., Turner S. M. R., Degryse P. and Shortland A. J. *Acta Cryst. A*, 2017, 73, 293.

Keywords: non-destructive analysis, cultural heritage artefacts, energy-dispersive XRD

Handheld XRD Methods for Applications in Mining and Metals Analysis

G. M. Hansford[a*]
[a] *Space Research Centre, University of Leicester, UK*
* *gmh14@leicester.ac.uk*

The application of energy-dispersive X-ray diffraction (EDXRD) in a back-reflection geometry, with 2θ close to 180°, results in a method that is insensitive both to the precise positioning of the sample and its morphology [1-4]. This technique can therefore be used to analyse unprepared samples such as whole rock specimens. The back-reflection EDXRD technique can be applied in a handheld instrument format through a modest adaptation of the geometry of handheld X-ray fluorescence (XRF) devices. This presentation will focus on the results derived from an instrument modified in this way.

As the described technique is inherently a powder XRD method, the sample must conform to the usual powder-averaging criterion in order that the diffraction peak intensities are representative. This criterion is met for almost all metals and for a large proportion of natural geological samples and, in a mining context, powder samples are usually readily available in any case. The spectral resolution of diffraction peaks afforded by a handheld instrument is low relative to standard laboratory diffractometers. Nevertheless, results show that mixtures of iron oxides can be identified and approximately quantified in iron ore samples, for example (see figure). The same instrumentation can be used in the phase and texture analysis of a wide variety of metals and alloys.

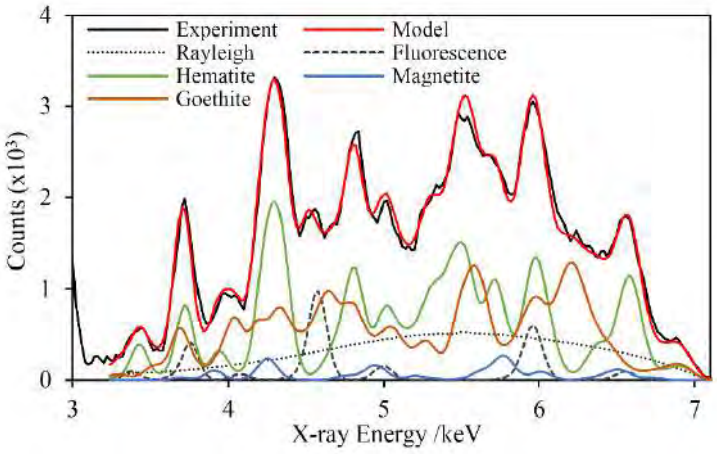

For applications in which the performance is sufficient to answer key questions relating to material properties, the advantages of *in situ*, non-destructive and rapid (~1 min) measurements means that the handheld technique has the potential to become the method of choice, saving considerable time and expense compared to sending samples to a laboratory for analysis.

[1] Hansford G. M. *J. Appl. Cryst.*, 2011, 44, 514.

[2] Hansford, G. M. *Nucl. Instr. and Meth. A*, 2013, 728, 102.

[3] Hansford G. M., Turner S. M. R., Staab D. and Vernon D. *J. Appl. Cryst.*, 2014, 47, 1708.

[4] Hansford G. M., Turner S. M. R., Degryse P. and Shortland A. J. *Acta Cryst. A*, 2017, 73, 293.

Keywords: handheld XRD, non-destructive analysis, energy-dispersive XRD

High resolution dispersive double bent crystal monochromators Si(111)+Si(311) and Si(111)+Si(400) with a strongly asymmetric diffraction geometry of the analyzer for powder diffractometry

P. Mikula[a*], J. Šaroun[a], V. Em[b]
[a] *Nuclear Physics Institute ASCR, v.v.i.25068 Řež, Czech Republic*
[b] *National Research Centre "Kurchatov Institute", Moscow, 123182, Russia*
** mikula@ujf.cas.cz*

In our contribution, some results of high-resolution neutron diffraction properties of the dispersive double-crystal Si(111) + Si(311) and Si(111) + Si(400) monochromators containing two bent perfect crystals but with the second one - analyzer in the strongly asymmetric diffraction geometry, are presented. For the sake of possible applications, both double crystal settings were tested in the orientation of the second crystal for the output beam compression (OBC) as well as the output beam expansion (OBE) of the diffracted beam (see Fig. 1 and Fig. 2). After the preparation of monochromatic beam by the double diffraction process, their resolution properties were tested on a standard α-Fe(211) polycrystalline pin of the diameter of 2 mm situated just 50 cm from the second crystal analyzer. The evaluation of the powder diffraction profiles has shown that the best resolution represented by *FWHM*($\Delta d/d$) has been achieved with the first double-bent-crystal setting providing the values of 1.6×10^{-3} and 2.5×10^{-3} for parallel and antiparallel diffraction geometry, respectively.

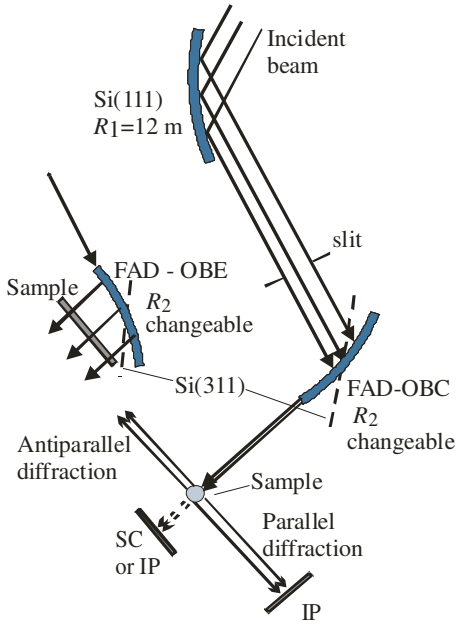

Fig. 1. The DBC setting with the FAD-geometry of the second Si(311) crystal in OBC as well as OBE orientations.

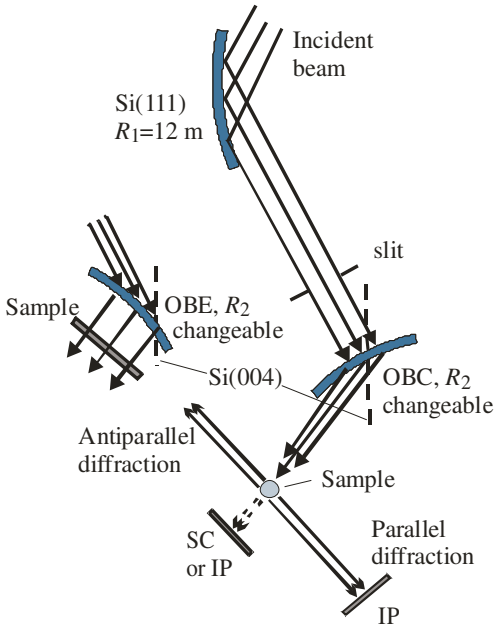

Fig. 2. The DBC setting with the asymmetric geometry of the second Si(004) crystal in OBC as well as OBE orientations.

Keywords: Neutron diffraction, dispersive monochromator, bent perfect crystal

The novel EIGER2 R 500K for Powder X-ray Diffraction

S. Brandstetter[a*], D. Sisak Jung[a], M. Müller[a]
[a] *Dectris Ltd., Täfernhof 1, 5405 Baden-Dättwil, Switzerland*
* *stefan.brandstetetter@dectris.com*

In the past years, Hybrid Photon Counting (HPC) detectors have become state of the art for powder X-ray diffraction. HPC detectors offer a number of unique advantages such as direct detection in a solid state sensor for high quantum efficiency and excellent resolution in addition to high local and global count rates. The recently introduced EIGER2 R 500K detector for laboratory powder diffraction features the established advantages of HPC technology. Furthermore, it provides the unique advantage of combining high pixel density and resolution with large active area. Superior count rate performance allows for accurate measurements of highest intensities. High frame rates enable instrument manufacturers to make sophisticated 0D, 1D, and 2D data acquisition modes available.

The presentation will give an overview of the EIGER2 R 500K's feature set and illustrate its benefits for powder X-ray diffraction.

Keywords: X-ray detectors, powder diffraction, laboratory

Event Based Powder Integration

J. P. Wright[a*], A. Elmaleh[b], B. Baptiste[b], S. C. Tarantino[c], E. Elkaïm[d].

[a] *ESRF, 71 Avenue des Martyrs, Grenoble, 38000 FRANCE*
* wright@esrf.fr
[b]*Sorbonne Université, umr CNRS 7590, IMPMC, Paris, France*
[c]*Università di Pavia, DSTA, Pavia, Italy*
[d]*Synchrotron SOLEIL, L'Orme des Merisiers Saint-Aubin, 91192 Gif-sur-Yvette, France*

How representative is a single crystal structure determination for a material? If we ask how much variation there is between different crystals then we will need to undertake a huge amount of work in measuring the same structure over and over again. Powder methods give an average over many crystallites but they do not tell us what is going on underneath a broad X-ray diffraction peak. Recent developments in X-ray sources and detectors are producing very high data rates and we can acquire thousands, or even millions, of 2D diffraction patterns in a reasonable amount of time. Serial crystallography [1] and diffraction tomography [2] methods are taking advantage of these new possibilities.

In our work in serpentinization in some chondrites [3] we came across a seemingly novel method for making a powder average from a very large number of crystallites. Conventionally researchers process 2D diffraction images by integrating around the rings and summing up the pixel-by-pixel intensity. Instead, we carried out a peak search on the frames and determined centroid positions and intensities for all of the isolated diffraction spots ("events"). We could then form a powder pattern by making histograms of the scattering angles and intensities of these events. The resulting angular resolution for the powder pattern is considerably improved in comparison to the conventional pixel-by-pixel integration. An automatic separation of highly crystalline minerals versus nano-crystalline or amorphous diffraction signals is made possible by comparing the different integration strategies.

[1] Standfuss and Spence IUCrJ (2017) 4, 100. [2] Bleuet et al Nature Materials (2008) 7, 468. [3] Elmaleh *et al*. Goldschmidt 2018.

Keywords: synchrotron, integration, area detectors

Beamline P02.1: A Workhorse for High-Resolution Powder Diffraction & Total Scattering Experiments at PETRA III, DESY

M. T. Wharmby,[a]* M. Etter,[a] J. Bednarcik,[a] J.-C. Tseng,[a]
M. Wendt,[a] S. Wenz,[a] A. Ehnes H.-P. Liermann,[a] O. H. Seeck[a]
[a] *PETRA III, DESY, Hamburg, Germany*
* *michael.wharmby@desy.de*

Powder diffraction is a standard tool for characterisation in a wide range of fields across the physical sciences: from materials science and metallurgy, to chemistry and solid state physics. Third generation synchrotron sources provide high fluxes of X-rays at higher energy than laboratory sources. These characteristics open the door not only to rapid data collection for high spatial-resolution structural studies, but also to time-resolved in situ/in operando measurements of functional materials under real conditions, thanks to high energy X-rays being able to penetrate operating environments. Furthermore, the use of high energy X-rays increases the region of reciprocal space which may be studied in an experiment, facilitating improved spatial resolution in total-scattering measurements.
Beamline P02.1 (PETRA III, DESY, Hamburg, Germany) is almost unique amongst high-resolution powder diffraction instruments in operating at a fixed energy of 60 keV [1],[2]. This energy is particularly well suited to the collection of powder diffraction data for Rietveld refinement (especially for high-Z materials, where absorption is a problem at lower energy) and for collection of total-scattering data (the high energy facilitating Q_{Max} of at least 20 $Å^{-1}$), which may be interpreted by Pair Distribution Function (PDF) analysis. Currently two detectors are available on the beamline (a two-dimensional Perkin Elmer XRD1621 and an in-house developed 10-channel Multi-Analyser Detector), whilst additional devices are available from a shared detector pool (including a Dectris Pilatus3 CdTe 2M designed for high-energy data collection).

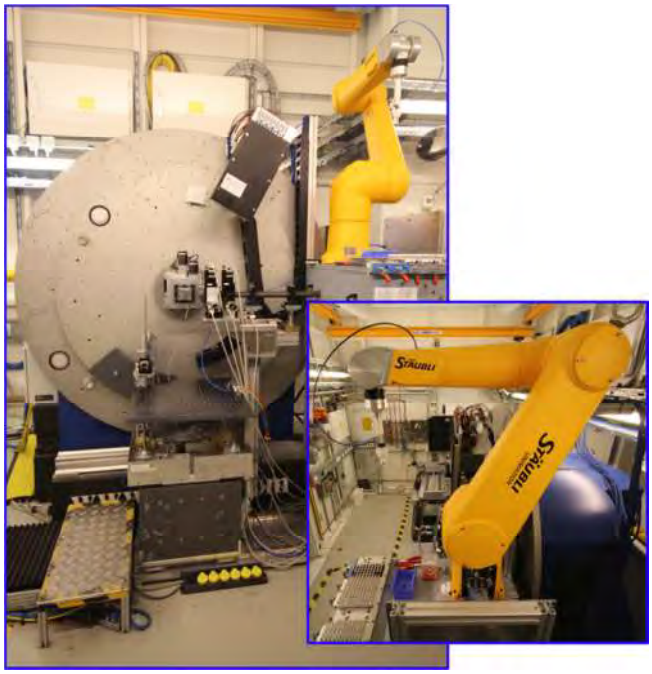

In addition to ambient temperature capillary measurements, P02.1 offers a range of standard sample environments (e.g. hot-air blower – RT-1100 K; cryostream – 90-500 K; cryostat – 10-300 K) whilst a number of others are under development (e.g. low pressure gas adsorption cell) or are maintained by the PETRA III sample environment group. Recently we have also brought a sample changing robot into operation, with capacity for 300 samples (see figure); this device is compatible with the cryostream and hot-air blower environments. Furthermore, the enormous amount of free space around the diffractometer, compared to many other powder diffraction beamlines, allows easy integration of complicated sample environments which are brought to the beamline by our users.
We report here the latest developments at P02.1 including planned changes to detector configurations, new sample environments, updates to the control software and possible remote access schemes.

[1] Dippel A.-C., Bindzus N., Saha D., Delitz J. T., Liermann H.-P., Wahlberg N., Becker J., Bøjesen E. D., Brummerstedt Iversen B., *Z. Anorg. Allg. Chem.* 2014, 640, 3094.

[2] Dippel A.-C., Liermann H.-P., Delitz J. T., Walter P., Schulte-Schrepping H., Seeck O. H., Franz H., *J. Synchrotron Radiat.* 2015, *22*, 675.

Keywords: beamline, sample environments, automation

New developments at the neutron powder diffraction facility of SAFARI-1

A. M. Venter[a*], D. Marais[a], J. C. Raaths[a] and P. R. van Heerden[a]
[a]*Research and Development Division, Necsa SOC Ltd., South Africa*
** andrew.venter@necsa.co.za*

The modernised neutron powder diffraction instrument PITSI [1] at the SAFARI-1 research reactor is available as a multi-purpose instrument rendering medium-resolution performance. Since its commissioning three years ago it has been applied extensively in in-situ chemical and magnetic phase transformation studies.

PITSI is equipped with a pseudo area detector of size 610 x 380 mm^2 comprising15 vertically stacked φ25.4 mm x 609.6 mm Reuter Stokes ^{3}He gas filled position sensitive detector tubes. At a sample-to-detector distance of 1.6 m it subtends a diffraction angle of 21°. The accessible diffraction range of 10° ≤ 2θ ≤ 115° is covered by step-scanning over 6 positions. The instrument is equipped with an extensive suite of in-situ temperature environments covering a wide temperature range that is attainable with the following cryogen-free units:

- 4.2 < T < 300 K: Janis system
- 1.5 < T < 800 K: Ice Oxford cryofurnace
- 400 < T < 1800 K: AS Scientific vacuum furnace

The variable double focused monochromator enables easy selection between the Si (551) and Si (331) reflections to deliver wavelengths of 1.07 and 1.76 Å respectively and access to a large Q-range. Instrument control scripts are programmed within the SINQ Instrument Control Software (SICS) environment with data treatment done with the in-house developed software ScanManipulator. In a recent development the analogue electronics were replaced with commercial Ethernet based units to ensure future upgradability and sustainability.

The need for more rapid data acquisition, especially with in-situ studies of temperature driven phase transformation of minority phases (small sample volume fractions) has been the main driving force to further improve the neutron detection efficiency by extending the detector bank angular coverage. Various configurations and technologies were considered. Biased by the superior neutron detection efficiency of ^{3}He, in conjunction with the resident expertise in the use of Reuter Stokes tubes, the solution being implemented is to have 3 independent banks each comprising 16 tube detectors, offset by 2θ = 18.5° at 1.6 m. This configuration will retain the present high detection efficiency at one setting and will require 2 steps of the assembly to cover a complete 2θ diffraction range. This will increase the instrument performance by a factor greater than 3. Additional flexibility will be built into the design to enable variation of the sample-to-detector distance from 1.6 to 1.2 m to enable larger angular coverage and reduced dead space at the expense of reduced instrumental resolution.

[1] Venter A.M., van Heerden P.R., Marais D., Raaths J.C., Sentsho Z.N., Physica B. In Press. doi: 10.1016/j.physb.2017.12.017

Keywords: neutron powder diffraction, SAFARI-1 research reactor, in-situ studies

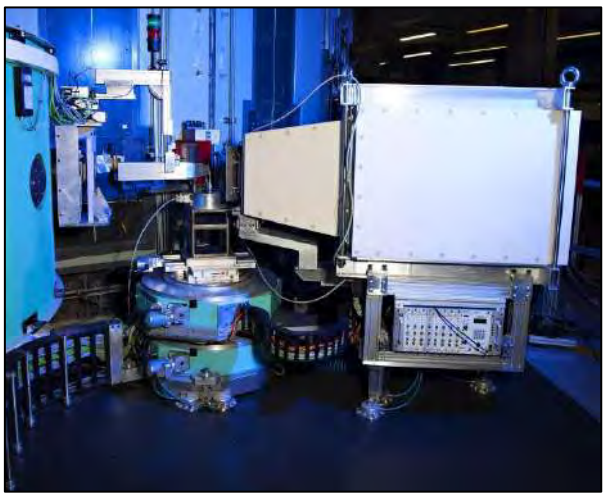

Is there a future for monochromatic neutron powder diffractometers at large-scale facilities?

P.F. Henry[a,b*]
[a] *ISIS Pulsed Neutron and Muon Source, Science and Technology Facilities Council, Rutherford Appleton Laboratory, Harwell Campus, Didcot, OC11 0Q, UK*
[b] *Department of Chemistry and Chemical Engineering, Chalmers University of Technology, Gothenburg, SE-41296, Sweden*
** paul.henry@stfc.ac.uk*

The determination of the real-space structure of materials on the atomic scale uses diffraction techniques. Accurate structure determination is essential in order to understand material properties. Neutron diffraction, although less commonly available due to its reliance on large-scale facilities, is highly complementary with X-ray diffraction. This is a result of the favourable properties of the neutron: high penetration depth, light element sensitivity, isotope dependent scattering, low energy and magnetic interaction.

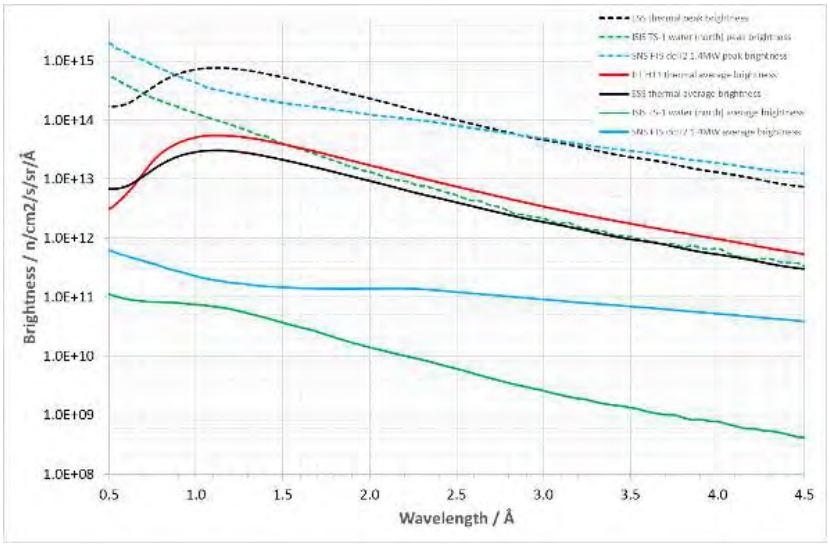

Two types of neutron powder diffractometer (NPD) are known, monochromatic and time-of-flight (TOF) respectively. The former uses a narrow wavelength band, selected by a monochromator, and either scans a set of point detectors over the scattering angle, D2B [1] type, or employ wide-angle area detectors, D20 [2] type. TOF diffractometers use a wavelength band, defined by the total instrument length, available time-window and moderator characteristics (related to the duty cycle of the source and/or chopper frequency), and fixed angle detector banks, e.g. POLARIS [3]. Each instrument type has a defined Q-coverage, resolution and count-rate adapted towards a particular science case.
Reactor neutron sources pioneered the development and use of monochromatic NPDs and spallation neutron sources brought the TOF method to powder diffractometers. The design of NPDs follows the general premise: *continuous sources build monochromatic instruments, except where significantly restricted geometry constraints are present, where TOF methods are preferred or necessary, and pulsed sources build TOF instruments.* With the planned closure of several national reactor-based neutron sources planned before 2020 and the rise of spallation-based sources for current and next generation of large-scale facilities in Europe and beyond, what impact is there on the design of future NPDs? If the reactor-based source has seen its heyday, what will become of the monochromatic NPD? Are there possibilities for next generation NPDs beyond TOF instruments? Are there science cases that remain better addressed with monochromatic NPDs? Here, we address the possibilities. [4]

[1] E. Suard, A.W. Hewat. *Neutron News* 2001, 12, 20-25.

[2] T.C. Hansen, P.F. Henry, H.E. Fischer, J. Torregrossa, P. Convert. *Meas. Sci. Technol.* 2008, 19(3), 034001.

[3] https://www.isis.stfc.ac.uk/Pages/polaris.aspx

[4] P.F. Henry, (submitted to NIMA).

Keywords: instrumentation, neutron, powder diffractometer

Developments in Certification of NIST SRMs for Lattice Parameter Dimensions

James P Cline*, Marcus H Mendenhall,
David R. Black and, Albert Henins
National Institute of Standards and Technology, USA
**james.cline@nist.gov*

The lattice parameters of NIST SRMs certified or re-certified since the year 2000 have been determined using data from the NIST-built Divergent Beam Diffractometer (DBD) [1]. While the machine can be set up in several configurations, the optical layout used for SRM certification conforms to that of a conventional divergent-beam diffractometer of Bragg-Brentano geometry. Data were analyzed with the *Fundamental Parameters Approach* for modeling of profile shape [2] using either the Pawley or Rietveld methods. The analysis of data from a divergent beam diffractometer requires knowledge of both the diffraction angle and the effective source-sample-detector distance(s). Therefore, two additional models must be included in the procedure to account for both the specimen displacement and linear attenuation. The inclusion of these models may place additional uncertainties on the measured lattice parameters relative to those determined from a parallel beam instrument. Assessment of systematic errors is considered with two approaches. The first is the consistency with respect to lattice parameter value obtained from each profile across the full Two-Theta range of the instrument. The second is an assessment of the "error space" depth/steepness from the rise in the residual error terms of a full-pattern fit as the lattice parameter is varied manually from the refined value. Both of these approaches indicate that 20 fm would be a conservative estimate of the potential systematic error in values obtained from the NIST DBD.

We now offer results from the NIST Parallel Beam Diffractometer (PBD) collected from NIST powder SRMs. The machine utilizes a rotating anode X-ray source and a graded parabolic optic to generate the parallel incident beam. Diffracted beam analysis is performed with a high-resolution, 0.07°, parallel slit analyzer before an area detector. Previous work was not inconsistent with the wavelength distribution of the incident beam being distorted from that of the Cu emission spectrum by the focusing optic. Therefore, the PBD was set up as a double crystal diffractometer and the emission spectrum of Cu was rigorously characterized [3]. Preliminary results from the PBD indicate that, with a properly aligned graded parabolic optic, the wavelength distribution of the $K\alpha_1$ line of the incident beam is identical to that of the Cu emission spectrum. Preliminary data from SRMs 640e, 660c and 1976b indicate a systematic discrepancy of approximately 20 fm between lattice parameter values obtained from the DBD relative to those from the PBD; the PBD being the lower of the two. An additional configuration used for this work included the insertion of a four-bounce Bartels monochromator, utilizing two asymmetric Si 220 channel cut crystals, after the parabolic optic. We realized a count rate of 35 cps from SRM 660c with this configuration. Results were in essential agreement with the PBD utilizing the parabolic optic alone.

[1] Cline, *et al.,* J. Res. NIST. 120 (2015)

[2] Cheary, *et al.,* J. Res. NIST. 109 (2004)

[3] Mendenhall, *et al.,* J. Phys. B: At. Mol. Opt. Phys. 50 (2017)

Keywords: lattice parameter, standard reference material, fundamental parameters approach

SI Traceable X-ray Wavelength Metrology at NIST

James P Cline[a]*, Marcus H Mendenhall[a], Csilla I. Szabo[b],
Lawrence Hudson[a], and, Albert Henins[a],
[a] *National Institute of Standards and Technology, USA*
[b] *Theiss Research, USA*
**james.cline@nist.gov*

We have reported on the Parallel Beam Diffractometer (PBD) configured as a double crystal diffractometer used to characterize the emission spectrum of the Cu Kα spectrum [1]. Features include the ability to determine absolute diffraction angles with scans in both the dispersive and non-dispersive configurations without altering the crystal mountings. Secondly the use of the 2D PSD allows for quantification of the degree to which various optical aberrations affect the results. We have recently re-commissioned the 45-year-old Vacuum Double Crystal Spectrometer (VDCS) [2] to include analogous capabilites. This affords us the ability to perform SI traceable measurement of emission spectra over a broad energy range; the VDCS provides results from 1 keV to 12 keV while the PBD can offer data at the higher energies.

We provide complete spectra of the line emission from various targets, rather than just peak positions, since X-ray emission lines are often not simply shaped. We present new data from the PBD on the molybdenum K spectrum, with improved determination of the K-L_3 ($K\alpha_1$) and K-L_2 ($K\alpha_2$) lines, shown in the figure, and K-M_2 and K-M_3 (the two more intense Kβ lines). The Kα lines have uncertainties in their energy scale of deltaE/E = 5×10^{-7}. The Kβ lines, which are much weaker, have uncertainties limited by counting statistics of 5×10^{-6}. We provide data from Cu collected on the VDCS in order to demonstrate full commissioning.

These two wavelength dispersive machines will be used to characterize the brighter X-ray transitions in an SI traceable manner. These will then serve as calibrations for high-resolution energy-dispersive methods that offer a higher sensitivity but are not directly traceable. We actively collaborate with the Quantum Sensors Group at NIST, Boulder, CO, developing large superconducting Transition Edge Sensor (TES) arrays with the goal of updating the NIST X-Ray Transition Energy database (SRD 128). This effort is intended to provide modern SI-traceable emission spectra within the framework of the International X-ray Fundamental Parameters Initiative.

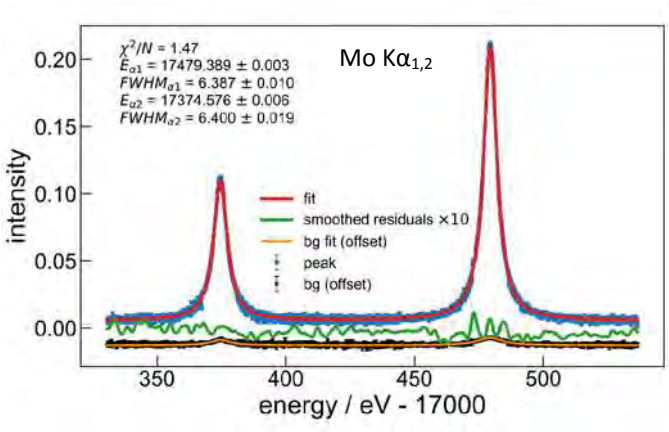

[1] Mendenhall, *et al.,* J. Phys. B: At. Mol. Opt. Phys. 50 (2017)

[2] Deslattes, RevSciInst. 38, 5 , 616-620 (1967)

Keywords: emission spectrum, double crystal spectrometer, X-ray Fundamental Parameters

MS11 - Materials under extreme conditions

MS11

Abstract Number	Title	Author	Corresponding Affiliation
MS11 - K1	Multiparametric studies of magnetocaloric materials in the system Mn5-xFexSi3	Dr Karen Friese	Technische Universitat Munchen, Garching
MS11 - K2	Unraveling the mechanical behaviour of an isoreticular family of Metal Organic Frameworks: UiO-66(M) with M=Zr, Hf, Ce	Dr Pascal G. Yot	Universite de Montpellier
MS11 - OR1	High Pressure Synthesis and Characterisation of MnFe3O5	Mr Ka Hou Hong	University of Edinburgh
MS11 - OR2	XRD and image based modelling to evaluate turbine blade failures	Prof Robert Cernik	Manchester
MS11 - OR3	Synthesis and characterization, by high pressure neutron powder diffraction, of the defect perovskite He2-x[CaZr]F6	Dr Angus Wilkinson	Georgia Institute of Technology
MS11 - P173	Strain induced martensitic Transformation in Austempered Ductile Iron (ADI)	Dr Michael Hofmann	Heinz Maier-Leibnitz Zentrum (MLZ), Technische Universität München
MS11 - P174	Crystalline swelling process of Mg-exchanged montmorillonite: effect of external environmental solicitation	Dr Walid Oueslati	Université de carthage/faculté des sciences de Bizerte/UR 05/13-01 Physique des Matériaux Lamellaires et Nano-Matériaux Hybrides (PMLNMH)
MS11 - P175	Water uptake mechanism in the case of Na-montmorillonite: XRD modeling profile approach	Dr Walid Oueslati	Université de carthage/faculté des sciences de Bizerte/
MS11 - P176	Alkali metal cesium under high pressure: electron core ionization	Dr Valentina Degtyareva	Institute of Solid State Physics, Russian Academy of Sciences
MS11 - P177	High-Pressure X-ray Diffraction and Computational Study of Fe1.087Te	Prof Jens-Erik Jørgensen	Aarhus University
MS11 - P178	Diffraction Based Determination of Single Crystalline Elastic Constants on Polycrystalline Alloys	Mr Alexander Heldmann	Technische Universität München, MLZ
MS11 - P179	Unraveling of the thermal and mechanical behaviour of Hydrazine Borane (NH2-NH2-BH3) using modelling techniques and synchrotron X-ray powder diffraction	Dr Pascal G. Yot	Universite de Montpellier
MS11 - P180	High-pressure synthesis, structure and magnetism of the novel double double perovskite CaMnMnReO6	Mr Padraig Kearins	University of Edinburgh
MS11 - P181	The Crystal Structures of α- and β-Fluorine	Dr Sergei Ivlev	Philipps-Universität Marburg
MS11 - P182	In-situ High Pressure Studies of SrGeO3 Polymorphs	Ms Camilla Kronbo	Dept. of Chemistry, Aarhus University
MS11 - P183	Effect of Thermal Expansion on Diffracted Intensities for Different Instrument Geometries	Dr Mark Styles	CSIRO

Multiparametric studies of magnetocaloric materials in the system $Mn_{5-x}Fe_xSi_3$

K. Friese[a*], A. Eich[b], C. Li[c] ,P. Hering[a], M. Maswada[a] M. Hanfland[d], A. Senyshyn[e], A. Grzechnik[b]
[a] *Jülich Centre for Neutron Science-2, Forschungszentrum Jülich GmbH, Germany*
[b] *Institute for Crystallography, RWTH University Aachen,Germany*
[c] *Jülich Centre for Neutron Science-SNS, Oak Ridge, USA*
[d] *European Synchrotron Radiation Facility, Grenoble, France*
[e] *Heinz Maier-Leibnitz Zentrum, Technische Universität München, Garching, Germany*
** k.friese@fz-juelich.de*

The magnetocaloric effect describes the change of the adiabatic temperature of a material with the application of a magnetic field [1]. This effect forms the basis of magnetic refrigeration technologies that could potentially replace conventional vapor compression cooling. Individual compounds in the system $Mn_{5-x}Fe_xSi_3$ (all of them hexagonal at ambient conditions) undergo a variety of magnetic phase transitions as a function of temperature and composition, which are accompanied by a significant (for some compounds inverse) magnetocaloric effect [2-4]. The magnetic transitions are also clearly reflected in changes of the crystal lattice [4].
We performed synchrotron powder diffraction experiments under a simultaneous variation of temperature and hydrostatic pressure for several compounds in the system $Mn_{5-x}Fe_xSi_3$. These measurements were complemented by temperature dependent neutron powder diffraction and neutron single crystal diffraction experiments both at ambient and high pressure [5], as well as magnetization measurements under high pressure.

The magnetic transitions are clearly reflected in anomalies in the lattice parameter, showing a close connection between the lattice and spin degrees of freedom. A detailed comparison of the influence of temperature, hydrostatic pressure and chemical substitution on the lattice parameter, the distortion of the unit cell, and the interatomic distances will be presented.

[1] Gschneidner K. A Jr. and Pecharsky V. K., Int. J. Refrigeration 2008, 31, 945.
[2] Songlin, et al., J. Alloys Comp. 2002, 334, 249.
[3] Binczycka H., et al., Phys. Stat. Sol. Sect. A,, 1973, 19, 13.
[4] Hering P., et.al., Chem. Mat. 2015, 27, 7128.
[5] Grzechnik A. , M. Meven and K. Friese, J. Appl. Cryst. 2018, 51, 351.

Keywords: hydrostatic pressure, magnetic materials, multiparametric study

Unraveling the mechanical behaviour of an isoreticular family of Metal Organic Frameworks: UiO-66(M) with M=Zr, Hf, Ce

V. Ortiz[a], J. Jacobsen[b], J. Dannewerk[b], I. Collings[c], S. Devautour-Vinot[a], G. Maurin[a], N.Stock[b] and P.G. Yot[a]
[a] *Institut Charles Gerhardt Montpellier, Université de Montpellier, France*
[b] *Institut für Anorganische Chemie, Christian Albrechts Universität zu Kiel, Germany*
[c] *European Synchrotron Radiation Facility, Grenoble, France*
* *pascal.yot@umontpellier.fr*

Metal Organic Framework (MOF) materials have been the focus of intense research activities over the past 20 years, with the emergence of a large variety of crystal structures built from the assembly of inorganic units (clusters, chains) linked by organic moieties. Some of these materials show promising performances for potential applications in diverse fields including storage of strategic gases, separation of fluids, catalysis etc…[1]. A significant effort has been devoted during the last few years to characterize the water stability of these materials, which is considered as one of the major drawbacks that would limit their uses for many applications. Their mechanical stability has received much less attention, although this feature is of utmost importance since the MOFs are required to retain their crystallinity and porosity during both their shaping (pellets and membranes) and the different types of compressions in play in the targeted applications.

Amongst the large number of MOFs reported so far, UiO-66 (Zr) (UiO stands for University of Oslo), have been the subject of a huge number of studies. This cage-like material has been demonstrated to possess good thermal and chemical stabilities that make it very attractive for further applications. We have previously reported that this material is one of the most resilience MOFs with a relatively high bulk modulus and this behavior has been correlated to the strength of the metal-oxygen [3]. Here, a systematic exploration of the effect of the metal present as single component (Zr,Hf,Ce) [3,4,5] and mixture (Zr/Hf) and (Zr/Ce) on the mechanical behavior of this topical MOF architecture is undertaken. High pressure *in-situ* synchrotron X-ray diffraction has been carried out up to 2 GPa using membrane diamond anvil cell at the European Synchrotron Radiation Facility (ESRF, Grenoble, France) in order to evaluate the Bulk modulus from the dependence of the unit cell volumes as a function of the applied pressure using the Birch Murnaghan equation of state.

We evidenced that (i) the crystallinity of all solids is maintained over the whole range of pressure without any phase transition, (ii) a well-pronounced dependence of the mechanical resilience on the nature of the metal and (iii) a modulation of the mechanical property of the architecture by using a mixture of metal center.

[1] G. Maurin, C. Serre, A. Cooper, G. Férey, *Chem. Soc. Rev.* 2017, 46, 3104.
[2] V. Guillerm, S. Gross, C. Serre, T. Devic, M. Bauer, G. Férey,Chem. Commun., 2010, 46, 767
[3] P. G. Yot, K. Yang, F. Ragon, V. Dmitriev, T. Devic, P. Horcajada, C. Serre G. Maurin, *Daton trans.*, 2016, 45, 4283.
[4] M. Lammert, M. T. Wharmby, S. Smolders, B. Bueken, A. Lieb, K. A. Lomachenko, D. De Vos, N. Stock, *Chem. Com.*, 205, 51, 12578.
[5] Z. Hu, A. Nalaparaju, Y. Peng, J. Jiang, D. Zhao, *Inorg. Chem.*, 2016, 55, 1134.

Keywords: Metal Organic Frameworks, Mechanical behaviour, High-pressure X-ray Diffraction

High Pressure Synthesis and Characterisation of $MnFe_3O_5$

K. H. Hong[a]*, Angel M. Arevalo-Lopez[b], Mauro Coduri[c], Graham M. McNally[a] and J. Paul Attfield[a]

[a] *Centre for Science at Extreme Conditions and School of Chemistry, University of Edinburgh, Mayfield Road, Edinburgh EH9 3JZ, UK.*

[b] *Univ. Lille, CNRS, Centrale Lille, ENSCL, Univ. Artois, UMR 8181 - UCCS - Unité de Catalyse et Chimie du Solide, F-59000 Lille, France.*

[c] *European Synchrotron Radiation Facility, 71 avenue des Martyrs, 38000 Grenoble, France.*

* *k.h.hong@sms.ed.ac.uk*

Many novel transition metal oxides are discovered at high pressure and high temperature conditions. Members of the $M^{2+}Fe_{n-1}O_{n+1}$ system are found to exhibit exotic electronic properties due to their complex and often competing ground states, and many of which are recently discovered at pressure. Fe_4O_5 (M = Fe, *n* =3), was reported to be synthesised at about 10 GPa and 1800 K.[1] Structural study shows anisotropic thermal expansion in the lattice parameters observed when cooled below room temperature and an incommensurate charge order is found at T_{CO} = 150 K, below which dimer and trimer like groups of Fe ions are formed.[2] Two magnetic transitions were found, an antiferromagnetic ordering at 320 K and a further spin canting transition at 85 K. The formation of dimers and trimers in Fe_4O_5 is similar what is reported in Fe_3O_4, where a complex charge and orbital ordered arrangement with weak Fe-Fe bonding interactions giving rise to trimerons, linear orbital molecule clusters of three Fe ions.[3,4] We report herein the synthesis of a novel member of the $MFe_{n-1}O_{n+1}$ family - $MnFe_3O_5$ a Mn analogue of Fe_4O_5, that displays a rich variety of magnetically ordered states on cooling. The synthesis was carried out under a pressure of 10 GPa at 1700 K. Rietveld fitting of high resolution synchrotron X-ray diffraction patterns, obtained from ID22 at the ESRF, confirms an orthorhombic structure (space group *Cmcm, a* = 2.920(1), *b* = 9.870(1) and *c* = 12.641(1) Å at 300 K). Variable temperature synchrotron X-ray diffraction shows that the structure undergoes anisotropic thermal expansion below 350 K, but no long range structural distortion is observed.[5] High resolution neutron diffraction experiment, carried out at WISH at the ISIS, shows Fe spins order antiferromagnetically below a Néel transition at 350 K. A second transition at 150 K marks Mn spin order that leads to spin canting of some of the Fe spins and ferrimagnetism. A further transition at 60 K is driven by charge ordering of Fe^{2+} and Fe^{3+} over two inequivalent Fe sites, with further canting of all spins. The magnetic structures of $MnFe_3O_5$ at 5, 75 and 300 K is shown below. Electrical resistivity measurements reveal semiconducting behaviour in $MnFe_3O_5$ with a change in activation energy at 285 K.[6]

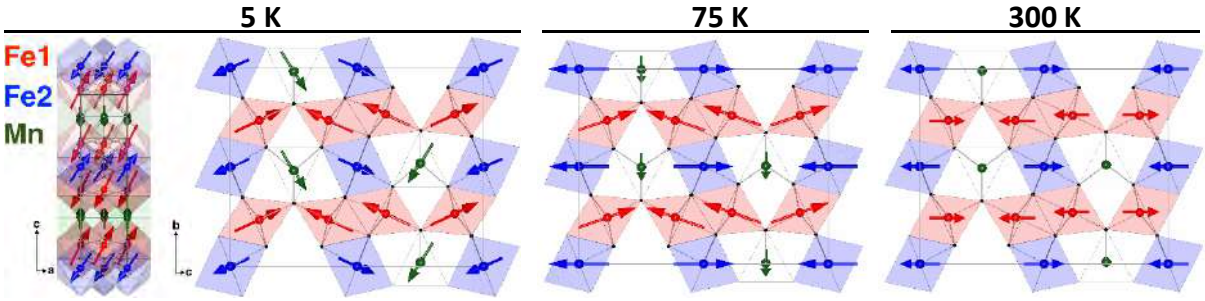

[1] Lavina B., et. al. *Proc. Natl. Acad. Sci. U. S. A.*, 2011, 108, 17281.

[2] Ovsyannikov S. V., et. al. *Nat. Chem.*, 2016, 1.

[3] Verwey E. J. W. *Nature*, 1939, 144, 327.

[4] Senn M. S., Wright J. P. and Attfield J. P. *Nature*, 2011, 481, 173.

[5] Hong K. H., McNally G. M., Coduri M. and Attfield J. P. *Zeitschrift für Anorg. und Allg. Chemie*, 2016, 642, 1355.

[6] Hong, K. H., Arevalo-Lopez, A. M., Coduri, M., McNally, G. M. and Attfield, J. P. *J. Mater. Chem. C*, 2018, 6, 3271.

R J Cernik and Chun Li

School of Materials, University of Manchester, UK

Jet engine turbine blade have to operate in hostile environments sometimes ~2000 °C. In service failures of the thermal barrier coatings (TBCs) used to protect the metal superalloy structures would be catastrophic. For this reason a method to non-destructively test would be highly advantageous. Residual stresses are considered to be the driving forces for the failure of thermal barrier coatings (TBCs). The residual stress distribution through an air plasma sprayed (APS) TBC has been experimentally measured by high energy synchrotron X-ray diffraction (XRD) showing two distinct features. Firstly a discontinuity or 'jump' in the residual stress trend at a depth of approximately 100 μm from the interface. Secondly we observed a much larger stress gradient than that theoretically predicted. To understand these observations the measured residual stress was compared with analytical and finite element models based on the real 2D and 3D microstructure of the coating visualized by scanning electron microscopy (SEM) and high energy X-ray microcomputed tomography (μ-CT). The effect of the pores in the coating and the rumpled interface between the top coat and the bond coat on the residual stress distribution was studied by image based modelling. It was found that the pores did not have an obvious effect on the overall residual stress distribution. The rumpled interface however was primarily responsible for the jump in the trend. This feature was observed to be located at a depth of approximately 120 μm from the surface with an overall magnitude of approximately 200 MPa. The identification of a specific failure inducing feature by X-ray diffraction means a non-destructive test can be developed for the whole fabricated component.

Synthesis and characterization, by high pressure neutron powder diffraction, of the defect perovskite $He_{2-x}[CaZr]F_6$

A.P. Wilkinson,[a] B. R. Hester,[a] A. M. Dos Santos,[b] J. J. Molaison,[b] J. C. Hancock [a]

[a] *School of Chemistry and Biochemistry, Georgia Institute of Technology, USA*

[b] *Neutron Science Directorate, Oak Ridge National Laboratory, USA*

* *angus.wilkinson@chemistry.gatech.edu*

ReO_3-type mixed metal fluorides, ABF_6, have been explored for their potential as low and negative thermal expansion materials (NTE). For example, $CaZrF_6$ displays strong NTE, α_V= -53 $ppmK^{-1}$ at 100 K, and remain cubic over a wide temperature range [1]. Most cubic ReO_3-type materials, including $CaZrF_6$, undergo symmetry lowering phase transitions below 1 GPa, which can be an obstacle to their application. In order to further our understanding of how $CaZrF_6$ behaves as a function of temperature and pressure, a variable temperature and pressure neutron diffraction study was conducted using helium as the pressure medium. Surprisingly, the unit cell volume was seen to increase on compression at room temperature (see figure). This is attributed to the insertion of helium into $CaZrF_6$. The behaviour of the lattice constants as a function of temperature and pressure, combined with Rietveld refinement of helium site occupancies, indicate that He is inserted into the empty "A-sites" of the pseudo-perovskite starting structure. The helium is trapped in the structure when cooled below 190 K at pressure. Gas uptake and release experiments indicate that pressurizing $CaZrF_6$ to ~500 MPa results in ~55% filling of the empty A sites leading to a defect perovskite $He_{2-x}[CaZr]F_6$. Compression in nitrogen leads to different behaviour. The volume of the material decreases steadily leading to a bulk modulus estimate of 36.7 GPa, which is consistent with earlier measurements using a DAC and a silicone oil medium. The inclusion of helium on the A-site of $CaZrF_6$ at ~450 MPa, reduces, but does not completely suppress, the material's NTE. If all of the A-sites in $CaZrF_6$ could be completely filled with hydrogen, rather than helium, the volumetric storage density would be ~0.044 kg H_2/L [2].

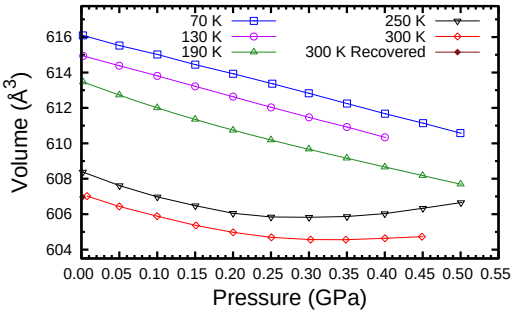

[1] Hancock J.C., Chapman K.W., Halder G.J., Morelock C.R., Kaplan B.S., Gallington L.C., Bongiorno A., Han C., Zhou S., Wilkinson A.P., Chem. Mater. 27 (2015) 3912-3918.

[2] Hester B.R., dos Santos A.M., Molaison J.J., Hancock, J.C., Wilkinson A.P., J. Am. Chem. Soc. 139 (2017) 13284-13287.

Keywords: perovskite, helium, high pressure

Strain induced martensitic Transformation in Austempered Ductile Iron (ADI)

M. Hofmann[a*], X. Li[a], P. Saal[b], W.M. Gan[c], M. Hoelzel[a]
[a] *Heinz Maier-Leibnitz Zentrum (MLZ), Technische Universität München, Germany*
[b] *Institute of metal forming and casting, Technische Universität München,Germany*
** michael.hofmann@frm2.tum.de*

Austempered ductile iron (ADI) is a nodular ductile iron which has undergone a special heat treatment to greatly enhance mechanical properties. The heat treatment process of ADI consists of austenitization, quenching to a temperature typically between 250°C and 450°C and isothermal austempering [1]. After such heat treatment the microstructure consists of acicular ferrite and high carbon enriched retained austenite. The microstructure of ADI strongly depends on the austenitizatin and austempering temperatures. Details on dependence of microstructure and temperature can be found in [1, 2]. In industrial applications alloying elements such as Ni, Mn or Cu are used in order to delay the phase transition kinetics, which improves the austemperability of thicker geometries.

The high carbon enriched retained austenite can transform to martenite during plastic deformation. Four different treatment parameters (austenitization temperature, austempering temperature, austempering time and alloying composition) can influence the retained austenite fraction, grain size and its stabilisation ([3],[4]), which in turn will influence the following martensitic transformation.

The influence of different treatment and composition parameters on the martensitic transformation has been investigated using in-situ neutron diffraction during applying either tension or compression to different plastic strains. In addition texture measurements using neutron diffraction have been performed to calculate the texture distribution of ferrite and austenite phases for different strain levels. Combining the detailed information on texture with the in-situ studies is necessary for quantitative phase analysis and extraction of martensite phase fractions.

The results from these experiments allowed us to develop a model of the martensitic transformation kinetic in ADI due to plastic strains with respect to austempering temperature and alloying element content.

[1] L. Meier, M.Hofmann, P.Saal, W. Volk, H. Hoffmann, Materials Characterization 85 (2013) 124-133

[2] M. A.l Yescas-González, Modelling the microstructure and mechannical properties of austempered ductile iron, Dissertation in department of materials science and metallurgy, University of Cambridge, (2001)

[3] S. Daber, K. S. Ravishankar and P. Prasad Rao, J.Mater.Sci (2008) 43:4929-4937

[4] C. Capdevila, F. G. Caballero and C. García de Andrés; Analysis of the effect of alloying elements on the martensite-start temperature of the steels; Department of Physical Metallurgy, CENIM

Keywords: texture, quantitative phase analysis, martensitic phase transformation

Crystalline swelling process of Mg-exchanged montmorillonite: effect of external environmental solicitation

M. Ammar, W.Oueslati*, A. Ben Haj Amara
UR 05/13-01 Physique des Matériaux Lamellaires et Nano-Matériaux Hybrides (PMLNMH), Faculté des Sciences de Bizerte, 7021 Zarzouna, Tunisia
** walidoueslati@ymail.com*

Smectite play important role in many geological processes, the phenomena of the petroleum migration, greenhouse gas sequestration, and oilfield and in engineering. For last decades montmorillonite (dioctahedral smectite) were widely used as crucial component for elaboration of natural barriers to isolate the hazardous wastes and for the heavy metal cations removal from various effluents of industrial and wastewater treatment. The present work investigate the damage that may affect the structural properties and the hydrous behaviour of an Mg-saturated montmorillonite undergoing a continuous variation of an environmental surroundings condition (i.e RH%). This environmental solicitation was performed by varying “in situ” the RH% in reverse sequence orientation upon two hydration/dehydration cycles. A primeval interpretation about the hydration states of the studied samples are achieved using qualitative XRD analysis. Semi quantitative XRD analysis was deduced through the d_{001} basal spacing values and a description of the 001 reflection profile geometry (profile symmetry and/or asymmetry). In addition, information about the hydration character of the studied samples (homogenous or interstratified) is supplied by the correlation between the calculated parameters including the full width at half maximum intensity (FWHM) for the 001 reflection and ξ parameters [1]. Nevertheless, the qualitative examination cannot provide information about structural transformation at the nanometer scale related to the position and organization of H_2O molecule and the exchangeable cations along the c* axis and distinguish the nature and the relative contributions of different hydration phases at different RH values.The quantitative analysis was based on the XRD profile modeling approach in order to propose theoretical structural models estimating respectively the gradual evolution of the interlamellar space (IS) content versus the hydration sequences, the nature of the different layer types coexisting within crystallites, their proportion and their structural composition at different stage of the both applied cycles. This method consists of adjusting the experimental XRD patterns (00*l* reflexions) to a theoretical ones where the calculated intensity is based on the algorithms developed by [2].The main results obtained through quantitative XRD investigation shows that :(i)The hydration behavior of the studied sample (i.e. SWy-2-Mg) was strongly depending on the sequence orientation of the RH that varied over cycles.(ii)The proposed theoretical models describing the evolution of the structural properties suggests the coexistence of more than one MLS indicating the hydration heterogeneity character for the SWy-2-Mg whatever the RH% sequence orientation. (iii) The montmorillonite's interlamellar water content growth was depending on the nature of the bivalent exchangeable cations. In fact, the presence of Mg^{2+} as well as Ni^{2+} ions in structure leads an irreversible interlayer water content process confirmed by the appearance of a hydration hysteresis. Whereas, the location of cations with largest ionic radius likes Ba^{2+} and Hg^{2+}, in exchangeable sites, was accompanied by more orderliness of systems and decreasing on the water content fluctuation.

[1] Bailey S.W. *American Mineralogist*, 1982, 67, 394.

[2] Drits, V.A . Tchoubar, C.X-ray Diffraction by Disordered Lamellar Structures: Theory and Applications to Microdivided Silicates and Carbons. Springer-Verlag, Berlin, 1990.

Keywords: Clay mineral; Ion exchange process; Environmental solicitation; Quantitative XRD analysis

Water uptake mechanism in the case of Na-montmorillonite: XRD modeling profile approach

W. Oueslati*, A. Ben Haj Amara
UR 05/13-01 Physique des Matériaux Lamellaires et Nano-Matériaux Hybrides (PMLNMH), Faculté des Sciences de Bizerte, 7021 Zarzouna, Tunisia
** walidoueslati@ymail.com*

This study aims at quantifying using XRD modeling approach, the effect of an in situ applied hydrous perturbation on the hydration behavior and the structural changes of Na exchanged montmorillonite. The structural parameters were determined by quantitative XRD analysis using an indirect method based on the comparison of the experimental *00l reflections* with those calculated from structural models [1]. This investigation allowed us to determine respectively the nature, amounts, position and organization of exchangeable cation in the interlamellar space, along the c* axis [2].

The obtained results in the case of SWy-2-Na sample before and after application of the atmospheric stress show:(i) A new hydration behavior of the "stressed" sample described by fluctuations in the hydration hysteresis as a function of the RH rates. (ii) The application of the sorption/desorption process by "in situ" variation of the %RH, before and after applying constraint, made it possible to identify the homogeneous hydration states and the hydration transition zones, which are characterized by a high heterogeneity degree.(iii) Structural heterogeneities are characterized by an elevated MLS number. Indeed, two possible configurations of IS contents, 0W / 1W / 2W and 1W / 2W / 3W with variable relative abundances, are discerned over a wide explored RH range.(iv) Iteration of the insertion / release phenomenon of the water molecules, during drying / wetting cycles, induces an increase in the relative abundance of the 0W and 3W population at the expense of the abundances of the 1W and 2W phases. This result explains the limits observed during sorption/desorption processes in the case of stressed sample.

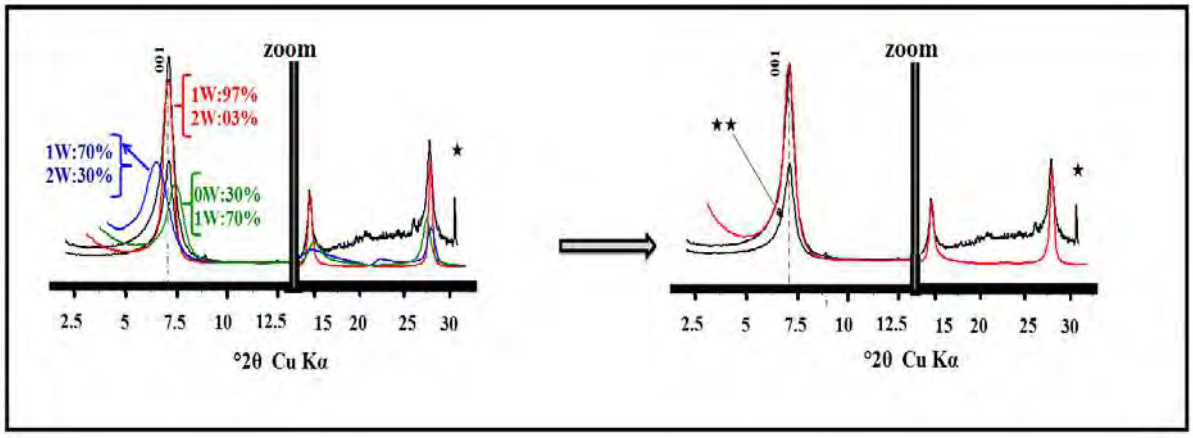

[1] Oueslati, W., Ben Rhaiem, H, Ben Haj Amara, A. *Applied Surface Science ,* 2012**,** 261, 396.

[2] Drits, V.A . Tchoubar, C.X-ray Diffraction by Disordered Lamellar Structures: Theory and Applications to Microdivided Silicates and Carbons. Springer-Verlag, Berlin, 1990.

Keywords: Sorption/Desorption process, hydrous perturbation, Hydration hysteresis.

Alkali metal cesium under high pressure: electron core ionization

V. F. Degtyareva
Institute of Solid State Physics, Russian Academy of Sciences, Chernogolovka, Moscow Region 14232, Russian
degtyar@issp.ac.ru

Elements of groups I and II in the Periodic table have valence electrons of *s*-type and are usually considered to be simple metals. Crystal structures of these elements at ambient pressure are closely-packed and high-symmetry structures of the *bcc* and *fcc* types, defined by electrostatic (Madelung) energy. Diverse structures have been found under high pressure that display a decrease of the coordination number, packing fraction and symmetry [1]. In the case of alkali metal Cs, the following structural sequence has been observed on compression: *bcc* – *fcc* – *oC*84 – *tI*4 – *oC*16 – *dhcp*. The formation of complex structures can be understood within the model of Fermi sphere – Brillouin zone interactions and supported by Hume-Rothery arguments [2]. Within this approach, for each high-pressure phase we consider their diffraction pattern and the $2k_F$ position (k_F is the Fermi sphere radius for a given valence electron number *z*). With the volume decrease there is a gain in band structure energy which is accompanied by a formation of many-faced Brillouin zones. As an example, a diffraction pattern of Cs-V at 12 GPa is shown with indication of $2k_F$ position and the constructed Brillouin zone related to diffraction peaks near $2k_F$.

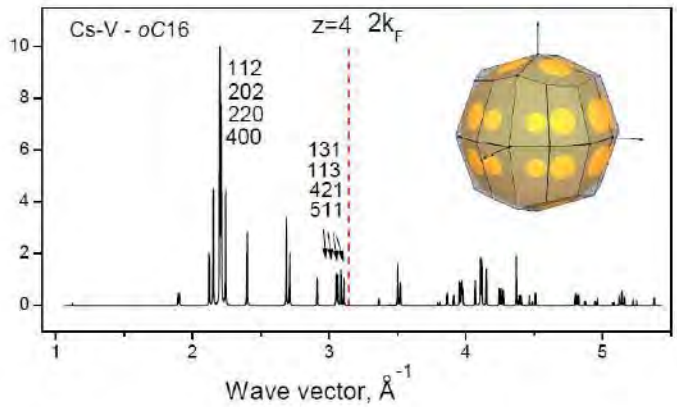

The number of valence electrons for Cs-V is assumed to be z=4. Similar *oC*16 structure has also been observed under pressure for Si and Ge – the four-valence elements [3]. For dense alkali metals K, Rb and Cs with this structure it is necessary to assume a similar valence electron state. Under compression to more than a half of the initial volume the interatomic distances become close to or smaller than the double ionic radius, which should lead to the electron core ionization. At strong compression it is necessary to assume for alkali and alkali-earth metals that there is a valence electron band overlap with the upper core electrons and an increase in the valence electron count.

[1] McMahon M.I. and Nelmes R.J. *Chem. Soc. Rev.,* 2006, 35, 943.

[2] Degtyareva V.F., Smirnova I.S. *Z. Kristallogr.,* 2007, 222, 718.

[3] Degtyareva V.F. *Crystals,* 2013, 3, 419.

Keywords: alkali metals, high pressure, electron core ionization

High-Pressure X-ray Diffraction and Computational Study of $Fe_{1.087}Te$

J.-E. Jørgensen[*], *M Bremholm*
Department of Chemistry, Aarhus University, DK-8000 Aarhus C, Denmark
**jenserik@chem.au.dk*

The $Fe_{1+x}Te$ compounds are isostructural with FeSe which is the simplest of the iron-based superconducting compounds. In contrast to FeSe, $Fe_{1+x}Te$ does not become superconducting at low temperatures but orders antiferromagnetically. Both $Fe_{1+x}Te$ and FeSe are layered materials composed of layers of edge-sharing FeX_4 tetrahedra where X = Te or Se but FeSe is Se deficient while Fe_{1+x} Te is stabilized by excess iron (*x*) located in the van der Waals like gap between the Te layers. The crystal structures of $Fe_{1.087}Te$ have been studied by high-pressure X-ray powder diffraction in the pressure range from 0.0001 to 25 GPa at ambient temperature. $Fe_{1.087}Te$ is tetragonal (space group *P4/nmm*) at ambient conditions and it was found that the tetragonal symmetry was preserved up to the highest measured pressure. Detailed information on the pressure-induced structural changes of the crystal structure was derived from Rietveld refinements of the recorded powder patterns. The volume of the $FeTe_4$ tetrahedra was found to be less compressible than the entire unit cell volume. The structural parameters obtained by high-pressure X-ray powder diffraction were used as input parameters for electronic band-structure calculation at the DFT level performed at selected pressures. For simplicity, the calculations were done for stoichiometric FeTe. Projected crystal orbital Hamilton population (pCOHP) curves and Fermi surfaces (FS) were extracted from the band-structure calculations. The pCOHP curves show that the chemical bonding between Te atoms across the van der Waals like gap is enhanced at elevated pressures while the strength of the Fe-Te bonds in the $FeTe_4$ tetrahedra is essentially unchanged. The FS of FeTe undergoes dramatic topological changes at elevated pressures as it changes from from two- to three-dimensional character at ≈4.3 GPa. The results obtained in the present study will be compared with the results of low-temperature high-pressure neutron diffraction studies of $Fe_{1+x}Te$ for x = 0.087 and 0.141 [1,2].

[1] J.-E. Jørgensen *et al*., *(2015) Eur. Phys. J. B 88 119*
[2] J.-E. Jørgensen *et al*., *(2016) Physica Status Solidi B 253 2257.*

Keywords: high-pressure diffraction, chemical bonding, fermi surface

Diffraction Based Determination of Single Crystalline Elastic Constants on Polycrystalline Alloys

A. E. Heldmann[a*], M. Hoelzel[a], M. Hofmann[a], W. M. Gan[b], W. W. Schmahl[c]
[a] *Forschungs-Neutronenquelle Heinz Maier-Leibnitz (MLZ), TU München, Germany*
[b] *German Engineering Materials Science Centre (GEMS), Helmholtz-Zentrum Geesthacht, Germany*
[c] *Department für Geo- und Umweltwissenschaften,LMU München,Germany*
** alexander.heldmann@frm2.tum.de*

The components of the stiffness tensor **c** or the compliance tensor **s** are directly related to material parameters such as the shear-, Young's- and bulk modulus. Also non-mechanical properties such as the Debye temperature can be calculated using the tensor components [1]. One major field of application is the stress analysis by diffraction, where from measured strains residual stresses are determined with use of the elastic constants.
The techniques for the derivation of the elastic constants are established methods like ultra-sonic techniques using single crystals. However, fabrication of single-crystalline specimen of most engineering-alloys is either difficult or even impossible. In such cases these methods are unable to determine the single-elastic constants properly.
Diffraction techniques allow the direct measurement of strains of all phases of poly-crystalline and multi-phase materials averaged over all possible orientations. Combining this with the knowledge of an external stress in a loading experiment enables a reversal of the classical stress analysis calculation with **c** or **s** as result [2].
For the derivation of the stiffness-constants **c** the exact knowledge of the lattice-plane distances, $\mathrm{d(hkl)}$, with respect to sample orientation is necessary. For this, a rotatable tensile-rig [3] was used to collect diffraction patterns for different orientations and applied stresses. From the lattice spacings the elastic strain tensor $\boldsymbol{\varepsilon}$ can be obtained. With the known stress tensor $\boldsymbol{\sigma}$ a system of equations for the elastic constants can be derived.

$$\begin{aligned}\varepsilon(\varphi,\psi,hkl) = {} & S_1(hkl)[\sigma_{11}+\sigma_{22}+\sigma_{33}] \\ & + \frac{1}{2}S_2(hkl)[\sigma_{11}\cos^2(\varphi)\sin^2(\psi)+\sigma_{22}\sin^2(\varphi)\sin^2(\psi)+\sigma_{33}\cos^2(\psi)] \\ & + \frac{1}{2}S_2(hkl)[\sigma_{12}\sin(2\varphi)\sin^2(\psi)+\sigma_{13}\cos(\varphi)\sin(2\psi)+\sigma_{23}\sin(\varphi)\sin(2\psi)].\end{aligned} \quad (1)$$

Here $S_1(\mathrm{hkl})$ and $S_2(\mathrm{hkl})$ are the diffraction elastic constants (DEC) and φ and ψ are the orientation angles of the specimen in sample system with respect to the measurement system [4]. There have been several approaches to calculate the single-crystal elastic constants by diffraction methods on polycrystals.

$$S_1(hkl) = s_{12} + s_0\Gamma, \text{and } \tfrac{1}{2}S_2(\mathrm{hkl}) = s_{11} - s_{12} - 3s_0\Gamma, \text{with } s_0 = s_{11} - s_{12} - 0.5s_{44}. \quad (2)$$

We have extended these approaches to lower symmetries and modified them by taking into account the texture. Validation of our technique was done on different types of steels S 235 JR (BCC), V2A (FCC) and duplex steel (BCC and FCC) for cubic symmetries on different models.
This technique was finally applied to hexagonal symmetry on different Ti-alloys, such as α-Ti (hexagonal), β-Ti (cubic) and α,β-Ti (two-phased, hexagonal and cubic).

[1] H. M. Ledbetter, N. V. Frederick and M. W. Austin. J. Appl. Phys. *51(1):*305-309, **1980**

[2] Gnäupel-Herold, T. , Brandt, P. C., Prask, H. J: J. Appl. Cryst. **1998**, 31, 929-935

[3] Hoelzel, M. , Gan, W. M., Hofmann, M., Randau, C., Seidl, G., Jüttner, Ph., Schmahl, W.W.: Nucl. Instr. **2013**, A711, 101-105

[4] H. Behnken: RWTH, Habil.-Schr. RWTH Aachen. **2002**. Berichte aus der Werkstofftechnik. Shaker, Aachen 2003. ISBN 3-8322-1384-8

Keywords: Elastic constants, Elasticity, Load experiments

Unraveling of the thermal and mechanical behaviour of Hydrazine Borane (NH_2-NH_2-BH_3) using modelling techniques and synchrotron X-ray powder diffraction

Salem Ould Amara,[a] Vibhav Yadav,[b] Guillaume Maurin,[b] Umit B. Demirci,[a] Pascal G. Yot,[b]
[a] *Institut Européen des Membranes, Université de Montpellier, France*
[b] *Institut Charles gerhardt Montpellier, Université de Montpellier, France*
** pascal.yot@umontpellier.fr*

Crystalline B–N–H compounds of low molecular weight have been intensively investigated over the past two decades owing to their promises for chemical hydrogen storage. [1-4] Boranes of low molecular weight are crystalline materials that have been much investigated over the past decade in the field of chemical hydrogen storage [5]. In the same time only few studies have been dedicated to their behaviour upon thermal stimuli [6]. Hydrazine borane NH_2-NH_2-BH_3 is one of the most recent examples of this family of materials [7]. In the present work, we explored its structural behaviour under (i) thermal stimulus over a wide range of temperature (80-300 K) upon heating and (ii) mechanical stimulus upon 2GPa by Synchrotron high pressure X-ray diffraction [8-9].

The thermo diffraction investigations shown that HB has an orthorhombic structure (S.G. *Pbcn*) over the whole temperature range and exhibits a unit cell volume decreases by ~1% in relation with an increase of the tilt angle between the *c*-axis and the B-N bond. In addition, the in-situ high pressure diffraction study has evidenced that hydrazine borane shows a gradual pressure-induced decrease of its unit cell dimension and that the process is reversible when the applied pressure is released. The compressibility of this material was established to be relatively low (high bulk modulus) and highly anisotropic. As revealed by molecular simulations based on Density Functional Theory calculations, the mechanical behaviour of NH_2-NH_2-BH_3 was correlated to the pressure-induced changes of its crystal structure in terms of intra- and intermolecular bond lengths and angles parameters. The equations of state have been determined for the two stimuli.

[1] Y.S. Chua, P. Chen, G. Wu, Z. Xiong, Chem. Commun,. 2011, 47, 5116.

[2] H.W. Li, Y. Yan, S.I.; Orimo, A.; Züttel, C.M. Jensen, Energies, 2011, 4, 185.

[4] Z. Huang, T. Autrey, Energy Environ. Sci., 2012, 5, 9257.

[5] L.H. Jepsen, M.B. Ley, Y.S. Lee, Y.W. Cho, M. Dornheim, J.O. Jensen, Y. Filinchuk, J.E. Jørgensen, F. Besenbacher, T.R. Jensen, Materials Today 2014, 17, 129.

[6] Y. Filinchuk, A.H. Nevidomskyy, D. Chernyshov, V. Dmitriev, Physical Review B 2009, 79, 214111:1-11.

[7] R. Moury, K. Robeyns, Y. Filinchuk, P. Miele, U.B. Demirci, Journal of Alloys and Compounds 2016, 659, 210

[8] P. G. Yot, P. Miele, U.B. Demirci, Crystals, 2016, 6, 16.

[9]. P. G. Yot, V. Yadav, S. Ould Amara,J.-P. Itiè, U. B. Demirci, G. Maurin, Phys. Chem. Chem. Phys., 2018,20, 2845.

Keywords: Chemical hydrogen storage materials, High pressure, Thermal behavior, Mechanical behavior

High-pressure synthesis, structure and magnetism of the novel double double perovskite $CaMnMnReO_6$

Padraig Kearins[a]*, Ángel M. Arévalo-López[1], Graham McNally[1], J. Paul Attfield[1]
[a]*Centre for Science at Extreme Conditions (CSEC), University of Edinburgh*
**s1245155@ed.ac.uk*

The double double perovskite structure was recently discovered in the high-pressure $MnRMnSbO_6$ (R = La, Pr, Nd, Sm) series of perovskites. [1] As for the $MnRMnSbO_6$ series, high-pressure conditions were necessary to synthesise this double double perovskite as it can be used to stabilise the incorporation of the small Mn^{2+} on the A-site, which is necessary as the larger Ca^{2+} would be favoured. This can be interesting as it will introduce magnetism on the A-site, from magnetic Mn^{2+}. $CaMnMnReO_6$ was synthesised by grinding $CaMnO_3$, MnO and ReO_2 and the ground powder was then placed into the high-pressure press in a Walker-type multi-anvil module. The pressure was increased to 10 GPa and the reagents heated to 1673 K over 20 minutes and left at temperature for 20 minutes before quenching. Neutron diffraction was carried out on the sample between temperatures of 2 and 300 K at the WISH diffractometer at the ISIS Neutron Facility. Refinement of the data showed that $CaMnMnReO_6$ has the space group $P4_2/n$ and that on the A-site the Mn are coordinated to four oxygens and have alternating square-planar and tetrahedral geometries and Ca is coordinated to 10 oxygens. On the B-site the Mn and Re are coordinated to six oxygens each and have octahedral geometry. [2] The ordering of the sites is clearly visible, where you can see the columnar A-sites and rocksalt B-sites. CaMnMnReO6 displays ferromagnetism on the A-site, with a magnetic moment of 3.10(4) μB and 2.79(7) μB for the square-planar and tetrahedral manganese respectively, and antiferromagnetism on the B-site with a magnetic moment of 2.50(2) μB. Magnetic susceptibility showed a Curie temperature of 130 K and an effective magnetic moment of 6.59 μB. Hysteresis showed that the material acts as a hard magnet at 3 K and has a saturated moment of 2.9 μB, which agrees with the magnetic moments of the A- and B-site.

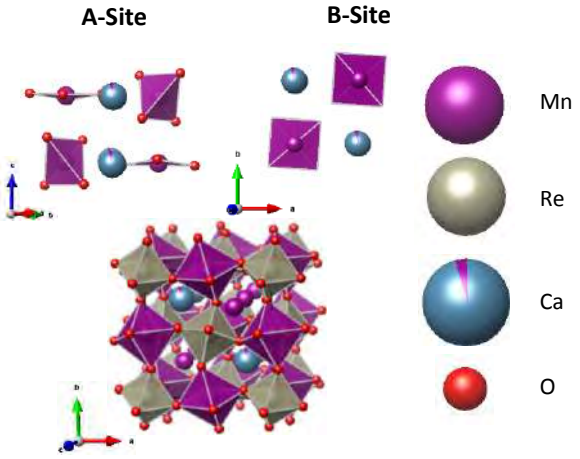

[1] E. Solana-Madruga, A. M. Arévalo-López, A. J Dos Santos-García, E. Urones-Garrote, D. Ávila-Brande, R. Sáez-Puche, and J. P. Attfield, Angew. Chem. Int. Ed. 2016, 55, 9340 –9344
[2] G .M. McNally, A. M. Arévalo-López, P. Kearins, F. Orlandi, P. Maniel, J. P. Attfield, Chem. Mater. 2017, 29, 8870-8874

Keywords : Double-double perovskite, neutron powder diffraction, magnetism.

The Crystal Structures of α- and β-Fluorine

S. I. Ivlev[a*], A. J. Karttunen[b], M. Hölzel[c], F. Kraus[a]
[a] *Fachbereich Chemie, Philipps-Universität Marburg, Germany*
[b] *Department of Chemistry and Materials Science, Aalto University, Finland*
[c] *Forschungs-Neutronenquelle Heinz Maier-Leibnitz, Garching, Germany*
** sergei.ivlev@chemie.uni-marburg.de*

The crystal structures of the chemical elements belong to the fundamental knowledge of chemistry as atom distances, bond lengths and angles can be determined precisely and the data serve as benchmarks for quantum chemistry. Surprisingly, the crystal structures of α-fluorine and β-fluorine have so far only once been investigated [1,2,3]. Probably this is due to the fact that solid F_2 is still extremely reactive and in the case of α-F_2 the authors reported several explosions due to the highly exothermic phase change and the subsequent reaction of F_2 with the sample holder [1]. It was concluded that α-F_2 crystallizes in the monoclinic crystal system, probably in space group type *C*2/*m*, but space group type *C*2/*c* could not be ruled out. Later the original diffraction data were reinterpreted by others and space group *C*2/*c* was found to be more likely correct [4]. The precise space group of α-F_2 remained, however, uncertain [5], which naturally has an influence on the determined atom positions, bond lengths and displacement parameters.

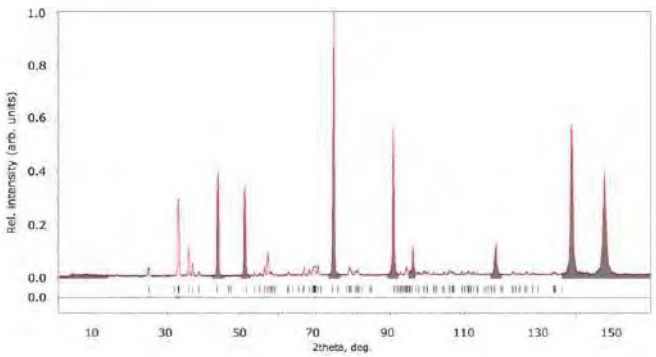

The crystal structure of β-F_2 was first reported in 1964 and determined by means of single crystal X-ray diffraction [3], the problem to distinguish between two cubic space group types, $P\bar{4}3n$ and $Pm\bar{3}n$, was faced. The higher symmetric space group type was chosen since a disordered structure was expected [3]. Neither the bond length of the F_2 molecules, and not the anisotropic displacement parameters of the fluorine atoms could be refined.

We therefore reinvestigated the crystal structures of α- and β-fluorine using powder neutron diffraction and Rietveld refinement. We will report on the obtained models providing much more precise lattice parameters, atomic coordinates as well as bond lengths for the two polymorphs of fluorine.

[1] L. Meyer, C. S. Barrett, S. C. Greer, J. Chem. Phys. 1968, 49, 1902.

[2] T. H. Jordan, W. D. Streib, H. W. Smith, W. N. Lipscomb, Acta Crystallogr. 1964, 17, 777.

[3] T. H. Jordan, W. E. Streib, W. N. Lipscomb, J. Chem. Phys. 1964, 41, 760.

[4] L. Pauling, I. Keaveny, A. B. Robinson, J. Solid State Chem. 1970, 2, 225.

[5] D. A. Young, Phase Diagrams of the Elements, University Of California Press, 1991.

Keywords: fluorine, neutron diffraction, Rietveld refinement

In-situ High Pressure Studies of $SrGeO_3$ Polymorphs

C. H. Kronbo[a*], M. Bremholm[a]
[a]*Center for Materials Crystallography (CMC), Department of Chemistry and iNANO, Aarhus University, DK*
** kronbo@chem.au.dk*

The high-pressure structural behaviors of $SrGeO_3$ polymorphs have been investigated in diamond anvil cells (DACs) using synchrotron powder X-ray diffraction (PXRD), single crystal diffraction (SC-XRD) and *in-situ* high-temperature high-pressure PXRD in a large volume press (LVP). The thermodynamically stable pseudo-wollastonite $SrGeO_3$ (space group *C*2/*c*) was synthesized at ambient pressure and subsequently a fraction was transformed in a LVP to the cubic perovskite $SrGeO_3$ (space group *Pm*-3*m*). Upon compression in a DAC at room temperature, Rietveld refinements showed that the perovskite retains the cubic symmetry up to the highest pressure of 45 GPa. For the pseudo-wollastonite $SrGeO_3$ it was seen that the sample gradually turns amorphous above 11 GPa as shown in the figure with selected refined PXRD patterns measured at ambient temperature in the pressure range 0 to 10 GPa and non-refined PXRD patterns in the range 11 to 45 GPa. Fitting a 3rd order Birch-Murnaghan equation of state to the obtained *P-V* data for the two polymorphs yielded bulk moduli of K_0 = 47(4) GPa and K_0 = 194(3) GPa for the pseudo-wollastonite and perovskite polymorphs, respectively, showing the perovskite structure is much less compressible. Previous studies of pseudo-wollastonite $SrGeO_3$ at high pressure and high temperature have shown a phase transition at 1 GPa, but the structure of the high pressure phase was not solved at the time [1]. To investigate the structural details of a subtle transition at 1 GPa and room temperature for pseudo-wollastonite $SrGeO_3$ we used SC-XRD in a DAC up to 10 GPa. The initial symmetry of the crystal was retained up to 10 GPa, with no indication of a phase transition. Above 10 GPa, the same transition as in the PXRD experiment to an amorphous phase was observed. In recent *in-situ* studies using high-temperature high-pressure PXRD at ESRF ID06, we extended the studies to include high temperature. The ongoing data analysis suggests several extensions to *P-T* phase diagram of $SrGeO_3$.

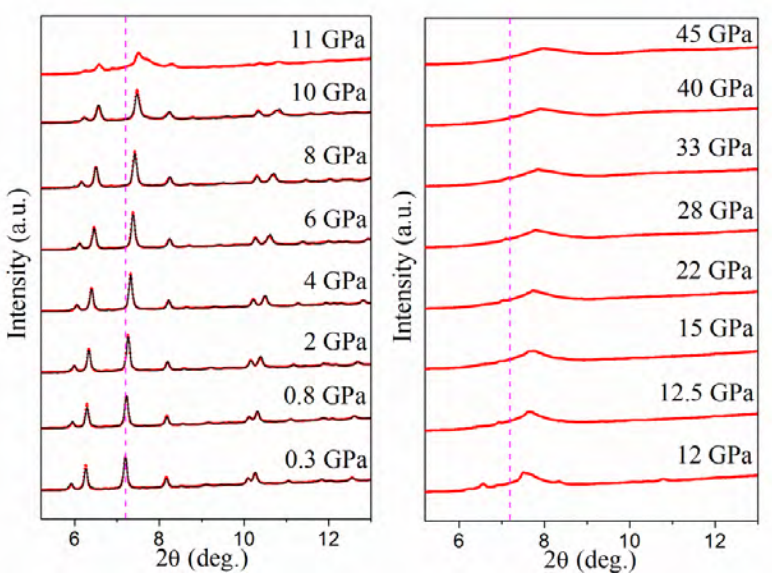

[1] Shimizu Y., Syono Y., and Akimoto S. *High Temperatures - High Pressures*, 1970, 2, 1.

Keywords: High Pressure, $SrGeO_3$, Polymorphism

Effect of Thermal Expansion on Diffracted Intensities for Different Instrument Geometries

M. J. Styles[a*], N. A. S. Webster[b], D. A. Sheppard[c], M. R. Rowles[d]
[a] *CSIRO Manufacturing, Clayton, VIC, Australia*
[b] *CSIRO Minerals Resources, Clayton, VIC, Australia*
[c] *Fuels and Energy Technology Institute, Curtin University, Bentley, WA, Australia*
[d] *John de Laeter Centre, Curtin University, Bentley, WA, Australia*
** Mark.Styles@csiro.au*

In situ powder diffraction is a powerful tool for studying temperature-dependent phenomena, including hydrothermal crystallisation [1], iron-ore sintering [2], and heat-treatment of metal alloys [3]. Using a variation of the external standard method [4], it is possible to evaluate the relative crystallinity of a sample in order to gain insight into the behaviour of any amorphous phases. For example, this approach has been used to quantitatively monitor the amorphous phase fraction in aluminium-based metallic glasses to understand the influence of alloy composition on the nucleation of crystalline phases during heat-treatment [5].

In general, the relative crystallinity method relies on there being a constant mass of material in the diffracting volume, so that the degree of crystallinity can be assessed relative to a maximum in the sum of the Rietveld scale factors. However, as the density of most materials varies as a function of temperature, with the majority of materials undergoing thermal expansion with increasing temperature, samples can displace from the diffracting volume. The degree to which thermal expansion affects the diffracted intensity (and hence scale factors) is dependent on the geometry of the instrument and the nature of the sample. In this presentation, the theoretical effects of thermal expansion on peak intensities in Bragg-Brentano, Debye-Scherrer, and asymmetric (fixed incident angle) diffraction geometries will be discussed and compared with experimental results collected for materials with large and small coefficients of thermal expansion.

[1] Christensen A.N., Jensen T.R., Scarlett N.V.Y., Madsen I.C., Hanson J.C. and Altomare A., *Dalton Transactions*, 2003, 3278–3282.

[2] Webster N.A.S., Pownceby M.I., Madsen I.C., Studer A.J., Manuel J.R., Kimpton J.A., *Metall. Mater. Trans B*. 2014, 45, 2097–2105.

[3] Styles M.J., Marceau R.K.W., Bastow T.J., Brand H.E.A., Gibson M.A., Hutchinson C.R., *Acta Mater.*, 2015, 98, 64–80.

[4] O'Connor B.H., Raven M.D., *Powder Diffraction*, 1988, 3, 2–6.

[5] Styles M.J., Sun W.W., East D.R., Kimpton J.A., Gibson M.A., Hutchinson C.R., *Acta Mater.*, 2016, 117, 170–187.

Keywords: Thermal expansion, diffracted intensity, instrument geometry

MS12 - Microstructure phemonena in thin films

MS12

Abstract Number	Title	Author	Corresponding Affiliation
MS12 - K1	Structure formation during sputter deposition of thin films	Dr Bärbel Krause	Karls
MS12 - K2	Materials science: in-situ, in-operando, time-resolved	Dr Jörg Grenzer	Helmholtz-Zentrum Dresden-Rossendorf e.V.
MS12 - OR1	Microstructure and properties of magnetron sputtered Pt, PtCu and PtNi polycrystalline coatings studied by the x-ray scattering methods	Dr Milan Dopita	Charles University, Faculty of Mathematics and Physics
MS12 - OR2	Film Texture as a Strain Relief Mechanism in the Cubic to Tetragonal Phase Transition in (CH3NH3)PbI3	Dr Kevin Stone	SLAC National Accelerator Laboratory
MS12 - OR3	Analysis of functional thin films via in plane diffraction methods	Dr Zoltán Balogh-Michels	Empa, Swiss Federal Instititue for Materials Science and Technology
MS12 - P184	Preparation and structural studies of thin films of hexagonal ferrites	Prof Radomir Kuzel	Charles University, Faculty of Mathematics and Physics

Structure formation during sputter deposition of thin films

B. Krause[a*], G. Abadias[b], T. Baumbach[a], C. Furgeaud[b], S. Ibrahimkutti[c], A. Michel[b], A. Resta[d], P. Wochner[c]

[a] *IPS, Karlsruhe Institute of Technology, Germany*
[b] *PPrime, CNRS, France*
[c] *Max-Planck-Institute for Solid State Physics, Germany*
[d] *Synchrotron Soleil, France*

* *baerbel.krause@kit.edu*

Depending on their application, the thickness of sputter-deposited thin films can range from few nm to several 100 micrometers. The relation between process parameters, structure formation, and resulting coating properties is very complex. The atomic ordering within sputter-deposited films ranges from amorphous to polycrystalline with various degrees of texture and microstrain. Metastable structures, induced, e.g., by the deposition of energetic particles or by the contribution of surface and interface energies, are quite common.
In situ x-ray diffraction is a versatile tool to access the microstructure evolution of thin films during deposition, giving information about thickness-dependent crystalline phases, texture, grain growth and microstrain. The method becomes even more powerful when combined with complementary thin film characterization methods such as x-ray reflectivity and optical curvature measurements [1]. This will be demonstrated on the example of the metal/amorphous silicon interface [1], comparing the interface formation and subsequent structure development during Pd and Mo deposition.

[1] Krause B. , Abadias G., Michel A., Wochner P., Ibrahimkutty S. and Baumbach T. *ACS Appl. Mater. Interfaces*, 2016, 8, 34888

Keywords: stress, silicides, sputter deposition

Materials science: in-situ, in-operando, time-resolved

J. Grenzer[a*], C. Bähtz[a], A. Rack[b]
[a] *Helmholtz-Zentrum Dresden-Rossendorf e.V., Germany*
[b] *ESRF—The European Synchrotron, Grenoble, France*
** j.grenzer@hzdr.de*

The development of new materials is today closely related to the “creation” of new functional nano structures. Structural investigations are the key to establish a connection between the functional and structural properties generating these functions. This knowledge makes it possible to design new materials with precisely predetermined properties. The function of nano structures is not only determined by their internal structure, but in large part by their morphology and surface properties.

Time-resolved in-situ or/and in-operando X-ray experiments open a very direct, natural way to study the formation and transformation of materials during the relevant technological processes. The talk will build a bridge from classical material science problems, like the formation of 3-dimensional Germanium nano crystal arrays embedded in a dielectric matrix using synchrotron radiation, or the crystallization process during a rapid thermal annealing (RTA) of an amorphous GeSn thin film using a laboratory setup, to experiments exploiting a µsec-time resolution and even behind that.

For example, material processing by laser beams is a widely used technology in industry. Many applications, like the fabrication of thin solar cells, require a large area processing in short times with a limited heat exposure. Therefore time resolved studies of laser driven processes are again of great scientific interest. If thousand of frames are needed to follow the materials evolution on an atomic level the regular bunch structure of a synchrotron source turns out to be an ideal probe to sense changes in the morphology and crystal structure during and after a laser-sample(target) interaction.

Keywords: in-situ, time-resolved, synchrotron

Microstructure and properties of magnetron sputtered Pt, PtCu and PtNi polycrystalline coatings studied by the x-ray scattering methods

M. Dopita[a*], I. Khalakhan[b]
[a] *Department of Condensed Matter Physics, Faculty of mathematics and Physics, Charles University, Prague, Czech Republic*
[b] *Department of Surface and Plasma Science, Faculty of Mathematics and Physics, Charles University, Czech Republic*
** dopita@gmail.com*

Huge boost in energy demand emerged a worldwide call for reducing the reliance on fossil fuels and harvesting of low-emission energy. Among many candidates, proton exchange membrane fuel cells (PEMFCs) are arguably one of the most promising candidates due to environmentally benign and a highly efficient electric power generation. They are expected to become a major power source for wide range of devices, ranging from portable electronics to electric vehicles. Among other obstacles a high cost of platinum, which still remains the only oxygen reduction reaction (ORR) catalyst that meets catalysis/durability requirements, is a serious problem breaking the commercialization. Extensive studies have been performed in order to find the ORR catalyst, which is more active, less expensive and more stable than pure platinum. One of the most promising strategies is the alloying of platinum with relatively cheap transition metals. It has been reported that Pt alloyed with Ni, Co and Fe enhances the electrocatalytic activity toward ORR, while at the same time lowers catalyst cost due to reduction of the amount of used platinum.
A series of Pt, PtCu and PtNi polycrystalline coatings varying in thickness from 5 nm to 100 nm were prepared by magnetron co-sputtering. The microstructure and the real structure of coatings were investigated in as-deposited as well as in as-treated (after the electrochemical treatment simulating the real function of fuel cell) using the x-ray scattering methods. A special emphasis was put on detailed description of the real structure of the coatings – the size of coherently diffracting domains, the defects of the crystal lattice, the preferred orientation of crystallites, the presence and the magnitude of the residual stress in coatings and the roughness of the coatings, because of its undisputable role and influence in the deterioration processes occurring during the materials operation as a cathode in a proton exchange membrane fuel cells.
The results of the x-ray scattering methods were correlated with the results of other experimental techniques as in situ electrochemical atomic force microscopy complemented with ex situ energy dispersive X-ray spectroscopy, X-ray photoelectron spectroscopy and synchrotron radiation photoelectron spectroscopy to get the complex insight into the coatings microstructural development and correlation of activity loss, dealloying and morphology changes induced by catalysts aging processes.
It was proven that the real structure of coatings plays enormously important role in the deterioration processes and influences the proton exchange membrane fuel cells life time significantly.

[1] I. Khalakhan, M. Vorokhta, P. Kúš, M. Dopita, M. Václavu, R. Fiala, N. Tsud, T. Skála, V. Matolín, Electrochim. Acta 245, 2017, 760–769

Keywords: Pt, PtCu, PtNi coatings, x-ray diffraction, fuel cells

Film Texture as a Strain Relief Mechanism in the Cubic to Tetragonal Phase Transition in $(CH_3NH_3)PbI_3$

K. H. Stone[a*] and L. T. Schelhas[a]
[a] *SSRL Materials Science Division, SLAC National Accelerator Laboratory, Menlo Park CA, USA*
* *khstone@slac.stanford.edu*

Hybrid organic-inorganic perovskite inspired materials have attracted a great deal of interest for their outstanding optoelectronic properties, especially for potential photovoltaic applications. In addition to their optoelectronic properties, these materials are promising for their wide range of gentle processing conditions from precursor solutions. Despite the low processing temperatures typically used for these materials, they tend to have quite high thermal expansion coefficients. As a result, cooling to room temperature after annealing can lead to a significant amount of shrinkage in the lattice parameters. When matched with common substrates, such as glass, this results in a large mismatch of thermal expansion resulting in the development of strain in thin films. Through the use of *in-situ* diffraction during the annealing step of perovskite thin film synthesis, we are able to observe the development of strain and have determined the level to which this development may be controlled through choice of substrate. Moreover, the prototypical perovskite material, methylammonium lead tri-iodide, cools through a phase transition after annealing. We will demonstrate how this phase transition may act as a strain relief mechanism and how this results in the formation of crystallographic texture in these thin film materials.

Keywords: Thin Film, Strain, Texture

Analysis of functional thin films via in plane diffraction methods

Z. Balogh-Michels[a*], M. Fisher[b], B. Sakar[c], O. Oztürk[c], F. Pagani[d], A. Neels[a]
[a] *Center for X-ray Analytics, Empa, Switzerland*
[b] *Nanoscale Materials Science, Empa, Switzerland*
[c] *Physics Dept, Gebze Technical University, Turkey*
[d] *Materials for Energy Conversion, Empa, Switzerland*

In this presentation we will review our recent results on the analysis of various thin film system using advanced X-ray diffraction methods. The key technique was in plane diffraction. Unlike the out of plane diffraction here the scatter plane, the plane defined by the incoming and the outgoing X-ray beam is parallel to the specimen surface. This means lattice planes perpendicular to the specimen normal can be directly investigated. This method is especially well suited to study the microstructure and symmetry of thin films.
We used a Bruked D8 Discover DaVinci XRD machine. The specimens were mounted on a tilt stage. This allowed us to record full sector scans in plane. These scans are based on radial scans of a suitable 2Θ range (e.g. 20-135°) at different specimen rotation (e.g. 0-140° with 1° step size). Such sectors contain enough substrate peaks to define the coordinate system in respect to the substrate.
Depending on the microstructure of the thin film specimen the sector scans contain different features. For 1:1 epitaxy other than the 1/x background and the substrate peaks nothing else will be visible. For other epitaxial conditions (like 2:1) new, weaker reflections appear. For polycrystalline or fiber textured specimens a ring structure will be observed, since the system has a rotational symmetry. The key difference between these subcases is the intensity ratio of the rings. For films with fiber texture only the rings belonging to the planar components of the texture will be visible.
In the presentation we are going to discuss the results of investigations in three different systems. A lithium-titanate based battery anode material [1], a nanoscale magnetic film [2], and an AlN(O) hard coating [3]. Using the in plane methods we could identify the microstructure in these systems. Based on the microstructural information we could explain important functional properties like conductivity, magnetization or vacancy concentration.

[1] F. Pagani *et al., to be published*

[2] B. Sakar *et al., to be published*

[3] M. Fischer *et al., to be published*

Keywords: thin films, in plane XRD, microstructure-property relationship

Preparation and structural studies of thin films of hexagonal ferrites

R. Kužel[a*], M. Dopita[a], J. Buršík[b], R. Uhrecký[b], M. Soroka[b]
[a]*Faculty of Mathematics and Physics, Charles University, Prague, Czech Republic,*
[b]*Institute of Inorganic Chemistry of the Czech Academy of Sciences, Husinec-Řež, Czech Republic*
** kuzel@karlov.mff.cuni.cz*

Thin films of M, Y and Z hexagonal ferrites with a potential of magnetoelectric effect were prepared by chemical solution deposition method and number of processing parameters were tested and optimized with the aim to minimize the amount of impurities that could spoil the magnetic properties of final material. In order to prepare highly oriented ferrite films, several substrates were used and different substrate/seeding layer/ferrite layer architectures were proposed.
The films were studied mainly by X-ray diffraction, atomic force microscopy and electron back-scatter diffraction. X-ray diffraction analysis was focused on the precise determination of lattice parameters, studies of out-of-plane and in-plane grain orientations, crystallite sizes and microstrains, and residual stresses. Most of studies were performed in parallel beam setup with the Eulerian cradle and polycapillary in primary beam. Different symmetric and asymmetric scans were performed. In most of cases strong out-of-plane orientations were found and only basal (00l) reflections were available in symmetric scans. Therefore, the lattice parameters, profile analysis and residual stresses were studied by combination of several asymmetric reflections scanned at specific suitable angles of inclinations φ and ψ (i.e. on the axis perpendicular to the film surface and axis perpendicular to the goniometer axis, respectively). For comparison of measured lattice parameters there was often a problem of either no data in the PDF-4+ database for specific phase or multiple but different data.
From seven M phases with different chemical composition, magnetic character and lattice misfit values investigated in their use as template and buffer layers for Y ferrite growth, the best results were achieved when the misfit values between seed layer and substrate, and between seed layer and top Y-layer are approximately equal and when the surface of seed layers are formed by hexagons for which the surface area formed by top surface of hexagons is much larger than surface area formed by side walls of hexagons [1, 2].
New Y-ferrite phases were prepared with the composition $BaSrZnCoFe_{11}(Me)O_{22}$ (Me = Al, Ga, In, Sc). and it was found that for Me = Al, Ga the magnetic structure is of non-colinear ferrimagnetic type with unspecified helical magnetic structure. For ME = Ga this is a new system with potential ME effect. Moreover, these films could be prepared as well-oriented both out-of-plane and in-plane on STO - $SrTiO_3$(111) substrates directly without any seeding layers.
ME Z-type ferrite $Sr_3Co_2Fe_{24}O_{41}$ and $Ba_xSr_{3-x}Co_2Fe_{24}O_{41}$ thin films were prepared and characterized for the first time [3]. According to the XRD texture analysis the orientation relationship between Z ferrite and substrate can be expressed as (00l)Z || (111)STO || and $[110]$Z || $[100]$STO. However, in these films the analysis was complicated by the presence of M and S (spinel) phases that were also oriented (aligned with the substrate) and therefore also many asymmetric reflections were overlapped and many of them were weak. Therefore, a careful selection of reflections suitable for the analysis had to be made.

[1] J. Buršík, R. Uhrecký, D. Kaščáková, M. Slušná, M. Dopita, R. Kužel, *Journal of the European Ceramic Society*, 2016, 26, 3173-3183.

[2] R. Uhrecký, J. Buršík, M. Soroka, R. Kužel, J. Prokleška, *Thin Solid Films*, 2017, 622, 104-110.

[3] J. Buršík, R. Uhrecký, M. Soroka, R. Kužel, J. Prokleška, *Journal of Magnetism and Magnetic Materials, 2018, submitted*

Keywords: thin films, hexagonal ferrites, out-of-plane and in-plane orientation

Platinum Sponsors

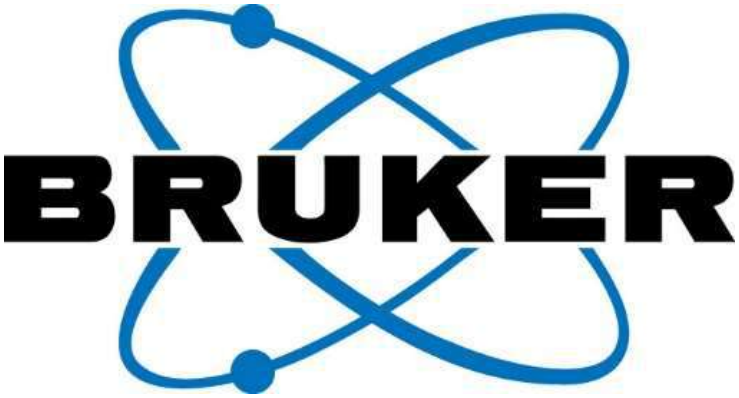

Gold Sponsors

Silver Sponsors

Exhibitors

Anton Paar

HUBER
Diffraction and Positioning Equipment

IUCr

OxfordCryosystems

PROTO
X-RAY DIFFRACTION

STOE

ThermoFisher
SCIENTIFIC
The world leader in serving science

Sponsors

crystals

CRYSTAL IMPACT

SIROQUANT
Sietronics Pty Ltd

X-Ray Laboratory Dr. Ermrich

ENTER A **NEW DIMENSION** WITH THE **3RD GENERATION EMPYREAN**

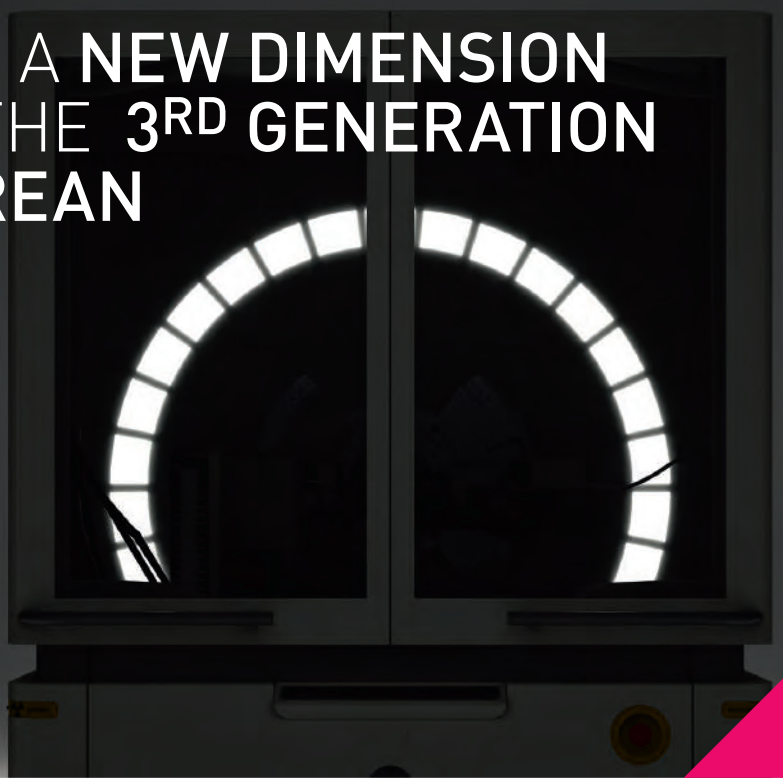

Visit our booth

UNVEILING A **REVOLUTION** IN THE WORLD OF X-RAY DIFFRACTION!

Do you want the highest sample throughput in a multi-user, multidisciplinary environment?

Would you like to increase the number of students who are able to perform advanced analyses and decrease the amount of training that is needed?

Do you want to reduce the possibility for mistakes in data collection?

Have you ever wondered why X-ray diffractometers are often not used during the nights or weekends?

Join our Lunch & Learn Seminar on Monday July 2nd in the Kirkland room, South Hall Complex from 12.30 until 14.00 (lunch included) where you will be among the first to discover what a difference an intelligent diffractometer can make. We will also feature our Aeris XRD benchtop and Morphologi 4 analytical imaging platform.

Stop by our booth and see the new Empyrean MultiCore Optics and our Aeris live in action

www.panalytical.com/empyrean

Malvern Panalytical

The 2018 Powder Diffraction File™

Diffraction Data You Can Trust

ICDD databases are the only crystallographic databases in the world with quality marks and quality review processes that are ISO certified.

PDF-4+
Identify and Quantitate
398,726 Entries
295,309 Atomic Coordinates

PDF-2
Phase Identification + Value
298,258 Entries

WebPDF-4+
Data on the Go
398,726 Entries
295,309 Atomic Coordinates

871,758 Entries

PDF-4/Organics
Solve Difficult Problems, Get Better Results
526,126 Entries
106,369 Atomic Coordinates

PDF-4/Minerals
Comprehensive Mineral Collection
45,497 Entries
37,210 Atomic Coordinates

Standardized Data

More Coverage

All Data Sets Evaluated For Quality

Reviewed, Edited and Corrected Prior To Publication

Targeted For Material Identification and Characterization

www.icdd.com

ICDD® International Centre for Diffraction Data

ISO 9001:2008 QUALITY ASSURED COMPANY CERT.NR. 11409.1

www.icdd.com | marketing@icdd.com

ICDD, the ICDD logo and PDF are registered in the U.S. Patent and Trademark Office.
Powder Diffraction File is a trademark of JCPDS – International Centre for Diffraction Data
©2018 JCPDS–International Centre for Diffraction Data – 6/18

Rigaku

Leading With Innovation

SmartLab

Automated Multipurpose X-ray Diffractometer

- Low-maintenance 9 kW X-ray source PhotonMAX
- High-energy resolution 2D detector HyPix-3000
- New CBO family, fully automated beam switchable CBO-auto and high-resolution micro area CBO-μ
- Lifetime perfect alignment
- SmartLab Studio II measurement and analysis software

COME TO OUR BOOTH FOR DETAILS

Rigaku Corporation and its Global Subsidiaries

Hugenottenallee 167 | 63263 Neu-Isenburg, Germany | TEL +49 610 277 99 - 951 | www.Rigaku.com | rese@Rigaku.com

The 2018 Powder Diffraction File™

Diffraction Data You Can Trust

ICDD databases are the only crystallographic databases in the world with quality marks and quality review processes that are ISO certified.

PDF-4+
Identify and Quantitate
398,726 Entries
295,309 Atomic Coordinates

PDF-2
Phase Identification + Value
298,258 Entries

WebPDF-4+
Data on the Go
398,726 Entries
295,309 Atomic Coordinates

871,758 Entries

PDF-4/Organics
Solve Difficult Problems, Get Better Results
526,126 Entries
106,369 Atomic Coordinates

PDF-4/Minerals
Comprehensive Mineral Collection
45,497 Entries
37,210 Atomic Coordinates

Standardized Data

More Coverage

All Data Sets Evaluated For Quality

Reviewed, Edited and Corrected Prior To Publication

Targeted For Material Identification and Characterization

www.icdd.com

ICDD® International Centre for Diffraction Data

ISO 9001:2008 QUALITY ASSURED COMPANY CERT.NR. 11409.1

www.icdd.com | marketing@icdd.com

ICDD, the ICDD logo and PDF are registered in the U.S. Patent and Trademark Office.
Powder Diffraction File is a trademark of JCPDS – International Centre for Diffraction Data
©2018 JCPDS–International Centre for Diffraction Data – 6/18

DECTRIS
detecting the future

Available in various diffractometers and stress robots

MYTHEN2 R

Detector Series

Microstrip X-ray detector for XRD and WD-XRF applications

- Noise-free single-photon counting from Ti to Ag radiation
- Compact design fits in any diffractometer
- 640- and 1280-strip modules
- Multi-modular systems for the laboratory

sales@dectris.com | www.dectris.com

EPDIC16
Delegate List

First name	Last name	Organisation	Email
A. M. Milinda	Abeykoon	Brookhaven National Laboratory	aabeykoon@bnl.gov
Paweł	Adamski	West Pomeranian University of Technology, Szczecin	adamski_pawel@zut.edu.pl
Jakob Voldum	Ahlburg	Department of chemistry, Aarhus University	Jakob.ahlburg@inano.au.dk
Xavier	Alcobe	Universitat de Barcelona	alcobe@ccit.ub.edu
André	Alker	F. Hoffmann-La Roche AG	andre_m.alker@roche.com
Phoebe	Allan	University of Birmingham	p.allan@bham.ac.uk
Mathieu	Allix	CEMHTI - CNRS (Orléans, FRANCE)	mathieu.allix@cnrs-orleans.fr
Angela	Altomare	Institute of Crystallography	angela.altomare@ic.cnr.it
Mahrez	Amri	Johnson Matthey	sarah.robinson@matthey.com
Henrik Lyder	Andersen	Aarhus University	hla@chem.au.dk
Georgios	Antipas	NanoMEGAS SPRL	yantipas@icloud.com
Angel	Arevalo	CNRS-UCCS	angel.arevalo-lopez@univ-lille1.fr
Grandeury	Arnaud	Novartis Pharma AG	arnaud.grandeury@novartis.com
Nicola	Ashcroft	IUCr	na@iucr.org
Paul	Attfield	University of Edinburgh	j.p.attfield@ed.ac.uk
Zoltan	Balogh-Michels	Empa	zoltan.balogh@empa.ch
Jethro	Beamish-Cook	University of Reading	j.beamish-cook@pgr.reading.ac.uk
Hanka	Becker	TU Bergakademie Freiberg, Institute of Materials Science	hanka.becker@iww.tu-freiberg.de
Detlef	Beckers	Malvern Panalytical B.V.	detlef.beckers@malvernpanalytical.com
Jozef	Bednarcik	DESY Hamburg	jozef.bednarcik@desy.de
Tony	Bell	Sheffield Hallam University	Anthony.Bell@shu.ac.uk
Hajar	Bellefqih	Hassan II University, Casablanca	hajar.bellefqih@gmail.com
Michela	Bellettato	eni S.p.A.	michela.bellettato@eni.com
Premysl	Beran	Nuclear Physics Institute, CAS	pberan@ujf.cas.cz
Federica	Bertolotti	Aarhus University	fbertolotti@aias.au.dk
Sebastian	Bette	Max Planck Institute for Solid State Research	S.Bette@fkf.mpg.de
Kenneth	Beyerlein	Max Planck Institute for the Structure and Dynamics of Matter	kenneth.beyerlein@mpsd.mpg.de
Dave	Billing	University of the Witwatersrand	dave.billing@wits.ac.za
David	Bish	Indiana University	bish@indiana.edu
Brigitte	Bitschnau	Graz University of Technology	bitschnau@tugraz.at
Thomas	Blanton	International Centre for Diffraction Data	tblanton@icdd.com
Carol	Blanton	International Centre for Diffraction Data	tblanton@icdd.com
Pierre	Bordet	Institut Neel, CNRS Grenoble	pierre.bordet@neel.cnrs.fr
Mauro	Bortolotti	University of Trento	mauro.bortolotti@unitn.it

EPDIC16
Delegate List

First name	Last name	Organisation	Email
Hanna	Boström	University of Oxford	hanna.bostrom@exeter.ox.ac.uk
Amarante	Böttger	Dr. Amarante Böttger - Delft University of Technology	a.j.bottger@tudelft.nl
Emil	Bozin	Brookhaven National Laboratory	bozin@bnl.gov
Stefan	Brandstetter	DECTRIS Ltd.	stefan.brandstetter@dectris.com
William	Brant	Uppsala University	william.brant@kemi.uu.se
Michael	Brogan	Malvern Panalytical Ltd.	michael.brogan@malvernpanalytical.com
Alexander	Browne	University of Edinburgh	A.J.Browne@sms.ed.ac.uk
Michela	Brunelli	DUBBLE / ESRF	brunelli@esrf.fr
Andrew	Cairns	Imperial College London	a.cairns@imperial.ac.uk
Chiara	Cappuccino	University of Bologna	chiara.cappuccino2@unibo.it
Johan	Cedervall	Uppsala University	johan.cedervall@kemi.uu.se
Robert	Cernik	University of Manchester	r.cernik@manchester.ac.uk
Radovan	Cerny	University of Geneva	Radovan.Cerny@unige.ch
Philip	Chater	Diamond Light Source	philip.chater@diamond.ac.uk
Stefano	Checchia	ESRF	stefano.checchia@esrf.fr
Mogens	Christensen	Aarhus University	mch@chem.au.dk
James	Cline	NIST	james.cline@nist.gov
Jeremy Karl	Cockcroft	Department of Chemistry, UCL, United Kingdom	jeremykarl@gmail.com
Mauro	Coduri	ESRF	coduri@esrf.fr
Alan	Coelho	Coelho Software	AlanCoelho@bigpond.com
Amy	Coleman	The University of Edinburgh	s0936764@sms.ed.ac.uk
Nicola	Corriero	Institute of Crystallography (IC-CNR)	nicola.corriero@ic.cnr.it
Fanny	Costa	UFACB	fanny.costa@ufabc.edu.br
Ana	Cuesta	UNIVERSIDAD DE MALAGA	a_cuesta@uma.es
James	Cumby	University of Edinburgh	james.cumby@ed.ac.uk
Eddie	Cussen	University of Strathclyde	edmund.cussen@strath.ac.uk
Gregorio	Dal Sasso	Istituto di Cristallografia (CNR)	gregorio.dalsasso@ic.cnr.it
Anita	D'Angelo	CSIRO	anita.dangelo@csiro.au
Monica	Dapiaggi	University of Milano	monica.dapiaggi@unimi.it
Partha Pratim	Das	NanoMEGAS	partha@nanomegas.com
William	David	STFC/Oxford	bill.david@stfc.ac.uk
Valentina	Degtyareva	Institute of Solid State Physics, Chernogolovka, Russia	degtyar@issp.ac.ru
Catherine	Dejoie	ESRF	catherine.dejoie@esrf.fr
Mariyam Susana	Dewi Darma	Karlsruhe Institute of Technology	mariyam.darma@kit.edu
Marco	Di Michiel	ESRF	dimichie@esrf.fr
Reiner	Dietsch	AXO DRESDEN GmbH	reiner.dietsch@axo-dresden.de
Robert	Dinnebier	MPI-FKF	r.dinnebier@fkf.mpg.de
Simone	Dolabella	Empa	simone.dolabella@empa.ch

EPDIC16
Delegate List

First name	Last name	Organisation	Email
ZhiLi	Dong	Nanyang Technological University, Singapore	zldong@ntu.edu.sg
Milan	Dopita	Charles University	dopita@gmail.com
Tlamsamani	Dounia	University of Moulay Ismail	douniayns@gmail.com
Christina	Drathen	Bruker AXS	christina.drathen@bruker.com
Sandra	Dressler	Loughborough University	s.dressler@lboro.ac.uk
Celine	Durniak	Data Management and Software Centre, The European Spallation Source ERIC	celine.durniak@esss.se
Gustav	Ek	Uppsala University	gustav.ek@kemi.uu.se
Erik	Elkaim	SOLEIL	missions@synchrotron-soleil.fr
Lars	Epple	Robert Bosch GmbH	lars.epple@de.bosch.com
Martin	Etter	Deutsches Elektronen-Synchrotron	martin.etter@desy.de
John	Evans	Durham University	john.evans@durham.ac.uk
Michael	Evans	Bruker AXS GmbH	michael.evans@bruker.com
Piotr	Fabrykiewicz	Faculty of Physics, University of Warsaw	Piotr.Fabrykiewicz@fuw.edu.pl
Hailiang	Fang	Department of Chemistry - Ångström Laboratory, Uppsala University	hailiang.fang@kemi.uu.se
François	Fauth	ALBA Synchrotron	ffauth@cells.es
Robert	Feidenhansl	European XFEL	robert.feidenhansl@xfel.eu
Daniella	Ferluccio	Heriot-Watt University	daf4@hw.ac.uk
William	Fernandes	UFPB - Brazil	williamvifer@hotmail.com
Maria Teresa	Fernandez-Diaz	Institut Laue Langevin	ferndiaz@ill.fr
Fabio Furlan	Ferreira	Federal University of ABC - UFABC	fabio.furlan@ufabc.edu.br
Evgeny	Filatov	NIIC SB RAS	decan@niic.nsc.ru
Andy	Fitch	ESRF	fitch@esrf.fr
Ekaterina	Fomina	Geological Institute of Kola Science Centre RAS	fomina_e.n@mail.ru
Sacha	Fop	University of Aberdeen	sachafop@gmail.com
Luca	Fornasari	University of Bologna	luca.fornasari3@unibo.it
Michel	Francois	IJL-University of Lorraine	michel.francois@univ-lorraine.fr
Karen	Friese	Research Centre Jülich	k.friese@fz-juelich.de
Pelle	Garbus	iNANO, Aarhus University	garbus@inano.au.dk
Luzia S.	Germann	Max Planck Institute for Solid State Research	l.germann@fkf.mpg.de
Holger	Geßwein	KIT IAM	holger.gesswein@kit.edu
Carlotta	Giacobbe	ESRF	travelstaff@esrf.fr
Lara	Gigli	Elettra-Sincrotrone Trieste	lara.gigli@elettra.eu
Chris	Gilmore	University of Glasgow	chris.gilmore@glasgow.ac.uk
Frederik	Gjørup	Aarhus University	fgjorup@chem.au.dk

EPDIC16
Delegate List

First name	Last name	Organisation	Email
Arianna	Gleason	SLAC / Stanford University	ariannag@stanford.edu
Jintaek	Gong	KAIST Natural Science Research Institute	kalimeriashd@kaist.ac.kr
Andrew	Goodwin	University of Oxford	andrew.goodwin@chem.ox.ac.uk
Fabia	Gozzo	Excelsus Structural Solutions	fabia.gozzo@excels.us
Georg	Gravogl	University of Vienna	georg.gravogl@univie.ac.at
Jörg	Grenzer	Helmholtz-Zentrum Dresden-Rossendorf e.V., Germany	J.Grenzer@HZDR.de
Stefan	Griessl	Huber Diffraction	epdic2018@nion.de
Flemming	Grumsen	Denmark tecnical university	fbgr@mek.dtu.dk
Maciej	Grzywa	Rigaku Europe SE	maciej.grzywa@rigaku.com
Antonietta	Guagliardi	Institute of Crystallography, CNR	antonella.guagliardi@ic.cnr.it
Marie	Guignard	ICMCB - CNRS	marie.guignard@icmcb.cnrs.fr
Nathalie	Guillou	Institut Lavoisier Versailles	nathalie.guillou@uvsq.fr
Yuanyuan	Guo	University of St Andrews	yg28@st-andrews.ac.uk
Paula	Haddad	Federal University of São Paulo - UNIFESP	haddadps@gmail.com
Clement	Haeck	Almac Group	clement.haeck@almacgroup.com
Ivan	Halasz	Rudjer Bošković Institute	ihalasz@irb.hr
Graeme	Hansford	University of Leicester	gmh14@leicester.ac.uk
Thomas	Hartmann	STOE & CIE GmbH	info@stoe.com
David	Havlicek	Faculty of Science, Charles University, Prague	havlicek@natur.cuni.cz
Michael	Hayward	University of Oxford	michael.hayward@chem.ox.ac.uk
Rajath	Hegde	Jawaharlal Nehru national College of Engineering	rajathhegdemm63@gmail.com
Alexander	Heldmann	Forschungs- Neutronenquelle Heinz Maier-Leibnitz (FRM2)	alexander.heldmann@frm2.tum.de
Paul	Henry	ISIS Pulsed Neutron & Muon Source	paul.henry@stfc.ac.uk
Stephen	Hillier	James Hutton Institute	stephen.hillier@hutton.ac.uk
Akihiro	Himeda	Rigaku	himeda@rigaku.co.jp
Manuel	Hinterstein	Karlsruhe Institute of Technology	m.hinterstein@kit.edu
Sophie	Hodgkiss	University of Liverpool	sgshodgk@student.liverpool.ac.uk
Jennifer	Hoelscher	Aarhus University	j.hoelscher@inano.au.dk
Markus	Hoelzel	MLZ / TU München	markus.hoelzel@frm2.tum.de
Michael	Hofmann	Heinz Maier-Leibnitz Zentrum (MLZ)	michael.hofmann@frm2.tum.de
Ka Hou	Hong	University of Edinburgh	k.h.hong@sms.ed.ac.uk
Steven	Horder	Malvern Panalytical	steven.horder@malvernpanalytical.com
Andreas	Houben	RWTH Aachen University	andreas.houben@ac.rwth-aachen.de
Sean	Injac	University of Sydney	ssta8177@uni.sydney.edu.au
Eleonora	Isotta	University of Trento	eleonora.isotta@unitn.it

EPDIC16
Delegate List

First name	Last name	Organisation	Email
Sergei	Ivlev	Philipps-Universität Marburg	sergei.ivlev@chemie.uni-marburg.de
Philipp	Jacobs	RWTH Aachen University	philipp.jacobs@ac.rwth-aachen.de
Dieter	Jehnichen	Leibniz-Institut für Polymerforschung Dresden e.V.	djeh@ipfdd.de
Kirsten Marie	Jensen	University of Copenhagen	kirsten@chem.ku.dk
Kunlang	Ji	The University of Edinburgh	s1301190@sms.ed.ac.uk
Mads Ry	Jørgensen	Aarhus University / MAX IV Laboratory	mads@chem.au.dk
Jens-Erik	Jørgensen	Aarhus University, Denmark	jenserik@chem.au.dk
Mikkel	Juelsholt	University of Copenhagen	mikkel.juelsholt@chem.ku.dk
James	Kaduk	North Central College	kaduk@polycrystallography.com
Il-Mo	Kang	Korea Institute of Geoscience and Mineral Resources (KIGAM)	imkang@kigam.re.kr
Paula	Kayser	University of Edinburgh	paula.kayser@ed.ac.uk
Padraig	Kearins	University of Edinburgh	s1245155@ed.ac.uk
Brendan	Kennedy	The University of Sydney	Brendan.Kennedy@Sydney.edu.au
Arnt	Kern	Bruker	arnt.kern@bruker.com
Peter	Khalifah	Stony Brook University & Brookhaven National Laboratory	kpete@bnl.gov
Mathias	Kiefer	University of the Witwatersrand	720957@students.wits.ac.za
Jungeun	Kim	Rigaku Corporation	jungeun@rigaku.co.jp
Jaehwan	Kim	KIGAM	jaehwankim@kigam.re.kr
Daeyoung	Kim	University of Science and Technology	daeyoung@kigam.re.kr
Caroline	Kirk	University of Edinburgh	Caroline.Kirk@ed.ac.uk
Charlotte	Kirk	University of Oxford	charlotte.kirk@new.ox.ac.uk
Daria	Kiseleva	Institute of Geology and Geochemistry, UB RAS	podarenka@mail.ru
Karin	Kleiner	Diamond Light Source	karin.kleiner@diamond.ac.uk
Patricia	Kloihofer	University of Edinburgh	s1138487@sms.ed.ac.uk
Michael	Knapp	KIT	michael.knapp@kit.edu
Karsten	Knorr	Bruker AXS	karsten.knorr@bruker.com
Robert	Koch	Alfred University	kochr@alfred.edu
Gabriele	Kociok-Kohn	University of Bath	chsgk@bath.ac.uk
Marek	Kojdecki	Military University of Technology	m_kojdecki@poczta.onet.pl
Takayuki	Konya	Rigaku corporation	konya@rigaku.co.jp
Katarzyna Małgorzata	Kosyl	Institute of Physics Polish Academy of Sciences	kosyl@ifpan.edu.pl
Bärbel	Krause	Karlsruhe Institute of Technology (KIT)	baerbel.krause@kit.edu
Aleksandar	Kremenovic	University of Belgrade	aleksandar.kremenovic@rgf.bg.ac.rs
Camilla	Kronbo	Aarhus University	kronbo@chem.au.dk
Krzysztof	Kudłacz	Codegopl	krzysiek.kudlacz@gmail.com

EPDIC16
Delegate List

First name	Last name	Organisation	Email
Radomir	Kuzel	Charles University, Faculty of Mathematics and Physics, Prague	kuzel@karlov.mff.cuni.cz
Ikram	Labtaini	University of Hassan 1 st Laboratory of Nanosciences and Modeling	ikram.labtaini@gmail.com
Kurt	Lawson	Loughborough University	k.lawson@lboro.ac.uk
Kriss	Lefwich	PROTO	kstrickland@protoxrd.com
Andreas	Leineweber	TU Bergakademie Freiberg	andreas.leineweber@iww.tu-freiberg.de
Christian	Lengauer	University of Vienna	christian.lengauer@univie.ac.at
Laura	Leon-Reina	Universidad de Málaga	lauralr@uma.es
Phil	Lightfoot	University of St Andrews	pl@st-andrews.ac.uk
YU	LIU	The University of Aberdeen	yu.liu@abdn.ac.uk
Henrik	Lund	Leibniz Institute for Catalysis at the University of Rostock	henrik.lund@catalysis.de
Josh	Makepeace	University of Oxford	josh.makepeace@chem.ox.ac.uk
Nishil	Malde	Anton Paar Ltd	kerrie.swindon@anton-paar.com
Asmaa	Marchoud	University Hassan II-Faculty of Sciences Ben M'ssik Casablanca	marchoud.asmaa@gmail.com
Irene	Margiolaki	University of Patras	imargiola@upatras.gr
Norberto	Masciocchi	University of Insubria & To.Sca.Lab	norberto.masciocchi@uninsubria.it
Fabio	Masiello	Malvern Panalytical	fabio.masiello@malvernpanalytical.com
Zdeněk	Matěj	MAX IV Laboratory, Lund University	zdenek.matej@maxiv.lu.se
Jette	Mathiesen	University of Copenhagen	jkm@chem.ku.dk
Dorota	Matras	University of Manchester	dorota.matras@rc-harwell.ac.uk
Kirstie	McCombie	University of Aberdeen	r01ksm15@abdn.ac.uk
Helen	McDonnell	International Centre for Diffraction Data	McDonnell@icdd.com
Kate	McHardy	Oxford Cryosystems Ltd	kate@oxcryo.com
Abbie	Mclaughlin	University of Aberdeen	a.c.mclaughlin@abdn.ac.uk
Malcolm	McMahon	The University of Edinburgh	mim@ph.ed.ac.uk
Graham	McNally	MPI for Solid State Sciences	G.McNally@fkf.mpg.de
Stefan	Michalik	Diamond Light Source	stefan.michalik@diamond.ac.uk
Pavol	Mikula	Nuclear Physics Institute ASCR, v.v.i.	mikula@ujf.cas.cz
Scott	Misture	Alfred University	misture@alfred.edu
Mashikoane Wilson	Mogodi	ESRF	mogodi@esrf.fr
Anna	Moliterni	Institute of Crystallography - CNR	annagrazia.moliterni@ic.cnr.it
Mathias	Mørch	Aarhus University	mmorch@chem.au.dk
Mickael	Morin	Excelsus Structural Solutions	mickael.morin@excels.us
Daniele	Moscheni	University of Insubria	d.moscheni@studenti.uninsubria.it

EPDIC16
Delegate List

First name	Last name	Organisation	Email
Heather	Mutch	University of Strathclyde	heather.mutch@strath.ac.uk
Antonia	Neels	Empa	antonia.neels@empa.ch
Gwilherm	Nenert	PANalytical B. V.	gwilherm.nenert@panalytical.com
Stavros	Nicolopoulos	NanoMEGAS SPRL	info@nanomegas.com
Beatriz	Noheda	University of Groningen, Zernike Institute for Advanced Materials	b.noheda@rug.nl
Ryoko	Oishi-Tomiyasu	Yamagata University	ryoko_tomiyasu@sci.kj.yamagata-u.ac.jp
Paul	O'Meara	Malvern Panalytical	paul.omeara@malvernpanalytical.com
Ezgi	Onur Sahin	Max-Planck-Institut für Kohlenforschung	onur@mpi-muelheim.mpg.de
Elise	Pachoud	University of Edinburgh	elise.pachoud@ed.ac.uk
Katharine	Page	Oak Ridge National Laboratory	pagekl@ornl.gov
Wojciech	Paszkowicz	Institute of Physics PAS, Warsaw	paszk@ifpan.edu.pl
Jan Skov	Pedersen	Aarhus University	jsp@chem.au.dk
Andreas	Pein	Anton-Paar GmbH	andreas.pein@anton-paar.com
Giuditta	Perversi	University of Edinburgh	mika-mika@hotmail.it
Giovanni	Pierri	University of Salerno	gpierri@unisa.it
Jiří	Plocek	Institute of Inorganic Chemistry of the Czech Academy of Sciences	plocek@iic.cas.cz
Jasminka	Popovic	Rudjer Boskovic Institute	jpopovic@irb.hr
Dragica	Prill	Goethe University Frankfurt am Main	prill@chemie.uni-frankfurt.de
Stjepan	Prugovečki	Malvern Panalytical B.V.	Stjepan.Prugovecki@panalytical.com
Estefanía	Quintero-Martos	Universidad de Málaga	estefaniaqm@uma.es
Rebecca	Rae	University of Edinburgh	rebecca.rae@ed.ac.uk
David	Rafaja	Freiberg University of Technology	rafaja@ww.tu-freiberg.de
Mark	Raven	CSIRO Land and Water	Mark.Raven@csiro.au
Luca	Rebuffi	Elettra-Sincrotrone Trieste S.C.p.A.	luca.rebuffi@elettra.eu
David	Rendle	Unaffiliated	drendle4@gmail.com
Emily	Reynolds	University of Oxford	emily.reynolds@chem.ox.ac.uk
Jordi	Ruius	Institut de Ciència de Materials de Barcelona (CSIC)	jordi.rius@icmab.es
Rosanna	Rizzi	Institute of Crystallography (IC-CNR)	rosanna.rizzi@ic.cnr.it
Kimin	Roh	Korea Institute of Geoscience and Mineral	kmroh@kigam.re.kr
Danilo	Rosa Nunes	Laboratoire de Physique des Solides/Université Paris-Sud	danilo.nunes@u-psud.fr
Gwenaelle	ROUSSE	Sorbonne Université - Collège de France	gwenaelle.rousse@upmc.fr
Matthew	Rowles	Curtin University	matthew.rowles@curtin.edu.au

EPDIC16
Delegate List

First name	Last name	Organisation	Email
Martin	Rudolph	TU Freiberg	M.Rudolph@iww.tu-freiberg.de
Anastasia	Ryanskaya	Institute of Geology and Geochemistry, UB RAS	tosenka2008@gmail.com
Amin	Sadeghpour	Empa	amin.sadeghpour@empa.ch
Martin	Sahlberg	Uppsala University	martin.sahlberg@kemi.uu.se
Matilde	Saura-Múzquiz	Aarhus University	msaura@chem.au.dk
Paolo	Scardi	University of Trento	Paolo.Scardi@unitn.it
Christian	Schimpf	TU Bergakademie Freiberg, Institute of Materials Science	schimpf@iww.tu-freiberg.de
Carina	Schlesinger	Goethe University, Frankfurt am Main, Germany	c.schlesinger@chemie.uni-frankfurt.de
Wolfgang	Schmidt	Max-Planck-Institut fuer Kohlenforschung	schmidt@kofo.mpg.de
Martin U.	Schmidt	Goethe University, Frankfurt a.M.	m.schmidt@chemie.uni-frankfurt.de
Peter	Schoderböck	Plansee SE	peter.schoderboeck@plansee.com
Pascal	Schouwink	Ecole polytechnique fédérale de Lausanne EPFL	pascal.schouwink@epfl.ch
Mark	Senn	University of Warwick	m.senn@warwick.ac.uk
Sung Man	Seo	KIGAM	smseo@kigam.re.kr
KENNETH	Shankland	UNIVERSITY OF READING	K.SHANKLAND@READING.AC.UK
Adam	Shnier	University of the Witwatersrand	608825@students.wits.ac.za
Priyank	Shyam	Aarhus University	priyank.shyam@gmail.com
Dubravka	Sisak Jung	DECTRIS Ltd.	dubravka.sisak@dectris.com
Oleksandr	Slipeniuk	Rigaku Europe SE	oleksandr.slipeniuk@rigaku.com
Stef	Smeets	Stockholm University	stef.smeets@mmk.su.se
Yoo Jung	Sohn	Forschungszentrum Jülich GmbH	y.sohn@fz-juelich.de
Elena	Solana Madruga	CSEC and School of Chemistry, The University of Edinburgh	esolana@ed.ac.uk
Timothy	Spain	Diamond Light Source	timothy.spain@diamond.ac.uk
Maria	Spiliopoulou	University of Patras, Department of Biology	mary.spiliopoulou94@gmail.com
Ashok	Sreekumar Menon	Uppsala University	ashok.menon@kemi.uu.se
Peter	Stephens	Stony Brook University	pstephens@stonybrook.edu
Kevin	Stone	SLAC National Accelerator Laboratory	khstone@slac.stanford.edu
Mark	Styles	CSIRO	Mark.Styles@csiro.au
Keith	Tame	Rigaku Europe SE	Keith.Tame@scimed.co.uk
Hao	Tang	Aarhus University	hao@inano.au.dk
Chiu	Tang	Diamond Light Source	c.c.tang@diamond.ac.uk
Lukas	Tapmeyer	Goethe University	tapmeyer@chemie.uni-frankfurt.de
Leszek	Tarkowski	Cztery Bity	leszek@tarkowski.org
Maxwell	Terban	Max Planck Institute FKF	M.Terban@fkf.mpg.de

EPDIC16
Delegate List

First name	Last name	Organisation	Email
Hideo	Toraya	Rigaku Corporation	toraya@rigaku.co.jp
Ivan	Trussov	University of Birmingham	ixt457@student.bham.ac.uk
Ivan	Trussov	University of Birmingham	ixt457@student.bham.ac.uk
Matt	Tucker	Oak Ridge National Lab'	tuckermg@ornl.gov
Kristian	Ufer	Federal Institute for Geosciences and Natural Resources (BGR)	kristian.ufer@bgr.de
Oriol	Vallcorba	ALBA Synchrotron	ovallcorba@cells.es
Jacco	van de Streek	Avant-garde Materials Simulation	jacco.vandestreek@avmatsim.eu
Geert	Vanhoyland	Bruker AXS	geert.vanhoyland@bruker.com
Andrew	Venter	Necsa SOC Limited	andrew.venter@necsa.co.za
Emmanuel	Veron	CEMHTI - CNRS (Orléans, FRANCE)	emmanuel.veron@cnrs-orleans.fr
Robert	Von Dreele	APS, Argonne National Laboratory	vondreele@anl.gov
Claudia	Weidenthaler	Max-Planck-Institut für Kohlenforschung	claudia.weidenthaler@mpi-muelheim.mpg.de
Simon	Welzmiller	Thermo Fisher Scientific	simon.welzmiller@thermofisher.com
Marius	Wetzel	Institute of Materials Science, TU Bergakademie Freiberg	marius.wetzel@iww.tu-freiberg.de
Michael	Wharmby	DESY	michael.wharmby@desy.de
Maggie	White	Newcastle University	maggie.white@newcastle.ac.uk
Pamela	Whitfield	Excelsus Structural Solutions	pamela.whitfield@excels.us
Angus	Wilkinson	Georgia Institute of Technology	angus.wilkinson@chemistry.gatech.edu
Andrzej	Wojtas	Dr Ir Andrzej Wojtas - METLAB	aswojtas@gmail.com
Tom	Wood	ISIS Neutron Source	thomas.wood@stfc.ac.uk
David	Wragg	University of Oslo	david.wragg@smn.uio.no
Jonathan	Wright	ESRF	wright@esrf.fr
Masao	Yonemura	High Energy Accelerator Research Organization (KEK)	yone@post.kek.jp
Tatchamapan	Yoskamtorn	The University of Oxford	tatchamapan.yoskamtorn@chem.ox.ac.uk
Pascal G.	Yot	Université de Montpellier	pascal.yot@umontpellier.fr
Debora	Zanolla	University of Trieste	debora.zanolla@phd.units.it
Asmaa	Zaraq	Université Hassan II Casablanca Morocco	assmaa.zaraq@gmail.com
Jesus David	Zea-Garcia	Universidad de malaga	jdavidzea@uma.es
Xiaodong	Zou	Stockholm University	xzou@mmk.su.se